

Title	Crystal engineering: exploiting variation of sulfur oxidation for the control of the solid state structure of organosulfur compounds
Authors	Daly, Carla A.
Publication date	2013
Original Citation	Daly, C.A. 2013. Crystal engineering: exploiting variation of sulfur oxidation for the control of the solid state structure of organosulfur compounds. PhD Thesis, University College Cork.
Type of publication	Doctoral thesis
Rights	© 2013, Carla A. Daly. - http://creativecommons.org/licenses/by-nc-nd/3.0/
Download date	2024-09-24 22:57:11
Item downloaded from	https://hdl.handle.net/10468/1181



UCC

University College Cork, Ireland
 Coláiste na hOllscoile Corcaigh

Crystal Engineering: Exploiting variation of sulfur oxidation for the control of the solid state structure of organosulfur compounds



Carla A. Daly, B.Sc.

A thesis presented for the degree of
Doctor of Philosophy

to

THE NATIONAL UNIVERSITY OF IRELAND, CORK

Department of Chemistry
University College Cork

Supervisors: Prof. Anita R. Maguire & Dr. Simon Lawrence

Head of Department: Prof. Michael Morris

January 2013

Contents

Chapter 1

Introduction.....1

Chapter 2

Design and synthesis of scaffolds to enable the study of weak hydrogen bond interactions in the solid state.....43

Chapter 3

Design and synthesis of a diphenylacetylene-based switching entity.....113

Chapter 4

Conclusions and Future work.....175

Chapter 5

Experimental.....181

Appendices

List of abbreviations*ii*

NCI-60 results.....*iv*

Abstract

This thesis is focused on the design and synthesis of a diverse range of novel organosulfur compounds (sulfides, sulfoxides and sulfones), with the objective of studying their solid state properties and thereby developing an understanding of how the molecular structure of the compounds impacts upon their solid state crystalline structure. In particular, robust intermolecular interactions which determine the overall structure were investigated. These synthons were then exploited in the development of a molecular switch.

Chapter One provides a brief overview of crystal engineering, the key hydrogen bonding interactions utilized in this work and also a general insight into “molecular machines” reported in the literature of relevance to this work.

Chapter Two outlines the design and synthetic strategies for the development of two scaffolds suitable for incorporation of terminal alkynes, organosulfur and ether functionalities, in order to investigate the robustness and predictability of the $S=O\cdots H-C\equiv C$ - and $S=O\cdots H-C(\alpha)$ supramolecular synthons. Crystal structures and a detailed analysis of the hydrogen bond interactions observed in these compounds are included in this chapter. Also the biological activities of four novel tertiary amines are discussed.

Chapter Three focuses on the design and synthesis of diphenylacetylene compounds bearing amide and sulfur functionalities, and the exploitation of the $N-H\cdots O=S$ interactions to develop a “molecular switch”. The crystal structures, hydrogen bonding patterns observed, NMR variable temperature studies and computer modelling studies are discussed in detail.

Chapter Four provides the overall conclusions from chapter two and chapter three and also gives an indication of how the results of this work may be developed in the future.

Chapter Five contains the full experimental details and spectral characterisation of all novel compounds synthesised in this project, while details of the NCI (National Cancer Institute) biological test results are included in the appendix.

Acknowledgements

The completion of this thesis would not have been possible without the help and support of several people. First and foremost I would like to express my sincerest gratitude to my supervisors, Prof. Anita Maguire and Dr. Simon Lawrence, for their guidance, encouragement, time and patience. Thank you both for affording me this wonderful opportunity and for remaining enthusiastic and supportive as various obstacles arose throughout the course of this work.

In addition, I have been very privileged to work and collaborate with many people in the Chemistry Department in UCC who became great friends over the past number of years. Many thanks to everyone in both my research groups – the ARM group (Aoife, Alan, Brian, Catherine, Denis, Francis, Graham, Leslie-Ann, Liam, Linda, Marie, Niamh, Naomi, Nuala, Orla, Paul, Rebecca, Sarah, Shane and Sinead) and the SEL group (Kevin Guiry, David, Kevin Eccles, Stephen, Robin and Lorraine) for always being so helpful and approachable. Thank you to all the researchers in Lab 4.27 for making the long days fun and enjoyable! To all my other fellow colleagues, from the various research groups in the Cavanagh and Kane buildings, who are too numerous to mention, but have all contributed to creating a friendly and enjoyable research atmosphere, thank you. A special word of thanks to Kevin Eccles for all his time and help with my crystal structures, Stephen for his expertise from computers to cars (someday I'll repay the €10,000!!!), Denis Lynch who always took the time to help me with any queries and Lorna for her lengthy discussions on 'Home and Away'!

I would like to thank all the technical staff in UCC. Thanks to Dr. Dan McCarthy and Dr. Lorraine Bateman for NMR work conducted, to Dr. Florence McCarthy and Mick O'Shea for mass spectrometry services, to Barry O' Mahony and Helen Kelly for microanalysis, to Derry Kearney for glass-blowing services, to Chrissie O'Flaherty, Tina Kent, Terry Horgan and Denis Duggan, to Noel Browne for solvent delivery, to Donnacha O'Connell for all his help with the demonstrating, Dr. Matthias Jauch for IT support, and Dr. Noel O'Boyle for the molecular modelling. Also a special thanks to Debbie Curran for all her help. Thanks to Dr. Florence McCarthy and Dr. Stuart Collins for their help with the NCI biological testing. I would also like to express my gratitude to Science Foundation Ireland (SFI) for funding my PhD studies.

A special word of thanks to Deirdre, Dan and Ernie for their friendship, laughs and chats, to Michelle for her singing and for keeping me company in a lab full of lads and to Roisin for her tea visits since I moved to Cork. I am also very grateful for being given the opportunity to play with the 'UCC United' ladies soccer team. It provided me with a welcome distraction

from the thesis typing and I've made some brilliant friends throughout the years. To Kevin and Niamh in No. 7, thank you for welcoming in a Clare girl, always looking out for me and being fantastic housemates over the past 4 years.

I would especially like to thank Larry for all his support and encouragement. I know it wasn't easy going through it all a second time! Thanks for your patience, advice and for keeping me smiling all the way to the end!

Finally, I'd like to thank all my family – my brother Kevin and sister Gina, Gran for all her candles and prayers, Ger for solving my many computer woes, Colette for her guidance, John, Mary, Dara and Ross for their hospitality in Dublin and constant encouragement. Last but not least, I'd like to thank Mam and Dad to whom I dedicate this thesis. Mam, thanks for all the soups and Shepherd's pies you sent to Cork for the past 8 years. You might get a break from it now! Dad, thanks for the hurling matches and giving me a few days out! Both of you, thanks for keeping me going through the hard times, getting me this far and always supporting me in whatever I choose to do.

To Mam and Dad

Chapter 1
Introduction

1 Contents

1.1	Supramolecular chemistry – a brief history	5
1.2	Crystal Engineering – the synthon approach.....	7
1.3	Hydrogen bonding in crystal engineering	10
1.3.1	Terminal alkynes as hydrogen bond donors	14
1.3.2	Sulfoxides as hydrogen bond acceptors	16
1.3.3	$C\equiv C-H\cdots O=S$ hydrogen bonding.....	17
1.3.4	$N-H\cdots S$ and $N-H\cdots O=S$ interactions.....	18
1.4	Molecular machines	20
1.4.1	Natural molecular machines	21
1.4.2	Rotaxanes, pseudorotaxanes, and catenanes.....	22
1.4.3	Crystalline molecular rotors	29
1.4.4	Molecular Switches	33
1.5	Future perspectives.....	34
1.6	References.....	35

1.1 Supramolecular chemistry – a brief history

Supramolecular chemistry is the ‘chemistry of molecular assemblies and of the intermolecular bond’ as defined by Jean-Marie Lehn, who won the Nobel Prize for his work on molecular recognition in 1987.^{1,2} Supramolecular chemistry is concerned with the ‘chemistry beyond the molecule’ *i.e.* the role of non-covalent forces and spatial fitting between molecular individuals in the formation of supramolecular clusters.³⁻⁵ It is one of today’s fastest growing and most active fields of chemistry. This relatively young area intertwines the areas of chemistry, biology and physics where a range of perspectives is a major feature of this discipline.⁶⁻⁹

Essentially supramolecular chemistry focuses on the study of systems containing more than one molecule and it aims to understand the structure, function and properties of these assemblies. These multi-component systems consisting of atoms, molecules or ions are held together by non-covalent interactions such as hydrogen bonding, van der Waals forces, π - π interactions and also electrostatic effects.¹⁰ Supramolecular chemistry uses these non-covalent interactions to create a variety of oligomeric and polymeric molecular ensembles from constituent molecules. This principle enables the development of new chemical species bearing an individual set of physical and chemical properties.¹¹

The initial inspiration for the design and synthesis of novel supramolecular architectures primarily came from natural molecules *e.g.* proteins, oligonucleotides, lipids.¹² When a drug attaches to its target, a substrate binds to an enzyme, or a signal is transmitted between cells, a particularly selective interaction occurs between these sites to control this process. Supramolecular chemistry arose from efforts to mimic these weak non-covalent interactions and the phenomenon of molecular recognition in biological systems. Molecular recognition first originated with Emil Fischer’s ‘lock and key’ mechanism which he proposed in 1894, to describe the enzyme-substrate recognition process, well before the idea of supramolecular chemistry came to light.¹³ In 1948, Powell coined the term ‘clathrate’ which describes supramolecular systems that are formed when guest molecules are incorporated into cavities formed by host molecules.¹⁴ He observed this behaviour on determining the structure of hydroquinone with SO₂ and other gases.¹⁵ A spatial complementarity exists between the molecules rather than formation of chemical bonds.¹¹ This implies that the chemical entities recognize each other and an information-recognition process is established. If the receptor is able to choose its partner among various substrates then it is selective which is very important.¹⁶ Interest gradually grew in this new area of science and in 1967, Pederson made

a significant breakthrough when he observed that the macrocyclic molecules, crown ethers, showed molecular recognition by coordinating with the cations of alkali metals.¹⁷ Lehn and Cram further explored this area and proceeded to develop more complex polycyclic ligands including 3D architectures such as cryptands and spherands.^{11,18-21}

The increased knowledge of intermolecular interactions and molecular recognition has led to significant advances in molecular self-assembly. The synthesis of multimolecular architectures with various shapes, compositions and functionalities is now possible in both the solution and the solid state.¹² Control of the geometry and rigidity of artificial molecules allows the building of molecules which can spontaneously generate well defined molecular structures *e.g.* porous organic cages, rotaxanes, helices and metal organic frameworks (MOFs), **Figure 1.1**.^{16,22-24}

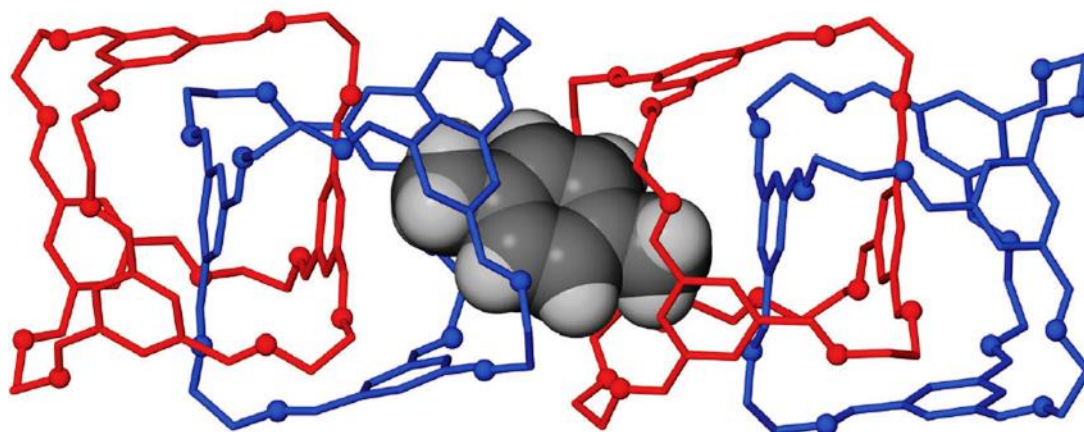


Figure 1.1: Triply interlocked cages synthesized by Cooper and co-workers joined by a *p*-xylene molecule that occupies well-defined cavities present within the assemblies.²²

Indeed recent research is focused on increasing the complexity of these supramolecular architectures and furthermore advancing their functionality. The development of molecular devices is one such approach to functionalising supramolecular systems. These supramolecular machines can carry out mechanical, electric, photochemical and other such functions in a similar manner to their macroscopic analogues *e.g.* motors, switches, muscles.^{11,25,26} For example, supermolecules that respond to light or that can conduct electricity suggest that supramolecular chemistry will be one of the major tools used for the development of nanotechnology. Supramolecular chemistry has the potential to answer many of the environmental and energy production problems faced by the world today by reducing our dependence on large devices and machines with poor energy efficiency.²⁷ Indeed significant progress has been achieved in the field of artificial photosynthetic systems.²⁸

In general, the chemical systems studied within the research field of supramolecular chemistry are broadly classified into two major categories: molecular recognition in solution is usually referred to as supramolecular chemistry and the organised self-assembly in the solid state as crystal engineering, **Figure 1.2**.

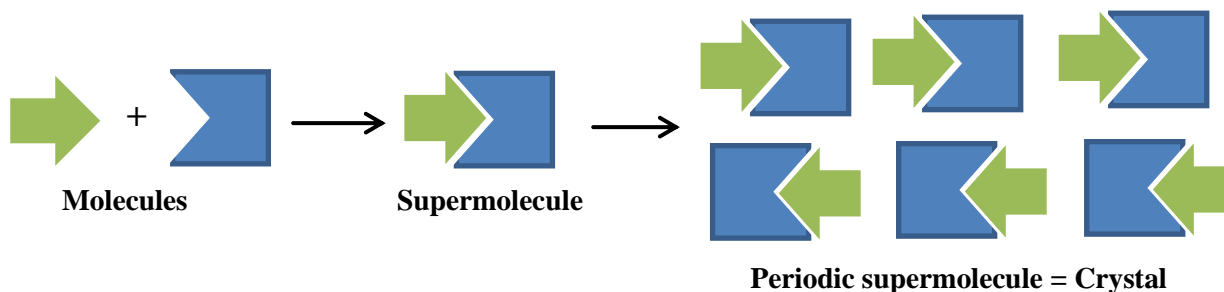


Figure 1.2: Molecular recognition of molecules to form a supermolecule and periodic arrangement of supermolecules in a crystal lattice. Reproduced from Nangia.²⁹

Since the solid state properties of organosulfur compounds are the major topic of this thesis, solid state supramolecular chemistry *i.e.* crystal engineering will be the main focus of this review.

1.2 Crystal Engineering – the synthon approach

Crystal engineering, the design and construction of a molecular crystal, is one branch of supramolecular chemistry that has flourished in recent years. Defined by Desiraju as ‘the understanding of intermolecular interactions in the context of crystal packing and the utilisation of such interactions in the design of new solids with desired physical and chemical properties’, the concept of crystal engineering can be applied to any kind of intermolecular assembly *e.g.* protein ligand recognition, supramolecular polymers or systems for drug delivery.^{30,31} This interdisciplinary subject attracts researchers from a wide variety of disciplines including organic chemistry, inorganic and organometallic chemistry, crystallography, material sciences and computational chemistry. The demand to broaden the understanding of how to control self-assembly and molecular recognition, and also the increased interest in developing sophisticated devices are the core reasons for this heightened interest.³²

Schmidt first coined the term ‘crystal engineering’ in 1971, with regard to his work on topochemical reactions of crystalline cinnamic acids.³³ However, the concept of crystal engineering emerged much earlier than this, possibly in the 1940s and 1950s, when Robertson was perhaps the first to relate the molecular structure of organic materials with

their crystal structure.³⁴ Dunitz was the first to describe the crystal in supramolecular terms - ‘supermolecule par excellence’, since the repetitive arrangement of molecules in three dimensions in the crystal has an incredible level of precision.^{35,36} Crystal engineering has often been compared to the supramolecular equivalent of organic synthesis since it rationally designs a particular solid state structure using appropriate intermolecular interactions and works backwards to identify precursor molecules that can assemble during crystallisation to form the target structure.³⁶

The purpose of crystal engineering is to predict and control the packing of molecular components in the solid state and thereby synthesise solid state supramolecular structures with specific functions from well-designed building blocks. However, the task of dissecting a complex target molecule into suitable building blocks is a significant challenge. Some strategies for structure simplification include: (i) the use of space group information to generate small clusters of molecules, (ii) hierarchical hydrogen bonding arrangement as exemplified by Etter, (iii) assembly through functional group recognition (supramolecular synthons) or molecular recognition (tectons).^{11,31,37}

The supramolecular synthon approach is highly advantageous as it offers a substantial simplification in the understanding of crystal structures. Corey first introduced the term ‘synthon’ with respect to organic chemistry retrosynthesis where he explained synthons as common building blocks with specific functionality.^{38,39} Similarly, in crystal engineering the term supramolecular synthon describes a repeating structural unit in crystal structures that directs the logical design of supramolecular architectures based on a small number of repeating hydrogen bond patterns.²⁹ These synthons contain the fundamental bond connectivity and stereochemical information required to synthesize the final target network. Robust synthons are those which can be transferred between different compounds bearing similar functional groups, **Figure 1.3**. However, other factors such as competing supramolecular synthons, interference from other molecular functionalities and undesirable interactions involving the hydrocarbon core will influence their reliability for controlling the solid state network. For example, in glycolanilide, **1**, **Figure 1.4**, both dimers and catemers can be observed depending on which polymorph is formed. In the more thermodynamically stable polymorph O-H···O=C chains are formed and the amide N-H is not involved in hydrogen bonding. However, in the metastable polymorph, a dimer is formed incorporating the N-H and O-H.⁴⁰

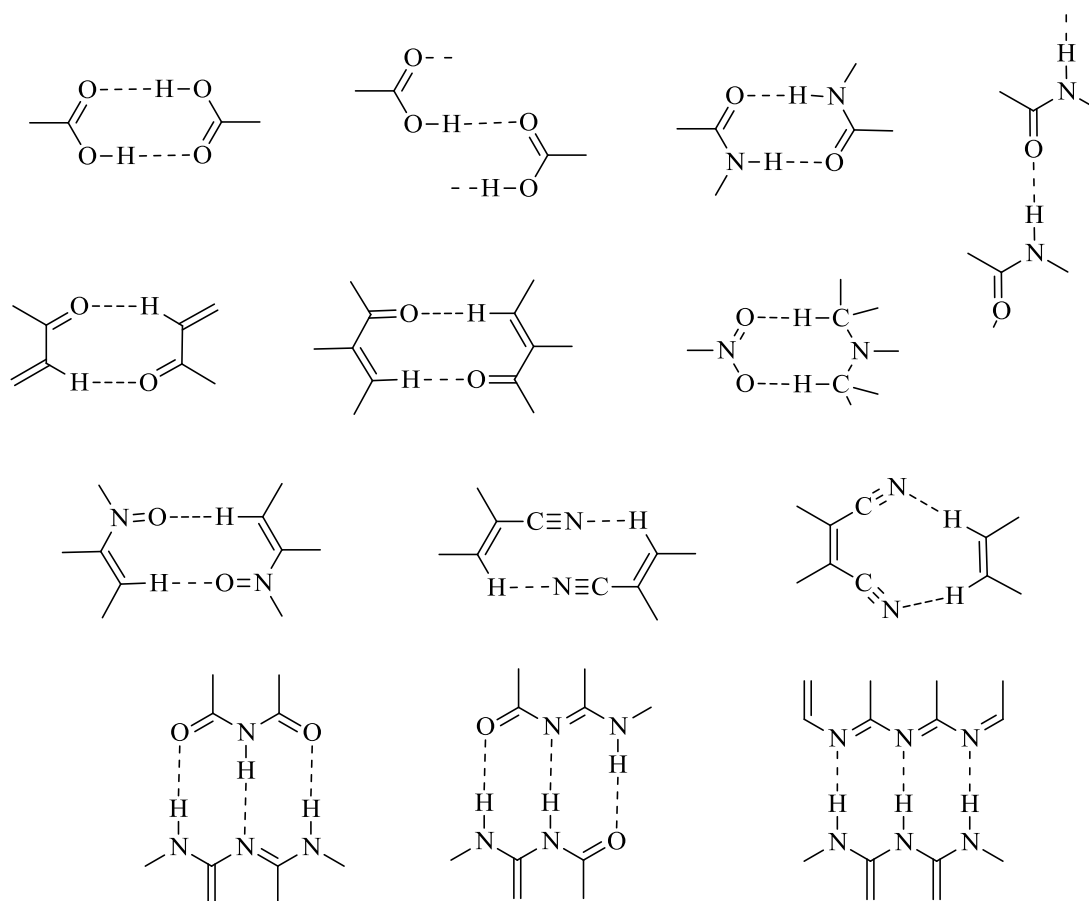


Figure 1.3: Common supramolecular synthons.

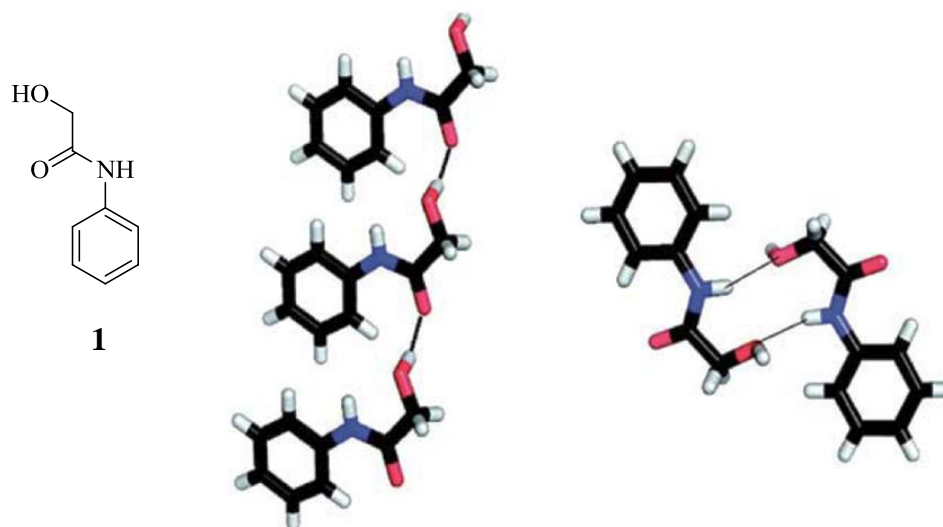


Figure 1.4: Glycolanilide, **1**, forming catemer (left) and dimer (right).⁴⁰

To form reliable and effective supramolecular synthons, it is necessary that the intermolecular interactions bear sufficient strength and directional characteristics. As a result, hydrogen bond interactions, which are often described as ‘the masterkey interaction in supramolecular chemistry’ due to their strong nature and directionality, have been widely

exploited in the construction of robust synthons and in crystal design *e.g.* O–H···O, N–H···O, C–H··· π .^{41,42}

1.3 Hydrogen bonding in crystal engineering

The hydrogen bond, usually characterized as X–H···Y, is an interaction between a hydrogen atom covalently bonded to an electronegative atom (X, where X = O, N, halogen) and another atom (Y, where Y = O, N, S, halide etc.) which has a lone pair of electrons or polarisable π electrons and is also reasonably electronegative.⁴³ The group X–H is referred to as the *donor* and Y is defined as the *acceptor*. The water dimer is the typical model system for hydrogen bonding, **Figure 1.5**.

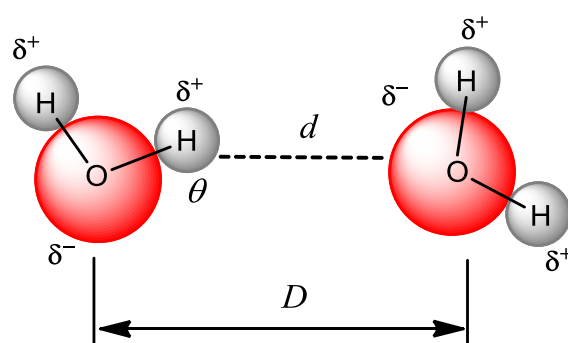


Figure 1.5: Hydrogen bonding between water molecules and the geometrical parameters associated in the characterisation of a hydrogen bond: $d = \text{H}\cdots\text{O}$ distance, $D = \text{O}\cdots\text{O}$ distance, $\theta = \text{O}-\text{H}\cdots\text{O}$ angle.

Hydrogen bonding is much more complex in reality than the classical case illustrated in **Figure 1.5**. A hydrogen bond can be so strong that it displays properties similar to a covalent bond or it can be extremely weak so that it resembles a van der Waals interaction. This has led to much discussion throughout the years on an accurate definition of hydrogen bonding.⁴⁴⁻⁴⁶ Initially, only strongly electrostatic X–H···Y interactions were considered as hydrogen bonds but evidence of weak hydrogen bonds such as C–H···O displaying geometrical, structural and spectroscopic characteristics similar to the stronger bonds resulted in a re-examination of this definition. As a result, only general explanations exist for this complex phenomenon so that strong and weak inter/intramolecular interactions are included. Hydrogen bonds have been defined in terms of their interaction geometries, IR characteristics and electron density distribution properties but these definitions are only applicable in their respective fields. It has also been suggested to consider the van der Waals radii as criterion for hydrogen bonding ('van der Waal cutoff'). This requires that the X···Y distance is significantly shorter than the sum of the van der Waals radii of X and Y.

However, this definition has been criticized as it is considered much too restrictive.⁴³ In 2011 a modern definition of the hydrogen bond was published by IUPAC including a list of criteria and characteristics important in hydrogen bonding.⁴⁷ It states that ‘the hydrogen bond is an attractive interaction between a hydrogen atom from a molecule or a molecular fragment X-H in which X is more electronegative than H, and an atom or group of atoms in the same or a different molecule, in which there is evidence for bond formation’.

One of the hallmarks of hydrogen bonding is a positive directionality preference, with the geometry of X-H...Y tending towards linearity. The polarity of the donor influences the degree of directionality. The directionality decreases as the polarity of the X-H group decreases *e.g.* O-H > C≡C-H > C=CH₂ > -CH₃.⁴³ **Figure 1.6** illustrates this concept with respect to X-H...O=C interactions. There is a gradual decrease in directionality from a) to d) as the donor acidity decreases. Although the C-H...O featured in d) displays weak linearity, it still displays a significant preference compared to the van der Waals C-H...H-C interaction depicted in e) in **Figure 1.6**.

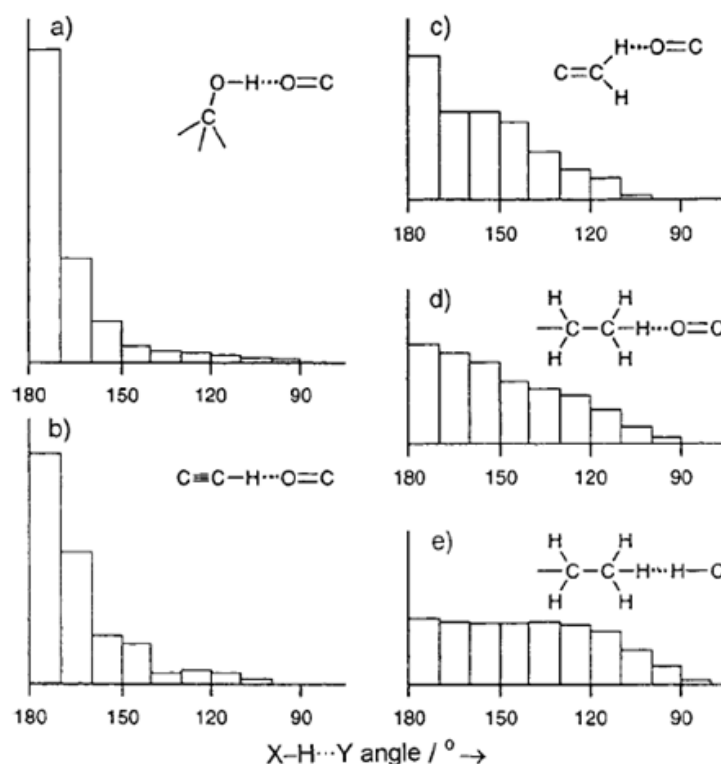


Figure 1.6: Histograms a) to d) depicting the decrease in directionality of X-H...O=C interactions as a result of a decrease in donor acidity. These are compared to the van der Waals contact in e).⁴⁴

Another unique feature of hydrogen bonds that distinguishes them from other dipole interactions is the ability of the hydrogen bond donor to interact with one, two or three acceptors simultaneously, **Figure 1.7**. The acceptor, however, can only partake in hydrogen bonding along the direction of its electron lone pairs and therefore this stoichiometry puts constraint on the number of neighbours located next to the acceptor site.⁴⁸

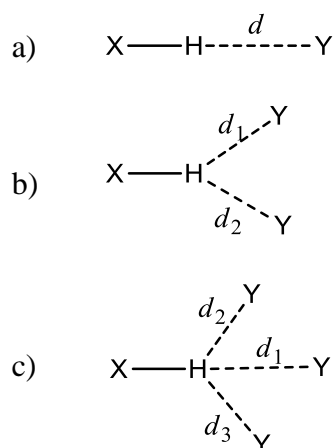


Figure 1.7: a) Simple hydrogen bond; b) bifurcated hydrogen bond; c) trifurcated hydrogen bond.⁴³

The task of predicting if a hydrogen bond will form between a potential donor (X-H) and acceptor (Y) is difficult. One method that has been investigated is to establish their probabilities of formation in order to identify the most robust and reproducible supramolecular synthons which can be reliably implemented in crystal engineering.⁴³ Hydrogen bonds that form sporadically are extremely difficult to control and therefore unreliable. Many factors can influence the ability of donors and acceptors to partake in motif formation, such as steric accessibility, donor/acceptor competition and cooperativity. Allen *et al.* developed a method, employing the Cambridge Structural Database (CSD), for identifying the most common intra- and intermolecular hydrogen-bonded ring motifs formed by N-H or O-H donors and N or O acceptors.^{49,50} Etter proposed a set of general guidelines with regard to hydrogen bonding patterns in organic compounds in order to help predict the resulting crystal structure. The first three rules can be applied to general functional groups and they state that all good proton donors and acceptors are used in hydrogen bonding, six-membered-ring intramolecular hydrogen bonds form in preference to intermolecular hydrogen bonds and the best proton donors and acceptors remaining after intramolecular hydrogen bond formation form intermolecular hydrogen bonds to one another.³⁷

The strength of a hydrogen bond ($\text{H}\cdots\text{Y}$) increases with an increased electronegativity of X, which leads to a highly polar covalent X-H bond. Also the closer the X-H \cdots Y angle is to 180° , the stronger the hydrogen bond and the shorter H \cdots Y distance.⁴⁷ Jeffrey classified hydrogen bonds as ‘strong’, ‘moderate’ and ‘weak’ and their respective properties are listed in **Table 1.1**. This table acts as a rough guide for categorising hydrogen bonds since their properties lie in continuous ranges with no strict borderlines.⁴³

Table 1.1: Properties of hydrogen bond interactions. Reproduced from reference.⁴³

	Strong	Moderate	Weak
Interaction Type	Strongly covalent	Mostly electrostatic	Electrostatic/ dispersion
Bond lengths (Å) ($\text{H}\cdots\text{Y}$)	1.2 - 1.5	1.5 - 2.2	> 2.2
Lengthening of X-H (Å)	0.08 - 0.25	0.02 - 0.08	< 0.02
X-H versus H \cdots Y	X-H \sim H \cdots Y	X-H < H \cdots Y	X-H \ll H \cdots Y
Directionality	strong	moderate	weak
Bond angle ($^\circ$) (X-H \cdots Y)	170 - 180	> 130	> 90
Bond energy (kcal mol ⁻¹)	15 - 40	4 - 15	< 4
Relat. IR shift $\delta\nu_{\text{XH}}$ (cm ⁻¹)	25%	10 - 25 %	< 10 %
¹ H downfield shift (%)	14 - 22	< 14	-

Weak hydrogen bonds have received increased attention in recent years due to their significant impact in crystal engineering and as a result, they are the major subject matter in this project. In weak hydrogen bonding the donor (X) or acceptor (Y), or even both are only of moderate to low electronegativity.⁴⁴ Similar to other hydrogen bonds, there are varying degrees of weak hydrogen bonds. Bonds formed between weak donors and strong acceptors have been studied extensively, particularly the C-H \cdots O bond.⁵¹ Strong donors associating with weak acceptors have also attracted attention *e.g.* O-H \cdots π , N-H \cdots π , O-H \cdots S. Finally at the lower end of the hydrogen bond scale are bonds formed with weak donors and weak acceptors *e.g.* C-H \cdots π , C-H \cdots F-C.⁵²

The task of crystal structure prediction can be extremely complicated as in most instances the interactions in the crystal packing are not hierarchical.⁴⁴ It is the combination of strong and weak interactions that determine the crystal packing, **Figure 1.8**. Therefore it is essential that weak interactions are studied carefully as they can have a significant influence on the overall packing and also may provide additional structural adaptability.

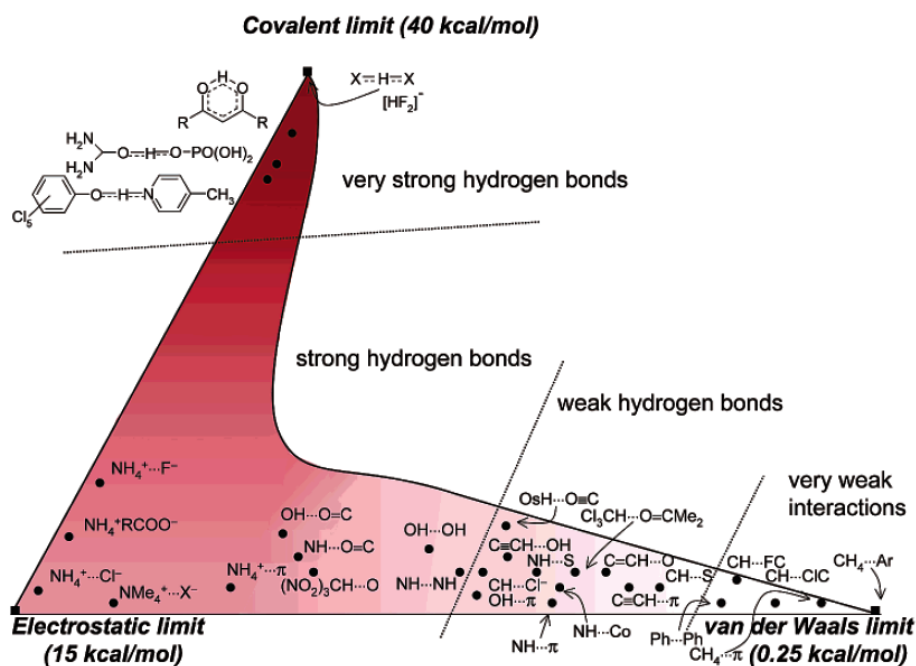


Figure 1.8: The vast continuum of hydrogen bonding ranging from near covalent in nature to almost complete van der Waals interactions. Reproduced from reference.⁴⁴

1.3.1 Terminal alkynes as hydrogen bond donors

The role of terminal alkynes in hydrogen bonding has previously been reviewed extensively by Lehane,⁵³ so for the purpose of this thesis terminal alkynes as hydrogen bond donors will be discussed briefly.

The hydrogen atom in a terminal alkyne forms stronger C-H...X hydrogen bonds than most hydrocarbons due to its relatively high acidity (Ethyne: pKa = 25). This acidity can be rationalised by examining the carbanion of the terminal alkyne. The lone pair of electrons on the carbanion lie in an *sp* hybrid orbital which consists of 50% *s* character and as a result these electrons are close to the carbon nucleus, which leads to greater electrostatic stabilisation of the electron pair, **Figure 1.9**. Therefore, the conjugate base of the alkyne is quite stable and easily formed.

Directionality is an important property of terminal alkynes in intermolecular interactions and when they act as hydrogen bond donors, a preference for linearity is observed.⁴³ Terminal alkynes have previously been exploited as hydrogen bond donors to effectively form C≡C-H...O₂N and C≡C-H...N≡C supramolecular synthons.⁵⁴ Marder and co-workers also

demonstrated that the $C\equiv C-H\cdots O$ motif forms in preference to $C\equiv C-H\cdots\pi$ interactions and as a result it can also be considered a robust supramolecular synthon, **Figure 1.10**.⁵⁵

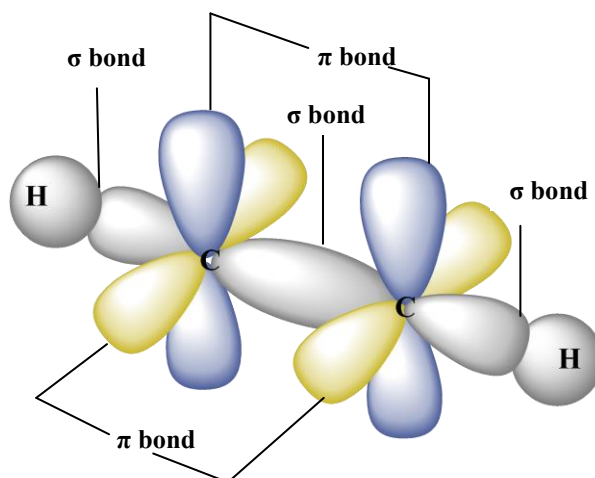


Figure 1.9: Structure of ethyne displaying orbital overlap.

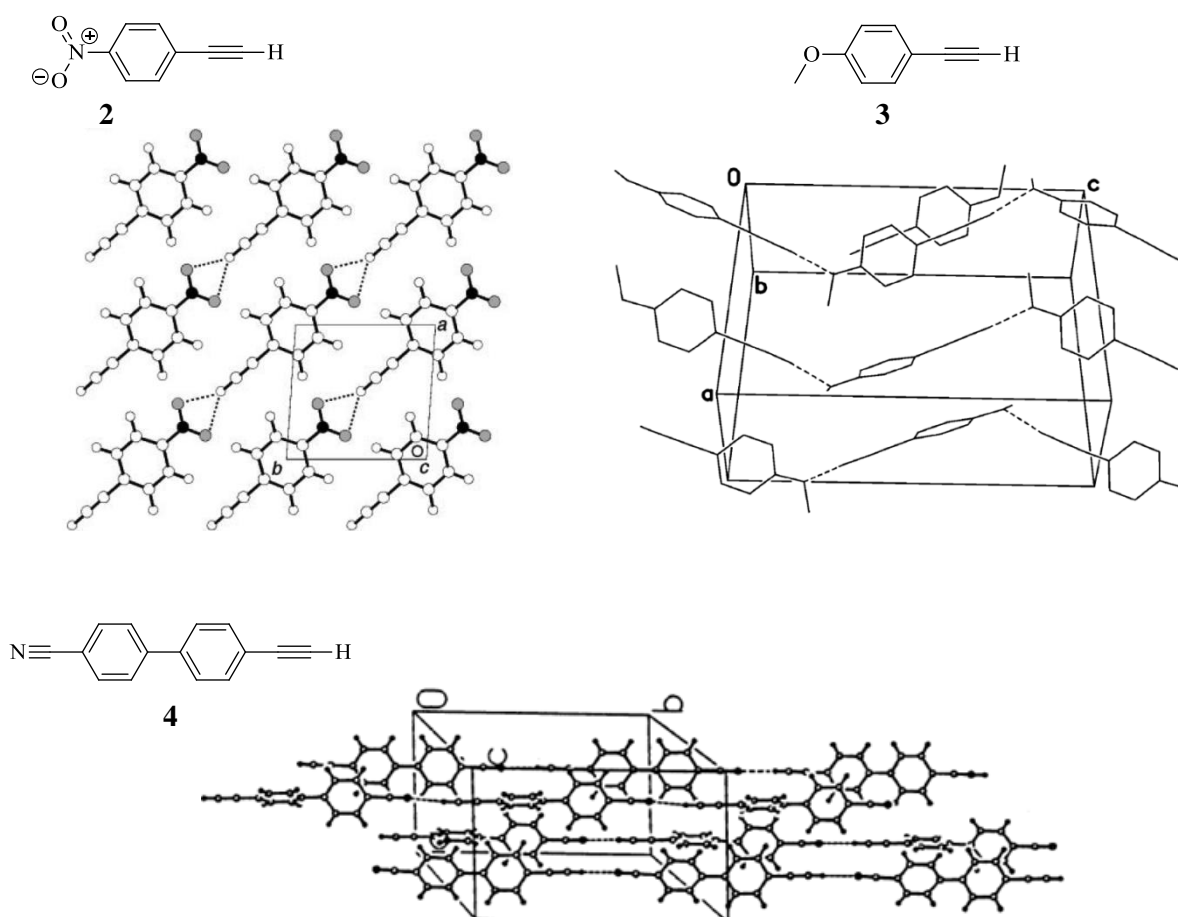


Figure 1.10: Crystal structures of 1-ethynyl-4-nitrobenzene, **2**, 4-ethynylanisole, **3**, and 4-cyano-4'-ethynylbiphenyl, **4**, illustrating $C\equiv C-H\cdots O_2N$, $C\equiv C-H\cdots O$ and $C\equiv C-H\cdots N\equiv C$ motifs respectively. Reproduced from references.⁵⁴⁻⁵⁶

1.3.2 Sulfoxides as hydrogen bond acceptors

Our research group has also reviewed sulfoxides as potent hydrogen bond acceptors in detail,⁵³ so a brief summary of their hydrogen bonding capabilities is outlined as follows.

Sulfoxides are polar functional groups with an electron rich oxygen, ideally suited to act as a hydrogen bond acceptor.^{57,58} According to Hunter, the sulfoxide is quite a strong hydrogen bond acceptor, much stronger than the carbonyl oxygen but weaker than a phosphinyl oxygen.⁵⁹ Similar to the hydrogen bond donor, directionality is an important feature for the hydrogen bond acceptor. Renault *et al.* investigated the average geometrical parameters associated with sulfoxides involved in hydrogen bonding through detailed analysis of the CSD, **Figure 1.11**.⁶⁰ The angle that the sulfinyl oxygen adopts when acting as a hydrogen bond acceptor is similar to a carbonyl oxygen, where the oxygen lone pair lobes direct hydrogen bonding at an angle of 120° with the C=O plane.⁴³ **Figure 1.12** illustrates the average distribution of O-H hydrogen bond donors around sulfoxides as determined from the CSD.⁶⁰ An additional feature of sulfoxides, which should be noted when studying their crystal structures, is their intrinsic chirality, when $X \neq Y$. This characteristic may significantly impact upon the crystal packing and the overall solid state structure.⁵⁸

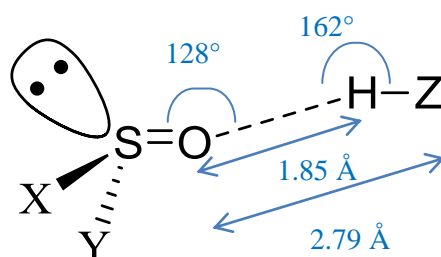


Figure 1.11: Geometrical parameters of sulfoxides involved in hydrogen bonding.

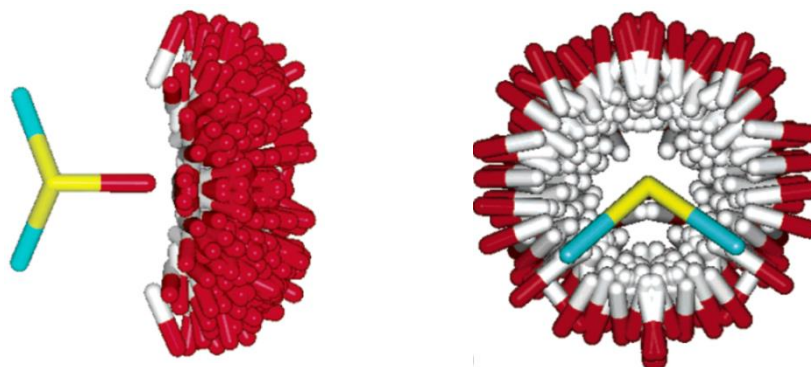


Figure 1.12: Experimental distribution of O-H donors around sulfoxides observed in the CSD reproduced from reference.⁶⁰

1.3.3 $C\equiv C-H\cdots O=S$ hydrogen bonding.

Weak hydrogen bonds involving the terminal alkyne as the donor and the sulfoxide as the acceptor are of particular interest to this research due to the recent developments by our group within this area.⁶¹ It has been widely documented that while C-H groups are often considered as poor hydrogen bond donors, many C-H \cdots O interactions display properties similar to stronger hydrogen bonds formed by N-H and O-H donors. Studies on the strength of C-H \cdots O interactions reveal that the most acidic C-H hydrogens and the best hydrogen bond acceptors *e.g.* P=O, H₂O form the strongest interactions.⁵⁶

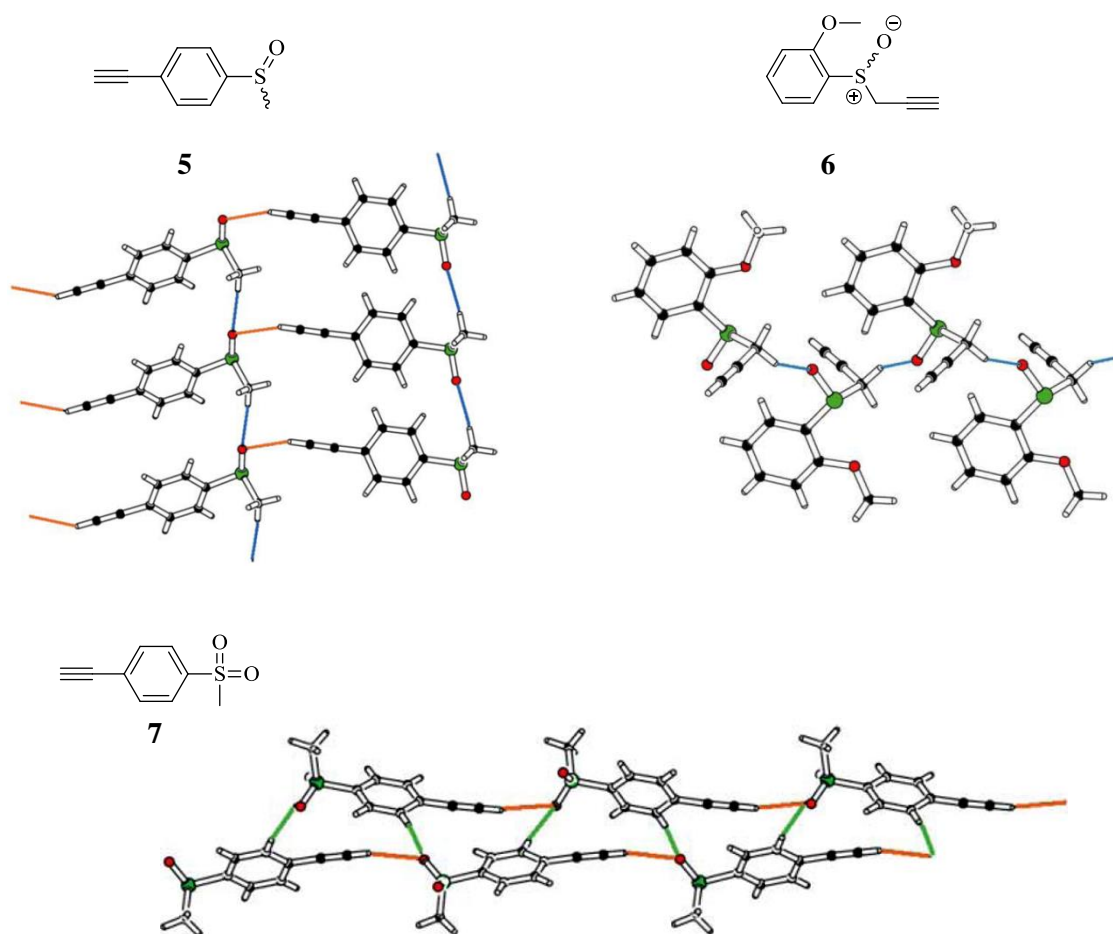


Figure 1.13: Crystal packing of sulfoxide, **5**, and sulfone, **7**, displaying $C\equiv C-H\cdots O=S$ interactions. Impact of sulfoxide on acidity of α hydrogens in **6**. Reproduced from reference.⁶¹

Prior to the investigation by our research group, surprisingly few studies involving C \equiv C-H \cdots O=S interactions were conducted.⁶²⁻⁶⁴ The most notable of these was Boese and co-workers co-crystal formation involving acetylene and dimethylsulfoxide.⁶² With such little literature precedent, this relatively unexplored interaction attracted our attention and

encouraged us to conduct a detailed investigation into the behaviour of $\text{C}\equiv\text{C}-\text{H}\cdots\text{O}=\text{S}$ interactions in the solid state.^{53,61} With evidence of terminal alkynes acting as effective hydrogen bond donors and sulfoxides acting as potent hydrogen bond acceptors, there is potential that the $\text{C}\equiv\text{C}-\text{H}\cdots\text{O}=\text{S}$ moiety could be utilized as a supramolecular synthon in crystal engineering. Lehane demonstrated that the $\text{C}\equiv\text{C}-\text{H}\cdots\text{O}=\text{S}$ interaction is an important structural feature in a series of both sulfoxide and sulfone substituted ethynylbenzenes, **5** and **7**, **Figure 1.13**. It was also established in the propynyl sulfoxide, **6**, that the acidity of the α hydrogens adjacent to sulfoxide functionality is enhanced and as a result they subsequently compete with the terminal alkyne as hydrogen bond donors.⁶¹

1.3.4 *N-H \cdots S and N-H \cdots O=S interactions.*

The versatility of amides to act as both a hydrogen bond donor and acceptor is a particularly appealing characteristic for molecular assembly and recognition. With regards to crystal engineering, it is usually their complementary $\text{N}-\text{H}\cdots\text{O}=\text{C}$ chains and dimers employed as supramolecular synthons.⁶⁵ However, the recent success in our group involving the co-crystallisation of sulfoxides with various primary amides, prompted further research of the $\text{N}-\text{H}\cdots\text{O}=\text{S}$ interaction as a reliable and robust synthon in crystal engineering.^{66,67} In the context of this particular project, the main focus was to incorporate amide and sulfur functionalities within a single molecule and exploit their hydrogen bond donor and acceptor capabilities for the formation of a molecular switch.

Sulfur has often been overlooked as a hydrogen bond acceptor due to its poor electronegativity compared to the first row elements extensively studied as hydrogen bonding entities. Early crystallographic data indicated that sulfur was a poor hydrogen bond acceptor,⁶⁸ but in recent years attention has focused on $\text{X}-\text{H}\cdots\text{S}$ hydrogen bonds where X is O or N, and reports have even suggested that hydrogen bonds involving sulfur can be just as strong as their oxygen analogues.^{69,70} The formation of $\text{N}-\text{H}\cdots\text{S}$ interactions have been observed in the crystal structures of β -lactam antibiotics, the active site of proteins such as cytochrome-P450 and also in iron-sulfur proteins.⁶⁹ This interaction is quite significant as sulfur atoms are present in the amino acids cysteine and methionine and as a result hydrogen bonding involving sulfur may play a key role in protein folding.⁷⁰ A recent study has indicated the major contribution that $\text{N}-\text{H}\cdots\text{S}$ interactions have in the stability of protein chains. It has been demonstrated that strong $\text{N}-\text{H}\cdots\text{S}$ bonds link the sulfur of methionine to

the backbone amide groups and therefore it has been suggested that the methionine residue should be considered as a strong hydrogen bond acceptor in proteins, **Figure 1.14**.⁷¹

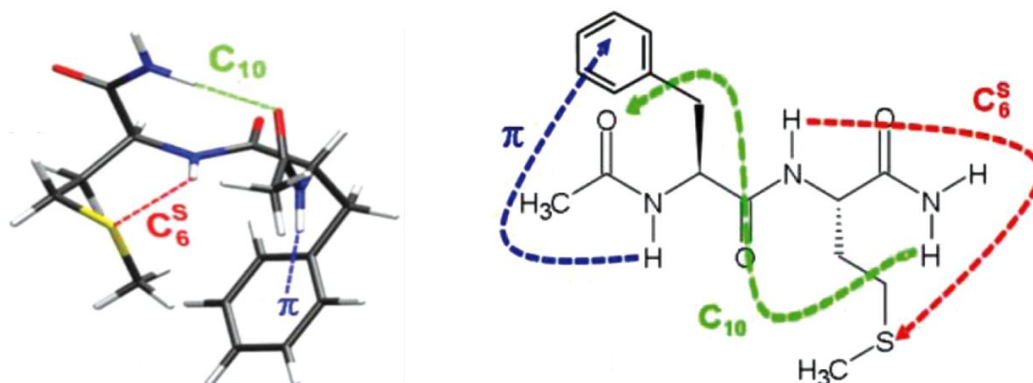


Figure 1.14: *N-H...S* hydrogen bond within *N*-acetyl-*L*-phenylalanyl-*L*-methionine-amide. Reproduced from reference.⁷¹

A search of the CSD reveals that $N-H\cdots O=S$ interactions are prevalent in the organic solid state.⁷² However, there have been few reports in the literature exploiting this interaction in crystal engineering.^{66,67} The relatively few studies that incorporate the $N-H\cdots O=S$ interaction involve the formation of co-crystals between simple amide and sulfoxide functionalities.^{73,74} Kagan *et al.* demonstrated that (*R*)-methyl *p*-tolyl sulfoxide crystallises with a secondary amide, however this work was in relation to asymmetric synthesis rather than the field of crystal engineering.⁷⁵ It is surprising that such little literature precedent exists for $N-H\cdots O=S$ acting as a supramolecular synthon, since amides are considered strong hydrogen bond donors and sulfoxides are such potent acceptors.⁵⁹ Hence, the limited exploitation of the $N-H\cdots O=S$ interaction in the solid state needs to be addressed promptly, as this synthon could potentially be a valuable contributor in the discipline of crystal engineering.

1.4 Molecular machines

‘What would be the utility of such machines? Who knows? I cannot see exactly what would happen, but I can hardly doubt that when we have some control of the arrangement of things on a molecular scale we will get an enormously greater range of possible properties that substances can have, and of the different things we can do’.^{76,77}

The above quote by Richard P. Feynman, the Nobel Laureate in Physics briefly discussed the topic of constructing artificial molecular machines in 1959.⁷⁸ One of the first reports of a synthetic molecular machine involved the photoisomerisation of azobenzene in the early 1980s.⁷⁹ However, it is only in the past 20-30 years that this field has achieved significant advancement. The ‘bottom-up approach’ for the construction of nanoscale motors and machines is an effective strategy and one actively pursued by chemists due to the potential impact these molecular-level machines may have in nanoscience and nanotechnology.⁸⁰

According to ‘The Oxford English Dictionary’, a machine is defined as ‘an apparatus using mechanical power and having several parts, each with a definite function and together performing a particular task’.⁸¹ This description of macroscopic machines also translates to their molecular counterparts. A molecular machine can be defined as an assembly of a discrete number of molecular components designed to perform mechanical-like movements as a consequence of appropriate external stimuli.⁷⁸ For a molecule to be considered as a machine, then it must contain a switching element that responds to an external stimulus *e.g.* chemical, electrochemical or photochemical, thereby imparting a change in shape or movement in the molecular structure. The motion may include rotation around covalent bonds or the making and breaking of intercomponent non-covalent bonds. This change must be directed, controlled and must not occur spontaneously. Another important requirement is that the functionality is reversible and can occur repetitively. The key factor in achieving reversible molecular switching is bi-stability so that the two independent forms of the molecule can be interconverted in a controlled manner by the application of an external stimulus.⁸² Therefore any chemical change that the system undergoes needs to be reversible. Chemical processes such as isomerisations, acid/base reactions, oxidation/reduction processes and complexation/decomplexation equilibria are suitable as reversible processes.⁷⁷

The topic of molecular machines is such a vast and multidisciplinary research field that for the purpose of this thesis specific examples are selected from the literature - namely how nature influences the design of artificial molecular machines, artificial molecular machines

that incorporate similarities in molecular features to this research and also the future perspectives in this contemporary area.

1.4.1 Natural molecular machines

The human body can be considered as a very complicated collection of molecular level machines. Indeed, nature very elegantly demonstrates how simple molecular mechanical components, once organised and assembled in a certain manner, can link motions efficiently from the nanometer scale to the macroscopic world and achieve extremely complex functions. The meticulous level of control that nature possesses over molecular architecture provides an inspiration for the development of artificial molecular machines. One of the most interesting molecular machines in the human body is ATP synthase, a molecular-level rotatory motor that occurs in mitochondria, bacteria and chloroplasts. Boyer first proposed the rotary motion of ATP synthases.⁸³ The enzyme consists of two domains F_0 and F_1 which both act as motors and are driven by protons and ATP respectively. F_1 represents the shaft and rotates relative to the surrounding F_0 . The protons flow through the F_0 portion and generate a torque which is transmitted to F_1 through the rod-shaped domain, γ . This changes the structure of the catalytic sites on F_1 and subsequently allows the uptake of adenosine diphosphate (ADP) and inorganic phosphate (P_i) and the synthesized ATP molecules are then released, **Figure 1.17**.^{77,84}

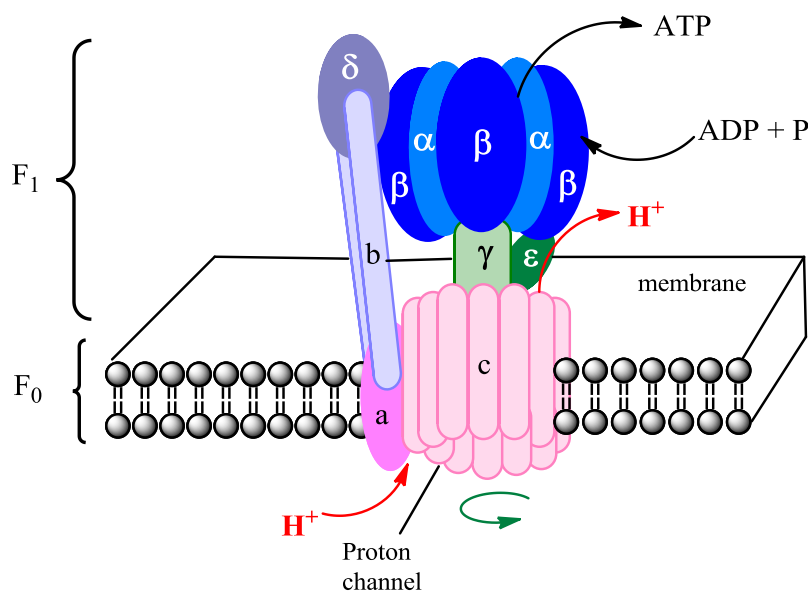


Figure 1.17: Structure of ATP synthase.

Other cytoplasmic proteins such as myosin, kinesin and dynein are also termed ‘molecular motors’ and they have been subjected to extensive study.⁸⁵ These linear motors transport

substrates by converting the energy of ATP hydrolysis into mechanical work. Myosin, which is responsible for all voluntary and involuntary muscle motions, binds to actin filaments and climbs unidirectionally along the filament resulting in the power stroke of muscle contraction, **Figure 1.18**.⁸⁴ RNA polymerases that move along DNA while accomplishing transcriptions are a further example of a biological process involving molecular motion.

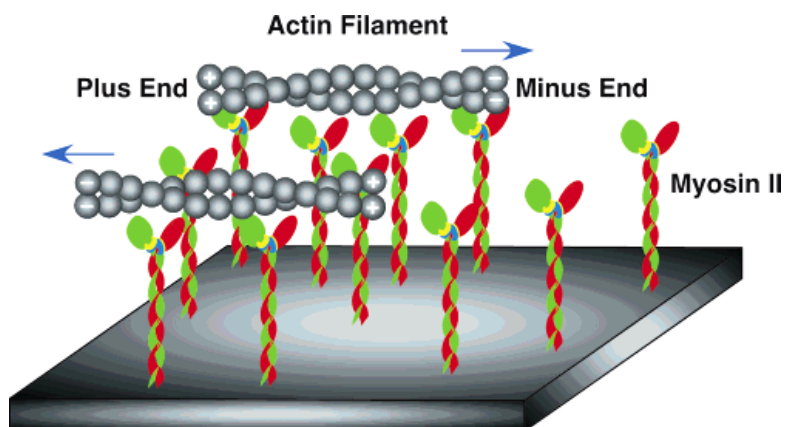


Figure 1.18: Directed motion of actin filaments from plus to minus end on an immobilised myosin surface. Reproduced from reference.⁸⁴

1.4.2 Rotaxanes, pseudorotaxanes, and catenanes

The sophisticated ability of natural processes to control molecular-level motion provides the inspiration for supramolecular research, which aims to create synthetic functioning molecular scale devices that mimic the function of these fascinating natural systems. Mechanically interlocked molecules, such as pseudorotaxanes, rotaxanes and catenanes, are at the heart of the development of molecular machine chemistry. The design of these systems employs the ‘bottom-up’ strategy where self-organisation, self-assembly and self-control is achieved at a molecular level, leading to potential applications as molecular devices for information storage and processing.^{86,87} Remarkable achievements have been witnessed involving these interlocked molecules including photodriven molecular machines,⁸⁸ porphyrin-containing catenanes and rotaxanes,^{89,90} anion- and active-metal-templated assemblies of mechanically interlocked structures,⁹¹ and bright functional rotaxanes,⁹² amongst others. The rapid development of this modern field has promoted the understanding of the concepts involved in the design, and the strategies needed for the self-assembly of structures, based on intermolecular interactions, in order to produce functional systems.

A rotaxane is composed of one or more macrocycles encircling a linear dumbbell-shaped unit, which is capped by two bulky stoppers at either terminal, thus preventing the components from dissociating from one another. This results in restricted motion of the interlocked components, to either gliding back and forth along the thread, often referred to as ‘shuttling’, or rotation around the dumbbell, referred to as ‘pirouetting’.^{93,94} Hence, the Latin origin of the name; ‘*rota*’ meaning wheel and ‘*axis*’ meaning axle.

The assembly of rotaxanes usually involves one of three major template-directed synthetic routes. One method that is often used involves threading a linear compound, which is stoppered at one end, through a pre-formed macrocycle, exploiting non-covalent bonding interactions, to form a pseudorotaxane, **Figure 1.19 a)**. A second bulky group can then be attached covalently in order to trap the macrocycle and form a rotaxane. A second strategy termed ‘clipping’ involves attaching a segmented macrocycle around the pre-formed dumbbell utilising non-covalent interactions, **Figure 1.19 b)**. Another common method for rotaxane synthesis, described as ‘slippage’, involves selecting a macrocycle of similar size to the dumbbell stopper. Following an increase in temperature, the macrocycle slips over the stopper and then, once cooled, the macrocycle remains trapped between the dumbbells, **Figure 1.19 c)**.⁷⁷

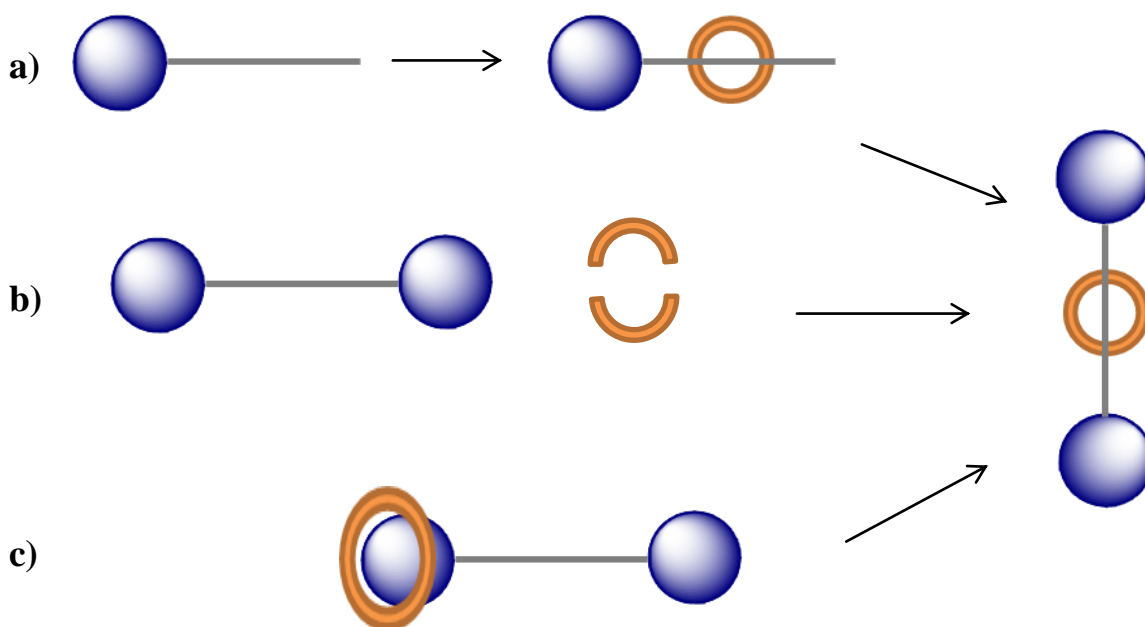


Figure 1.19: Assembly of rotaxanes by a) stoppering, b) clipping and c) slipping.

If the rotaxane contains two unique recognition sites on the linear dumbbell unit, then it is possible to switch the position of the macrocycle between the two sites or ‘stations’, thereby generating a molecular shuttle. The position of the ring is usually determined by the strength of the non-covalent bonding interactions it forms with each station. For instance, a macrocycle may preferentially occupy one site until a stimulus is applied, which would then turn off the stronger of the two recognition sites, and as a result the macrocycle would migrate to the second weaker recognition site. Effective stimuli that enable this type of reversibility include chemical, electrochemical or photochemical. Reactions that involve protonation/deprotonation or oxidation/reduction are also widely targeted.⁷⁸

A recent application involving rotaxanes and molecular shuttles utilised a concept that exploited the hydrogen bonding interactions involving amide and various sulfur-containing functionalities,⁹⁵ similar to the concept implied in this work. Altieri and co-workers synthesized a series of sulfide, sulfoxide and sulfone functionalised [2]rotaxanes, and by altering the oxidation level of the sulfur atom, the position of the macrocycle could be adjusted. This subsequently led to the development of a bi-stable molecular shuttle, **Figure 1.20**. Firstly the vinyl sulfide-succinamide thread, **8**, was synthesized and subjected to rotaxane-forming conditions. This involved the assembly of a benzylic amide macrocycle around **8** *via* five-component ‘clipping’ reaction and resulted in the formation of the interlocked architecture, **9**. Effective shuttling of the macrocycle was observed between two different sites on the thread by taking advantage of the different binding mechanisms of amide-sulfur functionalities. The macrocycle preferentially binds to the sulfoxide site, **10**, due to its strong hydrogen bond acceptor properties. Reduction to the sulfide, **8**, or oxidation to the sulfone, **11**, results in the macrocycle relocating to the succinamide binding site due to the weak nature of the amide-sulfide and amide-sulfone hydrogen bond interactions. This work successfully demonstrates that a molecular shuttle can be achieved through oxidation or reduction of the sulfur moiety.⁹⁵ Rotaxanes that respond to chemical oxidation/reduction are quite rare⁹⁶ but this example demonstrates that these systems incorporating N-H···S=O interactions could potentially be an important component of more advanced molecular machines.

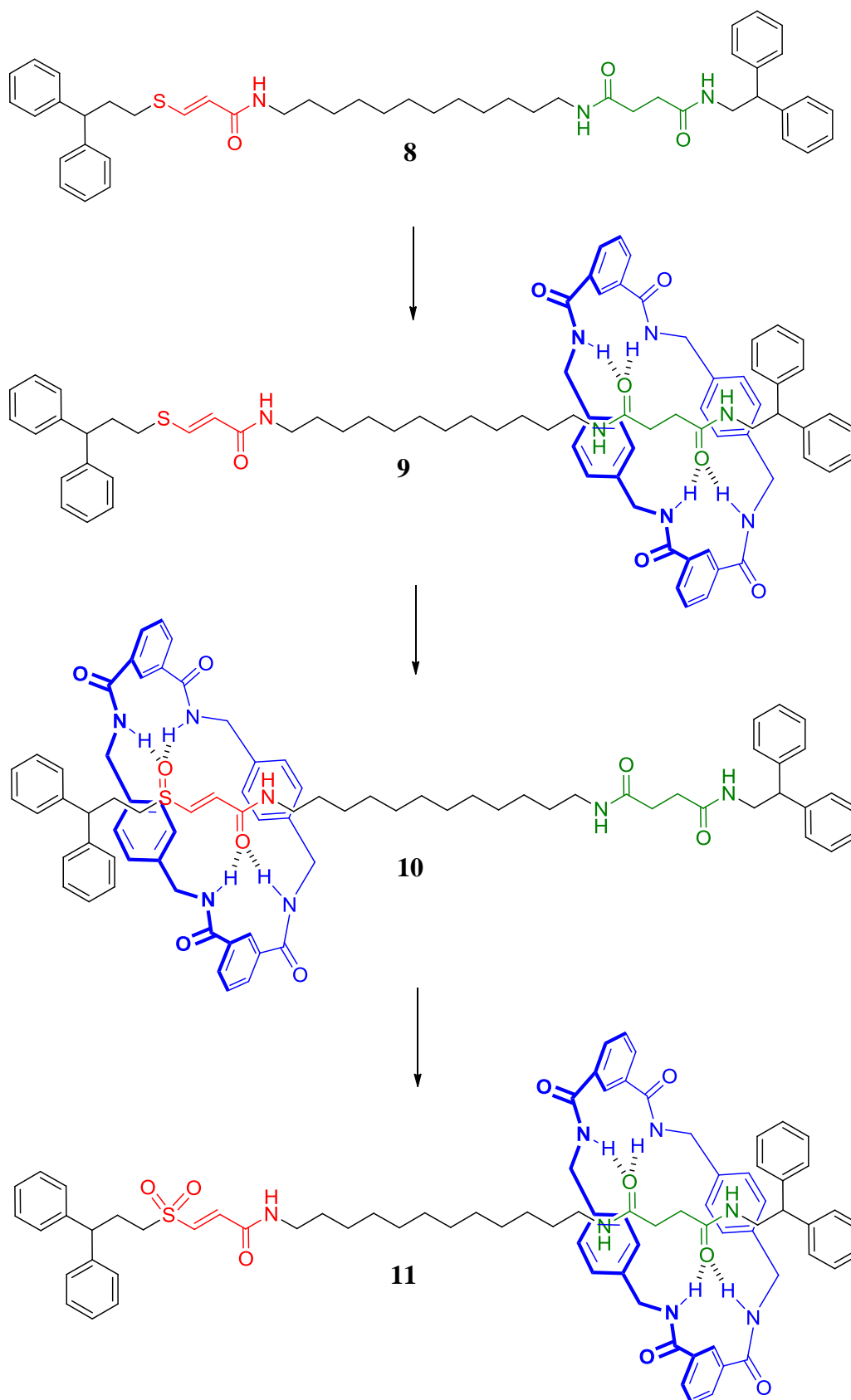


Figure 1.20: Sulfur-succinamide molecular shuttle. Reproduced from reference.⁹⁵

Pseudorotaxanes, as described previously, differ from rotaxanes as they can have one or both ends of the threading component sufficiently small to enable the macrocycle to thread or dethread.^{97,98} A particularly interesting application involving pseudorotaxanes is the formation of a molecular level plug/socket device. Similar to the macroscopic plug and socket electrical devices, the molecular analogue consists of connecting and disconnecting two components in a reversible manner so that an energy transfer occurs when the components are connected. Ishow *et al.* demonstrated this fascinating concept by employing an acid/base reversible process involving (\pm)-binaphthocrown ether, **12**, as the socket and the protonated form of **13**, as the plug.⁹⁹ On addition of the acid, the 'plugged in' state is represented by the binding of the anthracenyl unit to the crown ether, **14**. A photoinduced energy transfer process occurs involving the quenching of the binaphthyl fluorescence and sensitisation of the anthracenyl fluorescence. This energy-transfer process can be switched off following addition of a base.

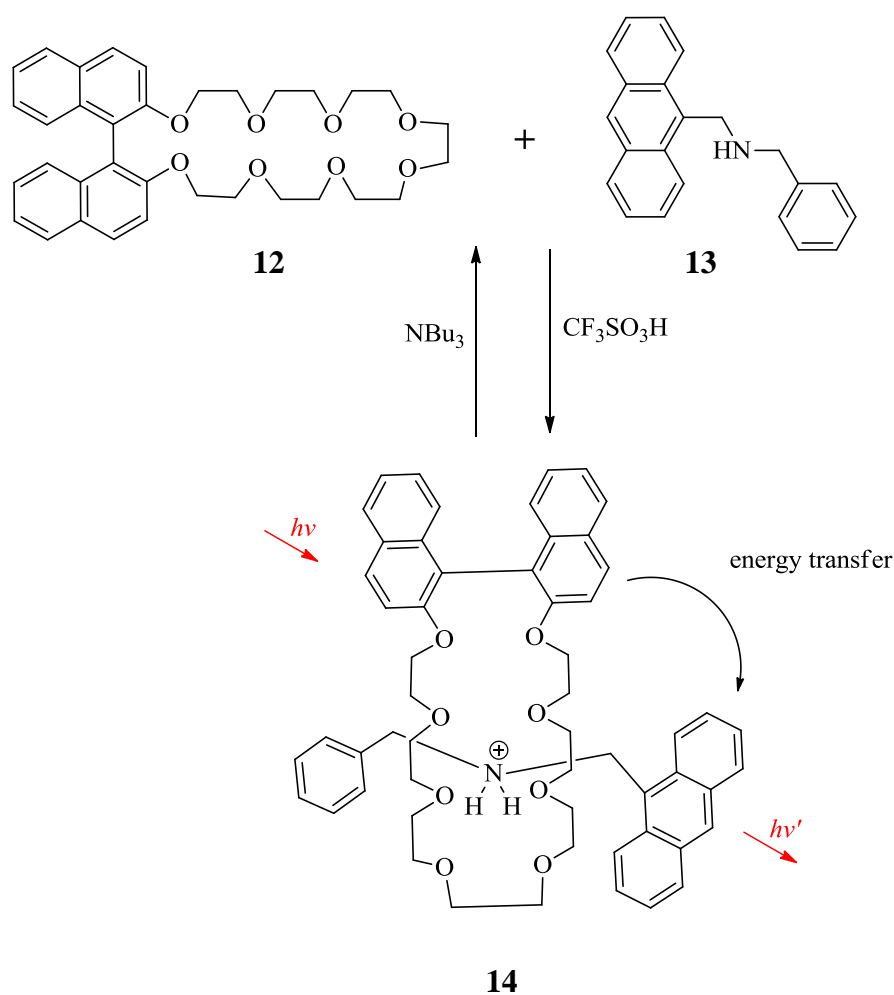


Figure 1.21: Plug and socket molecular device.⁹⁹

A recent study by Yu and co-workers displays the wide range applicability and benefits of the design and understanding of these mechanically interlocked molecules.¹⁰⁰ They discovered that a very stable [2]pseudorotaxane, **17**, could be formed between pillar[6]arene, **15**, and paraquat, **16**, in water. The paraquat molecule, **16**, can thread through **15** and bind very strongly due to a combination of electrostatic, hydrophobic and π - π stacking interactions, **Figure 1.22**. The significance of this system was the ability to reversibly control the binding, by altering the pH. It was observed that the formation of this pseudorotaxane subsequently played a key role in reducing the toxicity of paraquat.

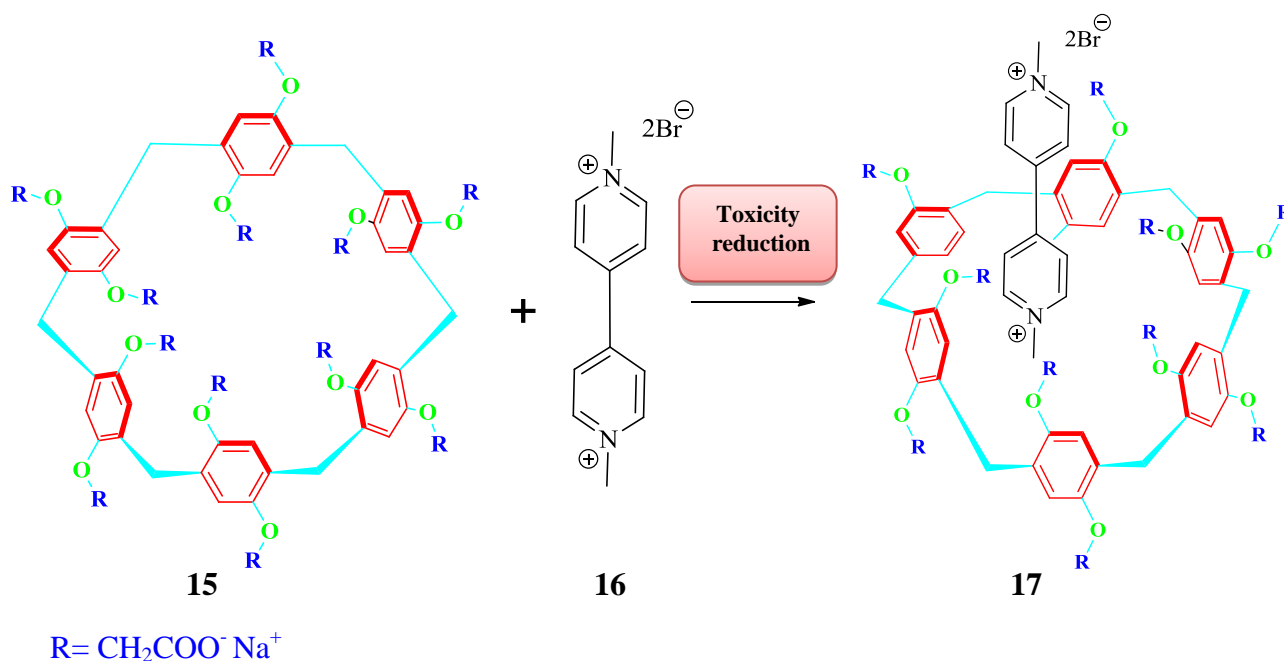


Figure 1.22: Pseudorotaxane formation between **15** and **16** which results in a reduction in toxicity of paraquat.

Similar molecular architectures related to rotaxanes and pseudorotaxanes are catenanes. These consist of two or more interlocked macrocycles which cannot be separated unless the covalent bonds of the macrocycles are broken.⁹⁴ The synthesis of [2]catenanes usually involves clipping one macrocycle around a second pre-formed macrocycle. In order to instill rotation in the catenanes, one of the macrocyclic rings may bear two different recognition sites while the second ring is usually symmetric. In this manner, the symmetric ring will preferentially dwell at one of the recognition sites by exploiting non-covalent bonding interactions.¹⁰¹ Then by applying a stimulus such as complexation/decomplexation of metal ions, protonation/deprotonation or oxidation/reduction processes, one macrocycle will circumrotate through the cavity of the other, **Figure 1.23**.⁷⁷

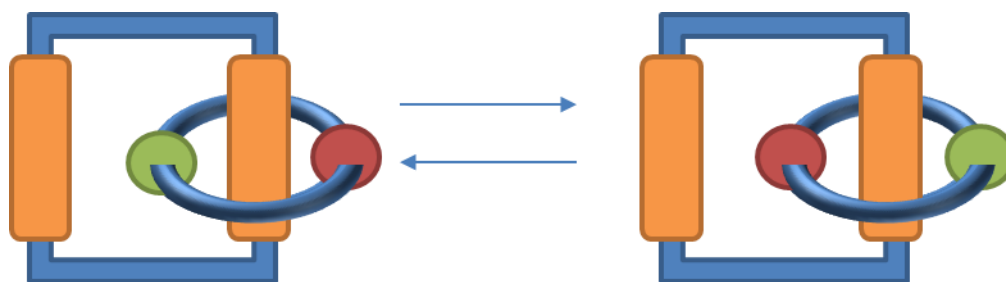


Figure 1.23: Illustration of a possible [2]catenane structure.

This methodology was employed by Asakawa *et al.*, in the construction of a [2]catenane, incorporating tetrathiafulvalene (TTF) and 1,5-dioxynaphthalene (DN) within one macrocycle, which act as two π -electron rich sites.¹⁰² Then cyclobis(paraquat-*p*-phenylene), which is π -electron deficient, is clipped on, and represents the symmetric macrocycle. It was demonstrated both by chemical and electrochemical oxidation/reduction processes that reversible switching could occur within this catenane. Initially, the TTF unit resides on the inside position, since it is the strongest electron donor and preferentially surrounds the tetracationic unit, **Figure 1.24**. On oxidation, the TTF becomes positively charged and repels the electron-acceptor unit, resulting in circumrotation of the polyether macrocycle with respect to the tetracationic cyclophane. In this position, the DN moiety is now inside the cyclophane. The original conformation can once again be restored on reduction. This reversibly switching catenane has been utilised in a solid-state electronic device.¹⁰³

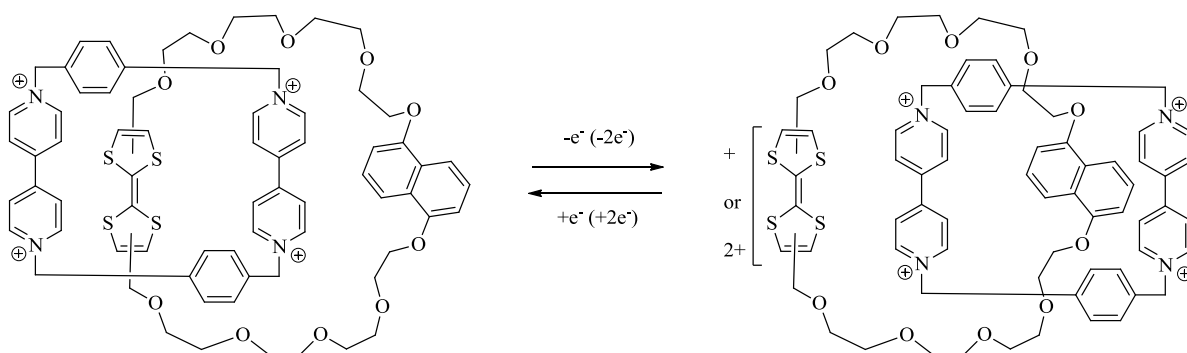


Figure 1.24: Effective formation of a [2]catenane switching entity based on electrochemical/chemical oxidation and reduction.

1.4.3 Crystalline molecular rotors

A molecular rotor describes molecules that consist of two parts which can easily rotate with respect to each other. The distinguishable structural feature of a molecular rotor is that the stator (the stationary frame of the system that contains the axle of rotation) is covalently attached to the rotator (the part of the molecule that rotates). This is in contrast to the molecular interlocked systems *e.g.* rotaxanes, pseudorotaxanes, catenanes, described previously which were characterized by non-covalent interactions.¹⁰⁴ The breadth of this subject is extremely vast ranging from random rotor molecules flowing freely in solution to rotors adhered to macroscopic surfaces.^{105,106} Hence, for the purpose of this review, the fundamental objective was to focus on certain aspects of solid state rotors that were applicable to this research.

Regarding crystalline molecular motors, construction of a structural assembly with precise alignment, orientation and intermolecular distances is necessary so that the dynamics of the system can be suitably controlled. To achieve high mobility and order then the crystalline molecular motors should ideally possess a symmetrical rotator that provides the motion of the molecule, a suitable axle to link the rotator to the stator, and a bulky static group that acts as a stator and shields the rotator from interfering adjacent molecules, **Figure 1.25**.^{107,108}

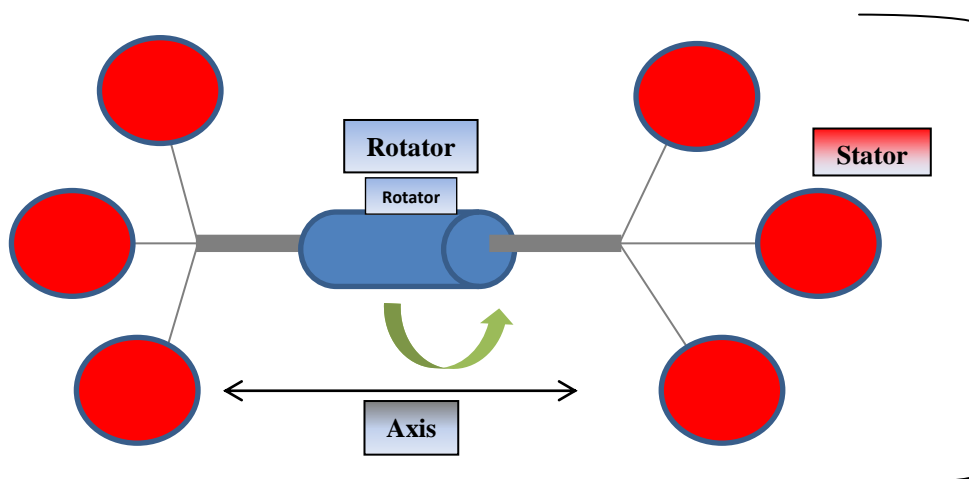


Figure 1.25: Diagram illustrating features of molecular rotor.

1.4.3.1 Phenyl-acetylene rotators

Phenyl-acetylene scaffolds, particularly in the design of supramolecular assemblies, have attracted increased interest in recent years. Their rigid and non-collapsible hydrocarbon backbone deem them as highly advantageous building blocks for the construction of ordered assemblies.^{109,110} In particular, the acetylene moiety possesses its own distinct advantages over other C-C bonds, most notably its enhanced rigidity and conjugation.¹¹¹ In the 1970's, Liberles and Matlosz investigated the planarity of diarylalkynes by studying the p orbital overlap of the aryl ring and the internal alkyne.¹¹² They deduced that a perpendicular geometry between the phenyl rings was more stable by ~ 1 kcal mol⁻¹ than a planar structure. However, the methods and calculations employed in this study have raised questions regarding the reliability of these results.¹⁰⁴ Several other studies have indicated that the energy barriers to bond rotations around the groups attached to the alkyne are very low.^{113,114} For diphenylacetylene derivatives the rotational barriers lie in the range 0.4-1.1 kcal mol⁻¹. Further studies have suggested that the steric bulk of the groups surrounding the ethynyl functionality increase the rotational barrier about this bond.^{104,115}

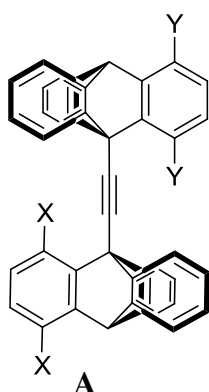


Table 1.1: Activation barriers for rotation for the compounds of general structure A.¹⁰⁴

No.	X	Y	ΔG^\ddagger_{273} (kcal mol ⁻¹)
18	H	CH ₃	10.1
19	H	OCH ₃	8
20	CH ₃	CH ₃	15.4
21	CH ₃	OCH ₃	12.7
22	OCH ₃	OCH ₃	9.4
23	F	CH ₃	11.6
24	Cl	CH ₃	14.7
25	Br	CH ₃	16.7
26	I	CH ₃	17.3
27	Ph	CH ₃	15.7

The rotational barrier of the diphenylacetylenes in **Table 1.1**, as measured by dynamic NMR (DNMR), increases as the steric size is increased. Comparing **20-22** it appears that the methyl group causes more steric interference than the methoxy group due to the restricted rotation of the Ph-CH₃ compared to the Ph-O-CH₃. Also the halo-substituted compounds **23-26** verify that an increase in the van der Waal radii results in an increase of the rotational barrier. From the above results, featured in **Table 1.1**, it appears that rotation about the triple bond increases in the order H < F < OCH₃ < Cl < CH₃ ~ Ph < Br < I.^{104,116-118}

Due to the relatively low rotational barrier that exists around the alkyne-aryl bond,¹¹³ it is no surprise that this structural feature has been harnessed to form crystals containing tailored rotor molecules. Macrobicyclic molecules incorporating a phenylene rotator have been extensively studied as effective molecular rotors. The *para*-substituted central phenyl ring behaves as an ideal rotator due to its symmetry. The acetylene groups act as the axle for rotation and links the rotator to the static framework. These ‘molecular turnstiles’, aptly named as a result of their motion, were firstly designed and synthesized by Moore and co-workers, **Figure 1.26**.¹¹⁹ It was also noted in the molecular turnstile that the size of the substituents influenced the rotation of the internal phenyl ring. For example, **28** rotated too quickly to be detected by NMR. Two conformations of **29** were identified by low temperature ¹H NMR spectroscopy, but at ambient temperature the barrier of rotation was calculated to be 13.4 kcal mol⁻¹, corresponding to fast rotation. In contrast, rotation was not observed for **30**, even at high temperatures and this may be attributed to the bulky substituent which cannot pass through the macrobicyclic framework.^{77,104}

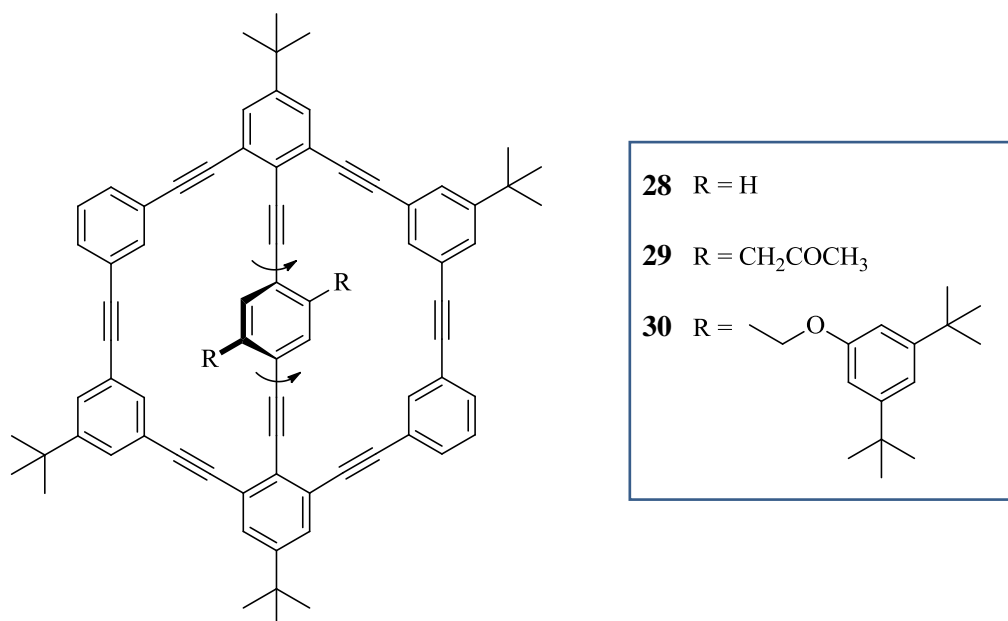


Figure 1.26: Molecular turnstile.¹¹⁹

One of the most exciting applications of ‘amphidynamic crystals’ that incorporate the 1,4-diethynylphenylene unit is in the field of molecular compasses and gyroscopes.^{107,120,121} A gyroscope is a device that consists of a spinning mass (rotator), with a spinning axis located through the centre of the mass and which is mounted within a rigid framework (stator).¹²² Macroscopic gyroscopes that are mounted on gimbals possess additional degrees of freedom and form the basis of inertial navigation systems utilised in airplanes and satellites. Macroscopic compasses, which are similar in topology, depend on the response of their magnetic dipole to the Earth’s magnetic field.¹⁰⁷

Garcia-Garibay *et al.*, designed ‘molecular gyroscopes’ by employing phenylene rotators linked by alkyne axles to triphenylmethyl (trityl) and triptycyl encapsulating stators. The bulky substituents form a cavity around the rotator which acts as a shield. Initially, simpler structures such as **31** and **32** were synthesised but due to the high activation barrier observed, compounds bearing bulkier groups such as **35** were targeted in order to increase the free space in which the phenylene unit can rotate, **Figure 1.27**.¹²³ More recently the *tert*-butyldiphenylsilyl-protected (TBDPS) derivatives, **33** and **34**, and the pentipycene substituted system, **36**, yielded very promising results towards the construction of molecular rotors.^{108,124}

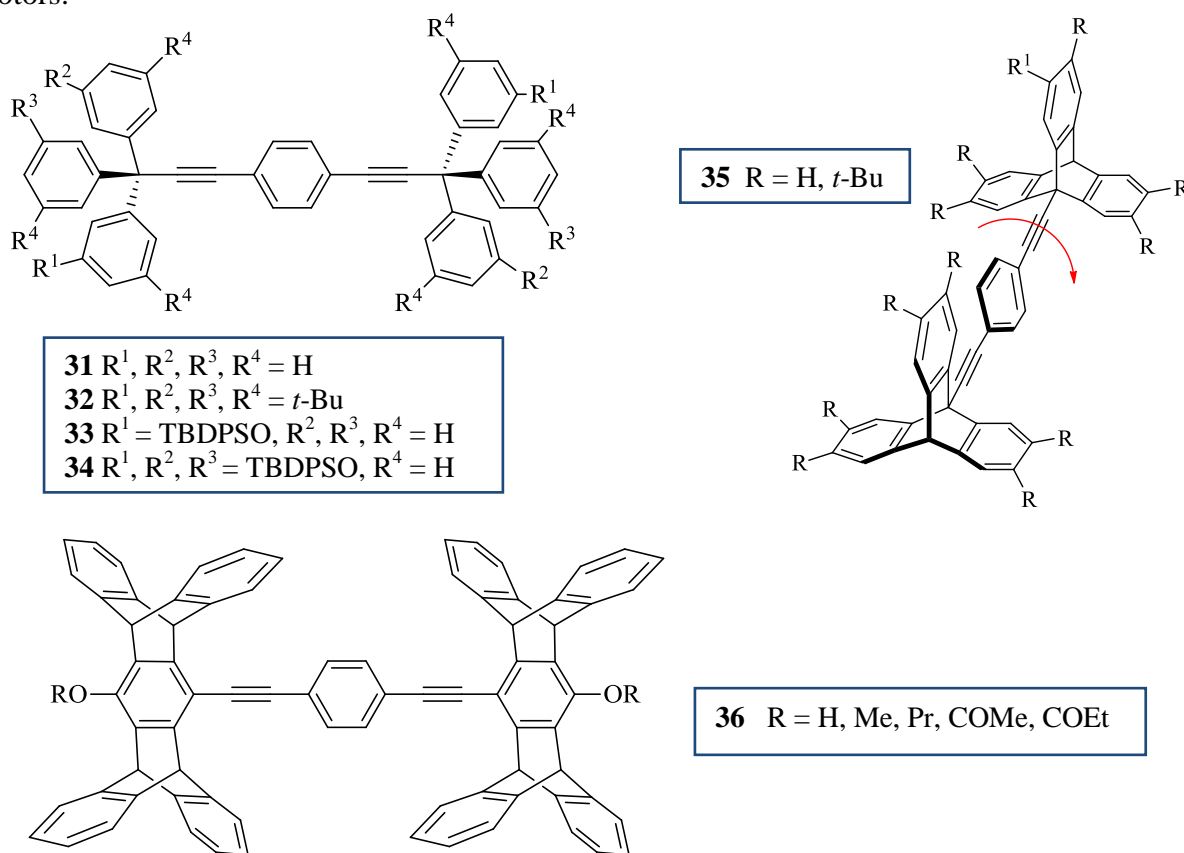


Figure 1.27: Currently pursued molecular rotors.

1.4.4 Molecular Switches

The definition of an artificial molecular switch is quite ambiguous since the term is often applied in conjunction with molecular machines.^{125,126} Molecules that exhibit a reversible conformational change in response to an external stimulus are considered switching entities.⁸² Therefore, molecular switches could be classified as a very simple molecular machine or as a necessary component in the ultimate formation of a molecular machine. The systems described in this review thus far all possess switching features. For example, the rotaxanes, pseudorotaxanes and catenanes can translate or circumrotate their internal components from one site to another, and the molecular rotors can rotate about an internal axis. Other examples include the formation of bi-stable daisy chains that involve contractions and extensions,¹²⁷ or *cis-trans* configurational changes as a result of heat or light activation.^{128,129} Therefore, it is difficult to categorise molecular switches into their own unique grouping. Since the terms ‘switch’ and ‘machine’ have often been used interchangeably in the past, it has been suggested that a molecular machine must ‘drive multifarious chemical reactions uphill and away from their inherent equilibria’, rather than just containing a switching element within their structures.¹²⁵

Molecular switches, recently described in the literature, with interesting and exciting applications include photochemical, pH and proton-controlled switches.^{82,130-141} Chiroptical molecular switches, as depicted in **Figure 1.28**, consists of a static lower half and an upper half that switches from right to left upon irradiation.⁸⁰ These switches may potentially have applications in molecular information storage systems and they have also been incorporated into the formation of a light-driven unidirectional molecular motor.

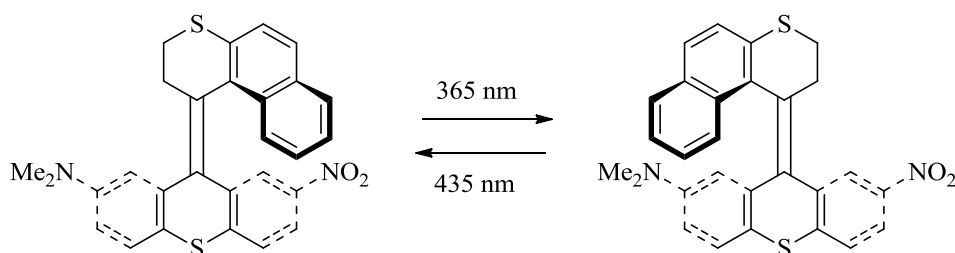


Figure 1.28: Chiroptical molecular switch.

1.5 Future perspectives

Nature's ability to control the molecular motion of intricate biological processes has provided the major inspiration for the design and construction of artificial molecular machines. While the molecular machines synthesised to date are primitive attempts compared to nature's complex systems, enormous progress has been achieved in this relatively new field in recent years. In particular, increasing our knowledge of non-covalent interactions at a fundamental level has led to the 'bottom-up' strategy. As a result, the successful design and construction of artificial molecular machines has been attributed to this simple approach. Therefore, in order to further progress and develop more complicated systems, investigating the specific non-covalent interactions in detail is the key to understanding the intricacies that lie at the heart of these machines.

While the exploitation of molecular machinery in a full technological sense still remains a distant ambition, promising achievements in controlling molecular motion by chemical, photochemical and electrochemical methods have led to the construction of practical devices, thereby encouraging future development in nanotechnology. The increased interest and activity from many science disciplines demonstrates the desire to successfully control and construct applicable molecular machines. In essence, with the significant progress being achieved in this field, Feynman's prediction quoted in **Section 1.4**, is quickly becoming a reality.^{77,78,82,104,105}

1.6 References

1. Lehn, J. M. *Science*, **1985**, *227*, 849-856.
2. Lehn, J. M. *Supramolecular Chemistry: Concepts and Perspectives*. VCH: Weinheim, 1995.
3. Steed, J. W.; Atwood, J. L. *Supramolecular Chemistry*; 2nd ed.; Wiley: UK, **2009**.
4. Desiraju, G. R. *Nature*, **2001**, *412*, 397-400.
5. Steed, J. W.; Atwood, J. L.; Gale, P. A. *Definition and emergence of supramolecular chemistry*. John Wiley & Sons Ltd.: **2012**; pp 3-7.
6. Atwood, J. L.; Davies, J. E. D.; MacNicol, D. D.; Vogtle, F.; Lehn, J. M. *Comprehensive Supramolecular Chemistry*. Pergamon: Oxford, 1996.
7. Kirkorian, K.; Ellis, A.; Twyman, L. J. *Chem. Soc. Rev.*, **2012**, *41*, 6138-6159.
8. Isaacs, L. *Adv. Drug Delivery Rev.*, **2012**, *64*, 763.
9. Kotchey, G. P.; Star, A. *Advances in supramolecular chemistry of carbon nanotubes*. John Wiley & Sons Ltd.: **2012**; pp 3767-3789.
10. Lehn, J. M. *Science*, **1993**, *260*, 1762-1763.
11. Soldatov, D. V.; Terekhova, I. S. *J. Struct. Chem.*, **2005**, *46*, S1-S8.
12. Uhlenheuer, D. A.; Petkau, K.; Brunsveld, L. *Chem. Soc. Rev.*, **2010**, *39*, 2817-2826.
13. Fischer, E. *Ber.*, **1894**, *27*, 2985-2993.
14. Powell, H. M. *J. Chem. Soc.*, **1948**, *16*, 61-73.
15. Palin, D. E.; Powell, H. M. *J. Chem. Soc.*, **1947**, 208-221.
16. Vicens, J.; Vicens, Q. *J. Inclusion Phenom. Macrocyclic Chem.*, **2011**, *71*, 251-274.
17. Pedersen, C. J. *J. Am. Chem. Soc.*, **1967**, *89*, 2495-2496.
18. Lehn, J. M. *Pure Appl. Chem.*, **1978**, *50*, 871-892.
19. Ariga, K.; Kunitake, T. *Supramolecular chemistry: fundamentals and applications*; Springer: Germany, **2006**.
20. Pederson, C. J.; Lehn, J. M.; Cram, D. J. *Resonance*, **2001**, *6*, 71-79.
21. Cram, D. J. *Science*, **1988**, *240*, 760-767.
22. Dalgarno, S. J. *Annu. Rep. Prog. Chem., Sect. B: Org. Chem.*, **2011**, *107*, 182-198.
23. Stang, P. J. *Chem. Eur. J.*, **1998**, *4*, 19-27.
24. Breault, G. A.; Hunter, C. A.; Mayers, P. C. *Tetrahedron*, **1999**, *55*, 5265-5293.

25. Lehn, J. M. *Chem. Soc. Rev.*, **2007**, *36*, 151-160.
26. Stoddart, J. F. *Acc. Chem. Res.*, **2001**, *34*, 410-411.
27. Schneider, H.-J. *Applications of Supramolecular Chemistry for 21st Century Technology*. CRC Press: USA, 2012.
28. Wasielewski, M. R. *Acc. Chem. Res.*, **2009**, *42*, 1910-1921.
29. Nangia, A.; Desiraju, G. R. *Chem. Commun.*, **1999**, 605-606.
30. Braga, D.; Desiraju, G. R.; Miller, J. S.; Orpen, A. G.; Price, S. L. *CrystEngComm*, **2002**, *4*, 500-509.
31. Desiraju, G. R. *J. Chem. Sci.*, **2010**, *122*, 667-675.
32. Desiraju, G. R. *Angew. Chem., Int. Ed.*, **2007**, *46*, 8342-8356.
33. Schmidt, G. M. J. *Pure Appl. Chem.*, **1971**, *27*, 647-678.
34. Robertson, J. M. *Proc. R. Soc., Ser. A*, **1951**, *207*, 101-110.
35. Dunitz, J. D. *Pure Appl. Chem.*, **1991**, *63*, 177-185.
36. Desiraju, G. R. *J. Mol. Struct.*, **1996**, *374*, 191-198.
37. Etter, M. C. *Acc. Chem. Res.*, **1990**, *23*, 120-126.
38. Corey, E. J. *Pure Appl. Chem.*, **1967**, *14*, 19-37.
39. Thalladi, V. R.; Goud, B. S.; Hoy, V. J.; Allen, F. H.; Howard, J. A. K.; Desiraju, G. R. *Chem. Commun.*, **1996**, 401-402.
40. Merz, K.; Vasylyeva, V. *CrystEngComm*, **2010**, *12*, 3989-4002.
41. Desiraju, G. R. *Chem. Commun.*, **1997**, 1475-1482.
42. Dunitz, J. D.; Gavezzotti, A. *Cryst. Growth Des.*, **2012**, *12*, 5873-5877.
43. Steiner, T. *Angew. Chem., Int. Ed.*, **2002**, *41*, 48-76.
44. Desiraju, G. R. *Acc Chem Res*, **2002**, *35*, 565-573.
45. Aakeroy, C. B.; Seddon, K. R. *Chem. Soc. Rev.*, **1993**, *22*, 397-407.
46. Steiner, T.; Desiraju, G. R. *Chem. Commun.*, **1998**, 891-892.
47. Arunan, E.; Desiraju, G. R.; Klein, R. A.; Sadlej, J.; Scheiner, S.; Alkorta, I.; Clary, D. C.; Crabtree, R. H.; Dannenberg, J. J.; Hobza, P.; Kjaergaard, H. G.; Legon, A. C.; Mennucci, B.; Nesbitt, D. J. *Pure Appl. Chem.*, **2011**, *83*, 1619-1636.
48. Videnova-Adrabinska, V. *J. Mol. Struct.*, **1996**, *374*, 199-222.

49. Allen, F. H.; Samuel, M.; Raithby, P. R.; Shields, G. P.; Taylor, R. *New J. Chem.*, **1999**, *23*, 25-34.
50. Bilton, C.; Allen, F. H.; Shields, G. P.; Howard, J. A. *Acta Crystallogr B*, **2000**, *56*, 849-856.
51. Desiraju, G. R. *Chem. Commun.*, **2005**, 2995-3001.
52. Desiraju, G. R.; Steiner, T. *The Weak Hydrogen Bond in Structural Chemistry and Biology*; Oxford University Press: Oxford, **1999**.
53. Lehane, K. N. *Ph.D. Thesis, NUI* **2007**.
54. Langley, P. J.; Hulliger, J.; Thaimattam, R.; Desiraju, G. R. *New J. Chem.*, **1998**, *22*, 1307-1309.
55. Dai, C.; Yuan, Z.; Collings, J. C.; Fasina, T. M.; Thomas, R. L.; Roscoe, K. P.; Stimson, L. M.; Yufit, D. S.; Batsanov, A. S.; Howard, J. A. K.; Marder, T. B. *CrystEngComm*, **2004**, *6*, 184-188.
56. Robinson, J. M. A.; Philp, D.; Kariuki, B. M.; Harris, K. D. M. *Chem. Commun.*, **1999**, 329-330.
57. Patai, S.; Rappaport, Z.; Stirlint, C. *The Chemistry of Sulphones and Sulphoxides*. John Wiley and Sons: New York, 1988; p 541.
58. Brondel, N.; Moynihan, E. J. A.; Lehane, K. N.; Eccles, K. S.; Elcoate, C. J.; Coles, S. J.; Lawrence, S. E.; Maguire, A. R. *CrystEngComm*, **2010**, *12*, 2910-2927.
59. Hunter, C. A. *Angew. Chem., Int. Ed.*, **2004**, *43*, 5310-5324.
60. Renault, E.; Le, Q. *J. Phys. Chem. A*, **2004**, *108*, 7232-7240.
61. Lehane, K. N.; Moynihan, E. J. A.; Brondel, N.; Lawrence, S. E.; Maguire, A. R. *CrystEngComm*, **2007**, *9*, 1041-1050.
62. Boese, R.; Kirchner, M. T.; Billups, W. E.; Norman, L. R. *Angew. Chem., Int. Ed.*, **2003**, *42*, 1961-1963.
63. Tsuchihashi, G.; Ogura, K.; Iriuchijima, S.; Tomisawa, S. *Synthesis*, **1971**, 89-91.
64. Tykwinski, R. R.; Williamson, B. L.; Fischer, D. R.; Stang, P. J.; Arif, A. M. *J. Org. Chem.*, **1993**, *58*, 5235-5237.
65. Seo, M.; Park, J.; Kim, S. Y. *Org. Biomol. Chem.*, **2012**, *10*, 5332-5342.
66. Eccles, K. S.; Elcoate, C. J.; Stokes, S. P.; Maguire, A. R.; Lawrence, S. E. *Cryst. Growth Des.*, **2010**, *10*, 4243-4245.
67. Eccles, K. S.; Elcoate, C. J.; Maguire, A. R.; Lawrence, S. E. *Cryst. Growth Des.*, **2011**, *11*, 4433-4439.

68. Allen, F. H.; Bird, C. M.; Rowland, R. S.; Raithby, P. R. *Acta Crystallogr., Sect. B: Struct. Sci.*, **1997**, *B53*, 696-701.
69. Biswal, H. S.; Wategaonkar, S. *J. Phys. Chem. A*, **2009**, *113*, 12763-12773.
70. Howard, D. L.; Kjaergaard, H. G. *Phys. Chem. Chem. Phys.*, **2008**, *10*, 4113-4118.
71. Biswal, H. S.; Gloaguen, E.; Loquais, Y.; Tardivel, B.; Mons, M. *J. Phys. Chem. Lett.*, **2012**, *3*, 755-759.
72. Eccles, K. S. *Ph.D. Thesis, NUI* **2012**.
73. Fleischman, S. G.; Kuduva, S. S.; McMahon, J. A.; Moulton, B.; Bailey, W.; Rodriguez-Hornedo, N.; Zaworotko, M. J. *Cryst. Growth Des.*, **2003**, *3*, 909-919.
74. Jagadish, B.; Carducci, M. D.; Bosshard, C.; Guenter, P.; Margolis, J. I.; Williams, L. J.; Mash, E. A. *Cryst. Growth Des.*, **2003**, *3*, 811-821.
75. Charpin, P.; Dunach, E.; Kagan, H. B.; Theobald, F. R. *Tetrahedron Lett.*, **1986**, *27*, 2989-2992.
76. Feynman, R. P. *Sat. Rev.*, **1960**, *43*, 45-47.
77. Balzani, V.; Credi, A.; Raymo, F. M.; Stoddart, J. F. *Angew. Chem., Int. Ed.*, **2000**, *39*, 3348-3391.
78. Ballardini, R.; Balzani, V.; Credi, A.; Gandolfi, M. T.; Venturi, M. *Acc. Chem. Res.*, **2001**, *34*, 445-455.
79. Shinkai, S.; Ishihara, M.; Ueda, K.; Manabe, O. *J. Inclusion Phenom.*, **1984**, *2*, 111-118.
80. Feringa, B. L. *Acc. Chem. Res.*, **2001**, *34*, 504-513.
81. <http://oxforddictionaries.com>, **2012**.
82. Feringa, B. L. *J. Org. Chem.*, **2007**, *72*, 6635-6652.
83. Boyer, P. D. *Annu. Rev. Biochem.*, **1997**, *66*, 717-749.
84. Kinbara, K.; Aida, T. *Chem. Rev.*, **2005**, *105*, 1377-1400.
85. Vale, R. D.; Milligan, R. A. *Science*, **2000**, *288*, 88-95.
86. Green, J. E.; Choi, J. W.; Boukai, A.; Bunimovich, Y.; Johnston-Halperin, E.; DeIonno, E.; Luo, Y.; Sheriff, B. A.; Xu, K.; Shin, Y. S.; Tseng, H. R.; Stoddart, J. F.; Heath, J. R. *Nature*, **2007**, *445*, 414-417.
87. Feng, M.; Gao, L.; Deng, Z.; Ji, W.; Guo, X.; Du, S.; Shi, D.; Zhang, D.; Zhu, D.; Gao, H. *J. Am. Chem. Soc.*, **2007**, *129*, 2204-2205.
88. Saha, S.; Stoddart, J. F. *Chem. Soc. Rev.*, **2007**, *36*, 77-92.

89. Faiz, J. A.; Heitz, V.; Sauvage, J. P. *Chem. Soc. Rev.*, **2009**, *38*, 422-442.
90. Brown, A.; Beer, P. D. *Dalton Trans.*, **2012**, *41*, 118-129.
91. Vickers, M. S.; Beer, P. D. *Chem. Soc. Rev.*, **2007**, *36*, 211-225.
92. Ma, X.; Tian, H. *Chem. Soc. Rev.*, **2010**, *39*, 70-80.
93. Kay, E. R.; Leigh, D. A. *Pure Appl. Chem.*, **2008**, *80*, 17-29.
94. Sauvage, J. P.; Dietrich-Buchecker, C. *Molecular Catenanes, Rotaxanes and Knots*. Wiley-VCH: Weinheim, 1999; pp 143-170.
95. Altieri, A.; Aucagne, V.; Carrillo, R.; Clarkson, G. J.; D'Souza, D. M.; Dunnett, J. A.; Leigh, D. A.; Mullen, K. M. *Chem. Sci.*, **2011**, *2*, 1922-1928.
96. Berna, J.; Alajarin, M.; Orenes, R. A. *J. Am. Chem. Soc.*, **2010**, *132*, 10741-10747.
97. Yerin, A.; Wilks, E. S.; Moss, G. P.; Harada, A.; Hartshorn, R. M.; Damhus, T.; Brecher, J.; Degtyarenko, K.; Heller, S. R.; Hellwich, K. H.; Hodge, P.; Hutton, A. T.; Leigh, G. J.; Wilson, J.; Kahovec, J.; Jones, R. G.; Lawson, A.; Norlander, E.; Nyitrai, J.; Powell, W. H.; Ansari, F. L.; Do, Y.; Dukov, I. L.; Hashem, M.; Lajunen, L. H. J.; Ogino, H.; Reedijk, J.; Schomburg, D.; Powell, W. H.; Metanomski, W. V.; Hellwich, K. H.; Favre, H. A.; Eller, G. *Pure Appl. Chem.*, **2008**, *80*, 2041-2068.
98. Ashton, P. R.; Philp, D.; Spencer, N.; Stoddart, J. F. *J. Chem. Soc., Chem. Commun.*, **1991**, 1677-1679.
99. Ishow, E.; Credi, A.; Balzani, V.; Spadola, F.; Mandolini, L. *Chem. Eur. J.*, **1999**, *5*, 984-989.
100. Yu, G.; Zhou, X.; Zhang, Z.; Han, C.; Mao, Z.; Gao, C.; Huang, F. *J. Am. Chem. Soc.*, **2012**, *134*, 19489-19497.
101. Dietrich-Buchecker, C. O.; Sauvage, J. P. *Chem. Rev.*, **1987**, *87*, 795-810.
102. Asakawa, M.; Ashton, P. R.; Balzani, V.; Credi, A.; Hamers, C.; Mattersteig, G.; Montalti, M.; Shipway, A. N.; Spencer, N.; Stoddart, J. F.; Tolley, M. S.; Venturi, M.; White, A. J. P.; Williams, D. J. *Angew. Chem., Int. Ed.*, **1998**, *37*, 333-337.
103. Collier, C. P.; Mattersteig, G.; Wong, E. W.; Luo, Y.; Beverly, K.; Sampaio, J.; Raymo, F. M.; Stoddart, J. F.; Heath, J. R. *Science*, **2000**, *289*, 1172-1175.
104. Kottas, G. S.; Clarke, L. I.; Horinek, D.; Michl, J. *Chem. Rev.*, **2005**, *105*, 1281-1376.
105. Browne, W. R.; Feringa, B. L. *Nat. Nanotechnol.*, **2006**, *1*, 25-35.
106. Rodriguez-Velamazán, J. A.; Gonzalez, M. A.; Real, J. A.; Castro, M.; Munoz, M. C.; Gaspar, A. B.; Ohtani, R.; Ohba, M.; Yoneda, K.; Hijikata, Y.; Yanai, N.; Mizuno, M.; Ando, H.; Kitagawa, S. *J. Am. Chem. Soc.*, **2012**, *134*, 5083-5089.
107. Garcia-Garibay, M. A. *Proc. Natl. Acad. Sci.*, **2005**, *102*, 10771-10776.

108. Arcos-Ramos, R.; Rodriguez-Molina, B.; Romero, M.; Mendez-Stivalet, J. M.; Ochoa, M. E.; Ramirez-Montes, P. I.; Santillan, R.; Garcia-Garibay, M. A.; Farfan, N. *J. Org. Chem.*, **2012**, *77*, 6887-6894.
109. Chinchilla, R.; Najera, C. *Chem. Rev.*, **2007**, *107*, 874-922.
110. Jenny, N. M.; Mayor, M.; Eaton, T. R. *Eur. J. Org. Chem.*, **2011**, *2011*, 4965-4983.
111. Diederich, F.; Stang, P. J.; Tykwinski, R. R. *Acetylene Chemistry - Chemistry, Biology and Material Science*. Wiley-VCH: Weinheim, Germany, 2005; pp 303-378.
112. Liberles, A.; Matlosz, B. *J. Org. Chem.*, **1971**, *36*, 2710-2713.
113. Sipachev, V. A.; Khaikin, L. S.; Grikina, O. E.; Nikitin, V. S.; Traetteberg, M. *J. Mol. Struct.*, **2000**, *523*, 1-22.
114. Stoelevik, R.; Bakken, P. *J. Mol. Struct.*, **1990**, *239*, 205-207.
115. Okuyama, K.; Hasegawa, T.; Ito, M.; Mikami, N. *J. Phys. Chem.*, **1984**, *88*, 1711-1716.
116. Toyota, S.; Yamamori, T.; Asakura, M.; Oki, M. *Bull. Chem. Soc. Jpn.*, **2000**, *73*, 205-213.
117. Toyota, S.; Yamamori, T.; Makino, T.; Oki, M. *Bull. Chem. Soc. Jpn.*, **2000**, *73*, 2591-2597.
118. Toyota, S.; Yamamori, T.; Makino, T. *Tetrahedron*, **2001**, *57*, 3521-3528.
119. Bedard, T. C.; Moore, J. S. *J. Am. Chem. Soc.*, **1995**, *117*, 10662-10671.
120. Dominguez, Z.; Dang, H.; Strouse, M. J.; Garcia-Garibay, M. A. *J. Am. Chem. Soc.*, **2002**, *124*, 2398-2399.
121. Khuong, T. A.; Zepeda, G.; Ruiz, R.; Khan, S. I.; Garcia-Garibay, M. A. *Cryst. Growth Des.*, **2004**, *4*, 15-18.
122. Khuong, T. A.; Nunez, J. E.; Godinez, C. E.; Garcia-Garibay, M. A. *Acc. Chem. Res.*, **2006**, *39*, 413-422.
123. Godinez, C. E.; Zepeda, G.; Garcia-Garibay, M. A. *J. Am. Chem. Soc.*, **2002**, *124*, 4701-4707.
124. Escalante-Sanchez, E.; Rodriguez-Molina, B.; Garcia-Garibay, M. A. *J. Org. Chem.*, **2012**, *77*, 7428-7434.
125. Coskun, A.; Banaszak, M.; Astumian, R. D.; Stoddart, J. F.; Grzybowski, B. A. *Chem. Soc. Rev.*, **2012**, *41*, 19-30.
126. Chatterjee, M. N.; Kay, E. R.; Leigh, D. A. *J. Am. Chem. Soc.*, **2006**, *128*, 4058-4073.
127. Wu, J.; Leung, K. C.-F.; Benitez, D.; Han, J. Y.; Cantrill, S. J.; Fang, L.; Stoddart, J. F. *Angew. Chem., Int. Ed.*, **2008**, *47*, 7470-7474.

128. Koshima, H.; Ojima, N.; Uchimoto, H. *J. Am. Chem. Soc.*, **2009**, *131*, 6890-6891.
129. Ferri, V.; Elbing, M.; Pace, G.; Dickey, M. D.; Zharnikov, M.; Samori, P.; Mayor, M.; Rampi, M. A. *Angew. Chem., Int. Ed.*, **2008**, *47*, 3407-3409.
130. Gust, D.; Moore, T. A.; Moore, A. L. *Chem. Commun.*, **2006**, 1169-1178.
131. Deetz, M. J.; Jonas, M.; Malerich, J. P.; Smith, B. D. *Supramol. Chem.*, **2002**, *14*, 487-489.
132. Brazdova, B.; Zhang, N.; Samoshin, V. V.; Guo, X. *Chem. Commun.*, **2008**, 4774-4776.
133. Ashton, P. R.; Ballardini, R.; Balzani, V.; Baxter, I.; Credi, A.; Fyfe, M. C. T.; Gandolfi, M. T.; Gomez-Lopez, M.; Martinez-Diaz, M. V.; Piersanti, A.; Spencer, N.; Stoddart, J. F.; Venturi, M.; White, A. J. P.; Williams, D. J. *J. Am. Chem. Soc.*, **1998**, *120*, 11932-11942.
134. Bissell, R. A.; Cordova, E.; Kaifer, A. E.; Stoddart, J. F. *Nature*, **1994**, *369*, 133-137.
135. Onoda, A.; Haruna, H.; Yamamoto, H.; Takahashi, K.; Kozuki, H.; Okamura, T. a.; Ueyama, N. *Eur. J. Org. Chem.*, **2005**, 641-645.
136. Spruell, J. M.; Paxton, W. F.; Olsen, J. C.; Benitez, D.; Tkatchouk, E.; Stern, C. L.; Trabolsi, A.; Friedman, D. C.; Goddard, W. A.; Stoddart, J. F. *J. Am. Chem. Soc.*, **2009**, *131*, 11571-11580.
137. Jones, I. M.; Hamilton, A. D. *Org. Lett.*, **2010**, *12*, 3651-3653.
138. Jones, I. M.; Hamilton, A. D. *Angew. Chem., Int. Ed.*, **2011**, *50*, 4597-4600.
139. Jones, I. M.; Lingard, H.; Hamilton, A. D. *Angew. Chem., Int. Ed.*, **2011**, *50*, 12569-12571.
140. Norikane, Y.; Tamaoki, N. *Org. Lett.*, **2004**, *6*, 2595-2598.
141. Tie, C.; Gallucci, J. C.; Parquette, J. R. *J. Am. Chem. Soc.*, **2006**, *128*, 1162-1171.

Chapter 2

Design and synthesis of scaffolds to enable the study of weak hydrogen bond interactions in the solid state

2. Contents

2.1. Introduction.....	47
2.1.1. Project Background	47
2.1.2. Project Objectives.....	49
2.2. Scaffold Design.....	50
2.3. Tertiary Amines	52
2.3.1. Synthetic Strategy.....	52
2.3.2. Linkers for Amine Scaffold.....	53
2.3.3. Reductive Amination.....	55
2.3.4. <i>N</i> -Alkylation	58
2.3.5. Oxidation to sulfoxide and sulfones	61
2.3.6. Crystal Structure Data	66
2.3.7. Conclusions	76
2.3.8. Biological Testing	77
2.4. Aromatic based systems	83
2.4.1. 1,2,3-substituted aromatic scaffold.....	83
2.4.2. Design and synthesis of linkers for rigid scaffold	84
2.4.3. Synthetic Strategy 1	87
2.4.4. Synthetic Strategy II	94
2.4.5. Synthetic Strategy III.....	99
2.4.6. Conclusions	105
2.5. Combination of Tertiary Amine and Aromatic Scaffold	106
2.5.1. Synthetic strategy	106
2.6. References.....	109

2.1. Introduction

The solid state physical properties of organic compounds are critically important to their application as pharmaceuticals. Solid pharmaceuticals can exist in a variety of crystalline or amorphous forms which can give rise to measurable differences in physical properties and processing. The particular form determines the physicochemical properties of the drug such as its hygroscopicity, bioavailability, solubility, stability and dissolution rate.¹ Drugs crystallising in more than one polymorphic form *e.g.* estradiol, ritonavir, carbamazepine have resulted in problematic quality release and stability testing of the finished dosage form.² Advances in crystal engineering and supramolecular chemistry has led us to consider new perspectives of the various solid state forms that molecules may adopt in terms of molecular assemblies.³ Control of the physical properties demands an understanding of the nature of interactions between molecules in the solid state at a fundamental level.

This research focused specifically on organosulfur functional groups (sulfides, sulfoxides and sulfones), with the aim to develop an understanding of how the molecular structure of the compounds impact upon the solid state crystalline structure and, in particular, to probe the relative importance of different inter/intramolecular non-covalent interactions. Our interest in exploring these interactions prompted us to investigate their use as switching entities. Molecular systems that can be induced to transform from one state to another by a certain stimuli are valued synthetic targets due to their wide range of applications.⁴ Initial work began by investigating weak hydrogen bond patterns between terminal alkynes and sulfur functional groups.⁵ As the research evolved, stronger hydrogen bonding interactions incorporating amides were investigated.

2.1.1. Project Background

The concept of this project emerged from recent research in the group which investigated the weak intermolecular hydrogen bond interactions in simple systems between a terminal alkyne ($C\equiv C-H$) and sulfur functional groups (sulfide, sulfoxide, sulfone) in the solid state.⁵ In particular, the research explored the ability of the terminal alkyne and sulfoxide hydrogen bond interaction to act as a robust synthon and as a recurring motif that directs molecular packing in crystal engineering.

Sulfoxides have been described as favourable hydrogen bond acceptors.⁶ The polar covalent nature of the sulfur oxygen bond is the key factor in allowing the sulfoxide group to partake in hydrogen bond interactions. The sulfoxide is a more potent hydrogen bond acceptor than a carbonyl oxygen,⁷ therefore it was anticipated that it would serve as a good hydrogen bond acceptor when the terminal alkyne was the donor.

Terminal alkynes have the ability to act as hydrogen bond donors via the acetylenic hydrogen.⁸ The hydrogen in a terminal alkyne forms stronger C-H...X hydrogen bonds than most hydrocarbon donors, due to its relatively high acidity (pKa ~26), and subsequently attracted our research group to investigate the involvement of terminal alkynes in weak hydrogen bond interactions in the solid state.⁵ Directionality is an important property of terminal alkynes in intermolecular interactions and when terminal alkynes act as hydrogen bond donors they show preference for linearity⁹, which is a key feature in the C≡C-H...O=S supramolecular synthon.

While investigating the viability of the C≡C-H...O=S synthon, a second important structure determining interaction was observed by Lehane and co-workers.⁵ It was demonstrated that terminal alkynes act as hydrogen bond donors in sulfides. Then by varying the level of oxidation at sulfur, the hydrogens α to the sulfur substituent compete with the terminal alkyne and dominate as hydrogen bond donors. The polar sulfoxide functional group enhances the acidity of the adjacent α hydrogens with the result that they become the major hydrogen bond donors. This phenomenon can then in turn be blocked by substitution at this position, as illustrated in **Figure 2.1**. Therefore, the overall crystal structure of the compound changes dramatically as a result of competing intermolecular hydrogen bond interactions.

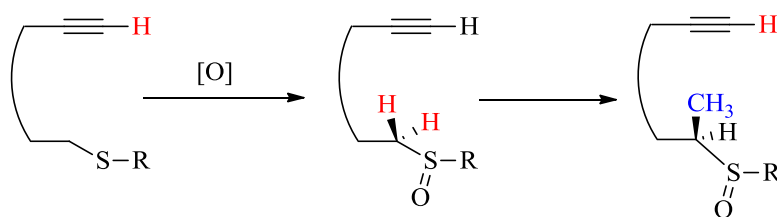


Figure 2.1: Demonstrating the effect of competing hydrogen bond donors by varying the acidity of the α hydrogens.

2.1.2. Project Objectives

The foundations of this project were established from the observation that the $C\equiv C-H\cdots O=S$ and the $S=O\cdots H-C(\alpha)$ interactions were viable supramolecular synthons in simple organic systems.^{5,10} The aim of this project was to further investigate the robustness of these synthons by combining the terminal alkyne and sulfur functional groups within a single molecule and studying the effect of including a second hydrogen bond acceptor (X), **Figure 2.2**. By introducing another hydrogen bond acceptor, it would compete with the $S=O$ for the hydrogen of the terminal alkyne, and therefore, explore the persistence of the $C\equiv C-H\cdots O=S$ and the $S=O\cdots H-C(\alpha)$ interactions as structural motifs in directing the supramolecular packing in the solid state of more complicated systems.

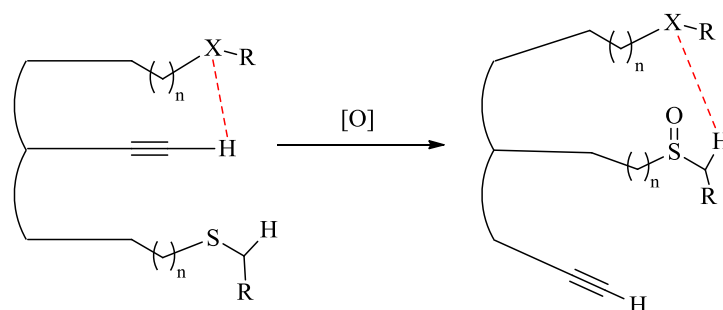


Figure 2.2: Initial proposal for the molecular switch. Terminal alkyne acts as hydrogen bond donor in sulfides. After oxidation the hydrogens α to the sulfoxide/sulfone would compete with the terminal alkyne to act as the hydrogen bond donor. (X = H-bond acceptor, R = alkyl/aryl).

Building further on this concept, it was decided to exploit the effect of varying the oxidation level of sulfur on the hydrogen bonding ability of the α hydrogens. If the hydrogen bond donor can be predictably switched from the hydrogen of the terminal alkyne to the hydrogens α to the sulfur, by a change in oxidation, then perhaps a molecular switch could be created. This particular idea is illustrated in **Figure 2.2**.

This particular investigation could be very useful in a more general sense with regards to crystal engineering as it may enhance the ability to predict and understand how individual molecules orientate themselves and the influence of their non-covalent interactions on the overall structure in the solid state. If the important structure determining interactions in the crystalline form of these compounds can be successfully identified, then control of the physical properties becomes easier to achieve.

The enormous challenge in this project was whether the molecular features designed into this compound at the outset, would deliver the predicted structure determining interactions. So the strategy to access this type of system had to be carefully planned and designed with this ultimate goal in mind.

2.2. Scaffold Design

Firstly a suitable scaffold had to be selected to act as an anchor point for attachment of the terminal alkyne, sulfur functionalities and hydrogen bond acceptors. The scaffold plays a key role in the structure of the molecule. It essentially will be the structural unit upon which the molecular switch is built, **Figure 2.3**.

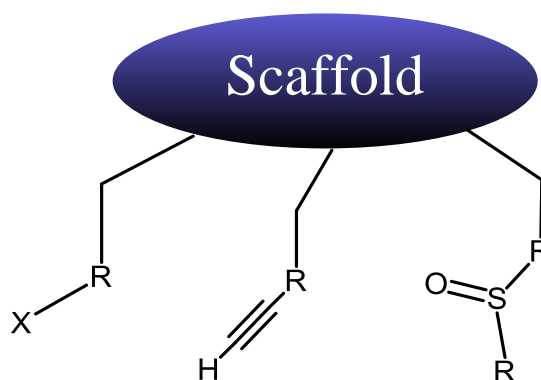


Figure 2.3: *The key role of the scaffold.*

The scaffold unit must be able to incorporate three ‘arms’ in which the functional groups are readily able to interact with each other. It would also be desirable if the target molecule could rotate so that maximum interaction could occur. Preferably the target molecule would be able to adjust and adapt to changes in chain length of the target synthons without huge difficulty. The scaffold must also have appropriate geometric constraints so that when the sulfur is at the sulfide oxidation level, then hydrogen bonding can occur selectively to the terminal alkyne, while in the compounds at higher oxidation levels (sulfoxide or sulfone) the hydrogen bonding can freely switch to the protons adjacent to the sulfur instead. In essence, the scaffold unit could be fixed or flexible and it would be preferable if the desired functional groups could be attached conveniently with the potential to readily vary the linkers and the sequence of attachment. Two systems were initially chosen to act as the scaffold – a tertiary amine and a tri-substituted aromatic system, **Figure 2.4**.

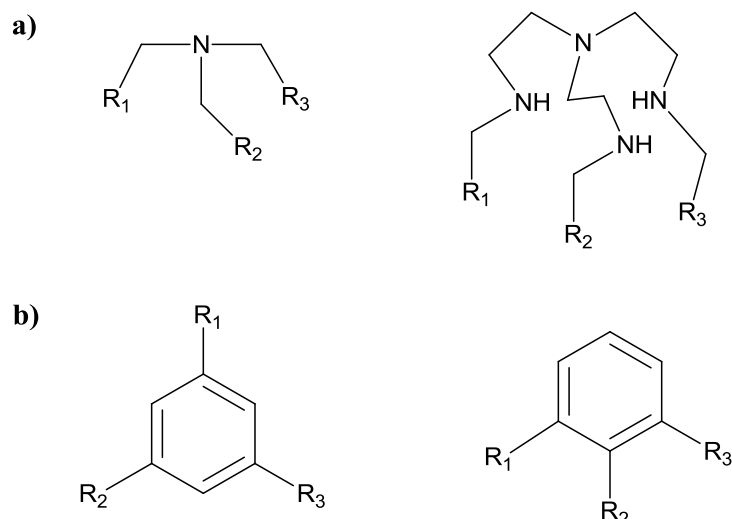


Figure 2.4: Examples of suitable scaffolds (a) Tertiary amine systems, (b) Aromatic systems.

In the tertiary amines, **Figure 2.4(a)**, the nitrogen acts as the scaffold and a series of terminal alkynes, sulfides and hydrogen bond acceptors could be readily attached. The attraction of using this tripodal amine was its ability to be quite a flexible system, thereby introducing the possibility of rotation between the functional groups and allowing the hydrogen bond donors to freely compete. Also the functional groups could be equidistant from each other and the chain length could be altered and expanded accordingly. First or second row metals could also be introduced to this amine system in order to orientate or chelate the ‘arms’.

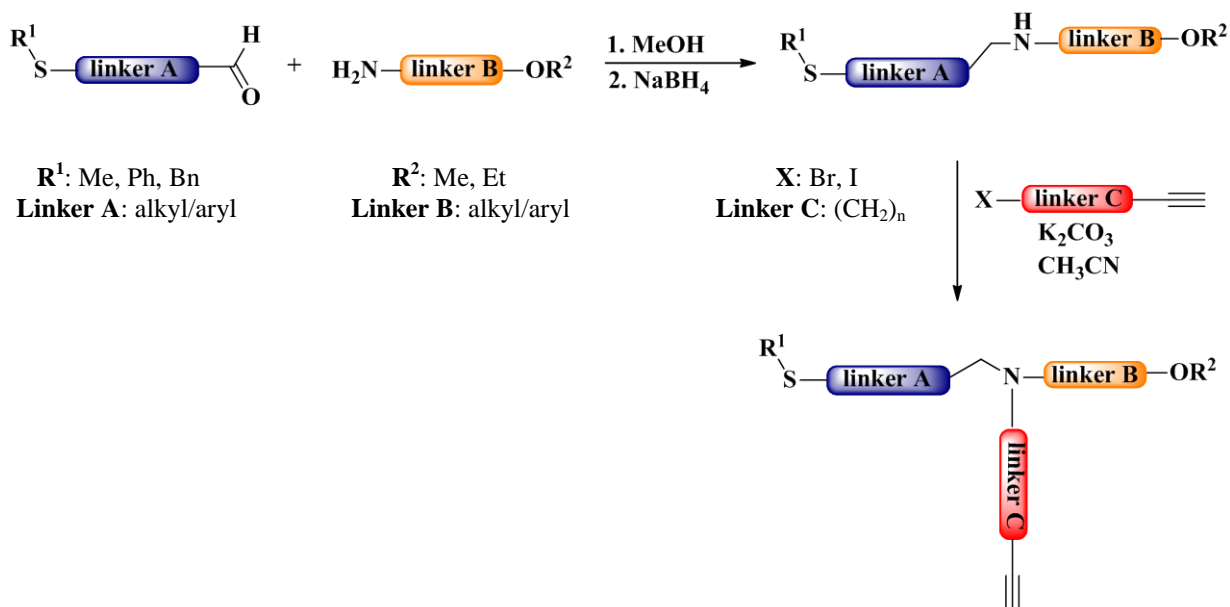
A 1,2,3- or 1,3,5-substituted aromatic ring, **Figure 2.4(b)**, was also an interesting system to pursue as the aromatic ring is a fixed and rigid system and would hold the structure of the molecule in a definite position for the ‘arms’ to interact with each other. The 1,2,3-substituted system was a more appealing scaffold than the 1,3,5-substituted aromatic ring as the ‘arms’ would be closer together and therefore, interaction may be achieved more easily. In the 1,3,5-substituted system, it may prove difficult for the linkers to reach each other so therefore this system may cause problems when studying the hydrogen bond interactions.

2.3. Tertiary Amines

2.3.1. Synthetic Strategy

The synthetic strategy devised to achieve the target tertiary amine is outlined in **Scheme 2.1**. Firstly, it was decided to use a reductive amination reaction to synthesise a variety of secondary amines, followed by an *N*-alkylation reaction to form the desired tripodal amine with the terminal alkyne, sulfur functionalities and hydrogen bond acceptors attached. Ether groups were chosen to act as the competitive hydrogen bond acceptor when the terminal alkyne was the donor. It was decided to synthesise the secondary amines with the sulfide and ether groups firstly attached, as these particular functional groups are more robust, and then alkylate the secondary amine with the terminal alkyne to produce the tertiary amine. In theory, intramolecular hydrogen bonding should take place between the hydrogen of the terminal alkyne and oxygen of the ether, when the sulfide is present. Then after oxidation to the sulfoxide or sulfone, an intramolecular hydrogen bond switch should occur and the sulfoxide/sulfone should act as the main hydrogen bond acceptor.

This synthetic strategy was quite flexible and robust which was a major advantage as a wide variety of functional groups could be attached easily. The linker chain lengths could be altered and the size and nature of the substituents could also be changed without severe disruption to the overall synthetic strategy.



Scheme 2.1: Synthetic strategy to access tertiary amines

2.3.2. Linkers for Amine Scaffold

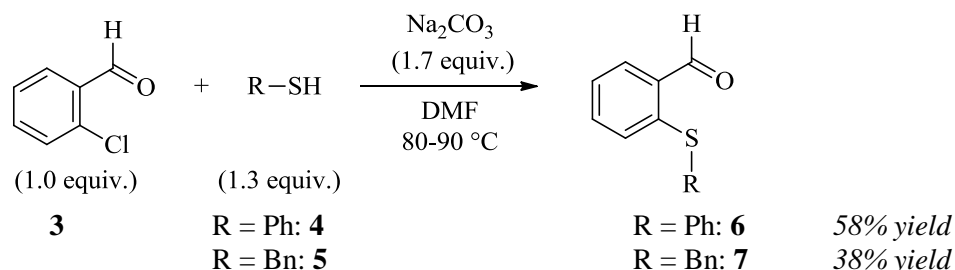
The choice of linker groups had to be carefully planned and designed before beginning the synthesis of the target tertiary amine. The linker groups act as tethers to which the desired functional groups are attached. The ease of altering the position of the functional groups, bulk of the substituents and chain length was the major factor in choosing suitable linkers.



Table 2.1: Linker groups and substituents.

Compound No.	Linker A	R ¹
1	(CH ₂) ₂	CH ₃
2	<i>p</i> -C ₆ H ₄	CH ₃
6	<i>o</i> -C ₆ H ₄	Ph
7	<i>o</i> -C ₆ H ₄	Bn

For linker A, alkyl and aryl substituents were obvious candidates to begin with and proved to be the most accommodating linkers. Compounds **1** and **2** are commercially available with the aldehyde and sulfide functional groups attached and so provided a good starting point, **Table 2.1**. The position and size of the sulfide also needed to be investigated, so phenyl and benzyl sulfides, **6** and **7**, were introduced at the *ortho* position utilising Heynderickx's procedure.¹¹ This involved a nucleophilic aromatic substitution of 2-chlorobenzaldehyde, **3**, with either thiophenol, **4**, or benzylmercaptan, **5**, to achieve the desired products **6** and **7** in 58% and 38% yields respectively, **Scheme 2.2**. In future reactions perhaps a more electronegative halogen at the *ortho* position *e.g.* fluorine would help to increase the yields of these particular sulfides.¹² The sulfide, **7**, which contains the benzyl group adds another dimension by introducing additional hydrogens α to the sulfide which may act as competing hydrogen bond donors when oxidation to the sulfoxide/sulfone occurs, as observed by Lehane in simpler systems.⁵



Scheme 2.2: Synthesis of **6** and **7**.

Similarly for linker B, the aryl and alkyl substituents proved to be the most accessible as **8** and **9** were commercially available with the amine and ether groups attached, **Table 2.2**. It was anticipated that the ether group at the end of a flexible chain, **8**, and in the *ortho* position, **9**, would provide sufficient variety when studying the weak hydrogen bond interactions.



Table 2.2: Suitable linkers and substituents

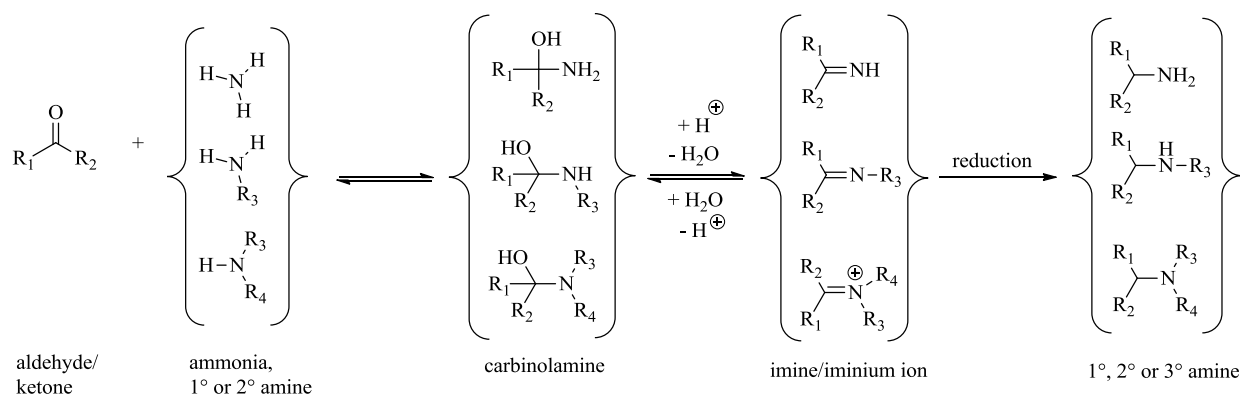
Compound No.	Linker B	R ²
8	(CH ₂) ₃	Et
9	CH ₂ (<i>o</i> -C ₆ H ₄)	CH ₃

It was decided to use straight alkyl chains for linker C containing the terminal alkyne and a good leaving group *e.g.* bromine and iodine, **Table 2.3**. The chain length could then be altered conveniently to increase the flexibility of the system in order to accommodate intramolecular hydrogen bonds.



Table 2.3: Suitable groups for Linker C.

Compound No.	X	Linker C
10	Br	CH ₂
11	Br	(CH ₂) ₂
14	I	(CH ₂) ₃
15	I	(CH ₂) ₄

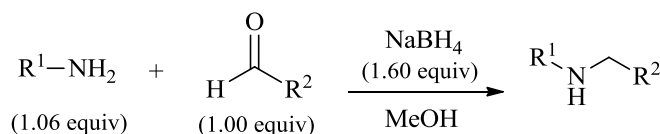


Scheme 2.4: General reductive amination pathway.¹⁶

Reductive amination reactions can be described as a *direct* or a *stepwise (indirect)* reaction.¹⁵ When the carbonyl compound and the amine are mixed with the appropriate reducing agent without prior formation of the intermediate imine or iminium salt, then this is referred to as the direct reaction. In this particular case it is vital that the correct reducing agent is used as the reducing agent must reduce the imines or iminium ions selectively over the aldehyde or ketone. Usually hydrogen, in the presence of metal catalysts or sodium cyanoborohydride (NaBH_3CN), is used as reducing agents for the direct reductive amination. Since this research project involves the use of terminal alkynes, hydrogenation would not be suitable to use as a method to access the secondary amines. Disadvantages of using sodium cyanoborohydride include its high toxicity and formation of toxic by-products. Sodium triacetoxymethylborohydride [$\text{NaBH}(\text{OAc})_3$] has also been detailed in the literature¹⁵ as an effective reducing agent, but due to the fact that it is flammable, water-reactive and poorly soluble in most commonly used organic solvents, an alternative method was used in this case for the reductive amination reactions.

The alternative stepwise or indirect reductive amination was a more appealing method to access the secondary amines due to the potential sensitivity of the functional groups involved (*e.g.* terminal alkynes). This reaction is still a one-pot reaction with an intermediate imine firstly formed and then reduction takes place in a separate step, **Scheme 2.5**. A key advantage of this method is the fact that the competing reduction of the carbonyl compound is not possible, so the choice of reducing agent is less restricted. Sodium borohydride was the reducing agent of choice as it is inexpensive, safe to handle and environmentally friendly.

The aldehyde was stirred in methanol with the primary amine to form the imine intermediate which was observed by TLC. Reduction then occurred *in situ* when sodium borohydride (1.60 eq.) was added.¹⁵ A wide variety of novel secondary amines were synthesised, varying the chain length, position of the functional groups and size of the substituents attached, **Table 2.4**.



Scheme 2.5: Formation of secondary amines by reductive amination.

Table 2.4: Series of secondary amines synthesised.

1° Amine	R ^{1a}	Aldehyde	R ²	2° Amine ^c	Yield %
8	EtO(CH ₂) ₃ -	1	-(CH ₂) ₂ SMe ^a	16	11 ^{d,e}
9	(2-MeO-C ₆ H ₄)CH ₂ -	1	-(CH ₂) ₂ SMe ^a	17	98 ^f
9	(2-MeO-C ₆ H ₄)CH ₂ -	2	-(4-MeS-C ₆ H ₄) ^a	18	98 ^{e,f}
9	(2-MeO-C ₆ H ₄)CH ₂ -	6	-(2-PhS-C ₆ H ₅) ^b	19	95 ^{e,f}
8	EtO(CH ₂) ₃ -	6	-(2-PhS-C ₆ H ₅) ^b	20	88 ^{e,f}
9	(2-MeO-C ₆ H ₄)CH ₂ -	7	-(2-BnS-C ₆ H ₅) ^b	21	86 ^{e,f}

a Commercially available (Sigma-Aldrich)

b Synthesised according to the Heynderickx procedure¹¹

c 2° amines (**16-21**) oils at room temperature

d Purified by column chromatography

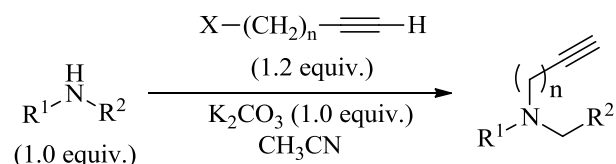
e Novel compounds and characterised by ¹H and ¹³C NMR, IR, *m/z* and HRMS

f Unpurified yield but sufficiently pure for next stage of synthesis

A variety of secondary amines, ranging from straight chain alkyl systems to aromatic based systems were successfully synthesised. The amines were isolated in good yields except for **16**, which resulted in a loss in yield after column chromatography due to the product adhering to the silica gel. Therefore, purification was not employed in the remaining transformations. The crude secondary amines (**17-21**) were sufficiently pure by ¹H NMR for the next stage of synthesis. In summary, this approach via the reductive amination proved an effective and convenient method for generating the secondary amines (**16-21**), bearing the sulfur and ether moieties.

2.3.4. N-Alkylation

The next stage in the synthetic strategy as outlined in **Scheme 2.1**, involved the alkylation of the secondary amines featured in **Table 2.4** with a number of terminal alkynes in order to complete the tripodal amine system.



(X=Br, n=1): **10**

(X=Br, n=2): **11**

(X=I, n=3): **14**

(X=I, n=4): **15**

* Δ for **10**, **14**, **15**; rt for **11**.

Scheme 2.6: N-Alkylation with terminal alkynes.

N-Alkylation, as illustrated in **Scheme 2.6**, using potassium carbonate as base in acetonitrile proved to be quite an effective route to yield a series of novel tertiary amine systems. Moderate to good yields were achieved with the exception of the tertiary amines **22** and **29**, which both included a long ether chain, **Table 2.5**. The best yields were obtained for **23**, **26** and **31** when the short chain propargyl bromide, **10**, was employed. The N-alkylation reactions were heated under reflux except when using 4-bromo-1-butyne, **11** which was stirred at room temperature for safety reasons (F.p. 23 °C). A loss in yield was noted for the tertiary amines **22**, **24**, **27**, **29**, and **32**, possibly due to these temperature constraints.

Table 2.5: Tertiary amines synthesised.

2° Amine	R ¹	R ²	Alkyne	n	3° Amine ^c	Yield (%) ^d
16	EtO(CH ₂) ₃ -	-(CH ₂) ₂ SMe	11 ^a	2	22	25
18	(2-MeO-C ₆ H ₄)CH ₂ -	-(4-MeS-C ₆ H ₄)	10 ^a	1	23	70
18	(2-MeO-C ₆ H ₄)CH ₂ -	-(4-MeS-C ₆ H ₄)	11 ^a	2	24	64
18	(2-MeO-C ₆ H ₄)CH ₂ -	-(4-MeS-C ₆ H ₄)	14 ^b	3	25	49
19	(2-MeO-C ₆ H ₄)CH ₂ -	-(2-PhS-C ₆ H ₅)	10 ^a	1	26	82 ^f
19	(2-MeO-C ₆ H ₄)CH ₂ -	-(2-PhS-C ₆ H ₅)	11 ^a	2	27	65
19	(2-MeO-C ₆ H ₄)CH ₂ -	-(2-PhS-C ₆ H ₅)	15 ^b	4	28	75 ^e
20	EtO(CH ₂) ₃ -	-(2-PhS-C ₆ H ₅)	11 ^a	2	29	29
20	EtO(CH ₂) ₃ -	-(2-PhS-C ₆ H ₅)	14 ^b	3	30	69
21	(2-MeO-C ₆ H ₄)CH ₂ -	-(2-BnS-C ₆ H ₅)	10 ^a	1	31	80
21	(2-MeO-C ₆ H ₄)CH ₂ -	-(2-BnS-C ₆ H ₅)	11 ^a	2	32	46

a Commercially available (Sigma-Aldrich)

b Synthesised according to the Borbas procedure¹³

c Novel 3° amines **22-32** characterised by ¹H and ¹³C NMR, IR, *m/z* and HRMS

d Purified yield after column chromatography.

e ~ 83% pure by ¹H NMR

f Crystal structure determined.

The characteristic bands for terminal alkynes were observed in the IR spectra of the compounds tabulated below in **Table 2.6** at 3289-3302 cm⁻¹ for the C≡C-H stretch and as a weak band at 2116-2118 cm⁻¹ for the C≡C stretch. Interestingly, for the short chain terminal alkynes where the carbon chain contains only one CH₂, the C≡C stretch was not observed in the IR spectra. The ν(C≡C) stretch in centrosymmetric acetylenes is not IR active and it has also been reported that the band may be too weak to be observed in cases where the substituents are of similar mass and have similar inductive effects.¹⁷

Table 2.6: IR and ¹H NMR data for tertiary amines.

3° Amine	$\nu_{\max}/\text{cm}^{-1}$ (C≡C-H)	$\nu_{\max}/\text{cm}^{-1}$ (C≡C)	δ_{H} (C≡C-H)*
22	3294	2118	1.94
23	3289	-	2.27
24	3293	2117	1.92
25	3295	2116	1.86
26	3292	-	2.26
27	3296	2116	1.90
28	3298	2116	1.90
29	3302	2117	1.92
30	3300	2116	1.88
31	3291	-	2.27
32	3295	2117	1.91

* ¹H NMR signal 300 MHz (δ_{H} ppm) in CDCl₃ for terminal alkyne proton

In the ¹H NMR spectra of the tertiary amines synthesised, the characteristic triplet of the terminal alkyne was observed between 1.86-2.27 ppm, (⁴J 2.3-2.6). It was noted that the proton signal (C≡C-H) for the shorter alkyl chain terminal alkynes **23**, **26**, and **31** was shifted further downfield than for the longer chain systems, due to the close proximity of the electronegative nitrogen which causes a deshielding effect.

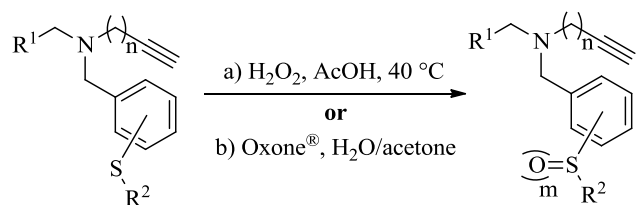
In conclusion, a series of novel tertiary amines bearing the sulfide, terminal alkyne and ether moieties was readily prepared following the synthetic strategy outlined in **Scheme 2.1**. The flexibility evident in this route provides sufficient scope for accessing further differentially substituted analogues.

2.3.5. Oxidation to sulfoxide and sulfones

While the synthetic strategy illustrated in **Scheme 2.1** was successfully completed and a number of novel target compounds were synthesised containing the sulfide, terminal alkyne and a competing hydrogen bond donor (ether), crystal structures of the novel tertiary amines in **Table 2.5** were quite difficult to obtain as these compounds were viscous oils at room temperature. This had not been envisaged at the outset of the design of these systems. Oxidation to the corresponding sulfoxides and sulfones was explored with a view to generate more crystalline solids. Obtaining crystal structures would further develop our knowledge of the weak interactions in these tertiary amine systems. **Scheme 2.7** illustrates the oxidation reactions of the tertiary amines to their corresponding sulfoxides and sulfones. With a large variety of oxidising agents available for the selective oxidation of sulfides,¹⁸ a metal catalyst-free and non-toxic process was the most attractive method to access the sulfoxides and sulfones.

For the synthesis of the sulfoxides, the use of hydrogen peroxide (H₂O₂) was quite an attractive method as it is environmentally friendly, cheap, and over-oxidation to the sulfone can be prevented.^{19,20} Also oxidation involving hydrogen peroxide proceeds under relatively mild conditions and so is suitable for use with sensitive sulfides *e.g.* terminal alkynes. The synthesis of the sulfoxides (**33-42**) was quite straightforward using H₂O₂ in acetic acid. Heating the reaction to ~40 °C reduced the reaction time and increased the efficiency with moderate to high yields obtained.

Oxone[®], which has many applications in the oxidation of various functional groups was the oxidant of choice for the conversion of sulfides to sulfones²¹ due to its mild, safe and stable properties. Sulfones (**43-52**) were obtained in moderate yields after column chromatography. A decrease in yield was noted for certain sulfones, namely **49** and **52** where complete oxidation to the sulfone had not occurred and unreacted sulfide and sulfoxide were recovered after column chromatography in each case.



Scheme 2.7: Oxidation of sulfides (SCH₃) to sulfoxides and sulfones.

Table 2.7: Summary of sulfides, sulfoxides and sulfones synthesised.

R ¹	R ²	n	Sulfide (m=0) ^a			a) Sulfoxide (m=1) ^a				b) Sulfone (m=2) ^a			
			No.	δ _H (SCH ₃)	δ _C (SCH ₃)	No.	Yield (%) ^c	δ _H (SCH ₃)	δ _C (SCH ₃)	No.	Yield (%) ^c	δ _H (SCH ₃)	δ _C (SCH ₃)
(2-MeO-C ₆ H ₄)-	<i>p</i> -SCH ₃	1	23	2.47	16.1	33^b	90 ^d	2.73	43.8	43	55	2.97	43.6
		2	24	2.47	16.2	34	57	2.72	43.9	44	42	3.04	44.6
		3	25	2.47	16.2	35	40	2.63	43.9	45^b	42	3.02	44.6
(2-MeO-C ₆ H ₄)-	<i>o</i> -SPh	1	26^b	-	-	36	68	-	-	46^b	28	-	-
		2	27	-	-	37	50	-	-	47	88	-	-
		4	28	-	-	38	48	-	-	48^{b,e}	19	-	-
		2	29	-	-	39	72	-	-	49^e	25	-	-
EtO(CH ₂) ₂ -	<i>o</i> -SPh	3	30	-	-	40	31	-	-	50	30	-	-
				δ _H (SCH ₂)	δ _C (SCH ₂)			δ _H (SCH ₂)	δ _C (SCH ₂)			δ _H (SCH ₂)	δ _C (SCH ₂)
		(2-MeO-C ₆ H ₄)-	<i>o</i> -SBn	1	31	3.72	38.9	41	45	4.01 (A of ABq, <i>J</i> 12.6) 4.15 (B of ABq, <i>J</i> 12.9)	61.7	51^b	33
		2	32	3.63	39.2	42	44	4.04 (A of ABq, <i>J</i> 12.6) 4.09 (B of ABq, <i>J</i> 12.6)	62.1	52	38	4.50	62.8

a Novel compounds characterised by ¹H and ¹³C NMR, IR, *m/z* and HRMS

b Crystal structure determined. For **51** crystal structure of HCl salt determined, (see section 2.3.6).

c Purified yield after column chromatography.

d Unpurified yield.

e Incomplete oxidation. Unreacted sulfide and sulfoxide was also recovered after column chromatography.

The sulfides (**23-25**), sulfoxides, (**33-35**), and sulfones, (**43-45**), summarised in **Table 2.7** were readily distinguished by ^1H and ^{13}C NMR with the methyl signals indicative of the oxidation state of sulfur. As the oxidation state of sulfur increases, the methyl hydrogens and carbon α to the sulfur moiety experience a decrease in electron density which results in a deshielding effect and therefore a downfield shift in signal.

In (**26-30**), while the methyl signals which had been very characteristic in the oxidations of (**23-25**) were absent, the oxidation products (**36-40**) and (**46-50**) were readily characterised by both ^1H NMR (**Figure 2.5**) and IR with the characteristic IR bands for sulfoxides ($\sim 1030\text{ cm}^{-1}$) and sulfones (~ 1307 and 1154 cm^{-1}) observed.

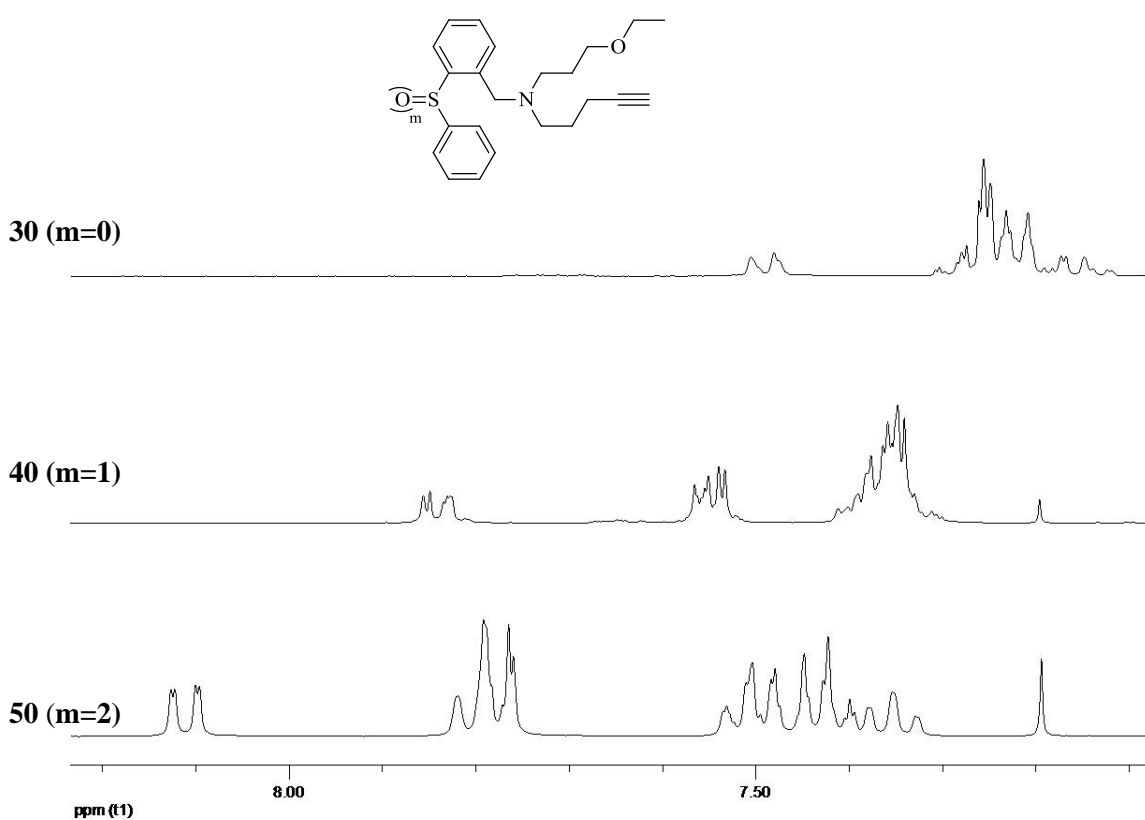


Figure 2.5: The ^1H NMR (300 MHz) spectra of the sulfide **30**, sulfoxide **40**, and sulfone **50**.

In the benzyl substituted sulfoxides, (**41** and **42**), due to the chiral centre at the sulfur, the hydrogens α to the sulfur are diastereotopic. Oxidation of the sulfide to the sulfoxide is indicated by these hydrogens appearing as an AB quartet in ^1H NMR, **Figure 2.6**. Further oxidation to their corresponding sulfones, (**51** and **52**), results in the α hydrogens shifting considerably downfield and appearing as a singlet due to the loss of chirality.

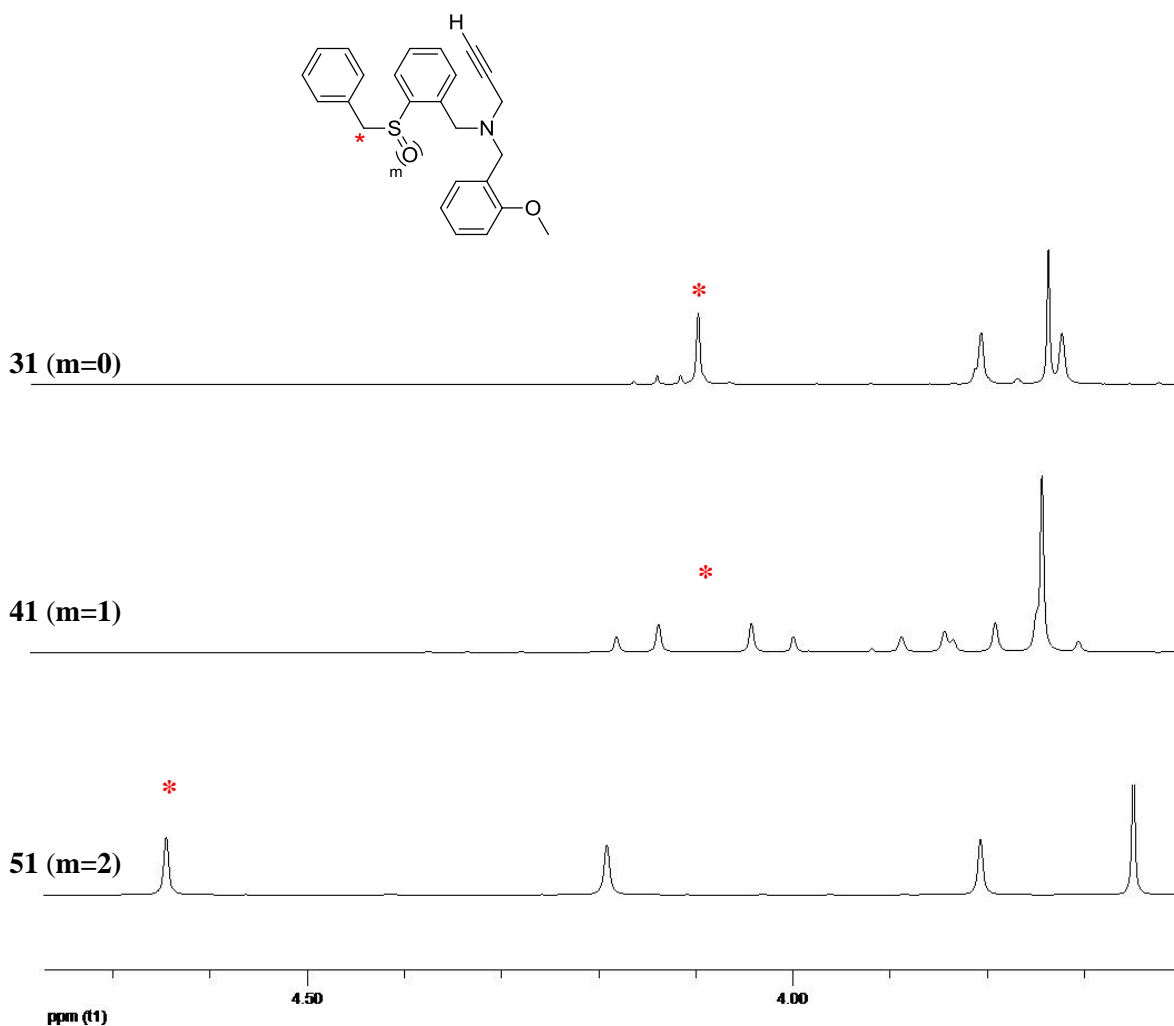


Figure 2.6: ^1H NMR (300 MHz) spectra of the sulfide, **31**, sulfoxide, **41**, and sulfone, **51**, at 3.60-4.70 ppm.

Further diastereotopic effects were evident in the ^1H NMR spectrum of **41**, **Figure 2.7**. The diastereotopic protons ($\text{H}_{\text{pro-R}}$ and $\text{H}_{\text{pro-S}}$) α to the alkyne have a non-equivalent chemical shift and appear as a finely split AB quartet at 3.15 ppm (J_{AB} 17.1, 4J 2.4) and 3.30 ppm (J_{AB} 17.1, 4J 2.4). In contrast these α hydrogens appear as doublets in the sulfide, **31**, at 3.26 ppm (4J 2.4) and the sulfone, **51**, at 3.27 ppm (4J 2.1).

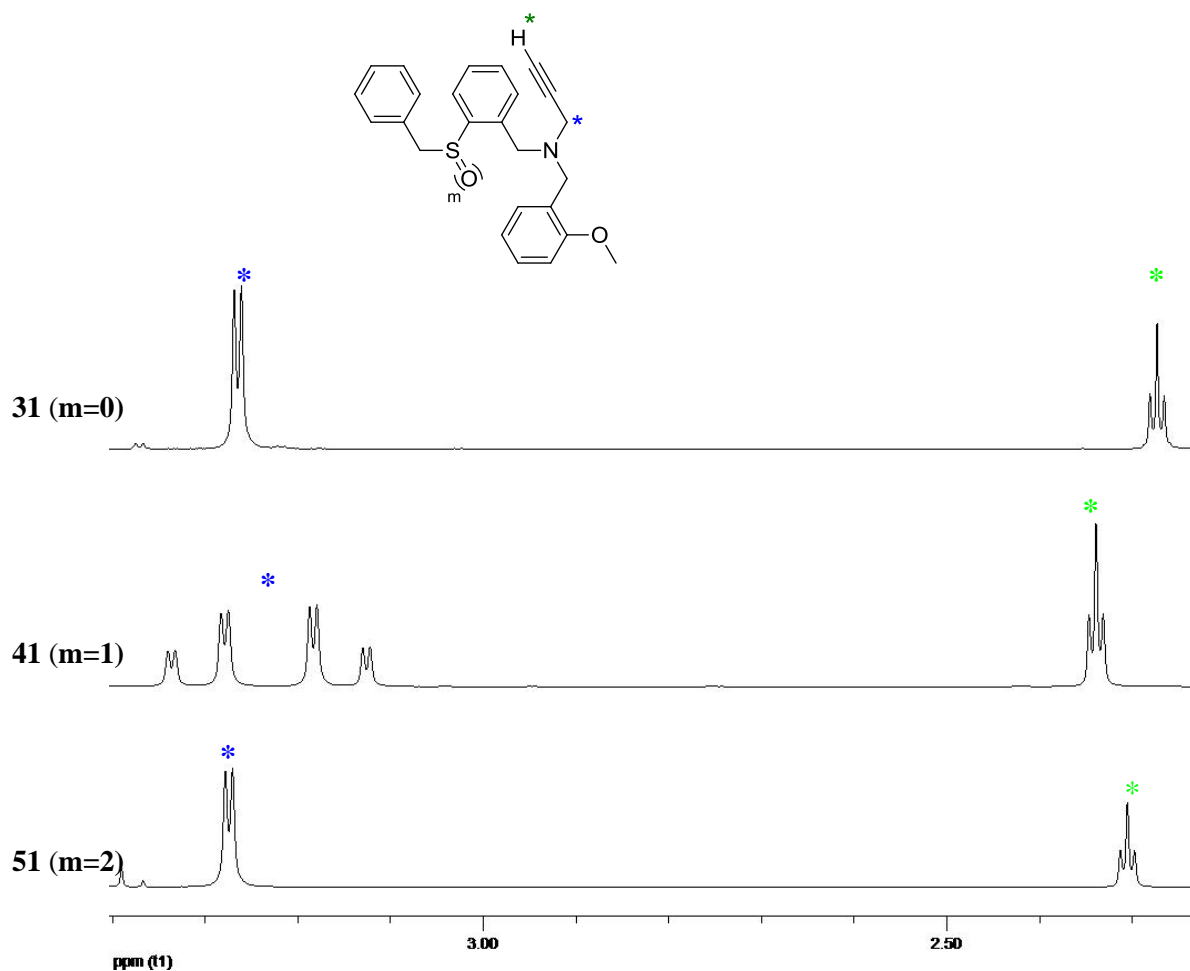


Figure 2.7: ^1H NMR (300 MHz) spectra of the sulfide, **31**, sulfoxide, **41**, and sulfone, **51**, at 2.30-3.40 ppm.

2.3.6. Crystal Structure Data

With a wide variety of tertiary amines synthesised and also the oxidation to their corresponding sulfoxides and sulfones successfully completed, the next challenge was to obtain crystal structures and study their intra/intermolecular hydrogen bonding patterns and preferred conformations. However, as the majority of these novel tripodal systems exist as oils at room temperature, our initial objective to investigate the hydrogen bonding network in these very interesting compounds proved challenging. It seemed that the systems designed were perhaps a little too flexible and exhibited too much conformational freedom. These simple short chain compounds however, provide a baseline from which second generation compounds, displaying the desired intramolecular interactions, could be constructed.

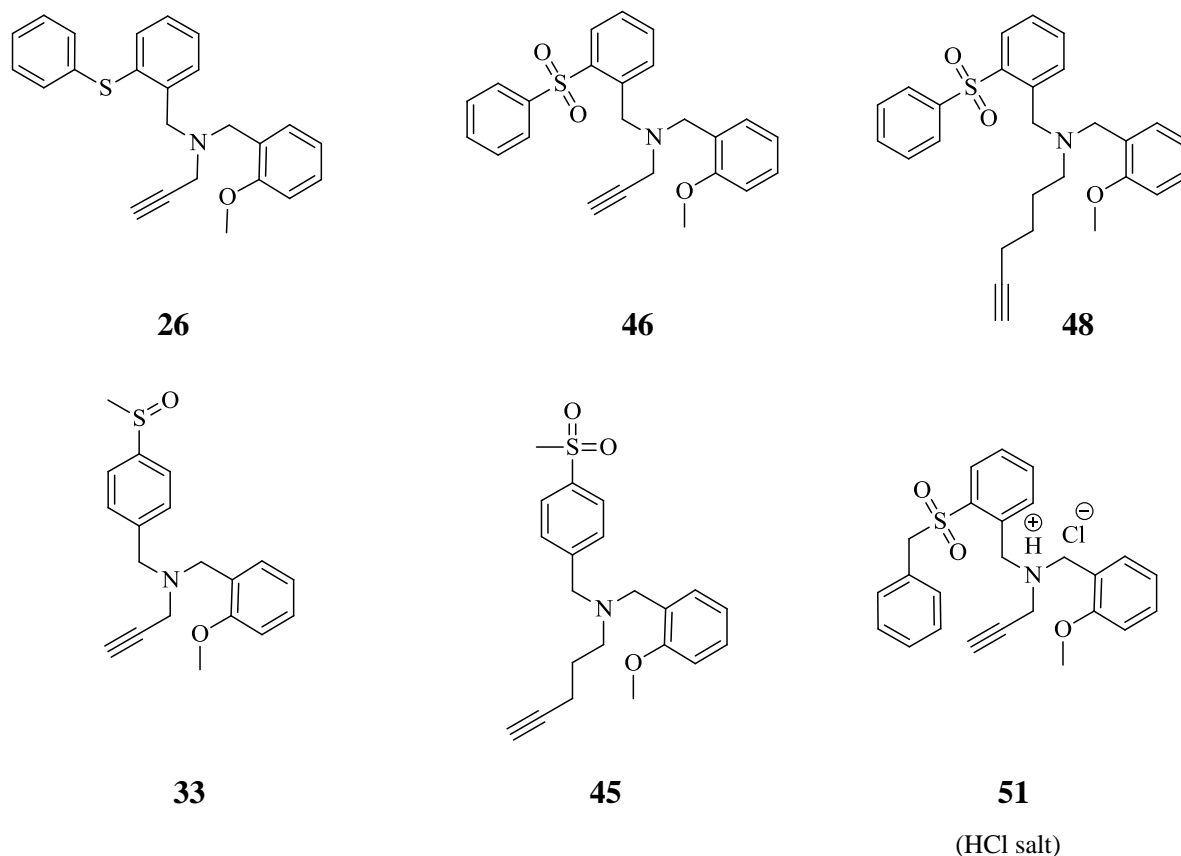


Figure 2.8: Crystal structures obtained for the tertiary amine systems.

Following considerable experimental effort, crystals were obtained for a small number of these tertiary amine systems (**26**, **46**, **48**, **33**, **45**, **51**), with the sulfones proving the most crystalline, **Figure 2.8**. Growing crystals of **26** and **33** proved to be very demanding as they existed as semi-solids or viscous oils at room temperature and required the use of *in situ* crystallisation, while the sulfones, **46**, **48**, **45** and **51**, were crystallised from solution in the normal manner. The *in situ* crystallisation procedure employed to obtain the crystal structures of the sulfide, **26**, and sulfoxide, **33**, involved mounting the material of interest on a pip, cooling and cycling the temperature above and below its melting point until a single crystal was obtained. This particular method of crystallisation is quite laborious and can fail due to glass formation.

When examining the crystal packing of these tertiary amine systems, some interesting packing motifs were noted. For example, **26**, which consists of a short chain terminal alkyne with both the methoxy and sulfide functional groups in the *ortho* position, as expected, did not display intramolecular interactions, due to the short chains and conformational constraint of the molecule. However, interesting intermolecular $\text{NCH}\cdots\pi(\text{C}\equiv\text{C})$ and $\text{NCH}\cdots\text{OME}$ interactions are holding the molecules together in weak hydrogen bonded dimers, **Figure 2.9**.

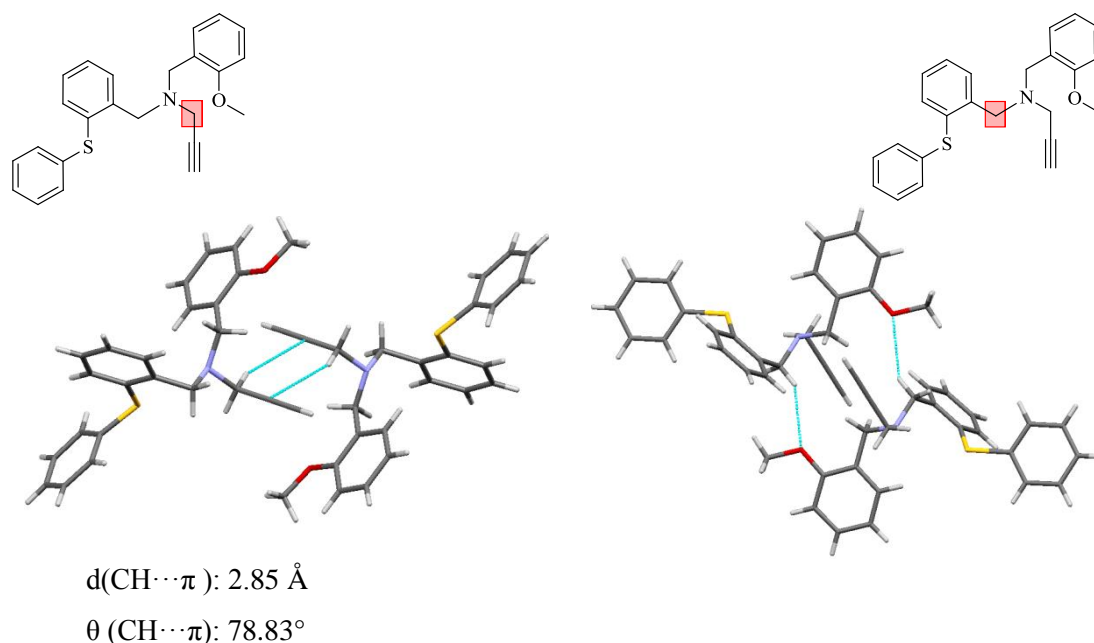


Figure 2.9: Intermolecular interactions observed in **26**.

The $\text{CH}\cdots\pi(\text{C}\equiv\text{C})$ dimer observed in **26** was of particular interest as this type of interaction was not previously observed in Lehané's simpler systems involving terminal alkynes.⁵ It is widely reported that terminal alkynes can act both as a hydrogen bond donor through the

alkynyl hydrogen and as a hydrogen bond acceptor through the π cloud of the triple bond. ^{22,23} A search of the Cambridge Structural Database (CSD) revealed that 199 structures contain the $N(CH_2)C\equiv CH$ moiety and 55 of these compounds contain the intermolecular $NCH\cdots\pi(C\equiv C)$ dimer formed between the CH of $N(CH_2)C\equiv C$ to the triple bond of the alkyne within the bond distance range of 1.00-3.50 Å, **Figure 2.10**. The bond distance observed in **26** of 2.85 Å is quite significant because it is at the lower range of intermolecular distances observed in the CSD.

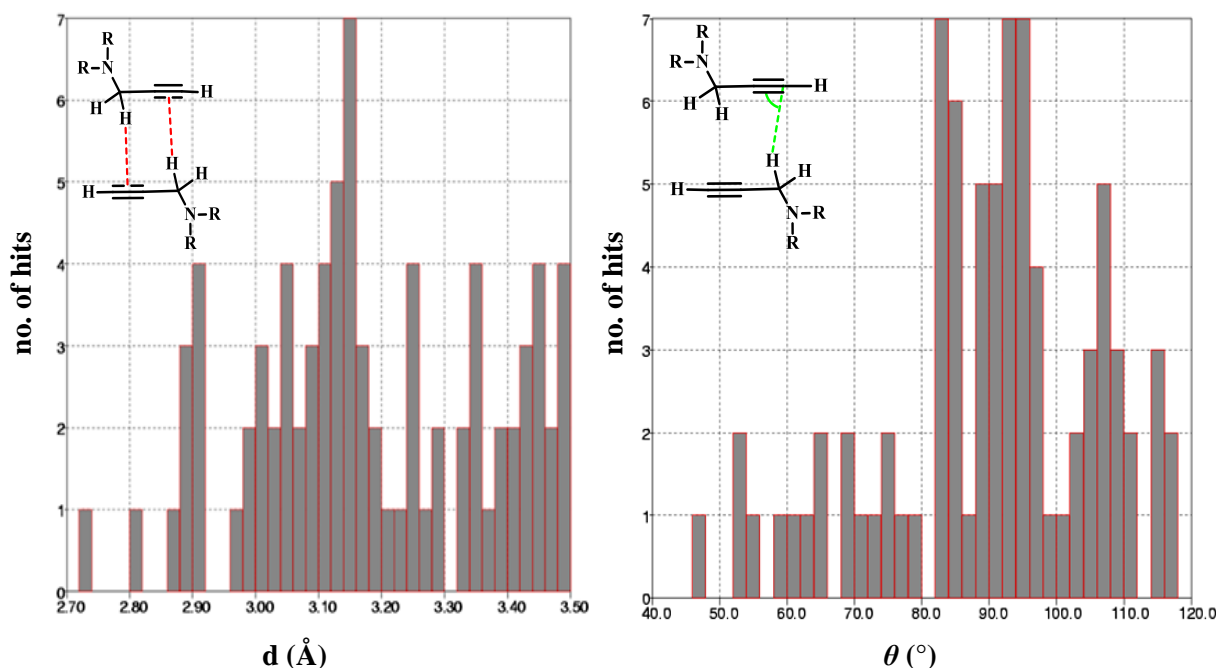


Figure 2.10: Histograms representing $NCH\cdots\pi$ bond distances (left) and $NCH_2\cdots\pi$ bond angles (right) reported for 55 structures from the CSD.

The intermolecular $CH\cdots\pi(C\equiv C)$ dimer angle (θ) adopted in these 55 structures varied considerably, ranging from 47°-118°, **Figure 2.10**. An angle of 78.83° exists in the dimer in **26** which seems to be the typical angle observed for these systems.

The structures of RUSYAG,²⁴ KAJRET²⁵ and JEVROS²⁶ are examples of simple structures similar to **26** that exhibit this $\text{NCH}\cdots\pi(\text{C}\equiv\text{C})$ interaction, even in the presence of stronger hydrogen bonding interactions, **Figure 2.11**. It appears that the propargylic CH_2 hydrogens directly attached to the nitrogen atom in **26**, and also in the structures featured in **Figure 2.11**, are competing with the terminal alkyne to act as the hydrogen bond donor. Therefore, perhaps these hydrogens are comparable in terms of acidity to the terminal alkyne hydrogen ($\text{pK}_a \sim 26$), which may explain the formation of the $\text{NCH}\cdots\pi(\text{C}\equiv\text{C})$ interactions.

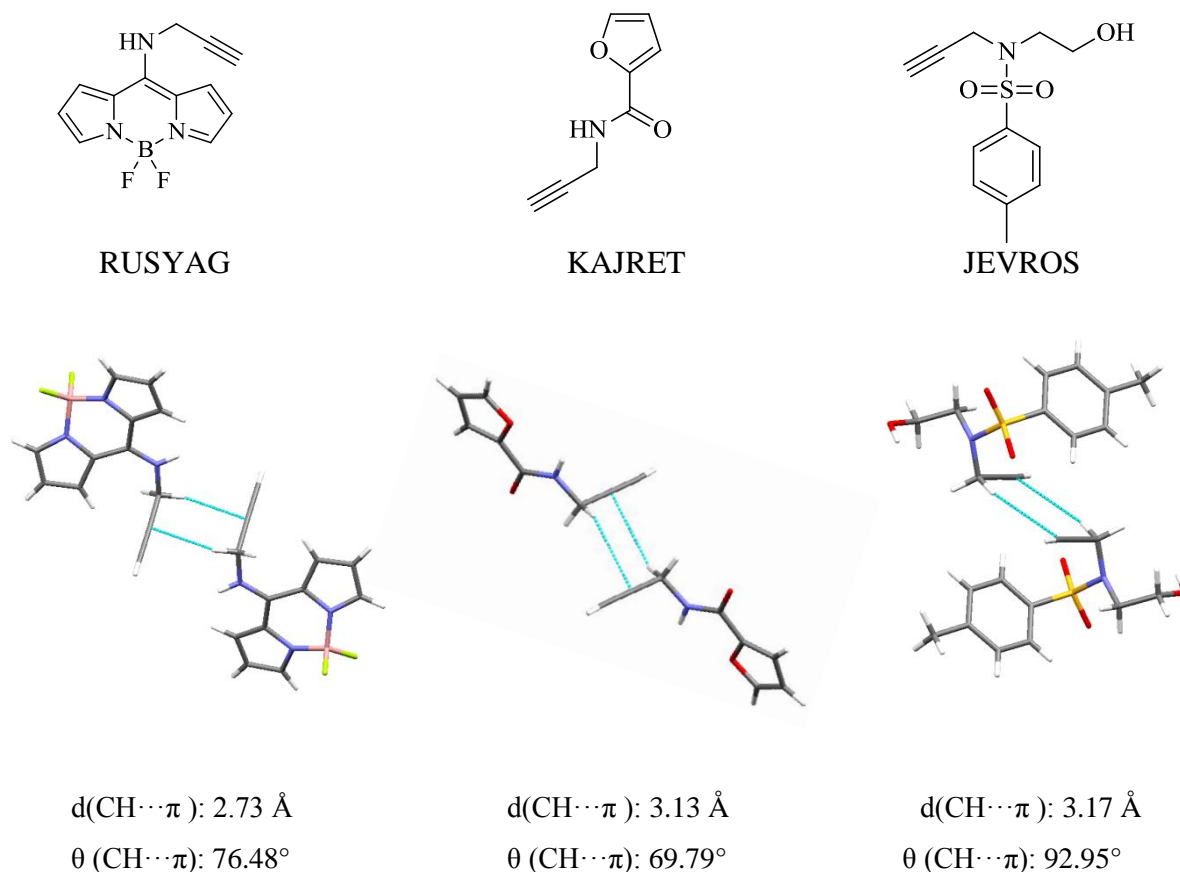


Figure 2.11: Crystal structures of RUSYAG,²⁴ KAJRET²⁵ and JEVROS.²⁶

The second intermolecular interaction observed in **26** involved the $\text{NCH}\cdots\text{OMe}$. In this case it is the NCH linked to the sulfide substituent which is participating in hydrogen bonding, as opposed to the NCH adjacent to the terminal alkyne, **Figure 2.9**. It is reasonable to assume that these α hydrogens are also relatively acidic and therefore good hydrogen bond donors, as they are adjacent to the electronegative nitrogen and also contain an *ortho* phenyl sulfide substituent. Both the $\text{NCH}\cdots\pi(\text{C}\equiv\text{C})$ and $\text{NCH}\cdots\text{OMe}$ intermolecular interactions occur simultaneously and it is unclear if these interactions are dependent on each other or form independently.

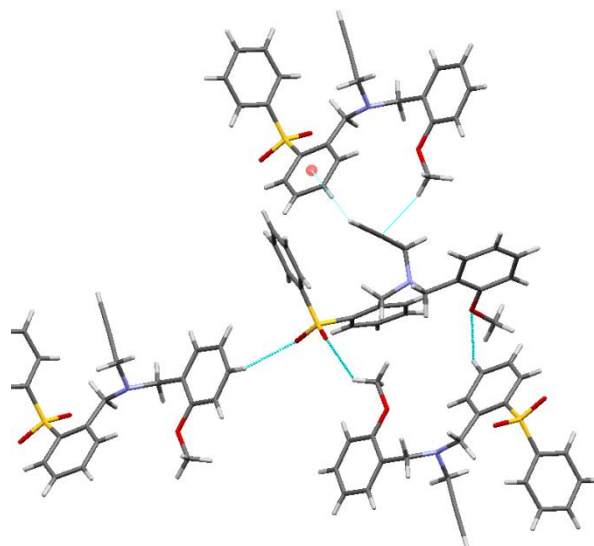


Figure 2.12: Intermolecular interactions for **46**.

Comparing the crystal packing of the sulfide, **26**, to its corresponding sulfone **46**, it was observed that the intermolecular interactions changed remarkably after oxidation, **Figure 2.12**. The oxygen of the sulfone is now participating in weak hydrogen bonding to nearby hydrogens of aromatic and methyl substituents and the $\text{NCH}\cdots\pi(\text{C}\equiv\text{C})$ dimer is no longer observed. Instead methoxy $\text{C-H}\cdots\pi(\text{C}\equiv\text{C})$ (2.89 Å) and $\text{C}\equiv\text{C-H}\cdots\pi(\text{arene})$ (2.84 Å) intermolecular interactions are now occurring. The terminal alkyne in **46** is acting as a hydrogen bond donor, pointing to the π -system of a neighbouring phenyl ring which is quite an unusual interaction. For example when both Boese and Harris investigated the crystal packing of 1,4-diethynylbenzene, **53**, and 1,3,5-triethynylbenzene, **54**, they found that competition exists between the $\text{C}\equiv\text{C-H}$ and the arene ring as acceptors for $\text{C}\equiv\text{C-H}\cdots\pi$ interactions, and suggested that the $\text{C}\equiv\text{C-H}\cdots\pi(\text{C}\equiv\text{C})$ is preferred over the $\text{C}\equiv\text{C-H}\cdots\pi(\text{arene})$ interaction, **Figure 2.13**.^{27,28} The crystal structure of **53** displays infinite zig-zag chains involving $\text{C}\equiv\text{C-H}\cdots\pi(\text{C}\equiv\text{C})$, while in **54** double helical chains involving the $\text{C}\equiv\text{C-H}\cdots\pi(\text{C}\equiv\text{C})$ interactions are adopted. In both cases the $\text{C}\equiv\text{C-H}\cdots\pi(\text{C}\equiv\text{C})$ interaction is only observed, even though arene systems are widely available for bonding in these compounds.

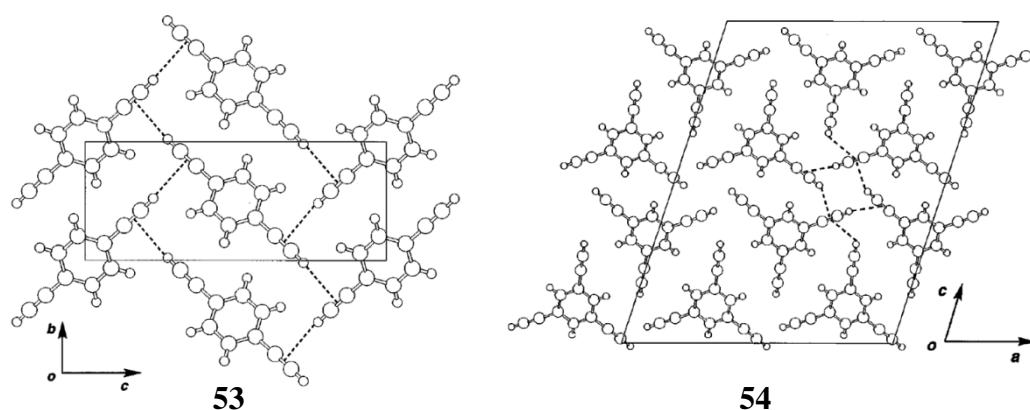


Figure 2.13: Crystal packing in and. Reproduced from Harris.²⁸

Boese *et al.* also discovered the unusual crystal packing of ethynylbenzene, **55**, which involved $\text{C}\equiv\text{C}-\text{H}\cdots\pi(\text{arene})$ interactions.²⁷ Similar to the interaction observed in the sulfone **46**, ethynylbenzene molecules adopt edge-to-face interactions. In addition, the melting point of **55** at $-45\text{ }^\circ\text{C}$ deviates remarkably from benzene ($5.5\text{ }^\circ\text{C}$) and from **53** and **54** ($97\text{ }^\circ\text{C}$ and $104\text{ }^\circ\text{C}$ respectively). The unusual packing behaviour of **55** is attributed to this substantial difference in physical properties.²⁷ This surprising packing motif may also contribute to the low melting point observed in the sulfides, sulfoxides and sulfones in this study. Recently, a new high pressure polymorph β of **55** was determined which is ‘nearly fully isostructural’ with the original α form, but formed $\text{C}\equiv\text{C}-\text{H}\cdots\pi(\text{C}\equiv\text{C})$ in preference to $\text{C}\equiv\text{C}-\text{H}\cdots\pi(\text{arene})$, **Figure 2.14.**²⁹

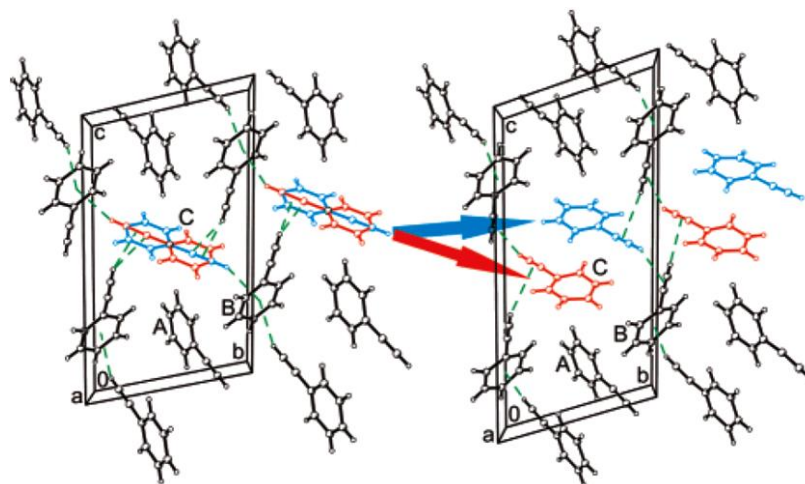


Figure 2.14: Crystal structure of 55α (left) and 55β (right). The two sites of disordered molecules C in 55α and the two corresponding displaced molecules in 55β are indicated in red and blue. The $\text{C}\equiv\text{C}-\text{H}\cdots\pi$ interactions are represented by green dashed lines. Reproduced from reference.²⁹

When the alkyne chain length was extended as in the case of the sulfone, **48**, the predicted interactions observed are similar to those described by Lehane in simpler systems.⁵ The terminal alkyne now acts as the major hydrogen bond donor forming weak hydrogen bond interactions to the strongest hydrogen bond acceptor in the molecule – the sulfone, **Figure 2.15**. This particular structure was obtained as a solvate. There is some uncertainty about the exact nature of the solvate, however the terminal alkyne hydrogen bond does appear to be present.

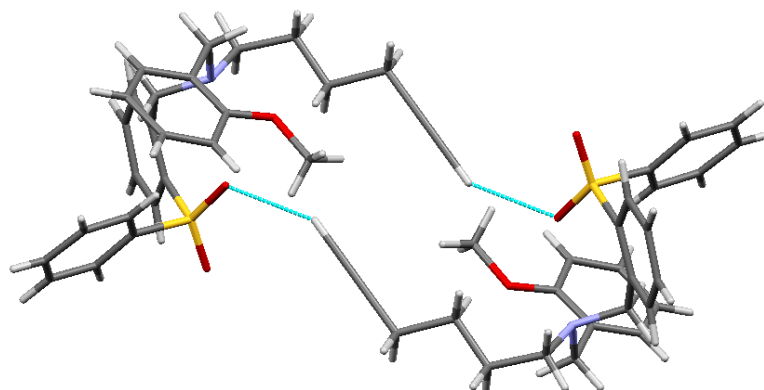


Figure 2.15: *The predicted interactions observed in 48 between the sulfone, and terminal alkyne. (only compound 48 shown for clarity)*

The weak hydrogen bond interactions observed so far have all occurred intermolecularly, as expected for the compounds synthesised with the sulfur functional groups in the *ortho* position. Next the crystal structures of compounds with the functional groups in different positions were studied in order to investigate the influence of substitution on the supramolecular architecture.

Interestingly, in **33** with the sulfoxide in the *para* position it was observed that the sulfoxide oxygen participates in bifurcated intermolecular hydrogen bonding to both the α NCH hydrogen and the terminal alkyne, **Figure 2.16**. In this particular case it is the α NCH hydrogen adjacent to the phenyl ring bearing the methoxy substituent that is involved in hydrogen bonding rather than the α NCH hydrogen linked to the sulfur substituent as observed in **26**.

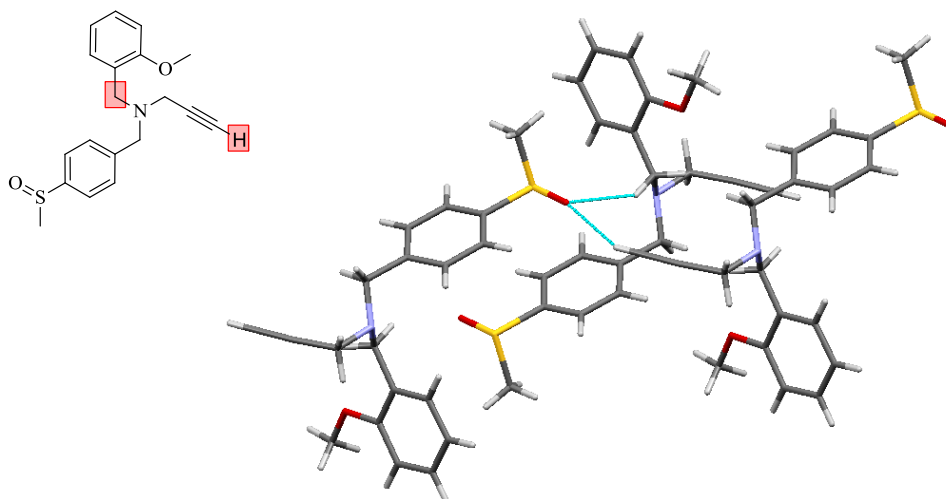


Figure 2.16: Interactions observed for the sulfoxide, **33**.

A crystal structure was also obtained for a similar compound varying the chain length of the terminal alkyne and the oxidation state at the sulfur. In **45**, the involvement of the α NCH hydrogens adjacent to the sulfur containing substituent in hydrogen bonding, which was observed in the crystal structures of the sulfide, **26**, once again presents itself as an interesting motif in this tertiary amine system, **Figure 2.17**. In this case, these α hydrogens are interacting with the oxygen of the sulfone. The terminal alkyne extends away from the sulfone as a result of its chain length and partakes in intermolecular hydrogen bonding to a methoxy group (2.88 Å). An interesting $R_2^2(8)$ dimer was also observed between neighbouring sulfones involving one of the α hydrogens of the methyl groups.

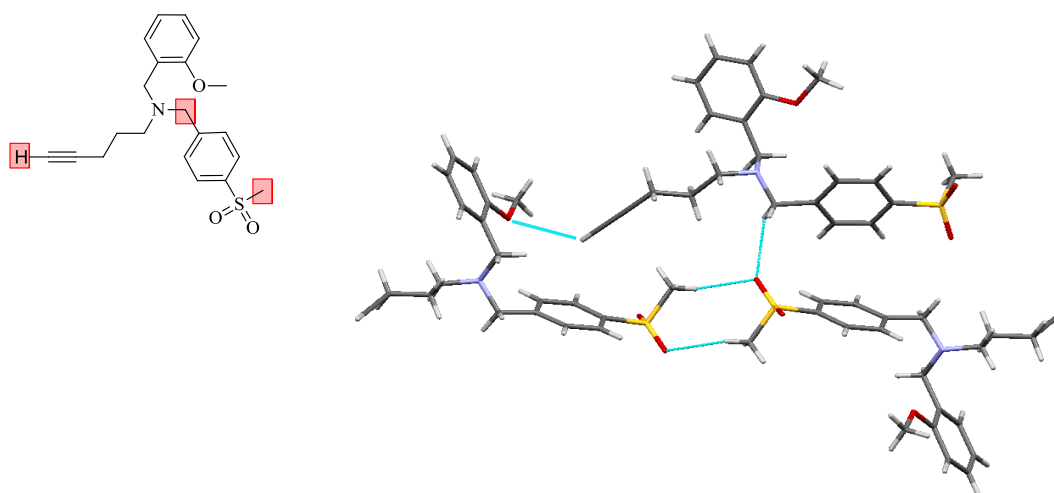


Figure 2.17: The hydrogen bonding network in the sulfone, **45**.

As these tertiary amine systems were difficult to crystallise, converting them to salts was also investigated. The sulfone, **51**, which was an oil at room temperature was dissolved in CH_2Cl_2 , and ethereal aqueous HCl [4:1(conc. HCl)] was added dropwise until the salt crashed out. Single crystal analysis was obtained for the HCl salt of **51**, **Figure 2.18**.

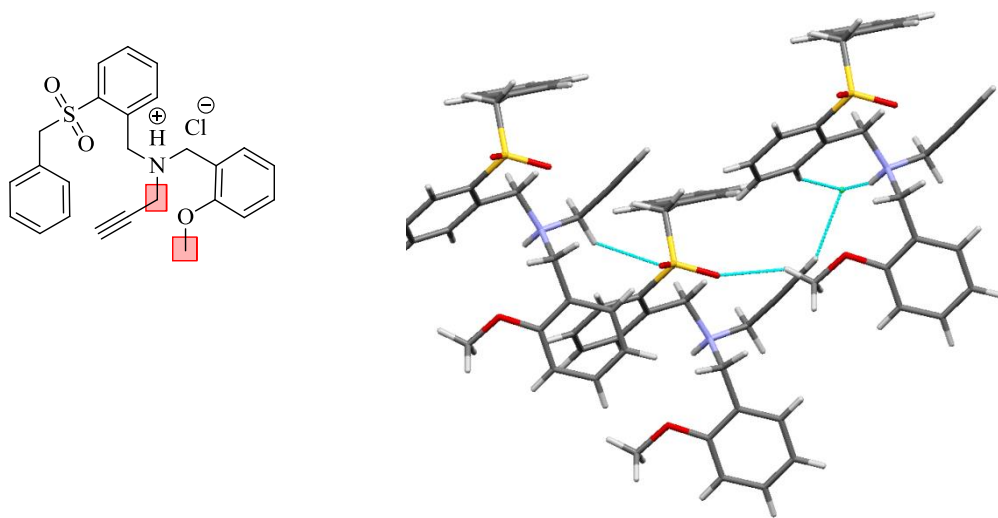


Figure 2.18: Crystal structure of the sulfone salt **51**.
(solvent omitted for clarity)

While salt formation of **51** enabled a crystal structure to be determined of the previously amorphous material, the electrostatic interactions may be disrupting the weak hydrogen bond interactions and therefore an accurate reflection of the hydrogen bonding network between the functional groups of interest is not possible. The terminal alkyne is now electrostatically attracted to the chloride, and so cannot partake in hydrogen bonding with the sulfone or methoxy functional groups. However, the $(\text{R})_2\text{NCH}\cdots\text{O}=\text{S}$ motif that was observed in the previously described sulfone and sulfoxide structures remains intact.

A CSD search for the $\text{C}\equiv\text{C}-\text{H}\cdots\text{Cl}^-$ interaction revealed only 27 structures in the CSD displaying this interaction. The structures ITUFAF³⁰ FADBUH³¹ and FOHLIY01³² are examples of quaternary ammonium salts similar in structure to **51** and displaying the $\text{C}\equiv\text{C}-\text{H}\cdots\text{Cl}^-$ interaction, **Figure 2.19**. A bond distance of 2.52 Å was noted for the $\text{C}\equiv\text{C}-\text{H}\cdots\text{Cl}^-$ interaction in **51**.^{*} The mean bond distance observed for this type of interaction tends to be 2.7 Å, **Figure 2.20**.

^{*} During the viva examination, the impact of coordination of water to the chloride on variation of hydrogen bond lengths was highlighted as discussed by Mitchell *et al.* (*J. Phys. Chem. A.*, **2001**, *105*, 9961-9971).

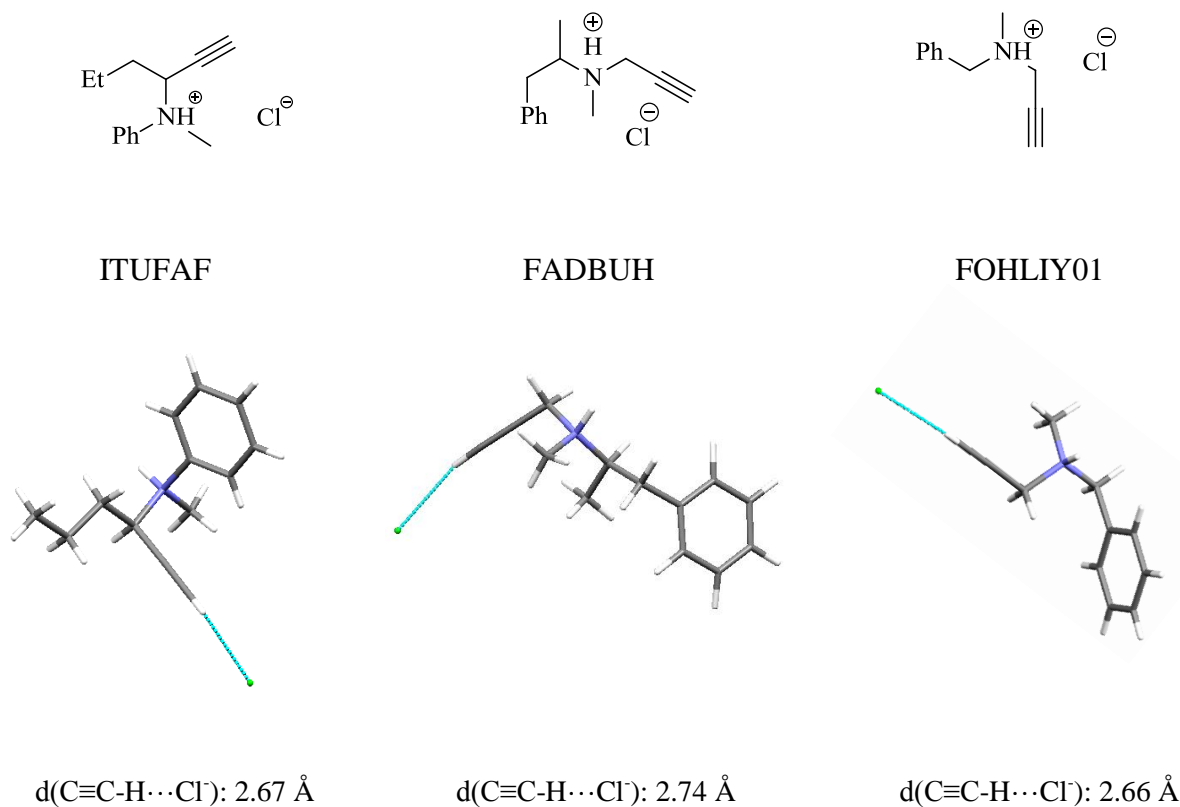


Figure 2.19: Crystal structures of ITUFAF³⁰, FADBUH³¹ and FOHLIY01³²

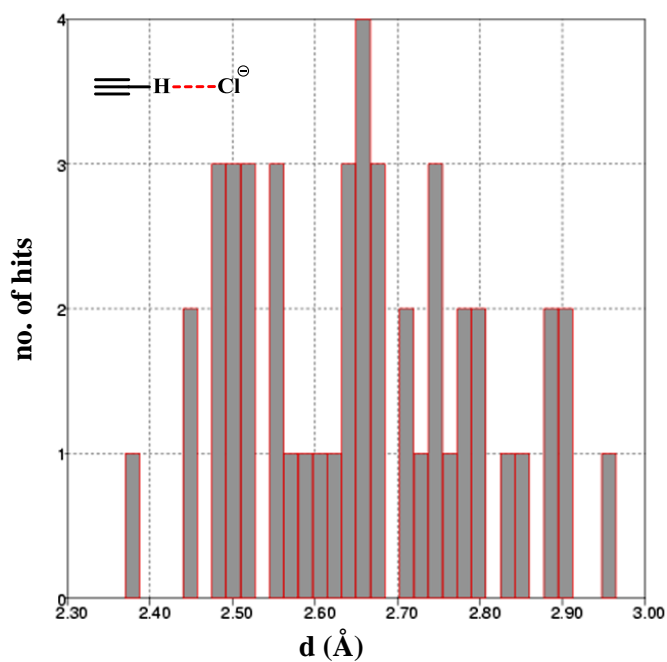


Figure 2.20: Histogram representing $\text{C}\equiv\text{C}-\text{H}\cdots\text{Cl}$ bond distances reported for 27 structures from the CSD. The mean bond distance was found to be 2.7 Å.

2.3.7. Conclusions

A series of novel tertiary amine systems at sulfide, sulfoxide and sulfone oxidation levels were successfully designed, synthesised and characterised. A synthetic route was effectively established and developed to access a wide range of these tripodal systems. The main objective of constructing these systems was to further investigate the robust nature of the $C\equiv C-H\cdots O=S$ and $S=O\cdots H-C(\alpha)$ interactions previously explored in our group and to utilise these interactions to create a molecular switch.

In retrospect, these particular systems are probably too flexible and have excessive conformational freedom to act as a molecular switch. The highly viscous nature of many of these compounds deemed them unsuitable targets for studying their solid state interactions. Despite this, some very interesting crystal structures were attained which displayed significant alterations in the supramolecular array upon oxidation from sulfide to sulfoxide and sulfone.

While no definite conclusions can be drawn from the structures obtained, many positive results have been observed. The $C\equiv C-H\cdots O=S$ interaction observed by Lehane⁵ was also a structure determining feature in some of the more complicated tertiary amines at the sulfoxide and sulfone oxidation levels *e.g.* **33** and **48**, but the steric restraints of the systems studied restricted the ability of these interactions to occur readily *e.g.* **45**. The unusual packing behaviour involving $CH\cdots\pi$ in **26** may explain the viscous nature of these compounds and bearing this in mind, structural adaptations may need to be investigated for future systems. The emergence of the α NCH hydrogens *e.g.* $(R)_2NCH\cdots O=S$, as dominant hydrogen bond donors and their significant directional role in the packing arrangement of these amine systems may lead to their development as potential supramolecular synthons. While direct literature reference to the pKa of $(R)_2NCH_2(\text{aryl})$ could not be identified, it appears that the acidity of these NCH hydrogens is of the order where they can compete with terminal alkynes as hydrogen bond donors. Investigation into these packing motifs can be expanded in future systems and may provide further insight into crystal packing in the solid state of organosulfur compounds.

2.3.8. Biological Testing

The recent exploration of pargyline, **56**, to act as a potential pro-apoptotic candidate in the treatment of cancer³³ prompted the investigation of the bioactivity of the structurally similar tertiary amine compounds (**23-52**), **Figure 2.21**, and also featured in **Table 2.7**. Pargyline, **56**, a monoamine oxidase inhibitor, has also been identified as an inhibitor of lysine specific demethylase 1 (LSD1). LSD1 is a histone modifying enzyme and is essential for mammalian development. It is implicated in many biological processes, such as cell-type differentiation and gene activation and repression. It has also been suggested that LSD1 over-expression might promote tumorigenesis.³⁴

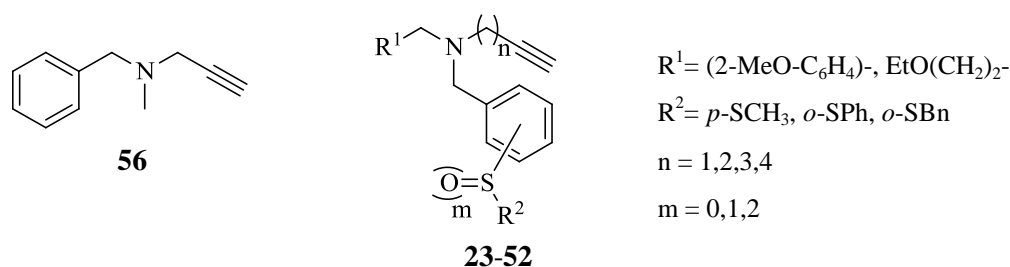


Figure 2.21: Structural similarity of **23-52** to pargyline, **56**.

Genetic alterations are a characteristic feature of human cancer. Histone modifications, such as acetylation, phosphorylation and methylation amongst others, have a significant effect on chromatin structure and are therefore linked to epigenetic changes. Thus, enzymes which play a role in these histone post-translational modifications have attracted interest as potential therapeutic targets for certain cancers. For example, histone deacetylase inhibitory agents display potential use as anti-tumour agents.³⁵ Recently, histone demethylases at specific lysine residues, which play a critical role in the regulation of gene expression, have been the subject of intense interest.³⁶ LSD1 is the first histone demethylase to have been discovered and specifically it removes the methyl groups from histone H3 lysine 4 (H3K4) or lysine 9 (H3K9) and represses transcription. Since LSD1 is a member of the flavin adenine dinucleotide (FAD)-dependent amine oxidases, certain inhibitors of monoamine oxidases, particularly 2-phenylcyclopropyl-amine (2-PCPA) and pargyline, **56**, are also capable of inhibiting LSD1.^{33,37} Several analogues of 2-PCPA tested against LSD1 have displayed induced differentiation of leukaemia cells and also slowed the growth of prostate and breast cancer cell lines.³⁸ Pargyline, **56**, has been reported to exhibit antiproliferative

effects on prostate cancer cells by blocking the demethylation of H3K9 by LSD1 and as a result androgen-receptor-dependent transcription.³³

The novel tertiary amines, **23-52**, synthesised in this work, possess the core structure of pargyline, **56**, and also contain ether and sulfur moieties which may help to increase their efficacy on cancer cell proliferation. For example, the terminal alkyne acts as a weak hydrogen bond donor whereas the ether, sulfoxide and sulfone act as good hydrogen bond acceptors and may lead to an increase in binding affinity at the desired site.

2.3.8.1. *NCI-60 cancer cell line screen*³⁹

The United States National Cancer Institute's Developmental Therapeutics Program's (NCI-DTP) 60 human tumour cell line anticancer drug screen (NCI-60) was developed in the 1980's as an *in vitro* strategic high-throughput screening tool for anticancer drug activity. Consisting of 60 cell lines derived from diverse human cancer types (leukaemia, lung, colon, central nervous system, melanoma, ovarian, renal, prostate and breast), the NCI-60 is the most comprehensive human cell panel in existence. The broad scope of the present day cell-based NCI-60 evolved from a government-sponsored drug discovery initiative with the objective of identifying compounds with growth-inhibitory or toxic effects on lung cancer cell lines ('disease orientated concept'). This screening model has since become a data-rich source which provides information on modes of tumorigenesis and cancer progression and additional biological details.⁴⁰⁻⁴³ Patterns of relative drug sensitivity and resistance of all the cell lines were generated with standard anticancer drugs using three response parameters: GI₅₀ (concentration at which growth of 50% of cells present is fully arrested), TGI (concentration for total inhibition or 0% cell growth) and LC₅₀ (lethal concentration causing cell death in 50% of cells originally present), and were rapidly found to reflect mechanisms of drug action. The activity profiles for the screening candidates can then be compared with the screening database by applying the automated 'COMPARE' algorithm and this can help to identify the mechanism of action. For example, the natural product Halichondrin B was submitted to the NCI-60 to determine its mechanism of action. The COMPARE algorithm successfully deduced that its activity was similar to compounds that were inhibitors of microtubule polymerisation. Experimental data confirmed that Halichondrin B indeed interacted with tubulin. The compound was further tested *in vivo*

where it also displayed anti-tumour activity. Following on from this successful result, the compound was accepted for further preclinical development.^{40,44}

The initial NCI-60 screening programme involves two stages. Firstly the compound of interest is tested against the 60 cell lines at a single dose of 10 μ M. If significant growth inhibition is observed at this stage then the compound is evaluated against the 60 cell lines at five concentration levels. Compounds which exhibit an interesting pattern of inhibition after the initial NCI-60 screening are then assessed by the Biological Evaluation Committee. If they generate useful activity profiles *via* potent and selective cytotoxicity across tumour cell lines, then they may progress to *in vivo* hollow-fibre implantation testing in mice and further evaluation in other xenograft assays. Successful candidates may then be authorised by the Drug Development Group to enter the NCI clinical development. Additional data returned to the compound supplier is also often important for licensing purposes or perhaps lead-hopping and rational 2nd generation drug design. This screening process has led to many significant discoveries, with the development of bortezomib, used in the treatment of myeloma, the most noteworthy of these. It took only 8 years from the initial NCI-60 hit identification to full FDA approval, which makes bortezomib probably the most rapidly developed anticancer drug in recent times.^{40,45}

2.3.8.2. *Tertiary amines submitted for biological investigation*

Fulfilling non-duplication criteria prescribed for NCI-60 compound selection, a preliminary panel of 4 novel tertiary amines (**26**, **36**, **45** and **47**) synthesised during this work were chosen as representative chemotypes for biological screening in the Developmental Therapeutics Program, **Figure 2.22**. It would be interesting to observe if varying the carbon chain length on the alkyne substituent and altering the position and oxidation state of the sulfur substituent would impact upon the biological activity of these compounds. These tertiary amines displaying structural similarity to pargyline, **56**, were successfully investigated for one-dose tumour cell line activity, and the pattern of quantifiable growth inhibition of these agents on the NCI-60 human tumour cell line panel is outlined.

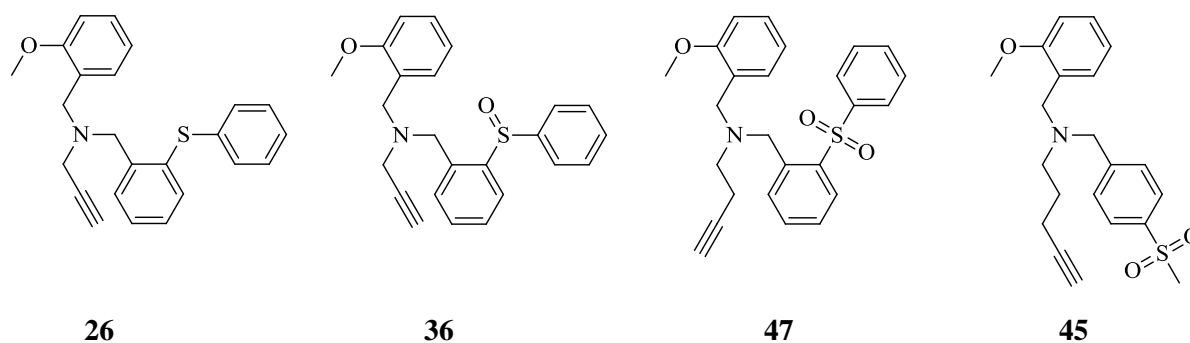


Figure 2.22: Tertiary amines submitted for NCI-60 testing.

2.3.8.3. NCI-60 cytotoxicity results

The reported methodology employed for evaluation of growth inhibition for the selected compounds (**26**, **36**, **45** and **47**) within the NCI-60 cell line panel involves initial formation of a 4 mM stock solution with DMSO, prior to dilution into RPMI 1640 medium containing 5% fetal bovine serum and 2 mM L-glutamine, and exposure to the human tumour cell lines that were previously cultured for 24 hours.^{40,46} After a 48 hour incubation period, the media was removed and cell fixation and staining with sulforhodamine B (SRB) was performed. The unbound dye was removed with several washes of 1% acetic acid and then the plates were air dried. The dye was dissolved in Tris buffer, and the absorbance was measured at 515 nm and calibrated against DMSO control.^{40,47} The one-dose data of each compound was reported as a ‘mean graph’ comprising a series of horizontal bar graphs representing units of nominal growth percent, deviating from the arithmetic mean growth inhibition for the entire 60 cell line array, *i.e.* centre line or ‘0’. In each case, graphs which extend to the right (-) denote selective cytotoxicity or positive growth inhibition, while those which extend to the left (+) of the centre line indicate a chemoprotective or non-cytotoxic effect on individual cell lines.^{40,48}

As demonstrated in the supplementary data (see Appendices), the novel tested compounds **26**, **36**, **45** and **47** displayed some interesting cytotoxicity profiles within 60 human tumours derived from 9 distinct tissue sites. Similar patterns of tumour chemosensitivity were observed, although critical differences in cytotoxicity profile could also be discerned based on small structural alterations, **Table 2.8**.

Table 2.8: Summary of notable growth inhibition after exposure of **26**, **36**, **45** and **47** to certain cell lines.

Compound no.	NCI-60 cell line	Tumour Site	% Growth after 48h ^a	Mean cell line growth
26	<i>HOP-92</i>	lung	70.40	95.88
	<i>CAKI-1</i>	kidney	75.34	
36	<i>HOP-92</i>	lung	47.74	79.71
	<i>HL-60(TB)</i>	blood	68.59	
	<i>K-562</i>	blood	52.54	
	<i>MOLT-4</i>	blood	70.65	
	<i>RPMI-8226</i>	blood	53.01	
	<i>HCT-116</i>	colon	66.57	
	<i>SK-MEL-5</i>	skin	62.69	
	<i>UACC-62</i>	skin	57.24	
	<i>CAKI-1</i>	kidney	56.29	
	<i>PC-3</i>	prostate	53.21	
	<i>T-47D</i>	breast	58.33	
	<i>MDA-MB-468</i>	breast	53.61	
47	<i>K-562</i>	blood	49.61	82.75
	<i>MOLT-4</i>	blood	68.40	
	<i>RPMI-8226</i>	blood	66.36	
	<i>HOP-92</i>	lung	69.27	
	<i>HCT-116</i>	colon	60.94	
	<i>UACC-62</i>	skin	63.46	
	<i>CAKI-1</i>	kidney	62.40	
	<i>PC-3</i>	prostate	50.33	
	<i>MDA-MB-468</i>	breast	65.44	
45	<i>HCT-116</i>	colon	74.37	95.53

a Cultured cells were tested on RPMI 1640 medium at an initial compound concentration of 10 μ M.

The majority of the human cell lines were deemed relatively refractory to growth arrest by the sulfide, **26**, and the sulfone, **45**. Slight selective cytotoxicity was expressed for **26** within HOP-92 (lung adenocarcinoma) and CAKI-1 (renal cell carcinoma), and for **45** within HCT-116 (colorectal carcinoma), compared with related tissue cell lines. In addition, a chemoprotective effect (>100%) was observed in the CNS tumours with all the four

compounds submitted for testing. It was particularly interesting to observe the increase in growth inhibition of specific cell lines following incubation with the novel sulfoxide, **36**, and the sulfone, **47**. Comparing the sulfide, **26**, to its corresponding sulfoxide, **36**, a significant increase in growth inhibition of the HOP-92 cells is observed. The compounds **36** and **47** also display significant selectivity for leukemia, and also for the PC-3 (prostate) and MDA-MB-468 (breast) cell lines. This is particularly noteworthy as analogues of 2-PCPA and pargyline, **56**, also display growth inhibition against these cancers. Although **36** and **47** are structurally similar to **26**, it appears that the additional hydrogen bond acceptor present may result in an increased binding affinity of the compounds to the desired site. Also the increased polarity, particularly in the sulfoxide, **36**, will result in increased solubility in the DMSO, prior to addition to the human tumour cell lines. Comparing the sulfones, **45** and **47**, it also appears that the position and substituent on the sulfur moiety and perhaps the carbon chain length of the alkyne moiety may have an additional impact on the biological activity of these tertiary amines. These structural implications should be considered if future systems are submitted for NCI-60 testing. While **47** displays some interesting selectivity and growth inhibition for the K-562 (leukemic) and PC-3 (prostate) cancer cell lines, the sulfone, **45**, only displays a mean growth inhibition of 5 % with slight selectivity for HCT-116 (colon carcinoma). At this level of activity, the compounds were not progressed to the further five-dose testing.

2.4. Aromatic based systems

2.4.1. 1,2,3-substituted aromatic scaffold

As discussed previously in **Section 2.2, Figure 2.4(b)**, the 1,2,3-substituted aromatic ring system, may be a more rigid scaffold than the tertiary amine systems for the development of a molecular switch. In this particular scaffold, the functional groups of interest can be tethered to the fixed, planar aromatic ring without hindering the inter/intramolecular interactions between the desired groups. The commercially available triol, 2,6-bis(hydroxymethyl)-4-methylphenol, **57**, was very well suited for the purpose of an aromatic scaffold as it is inexpensive, readily available and a series of alkylation reactions can be performed on the available alcohol groups to attach chains incorporating the desired functional groups, **Figure 2.23**.

The functional groups selected for investigation, in line with the earlier work involving tertiary amines, were ethers, sulfur functionalities and terminal alkynes. The sulfide can then be oxidised, and competition is envisaged to occur between the ether and sulfoxide/sulfone to act as the hydrogen bond acceptor when the terminal alkyne is the donor, therefore potentially generating a molecular switch.

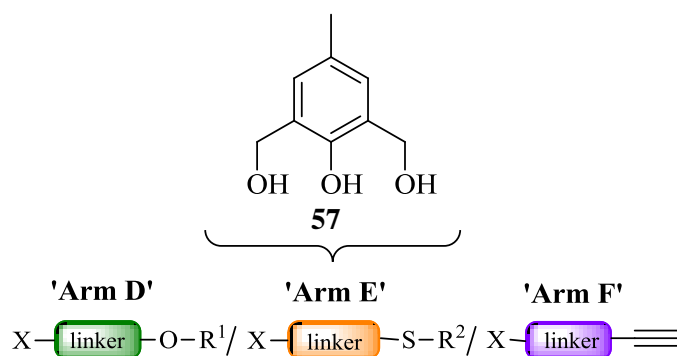


Figure 2.23: 2,6-Bis(hydroxymethyl)-4-methylphenol, **57**, as aromatic scaffold to attach 'Arms D, E and F' for hydrogen bonding investigations.

2.4.2. Design and synthesis of linkers for rigid scaffold

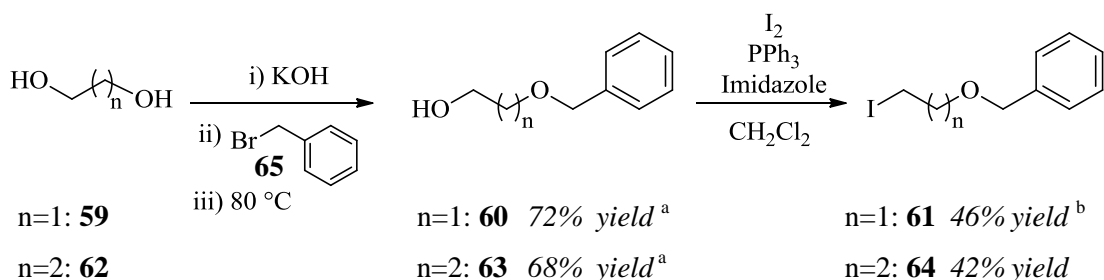
With a suitable scaffold in place, the next stage involved the design and synthesis of ‘arms’ incorporating versatile linkers and hydrogen donors/acceptors of interest for attachment to the triol, **57**. Alkyl ether groups, similar to those employed in the tertiary amine systems, were ideally suited to act as hydrogen bond acceptors. The carbon chain in alkyl ethers can also be easily modified to adopt a suitable length for hydrogen bond interactions.



Table 2.9: ‘Arm D’ systems.

Compound No.	X	Linker	R ¹
58	Br	(CH ₂) ₂	CH ₃
61	I	(CH ₂) ₂	Bn
64	I	(CH ₂) ₃	Bn

Various alkyl ether groups containing good leaving groups (*e.g.* Br, I) and differing in chain length and steric bulk were chosen for the alkylation reactions, **Table 2.9**. 2-Bromoethyl methyl ether, **58**, which is commercially available contains a small methoxy functional group and short carbon chain. In contrast, the benzyl ethers, **61** and **64**, with different steric and electronic properties, were synthesised from their corresponding alcohols, **60** and **63**, according to **Scheme 2.8**, illustrated below. Monobenylation of the diols, **59** and **62**, occurred readily using benzyl bromide, **65**, as did the iodination reaction using the Borbas procedure¹³ described earlier in **Scheme 2.3**. Both iodides, **61** and **64**, were purified by column chromatography. However, unidentified signals were observed in the ¹³C NMR of **61** after purification (see Chapter 5 for details).



a unpurified yield

b impurities present

Scheme 2.8: Synthesis of compounds **61** and **64**.

Straight chain thioethers, similar in structure to the alkyl ethers were also designed and synthesised successfully. Again, both medium and short alkyl chain systems were explored to accommodate intramolecular hydrogen bonds. Iodo-substituted compounds were targeted due to their better leaving group capabilities for the future alkylation reactions, **Table 2.10**.

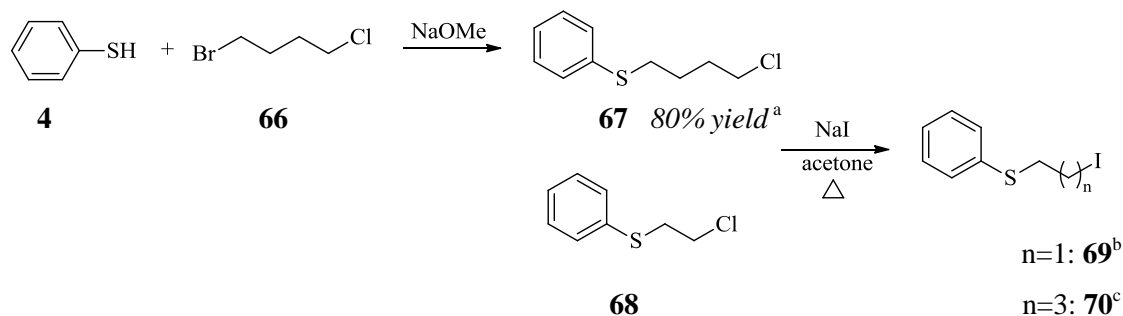


Table 2.10: 'Arm E' systems.

Compound No.	X	Linker	R ²
69	I	(CH ₂) ₂	Ph
70	I	(CH ₂) ₄	Ph

The thioethers, **69** and **70**, were synthesised from their respective chloro-substituted compounds, **67** and **68**, utilising the Finkelstein reaction which involves S_N2 substitution converting the alkyl chloride to the alkyl iodide, **Scheme 2.9**.^{49,50} These reactions were difficult to monitor for completion by TLC. However, the indicative strongly shielded C-I δ_C signals at 2.7 and 5.9 ppm for **69** and **70** implied that successful halogen exchange had occurred. Purification of **69** and **70** by column chromatography was challenging due to the similar R_f values between the starting material and product. Therefore, it was not surprising to observe the presence of some unreacted **67** (~53%) and **68** (~33%) in the ¹H and ¹³C NMR spectra of **69** and **70** respectively (see Chapter 5 for details). The mixed chlorides and iodides, **67/70** and **68/69**, were brought forward in the subsequent alkylations without further purification. The chloro-substituted thioether, **68**, was commercially available but **67** was

synthesised from thiophenol **4**, and 1-bromo-4-chlorobutane **66**, in sodium methoxide solution.



a unpurified yield

b isolated as a mixture with **68** (~33%)

c isolated as a mixture with **67** (~53%)

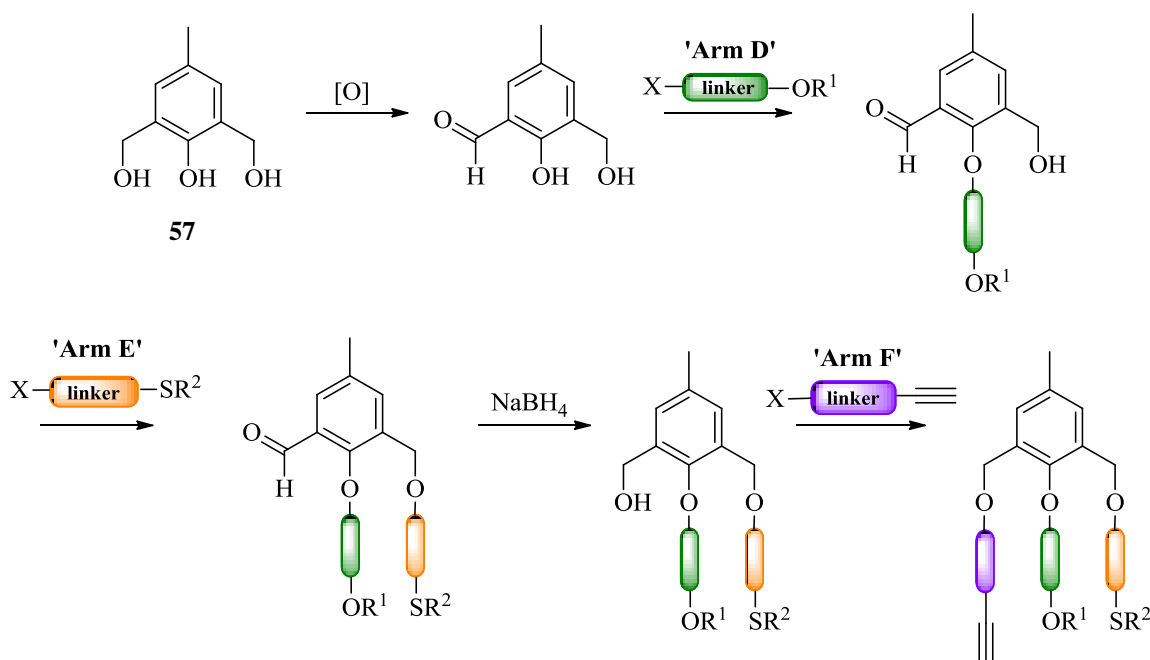
Scheme 2.9: Synthetic scheme to access the thioethers **69** and **70**.

For ‘Arm F’, containing the terminal alkyne moiety, **Figure 2.23**, it was decided to firstly attach a simple short alkyl system *e.g.* propargyl bromide, **10**, and then extend the chain length if necessary to enable intramolecular hydrogen bonding.

Attachment of the described ‘Arms D, E and F’ to the triol, **57**, proved to be quite complicated and challenging, with the result that various synthetic strategies were tested to achieve the target tri-alkylated system.

2.4.3. Synthetic Strategy 1

The synthetic strategy outlined in **Scheme 2.10** was designed to effectively access a wide range of target compounds with the sulfur, ether and terminal alkyne functional groups attached. The synthetic challenge was to achieve sequential selective reactions at each of the three alcohol moieties in **57**.



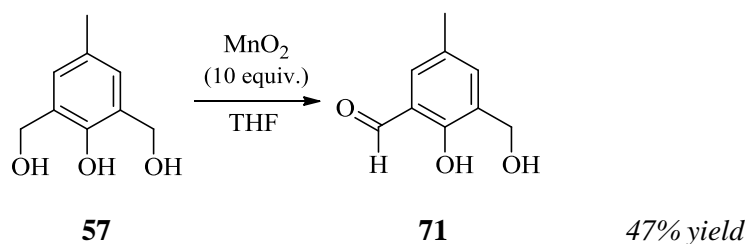
Scheme 2.10: ‘Synthetic Strategy I’: tri-substituted aromatic system with ‘Arms D, E and F’ attached.

The strategy firstly involved selective oxidation of 2,6-bis(hydroxymethyl)-4-methylphenol, **57**, to its respective aldehyde, in order to protect one of the primary alcohol sites. Then in the next step, the phenol would be the preferred site for regioselective alkylation with ‘Arm D’ due to the significant difference in acidity between the phenol (pKa ~10) and primary alcohol (pKa ~16). The remaining available primary alcohol could then be alkylated with ‘Arm E’ to provide a compound with two of the three ‘Arms’ attached. Reduction of the aldehyde to a primary alcohol should then allow for a third alkylation with the final ‘Arm F’. The effect of varying the oxidation level at sulfur on the inter/intramolecular hydrogen bond interactions between the functional groups of interest could then be studied.

As outlined in **Scheme 2.10**, the sequence of the introduction of the substituents was initially the ether, sulfide and then the alkyne. However, the order and position of attachment of the various groups can potentially be altered in the above strategy.

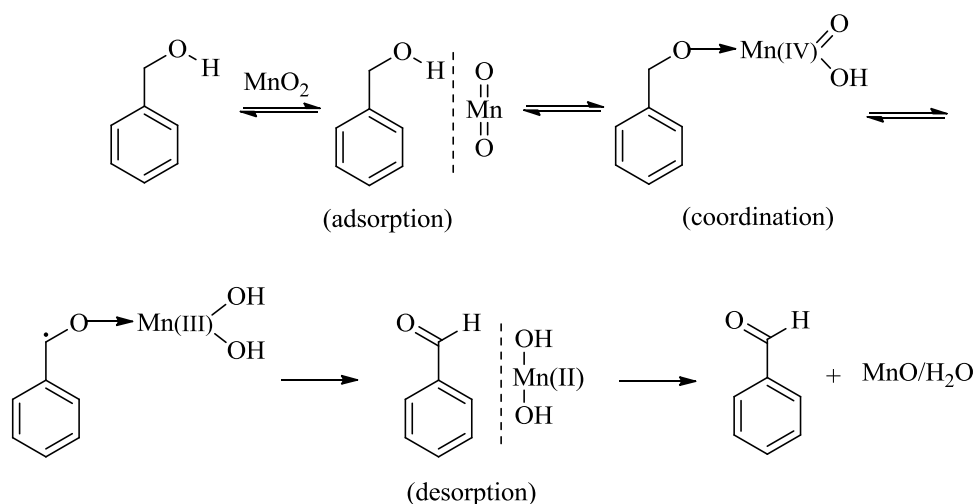
2.4.3.1. Selective oxidation of primary alcohol

The initial step in achieving the final target molecule was to protect one of the primary alcohols in 2,6-bis(hydroxymethyl)-4-methylphenol, **57**, by selective oxidation, **Scheme 2.11**. The influences of oxidant activity, reaction solvent and temperature on the selectivity were investigated and favourable conditions were developed to yield the desired aldehyde, **71**.



Scheme 2.11: Selective oxidation of primary alcohol **57** to aldehyde **71**.

Manganese dioxide (MnO_2) was chosen as oxidant as it is widely used for the selective transformation of allylic and benzylic alcohols into aldehydes and ketones without over-oxidation to the carboxylic acid.⁵¹ The simple work-up involving just a filtration of the suspended solid and isolation of the filtrate was also quite attractive. The selectivity of active MnO_2 can be attributed to the formation of a π -complex between the olefin or aromatic ring in the alcohol and some Lewis acid site on the surface of the manganese dioxide particles.⁵² There has been much speculation over the precise mechanism that MnO_2 undergoes when oxidising alcohols. It is believed that oxidation occurs when the alcohol complexes to the surface of MnO_2 and then the carbonyl compound diffuses away from the surface. Goldman proposed a free radical mechanism for benzyl alcohol, as illustrated in **Scheme 2.12**.^{53,54} This involves adsorption of the alcohol on MnO_2 which allows formation of a coordination complex. A radical is then generated by electron transfer in the coordination complex and Mn(IV) is reduced to Mn(III) . A second electron transfer generates the carbonyl compound adsorbed onto Mn(OH)_2 . Oxidation is completed by desorption of the aldehyde with loss of water.⁵⁵ An alternative mechanism, suggested by Hall and Story, which includes an intermediate manganese ester is also accepted as a viable mechanism.⁵⁶



Scheme 2.12: Goldman's proposed free radical mechanism.

It is widely accepted that many factors influence the rate of this reaction including activity of the oxidant, impurities present, solvent, temperature, structure of the substrate and the ratios of reactants.⁵⁷ These factors had to be considered and tested when developing the optimum conditions for successful oxidation of **57**. Initially active MnO_2 was prepared according to literature procedure,⁵⁷ but due to the long preparation time and unsatisfactory yields obtained, attention turned to the commercially available electronic grade MnO_2 which has a greater surface area and can potentially lead to increased activity. Typically 5-20 equivalents of active MnO_2 is recommended for the selective oxidation of allylic or benzylic alcohols.⁵² Previous reports in the literature for the synthesis of **71** and similar compounds have achieved successful oxidation using 10 equivalents of MnO_2 .^{58,59}

The oxidations of allylic and benzylic alcohols are most efficient in apolar solvents that do not compete with the alcohol for the surface of the MnO_2 particles. Thus, primary and secondary alcohols are unsuitable solvents as they cause a deactivating effect of the MnO_2 .⁵¹ Alkanes, chlorinated hydrocarbons, ethers, acetone and acetonitrile are the most commonly used solvents for these transformations.⁵⁵ In this particular oxidation of **57** to **71**, chloroform, acetone and THF were the solvents investigated. The starting material **57** was completely soluble in THF, unlike in chloroform and acetone where a suspension was observed, and therefore THF was the solvent of choice for this reaction.

Purification of **71** by column chromatography initially proved quite challenging with a significant loss in yield after purification. The desired product was perhaps adhering to or even degrading on the silica gel. Addition of 1% triethylamine to the eluent helped to

deactivate the silica and/or increase the polarity of the eluent, therefore separation of the target compound became much more manageable. A purified yield of 47% was obtained with literature yields tending to vary from 38% to 58%.^{58,60,61}

Structural analysis of **71** shows that it crystallises in the $P2_1/n$ space group with two molecules in the asymmetric unit. Significant intermolecular CH \cdots OH (2.69 Å) and S(6) intramolecular OH \cdots O=C (1.89 Å) hydrogen bond interactions are evident within **71**, **Figure 2.24**.

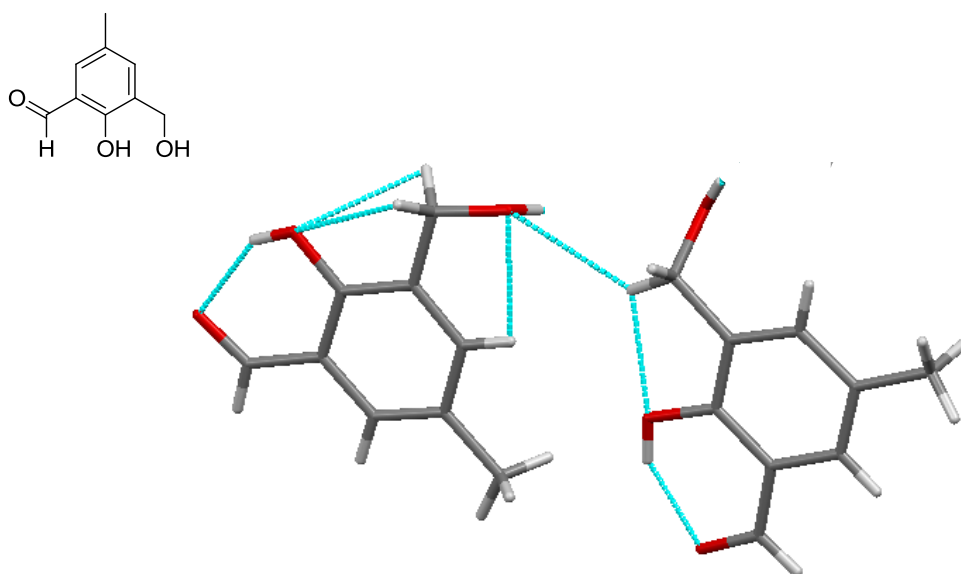


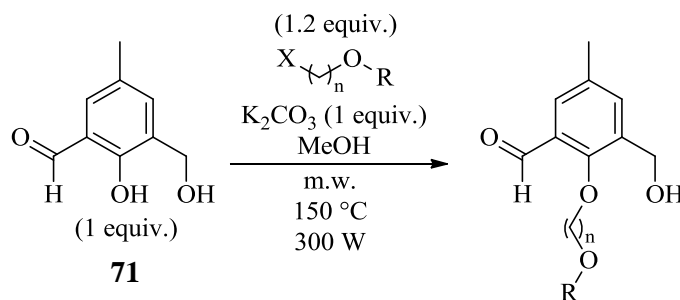
Figure 2.24: Asymmetric unit of **71**.

2.4.3.2. Attachment of 'Arm D'

Once the formation of the aldehyde, **71**, was achieved in satisfactory yields, the next stage of the synthetic strategy involved alkylation of the phenol site with 'Arm D', **Scheme 2.10**. The Williamson synthesis is employed for the preparation of ethers from an alkyl halide and an alkoxide or phenoxide salt. A mild base such as K_2CO_3 is suitable for this reaction since phenols are more acidic than aliphatic alcohols. However, under thermal conditions use of K_2CO_3 for these alkylations has been reported as sluggish with reaction times up to 72 h.⁶² This was indeed the case in this work when attempting to alkylate the phenol.

Research into microwave-assisted reactions proved to be much more worthwhile with shorter reaction times and easier isolation of the product being the main advantages. Literature reports involving alkylation of phenols by microwave irradiation usually require a large excess of NaOH or KOH which can lead to undesirable side reactions, high boiling point solvents which are difficult to remove, or the addition of organic phase transfer catalysts which can cause contamination of the product.⁶²⁻⁶⁴ A recent literature procedure by Sarju *et al.* involving microwave-assisted alkylation of phenols proved very successful in forming the desired product.⁶² K_2CO_3 as base in stoichiometric amounts, and methanol employed as solvent provided very mild conditions which is ideal for this reaction. Moderate but synthetically practical yields were achieved using this method, **Scheme 2.13**.

The three desired ethers, **58**, **61** and **64**, were successfully attached to the phenol, **71**, to afford the novel alkylated products, **72**, **73** and **74** respectively. It was noted that the iodoethers underwent alkylation faster than the bromo-ether substituent which can be attributed to the better leaving group capabilities of the iodide, **Table 2.11**.



Scheme 2.13: Alkylation of phenol **71**.

Table 2.11: Yields obtained for **72**, **73** and **74** after successful alkylations.

Arm D	X	n	R	Time (mins)	Product	Yield (%) ^a
58	Br	2	CH ₃	80	72	47 ^b
61^d	I	2	Bn	60	73	47 ^c
64	I	3	Bn	40	74	53 ^c

a Novel compounds characterised by ¹H and ¹³C NMR, IR, *m/z* and HRMS.

b Purified yield.

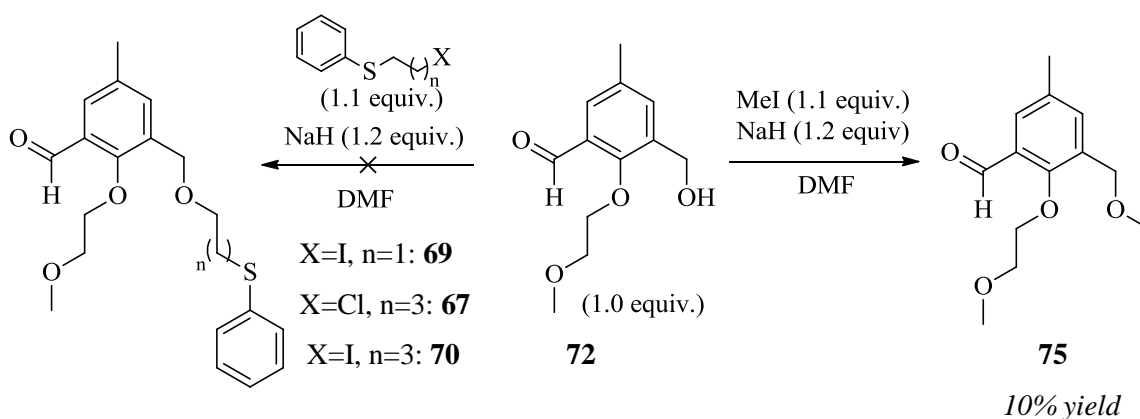
c ~80% pure as determined by ¹H NMR.

d Impurities present (**Scheme 2.8**)

Most importantly the selective alkylation of the phenolic site in **71** with the desired ‘Arm D’ systems, in the presence of a primary alcohol was achieved with modest efficiency by microwave irradiation. The methyl ether system, **72**, was successfully purified by column chromatography. The benzyl ethers, **73** and **74**, could only be achieved in ~80% purity, with unidentifiable impurities present after column chromatography, but these compounds were deemed sufficiently pure to continue the next stage of the synthetic strategy. While the iodide, **64**, was clean prior to use, impurities were observed in **61** which may have influenced the outcome.

2.4.3.3. Attachment of 'Arm E'

The next stage of the synthetic strategy outlined in **Scheme 2.10** involved the attachment of 'Arm E' containing the sulfur functionality. This proved to be quite a difficult task to accomplish. Initial attempts to attach **69** and **70** (which contained mixtures of the iodide/chloride) to the primary alcohol, **72**, were unsuccessful, with no evidence of attachment. To explore if alkylation at this position is possible, methylation with methyl iodide was attempted using sodium hydride in DMF, **Scheme 2.14**. The crude reaction mixture consisted of unreacted starting material (~21%), unknown impurity (~25%), and the desired product (~54%) which was subsequently purified to give **75** as a clear oil. While the methylated ether, **75**, was isolated in very low yield (10%), this demonstrated that, in principle at least, the primary alcohol can undergo alkylation. Extension to the primary alkyl halides bearing the sulfide chain was not achieved during this work.

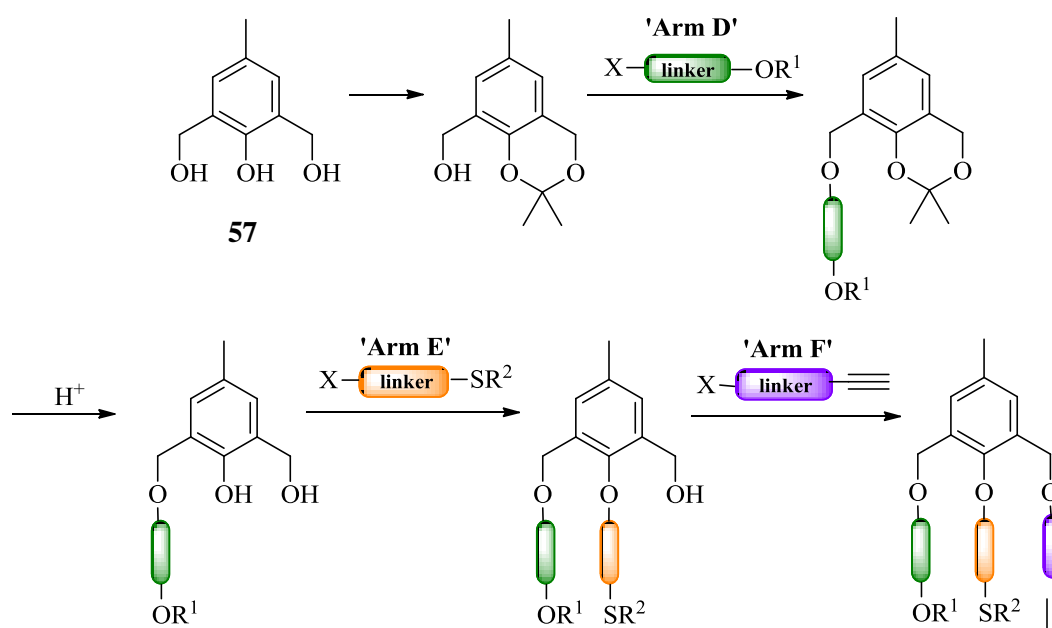


Scheme 2.14: Methylation of primary alcohol to form **75**.

As this particular synthetic pathway was proving quite problematic especially in attaining sufficient yields, for example in the initial selective oxidation to form the aldehyde, **71**, and also in the inability to alkylate with the desired functional groups, attention turned to developing a different synthetic approach to access the target molecule.

2.4.4. Synthetic Strategy II

The major limiting step that was identified in ‘Synthetic Strategy I’ was the selective oxidation of the triol, **57**, to the aldehyde, **71**. This particular step, which was the first step in the sequence, resulted in a reduced yield even before ‘Arms D, E and F’ had been attached. ‘Synthetic Strategy II’ focused on an alternative route to protect one of the primary alcohols with the aim of improving the yield of this step so that there would be sufficient material available for alkylation with the previously designed arms.

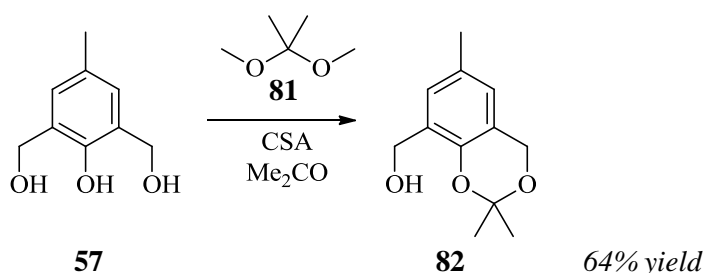


Scheme 2.15: ‘Synthetic Strategy II’

Scheme 2.15 highlights the alternative and improved strategy to access the target compound. 2,6-Bis(hydroxymethyl)-4-methylphenol, **57**, was once again chosen as starting material. Introduction of an acetal protecting group should allow for alkylation of the only available primary alcohol site with ‘Arm D’. The acetal group can then be easily cleaved by simple acid hydrolysis. Subsequently the sulfide and alkyne functionalities could then be attached by S_N2 alkylation reactions in either sequence.

2.4.4.1. Acetal Formation

Selective protection of 2,6-bis(hydroxymethyl)-4-methylphenol, **57**, and similar triols to form their respective acetonides have previously been described in the literature.⁶⁵⁻⁶⁷ Using these methods the phenolic hydroxyl group and one of the hydroxymethyl groups were effectively protected using 2,2-dimethoxypropane, **81**, in the presence of camphorsulfonic acid (CSA) and acetone to give **82** in 64% yield without the need for further purification, **Scheme 2.16**.



Scheme 2.16: Formation of the acetonide, **82**.

The formation of the acetal to act as a protecting group was a much more satisfactory and reliable strategy than the previously described selective oxidation, **Scheme 2.11**. This very accessible route to the acetonide, **82**, enabled access to multi-gram quantities without difficulty, providing the key starting compound for attachment of the ‘Arms’. Single crystals of the acetonide, **82**, were grown from CH₂Cl₂, and a novel crystal structure was obtained, **Figure 2.25**. The molecule crystallises in a *P2*₁/*c* space group with intermolecular OH...O hydrogen bond interactions observed in the crystal packing of the molecule.⁶⁸

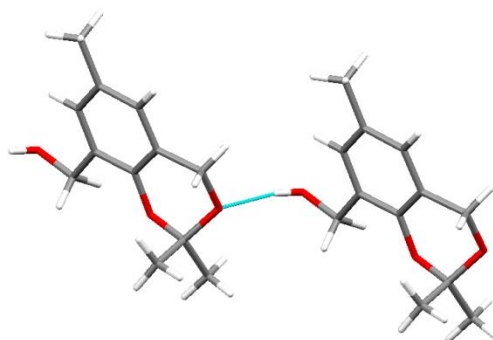
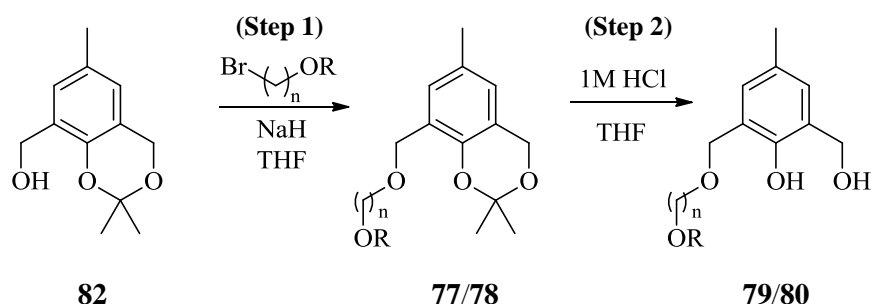


Figure 2.25: Crystal Structure of **82**.

2.4.4.2. Alkylation of primary alcohol with 'Arm D' and acetal cleavage

The primary alcohol, **82**, was successfully alkylated with the commercially available 'Arm D' ethers, **58** and **76**, to form the novel alkylated products, **77** and **78**, **Scheme 2.17**, (**Step 1**). Singh's procedure for a similar system was adopted to achieve this particular alkylation.⁶⁷ It involves deprotonation of the primary alcohol with sodium hydride, followed by alkylation with a suitable alkyl halide. The shorter chain system, **77**, was synthesised in excellent yield and was deemed sufficiently pure by ¹H and ¹³C NMR to proceed to the next stage of synthesis. However, a reduced yield was noted for **78**, **Table 2.12**. The crude material isolated after alkylation with the ether, **76**, consisted of a much more complex mixture and therefore required purification by column chromatography.



Scheme 2.17: Alkylation with ether functionalities and acetal cleavage.

Table 2.12: Yields obtained for **77,78,79** and **80**

Arm D	n	R	Product (Step 1) ^a	Yield (%) (Step 1)	Product (Step 2) ^a	Yield (%) (Step 2)
58	2	CH ₃	77	96 ^c	79	85 ^c
76	3	Bn	78	31 ^b	80	56 ^c

a Novel compounds.

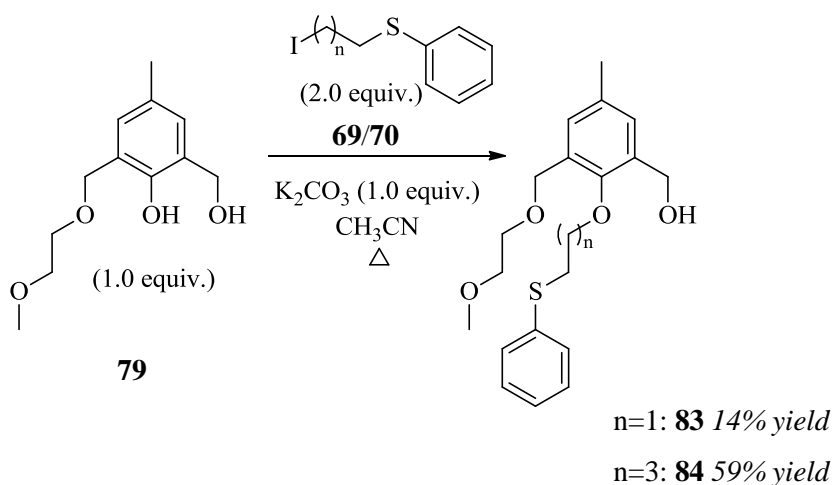
b Purified yield.

c Unpurified yield.

The acetal group that acted as an effective protecting group for two of the three hydroxyl groups was easily cleaved by the addition of HCl (1 M) to afford **79** and **80** in good yields, as oils at room temperature, **Scheme 2.17**, (**Step 2**). Purification of these highly polar compounds by column chromatography was avoided. The crude material was sufficiently pure for the further alkylation reactions. Overall, this approach involving the acetal group led to the efficient introduction of 'Arm D'.

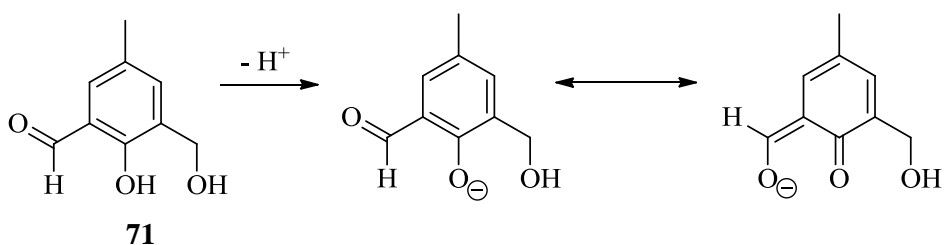
2.4.4.3. Alkylation of phenol with 'Arm E'

The difference in acidity between the phenol and primary alcohol was again exploited in this synthetic route to achieve selective alkylation of the phenol with 'Arm E'. Alkylation at this phenolic site was very difficult to accomplish in 'Synthetic Scheme I' and required microwave-assisted reactions, **Scheme 2.13**. However, heating **79** under reflux in acetonitrile in the presence of K_2CO_3 and the previously synthesised iodo-substituted thioethers, **69** and **70**, resulted in the formation of the novel desired products, **83** and **84**, which were subsequently purified and isolated as oils at room temperature, **Scheme 2.18**.



Scheme 2.18: Alkylation of phenol with purified yields obtained for **83** and **84**.

The observation that alkylation of the phenol occurs much more readily in **79** than in the aldehyde-containing **71** indicates that conjugation plays a significant role in the reactivity of the phenoxide. The presence of the electron withdrawing aldehyde in **71** significantly stabilises the phenoxide by extended resonance delocalisation, relative to the phenoxide derived from **79**, and thereby reduces its activity, **Scheme 2.19**.



Scheme 2.19: Possible resonance structures of **71**.

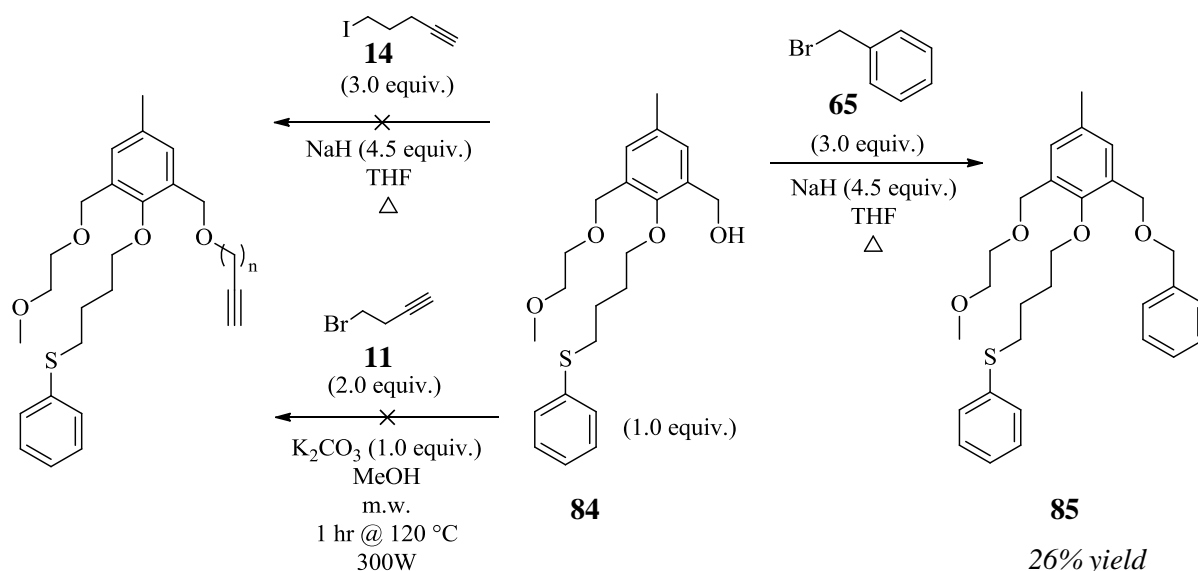
A very noticeable reduction in yield was observed between the alkylated products, **83** and **84**, which indicates that electronic effects play a key role in the efficiency of alkylation at the

phenolic site. In **69**, where the sulfide lies on the adjacent carbon to the alkyl iodide, the efficiency of the alkylation could be reduced by the inductive electron withdrawing effect of the sulfide, or alternatively by a competing E2 elimination.

2.4.4.4. Alkylation of primary alcohol

The final alkylation reaction with ‘Arm F’ to achieve the target molecule also proved quite challenging. Alkylation of the benzyl alcohol, **84**, with either the alkyl iodide, **14**, using conditions similar to **Scheme 2.17 (Step 1)**, or with the alkyl bromide, **11**, involving a microwave-assisted reaction proved unsuccessful, with only the unreacted starting material, **84**, recovered, **Scheme 2.20**. To explore if alkylation at the benzyl alcohol could be achieved with simpler electrophiles, benzylation was undertaken with benzyl bromide, **65**, while heating under reflux with NaH in THF. With this more reactive electrophile, benzylation to form the ether, **85**, was indeed achieved, albeit in modest yield with substantial recovery of the unreacted starting material, **84**. Thus it is clear that alkylation at this position is challenging but not impossible.

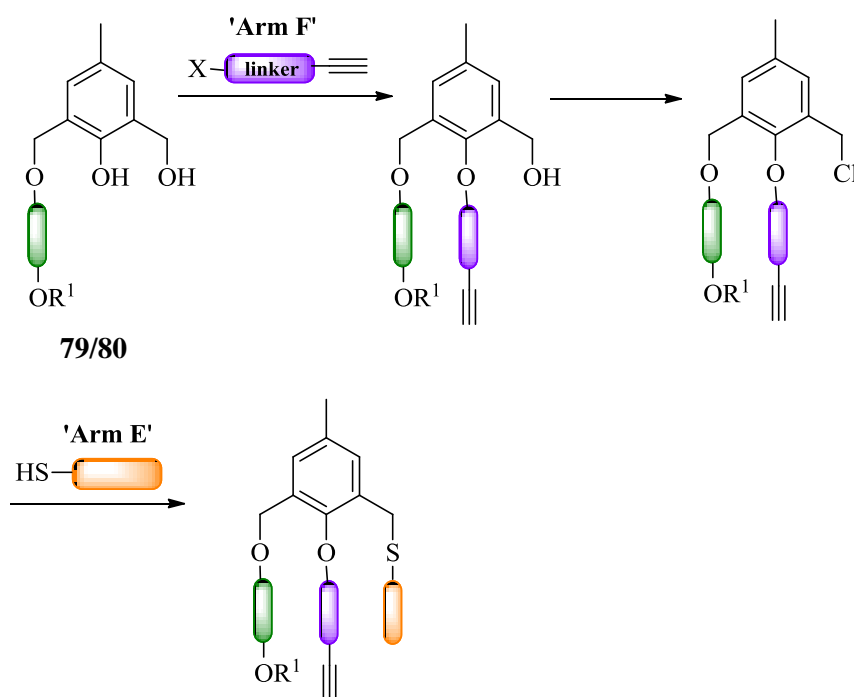
The results from ‘Synthetic Strategy II’ were very positive and further advanced the possibility of completing the synthesis of the tri-alkylated system outlined in **Scheme 2.15**. Clearly this strategy needed to be further modified, to enable the introduction of the terminal alkyne.



Scheme 2.20: Synthesis of tri-alkylated system, **85**.

2.4.5. Synthetic Strategy III

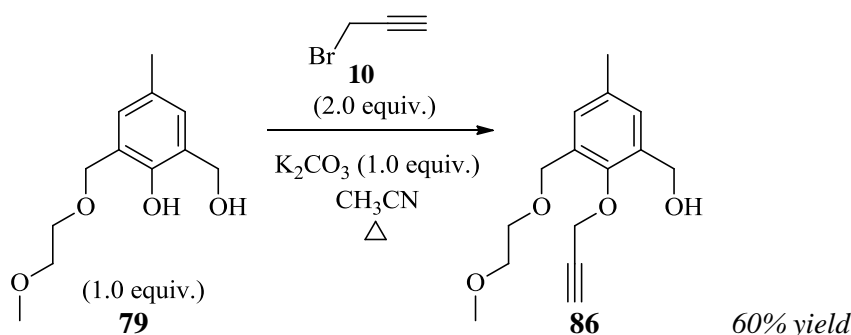
'Synthetic Strategy II' proved extremely effective for the generation of the mono-substituted derivatives, **79** and **80**, bearing the ether arm, but the efficiency of the introduction of the remaining two arms incorporating the sulfide and terminal alkyne required further work. Thus, 'Synthetic Strategy III' involved the introduction of the alkyne arm *i.e.* 'Arm F', at the phenol site through alkylation, **Scheme 2.21**, resulting in a different arrangement of the 'arms' compared to the 'Synthetic Strategies I and II'. It was envisaged that this would enable attachment of the terminal alkyne, which had not been possible in 'Synthetic Strategy II'. To overcome the difficulty in alkylating the final benzyl alcohol position in 'Synthetic Strategy II', an alternative strategy for the introduction of the sulfide arm was envisaged as outlined in **Scheme 2.21**, through conversion of the benzyl alcohol to a benzyl chloride followed by substitution with a thiolate. Use of the benzyl chloride rather than the benzyl alcohol in this key final step was envisaged to overcome the challenges in alkylation at this site.



Scheme 2.21: 'Synthetic Strategy III'

2.4.5.1. Alkylation of phenol with terminal alkyne

As anticipated, attachment of the short chain terminal alkyne, **10**, at the phenolic site of **79** was achieved without difficulty to form **86** in moderate yield after purification by column chromatography, **Scheme 2.22**. While the reaction conditions employed were essentially the same as those employed in **Scheme 2.18** for the introduction of the sulfide chain, the efficiency of the propargylation was notably higher, resulting in a cleaner product with the more reactive electrophile.



Scheme 2.22: Attachment of terminal alkyne to form **86**.

While the majority of the compounds synthesised to date were oils, the propargyl ether, **86**, was isolated as a crystalline solid and its novel single crystal structure was determined after recrystallisation from CH_2Cl_2 , **Figure 2.26**. This enabled, for the first time, direct observation of the solid state behaviour, albeit with two of the three desired arms attached. As anticipated, the key intermolecular interaction involves hydrogen bonding between the benzyl alcohol moieties $\text{CH}_2\text{OH}\cdots\text{OCH}_2$ (1.83 Å), as illustrated in **Figure 2.26**. Also the predicted weak $\text{C}\equiv\text{C-H}\cdots\text{O}$ intermolecular hydrogen bond interaction is observed with the terminal alkyne hydrogen participating in bifurcated bonding with the ether oxygens of a neighbouring molecule (2.70 Å). Intramolecular interactions involving the benzylic hydrogens to the central oxygen of the scaffold and the propargylic hydrogens to a neighbouring ether moiety were also noted. This significant result indicates that crystalline material can be obtained from the aromatic scaffold and also the predicted solid state interactions involving the terminal alkyne were successfully detected using single crystal analysis.

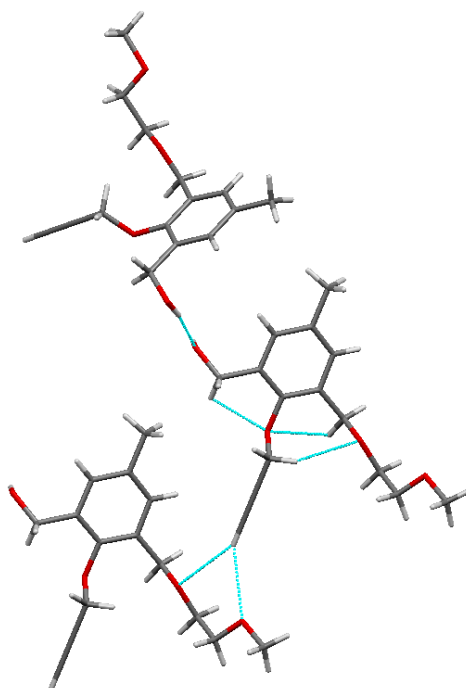
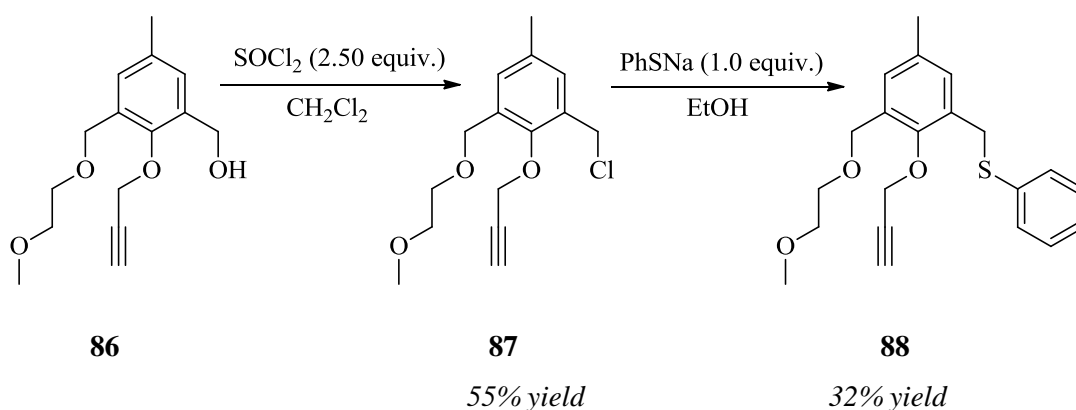


Figure 2.26: *Crystal packing of 86.*

2.4.5.2. Chlorination of primary alcohol and *S*-alkylation

Due to the challenges that arose when alkylating the primary alcohol, **84**, in ‘Synthetic Strategy II’, conversion of the alcohol, **86**, to a reactive benzyl halide was explored in order to increase the reactivity at this site. Chlorination was achieved employing thionyl chloride in CH_2Cl_2 to afford the novel benzyl chloride, **87**, in 55% yield after purification by column chromatography, **Scheme 2.23**. The chloride, **87**, existed as an oil at room temperature confirming the critical role of hydrogen bonding between the alcohols in **86** in the provision of a crystalline solid, **Figure 2.26**.

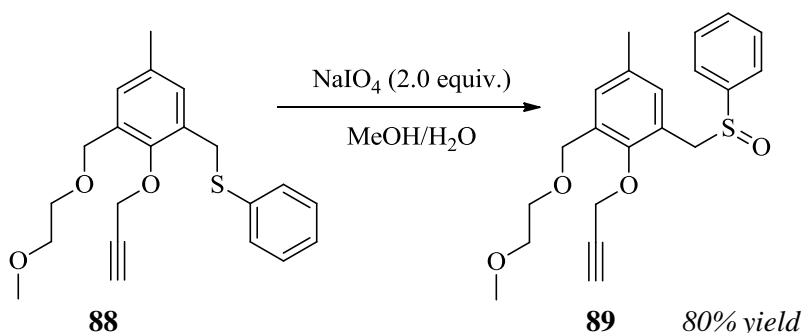


Scheme 2.23: *Conversion of 86 to 87 and 88.*

Introduction of the sulfur functionality was successfully achieved through an S-alkylation reaction of **87** with sodium thiophenoxide, using reaction conditions similar to Cronin,⁶⁹ to afford the novel tri-substituted aromatic system, **88**, together with unreacted **87**. Purification of **88** was attempted by column chromatography but the product obtained still contained evidence of the starting material, **87**, in the ¹H NMR spectrum (15%). The tri-alkylated compound, **88**, was obtained as an oil at room temperature, perhaps as a result of the impurity and/or due to the lack of significant hydrogen bonding within the molecule. Synthesis of **88** was a significant milestone as it demonstrated that the target aromatic scaffold containing all three functional groups of interest – ether, terminal alkyne and sulfide, as illustrated in **Figure 2.23**, could be obtained.

2.4.5.3. Oxidation to sulfoxide

As the sulfide, **88**, was an oil at room temperature, oxidation to the sulfoxide was undertaken with the objective of forming a crystalline solid on introduction of a strong hydrogen bond acceptor. Sodium meta-periodate (NaIO₄) was chosen as oxidant to selectively oxidise the sulfide, **88**, to the sulfoxide, **89**, without over-oxidation to the sulfone, **Scheme 2.24**.²⁰



Scheme 2.24: Oxidation of sulfide **88** to sulfoxide **89**.

Chemoselective oxidation to the sulfoxide, **89**, was achieved successfully in 80% yield after column chromatography and **89** was isolated as an oil at room temperature with no evidence of over-oxidation to the sulfone or of a competing reaction at the alkyne. Comparing the ¹H NMR spectra of the sulfide, **88**, and sulfoxide, **89**, a downfield shift was observed for the sulfoxide protons. The protons α to the sulfoxide are now diastereotopic and appear as an AB quartet at 4.11 ppm (J_{AB} 12.3) and 4.15 ppm (J_{AB} 12.3). The protons α to the alkyne are also diastereotopic after oxidation and interestingly a finely split AB quartet at 4.58 ppm

(J_{AB} 15.6, 4J 2.4) and 4.65 ppm (J_{AB} 15.6, 4J 2.4) was detected, despite the distance from the stereogenic centre at sulfur, **Figure 2.27**.

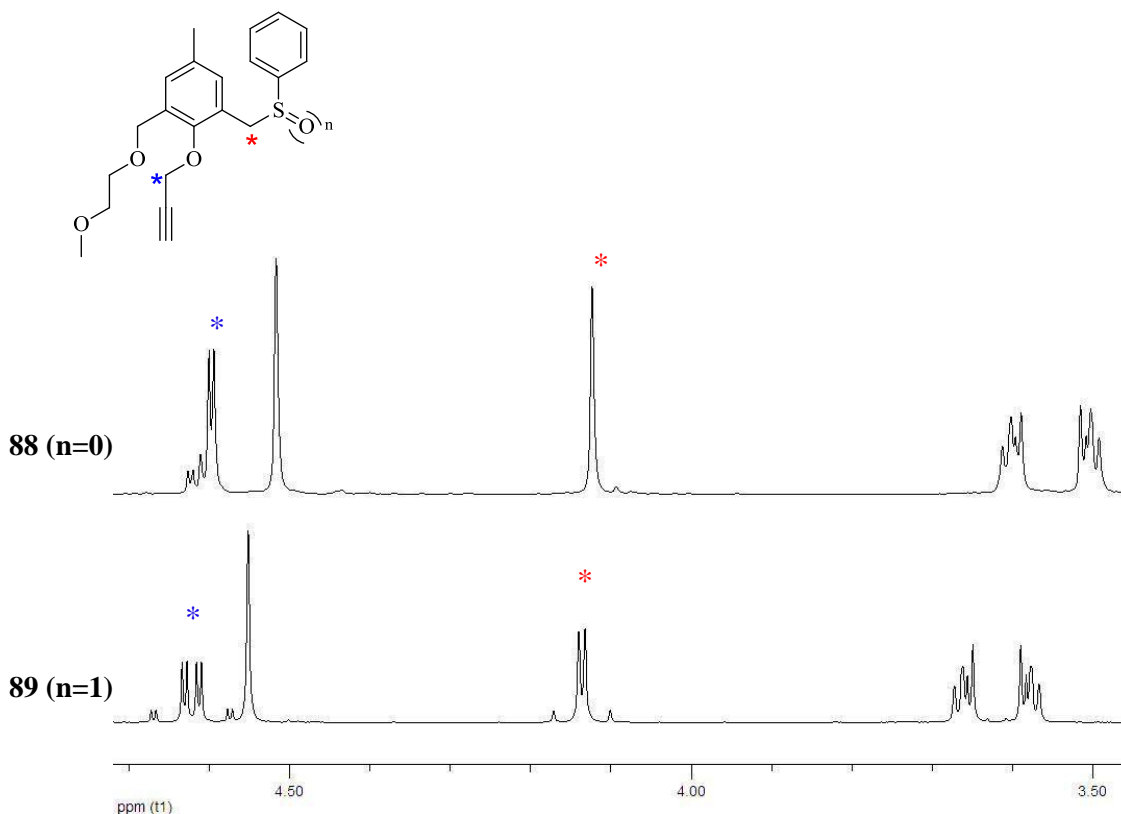


Figure 2.27: ^1H NMR (400 MHz) spectra of the sulfide, **88**, and sulfoxide, **89**, at 3.49–4.80 ppm.

The signals for the protons on the tetrasubstituted aromatic system, which appear as two finely split singlets at 6.94 and 7.05 ppm in the sulfide, **88**, are visibly shifted on oxidation to the sulfoxide, **89**, and appear at 6.82 and 7.19 ppm again with fine splitting, due to the mutual long range coupling, **Figure 2.28**. The protons (H_A and H_B) were identified by HMBC and NOESY 2D NMR experiments. A downfield shift of these aromatic protons would be expected on oxidation from sulfide to sulfoxide. However, while the signal for H_A was shifted downfield, it was interesting to note that the signal for H_B was shifted upfield after oxidation. Since H_B , according to the NOESY data, **Figure 2.29**, is in close proximity to the benzyl sulfoxide protons, it is reasonable to assume that this upfield shift can be attributed to intramolecular hydrogen bonding between the sulfoxide oxygen and the H_B proton, as illustrated in **Figure 2.28**.

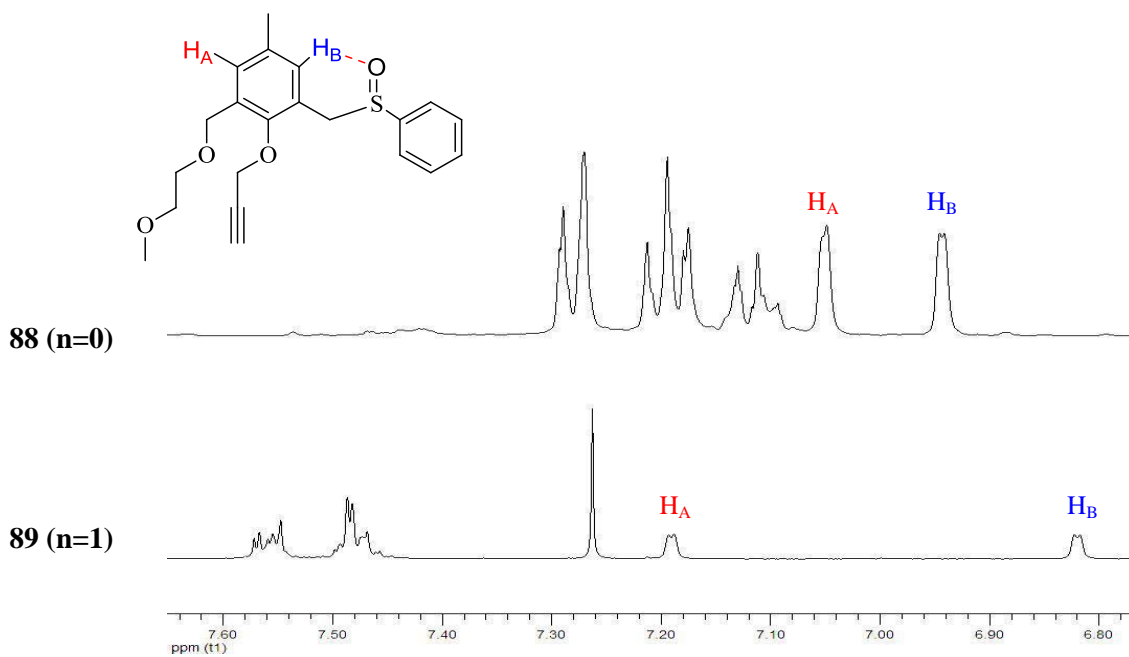


Figure 2.28: 1H NMR spectra of the aromatic region of the sulfide, **88**, and sulfoxide, **89**, (400 MHz).

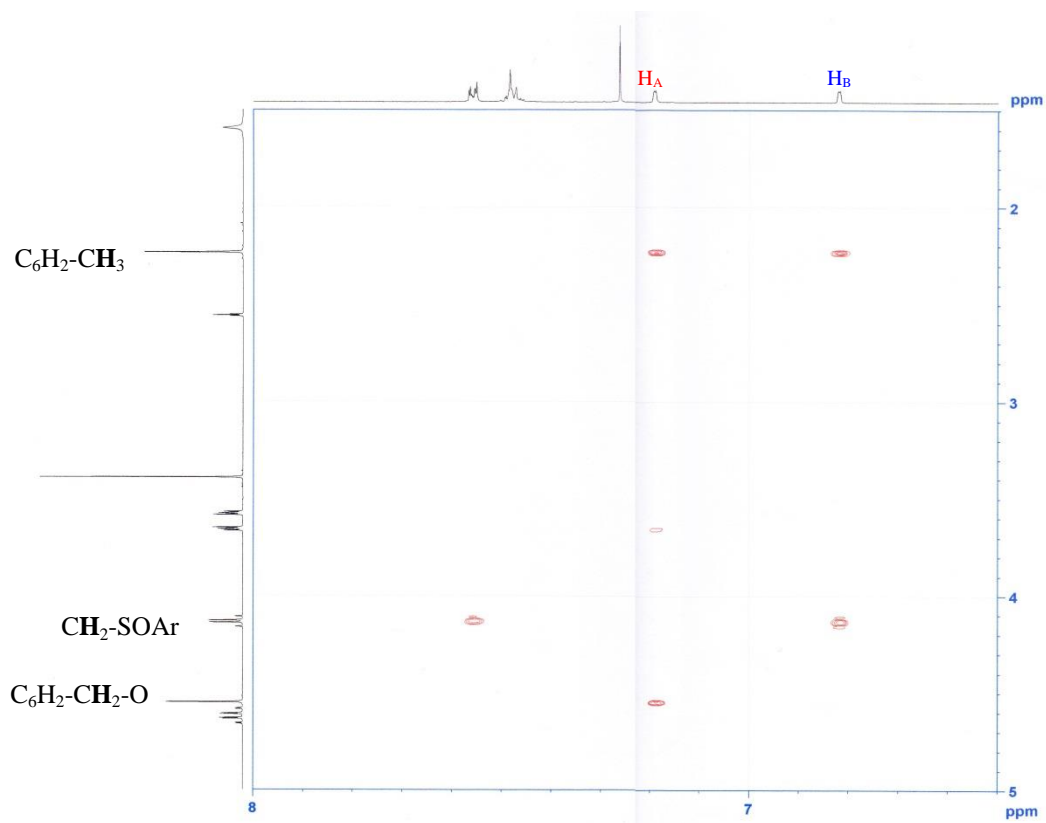


Figure 2.29: NOESY NMR of sulfoxide, **89**, (400 MHz).

'Synthetic Strategy III' afforded the most positive results with successful attachment of the 'Arms' incorporating the ether, terminal alkyne and sulfide functional groups, at each of the three sites of the aromatic triol scaffold. In addition the sulfide was then chemoselectively oxidised to the corresponding sulfoxide. This synthetic strategy is a significant breakthrough as it now provides a robust synthetic route which can be exploited for the synthesis of structurally related compounds.

2.4.6. Conclusions

In summary, the triol, **57**, was an effective compound to act as a scaffold on which to tether the desired functional groups of interest. A number of synthetic strategies were designed and attempted to ultimately alkylate each of the three hydroxyl groups with a hydrogen bond acceptor (ether), a hydrogen donor (terminal alkyne) and sulfur functionalities which could potentially act as competitive hydrogen bond acceptors depending on the oxidation level. Many challenges arose throughout these synthetic attempts including poor reactivity at certain sites, electronic effects, competing side reactions which resulted in a loss in yield in specific steps, and the difficulty in selectively alkylating the three alcohol sites with three different functional groups. Ultimately, each of these obstacles were overcome to produce a synthetic strategy that was both novel and adaptable for future systems.

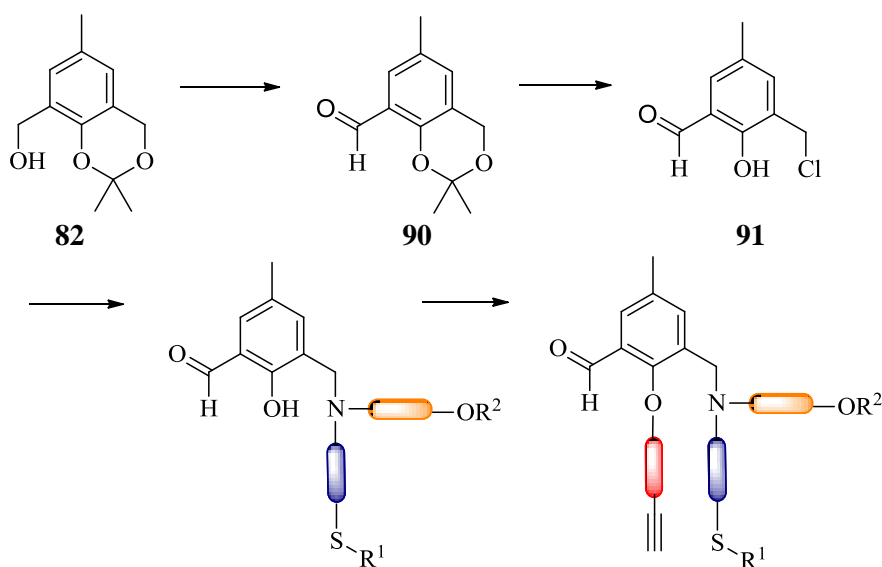
While **88** and **89** were obtained as model systems, it was recognised at the outset that for conformational reasons it was extremely unlikely that these compounds would yield the desired intramolecular hydrogen bonding patterns in the solid state. However, building on this work, design of related compounds with extended linkers which would enable the conformational flexibility to access the hydrogen bonded structures can be envisaged. Given the challenges in obtaining crystalline material in this series, this work has not been progressed to date.

2.5. Combination of Tertiary Amine and Aromatic Scaffold

2.5.1. Synthetic strategy

With the successful design and synthesis of the tertiary amine and tri-alkylated aromatic scaffold, the investigation of combining these two core structures within a single molecule was an interesting pursuit. It was envisaged that the more rigid triol scaffold would act as an anchor for attachment of the flexible tertiary amines, and the positive attributes from both scaffolds would be utilised effectively. The rotation of the flexible ‘arms’ in the tertiary amine may increase the possibility of intramolecular interactions and the incorporation of the triol may lead to the formation of more crystalline material, **Scheme 2.25**.

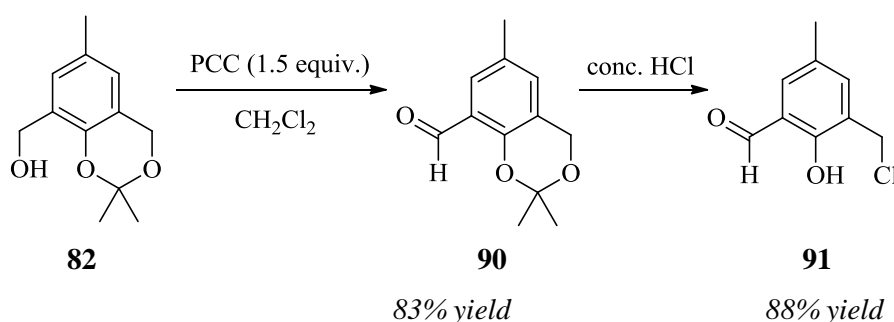
The synthetic strategy involved forming the acetonide, **82**, as previously described in ‘Synthetic Strategy II’, **Scheme 2.15**. Then oxidation of the benzyl alcohol to the corresponding aldehyde, **90**, would protect this site from alkylation in the subsequent steps. Deprotection of the acetal and conversion of the second benzyl alcohol to the benzyl chloride, **91**, would form a compound suitable to undergo an *N*-alkylation reaction with one of the previously synthesised secondary amines, **Section 2.3.3, Table 2.4**. Attachment of the terminal alkyne could then be achieved by an S_N2 substitution reaction to afford the target molecule. It was envisaged that the aldehyde could subsequently be modified to provide a series of compounds with differing solid state properties. The synthetic flexibility of the aldehyde, potentially through oxidation, reduction or condensation processes is of value in this context.



Scheme 2.25: Synthetic strategy for combining the two scaffolds.

2.5.1.1. Oxidation to aldehyde and chlorination of primary alcohol

Chirakul *et al.* had previously described the transformation of **82** to **91** and similar conditions were adopted in this work, **Scheme 2.26**.⁷⁰ Pyridinium chlorochromate (PCC) successfully oxidised the primary alcohol, **82**, to the aldehyde, **90**, in 83% yield after column chromatography. Then **90** was effectively deprotected and chlorinated with concentrated HCl in a one-pot reaction which afforded **91** in 88% yield after recrystallisation from hexane.



Scheme 2.26: Preparation of **91** from **82**.

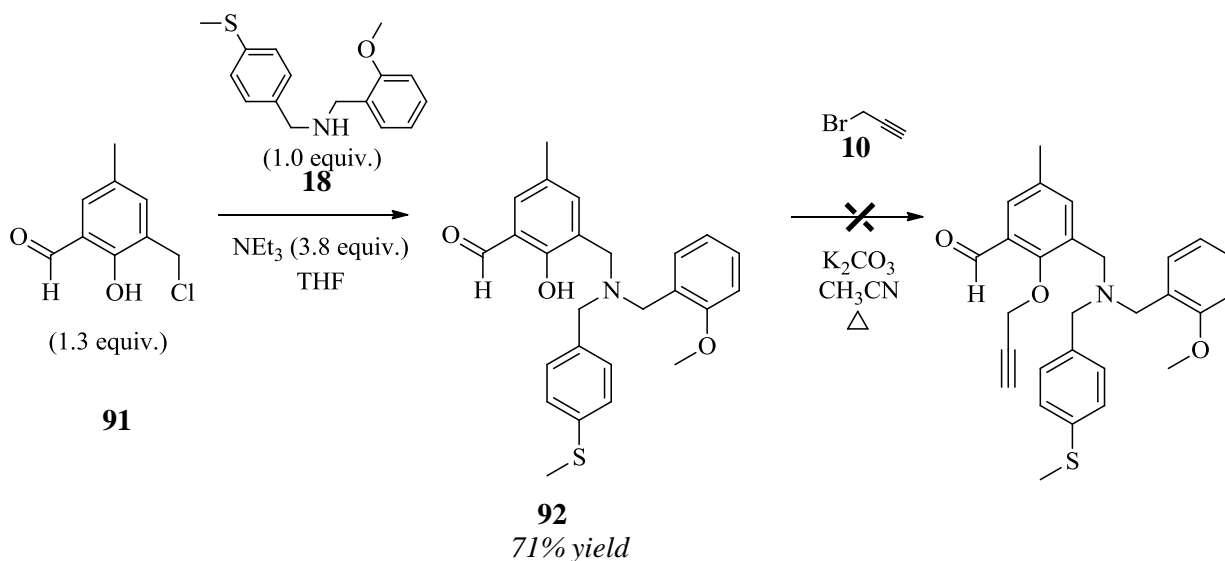
This synthetic route efficiently provided a suitable intermediate that could be alkylated with the secondary amines containing the functional groups of interest *i.e.* ether and sulfur moieties.

2.5.1.2. N-Alkylation and alkylation of the phenol

N-Alkylation of the secondary amine, **18**, with the benzyl chloride, **91**, was achieved utilising conditions similar to Boudalis *et al.* involving triethylamine (NEt₃) and THF.⁷¹ While Boudalis and co-workers had not synthesised specifically the tertiary amine, **92**, they had demonstrated benzylation of secondary amines under these conditions. The novel tertiary amine, **92**, was isolated as an oil in 71% yield after column chromatography, **Scheme 2.27**.

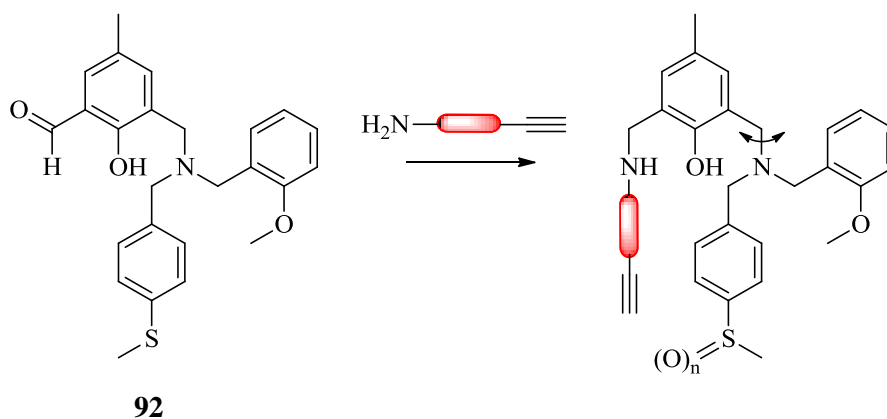
Next, to alkylate the phenolic site in **92**, identical reaction conditions to those used for the successful alkylation of **79** in **Scheme 2.22**, involving propargyl bromide, **10**, were attempted. However alkylation was not achieved in this particular case with only the starting material, **92**, isolated after a 24 h reflux. Once again, as described previously in **Scheme 2.19**, conjugation to the aldehyde reduces the activity of the phenoxide ion, thereby hindering alkylation. Steric effects may also be envisaged with the bulky amine in close

proximity to the phenoxide. As other aspects of the project were proving effective, this route was not further pursued.



Scheme 2.27: Formation of **92** which combines the triol and tertiary amine scaffolds.

To further develop this strategy in the future, perhaps a reductive amination reaction between the aldehyde, **92**, and an amine incorporating a terminal alkyne, could be attempted. Through sulfur oxidation the hydrogen bond acceptor could then be varied, **Scheme 2.28**.



Scheme 2.28: Future concept involving the combination of scaffolds.

2.6. References

1. Huang, L. F.; Tong, W. Q. *Adv. Drug Delivery Rev.*, **2004**, *56*, 321-334.
2. Snider, D. A.; Addicks, W.; Owens, W. *Adv. Drug Delivery Rev.*, **2004**, *56*, 391-395.
3. Rodriguez-Spong, B.; Price, C. P.; Jayasankar, A.; Matzger, A. J.; Rodriguez-Hornedo, N. *Adv. Drug Delivery Rev.*, **2004**, *56*, 241-274.
4. Jones, I. M.; Hamilton, A. D. *Org. Lett.*, **2010**, *12*, 3651-3653.
5. Lehane, K. N.; Moynihan, E. J. A.; Brondel, N.; Lawrence, S. E.; Maguire, A. R. *CrystEngComm*, **2007**, *9*, 1041-1050.
6. Patai, S.; Rappaport, Z.; Stirlint, C. *The Chemistry of Sulphones and Sulphoxides*. John Wiley and Sons: New York, 1988; p 541.
7. Hunter, C. A. *Angew. Chem., Int. Ed.*, **2004**, *43*, 5310-5324.
8. Dai, C.; Yuan, Z.; Collings, J. C.; Fasina, T. M.; Thomas, R. L.; Roscoe, K. P.; Stimson, L. M.; Yufit, D. S.; Batsanov, A. S.; Howard, J. A. K.; Marder, T. B. *CrystEngComm*, **2004**, *6*, 184-188.
9. Steiner, T. *Angew. Chem., Int. Ed.*, **2002**, *41*, 48-76.
10. Brondel, N.; Moynihan, E. J. A.; Lehane, K. N.; Eccles, K. S.; Elcoate, C. J.; Coles, S. J.; Lawrence, S. E.; Maguire, A. R. *CrystEngComm*, **2010**, *12*, 2910-2927.
11. Heynderickx, A.; Samat, A.; Guglielmetti, R. *J. Heterocycl. Chem.*, **2001**, *38*, 737-742.
12. Creed, T.; Leardini, R.; McNab, H.; Nanni, D.; Nicolson, I. S.; Reed, D. *J. Chem. Soc., Perkin Trans. 1*, **2001**, 1079-1085.
13. Borbas, K. E.; Chandrashaker, V.; Muthiah, C.; Kee, H. L.; Holten, D.; Lindsey, J. S. *J. Org. Chem.*, **2008**, *73*, 3145-3158.
14. Gomez, S.; Peters, J. A.; Maschmeyer, T. *Adv. Synth. Catal.*, **2002**, *344*, 1037-1057.
15. Abdel-Magid, A. F.; Carson, K. G.; Harris, B. D.; Maryanoff, C. A.; Shah, R. D. *J. Org. Chem.*, **1996**, *61*, 3849-3862.
16. Abdel-Magid, A. F.; Mehrman, S. J. *Org. Process Res. Dev.*, **2006**, *10*, 971-1031.
17. Silverstein, R. M.; Webster, F. X. *Spectrometric identification of organic compounds*. Wiley: New York, 1998; pp 85-86.
18. O'Mahony, G. E.; Kelly, P.; Lawrence, S. E.; Maguire, A. R. *ARKIVOC*, **2011**, 1-110.
19. Kaczorowska, K.; Kolarska, Z.; Mitka, K.; Kowalski, P. *Tetrahedron*, **2005**, *61*, 8315-8327.

20. Collins, S. G.; Maguire, A. R. *Sci. Synth.*, **2007**, *31a*, 907-948.
21. Yu, B.; Liu, A. H.; He, L. N.; Li, B.; Diao, Z. F.; Li, Y. N. *Green Chem.*, **2012**, *14*, 957-962.
22. Steiner, T.; Tamm, M.; Grzegorzewski, A.; Schulte, N.; Veldman, N.; Schreurs, A. M. M.; Kanters, J. A.; Kroon, J.; van, d. M.; Lutz, B. *J. Chem. Soc., Perkin Trans. 2*, **1996**, 2441-2446.
23. Nishio, M. *CrystEngComm*, **2004**, *6*, 130-158.
24. Gomez-Duran, C. F. A.; Garcia-Moreno, I.; Costela, A.; Martin, V.; Sastre, R.; Banuelos, J.; Lopez, A.; Lopez, A., I; Pena-Cabrera, E. *Chem. Commun.*, **2010**, *46*, 5103-5105.
25. Hashmi, A. S.; Weyrauch, J. P.; Frey, W.; Bats, J. W. *Org. Lett.*, **2004**, *6*, 4391-4394.
26. Chinnakali, K.; Poornachandran, M.; Raghunathan, R.; Fun, H. K. *Acta Crystallogr., Sect. E: Struct. Rep. Online*, **2007**, *E63*, o980-o981.
27. Weiss, H. C.; Blaser, D.; Boese, R.; Doughan, B. M.; Haley, M. M. *Chem. Commun.*, **1997**, 1703-1704.
28. Robinson, J. M. A.; Kariuki, B. M.; Gough, R. J.; Harris, K. D.; Philp, D. *J. Solid State Chem.*, **1997**, *134*, 203-206.
29. Dziubek, K.; Podsiadlo, M.; Katrusiak, A. *J. Am. Chem. Soc.*, **2007**, *129*, 12620-12621.
30. Yoshida, A.; Hattori, G.; Miyake, Y.; Nishibayashi, Y. *Org. Lett.*, **2011**, *13*, 2460-2463.
31. Simon, K.; Podanyi, B.; Ecsery, Z.; Toth, G. *J. Chem. Soc., Perkin Trans. 2*, **1986**, 111-115.
32. Hempel, A.; Camerman, N.; Camerman, A.; Mastropaolo, D. *Acta Crystallogr., Sect. E: Struct. Rep. Online*, **2005**, *E61*, o1598-o1600.
33. Metzger, E.; Wissmann, M.; Yin, N.; Mueller, J. M.; Schneider, R.; Peters, A. H. F. M.; Guenther, T.; Buettner, R.; Schuele, R. *Nature*, **2005**, *437*, 436-439.
34. Lv, T.; Yuan, D.; Miao, X.; Lv, Y.; Zhan, P.; Shen, X.; Song, Y. *PLoS One*, **2012**, *7*, e35065.
35. Tan, J.; Cang, S.; Ma, Y.; Petrillo, R. L.; Liu, D. *J. Hematol. Oncol.*, **2010**, *3*, 5.
36. Ueda, R.; Suzuki, T.; Mino, K.; Tsumoto, H.; Nakagawa, H.; Hasegawa, M.; Sasaki, R.; Mizukami, T.; Miyata, N. *J. Am. Chem. Soc.*, **2009**, *131*, 17536-17537.
37. Schmidt, D. M. Z.; McCafferty, D. G. *Biochemistry*, **2007**, *46*, 4408-4416.
38. Pollock, J. A.; Larrea, M. D.; Jasper, J. S.; McDonnell, D. P.; McCafferty, D. G. *ACS Chem. Biol.*, **2012**, *7*, 1221-1231.

39. <http://dtp.nci.nih.gov>, **2012**
40. Shoemaker, R. H. *Nat. Rev. Cancer*, **2006**, *6*, 813-823.
41. Smith, S. C.; Baras, A. S.; Lee, J. K.; Theodorescu, D. *Cancer Res.*, **2010**, *70*, 1753-1758.
42. Weinstein, J. N. *Mol. Cancer Ther.*, **2006**, *5*, 2601-2605.
43. Adams, S.; Robbins, F. M.; Chen, D.; Wagage, D.; Holbeck, S. L.; Morse, H. C., III; Stroncek, D.; Marincola, F. M. *J. Transl. Med.*, **2005**, *3*, No.
44. Ikediobi, O. N.; Davies, H.; Bignell, G.; Edkins, S.; Stevens, C.; O'Meara, S.; Santarius, T.; Avis, T.; Barthorpe, S.; Brackenbury, L.; Buck, G.; Butler, A.; Clements, J.; Cole, J.; Dicks, E.; Forbes, S.; Gray, K.; Halliday, K.; Harrison, R.; Hills, K.; Hinton, J.; Hunter, C.; Jenkinson, A.; Jones, D.; Kosmidou, V.; Lugg, R.; Menzies, A.; Mironenko, T.; Parker, A.; Perry, J.; Raine, K.; Richardson, D.; Shepherd, R.; Small, A.; Smith, R.; Solomon, H.; Stephens, P.; Teague, J.; Tofts, C.; Varian, J.; Webb, T.; West, S.; Widaa, S.; Yates, A.; Reinhold, W.; Weinstein, J. N.; Stratton, M. R.; Futreal, P. A.; Wooster, R. *Mol. Cancer Ther.*, **2006**, *5*, 2606-2612.
45. Boyd, M. R.; Paull, K. D. *Drug Dev. Res.*, **1995**, *34*, 91-109.
46. Gills, J. J.; Holbeck, S.; Hollingshead, M.; Hewitt, S. M.; Kozikowski, A. P.; Dennis, P. A. *Mol. Cancer Ther.*, **2006**, *5*, 713-722.
47. Rubinstein, L. V.; Shoemaker, R. H.; Paull, K. D.; Simon, R. M.; Tosini, S.; Skehan, P.; Scudiero, D. A.; Monks, A.; Boyd, M. R. *J. Natl. Cancer Inst.*, **1990**, *82*, 1113-1118.
48. Boyd, M. R. *The NCI human tumor cell line (60-cell) screen: Concept, implementation, and applications*. Humana Press Inc.: **2004**; pp 41-61.
49. Finkelstein, H. *Ber. Dtsch. Chem. Ges.*, **1910**, *43*, 1528-1532.
50. Coleman, G. H.; Hauser, C. R. *J. Am. Chem. Soc.*, **1928**, *50*, 1193-1196.
51. Lou, J. D.; Xu, Z. N. *Tetrahedron Lett.*, **2002**, *43*, 6149-6150.
52. Tojo, G.; Fernandez, M. *Oxidation of Alcohols to Aldehydes and Ketones: a guide to current common practice*. Springer: USA, 2006; pp 290-293.
53. Goldman, I. M. *J. Org. Chem.*, **1969**, *34*, 3289-3295.
54. Lou, J. D.; Zou, X. N.; Zhang, C.; Wang, Q.; Ma, Y. C. *Oxid. Commun.*, **2011**, *34*, 355-360.
55. Smith, M. B. *Organic Synthesis*. 3rd ed.; Academic Press: USA, 2011; pp 252-255.
56. Hall, T. K.; Story, P. R. *J. Amer. Chem. Soc.*, **1967**, *89*, 6759-6761.
57. Constantinides, I.; Macomber, R. S. *J. Org. Chem.*, **1992**, *57*, 6063-6067.

58. Sun, G. C.; He, Z. H.; Li, Z. J.; Yuan, X. D.; Yang, Z. J.; Wang, G. X.; Wang, L. F.; Liu, C. R. *Molecules*, **2001**, *6*, 1001-1005.
59. Amato, M. E.; Ballistreri, F. P.; Pappalardo, A.; Sciotto, D.; Tomaselli, G. A.; Toscano, R. M. *Tetrahedron*, **2007**, *63*, 9751-9757.
60. Carlsson, H.; Haukka, M.; Bousseksou, A.; Latour, J. M.; Nordlander, E. *Inorg. Chem.*, **2004**, *43*, 8252-8262.
61. Lambert, E.; Chabut, B.; Chardon-Noblat, S.; Deronzier, A.; Chottard, G.; Bousseksou, A.; Tuchagues, J. P.; Laugier, J.; Bardet, M.; Latour, J. M. *J. Am. Chem. Soc.*, **1997**, *119*, 9424-9437.
62. Sarju, J.; Danks, T. N.; Wagner, G. *Tetrahedron Lett.*, **2004**, *45*, 7675-7677.
63. Wang, Z.; Gu, J.; Jing, H.; Liang, Y. *Synth. Commun.*, **2009**, *39*, 4079-4087.
64. Keglevich, G.; Balint, E.; Karsai, E.; Grun, A.; Balint, M.; Greiner, I. *Tetrahedron Lett.*, **2008**, *49*, 5039-5042.
65. Abe, A. M. M.; Helaja, J.; Koskinen, A. M. P. *Org. Lett.*, **2006**, *8*, 4537-4540.
66. Clark, D. A.; Riccardis, F. D.; Nicolaou, K. C. *Tetrahedron*, **1994**, *50*, 11391-11426.
67. Singh, V.; Alam, S. Q.; Praveena, G. D. *Tetrahedron*, **2002**, *58*, 9729-9736.
68. Eccles, K. S.; Stokes, S. P.; Daly, C. A.; Barry, N. M.; McSweeney, S. P.; O'Neill, D. J.; Kelly, D. M.; Jennings, W. B.; Dhubhghaill, O. M. N.; Moynihan, H. A.; Maguire, A. R.; Lawrence, S. E. *J. Appl. Crystallogr.*, **2011**, *44*, 213-215, S213-1.
69. Cronin, M. *Ph.D. Thesis, NUI 1998*.
70. Chirakul, P.; Hampton, P. D.; Bencze, Z. *J. Org. Chem.*, **2000**, *65*, 8297-8300.
71. Boudalis, A. K.; Aston, R. E.; Smith, S. J.; Mirams, R. E.; Riley, M. J.; Schenk, G.; Blackman, A. G.; Hanton, L. R.; Gahan, L. R. *Dalton Trans.*, **2007**, 5132-5139.

Chapter 3

Design and synthesis of a diphenylacetylene-based switching entity

3. Contents

3.1. Diphenylacetylene Scaffold	117
3.1.1. Introduction	117
3.1.2. Hunter's Rationale	120
3.1.3. Design of diphenylacetylene targets	121
3.1.4. Synthetic Strategies for A, B and C	125
3.1.5. Iodo-amide precursors	128
3.1.6. Terminal alkyne precursors	130
3.1.7. Sonogashira Coupling	133
3.1.8. Crystal Structure Data	137
3.1.9. Variable-temperature NMR spectroscopic studies	158
3.2. Introduction of a competing hydrogen bond donor	162
3.2.1. Introduction	162
3.2.2. Preparation of <i>N</i> -(2-Iodo-3-aminophenyl)benzamide	163
3.2.3. Sonogashira coupling and functionalisation of amine	164
3.2.4. Crystal Structures	167
3.2.5. Computer Modelling	169
3.2.6. Conclusion	170
3.3. References	172

3.1. Diphenylacetylene Scaffold

3.1.1. Introduction

Diphenylacetylene units have recently been explored to act as effective switching entities. The very small rotational barrier of ~ 0.6 kcal/mol that exists for the internal rotation of diphenylacetylene results in conformations that are very flexible and unpredictable. This is readily explained on the basis of symmetry, where overlap of one $p\pi$ -orbital occurs in the planar geometry, and overlap with the other $p\pi$ -orbital in the perpendicular geometry.¹ Experiments undertaken by Liberles *et al.* involving X-ray diffraction studies, solution studies (UV experiments), and dipole moment calculations indicate that diphenylacetylene adopts a coplanar geometry.² It has been suggested that the p orbitals of the aromatic rings overlap with the same set of p orbitals of the alkyne which leads to the planar conformation.²

Kemp and Gong demonstrated in their studies of β -turn mimetics that by introducing an intramolecular hydrogen bond into diphenylacetylene systems, **93** and **94**, then the rotational barrier is increased to 7.19 kcal/mol around the phenyl-alkyne bond and the system is stabilised into well-defined conformations, **Figure 3.1**.^{1,3,4} Hamilton further expanded this design in synthetic mimetics by synthesising a foldamer scaffold based on 2,2-disubstituted indolin-3-ones, **95**.⁵ Intramolecular hydrogen bonding occurs between the carbonyl oxygen of an indolinone and a neighbouring N-H which favours the substituents lying on the same side of the molecule, thereby adopting the desired conformation and mimicking a β -strand.

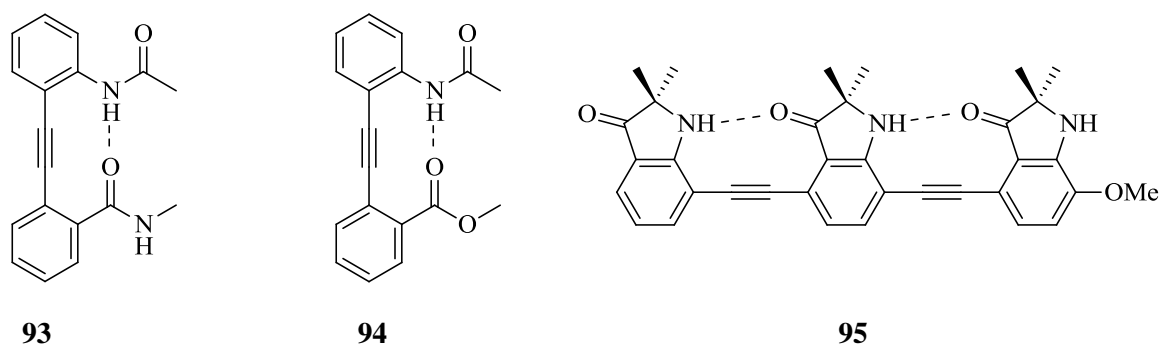


Figure 3.1: Previously described diphenylacetylene units.

These observations prompted Hamilton and co-workers to transform the stabilised intramolecular diphenylacetylene units, namely **94**, into a molecular switch.⁶ By introducing a second hydrogen bond donor in the form of a competing amide *ortho* to the alkyne spacer unit, it was demonstrated that the ester hydrogen bond acceptor preferred one amide over the other depending on the acidity of the N-H. By attaching electron-withdrawing/donating groups it was possible to predict which N-H was the preferred hydrogen bond donor. An electron rich carbonyl results in the N-H bond being less acidic and therefore a weaker hydrogen bond donor. In contrast, an electron poor carbonyl has the effect of increasing the acidity of the N-H, making it a stronger hydrogen bond donor. Hamilton *et al.* successfully delivered this concept by synthesising **96**. By single crystal X-ray diffraction and ¹H NMR studies it was demonstrated that indeed **96** adopted the predicted conformation and intramolecular hydrogen bonding occurred between the more acidic *p*-NO₂-amide and the ester, **Figure 3.2**.

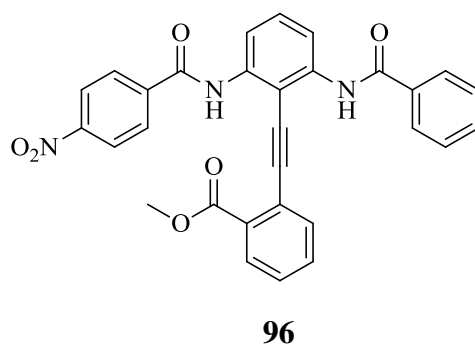


Figure 3.2: Varying the acidity of NH influences the conformational equilibrium.

Further developing this concept, Hamilton and co-workers recently reported a pH-dependent molecular switch exploiting the 2,6-benzamidodiphenylacetylene system.⁷ Firstly, **97** was synthesised and it was established by single crystal X-ray diffraction that the ester was biased towards the benzamide N-H since *p*-NMe₂ is electron-donating therefore weakening the hydrogen bond strength of the *p*-NMe₂-benzamide. Next, it was discovered by ¹H NMR that conversion to the dimethyl-ammonium ion, **98**, formed a conformational switch, since protonation results in the formation of an electron-withdrawing group and the ester group now favours intramolecular hydrogen bonding to the stronger hydrogen bond donor *i.e.* *p*-N(H)Me₂⁺, **Figure 3.3**.

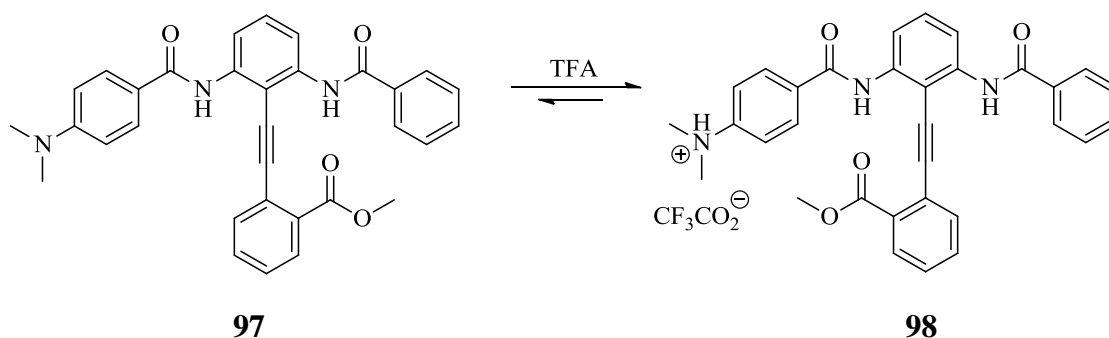


Figure 3.3: *pH dependent molecular switch.*

Hamilton also extended his research to develop an anion-dependent intramolecular hydrogen bond switch, **Figure 3.4**.⁸ Building on the diphenylacetylene scaffold, a urea group was incorporated into the structure since ureas are known to form strong complexes with anions. ¹H NMR studies were conducted before and after the addition of tetrabutylammonium chloride (NBu₄Cl). A switch in conformation was observed between the urea protons and amide proton after the addition of Cl⁻. The phenylurea is a stronger hydrogen bond donor than the acetamide in **109**. However, once the Cl⁻ binds to the urea, a switching effect occurs in **110**.

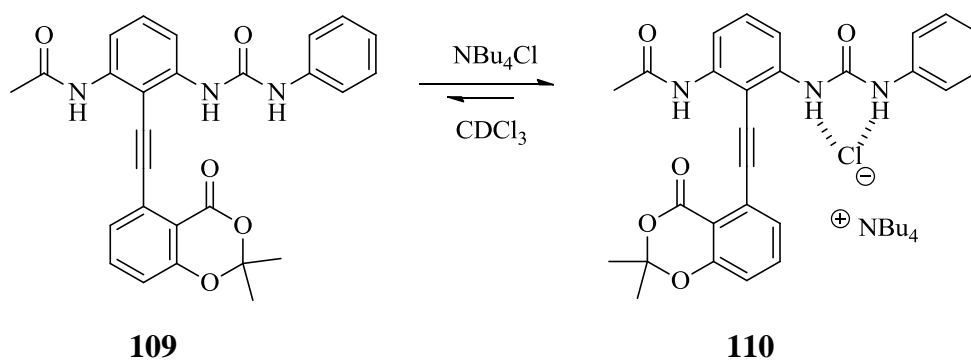


Figure 3.4: *Anion dependent molecular switch.*

The significant development by Hamilton of exploiting the diphenylacetylene unit as a switching entity prompted the exploration of its ability to act as a scaffold in this particular study, incorporating amide and sulfur functional groups. Recent work in our group has demonstrated that sulfoxides, in particular, form strong hydrogen bonds with amides, while the analogous sulfides and sulfones are much weaker hydrogen bond acceptors.⁹ The diphenylacetylene unit provided an excellent backbone on which to construct a molecule in

which the effects of varying the oxidation level of sulfur on the hydrogen bond interactions in the solid state could be studied, with a view to the development of a molecular switch.

3.1.2. Hunter's Rationale

The initial concept of this study was based on Hunter's observations of the abilities of specific functional groups to act as hydrogen bond donors and acceptors.¹⁰ Previous to Hunter's experiments, pKa values were employed to classify the strengths of hydrogen bond donors and acceptors. However, pKa is a measure of proton transfer rather than a direct measure of hydrogen bond strength and therefore is not ideal for comparing the hydrogen bond donor/acceptor strength of different functional groups.

Hunter developed a method based on molecular electrostatic potentials (MEPs) to quantify relative hydrogen bond donor/acceptor strengths across a series of functionalities. The values of the hydrogen bond donor (α) and acceptor (β) are calculated from the MEP. It was demonstrated that although a carboxylic acid (pKa ~ 4.2) is more acidic than a phenol (pKa ~ 10), the calculated MEPs suggest that phenols are better hydrogen bond donors. Since the hydrogen bond is the attraction of two opposite charges, the best hydrogen bond donor has the highest positive charge *i.e.* high α value, and the best acceptor has the highest negative charge *i.e.* high β value. Therefore, Hunter's approach enables a hierarchy of hydrogen bond interactions to be developed. This classification was extremely useful in the design of a hydrogen bond dependent molecular switch. **Table 3.1** highlights some of the functional groups featured in Hunter's table.¹⁰ The sulfoxide, sulfone and amide functional groups are of particular interest to this study. The sulfoxide is a particularly good hydrogen bond acceptor with its β value higher than esters or sulfones.

Table 3.1: Hunter's table for hydrogen bond donors and acceptors.¹⁰

H-bond donors	$\alpha^{[a]}$	$\alpha^{[b]}$	H-bond donors	$\alpha^{[a]}$	$\alpha^{[b]}$	H-bond donors	$\alpha^{[a]}$	$\alpha^{[b]}$
alkane		0.4	amine		1.5	amide		2.9
alkene		0.7	aldehyde		1.6	urea		3.0
benzene		1.0	thiol		1.7	thioamide		3.3
alkyl thioether		1.0	thiophenol	1.8		carboxylic acid		3.6
alkyl chloride		1.3	alkyne	1.9		phenol		3.8
carbon tetrachloride	1.4		aniline	2.1		phosphoric acid		4.0
alkyl ester		1.5	alcohol	2.7		perfluoro- <i>tert</i> -butanol		4.9
H-bond acceptors	$\beta^{[a]}$	$\beta^{[b]}$	H-bond acceptors	$\beta^{[a]}$	$\beta^{[b]}$	H-bond acceptors	$\beta^{[a]}$	$\beta^{[b]}$
alkane		0.3	alkyne	2.7		alcohol		5.8
carbon tetrachloride	0.6		thiol	2.7		sulfone		6.3
alkene	1.1		thioether	3.6		amine		7.8
alkyl chloride	2.2		water	4.5		amide		8.3
benzene	2.2		aldehyde	4.7		urea		8.3
thiophenol	2.2		carboxylic acid	5.3		sulfoxide		8.9
phenol	2.7		ester	5.3		phosphine oxide		9.9

[a] Values based on literature values.

[b] Values based on the molecular electrostatic potential surface.

3.1.3. Design of diphenylacetylene targets

Before synthesis could commence, a system suitable to act as a molecular switch, influenced by sulfur oxidation was designed. Many different compounds, along with their synthetic strategies were devised and considered as suitable targets. Compounds **A**, **B** and **C** were initially envisaged to act as a potential switch, **Figure 3.5**.

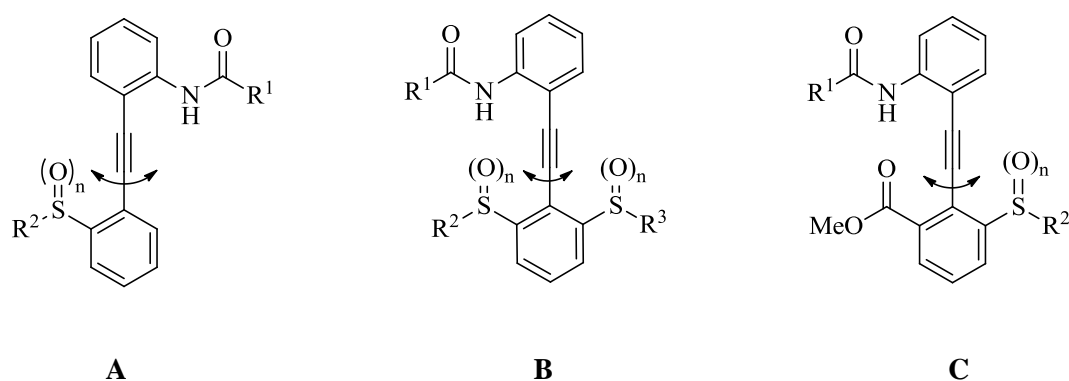
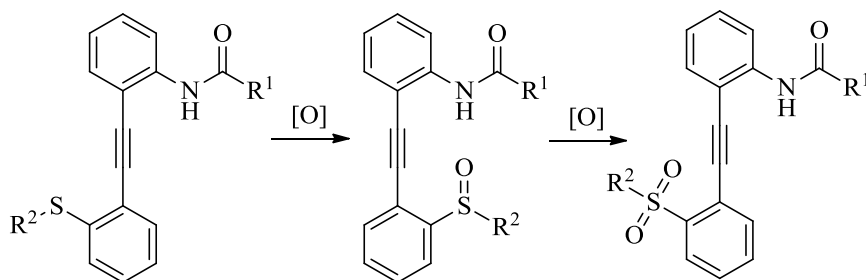


Figure 3.5: Initial candidates **A**, **B** and **C** to act as a molecular switch. $n = 0, 1, 2$.

By applying Hunter's rationale it was envisaged that in **A** at the sulfide level, interaction between the sulfur and amide is not expected and the dominant solid state interaction predicted is the $\text{N-H}\cdots\text{O}=\text{C}$ intermolecular interaction. As a result, it would be expected that the sulfide should lie on the opposite side to the amide, as illustrated in **Scheme 3.1**, thereby enabling the intermolecular $\text{N-H}\cdots\text{O}=\text{C}$ interaction. On oxidation to the sulfoxide, the strong intramolecular $\text{N-H}\cdots\text{O}=\text{S}$ interaction should compete effectively with the intermolecular $\text{N-H}\cdots\text{O}=\text{C}$ interaction as sulfoxides are potent hydrogen bond acceptors.¹¹ In this case, the sulfoxide should lie on the same side as the amide, according to Hamilton's model. On further oxidation to the sulfone, which is a weaker hydrogen bond acceptor than the sulfoxide, it was anticipated at the outset that the strong $\text{N-H}\cdots\text{O}=\text{C}$ intermolecular interaction should once again dominate, resulting in the sulfone lying on the opposite side to the amide.



Scheme 3.1: Envisaged change in conformation of **A** as a result of varying the oxidation level of sulfur.

Further developing this concept in **B**, the introduction of two competing sulfur-containing moieties was envisaged, **Figure 3.5**. Competition between the two groups for intramolecular hydrogen bonding to the amide should influence the conformation of the phenylacetylene moiety. Thus, selective oxidation of the sulfur groups so that one is a sulfoxide while the other is a sulfide or sulfone should have a powerful influence on the preferred conformation. Alternatively, varying the electronic properties of the sulfur substituents through variation of 'R²' and 'R³', while maintaining the same oxidation level at sulfur should provide a more subtle influence on the conformation.

Another interesting approach would involve developing a system resembling **C**, in which competition would exist between different hydrogen bond acceptors for the amide donor, **Figure 3.5**. Hunter's table clearly indicates that while an ester is a stronger hydrogen bond acceptor than a sulfide, both the sulfoxide and sulfone moieties are more powerful hydrogen

bond acceptors than the ester, **Table 3.1**. Thus in **C**, at the sulfide level, the conformation is envisaged to be controlled by an intramolecular N-H...O=C hydrogen bond between the amide and ester, but at higher levels of oxidation rotation is envisaged to enable N-H...O=S intramolecular hydrogen bonding between the amide and sulfoxide or sulfone.

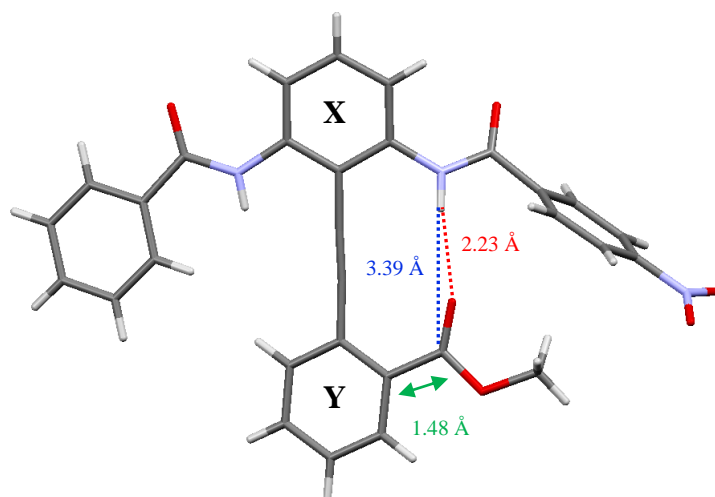


Figure 3.6: *Crystal Structure of 96.*

At the outset of this work, a key question to be considered was if the diphenylacetylene backbone provided sufficient space to replace the carbonyl group in Hamilton's system with sulfur-containing substituents in **A**, **B** and **C**, while still enabling a planar N-H...O=S hydrogen bond. Examining the crystal structure of Hamilton's amide-ester, **96**, an intramolecular N-H...O=C hydrogen bond (2.23 Å) is observed. The distance between the N-H of the amide and the carbon of the ester is approximately 3.39 Å, **Figure 3.6**. The diphenylacetylene rings **X** and **Y** are also slightly out of plane with each other (~12.90°). According to Allen the average S...O bond length for a sulfoxide is 1.497 Å and 1.436 Å for a sulfone.¹² In the first instance, substituting the C=O in **96** with an S=O, and ignoring the difference between C...C and C...S bond distances, then a theoretical intramolecular N-H...O=S pocket distance of 1.89 Å for a sulfoxide and 1.95 Å for a sulfone would exist. However, it must be considered that the C...C bond distance (1.48 Å) in **96** is notably shorter than a typical C...S bond distance (1.80 Å), which is likely to impact on the N-H...O=S bond distance, potentially increasing it. Also it must be taken into account that while the ester functionality in **96** is in a planar conformation with the **Y** ring, it is unlikely that a sulfoxide would adopt this planarity since it is tetrahedral in geometry. This geometry could also potentially increase the N-H...O=S bond distance. A search of the CSD for N-H...O=S

hydrogen bond distances 1.00-2.30 Å, revealed 11 hits for intramolecular bonding and 37 hits for intermolecular bonding within the specified range, **Figure 3.7**. These results indicate that intramolecular N-H···O=S hydrogen bond interactions should be feasible within this diphenylacetylene system.

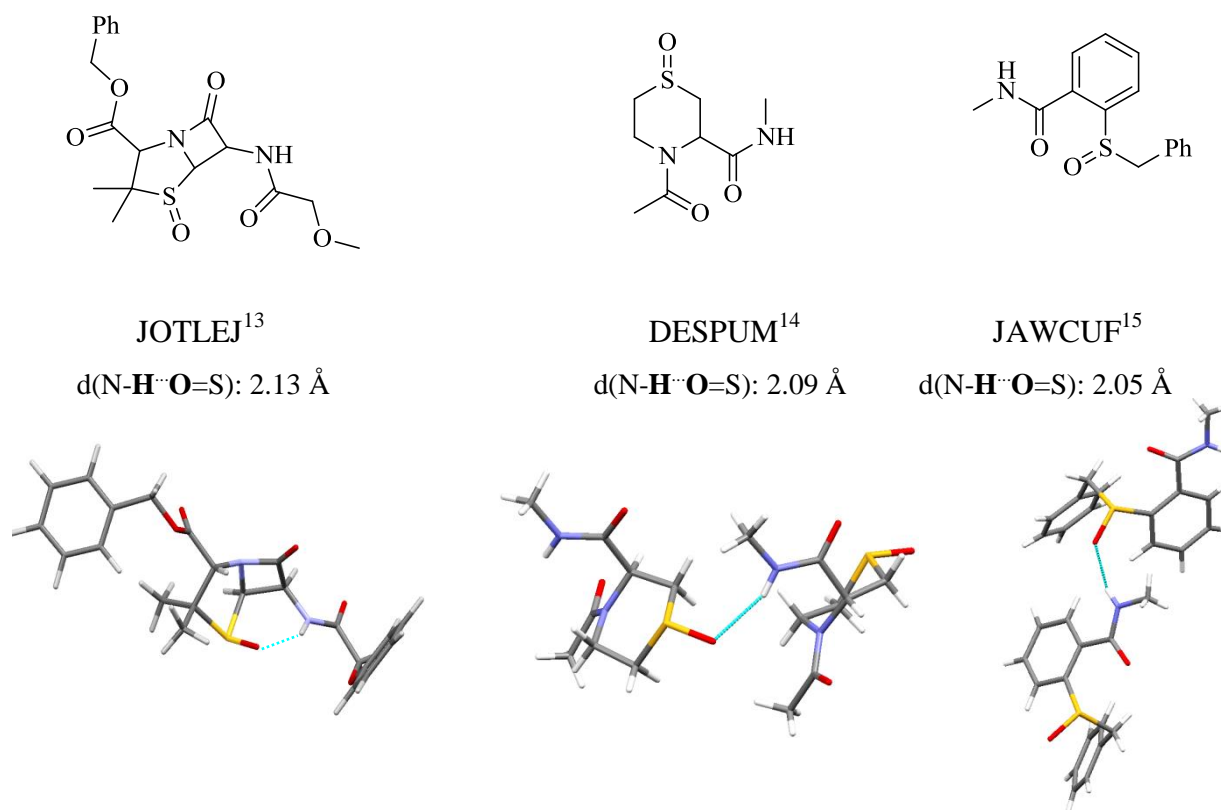
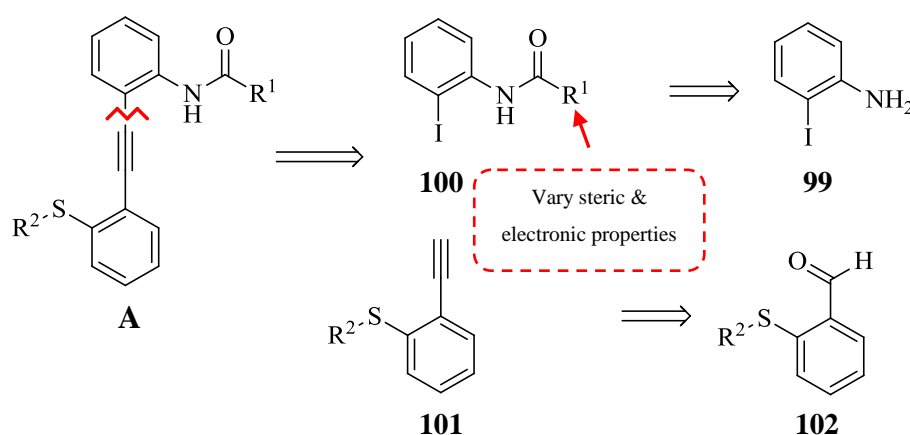


Figure 3.7: Crystal structures of JOTLEJ, DESPUM and JAWCUF displaying inter/intramolecular N-H···O=S interactions.

3.1.4. Synthetic Strategies for A, B and C

3.1.4.1. Synthetic Strategy A

To synthesise the core diphenylacetylene unit, the Sonogashira coupling approach has been widely described in the literature.^{1,5,6} The most efficient strategy to form **A** involved disconnecting the diphenylacetylene so that iodo-amides and sulfur substituted terminal alkynes would act as suitable precursors for the carbon-carbon bond forming reaction, **Scheme 3.2**. A series of iodo-amides, **100**, containing substituents with differing steric and electronic properties could be readily accessed from the widely available 2-iodoaniline, **99**, and a range of acyl chlorides. The sulfide-containing alkynes, **102**, can be attained from their respective aldehydes, **101**, by either the Corey Fuchs¹⁶ or the Bestmann-Ohira¹⁷ approaches. To the best of our knowledge the Sonogashira coupling in the presence of a sulfide has not been widely described in the literature, other than reports by Chen and Schneider.^{18,19}



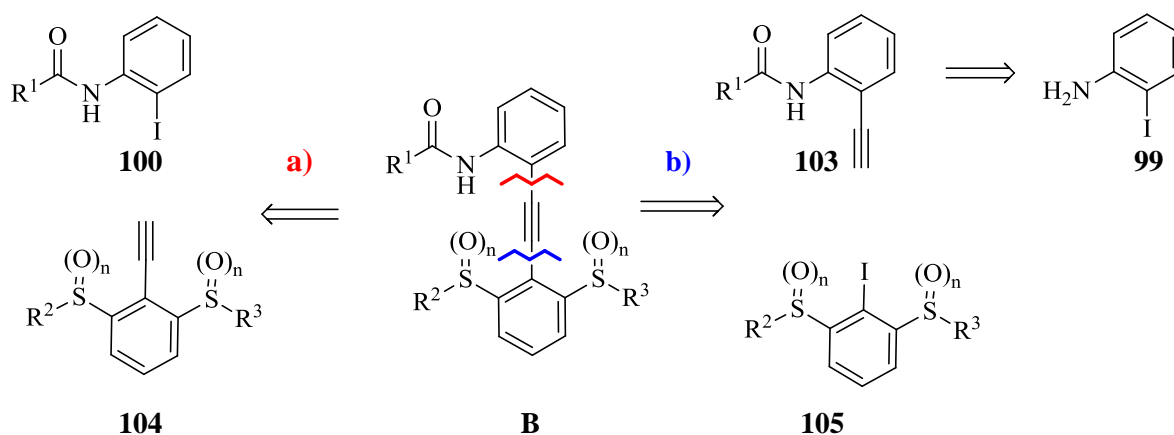
Scheme 3.2: Synthetic Strategy to access **A**.

This particular route would be a good starting point on which to access a large variety of compounds and study their hydrogen bond interactions. Also, the system could be adapted to include a second competing amide in the *ortho* position, similar to Hamilton's system, **Figure 3.2**.

3.1.4.2. Synthetic Strategy B

Two potential strategies were identified to access compound **B**, which incorporates two different sulfur functionalities in the *ortho* positions. A similar route to **A** could be adopted which involves preparing iodo-amides, **100**, and sulfide substituted terminal alkynes **104**, **Scheme 3.3a**). The synthesis of **104** would prove much more challenging than in the simpler compound **A** since now two sulfur functionalities would have to be in the *ortho* position and potentially contain different substituents. Also, the selective oxidation of each sulfide would be very difficult to achieve.

The second strategy would involve assembling the diphenylacetylene from a terminal alkyne bearing amide, **103**, and an iodo-substituted sulfide, **105**, *via* Sonogashira reaction, **Scheme 3.3b**). The amide moiety, **103**, could be readily accessed from 2-iodoaniline, **99**, using a procedure similar to Costa *et al.*²⁰ Again, synthesis of the tri-substituted **105** could be quite difficult to achieve in sufficient yields for coupling.



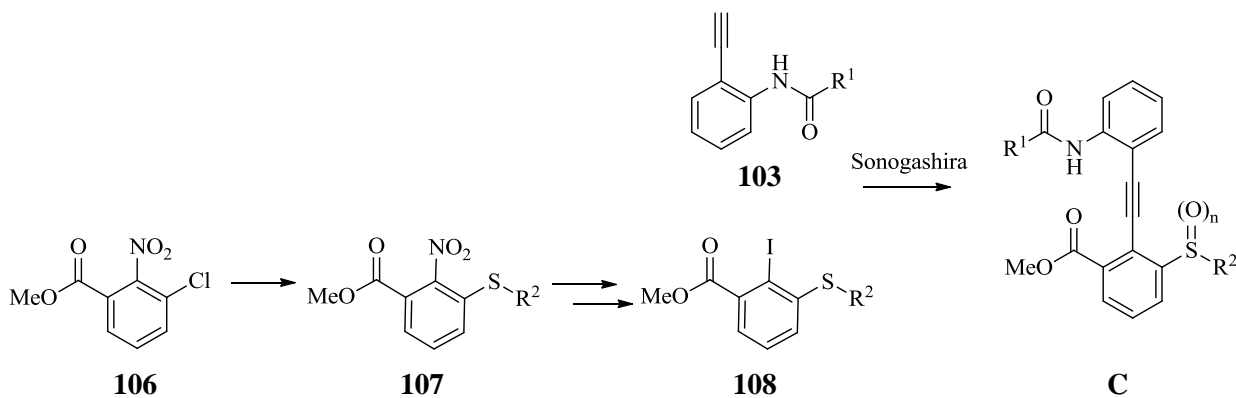
Scheme 3.3: Potential synthetic strategy to access **B**.

While **B** would be a very desirable system to investigate, the synthesis could be quite challenging and the ability to form a wide series of related systems could be difficult to achieve. Therefore, this particular route was not pursued for this project.

3.1.4.3. Synthetic Strategy C

To assemble a system similar to **C**, again the amide and ester/sulfide moieties would have to be synthesised separately and coupled utilising the Sonogashira reaction, **Scheme 3.4**. Synthesis of **106** has been described previously by Ashburn *et al.* from the corresponding commercially available acid.²¹ The sulfide could be attached by an S_NAr reaction to form **107**. Banzatti *et al.* have described a procedure for the reduction of a nitro group to an amine, followed by conversion to its corresponding iodide for 1,2,3-trisubstituted aromatics containing ester and carboxylic acid functionalities.²² This procedure could be attempted for the synthesis of **108**. The amide, **103**, could be synthesised as previously described for **B**. The coupling of **103** and **108** to lead to system **C** for solid state investigation is envisaged to be feasible using Sonogashira conditions.

A major challenge involving this approach is that it is envisaged that the sulfoxide and the sulfone may well lead to the same conformation. The sulfone, while a weaker hydrogen bond acceptor than the sulfoxide, is at the same time a stronger hydrogen bond acceptor than the ester, **Table 3.1**. Nonetheless, this may be an interesting strategy to pursue in the future and could be further developed.

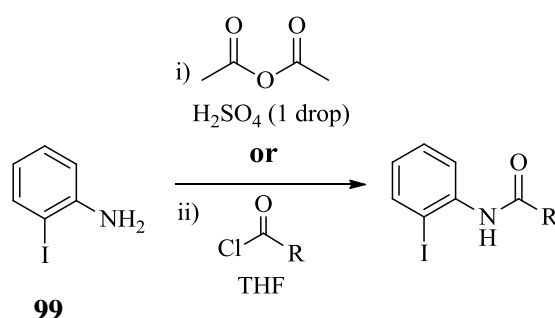


Scheme 3.4: Synthetic strategy to form **C**.

‘Synthetic Strategy A’ was the most advantageous route to pursue due to its accessibility and versatility. The Sonogashira precursors can be synthesised in two-step reactions and different electronic and steric properties can be easily introduced. Using this strategy, a wide range of compounds of the general structure **A** can be readily assembled and their solid state interactions can be studied in detail. This route is also quite flexible for expansion, and if necessary, the core structure can be adjusted to include other functional groups of interest.

3.1.5. Iodo-amide precursors

A series of iodo-amides, **116-119**, substituted with various electron-withdrawing/donating substituents, were readily synthesised in one step by reacting the commercially available 2-iodoaniline, **99** with a series of acid chlorides, **111-114**, according to a procedure similar to Barbero *et al.*²³ For the methyl derivative, **115**, the iodoamine, **99**, was stirred in acetic anhydride containing a drop of sulfuric acid, **Scheme 3.5**.²⁴ Different electron-withdrawing and donating groups were attached to investigate their effect on the acidity of the N-H and therefore influence the hydrogen bonding ability of the amide.



Scheme 3.5: Synthesis of iodoamides **115-119**.

Table 3.2: Yields obtained for iodoamides **115-119**.

Method	RCOCl ^a	R	Product	Yield %	Planar Angle (°) C ₆ H ₄ -I/HN-C=O
i	-	Me	115	59 ^{b,e}	45.8
ii	111	Ph	116	50 ^b	64.8
ii	112	<i>p</i> -NO ₂ -C ₆ H ₄	117	82 ^c	37.7
ii	113	<i>p</i> -F-C ₆ H ₄	118	60 ^d	74.7
ii	114	<i>p</i> -Me-C ₆ H ₄	119	54 ^d	-

a Commercially available (Sigma-Aldrich).

b Purified yield after recrystallisation from hexane.

c Unpurified yield but sufficiently pure for next stage of synthesis.

d Purified yield after column chromatography.

e Crystal structure determined.

Table 3.2 indicates the yields obtained for the iodoamides, **115-119**, which were all isolated as solids. Crystal structures for **116**,²⁵ **117**²⁶ and **118**²⁷ have previously been reported in the CSD. While the *p*-Me substituted benzamide, **119**, was obtained as a white solid, it was not crystalline and its structure could not be determined. A novel crystal structure was determined for the acetamide, **115**, after recrystallisation from CH₂Cl₂, **Figure 3.8**. It

crystallises in the $P2_12_12_1$ space group with $\text{NH}\cdots\text{O}=\text{C}$ C(4) chains dominating the structure. A polymorph of this material was also obtained after recrystallisation from hexane/ethyl acetate (9:1) with a $P1$ space group observed.

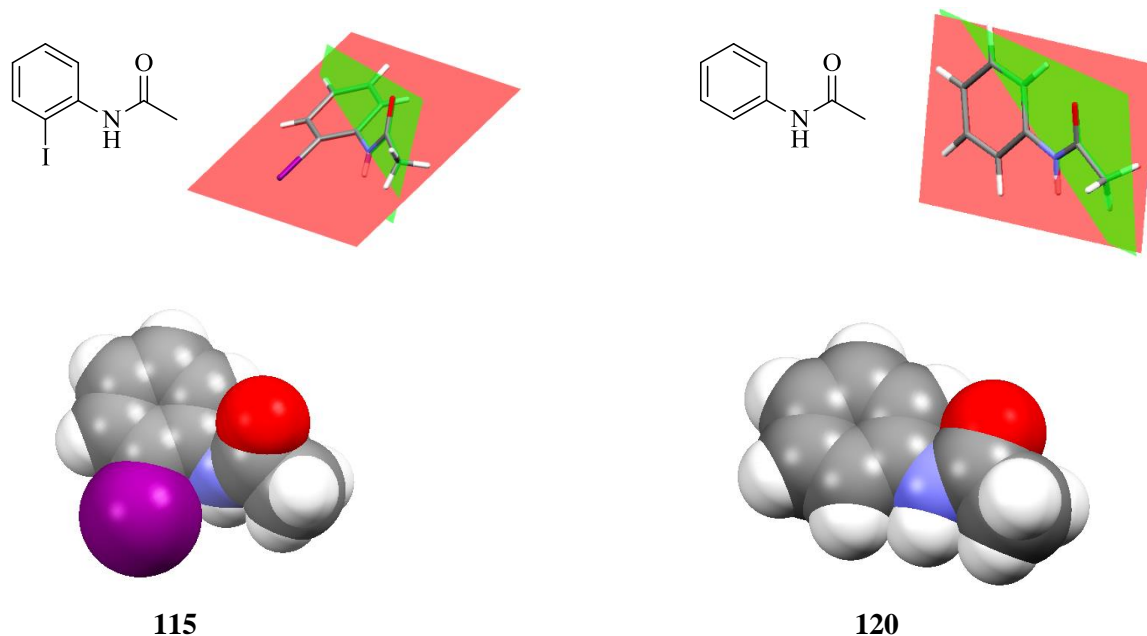
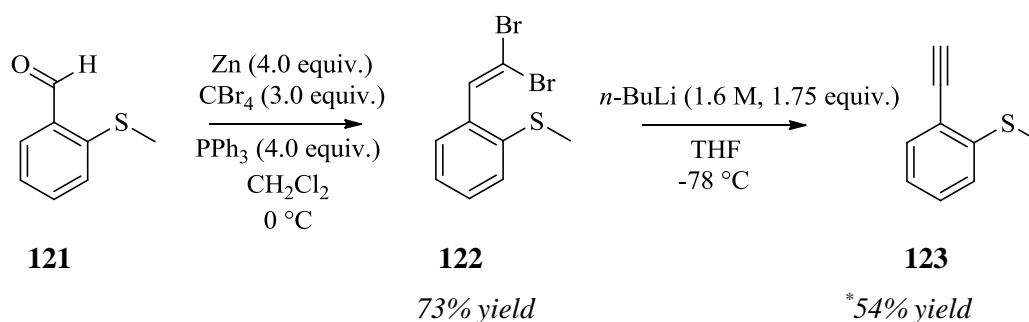


Figure 3.8: Comparing planar angles between iodo-amides **115** and **120**.

The amide ($\text{H}-\text{N}-\text{C}=\text{O}$) and aryl iodide ($\text{C}_6\text{H}_4-\text{I}$) moieties in the iodophenylacetamides (**115-118**) are not coplanar compared to their phenylacetamide counterparts. **Figure 3.8** displays this significant conformational variation between **115** and **120**. In **115**, the planar angle between the amide and aryl functionalities (45.8°) differs substantially from **120** (17.3°) because the larger size and electron density of the iodine atom compared to the hydrogen atom forces the amide further out of the plane in **115**. This is illustrated in the space-fill diagram featured in **Figure 3.8**. The iodophenylamides, **115-119**, are precursors for the Sonogashira reaction, so the iodine will be replaced with a carbon and the conformation of the amide in the coupled product should not differ substantially from the conformation of **120**. Also the rotation that exists about the $\text{HN}-\text{C}_6\text{H}_4$ bond suggests that sufficient flexibility exists to accommodate intramolecular hydrogen bonding when the sulfur functionalities are attached. Accordingly, examination of these planar angles after the Sonogashira coupling is of particular interest.

3.1.6. Terminal alkyne precursors

With a series of iodoamides successfully synthesised, the next stage in the strategy, as outlined in **Scheme 3.2**, involved the synthesis of terminal alkynes incorporating sulfur functionalities in the *ortho* position. The simple methyl sulfide, **123**, was initially targeted to minimise steric hindrance, once coupled to the iodoamides in **Table 3.2**, in order to maximise the possibility of intramolecular N-H...O=S interactions occurring. Lehane had previously described the synthesis of **123** utilising Corey-Fuchs methodology.²⁸ The commercially available aldehyde, **121**, was firstly converted by a C₁-homologation reaction to the dibromoalkene, **122**, in a solution of zinc, carbon tetrabromide (CBr₄) and triphenylphosphine (PPh₃), **Scheme 3.6**. Lehane had isolated **122** as a yellow brown oil but in this study **122** was obtained as a white solid in 73% yield after column chromatography. This was subsequently recrystallised from CH₂Cl₂ to form a white crystalline solid and the novel crystal structure was then determined, **Figure 3.9**.



* (~60% pure after column chromatography)

Scheme 3.6: Corey Fuchs reaction to form **123**.

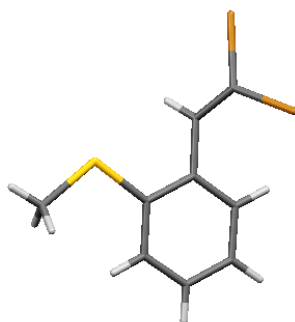
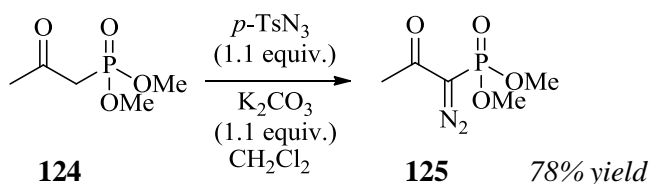


Figure 3.9: Crystal structure of **122**.

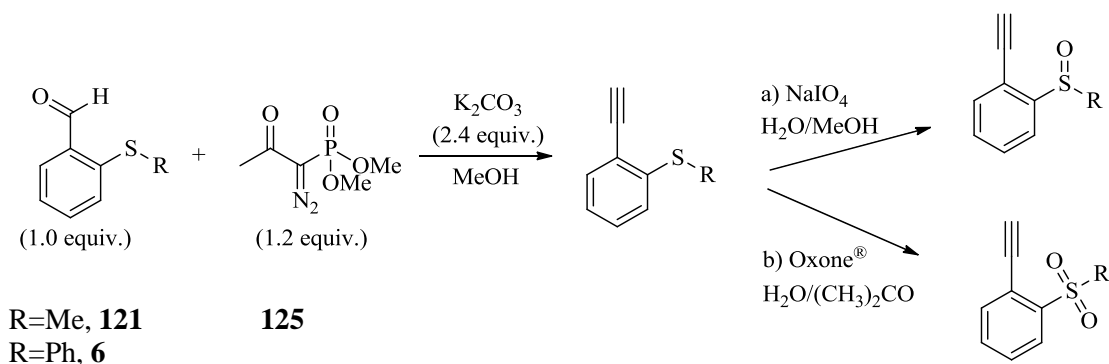
The acetylenic derivative, **123**, was prepared by reaction of **122** with *n*-butyllithium at -78 °C. The purification of **123** was very difficult to achieve by column chromatography with a number of unidentifiable materials co-eluting with the desired compound. Thus **123** was isolated in approximately 60% purity after column chromatography. The preparation of the phenyl substituted sulfide, **130**, was also attempted using this method but complete decomposition was observed after the addition of *n*-BuLi. These terminal alkynes which are the precursors for the subsequent Sonogashira reaction needed to be attained in good yields and purity. As the Corey-Fuchs method proved unsatisfactory as a means to access these precursors, presumably due to the strong basic conditions, an alternative strategy was required.

Diazoalkylphosphonate reagents have also been widely reported for the conversion of aldehydes to terminal alkynes.²⁹ These reagents are very appealing due to their mild nature and their ability to complete the transformation in one step. Seyferth,³⁰ Gilbert³¹ and Colvin³² were the first to show that aldehydes could be converted to terminal alkynes using dialkyl diazomethylphosphonates. The more recent Ohira and Bestmann method involves a significant modification to the Seyferth-Gilbert procedure in which 1-diazo-2-oxopropylphosphonate, **125**, (Bestmann-Ohira reagent) allows for the direct conversion of a wide range of alkyl and aromatic aldehydes, including base-labile substrates, to alkynes *in situ* at room temperature. The Bestmann-Ohira one-pot procedure was highly advantageous in this study to access the *ortho* substituted terminal alkynes due to the mild conditions employed. The Bestmann-Ohira reagent, **125**, was firstly prepared from the commercially available **124**, as illustrated in **Scheme 3.7**.²⁹



Scheme 3.7: Preparation of the Bestmann-Ohira reagent, **125**.

The benzaldehydes, **6**, which was prepared according to **Scheme 2.2**, and **121** which is commercially available, were reacted with the Bestmann-Ohira reagent, **125**, to form the desired alkynyl sulfides, **123** and **128**, in analytically pure form after column chromatography, **Table 3.3**. The sulfides, **123** and **128**, were then oxidised to their respective sulfoxides (**126** and **129**) and sulfones (**127** and **130**) in moderate to excellent yields after column chromatography, as illustrated in **Scheme 3.8**.



Scheme 3.8: The preparation of alkynyl sulfides, sulfoxides and sulfones.

Table 3.3: Yields obtained for alkynyl sulfides, sulfoxides and sulfones.

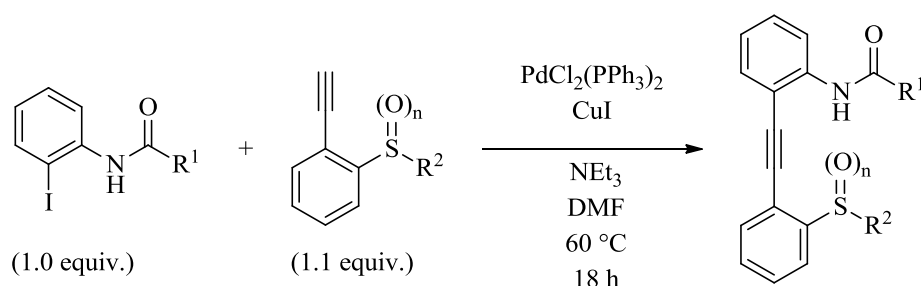
R	Sulfide	% Yield	Sulfoxide	% Yield	Sulfone	% Yield
Me	123	86	126	90	127	91
Ph	128	77	129	43	130	52

3.1.7. Sonogashira Coupling

Sonogashira cross-coupling reactions have been widely used in the construction of nanoscale architectures through the formation of acetylene-phenyl bonds.³³ Typically this involves the coupling of an acetylene to an aryl halogen centre. In this particular case the previously synthesised iodo-amides, **Table 3.2**, and the 2-alkynylphenyl sulfur functionalities, **Table 3.3**, are the building blocks of interest for the formation of the conjugated π system, as illustrated in **Scheme 3.2**. Sonogashira couplings have previously been successfully achieved in the presence of 2-alkynylbenzyl sulfides¹⁹ and simple *ortho* substituted methylthiophenylacetylenes¹⁸ in reasonable yields. However, Larock reported obtaining an inseparable mixture after attempting to couple the amide, **116**, and the alkynylsulfide, **123**, using Sonogashira conditions.³⁴

The reaction conditions for this study, as outlined in **Scheme 3.9**, employed bis(triphenylphosphine)palladium(II) dichloride as the palladium source, copper(I) iodide as the co-catalyst and triethylamine as base at 60 °C for 18 hours, which were similar conditions to those utilised by Hamilton for the amide-ester compounds.⁸ Using this sequence a number of novel diphenylacetylenes were prepared in which the substituents were varied to investigate electronic effects, **Table 3.4**. The sulfoxide, **132**, was synthesised by the oxidation of the sulfide, **131**, using sodium periodate in a water/methanol mixture, rather than by the Sonogashira coupling reaction. This demonstrates that the coupled products are suitably stable to further oxidation and functionalisation.

The successfully coupled products, featured in **Table 3.4**, are all novel, fully characterised by ¹H and ¹³C NMR, IR, *m/z* and HRMS and stable at room temperature. The majority of the compounds, except for **142** and **145**, were solids at room temperature and their crystal structures were determined where indicated.



Scheme 3.9: Sonogashira coupling conditions.

Table 3.4: Novel sulfides, sulfoxides and sulfones synthesised using Sonogashira coupling.

Amide	R ¹	Alkyne	R ²	n	Product ^f	% Yield ^a	PdCl ₂ (PPh ₃) ₂ (mol%)
115	Me	123	Me	0	131 ^{b,c}	70	5
-		-		1	132 ^{c,d}	88	-
		127		2	133 ^c	34	10
116	Ph	123		0	134 ^{b,c}	15	6
		126		1	135 ^c	15	10
		127		2	136 ^c	55	10
118	<i>p</i> -F-C ₆ H ₄	123		0	137 ^c	33	11
		126		1	138 ^c	81	12
		127		2	139 ^c	26	10
119	<i>p</i> -Me-C ₆ H ₄	123		0	140 ^c	56	11
		126		1	141 ^c	48	5
		127		2	142	28	10
115	Me	128	Ph	0	143 ^{c,e}	22	6
		130		2	144 ^{c,e}	95	12
116	Ph	128		0	145	15	10
118	<i>p</i> -F-C ₆ H ₄	128		0	146 ^c	37	12
		129		1	147 ^c	37	13
		130		2	148 ^c	82	13
119	<i>p</i> -Me-C ₆ H ₄	128		0	149 ^c	9	12

a Purified yield after column chromatography.

b Iodo-amide (2.0 equiv.), terminal alkyne (1.0 equiv.)

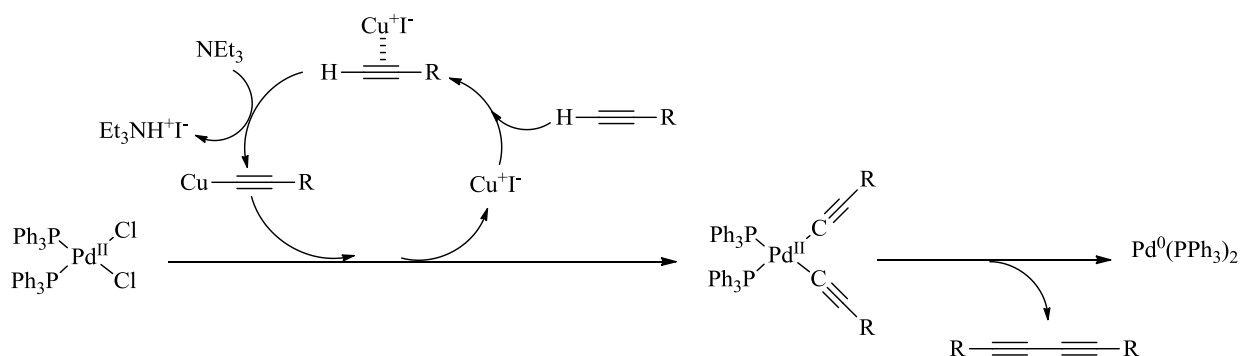
c Crystal structure determined.

d Synthesised from **131** using NaIO₄ (3.0 equiv.) in H₂O/MeOH, not by coupling of the sulfoxide in this instance.

e Heated at 60 °C for 2.5 hr.

f Novel compounds and characterised by ¹H and ¹³C NMR, IR, *m/z* and HRMS.

The yields obtained varied quite substantially between the products, featured in **Table 3.4**, after the Sonogashira coupling. Different catalyst loadings were employed in different experiments but no major improvement in the percentage yield was observed. It was noted in the crude ^1H NMR of the products in **Table 3.4**, that a substantial proportion of undesirable side products were formed. These side products had similar R_f values to the target compound and as a result, purification of the crude mixtures by column chromatography proved quite challenging. One particular problematic side-reaction for Sonogashira reactions, that has been widely documented in the literature, is Glaser coupling.³³ This is associated with the addition of copper salts as co-catalysts, which can lead to the generation of copper acetylides, resulting in the homocoupling of the terminal alkynes, in the presence of trace quantities of oxygen, **Scheme 3.10**.^{35,36}



Scheme 3.10: Mechanism for the palladium-catalysed oxidative homocoupling of terminal alkynes.^{33,37}

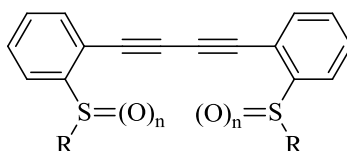


Table 3.5: Homocoupled by-products isolated after column chromatography.

Terminal Alkyne	n	R	Homocoupled Product
123	0	Me	150
126	1	Me	151
127	2	Me	152
128	0	Ph	153

Diacetylene homocoupling of the sulfides, **123** and **128**, the sulfoxide, **126**, and the sulfone, **127**, were readily identified in the crude ^1H NMR spectra of the products in **Table 3.4**. In most instances, in the synthesis of **131**, **134**, **135**, **137**, **139**, **142**, **143**, **145**, and **149**, featured in **Table 3.4**, pure samples of the homocoupled alkynes, **150-153**, were isolated by column chromatography, **Table 3.5**.

Copper-free Sonogashira couplings have been of intense interest in recent years to overcome these problematic side reactions. Since this project was focused on the strategic approach to access diphenylacetylenes bearing amide and sulfur functionalities, the optimisation of the coupling was not the primary objective. However, in the future, to overcome the formation of side-products, it may be worthwhile to introduce a suitable acetylene protecting group *e.g.* TMS, as it has been reported that *in situ* deprotection of the acetylene moiety in the presence of the Sonogashira coupling agents may lead to improved yields due to the cross-coupled product being favoured over the homocoupled product.³⁸

As summarised in **Table 3.4**, successful coupling of the two components bearing the amide and sulfur substituents was achieved, albeit in modest yields. Most significantly, we demonstrated coupling could be achieved with the sulfide, sulfoxide and sulfone moieties, with better yields in general at the higher level of oxidation, possibly reflecting coordination of the sulfide to the metal. These results are also very significant as a successful synthetic route has now been developed to access a wide range of novel diphenylacetylene compounds incorporating amide and sulfur functionalities and also provides a route to construct future systems.

3.1.8. Crystal Structure Data

The majority of the diphenylacetylenes featured in **Table 3.4** were isolated as solids after column chromatography and recrystallised from acetonitrile, to give crystals suitable for single crystal analysis. Analysis of the crystal structures of the diphenylacetylenes bearing the amide and sulfur moieties allowed the influence of varying the oxidation level of sulfur on inter/intramolecular hydrogen bond interactions to be investigated.

Beginning with a detailed examination of the crystal structures for the methyl substituted derivatives, **131**, **132** and **133**, some interesting packing motifs were observed. As discussed earlier in **Scheme 3.1**, it was expected that the amide functionality would be on the opposite side to the sulfide for compounds similar to **131**, since sulfur is considered to be a poor hydrogen bond acceptor.³⁹ Interestingly, the crystal structure of **131** revealed that the sulfide lies on the same side as the amide, **Figure 3.10**, and surprisingly the strong intermolecular NH...O=C interaction between neighbouring amides is not present. Instead, the carbonyl of the amide participates in bifurcated intermolecular hydrogen bonding to methyl hydrogens of neighbouring molecules, involving both the sulfide and amide functionalities. The phenyl rings are very slightly out of plane in relation to each other (~6.4°) which places the sulfide directly opposite the amide N-H. This is significant as the amide-sulfide pocket distance is 3.18 Å which is slightly shorter than that observed for Hamilton's amide-ester system (3.39 Å), **Figure 3.6**.

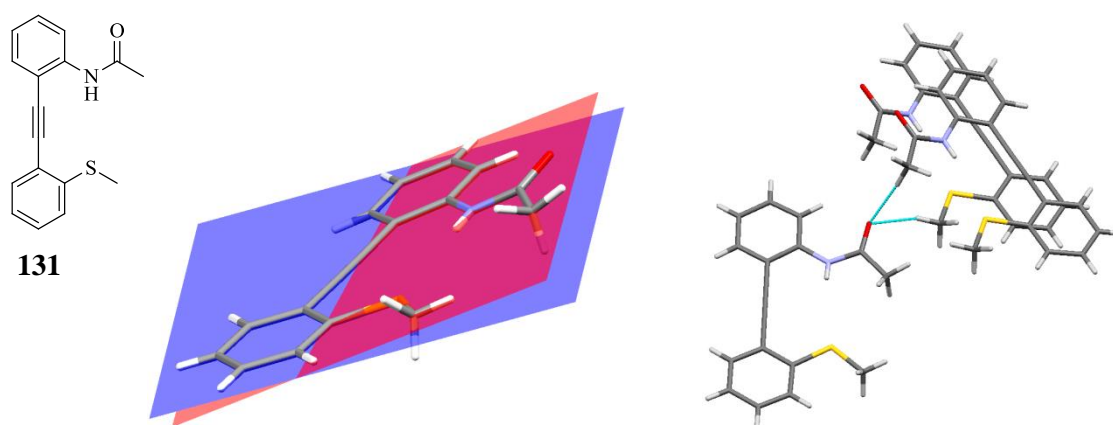


Figure 3.10: Crystal structure of **131** illustrating the conformation and intermolecular interactions.

Following oxidation of the sulfide, **131**, to the sulfoxide, **132**, an interesting conformation is adopted, **Figure 3.11**. The sulfoxide is positioned on the same side as the amide but points away from the N-H and instead forms an intermolecular $R_2^2(8)$ dimer with a neighbouring sulfoxide. It is interesting to note that the sulfoxide which is a stronger hydrogen bond acceptor than the amide now participates in intermolecular hydrogen bonding to the two methyl groups of a neighbouring molecule. This is in contrast to the sulfide, **131**, where the amide formed intermolecular interactions with the methyl groups.

The conformation that the sulfoxide functional group adopts in **132** can perhaps be attributed to the intramolecular spatial constraints. According to the sulfide, **131**, a distance of 3.18 Å exists between the sulfur and amide. Taking into consideration that the average sulfur oxygen bond distance in the sulfoxide, **132**, is 1.497 Å¹² suggests that a minimum intramolecular bond distance of 1.68 Å is available, if the system remains planar. Calculations at the AM1 level suggest that a small amount of out of plane twisting can be accommodated to give a N-H...O=S distance of 2.07 Å.* While results from the CSD search indicate that N-H...O=S intramolecular hydrogen bonds can form within this distance,⁴⁰ perhaps this particular diphenylacetylene is too constrained to accommodate such an interaction. Also the phenyl rings are twisted further out of planarity in relation to each other (15.6°) compared to the sulfide, **131**, possibly as a result of the added strain to accommodate the intermolecular hydrogen bond.

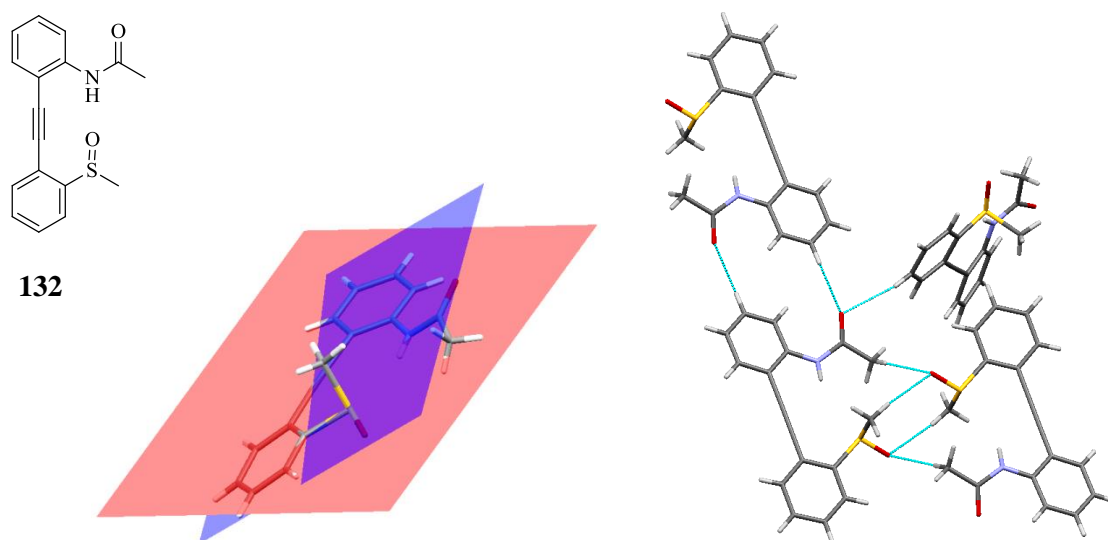


Figure 3.11: *Crystal structure of 132 and intermolecular interactions.*

* The AM1 calculation was discussed during the viva

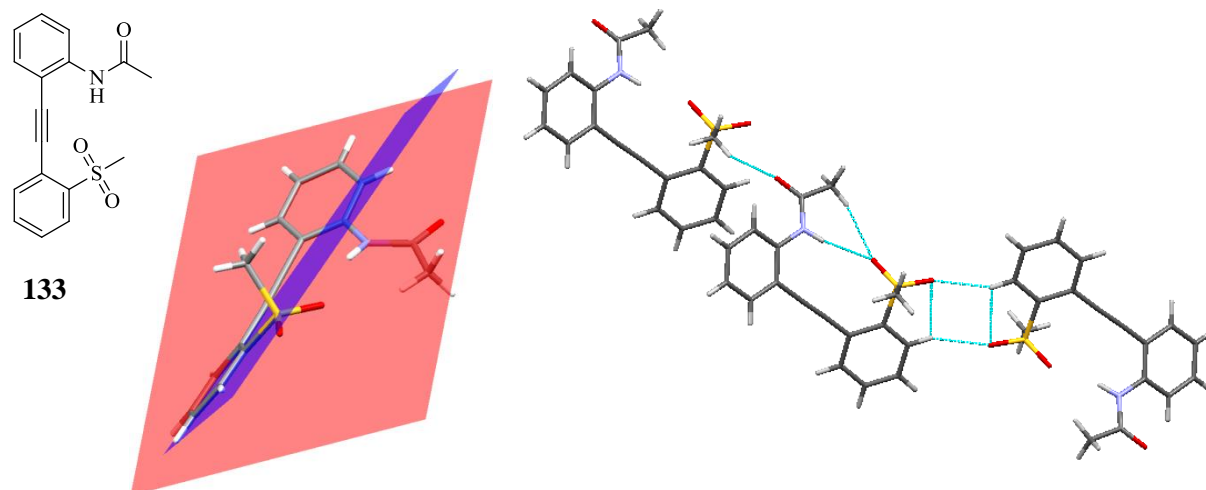


Figure 3.12: Crystal structure of **133** and intermolecular interactions.

Examining the crystal structure of the corresponding methyl sulfone, **133**, the amide and sulfur functionalities remain on the same side of the diphenylacetylene, as seen for both **131** and **132**, **Figure 3.12**. However, the phenyl sulfone twists further out of planarity with the phenyl amide with the angle between these phenyl rings substantially increasing after oxidation (34.4°). This significant twist in conformation is as a result of the extra oxygen in the sulfone compared to the sulfoxide. Due to the tetrahedral arrangement at sulfur, interaction between one of the sulfonyl oxygens with the amide N-H is increasingly likely. The spatial constrictions as described previously for the sulfoxide, **132**, forces the phenyl ring to twist significantly so that the sulfone functional group can fit within the available space. It is somewhat surprising that the sulfone does not lie on the opposite side to the amide so that the diphenylacetylene core adopts a more planar conformation. This observation may suggest that despite the spatial constraints, significant inter/intramolecular interactions play a key role in the conformation the molecule adopts. Specifically, the stabilisation associated with the N-H \cdots O=S hydrogen bond must be sufficient to compensate for the deviation from planarity in the diphenylacetylene system.

In **133**, intramolecular hydrogen bonding is observed for the first time within this diphenylacetylene system. An intramolecular N-H \cdots O=S hydrogen bond (2.29 \AA) and C-H \cdots O=S hydrogen bond occurs between the amide and a sulfonyl oxygen. The other sulfonyl oxygen forms an $R_2^2(10)$ intermolecular dimer with a neighbouring molecule. It is interesting to note, that in all cases (**131**, **132** and **133**), it is as anticipated the strongest hydrogen bond acceptor (the carbonyl oxygen for **131** and **133**; the sulfoxide oxygen for **132**) which is interacting, although with the neighbouring methyl groups.

Table 3.6 summarises the various planar angles observed for the methyl sulfide, **131**, sulfoxide, **132**, and sulfone, **133**. The angle between the planes of the two aromatic rings in the diphenylacetylene backbone, together with the angle between the amide functionality (H-N-C=O) and the phenyl ring to which its attached (C_6H_4), are compared for each compound, **Figure 3.13**. It is interesting to observe that the angles between the phenylacetylenes and the planar angles involving the amide increase as the oxidation level increases from sulfide to sulfoxide and sulfone, presumably to accommodate intramolecular hydrogen bonding motifs.

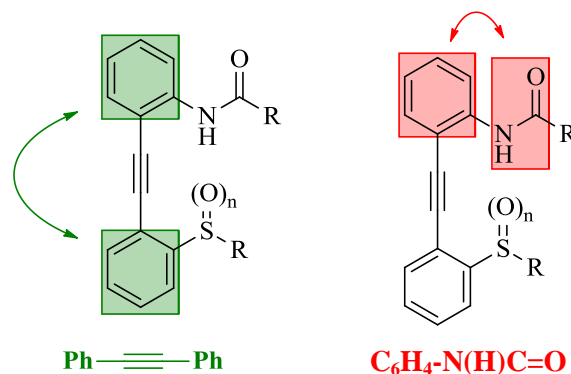


Figure 3.13: Comparison of planar angles.

Table 3.6: Summary of the angles observed in the methyl amide derivatives.

No.	n	Ph≡Ph (°)*	C ₆ H ₄ -N(H)C=O (°)**
131	0	6.4	8.6
132	1	15.6	23.3
133	2	34.4	26.3

* refers to the deviation from planarity of the aromatic rings in the diphenylacetylene backbone (green)

** refers to the angle between the planes of the amide and the aryl ring (red)

Attention then focused on the amide bearing a phenyl substituent. An almost planar geometry between the phenylacetylene rings exists for the sulfide, **134**, ($\sim 4.4^\circ$) similar to the simpler sulfide, **131**, **Figure 3.14**. The methyl sulfide once again lies on the same side as amide. The intramolecular distance between the sulfur and N-H is 2.96 Å which is a slightly smaller pocket distance than observed in **131**. Again for this particular sulfide, the expected strong intermolecular N-H \cdots O=C hydrogen bond interaction does not occur and instead the carbonyl oxygen is bifurcated to participate in weak intermolecular interactions to phenyl rings on neighbouring molecules. Steric hindrance may be a contributing factor in this unusual behaviour.

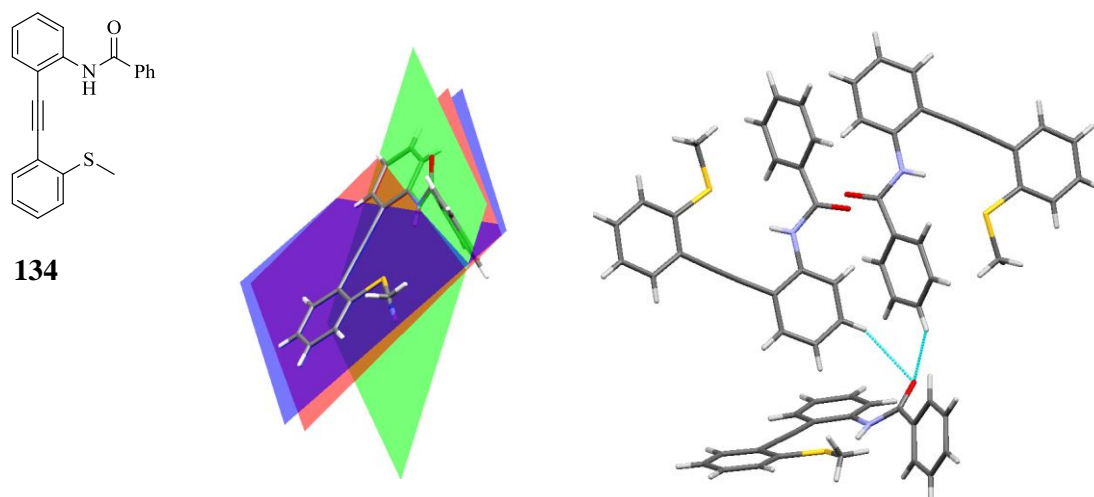


Figure 3.14: Crystal structure of **134** illustrating the conformation and intermolecular interactions.

A crystal structure of the corresponding sulfoxide, **135**, was successfully determined as an acetonitrile solvate, **Figure 3.15**. The phenylacetylene rings still remain almost completely planar in relation to each other ($\sim 4.7^\circ$) after oxidation which is in contrast to the sulfoxide, **132**, where a significant twist out of planarity was observed. The sulfoxide moiety remains on the same side as the amide and again the sulfoxide oxygen points away from the N-H of the amide, possibly as a result of the spatial limitations. The conformation of the amide (green) is also altered substantially after oxidation.

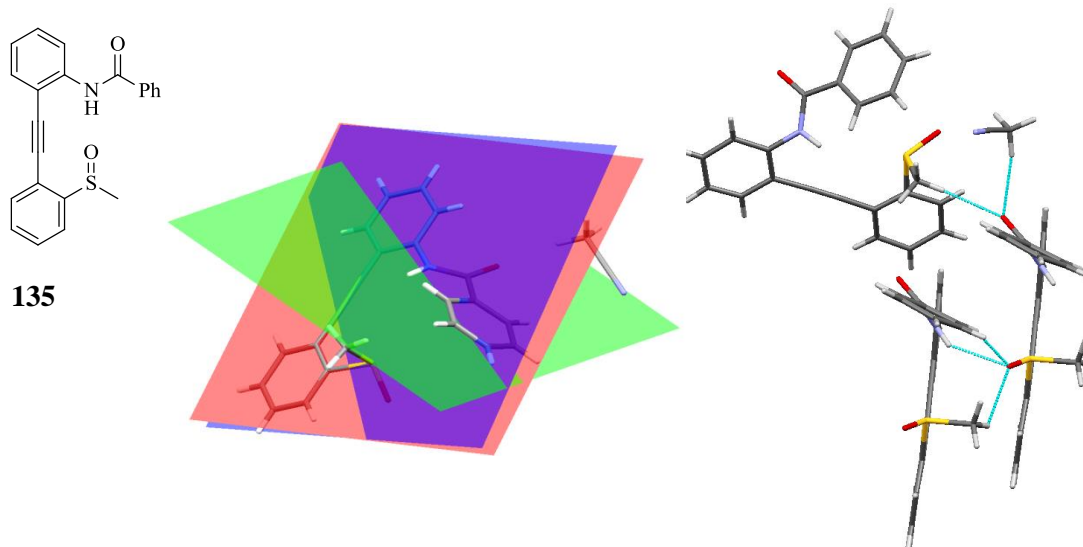


Figure 3.15: Crystal structure of **135** and intermolecular interactions.

The predicted N-H \cdots O=S hydrogen bond is observed between the sulfoxide and amide, although this interaction occurs intermolecularly (2.33 Å). However, this observation is significant as it verifies that the sulfoxide and amide moieties are forming hydrogen bonds and perhaps the system needs to be slightly adjusted so that this interaction occurs

intramolecularly. The sulfoxide oxygen is also involved in C-H...O=S intermolecular interactions to an aromatic ring and a methyl sulfoxide of a neighbouring molecule. The carbonyl of the amide is bifurcated, interacting with the acetonitrile molecule to form a solvate and also with a methyl sulfoxide.

The predicted switch in conformation is observed after oxidation to the sulfone, **136**, **Figure 3.16**. The phenyl sulfone rotates further out of the plane in relation to the amide (19.9°) and lies on the opposite side to the amide. A combination of factors may influence the switch in conformation, such as the bulky phenyl substituent on the amide, the narrow space available between the sulfone and amide or the intermolecular interactions. The predicted intermolecular N-H...O=C hydrogen bond interaction was confirmed by the presence of C(4) chains between neighbouring amides when the sulfone rotated to the opposite side of the molecule (2.28 \AA). The sulfone adopts a ladder like network of intermolecular hydrogen bonding interactions to adjacent sulfones, forming repeating $R_2^2(8)$ dimers. This particular molecule is the first instance where rotation around the alkyne is observed in response to altering the oxidation level at the sulfone.

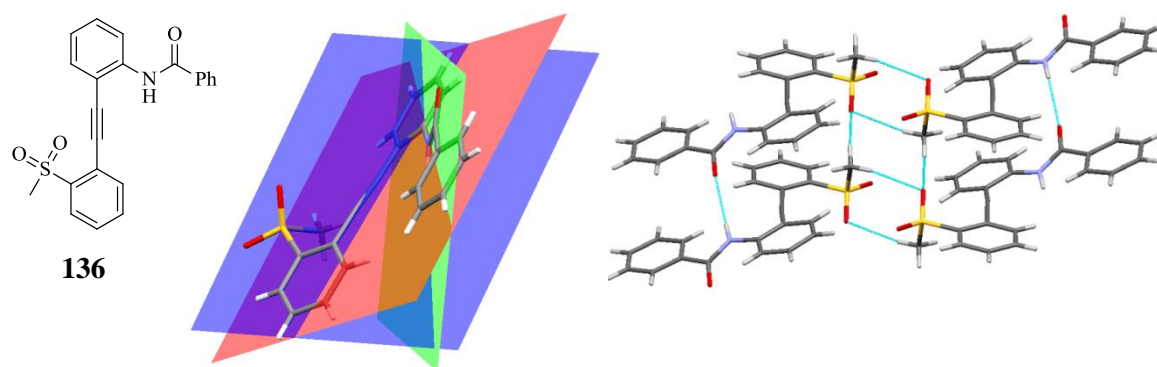


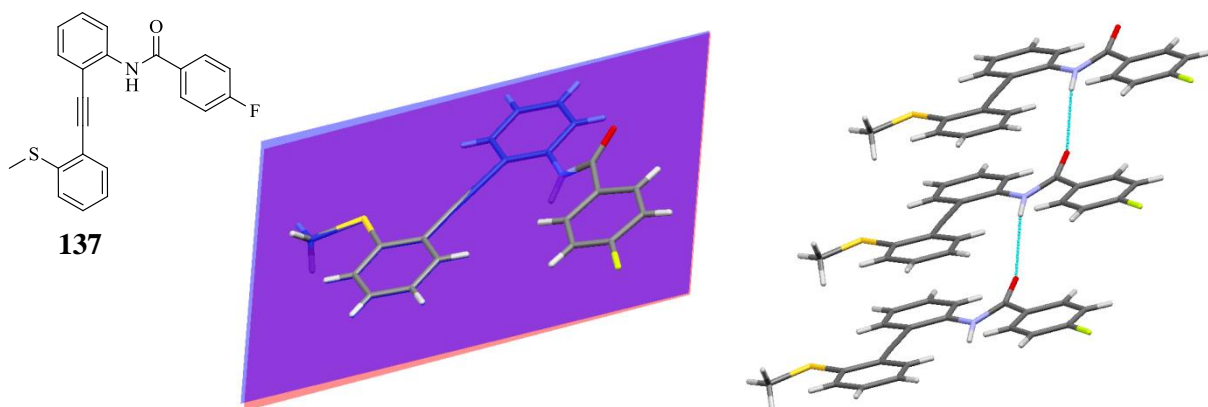
Figure 3.16: Crystal Structure of **136** where a switch in conformation is observed.

A summary of the planar angles, which are defined in **Figure 3.13**, are indicated in **Table 3.7** for the sulfide, **134**, sulfoxide, **135**, and sulfone, **136**. Again it was observed for the phenyl substituted amides that the angle between the phenylacetylene rings increased as the oxidation level increased. The amide functionality twisted further out of planarity when participating in N-H...O=C interactions as observed in the sulfoxide, **135**.

Table 3.7: Angles observed for phenyl amide derivatives.

No.	n	Ph—≡—Ph (°)	C ₆ H ₄ -N(H)C=O (°)
134	0	4.4	29.9
135	1	4.7	43.9
136	2	19.9	30.0

A very interesting result arose when the *para* fluoro substituted amide, **118**, was coupled to the alkynyl sulfide, **123**, and the crystal structure of **137** was determined, **Figure 3.17**. In this particular case the sulfide lies on the opposite side to the amide and adopts the conformation that was initially predicted in the design of these diphenylacetylene systems, **Scheme 3.1**. It appears that electronic effects play a key role within these compounds. The *p*-F substituent has an electron withdrawing effect on the carbonyl of the amide and therefore the N-H becomes more acidic and a stronger hydrogen bond donor. The enhanced acidity of the N-H in **137** therefore leads to the preferential formation of N-H···O=C C(4) chains (2.46 Å), above any other intermolecular interaction. The formation of these amide chains results in the sulfide lying on the opposite side to the amide. Perhaps in the previous crystal structures of the sulfides, **131** and **134**, the amide N-H was not sufficiently acidic to dominate as the main hydrogen bond donor and competing intermolecular interactions were influencing the crystal packing of the molecule and as a result the sulfide lay on the same side as the amide. A very small angle of 0.9° exists between the phenyl rings of the diphenylacetylene unit. This planar conformation results in a stacking effect being observed between the phenyl rings in the packing of the molecule.

**Figure 3.17:** Crystal packing observed for **137**.

When the iodoamide, **118**, was coupled to the sulfoxide, **126**, the crystal structure of **138** revealed that the sulfur moiety remained on the opposite side to the amide, **Figure 3.18**. The phenylacetylene rings are also bent out of plane (16.6°), in contrast to its sulfide analogue, **137**. It is interesting to observe that the sulfoxide oxygen is once again facing out of the plane, similar to the conformation that other sulfoxides in the series displayed, *e.g.* **132** and **135**, although on the opposite side of the molecule. It was believed that spatial constraints between the amide and the sulfoxide functional group in **132** and **135** were perhaps forcing the sulfoxide oxygen out of the plane. However, the structure of **138** suggests that intermolecular interactions may be responsible for this behaviour. The N-H \cdots O=C C(4) chains observed in **137** are broken in the sulfoxide, **138**. Instead the amide is now partaking in N-H \cdots O=S intermolecular interactions (2.34 \AA), bonding to the strongest hydrogen bond acceptor in the molecule *i.e.* the sulfoxide oxygen. Intermolecular N-H \cdots O=S hydrogen bonds are formed in preference to intramolecular bonds.⁴¹

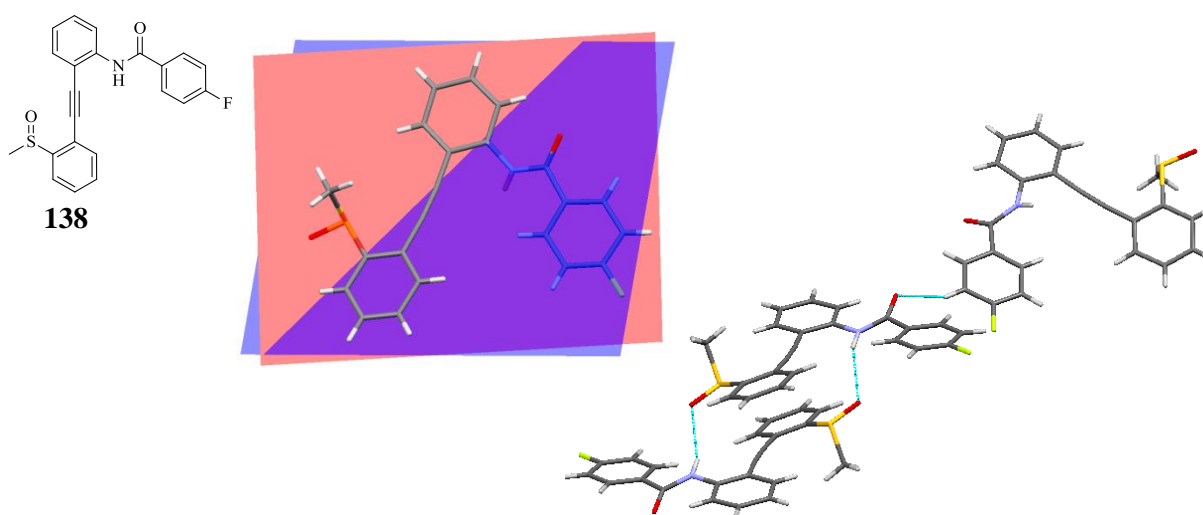


Figure 3.18: Crystal structure of **138**.

The sulfone, **139**, adopts the predicted conformation with the sulfone functionality lying on the opposite side to the amide. The diphenylacetylene backbone of the sulfone, **139**, twists further out of planarity (20.7°), as illustrated in **Figure 3.19**. The predicted interactions are also displayed with the amide reverting back to N-H \cdots O=C intermolecular interactions (2.32 \AA), which are comparable to the corresponding sulfide, **137**, as amides are stronger hydrogen bond acceptors than sulfones. The sulfones are linked by C-H \cdots O=S intermolecular interactions (2.49 \AA).

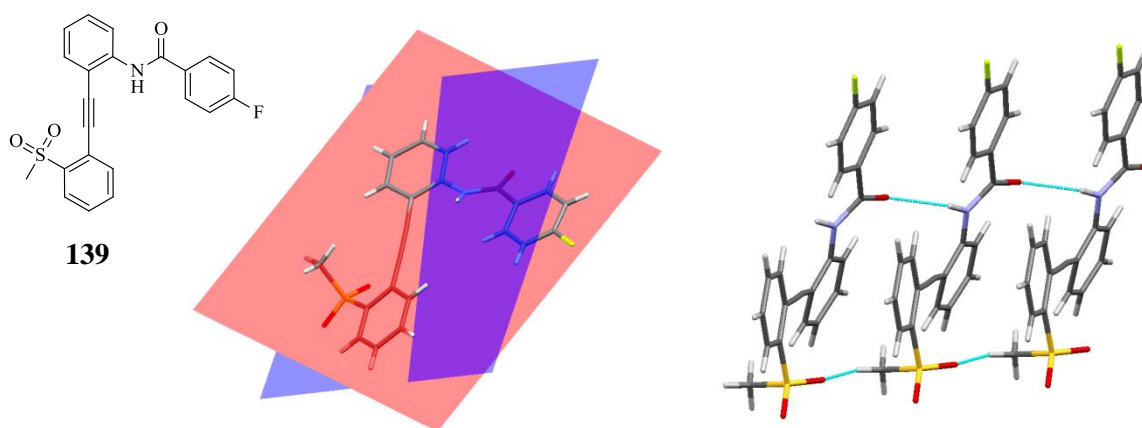


Figure 3.19: Crystal structure and intermolecular interactions for **139**.

The planar angles for the *p*-F amides* at the sulfide, **137**, sulfoxide, **138**, and sulfone, **139**, oxidation levels are compared in **Table 3.8**, as defined in **Figure 3.13**. Again, as observed in the methyl and phenyl substituted amides, the degree of rotation between the phenylacetylene rings increases as the oxidation level increases. The *p*-F substituted diphenylacetylenes gave very encouraging results as the predicted interactions were observed. Although the sulfoxide, **138**, did not adopt the desired conformation, the N-H...O=S interaction occurred intermolecularly.

Table 3.8: Angles observed for *p*-F derivatives.

No.	n	Ph—≡—Ph (°)	C ₆ H ₄ -N(H)C=O (°)
137	0	0.9	27.7
138	1	16.6	24.4
139	2	20.7	28.0

The results from the *p*-F substituted diphenylacetylenes suggests that the N-H...O=C intermolecular interactions are more likely to form when the amide is electron poor, therefore resulting in the N-H being more acidic. The formation of the N-H...O=C C(4) chains blocks the sulfur functionality from lying on the same side as the amide. To further investigate the theory that varying the acidity of the amide N-H influences the intermolecular interactions and therefore the overall conformation of the molecule, a *para* methyl substituted amide was introduced. Since *p*-Me is electron donating, the amide N-H is expected to be less acidic than the unsubstituted or *p*-F analogues, **137-139**. Therefore, by attaching *p*-Me substituted amides to the diphenylacetylene core, competing hydrogen bond

* *p*-F/*p*-Me amide refers to the substituent on the amide (see **Table 3.4**)

donors should partake in hydrogen bonding to the carbonyl, overcoming the formation of the N-H \cdots O=C C(4) chains in this compound. At the outset, the *p*-Me diphenylacetylenes were expected to display conformations similar to the methyl (**131**, **132**, **133**) and phenylamide (**134**, **135**, **136**) derivatives, rather than the *p*-F phenyl derivatives.

The crystal structure of the sulfide, **140**, suggests the hypothesis that the acidity of the amide N-H plays a key role in determining the conformation that the molecule adopts, **Figure 3.20**. The methyl sulfide is positioned on the same side as the amide due to the lack of formation of N-H \cdots O=C intermolecular hydrogen bond interactions which would ultimately block this site. Instead the carbonyl participates in intermolecular C-H \cdots O=C interactions involving methyl and aromatic hydrogens from neighbouring molecules as these are possibly competing with the amide N-H to act as the major hydrogen bond donors. These interactions are very similar to the interactions observed in the sulfides, **131** and **134**.

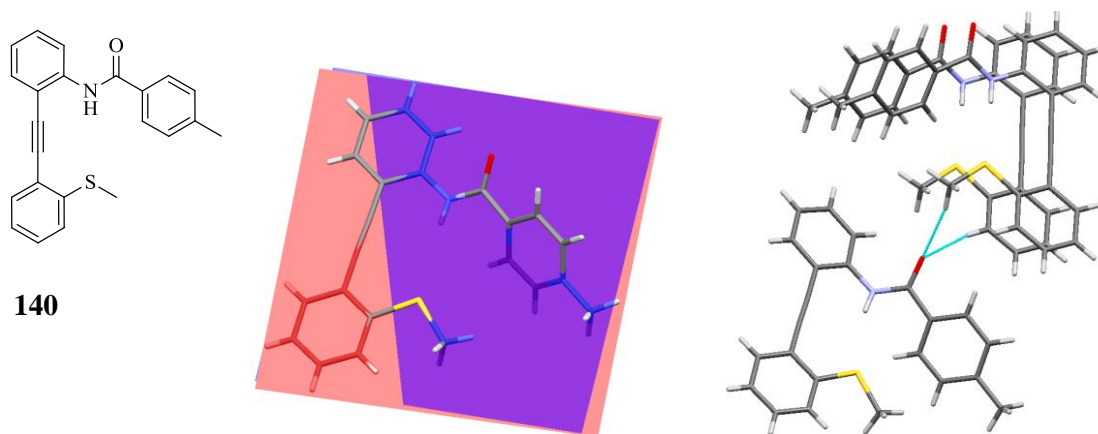


Figure 3.20: Crystal structure of **140** and hydrogen bond interactions observed.

The sulfoxide, **141**, adopts a similar conformation in the diphenylacetylene backbone to that of its corresponding sulfide, **140**, with the sulfur functionality lying on the same side as the amide, **Figure 3.21**. The predicted N-H \cdots O=S interaction is once again observed in an intermolecular fashion (2.29 Å). While in the sulfide, **140**, it was the C-H \cdots O=C forming weak intermolecular hydrogen bonding interactions, in the sulfoxide, **141**, this switches to C-H \cdots O=S interactions, as sulfoxides are stronger hydrogen bond acceptors than amides.

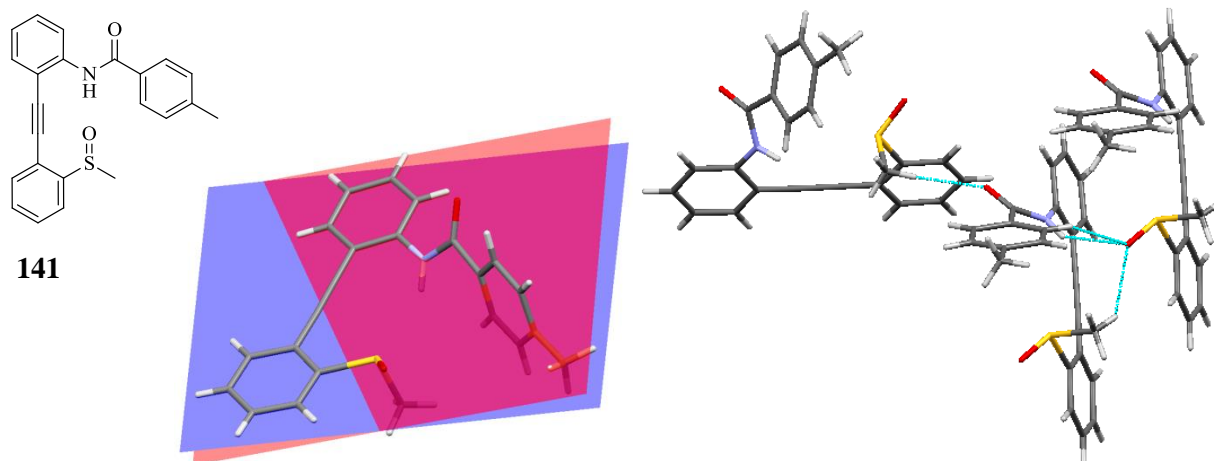


Figure 3.21: Crystal structure of **141** and intermolecular interactions observed.

The sulfoxide oxygen once again adopts a conformation out of the plane, with the intramolecular distance between the sulfur and amide N-H approximately 3.41 Å. Although this pocket distance seems feasible for the N-H \cdots O=S intramolecular interaction to occur, consideration of Etter's rules,⁴¹ suggests that the sulfoxide in **141** would favour intermolecular hydrogen bonding since N-H \cdots O=S intramolecular bonding would involve the formation of a ten-membered-ring.

Table 3.9 indicates the angles observed for the sulfide, **140**, and the sulfoxide, **141**. In both cases the phenylacetylene rings are relatively coplanar. However the amide functionality is forced further out of planarity in **141** to enable formation of the N-H \cdots O=S intermolecular hydrogen bond. Thus, the energetic benefit gained from the intermolecular hydrogen bond is sufficient to compensate for the decrease in planarity around the amide. The sulfone, **142**, was obtained as a white solid after column chromatography. However, after multiple recrystallisation attempts from acetonitrile and CH₂Cl₂, a sufficiently crystalline sample could not be isolated and therefore its crystal structure could not be determined.

Table 3.9: Angles observed for p-Me derivatives.

No.	n	Ph—≡—Ph (°)	C ₆ H ₄ -N(H)C=O (°)
140	0	6.1	28.8
141	1	6.1	44.5

Next, the sulfur substituent was altered from a methyl to a phenyl group to investigate if steric factors impact on the rotation of the molecule. The sulfide, **143**, adopts a similar conformation to the simpler methyl substituted derivative, **131**, with the sulfide functional group lying on the same side as the amide, **Figure 3.22**. The intermolecular interactions are also similar to those observed in **131**, with bifurcated C-H \cdots O=C interactions occurring between the carbonyl of the amide to methyl and phenyl groups of neighbouring molecules. The phenylacetylene rings are almost completely planar in relation to each other (3.9°).

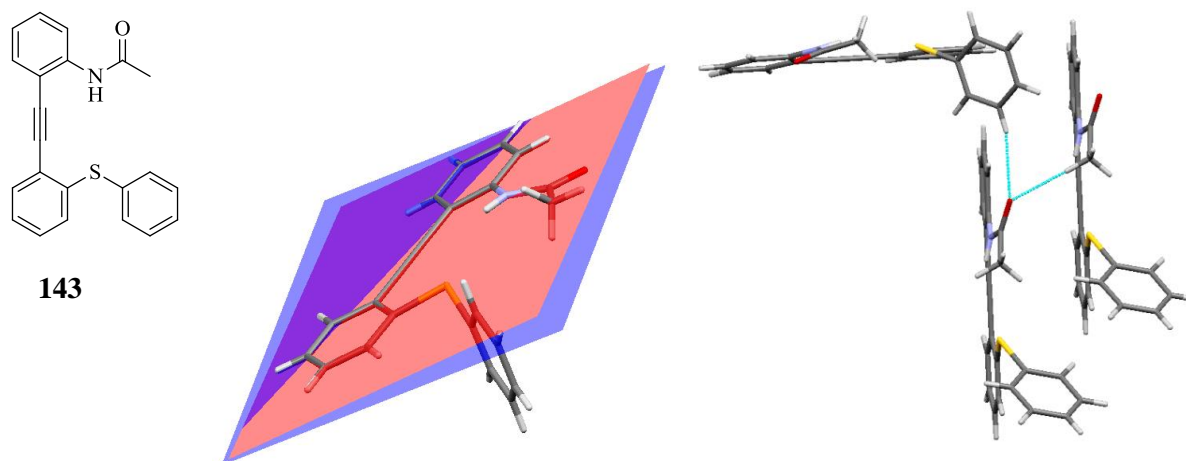


Figure 3.22: *Crystal structure of 143 and intermolecular interactions observed.*

The intramolecular N-H \cdots S distance in **143** is ~ 2.93 Å. Taking into account the typical sulfur-oxygen bond distance in sulfoxides and sulfones, it is reasonable to assume that the available space would be insufficient to accommodate N-H \cdots O=S intramolecular interactions. This observation would explain the change in conformation when the crystal structure of the sulfone analogue, **144**, was determined, **Figure 3.23**. The sulfone moiety lies on the opposite side to the amide. Although the methyl sulfone derivative, **133**, displayed an intramolecular N-H \cdots O=S interaction, in this particular sulfone, **144**, the additional phenyl group introduces further constraint and reduces the space available for an intramolecular interaction to occur. The phenylacetylene rings are bent further out of planarity (14.3°) compared to the sulfide, **143**, **Table 3.10**. The predicted N-H \cdots O=C intermolecular interaction between the amides dominate in the crystal packing of **144**. The sulfone partakes in intermolecular hydrogen bonding to neighbouring aromatic hydrogens.

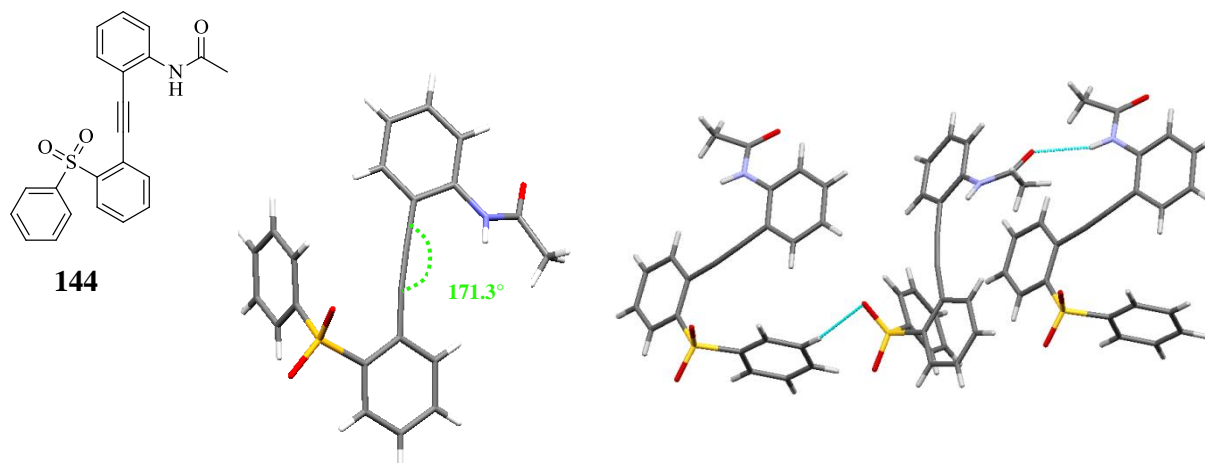


Figure 3.23: Crystal structure of **144** and intermolecular interactions observed.

Table 3.10: Angles observed for **143** and **144**.

No.	n	Ph—≡—Ph (°)	C ₆ H ₄ -N(H)C=O (°)
143	0	3.9	15.7
144	2	14.3	31.8

The internal alkyne in **144** also bends significantly (171.3°) out of its usual planar 180° conformation. A search of the CSD reveals that this bend is at the upper limit compared to the mean alkyne bend (176°) for various substituted diphenylacetylene systems, **Figure 3.24**.

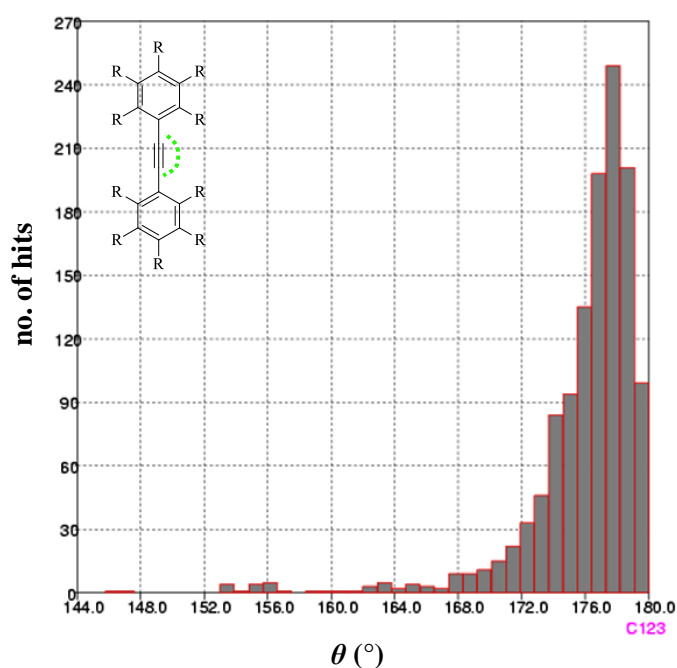


Figure 3.24: CSD search of alkyne angles in diphenylacetylenes.

Reports have suggested that alkyne distortion may occur when an electron rich atom is adjacent to an electron poor alkyne. Rice and co-workers first noted this *trans* bend in 2-nitrophenylalkyne, **154**, where a nitro oxygen atom was forming a short (1,5) contact with the sp C atom of the alkyne resulting in a displacement of the sp C atom towards the oxygen atom.⁴² Further studies also revealed the presence of the *trans* bend in diphenylacetylene compounds, bearing ester, **155**, or carboxylic acid, **156**, functionalities in close proximity to the internal alkyne.^{43,44} It is therefore reasonable to assume that this type of alkyne bending is occurring in the sulfone, **144**, where the sulfonyl oxygen is forming a short contact to the sp C atom of the alkyne, **Figure 3.25**. The S=O \cdots C \equiv C distance (3.08 Å) is within the sum of the O \cdots C van der Waal radii (3.24 Å).⁴⁴

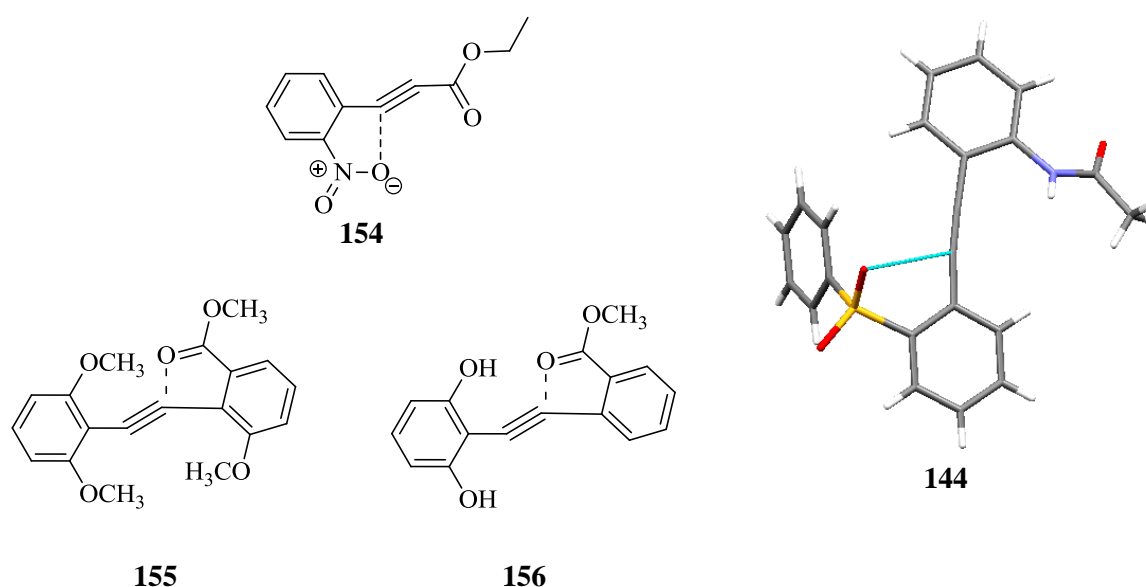


Figure 3.25: Alkyne bending observed in **144**, **154**, **155** and **156**.

The sulfide, **146**, exhibits similar behaviour to the related *p*-F sulfide, **137**, with the sulfide functionality located on the opposite side to the amide, **Figure 3.26**. Again, it was observed that the *p*-F substituent on the amide, due to its electron withdrawing properties, increases the likelihood of the formation of N-H \cdots O=C C(4) chains. The formation of these strong amide intermolecular interactions forces the phenylacetylene containing the phenylsulfide to rotate and lie on the opposite side of the molecule. In addition there is $\pi(\text{arene})\cdots\pi(\text{C}\equiv\text{C})$ stacking of the aromatic ring over the internal alkyne.

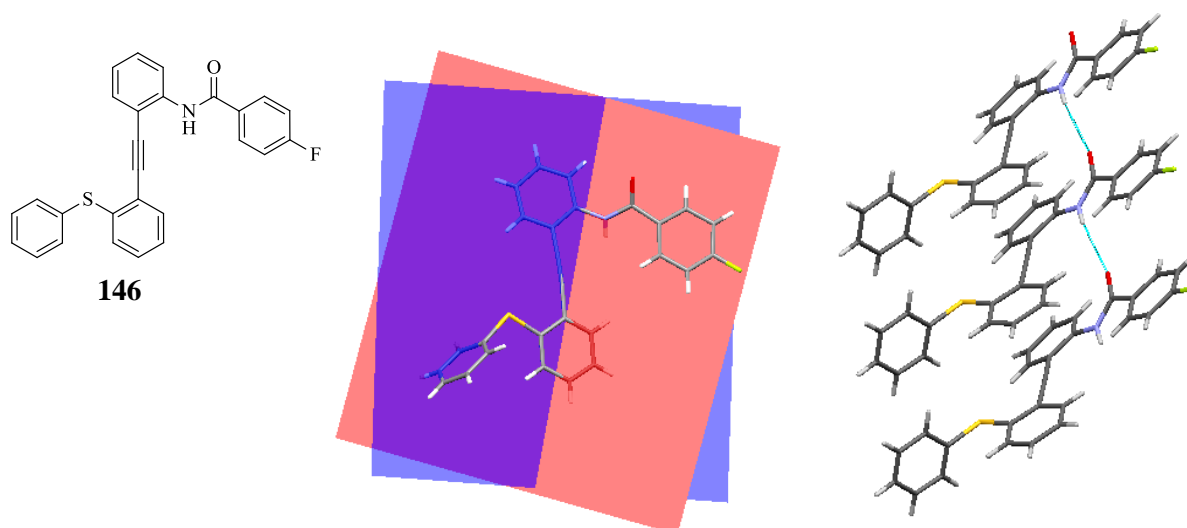


Figure 3.26: Crystal structure of **146** and $N-H\cdots O=C$ intermolecular interactions.

When the *p*-F substituted iodoamide, **118**, was coupled with the alkynyl sulfoxide, **129**, to form the diphenylacetylene, **147**, some interesting intermolecular interactions were observed. The phenylacetylene rings are significantly out of plane in relation to each other (36.2°). The sulfoxide functionality remains on the opposite side to the amide and the sulfoxide oxygen once again points away in a downward direction so that it cannot be involved in intramolecular hydrogen bonding, **Figure 3.27**. In the similar sulfoxide, **138**, $N-H\cdots O=S$ intermolecular interactions were observed since the sulfoxide is the strongest hydrogen bond donor and as a result the $N-H\cdots O=C$ C(4) chains were prevented from forming. However, in **147**, the $N-H\cdots O=C$ intermolecular interactions between the amides prevail and the sulfoxide forms $C-H\cdots O=S$ intermolecular interactions to aromatic hydrogens of neighbouring molecules. The additional phenyl group attached to the sulfoxide adds extra steric bulk to the molecule and may prevent the sulfoxide oxygen from easily accessing the amide N-H. As a result the $N-H\cdots O=C$ intermolecular interactions dominate this structure.

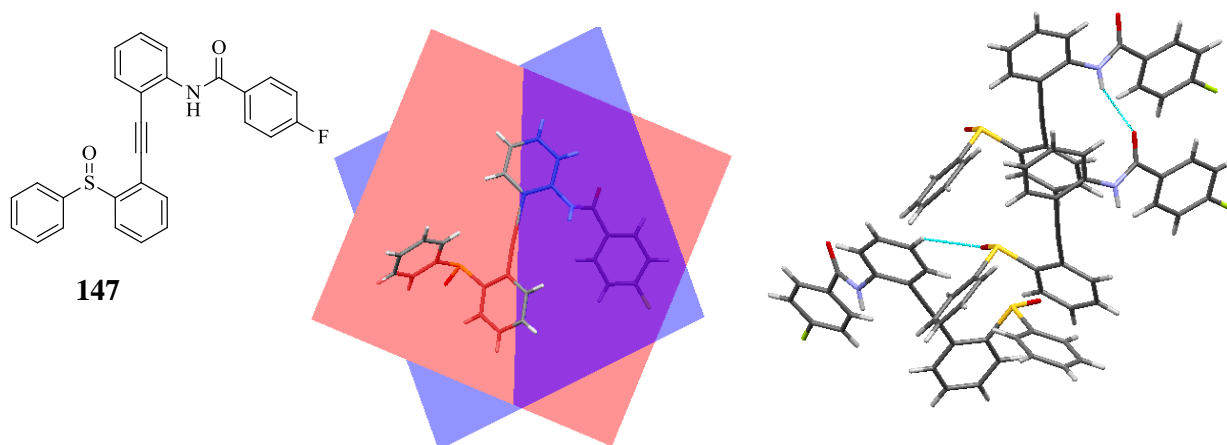


Figure 3.27: Crystal structure of **147** and intermolecular interactions.

The structure of the sulfone, **148**, is also quite remarkable, with the sulfone functionality remaining on the opposite side to the amide. The angle between the diphenylacetylene rings are approximately the same as that observed in **147**, **Table 3.11**, but the intermolecular interactions observed in **148** are notably different. The N-H \cdots O=C C(4) chains that were observed in the sulfide, **146**, and in the sulfoxide, **147**, are unexpectedly broken in the sulfone, **148**, **Figure 3.28**. Instead, $\pi(\text{arene})\cdots\pi(\text{arene})$, weak C-H \cdots O=C and C-H \cdots O=S intermolecular interactions are dominating the crystal packing in **148**. This behaviour is quite unusual as sulfones are weaker hydrogen bond acceptors than amides, and particularly with the *p*-F substituent attached to the amide, one would expect the strong N-H \cdots O=C to prevail in **148**.

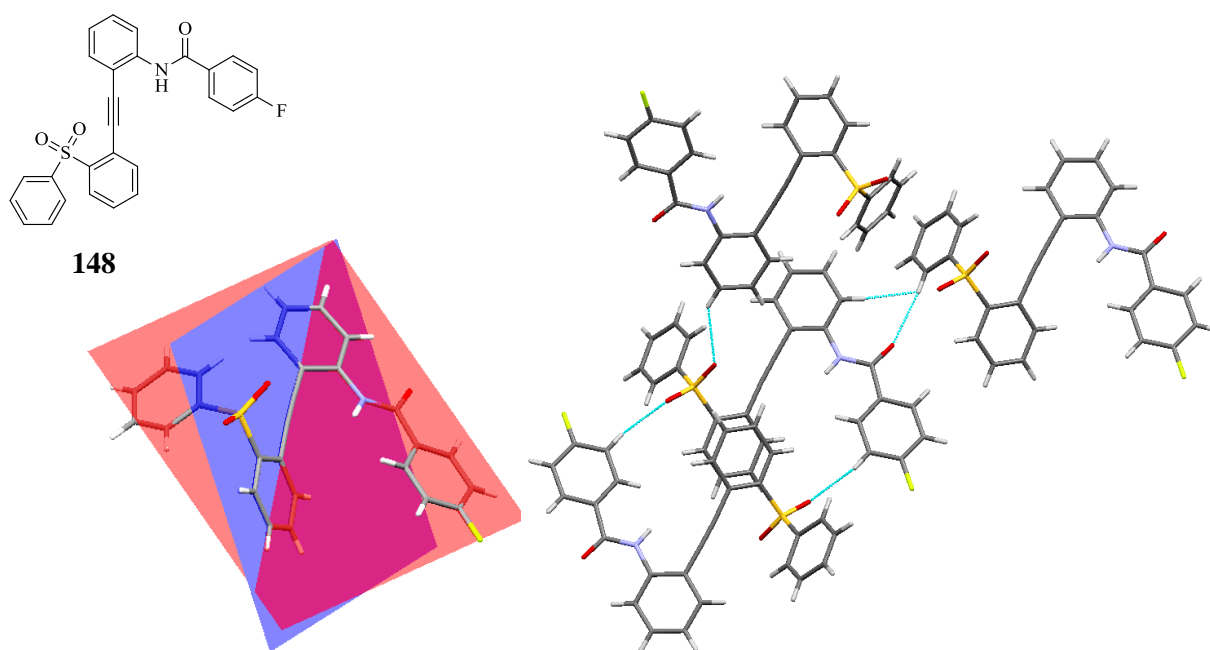


Figure 3.28: Crystal structure of **148** and intermolecular interactions observed.

Table 3.11: Angles observed for **146**, **147** and **148**.

No.	n	Ph \equiv Ph ($^{\circ}$)	C ₆ H ₄ -N(H)C=O ($^{\circ}$)
146	0	14.3	31.0
147	1	36.2	39.1
148	2	35.4	31.0

The crystal structure of the sulfide, **149**, can be compared to the similar *p*-Me substituted diphenylacetylene, **140**. The sulfide, **149**, adopts the same conformation as **140** and the intermolecular interactions are also very similar, **Figure 3.29**. The electron-donating effects of the *p*-Me substituent weakens the hydrogen bond donor capabilities of the amide N-H and as a result the N-H \cdots O=C C(4) chains fail to form. Therefore, the sulfide functionality lies on the same side as the amide. This orientation is precisely what was observed in the crystal structure of **140**.

In **149** the phenylacetylene rings are only slightly out of plane with each other (3.4°). Also, the intramolecular distance between the amide N-H and the sulfide is 3.19 Å. Since the sulfoxide oxygen pointed away from the amide N-H in **141**, it was decided not to investigate further the sulfoxide and sulfone analogues of the *p*-Me substituted amide.

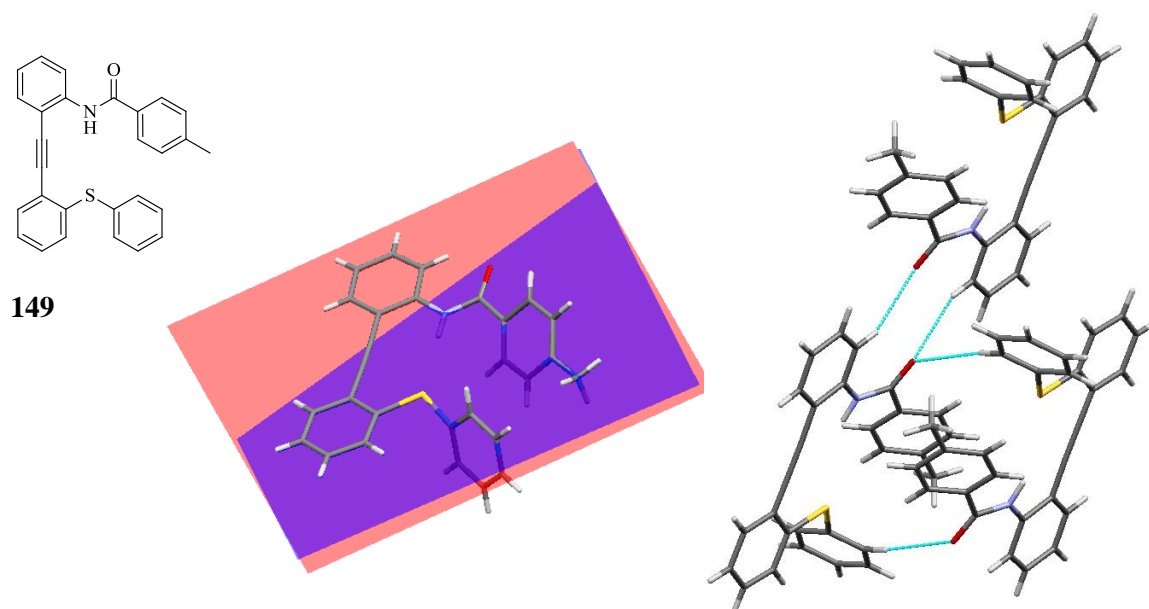


Figure 3.29: Crystal structure and interactions observed in **149**.

With a wide range of crystal structures obtained for the diphenylacetylene compounds containing the amide, sulfide, sulfoxide and sulfone functionalities, some clear trends emerged regarding the orientation of the molecules and the intermolecular interactions observed. As illustrated in **Figure 3.30**, in the majority of the sulfides, the amide and sulfide functionalities lie on the same side. This unanticipated result in **131**, **134**, **140**, **143**, and **149** could be occurring for a number of reasons. It appears, in these cases, that the energy associated with the predicted N-H \cdots O=C intermolecular interactions is not sufficient to overcome other competing factors and determine the solid state structure. Therefore, the sulfide remains on the same side as the amide. This appears a reasonable explanation as it

was demonstrated that increasing the acidity of the amide N-H using *p*-F substituents in **137** and **146**, resulted in the sulfides lying on the opposite side to the amides. When the electron donating *p*-Me substituent was introduced in **140** and **149**, then the sulfides once again stayed on the same side as the amide. Another possible explanation for the sulfides exhibiting this unusual behaviour could be the formation of weak N-H...S hydrogen bond interactions between the amide and sulfide. Although early crystallographic studies considered sulfur to be a poor hydrogen bond acceptor,³⁹ recently more attention has been focused on the role of sulfur in hydrogen bonding.⁴⁵ Howard *et al.*, using binding energy calculations have demonstrated that the hydrogen bond strength of sulfur in dimethyl sulfide is quite significant when compared to oxygen in dimethyl ether.⁴⁶ Perhaps the formation of the weak N-H...S intramolecular interaction, (see **Section 1.3.4**), is part of the overall combination of features overcoming the formation of the N-H...O=C C(4) chains, and thus the sulfide favours the same side as the amide.

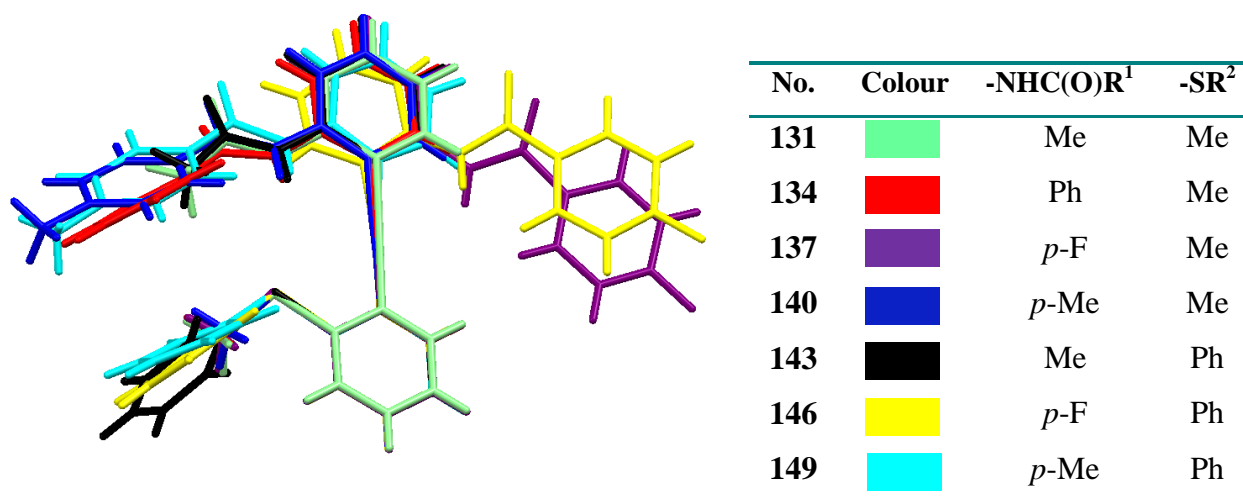


Figure 3.30: Stacked crystal structures of the sulfides.

The crystal structures of the sulfoxides, **135**, **138** and **141**, reveal the predicted N-H...O=S although these interactions are occurring intermolecularly. The sulfoxide oxygen adopts an unanticipated conformation and points out of the plane. While it could be argued that intramolecular spatial constraints could be the reason for this in **132**, **135** and **141**, the sulfoxide remains out of planarity in **138** and **147** where spatial limitation relative to the amide is not an issue. Interestingly, a review of the CSD indicates that for phenyl substituted sulfoxides, the sulfoxide functionality is usually in a planar conformation with the phenyl ring, with a mean torsional angle of -4.24° , **Figure 3.31**. Perhaps the strong N-H...O=S intermolecular interactions in the sulfoxides synthesised in this project force the sulfoxide oxygen out of planarity.

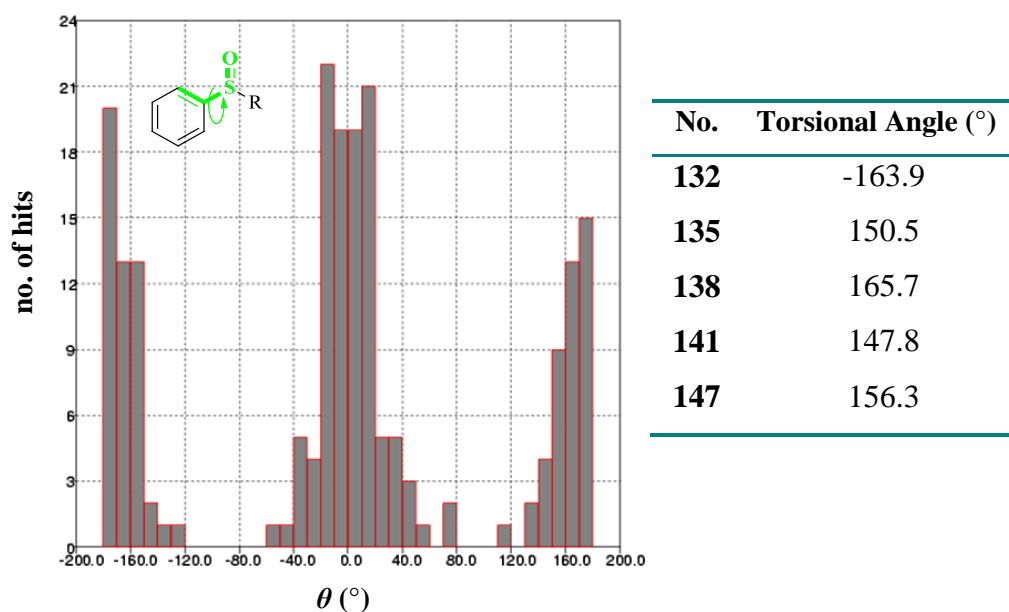


Figure 3.31: Torsional angles observed in the CSD for general phenylsulfoxides compared to sulfoxides synthesised in this work.

In **132**, **135**, **138** and **141**, the sulfoxide oxygen acts as the major hydrogen bond acceptor and dramatically alters the solid state interactions when compared to their respective sulfides. The only exception to this was observed in the crystal structure of **147** where the N-H...O=C remained unchanged compared to the sulfide **146**. It appears that steric reasons may be preventing N-H...O=S from occurring in this instance. In the initial concept, it was envisaged that the sulfoxide would lie on the same side as the amide. This was observed in **132**, **135** and **141**. However, when the *p*-F substituent was introduced in **138** and **147**, the sulfoxide remained on the opposite side to the amide, **Figure 3.32**. This is interesting as in **138**, the N-H...O=C C(4) chains are broken and replaced with N-H...O=S intermolecular chains, yet the sulfoxide remains on the opposite side to the amide. In contrast, in **147**, the N-H...O=C C(4) chains remain intact and the sulfoxide group is still on the opposite side to the amide.

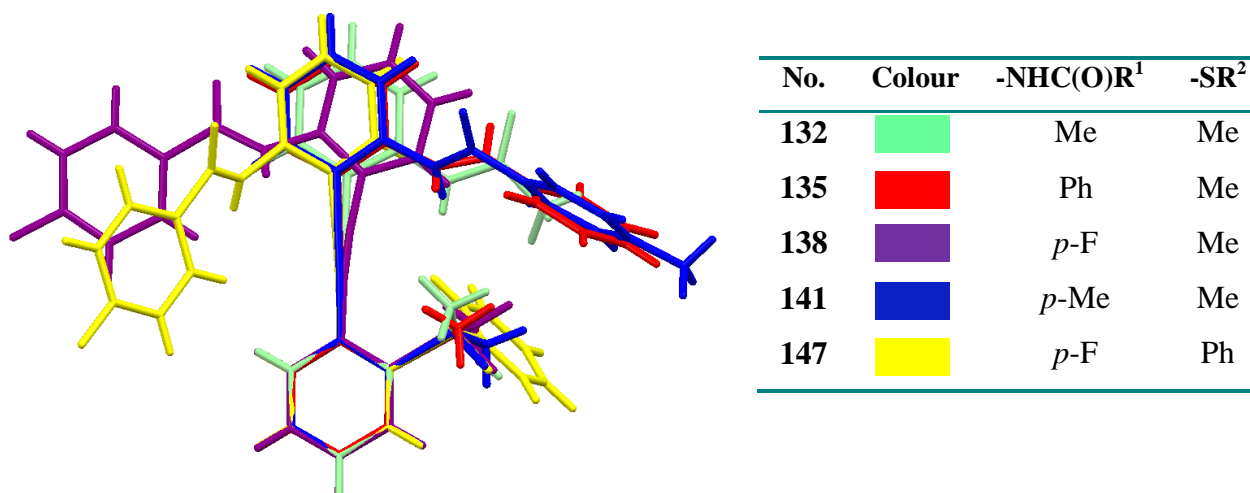


Figure 3.32: Stacked structures of sulfoxides.

The sulfones, **136**, **139**, **144** and **148**, display the predicted conformation and lie on the opposite side to the amide, **Figure 3.33**. Also, their interactions are exactly as predicted with the N-H \cdots O=C C(4) amide chains dominating their crystal structures. The only exception to this is in the crystal packing of **133** where the sulfone group is on the same side as the amide and an intramolecular N-H \cdots O=S interaction is observed. However, since the N-H \cdots O=C C(4) chains were not displayed in its corresponding sulfide **131**, it is not surprising that they do not form in the sulfone. Instead, C(H₂)H \cdots O=C were observed in the sulfide, **131**, and were broken in the sulfoxide, **132**, but were observed again in the sulfone, **133**.

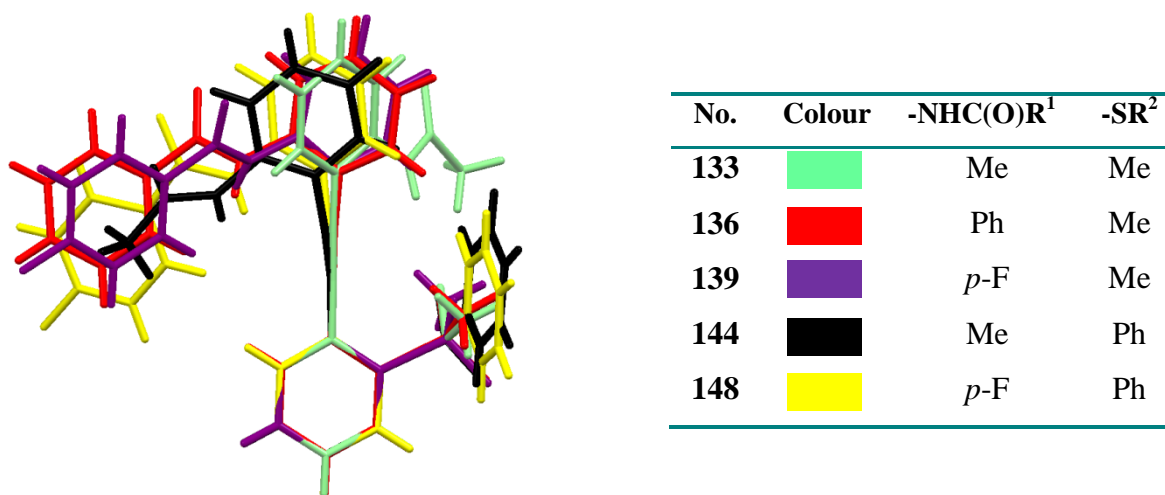


Figure 3.33: Stacked crystal structures of sulfones.

It was noted for all the diphenylacetylene systems synthesised, particularly for the sulfoxide and sulfone substituted compounds, that the aryl rings in the diphenylacetylene core structure, were noticeably out of plane in relation to each other. Particularly the sulfoxide, **147** (36.2°), and the sulfones, **133** (34.4°) and **148** (35.4°), displayed quite a significant distortion. While the CSD reveals that it is not uncommon for substituted diphenylacetylenes to exist out of planarity, the majority of the aryl rings within these structures are coplanar with each other, **Figure 3.34**. As noted in **Section 3.1.1**, the rotational barrier in unsubstituted diphenylacetylenes is negligible and the observation in the solid state that the aryl rings are commonly coplanar is more likely explained due to the ease of packing rather than due to stability in the coplanar conformation.

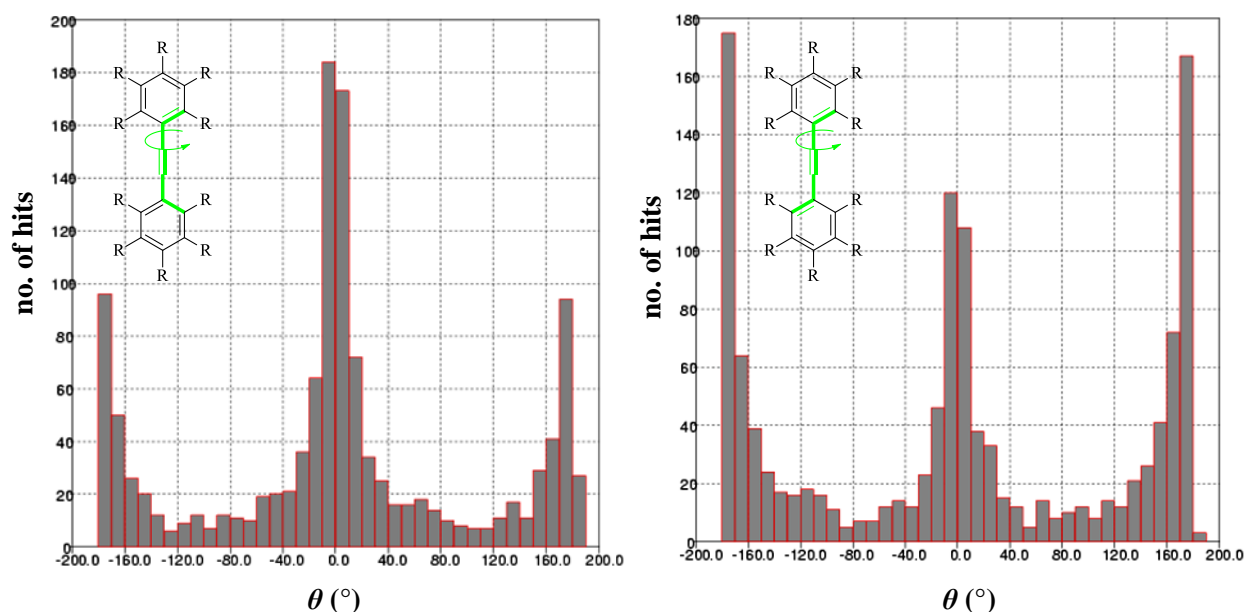


Figure 3.34: Histograms of torsional angles for aryl rings in diphenylacetylene systems observed in CSD.

Overall, the results demonstrate that crystal structures can be obtained for these very interesting systems at all sulfur oxidation levels (sulfide, sulfoxide and sulfone). Also, it was demonstrated that varying the oxidation level of sulfur dramatically alters the solid state interactions, and in some cases caused rotation of the phenylacetylene core unit. It is clear that one of the key structure determining features in the solid state properties of these compounds is the level of sulfur oxidation and the associated variation in hydrogen bond accepting strengths. There is a fine balance between the hydrogen bonding arrays involving the sulfur functionalities and the well-established $\text{N-H}\cdots\text{O}=\text{C}$ bonding in determining the overall structure. Evidently, this can be manipulated in a predictable manner *e.g.* increasing the acidity of the N-H bond tipped the balance towards the $\text{N-H}\cdots\text{O}=\text{C}$ interactions dominating in the crystal structures. The deviation from planarity in the diphenylacetylene backbone confirms that the stabilising effect of the specific hydrogen bonding interactions is sufficient to compensate energetically. While this investigation provides a reasonable insight into the relationship between molecular structure and the orientation of the solid state, further work is warranted to probe this in more detail.

3.1.9. Variable-temperature NMR spectroscopic studies

Variable temperature NMR spectroscopic studies were conducted on the simpler sulfoxide, **132**, and sulfone, **133**, in conjunction with Dr Lorraine Bateman in University College Cork. It was decided to investigate if restricted rotation of these compounds could be observed in solution. The assignment of each proton in both **132** and **133** was aided by HMBC, HSQC, COSY and NOESY 2D NMR experiments. ^1H NMR, NOESY and NOE experiments were then conducted at 290, 300 and 320 K. At the time this work was undertaken, the temperature range accessible on the NMR was limited to 290-320 K.

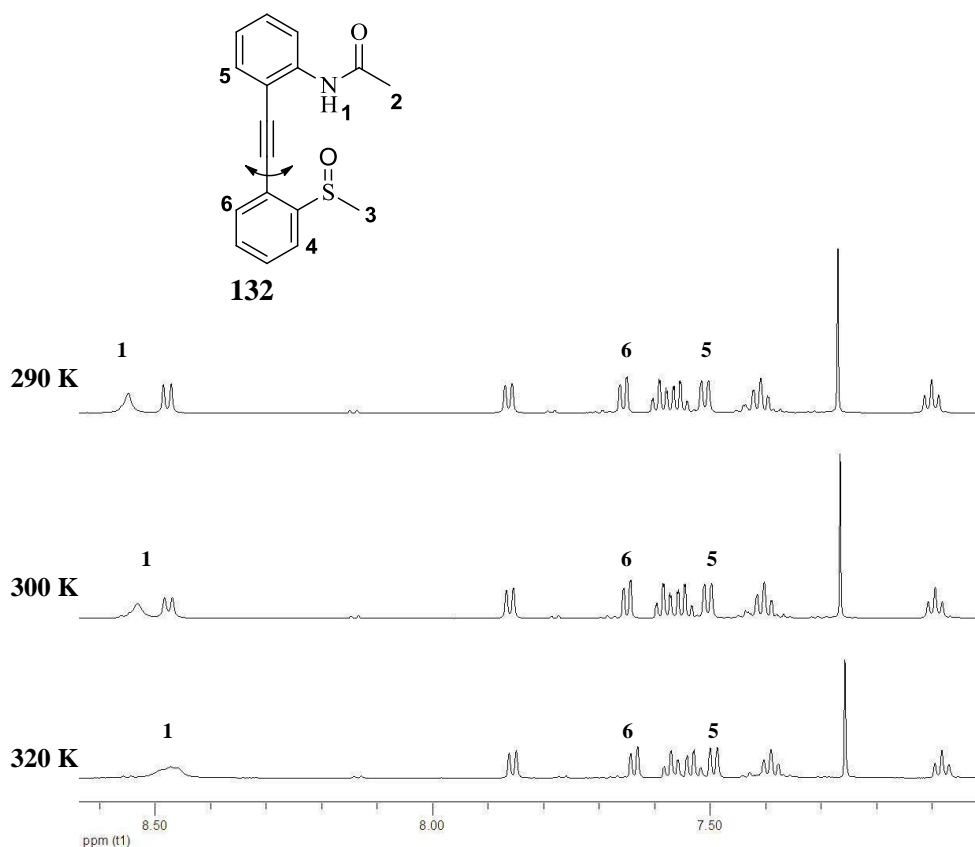


Figure 3.35: Stacked ^1H NMR spectra of **132** in CDCl_3 at 600 MHz at 290, 300 and 320 K.

The variable-temperature ^1H NMR studies of the sulfoxide, **132**, reveals a slight upfield shift and peak broadening of the amide N-H signal, as the temperature is increased from 290-320 K, **Figure 3.35**. The signal shifts from 8.53 ppm to 8.49 ppm, where it merges with the doublet at 8.47 ppm. No other significant shifts in the ^1H NMR of **132** were noted as the temperature was varied. It is difficult to draw definite conclusions from these results as amide N-H signals tend to shift quite easily and here the N-H signal is probably shifting as a result of a change of temperature rather than the effect of the molecule rotating. Also, the

methyl protons attached to the amide and sulfoxide moieties undergo no significant shift and therefore do not experience any detectable change in environment with varying temperature.

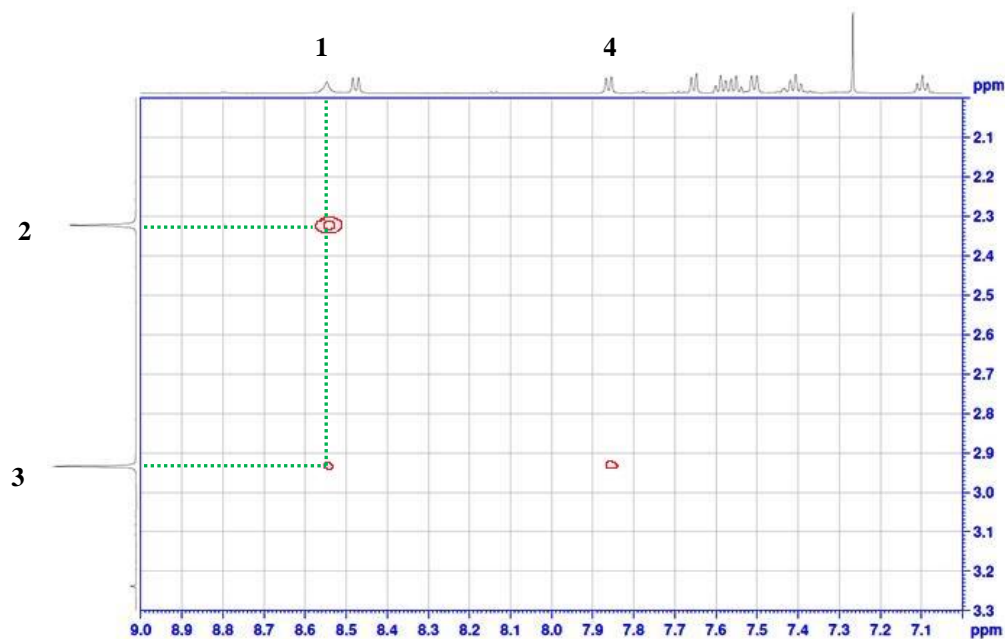


Figure 3.36: NOESY NMR data for **132** in CDCl_3 at 600 MHz.

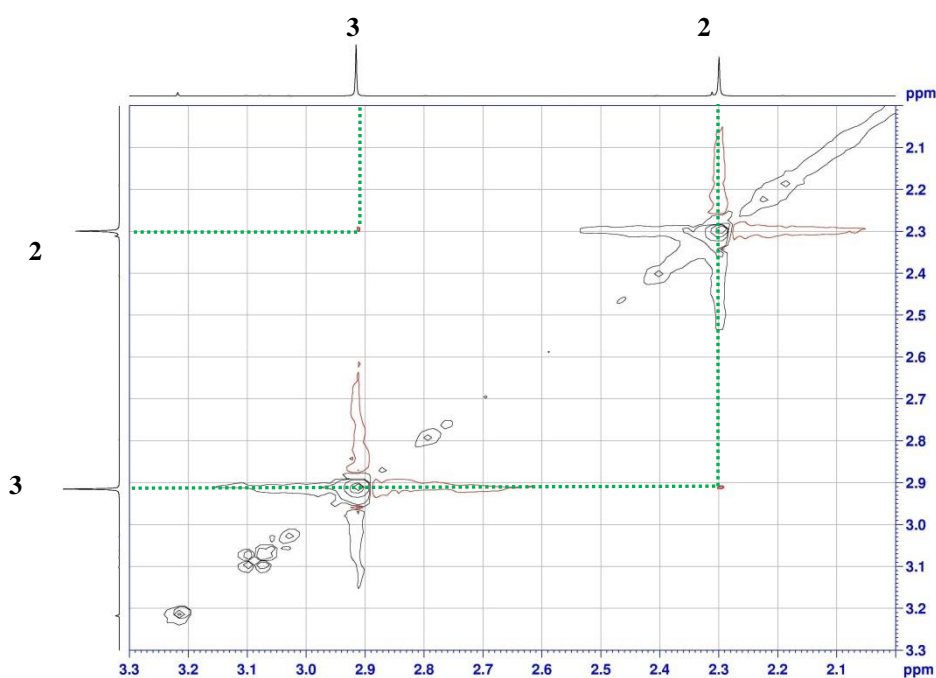


Figure 3.37: NOESY NMR data for **132** (2.0–3.3 ppm) in CDCl_3 at 600 MHz.

The NOESY NMR data of **132** provides additional information about the conformation that the molecule adopts. It appears that the N-H proton is in close proximity to the methyl sulfoxide protons, **Figure 3.36**. Also, both sets of methyl protons interact with each other so it is reasonable to assume that the sulfoxide lies on the same side as the amide, for at least a substantial proportion of time, **Figure 3.37**. A NOESY signal could not be detected between the aromatic protons, **5** and **6**. It is generally accepted that for a correlation between two protons to be detected in NOESY NMR, then the distance between them has to be smaller than 5.0 Å. The crystal structure data previously attained for **132** revealed that the distance between the protons **5** and **6** is 4.63 Å, which is just within the limit for detection and so it is envisaged that the signal would be difficult to observe, if present. Overall, the NOESY signals observed for **132** do not detectably alter as the temperature is varied from 290-320 K, confirming the limited change in conformation over this temperature range. NOE experiments were also performed on **132** at 290, 300 and 320 K but no definite conclusions could be determined from these results.

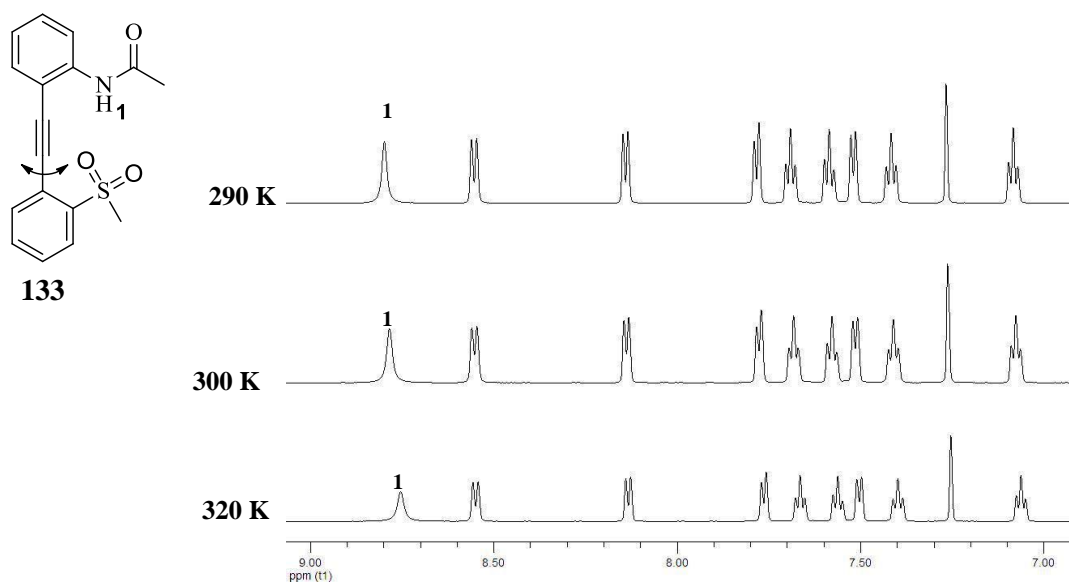


Figure 3.38: Stacked ^1H NMR spectra of **133** in CDCl_3 at 600 MHz at 290, 300 and 320 K.

Comparing the ^1H NMR data between the sulfoxide, **132**, and the sulfone, **133**, a downfield shift in the signals for the aromatic protons is observed for **133**, **Figure 3.38**. In particular, the amide N-H signal moves from 8.53 ppm to 8.79 ppm. Previous reports have shown that signals for non-hydrogen bonded amides appear around 8 ppm, and amides that partake in hydrogen bonding appear around ~9.0-9.2 ppm in the ^1H NMR spectra of diphenylacetylene-type compounds.^{1,6} As described previously, the crystal structure of **133** reveals intramolecular $\text{NH}\cdots\text{O}=\text{S}$ hydrogen bond interactions, whereas in the crystal structure of

132, the amide N-H does not participate in any significant inter/intramolecular interactions. This difference in hydrogen bonding participation may explain the slight shift of the amide N-H signal between **132** and **133** in the ^1H NMR spectra.

Similar trends to the sulfoxide, **132**, were observed for the sulfone, **133**, in the variable-temperature NMR experiments. The temperature was increased from 290 K to 300 K and then to 320 K with only a slight upfield shift of the N-H signal observed, **Figure 3.38**. The aromatic and methyl signals remained at the same chemical shift on increase of temperature. The NOESY data seems to also suggest that the sulfone lies on the same side as the amide, at least for a substantial proportion of time, **Figure 3.39**. NOE experiments were also performed at the various temperatures but no definite conclusions could be determined from these results.

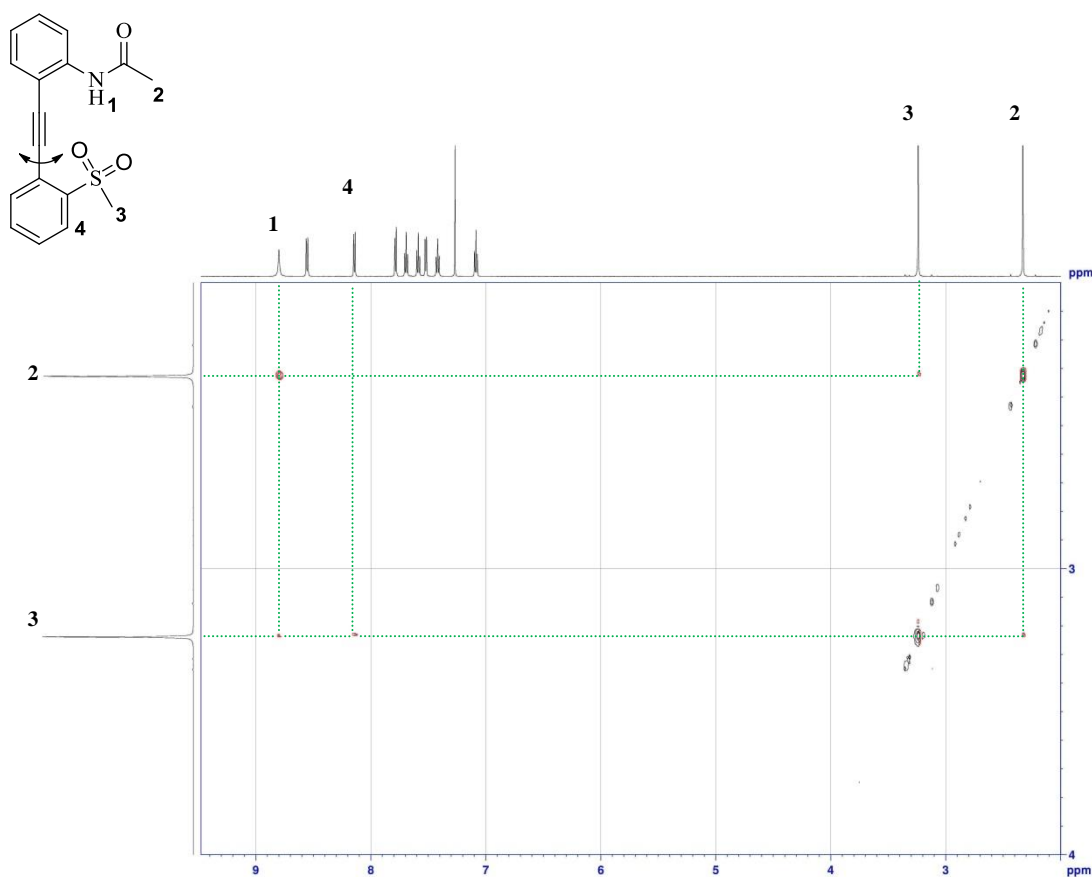
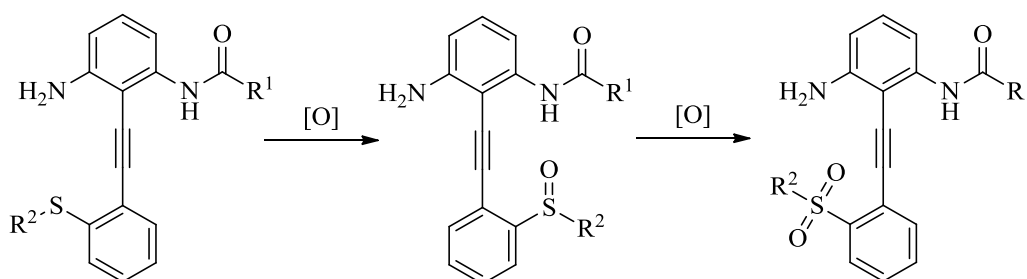


Figure 3.39: NOESY NMR data for **133** in CDCl_3 at 600 MHz.

3.2. Introduction of a competing hydrogen bond donor

3.2.1. Introduction

The initial concept, as illustrated in **Scheme 3.1**, needed to be further adjusted in order to fully control the conformation and orientation adopted by these compounds. To introduce more control into the orientation of these molecules, the addition of a second hydrogen bond donor seemed a plausible approach. Amine functionalities were initially considered as they are weaker hydrogen bond donors than amides.¹⁰ This concept would involve creating competition between the hydrogen bond acceptors for the strongest hydrogen bond donor by altering the oxidation level of the sulfur and exploiting the difference in acidity and hydrogen bond strength between amides and amines, **Scheme 3.11**.

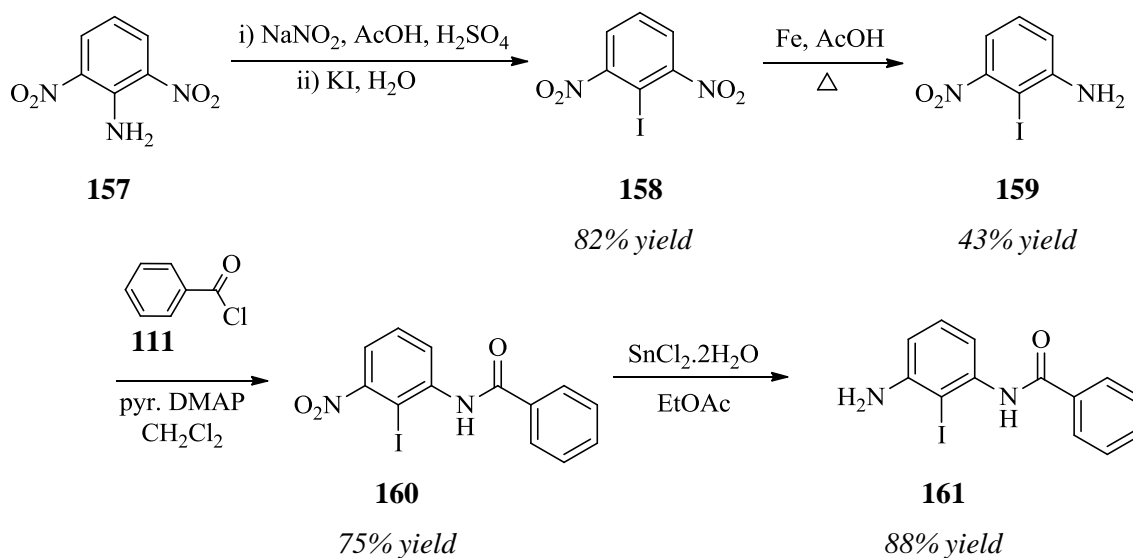


Scheme 3.11: Concept involving competing hydrogen bond donors.

It was envisaged using this approach, that at the sulfide level, interaction between the sulfur and amide or amine is not expected and the dominant solid state interaction predicted is the N-H...O=C intermolecular interaction. As a result, one would expect the sulfide to lie on the opposite side to the amide, as illustrated in **Scheme 3.11**, thereby enabling the intermolecular N-H...O=C interaction. On oxidation to the sulfoxide, the strong intramolecular N-H...O=S interaction should compete effectively with the intermolecular N-H...O=C interaction as sulfoxides are potent hydrogen bond acceptors¹¹ and amides are stronger hydrogen bond donors than amines.¹⁰ In this case, it is expected that the sulfoxide will lie on the same side as the amide. On further oxidation to the sulfone, which is a weaker hydrogen bond acceptor than the sulfoxide, it was anticipated at the outset that the strong N-H...O=C intermolecular interaction would once again dominate, resulting in the sulfone lying on the opposite side to the amide.

3.2.2. Preparation of *N*-(2-Iodo-3-aminophenyl)benzamide

Firstly an iodoamide bearing an amine group was synthesised as a precursor for the Sonogashira coupling reaction. The aminophenylbenzamide, **161**, fitted this particular profile and the four-step synthesis had been previously described by Hamilton and co-workers.⁶ This route involved firstly preparing **158** by the diazotisation of the commercially available aniline, **157**, and then treating the diazonium salt with potassium iodide, **Scheme 3.12**. One of the nitro groups in **158** was then selectively reduced using iron powder in acetic acid (Béchamp reduction) to form **159**. Although a significant loss in yield was noted for this step, the results are comparable with the literature yield (40%).^{6,47} The nitroaniline, **159**, was converted to the benzamide, **160**, using benzoyl chloride, **111**, in CH₂Cl₂. Stannous chloride which is widely described in the literature for the reduction of aryl nitro compounds with sensitive functionalities,⁴⁸ proved effective in the final step to form **161** in 88% yield after column chromatography.

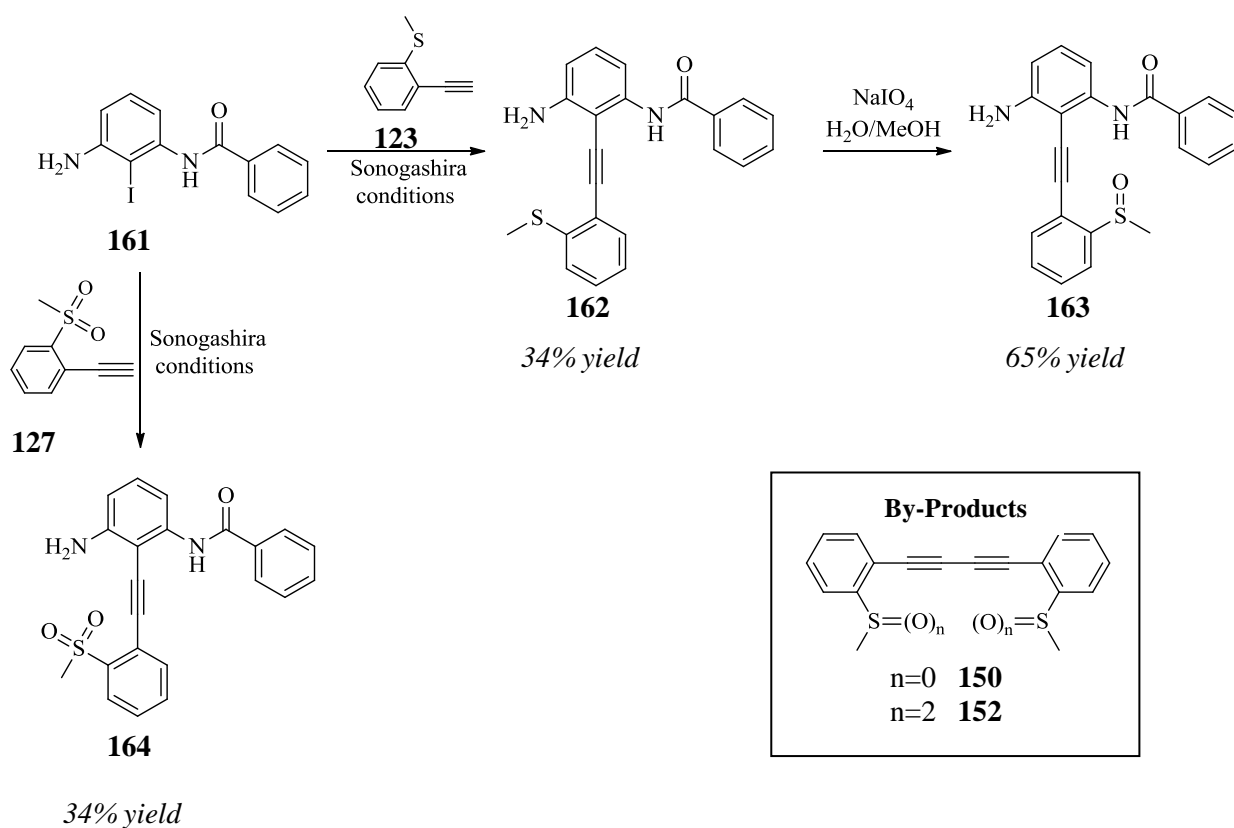


Scheme 3.12: Synthetic strategy to form **161**⁶ with yields obtained for each step.

With a robust synthetic route in place, **161** could be achieved in excellent yields. The remaining amine could also be easily converted to an amide if required, in order to investigate differing electronic properties on the hydrogen bond donor capabilities between the two benzamides once coupled to the alkynyl sulfur functionalities.

3.2.3. Sonogashira coupling and functionalisation of amine

The Sonogashira reaction was employed to couple the sulfur moieties, **123** and **127**, with aminophenylbenzamide, **161**, using conditions similar to those in **Scheme 3.9**. The novel sulfide, **162**, and sulfone, **164**, were isolated as solids, each in 34% yield after column chromatography, **Scheme 3.13**. The moderate yields obtained are similar to the trends observed in **Table 3.4**, for the Sonogashira reactions involving the mono-substituted phenylacetylenes. The competing side reactions, in particular the Glaser coupling (**Section 3.1.7, Scheme 3.10**), once again contributed to the loss in yield. The homo-coupled products, **150** and **152**, formed from the alkynyl sulfide, **123**, and the alkynyl sulfone, **127**, respectively, were isolated after column chromatography, **Scheme 3.13**.



*Sonogashira conditions: $\text{PdCl}_2(\text{PPh}_3)_2$, CuI , NEt_3 , DMF, 60°C

Scheme 3.13: Synthesis of **162**, **163** and **164**.

The novel sulfoxide, **163**, was readily obtained by the oxidation of the sulfide, **162**. This demonstrates that these compounds are sufficiently stable for further derivatisation. All three novel products **162**, **163**, and **164** existed as solids and were stable at room temperature. They were fully characterised by ^1H and ^{13}C NMR, IR, m/z and HRMS and their crystal structures were determined. The characteristic downfield shift of the methyl and aromatic protons were noted on oxidation from sulfide, **162**, to sulfoxide, **163**, and sulfone, **164**, **Figure 4.40**.

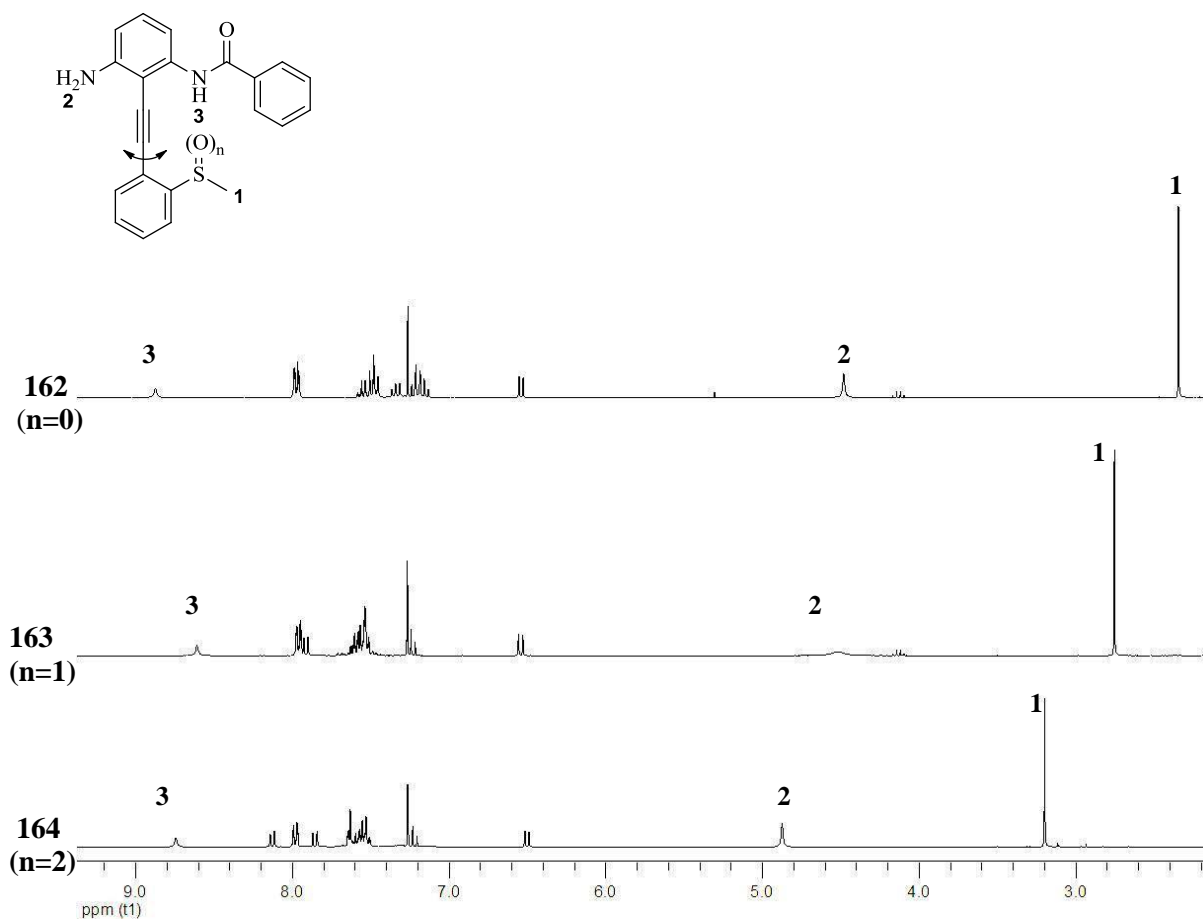
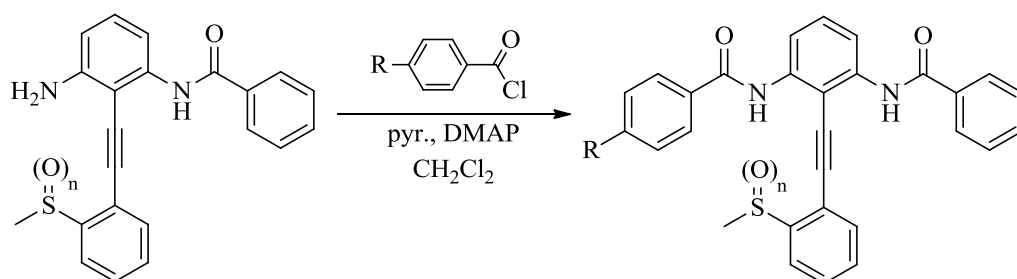


Figure 4.40: ^1H NMR (300 MHz) data in CDCl_3 for **162**, **163** and **164**.

It was decided to convert the amines, to the benzamides, bearing *p*-NO₂ and *p*-F substituents, in order to investigate the electronic effects on the hydrogen bonding interactions in the solid state, **Scheme 3.14**. It would be interesting to observe if the sulfur functionalities favoured hydrogen bonding to one amide N-H over the other. A bias could be created between the two amides by altering their electronic properties and therefore competition would exist between these amides to act as the major hydrogen bond donor. The amines, **162** and **164**, were reacted with the acid chlorides, **112** and **113**, in the presence of pyridine and DMAP, to form the novel bisbenzamido compounds, **165**, **166**, and **167**, in excellent yields, **Table 3.12**.



Scheme 3.14: Formation of bisbenzamido-diphenylacetylenes **165,166,167**.

Table 3.12: Yields obtained for **165,166,167**.

Amine	n	R-C ₆ H ₄ -C(O)Cl	R	Product ^a	Yield (%)
162	0	112	NO ₂	165	79
162	0	113	F	166	98
164	2	113	F	167	97 ^b

a Novel compounds and characterised by ¹H and ¹³C NMR, IR, *m/z*, HRMS and elemental analysis.

b Purified yield after column chromatography

The desired compounds **165**, **166**, and **167** were isolated as solids but they were not sufficiently crystalline for single crystal analysis. Nonetheless, this route highlights that the bisbenzamido-diphenylacetylenes are readily accessible and various substituents could be attached in the future to further explore the hydrogen bonding patterns in these interesting systems.

In summary, it has been successfully demonstrated that the diphenylacetylenes bearing amine, amide and sulfur functionalities can be constructed utilising Sonogashira conditions in reasonable yields. Also, these compounds can be oxidised and further functionalised with various amide groups in excellent yields. Now that the envisaged compounds have been successfully synthesised and a synthetic strategy has been put in place, there is scope to further expand and functionalise these systems in the future.

3.2.4. Crystal Structures

Single crystal X-ray diffractions of **162**, **163** and **164**, each recrystallised from the same solvent, CH_2Cl_2 , demonstrated the predicted conformational change as a result of altering the oxidation level of sulfur, **Scheme 3.11**. As expected the sulfide lies on the opposite side to the amide, then switches after oxidation to the sulfoxide and switches back again when the sulfone is formed.

For **162**, the phenylacetylene rings are almost completely planar in relation to each other (1.43°). As predicted, the sulfide group lies on the same side as the amine with a distance of 2.93 \AA between the functionalities, so if hydrogen bonding is occurring between these functional groups it is extremely weak, **Figure 3.41**. The strong intermolecular $\text{N-H}\cdots\text{O}=\text{C}$ dominates the crystal packing, and the $\text{C}=\text{O}$ of the amide is involved in bifurcated hydrogen bonding to both a neighbouring N-H of an amide (2.12 \AA) and C-H of a methyl group (2.66 \AA).

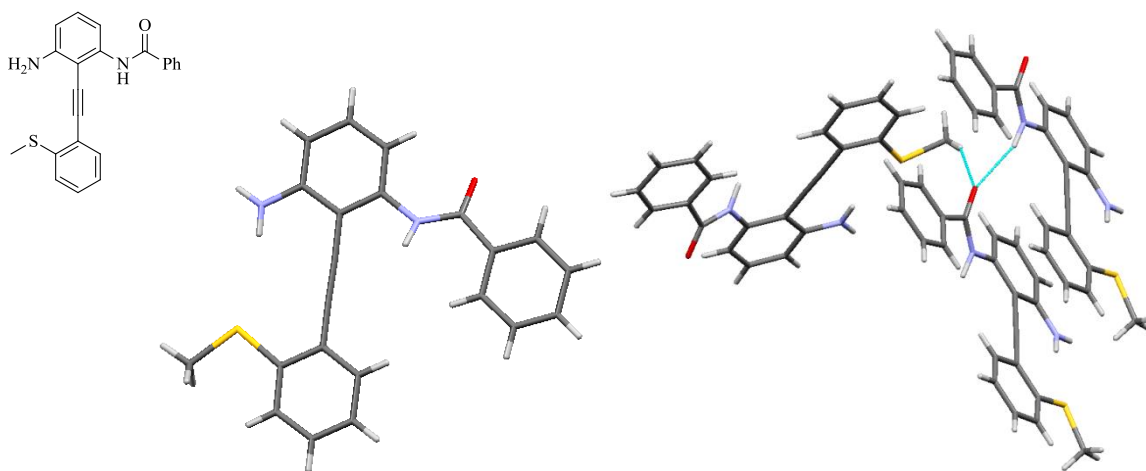


Figure 3.41: Crystal structure and interactions observed for sulfide, **162**.

Interestingly, although the conformation switches in the sulfoxide, **163**, the key non-covalent interactions observed were not as anticipated, **Figure 3.42**. Instead of an intramolecular N-H \cdots O=S bond occurring between the amide and sulfoxide, an intermolecular N-H \cdots O=S is formed between the sulfoxide and a neighbouring amine. The phenylacetylene rings are twisted further out of planarity (11.4°) after oxidation, and the oxygen from the sulfoxide points away from the amide, with the result that intramolecular hydrogen bonding does not occur. The strong N-H \cdots O=C interaction prevails in the crystal structure and oxidation to the sulfoxide has not disrupted this interaction. Comparison of the structural features of Hamilton's amide-ester system with our amide-sulfoxide system is very interesting. Although the sulfoxide is expected to be a stronger hydrogen bond acceptor than the ester, the planar intramolecular hydrogen bond which we anticipated to form did not occur in practice. Examination of the amide to sulfoxide N-H \cdots O=S intramolecular distance available in **163** (~2.05 Å), together with analysis of the Cambridge Structural Database, **Figure 3.7**, and comparison with the amide-ester N-H \cdots O=C hydrogen bond distance (2.23 Å), **Figure 3.6**, suggests that intramolecular hydrogen bonding, while not observed, is feasible in our system.

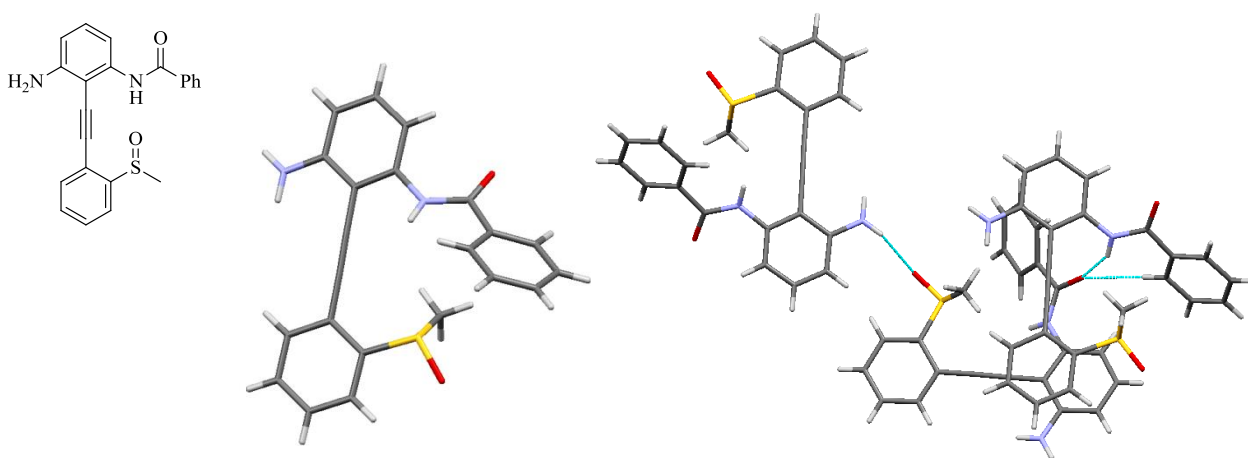


Figure 3.42: *Crystal structure and interactions observed for sulfoxide, 163.*

The sulfone, **164**, crystallises with $Z' = 2$, with both molecules adopting the same conformation as seen in the sulfide, **162**, *i.e.* the sulfone lies on the opposite side to the amide, **Figure 3.43**. Similar to **162** the phenylacetylene rings in **164** adopt almost complete planarity (1.2°), **Table 3.13**. The key interactions involving the two crystallographically independent molecules are intra- and intermolecular N-H \cdots O=S hydrogen bonds. The combination gives rise to a visually appealing $R_4^4(12)$ motif at the binary level. Also present

within this motif is a C-H...O=S intermolecular interaction between one of the sulfone oxygen atoms and a methyl group. Significantly, the strong intermolecular N-H...O=C between the amides, which was the key structure-defining feature in the sulfide and sulfoxide structures, was disrupted on oxidation to the sulfone, therefore altering very substantially the crystal packing of the molecule.

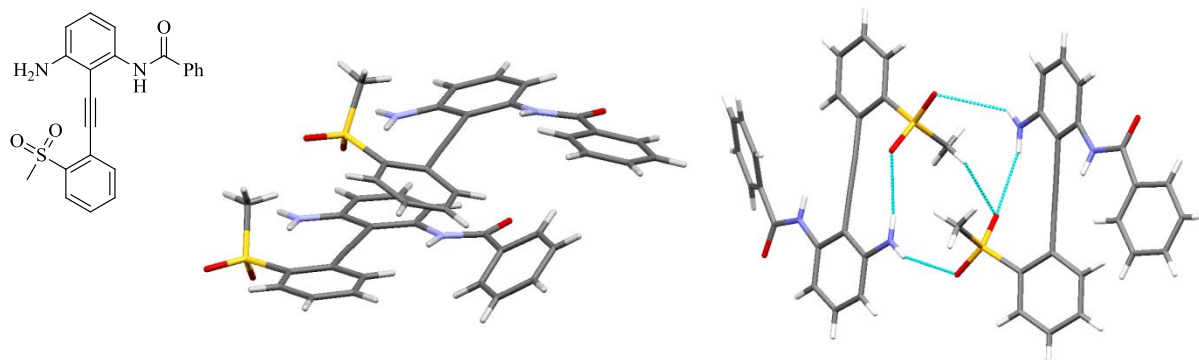


Figure 3.43: Crystal structure and interactions observed for sulfone, **164**.

Table 3.13: Angles observed for **162**, **163** and **164**.

No.	n	Ph—≡—Ph (°)	Planar Angle (°) C ₆ H ₄ /HN-C=O
162	0	1.43	32.9
163	1	11.4	40.5
164	2	1.2	3.1

3.2.5. Computer Modelling

To further investigate why the sulfoxide, **163**, does not have an intramolecular N-H...O=S hydrogen bond between the sulfoxide and the amide moieties, modelling studies were conducted in conjunction with Dr. Noel O' Boyle in University College Cork. Density functional theory calculations were carried out with Gaussian 09⁴⁹ using the B3LYP^{50,51} hybrid exchange and correlation functional and the 6-31G(d) basis set. The results obtained from this study are presented in **Figure 3.44**. For comparison, two conformers of **163** were energy-minimised: the first as in the crystal structure (structure **I**) with the electron lone pair of the sulfoxide pointing towards the amide, and the second (structure **II**) with the sulfoxide oxygen pointing towards the amide, thereby forming a hydrogen bond.

After optimising the structures, the main structural difference apart from the orientation of the sulfoxide group, is a rotation of the axial phenyl rings with respect to each other; in structure **I** the two phenyl rings are planar with respect to each other while in structure **II** they exhibit a torsion angle of 56° . Given that structure **I** is slightly lower in energy than **II** (~ 2.8 kJ/mol), essentially negligible, despite the absence of the intramolecular hydrogen bond, this suggests that the formation of the hydrogen bond is energetically unfavourable as the stabilisation energy thus obtained is offset by the energy associated with the loss of extended conjugation of the phenyl rings.

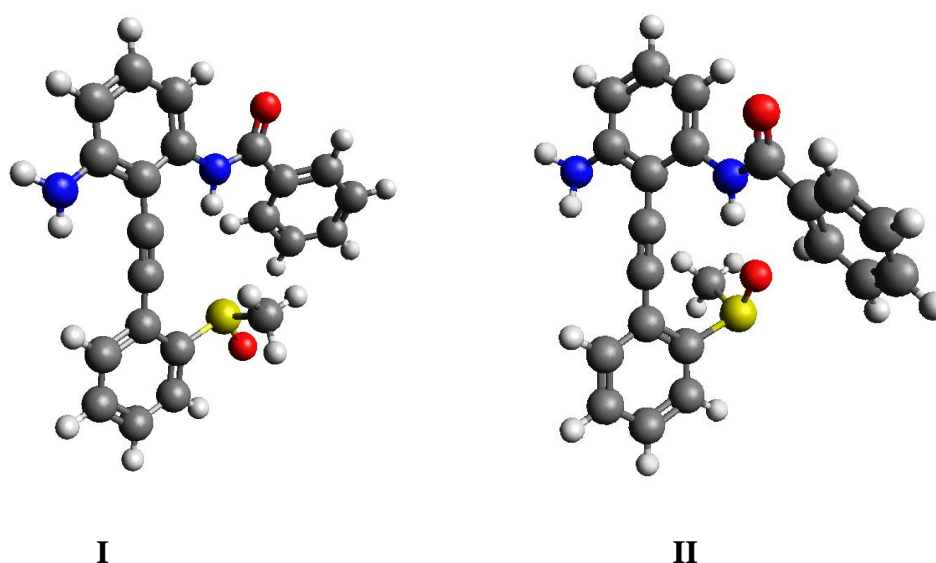


Figure 3.44: Computational studies on **163**.

3.2.6. Conclusion

The introduction of competing hydrogen bond donors into the diphenylacetylene core structure resulted in many very interesting observations. A robust synthetic pathway has been successfully developed to incorporate amine, amide and sulfur functionalities into a single diphenylacetylene unit. This is the first time that such novel compounds have been reported.⁵² Also, it has been demonstrated that the Sonogashira couplings involving the *N*-(2-iodo-3-aminophenyl)benzamide, **161**, are effective at sulfide, sulfoxide and sulfone oxidation states. After coupling, the amine group can be further functionalised to form benzamides as demonstrated with the synthesis of **165**, **166**, and **167**.

Crystal structures were obtained for **162**, **163**, and **164**. The predicted change in molecular conformation of the sulfide, **162**, to the sulfoxide, **163**, and sulfone, **164**, was observed as a direct result of altering the oxidation state of sulfur and therefore impacting on the key

hydrogen bonding features in the solid state. It is very interesting to note that when no amine is present in the sulfide, **134**, then the sulfide functionality is on the same side as the amide, **Figure 3.14**. However when the amine functionality is introduced in **162**, then the sulfide is on the same side as the amine, **Figure 3.41**. Although in **162** quite a distance exists between the amine N-H and the sulfide (2.93 Å), perhaps weak intramolecular hydrogen bonding is occurring between these groups. The predicted intermolecular N-H...O=C interactions were observed in **162**, which blocks the sulfide from lying on the same side as the amide. The solid state structure of the sulfoxide, **163**, adopts a conformation that enables two structure-defining intermolecular interactions: the amine N-H...O=S and the amide N-H...O=C. The key feature that arose was the unanticipated orientation of the sulfoxide out of the plane. While computational studies demonstrate that an intramolecular hydrogen bond is possible, it would require the axial phenyl rings to twist out of planarity, therefore leading to a decrease of extended conjugation and stabilisation. As a result, the observed conformation, which has the sulfoxide oxygen pointing away from the amide, is predicted to be slightly lower in energy. It was observed that at the sulfone level of oxidation in **164**, the molecule rotated to adopt a conformation similar to **162**. The N-H...O=C C(4) chains were broken and N-H...O=S intramolecular interactions between the amine and sulfone were noted. To investigate the solution properties of compounds **162** and **163**, NMR studies were undertaken. Results from NOESY 2D NMR experiments did not result in any substantial correlation between spectroscopic features and the solid state interactions.

The observed rotation of the diphenylacetylene unit after oxidation is a significant breakthrough in this research as it has now been demonstrated that solid state structures can be controlled in a rational manner, albeit with the key hydrogen bonding interactions somewhat different to the predicted patterns. These results may lead to future applications in the development of an innovative molecular switching mechanism.

3.3. References

1. (a) Yang, X.; Yuan, L.; Yamato, K.; Brown, A. L.; Feng, W.; Furukawa, M.; Zeng, X. C.; Gong, B. *J. Am. Chem. Soc.*, **2004**, *126*, 3148-3162. (b) Abramenkov, A. V.; Almenningen, A.; Cyvin, B. N.; Cyvin, S.J.; Jonvik, T.; Khaikin, L. S.; Romming, C.; Vilkov, L.V. *Acta Chem. Scand.*, **1988**, *A42*, 674-684.
2. Liberles, A.; Matlosz, B. *J. Org. Chem.*, **1971**, *36*, 2710-2713.
3. Kemp, D. S.; Li, Z. Q. *Tetrahedron Lett.*, **1995**, *36*, 4175-4178.
4. Kemp, D. S.; Li, Z. Q. *Tetrahedron Lett.*, **1995**, *36*, 4179-4180.
5. Wyrembak, P. N.; Hamilton, A. D. *J. Am. Chem. Soc.*, **2009**, *131*, 4566-4567.
6. Jones, I. M.; Hamilton, A. D. *Org. Lett.*, **2010**, *12*, 3651-3653.
7. Jones, I. M.; Lingard, H.; Hamilton, A. D. *Angew. Chem., Int. Ed.*, **2011**, *50*, 12569-12571.
8. Jones, I. M.; Hamilton, A. D. *Angew. Chem., Int. Ed.*, **2011**, *50*, 4597-4600.
9. Eccles, K. S.; Elcoate, C. J.; Maguire, A. R.; Lawrence, S. E. *Cryst. Growth Des.*, **2011**, *11*, 4433-4439.
10. Hunter, C. A. *Angew. Chem., Int. Ed.*, **2004**, *43*, 5310-5324.
11. Nangia, A.; Desiraju, G. R. *Chem. Commun.*, **1999**, 605-606.
12. Allen, F. H.; Kennard, O.; Watson, D. G.; Brammer, L.; Orpen, A. G.; Taylor, R. *J. Chem. Soc., Perkin Trans. 2*, **1987**, S1-S19.
13. Shin, W.; Cho, S. W. *Acta Crystallogr., Sect. C: Cryst. Struct. Commun.*, **1992**, *C48*, 1447-1449.
14. Vanhouteghem, F.; Lenstra, A. T. H.; Geise, H. J.; Van, d. A.; Anteunis, M. J. *Acta Crystallogr., Sect. C: Cryst. Struct. Commun.*, **1985**, *C41*, 1818-1821.
15. Iwasaki, F.; Toyoda, N.; Yamazaki, N. *Acta Crystallogr., Sect. C: Cryst. Struct. Commun.*, **1989**, *C45*, 1914-1917.
16. Corey, E. J.; Fuchs, P. L. *Tetrahedron Lett.*, **1972**, 3769-3772.
17. Mueller, S.; Liepold, B.; Roth, G. J.; Bestmann, H. J. *Synlett*, **1996**, 521-522.
18. Chen, Q. H.; Rao, P. N. P.; Knaus, E. E. *Bioorg. Med. Chem.*, **2005**, *13*, 6425-6434.
19. Schneider, C. C.; Bortolatto, C.; Back, D. F.; Menezes, P. H.; Zeni, G. *Synthesis*, **2011**, 413-418.
20. Costa, M.; Della, C.; Gabriele, B.; Massera, C.; Salerno, G.; Soliani, M. *J. Org. Chem.*, **2004**, *69*, 2469-2477.

21. Ashburn, B. O.; Rathbone, L. K.; Camp, E. H.; Carter, R. G. *Tetrahedron*, **2007**, *64*, 856-865.
22. Banzatti, C.; Carfagna, N.; Commisso, R.; Heidempergher, F.; Pegrassi, L.; Melloni, P. *J. Med. Chem.*, **1988**, *31*, 1466-1471.
23. Barbero, N.; Carril, M.; San, M.; Dominguez, E. *Tetrahedron*, **2007**, *63*, 10425-10432.
24. Kotha, S.; Shah, V. R. *Eur. J. Org. Chem.*, **2008**, 1054-1064.
25. Zhu, Y. Y.; Yi, H. P.; Li, C.; Jiang, X. K.; Li, Z. T. *Cryst. Growth Des.*, **2008**, *8*, 1294-1300.
26. Wardell, J. L.; Low, J. N.; Skakle, J. M. S.; Glidewell, C. *Acta Crystallogr., Sect. B: Struct. Sci.*, **2006**, *B62*, 931-943.
27. Nayak, S. K.; Reddy, M. K.; Guru, R.; Chopra, D. *Cryst. Growth Des.*, **2011**, *11*, 1578-1596.
28. Lehane, K. N.; Moynihan, E. J. A.; Brondel, N.; Lawrence, S. E.; Maguire, A. R. *CrystEngComm*, **2007**, *9*, 1041-1050.
29. Quesada, E.; Raw, S. A.; Reid, M.; Roman, E.; Taylor, R. J. K. *Tetrahedron*, **2006**, *62*, 6673-6680.
30. Seyferth, D.; Marmor, R. S.; Hilbert, P. *J. Org. Chem.*, **1971**, *36*, 1379-1386.
31. Gilbert, J. C.; Weerasooriya, U. *J. Org. Chem.*, **1982**, *47*, 1837-1845.
32. Colvin, E. W.; Hamill, B. J. *J. Chem. Soc., Perkin Trans. 1*, **1977**, 869-874.
33. Jenny, N. M.; Mayor, M.; Eaton, T. R. *Eur. J. Org. Chem.*, **2011**, *2011*, 4965-4983.
34. Larock, R. C.; Yum, E. K.; Refvik, M. D. *J. Org. Chem.*, **1998**, *63*, 7652-7662.
35. Chinchilla, R.; Najera, C. *Chem. Rev.*, **2007**, *107*, 874-922.
36. Trost, B. M.; Sorum, M. T.; Chan, C.; Ruehter, G. *J. Am. Chem. Soc.*, **1997**, *119*, 698-708.
37. Siemsen, P.; Livingston, R. C.; Diederich, F. *Angew. Chem., Int. Ed.*, **2000**, *39*, 2632-2657.
38. Haley, M. M.; Bell, M. L.; English, J. J.; Johnson, C. A.; Weakley, T. J. R. *J. Am. Chem. Soc.*, **1997**, *119*, 2956-2957.
39. Allen, F. H.; Bird, C. M.; Rowland, R. S.; Raithby, P. R. *Acta Crystallogr., Sect. B: Struct. Sci.*, **1997**, *B53*, 696-701.
40. Jiang, R. W.; Lu, Y.; Min, Z. D.; Zheng, Q. T. *J. Mol. Struct.*, **2003**, *655*, 157-162.
41. Etter, M. C. *Acc. Chem. Res.*, **1990**, *23*, 120-126.

42. Rice, C. R.; Wallis, J. D. *J. Chem. Soc., Chem. Commun.*, **1993**, 572-574.
43. Pilkington, M.; Wallis, J. D.; Smith, G. T.; Howard, J. A. K. *J. Chem. Soc., Perkin Trans. 2*, **1996**, 1849-1854.
44. Smith, G. T.; Howard, J. A. K.; Wallis, J. D. *Phys. Chem. Chem. Phys.*, **2001**, 3, 4501-4507.
45. Francuski, B. M.; Novakovic, S. B.; Bogdanovic, G. A. *CrystEngComm*, **2011**, 13, 3580-3591.
46. Howard, D. L.; Kjaergaard, H. G. *Phys. Chem. Chem. Phys.*, **2008**, 10, 4113-4118.
47. Liu, Y.; Lu, Y.; Prashad, M.; Repic, O.; Blacklock, T. J. *Adv. Synth. Catal.*, **2005**, 347, 217-219.
48. Bellamy, F. D.; Ou, K. *Tetrahedron Lett.*, **1984**, 25, 839-842.
49. Frisch, M. J.; Trucks, G. W.; Schlegel, H. B.; Scuseria, G. E.; Robb, M. A.; Cheeseman, J. R.; Scalmani, G.; Barone, V.; Mennucci, B.; Petersson, G. A.; Nakatsuji, H.; Caricato, M.; Li, X.; Hratchian, H. P.; Izmaylov, A. F.; Bloino, J.; Zheng, G.; Sonnenberg, J. L.; Hada, M.; Ehara, M.; Toyota, K.; Fukuda, R.; Hasegawa, J.; Ishida, M.; Nakajima, T.; Honda, Y.; Kitao, O.; Nakai, H.; Vreven, T.; Montgomery, J. A. Jr.; Peralta, J. E.; Ogliara, F.; Bearpark, M.; Heyd, J. J.; Brothers, E.; Kudin, K. N.; Staroverov, V. N.; Kobayashi, R.; Normand, J.; Raghavachari, K.; Rendell, A.; Burant, J. C.; Iyengar, S. S.; Tomasi, J.; Cossi, M.; Rega, N.; Millam, N. J.; Klene, M.; Knox, J. E.; Cross, J. B.; Bakken, V.; Adamo, C.; Jaramillo, J.; Gomperts, R.; Stratmann, R. E.; Yazyev, O.; Austin, A. J.; Cammi, R.; Pomelli, C.; Ochterski, J. W.; Martin, R. L.; Morokuma, K.; Zakrzewski, V. G.; Voth, G. A.; Salvador, P.; Dannenberg, J. J.; Dapprich, S.; Daniels, A. D.; Farkas, O.; Foresman, J. B.; Ortiz, J. V.; Cioslowski, J.; Fox, D. J. *Gaussian 09, Revision B. 1*, **2012**, Gaussian, Inc.: Wallingford, CT, 2009.
50. Becke, A. D. *J. Chem. Phys.*, **1993**, 98, 5648-5652.
51. Lee, C.; Yang, W.; Parr, R. G. *Phys. Rev. B: Condens. Matter*, **1988**, 37, 785-789.
52. Daly, C. A.; Eccles, K. S.; Bateman, L. M.; O'Boyle, N. M.; Lawrence, S. E.; Maguire, A. R. *CrystEngComm*, **2012**, 14, 7848-7850.

Chapter 4

Conclusions and Future Work

4. Conclusions and Future Work

4.1. Conclusions

This work began with an overall aim to understand how the solid state can be varied in a predictive and rational manner based on subtle alterations in the molecular structure. Based on earlier research from within the group, specifically by Lehane *et al.*,^{1,2} this work focused on the design of a solid state structure that could be manipulated by varying the level of oxidation of sulfur. While Lehane demonstrated that hydrogen bonding involving terminal alkynes as hydrogen bond donors could be predictably controlled as a structure determining feature, depending on the oxidation state of sulfur in simple organic molecules, this research significantly expanded this concept to include more complex systems and investigate the impact of altering the oxidation level of sulfur on hydrogen bond interactions in the solid state. Firstly, suitable compounds that could be assembled easily and could incorporate terminal alkyne, ether and sulfur functionalities were designed. Tertiary amines and 1,2,3-substituted aromatic systems best suited this purpose.

A synthetic strategy was developed which yielded 31 novel tertiary amines incorporating a variety of terminal alkynes, ethers, sulfides (**22-32**), sulfoxides (**33-42**) and sulfones (**43-52**). While the majority of these tertiary amines were isolated as oils at room temperature, crystal structures were obtained for a small portion using low temperature techniques. As a result, it is difficult to discern a definite trend in the hydrogen bonding patterns for these tertiary amines. However, the $C\equiv C-H\cdots O=S$ interaction identified by Lehane, emerged once again as a dominant interaction in some of the tertiary amine systems (**33** and **43**). In many of the structures obtained $(R)_2NCH\cdots O=S$ interactions were a frequent occurrence due to the relatively acidic nature of the α hydrogens adjacent to the nitrogen. A most unusual interaction involving $C\equiv C-H\cdots \pi(\text{arene})$ was also observed which has been previously described to be a feature in particularly viscous compounds.³

Many synthetic strategies were attempted to tri-alkylate the triol, **57**. After a number of attempts, the ether, terminal alkyne and sulfide functionalities were attached, to form **88**. Successful oxidation was also achieved to afford the corresponding sulfoxide, **89**. While **88** and **89** were not crystalline at room temperature, ¹H NMR data suggests that the functional groups are not in an orientation to accommodate $C\equiv C-H\cdots O=S$ intramolecular hydrogen bonding. Nonetheless, with a suitable synthetic strategy in place and also the possibility of

combining this aromatic system with the tertiary amine, future expansion could result in obtaining crystalline material and studying the hydrogen bond interactions.

The ability to control the orientation of a molecule by altering its hydrogen bonding properties through varying the oxidation level of sulfur was a particularly exciting prospect to explore in this research. However, this was unlikely to be achieved in the tertiary amine and aromatic systems previously discussed, as they contain terminal alkynes which form weak hydrogen bonds. Controlling the conformation of a molecule would be too difficult to achieve based solely on weak hydrogen bond interactions. Therefore, a stronger hydrogen bond donor was required. Previous research in the group highlighted the effective use of sulfoxide-amide interactions in supramolecular synthons.⁴ As a result, the research expanded to incorporate sulfur and amide functionalities within a single molecule and study the effects of varying the oxidation level of sulfur on the hydrogen bond interactions in the solid state. The diphenylacetylene unit involving ester and amide functionalities recently explored by Hamilton *et al.*, provided a suitable scaffold on which to construct this system.⁵ Their success in controlling the conformation of the molecule by varying the acidity of the amide encouraged us to expand this system by incorporating sulfur functionalities. Applying Hunter's rationale, it was envisaged that competition could be created between hydrogen bond acceptors for the strongest donor by varying the oxidation state of sulfur.⁶

A synthetic strategy was designed to access the diphenylacetylenes bearing amide and sulfur functionalities. Iodo-amides, (**115-119**), with varying electronic properties, and alkynyl sulfur compounds, (**123**, **126-130**), were prepared and coupled *via* Sonogashira reaction conditions. While Sonogashira couplings involving amide and sulfur functionalities have not been widely reported in the literature, it was successfully achieved in this research to afford a wide range of compounds differing in size, electronic properties and oxidation states. Their crystal structures were subsequently determined to reveal some very interesting conformations and hydrogen bonding interactions.

In general, as predicted, it was observed that the hydrogen bonding network altered remarkably as the oxidation of sulfur was varied. It was noted in the majority of the structures obtained, that the amide acted as the major hydrogen bond acceptor in sulfides and usually formed C-H...O=C and N-H...O=C interactions. In the sulfoxides, these interactions were then replaced by C-H...O=S and N-H...O=S interactions as sulfoxides are stronger hydrogen bond acceptors than amides. The amide once again acted as the major hydrogen

bond donor in the sulfones where once again C-H...O=C and N-H...O=C interactions were observed. At the outset of this research, it was envisaged that a clean switching effect would be observed on oxidation from sulfide to sulfoxide and sulfone. While this switching was observed, the unanticipated orientation of the sulfoxide oxygen out of the plane means that the original concept was too simple, and as a result, it would be difficult to predict the precise solid state properties based on this approach. Depending on the electronic nature of the amide, it appeared that the solid state structures of the diphenylacetylene units were influenced by steric and electronic effects. For example, it was observed that by attaching electron withdrawing/donating substituents to the amide, then the acidity and hydrogen bonding capability of the amide N-H could be controlled *e.g.* **137** and **140**.

Ultimately, the desired switch in conformation was observed when an amine was introduced to act as a competing hydrogen bond donor. It was demonstrated through single X-ray diffraction studies that the sulfur functionality could be manipulated to lie on a specific side of the molecule by altering its oxidation level. As a sulfide, **162**, the conformation with the sulfide on the same side of the molecule as the amine was favoured. In the sulfoxide, **163**, a switch in conformation was observed due to the disruption of the strong N-H...O=C C(4) chains. Then, in the sulfone, **164**, the molecule adopted a similar conformation to its corresponding sulfide. This rotation in conformation demonstrates that by making subtle alterations in the molecular structure *i.e.* varying the oxidation level of sulfur, then the solid state is affected significantly. Specifically, it was demonstrated that by controlling the hydrogen bond donor/acceptor capabilities of certain functional groups, then the conformation of a molecule can be altered. The exploitation of these interactions resulted in the development of a molecular switch.

Further development of these preliminary results is warranted to lead to improved molecular switches through control of electronic features including amide acidity and sulfur oxidation. Critically, robust synthetic methods have now been developed to lead to a range of building blocks for solid state investigation based on these exciting hydrogen bonding motifs.

4.2. Future Work

Many areas in this research could potentially be expanded and further investigated. Now with robust synthetic strategies in place, the tertiary amine and aromatic systems described in Chapter 2 can be further functionalised and even combined to further study the $C\equiv C-H\cdots O=S$ and $(R)_2NCH\cdots O=S$ interactions in the solid state.

Also, perhaps the observation in Chapter 2 of the involvement of the $(R)_2NCH_2$ moiety in hydrogen bonding could potentially be linked with the diphenylacetylene core structure that effectively worked as a switching entity in Chapter 3. Furthermore, additional functional groups could be attached to the diphenylacetylenes bearing the amide and sulfur functionalities discussed in Chapter 3. Since the orientation of the sulfoxide out of the plane impacted upon the hydrogen bonding interactions in these diphenylacetylene systems, perhaps the addition of a benzyl-sulfur functionality would alter the orientation of the sulfoxide and result in an $N-H\cdots O=S$ intramolecular interaction, **Figure 4.1**.

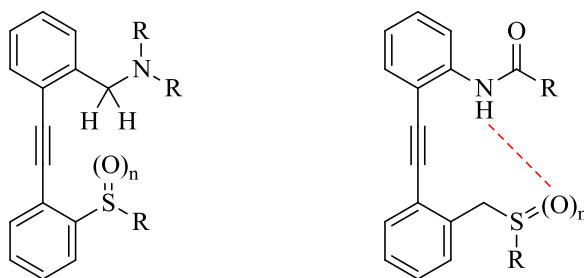


Figure 4.1: Potential target compounds.

4.3. References

1. Lehane, K. N.; Moynihan, E. J. A.; Brondel, N.; Lawrence, S. E.; Maguire, A. R. *CrystEngComm*, **2007**, *9*, 1041-1050.
2. Brondel, N.; Moynihan, E. J. A.; Lehane, K. N.; Eccles, K. S.; Elcoate, C. J.; Coles, S. J.; Lawrence, S. E.; Maguire, A. R. *CrystEngComm*, **2010**, *12*, 2910-2927.
3. Weiss, H. C.; Blaser, D.; Boese, R.; Doughan, B. M.; Haley, M. M. *Chem. Commun.*, **1997**, 1703-1704.
4. Eccles, K. S.; Elcoate, C. J.; Maguire, A. R.; Lawrence, S. E. *Cryst. Growth Des.*, **2011**, *11*, 4433-4439.
5. Jones, I. M.; Hamilton, A. D. *Org. Lett.*, **2010**, *12*, 3651-3653.
6. Hunter, C. A. *Angew. Chem., Int. Ed.*, **2004**, *43*, 5310-5324.

Chapter 5

Experimental

5. Contents

5.1. General Procedures	185
5.2. Tertiary Amine Synthesis.....	187
5.2.1. Linkers A and C.....	187
5.2.2. Secondary Amines.....	189
5.2.3. Preparation of tertiary amine sulfides.....	193
5.2.4. Preparation of tertiary amine sulfoxides.....	202
5.2.5. Preparation of tertiary amine sulfones.....	210
5.3. Aromatic based systems	218
5.3.1. Arms D, E and F.....	218
5.3.2. Synthetic Strategy I	222
5.3.3. Synthetic Strategy II	226
5.3.4. Synthetic Strategy III.....	232
5.4. Combination of tertiary amine and aromatic scaffolds	235
5.5. Diphenylacetylene Scaffold	237
5.5.1. Iodoamide precursors	237
5.5.2. Terminal alkyne precursors	240
5.5.3. Sonogashira coupled products	246
5.6. Introduction of competing hydrogen bond donor	265
5.7. References.....	273

5.1. General Procedures

All solvents used were HPLC grade or were distilled prior to use by the following methods: acetonitrile was distilled from calcium hydride, dichloromethane was distilled from phosphorous pentoxide and ethyl acetate was distilled from potassium carbonate. Methanol was distilled from magnesium in the presence of iodine and stored over 3 Å molecular sieves.¹ Tetrahydrofuran (THF) was distilled from sodium and benzophenone.¹ Molecular sieves were dried by heating at 150 °C overnight. Organic phases were dried using anhydrous magnesium sulphate. All commercial reagents were supplied by Sigma-Aldrich and were used without further purification.

Infrared spectra were recorded as thin films on sodium chloride plates for oils or as potassium bromide (KBr) discs for solids on a Perkin Elmer Paragon 1000 FT-IR spectrometer. Melting points were measured on an Electrothermal 9100-Melting Point apparatus. Microwave assisted synthesis was conducted using the CEM Discover Synthesiser in conjunction with ChemDriver software (Version 3.5.0).

¹H (300 MHz) and ¹³C (75.5 MHz) NMR spectra were recorded on a Bruker Avance 300 MHz NMR spectrometer. ¹H (400 MHz) NMR spectra were recorded on a Bruker Avance 400 MHz NMR spectrometer. ¹H (600 MHz) and ¹³C (600 MHz) NMR spectra were recorded on a Bruker Avance 600 MHz NMR spectrometer. All spectra were recorded at room temperature (~20 °C) in deuterated chloroform (CDCl₃), unless otherwise stated using tetramethylsilane (TMS) as an internal standard. Chemical shifts (δ_{H} & δ_{C}) are reported in parts per million (ppm) relative to TMS and coupling constants are expressed in Hertz (Hz). Splitting patterns in ¹H spectra are designated as follows: singlet (s), broad singlet (bs), doublet (d), doublet of doublets (dd), triplet of doublets (td), triplet (t), quartet (q), AB quartet (ABq) and m (multiplet). ¹³C NMR spectra were calibrated using the solvent signals, *i.e.* δ_{C} 77.0 ppm, and were assigned with the aid of DEPT experiments. On occasion *J* values measured from the spectra do not exactly match up, but always fall within experimental error.

Thin layer chromatography (TLC) was carried out on precoated silica gel plates (Merck 60 PF₂₅₄). Visualisation was achieved by UV (254nm) light detection and potassium permanganate staining. Wet flash chromatography was performed using Kieselgel silica gel 60, 0.040-0.063 mm (Merck).

Low resolution mass spectra (LRMS) were recorded on a Waters Quattro Micro triple quadrupole spectrometer in electrospray ionisation (ESI) mode using 50% water/acetonitrile containing 0.1% formic acid as eluent; samples were made up in acetonitrile. High resolution precise mass spectra (HRMS) were recorded on a Waters LCT Premier Tof LC-MS instrument in electrospray ionisation (ESI) mode using 50% water/acetonitrile containing 0.1% formic acid as eluent; samples were prepared in acetonitrile.

Elemental analysis were performed by the Microanalysis Laboratory, National University of Ireland, Cork, using Perkin-Elmer 240 and Exeter Analytical CE440 elemental analysers.

Single crystal X-ray diffraction data were collected at University College Cork on either a Bruker APEX II DUO diffractometer or a Bruker SMART X2S diffractometer.² The APEX II DUO allows either Mo K α radiation (graphite monochromator, $\lambda = 0.7107 \text{ \AA}$) or Cu K α radiation (doubly curved silicon monochromator, $\lambda = 1.54178 \text{ \AA}$). An Oxford Cryosystems COBRA fitted with an N₂ generator was used for cooling. All calculations were performed using the APEX2 software suite,^{3,4} and the diagrams were prepared using Mercury 3.0.⁵ The N-H and O-H hydrogen atoms were found and refined where possible and the positions of the other hydrogen atoms were calculated and allowed to ride on the parent atom.

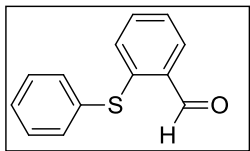
References:

1. Leonard, J.; Lygo, B.; Procter, G.; Editors. *Advanced Practical Organic Chemistry, 2nd Edition*; **1995**.
2. Eccles, K. S.; Stokes, S. P.; Daly, C. A.; Barry, N. M.; McSweeney, S. P.; O'Neill, D. J.; Kelly, D. M.; Jennings, W. B.; Ní Dhubhghaill, O. M.; Moynihan, H. A.; Maguire, A. R.; Lawrence, S. E. *J. Appl. Cryst.* **2011**, *44*, 213–215.
3. *APEX2 v2009.3-0*; Bruker AXS: Madison, WI, 2009.
4. Sheldrick, G. M. *Acta Crystallogr., Sect. A* **2008**, *64*, 112–122.
5. Macrae, C. F.; Bruno, I. J.; Chisholm, J. A.; Edgington, P. R.; McCabe, P.; Pidcock, E.; Rodriguez-Monge, L.; Taylor, R.; van de Streek, J.; Wood, P. A. *J. Appl. Crystallogr.* **2008**, *41*, 466–470.

5.2. Tertiary Amine Synthesis

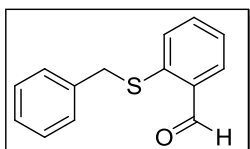
5.2.1. Linkers A and C

2-(Phenylthio)benzaldehyde (**6**)¹



This compound was synthesised using a modified version of the Heynderickx procedure.¹ 2-Chlorobenzaldehyde, **3**, (1.73 mL, 15.0 mmol) was added dropwise over 10 mins, to a stirred solution of thiophenol, **4**, (2.0 mL, 19.0 mmol) and anhydrous sodium carbonate (2.68 g, 25.0 mmol) in dry DMF (20 mL) at 80-90 °C under nitrogen. The resulting mixture was stirred at the same temperature for 4 h. After cooling, the reaction mixture was poured onto water (100 mL) and extracted with ether (2 x 50 mL). The extract was washed with water (2 x 50 mL), dried with MgSO₄, and concentrated to afford an oil that crystallised by adding hexane. Recrystallisation from hexane gave 2-(phenylthio)benzaldehyde, **6**, (1.87 g, 58 %), as pale yellow crystals. m.p: 49-50 °C (Lit.¹ 50 °C); $\nu_{\max}/\text{cm}^{-1}$ (KBr): 3067 (=C-H), 2843 (CH), 1673 (C=O), 1552 (ring stretch), 1456 (ring stretch), 1440 (H-C=O); δ_{H} (300 MHz): 7.11 (1H, dd, *J* 7.8, 1.2, ArH), 7.29-7.46 (7H, m, ArH), 7.87 (1H, dd, *J* 7.5, 1.5, ArH), 10.39 (1H, s, CHO); Spectral characteristics were in agreement with those previously reported.¹

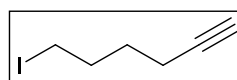
2-(Benzylthio)benzaldehyde (**7**)²



This compound was synthesised using using a modified version of the Heynderickx procedure.¹ 2-Chlorobenzaldehyde, **3**, (1.38 mL, 12.0 mmol) was added dropwise over 10 mins to a stirred solution of benzylmercaptan, **5**, (2.0 mL, 16.0 mmol) and anhydrous sodium carbonate (2.14 g, 20.0 mmol) in dry DMF (20 mL) at 80-90 °C under nitrogen. The resulting mixture was stirred at the same temperature for 4 h. After cooling, the reaction mixture was poured onto water (100 mL) and extracted with ether (2 x 50 mL). The extract was washed with water (2 x 50 mL), dried with MgSO₄, and concentrated to afford an oil that crystallised by adding hexane. Recrystallisation from hexane gave 2-(benzylthio)benzaldehyde, **7**, (1.04 g, 38 %), as a pale yellow crystals. m.p: 74-76 °C (Lit.³ 75 °C); $\nu_{\max}/\text{cm}^{-1}$ (KBr): 3060 (=C-H), 1691 (C=O), 1587 (ring stretch), 1460 (H-C=O); δ_{H} (300 MHz): 4.13 (2H, s, CH₂S), 7.21-7.37 (6H, m, ArH), 7.43-7.53 (2H, m, ArH), 7.81 (1H, dd, *J* 7.7, 1.4, ArH), 10.26 (1H, s, CHO); Spectral characteristics were in agreement with those previously reported.²

5-Iodopent-1-yne (14)⁴

This compound was synthesised using a modified version of the Borbas procedure.⁵ Triphenylphosphine (1.87 g, 7.13 mmol), imidazole (0.49 g, 7.13 mmol) and CH₂Cl₂ (10 mL) were added to a two-necked round bottom flask under a flow of nitrogen and stirred at room temperature until the solids had dissolved resulting in a clear solution. The reaction mixture was cooled to 0 °C using an ice bath. Iodine (1.81 g, 7.13 mmol) was then added portionwise to the mixture. Once all the iodine had dissolved, 4-pentyn-1-ol, **12**, (0.50 mL, 5.40 mmol) in CH₂Cl₂ (2 mL) was added slowly by syringe over 10-15 mins. Stirring of the reaction mixture was continued for 24 h. The mixture was then washed with portions of aqueous sodium thiosulfate (1 M, 4 x 20 mL) and the phases separated. The organic extracts were washed repeatedly with water until colourless, dried over MgSO₄, filtered, and the solvent was removed *in vacuo*. Purification by column chromatography using hexane/ethyl acetate (9:1) as eluent, gave the alkyne **14**, as a pale yellow oil (0.47 g, 45%). $\nu_{\max}/\text{cm}^{-1}$ (film): (C≡C-H stretch not observed), 2961 (CH), 2918 (CH), (C≡C stretch not observed), 801 (C-I); δ_{H} (400 MHz): 1.97-2.05 (3H, m, CH₂CH₂I and C≡C-H), 2.34 (2H, td, *J* 6.7, 2.5, CH₂C≡C-H), 3.32 (2H, t, *J* 6.8, CH₂I); Spectral characteristics were in agreement with those previously reported.⁴

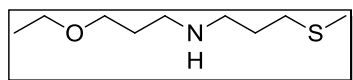
6-Iodohept-1-yne (15)⁴

Triphenylphosphine (3.15 g, 12.0 mmol), imidazole (0.82 g, 12.0 mmol), CH₂Cl₂ (20 mL), iodine (3.05 g, 12.0 mmol) and 5-hexyn-1-ol, **13** (1.0 mL, 9.07 mmol) were used in the same way as described in **14** to give the alkyne **15**, as a pale yellow oil after column chromatography (1.16 g, 62%). $\nu_{\max}/\text{cm}^{-1}$ (film): (C≡C-H not observed), 2963 (CH), (C≡C stretch not observed), 1260 (CH₂), 799 (C-I); δ_{H} (300 MHz): 1.59-1.70 (2H, m, CH₂CH₂CH₂I), 1.90-2.01 (3H, m, CH₂CH₂I and C≡C-H), 2.23 (2H, td, *J* 6.9, 2.7, CH₂C≡C-H), 3.22 (2H, t, *J* 6.9, CH₂I); δ_{C} (75 MHz): 6.1 (CH₂, CH₂I), 17.4 (CH₂, CH₂C≡CH), 29.1, 32.2 (2 x CH₂, CH₂CH₂CH₂C≡CH), 68.9 (CH, C≡CH), 83.6 (C, C≡CH); Spectral characteristics were in agreement with those previously reported.⁴

5.2.2. Secondary Amines

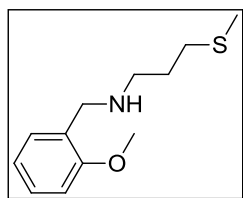
The following secondary amines were synthesised according to a modified version of the Abdel-Magid procedure.⁶

3-Ethoxy-*N*-[3-(methylthio)propyl]propan-1-amine (16)



3-(Methylthio)-propionaldehyde, **1**, (0.91 mL, 9.6 mmol) was added to a solution of 3-ethoxypropylamine, **8**, (1.22 mL, 10.0 mmol) in methanol (15 mL) and the resulting solution was heated under reflux for 16 h under nitrogen. The reaction progress was monitored by TLC, until complete formation of the aldimine was observed. Solid sodium borohydride (0.58 g, 15.0 mmol) was then added to the solution in small portions over a period of 10-15 mins. The reaction mixture was stirred for 1 h at room temperature and then quenched with aqueous NaOH (1 M, 10 mL). The product was extracted with ether (3 x 20 mL). The combined organic phases were washed with brine (30 mL), dried over MgSO₄ and concentrated *in vacuo* to give the crude product. Purification was achieved by column chromatography using hexane/ethyl acetate (3:2) as eluent, to give **16**, as a colourless oil (0.19 g, 11%). $\nu_{\max}/\text{cm}^{-1}$ (film): 2931 (CH), 2860 (CH), 1442 (CH₃), 1376 (CH₃), 1114 (COC), 511 (CNC); δ_{H} (300 MHz): 1.19 (3H, t, *J* 7.0, OCH₂CH₃), 1.74-1.87 (4H, m, 2 x CH₂CH₂NH), 2.10 (3H, s, CH₃S), 2.24 (1H, bs, NH), 2.55 (2H, t, *J* 7.0, CH₂S), 2.73 (4H, t, *J* 7.0, CH₂NCH₂), 3.41-3.53 (4H, m, 2 x CH₂OCH₂); δ_{C} (75 MHz): 15.2, 15.5 (CH₃, 2 x CH₃), 29.1, 29.8 (2 x CH₂, CH₂CH₂NHCH₂CH₂), 32.1 (CH₂, CH₂SCH₃), 47.4, 48.7 (2 x CH₂, CH₂NHCH₂), 66.2, 69.2 (2 x CH₂, CH₂OCH₂); *m/z* (ESI) 192.5 [(M+H)⁺]; HRMS (ESI): exact mass calculated for C₉H₂₂NOS [(M+H)⁺], 192.1422. Found 192.1423.

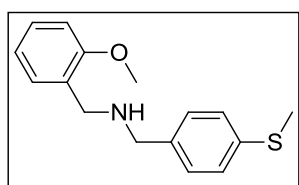
N-(2-Methoxybenzyl)-3-(methylthio)propan-1-amine (17)⁷



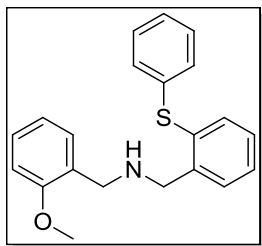
3-(Methylthio)-propionaldehyde, **1**, (0.91 mL, 9.6 mmol) was added to a solution of 2-methoxybenzylamine, **9**, (1.33 mL, 10.0 mmol) in methanol (15 mL) and the resulting solution was stirred at room temperature for 16 h under nitrogen. The reaction progress was monitored by TLC, until complete formation of the aldimine was observed. Solid sodium borohydride (0.58 g, 15.0 mmol) was then added to the solution in small portions over a period of 10-15 mins. The reaction mixture was stirred for 1 h at room temperature and then quenched with aqueous NaOH (1 M, 10 mL). The product was extracted with ether (3 x 20

mL). The ether layers were combined, washed with brine (30 mL) and dried over MgSO_4 . The solvent was removed *in vacuo* to give the amine **17**, as a colourless oil without the need for further purification (2.42 g, 98%). $\nu_{\text{max}}/\text{cm}^{-1}$ (film): 3304 (NH), 2915 (CH), 2836 (CH), 1601 (ring stretch), 1495 (ring stretch), 1463 (CH_3), 1242 (CN), 755 (CS); δ_{H} (300 MHz): 1.61 (1H, bs, NH), 1.74-1.87 (2H, m, NHCH_2CH_2), 2.09 (3H, s, SCH_3), 2.55 (2H, t, J 7.4, CH_2S), 2.69 (2H, t, J 7.0, NHCH_2CH_2), 3.78 (2H, s, $\text{NHCH}_2\text{C}_6\text{H}_4$), 3.78 (3H, s, OCH_3), 6.80-6.96 (2H, m, ArH), 7.181-7.27 (2H, m, ArH). Spectral characteristics were in agreement with those previously reported.⁷

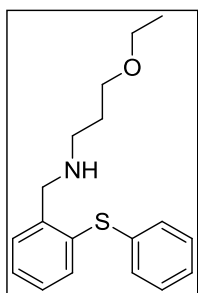
***N*-(2-Methoxybenzyl)-1-[4-(methylthio)phenyl]methanamine (18)**



4-(Methylthio)benzaldehyde, **2**, (0.44 mL, 3.29 mmol) was added to a solution of 2-methoxybenzylamine, **9**, (0.45 mL, 3.48 mmol) in methanol (10 mL) and the resulting solution was stirred at room temperature for 16 h under nitrogen. The reaction progress was monitored by TLC, until complete formation of the aldimine was observed. Solid sodium borohydride (0.20 g, 5.26 mmol) was then added to the solution in small portions over a period of 10-15 mins. The reaction mixture was stirred for 1 h at room temperature and then quenched with aqueous NaOH (1 M, 5 mL). The product was extracted with ether (3 x 10 mL). The organic extracts were combined, washed with brine (20 mL), dried over MgSO_4 and the solvent was removed *in vacuo*. The resulting amine **18** was obtained as a colourless oil, without the need for further purification (0.89 g, 98%). $\nu_{\text{max}}/\text{cm}^{-1}$ (film): 3332 (NH), 2920 (CH), 2835 (CH), 1601 (ring stretch), 1495 (ring stretch), 1463 (CH_2), 1456 (CH_3), 1242 (CN); δ_{H} (400 MHz): 1.88 (1H, bs, NH), 2.47 (3H, s, CH_3), 3.73, 3.79 (2 x 2H, 2 x s, CH_2NHCH_2), 3.82 (3H, s, OCH_3), 6.86 (1H, d, J 8.0, ArH), 6.92 (1H, td, J 7.4, 0.8, ArH), 7.20-7.29 (6H, m, ArH); δ_{C} (75 MHz): 16.2 (CH_3 , SCH_3), 48.7, 52.5 (2 x CH_2 , CH_2NHCH_2), 55.2 (CH_3 , OCH_3), 110.3 (CH, aromatic CH), 120.4 (CH, aromatic CH), 126.9 (2 x CH, aromatic CH), 128.3 (CH, aromatic CH), 128.4 (C, quaternary aromatic C), 128.8 (2 x CH, aromatic CH), 129.9 (CH, aromatic CH), 136.5 (C, quaternary aromatic C), 137.7 (C, quaternary aromatic C), 157.7 (C, quaternary aromatic C); m/z (ESI) 274.4 [(M+H)⁺]; HRMS (ESI): exact mass calculated for $\text{C}_{16}\text{H}_{20}\text{NOS}$ [(M+H)⁺], 274.1266. Found 274.1266.

***N*-(2-Methoxybenzyl)-1-[2-(phenylthio)phenyl]methanamine (19)**

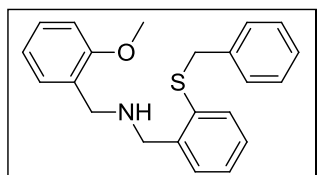
2-(Phenylthio)benzaldehyde, **6**, (0.50 g, 2.33 mmol) was added to a solution of 2-methoxybenzylamine (0.32 mL, 2.47 mmol) in methanol (10 mL) and the resulting solution was stirred at room temperature for 16 h under nitrogen. The reaction progress was monitored by TLC, until complete formation of the aldimine was observed. Solid sodium borohydride (0.14 g, 3.73 mmol) was then added to the solution in small portions over a period of 10-15 mins. The reaction mixture was stirred for 1 h at room temperature and then quenched with aqueous NaOH (1 M, 5 mL). The product was extracted with ether (3 x 10 mL). The ether layers were combined, washed with brine (20 mL) and dried over MgSO₄. The solvent was removed *in vacuo* to give the title compound **19**, as a pale yellow oil (0.74 g, 95%). No purification was undertaken. $\nu_{\max}/\text{cm}^{-1}$ (film): 3316 (NH), 3059 (=CH), 2937 (CH), 2835 (CH), 1601 (ring stretch), 1587 (NH), 1494 (ring stretch), 1464 (CH₃), 1439 (CN), 1289 (CO), 1242 (COC), 691 (CS); δ_{H} (300 MHz): 2.00 (1H, bs, NH), 3.78 (3H, s, OCH₃), 3.79, 3.89 (2 x 2H, 2 x s, CH₂NHCH₂), 6.83 (1H, d, *J* 8.4, ArH), 6.89 (1H, td, *J* 7.4, 1.0, ArH), 7.14-7.39 (10H, m, ArH), 7.48 (1H, dd, *J* 7.4, 1.0, ArH); δ_{C} (75 MHz): 48.9, 51.5 (2 x CH₂, CH₂NHCH₂), 55.2 (CH₃, OCH₃), 110.2 (CH, aromatic CH), 120.4 (CH, aromatic CH), 126.5 (CH, aromatic CH), 127.8 (CH, aromatic CH), 127.9 (CH, aromatic CH), 128.2 (CH, aromatic CH), 128.3 (C, quaternary aromatic C), 129.1 (CH, 2 x aromatic CH), 129.7 (CH, aromatic CH), 129.9 (CH, aromatic CH), 129.9 (CH, 2 x aromatic CH), 133.5 (CH, aromatic CH), 133.8 (C, quaternary aromatic C), 136.5 (C, quaternary aromatic C), 141.8 (C, quaternary aromatic C), 157.7 (C, quaternary aromatic C); *m/z* (ESI) 336.1 [(M+H)⁺]; HRMS (ESI): exact mass calculated for C₂₁H₂₂NOS [(M+H)⁺], 336.1422. Found 336.1419.

3-Ethoxy-*N*-[2-(phenylthio)benzyl]propan-1-amine (20)

2-(Phenylthio)benzaldehyde, **6**, (0.90 g, 4.20 mmol) was added to a solution of 3-ethoxypropylamine (0.53 mL, 4.45 mmol) in methanol (10 mL) and the resulting solution was stirred at room temperature for 16 h under nitrogen. The reaction progress was monitored by TLC, until complete formation of the aldimine was observed. Solid sodium borohydride (0.25 g, 6.72 mmol) was then added to the solution in small portions over a period of 10-15 mins and the resulting mixture was stirred for 1 h at room temperature. Aqueous NaOH (1 M, 5 mL) was then added to quench the reaction. The product was extracted with ether (3 x 10 mL). The combined organic layers were washed

with brine (20 mL), dried over MgSO_4 and the solvent was removed *in vacuo*. The amine **20** was obtained as a pale yellow oil, without the need for further purification (1.12 g, 88%). (Found: C, 71.70; H, 7.60; N, 4.65%. $\text{C}_{18}\text{H}_{23}\text{NOS}$ requires C, 71.72; H, 7.69; N, 4.65%); $\nu_{\text{max}}/\text{cm}^{-1}$ (film): 3327 (NH), 3059 (=CH), 2972 (CH), 2933 (CH), 2861 (CH), 1582 (ring stretch), 1471 (CH_2), 1444 (CH_3), 1377 (CH_3), 1115 (COC), 693 (CS); δ_{H} (400 MHz): 1.17 (3H, t, J 7.0, OCH_2CH_3), 1.65 (1H, bs, NH), 1.69-1.78 (2H, m, $\text{CH}_2\text{CH}_2\text{NH}$), 2.67 (2H, t, J 6.9, $\text{CH}_2\text{CH}_2\text{NH}$), 3.41-3.48 (4H, m, CH_2OCH_2), 3.90 (2H, s, $\text{NHCH}_2\text{C}_6\text{H}_4\text{S}$), 7.17-7.23 (4H, m, ArH), 7.24-7.34 (4H, m, ArH), 7.43 (1H, dd, J 7.5, 1.4, ArH); δ_{C} (75 MHz): 15.2 (CH_3 , CH_3), 30.1 (CH_2 , $\text{CH}_2\text{CH}_2\text{NH}$), 46.7, 52.2 (2 x CH_2 , CH_2NHCH_2), 66.2, 69.1 (CH_2 , CH_2OCH_2), 126.5 (CH, aromatic CH), 127.9 (CH, aromatic CH), 128.1 (CH, aromatic CH), 129.2 (2 x CH, aromatic CH), 129.7 (2 x CH, aromatic CH), 129.8 (CH, aromatic CH), 133.6 (C, quaternary aromatic C), 133.8 (CH, aromatic CH), 136.5 (C, quaternary aromatic C), 141.8 (C, quaternary aromatic C); m/z (ESI) 302.1 [(M+H)⁺]; HRMS (ESI): exact mass calculated for $\text{C}_{18}\text{H}_{24}\text{NOS}$ [(M+H)⁺], 302.1579. Found 302.1577.

***N*-(2-(Benzylthio)benzyl)-1-(2-methoxyphenyl)methanamine (21)**

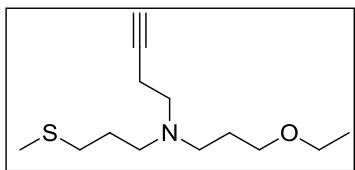


2-(Benzylthio)benzaldehyde, **7**, (0.19 g, 0.83 mmol) was added to a solution of 2-methoxybenzylamine (0.12 mL, 0.88 mmol) in methanol (5 mL) and the resulting solution was stirred at room temperature for 16 h under nitrogen. The reaction progress was monitored by TLC, until complete formation of the aldimine was observed. Solid sodium borohydride (0.05 g, 1.33 mmol) was then added to the solution in small portions over a period of 10-15 mins. The reaction mixture was stirred for 1 h at room temperature and then quenched with aqueous NaOH (1 M, 2 mL). The product was extracted with ether (3 x 5 mL). The ether layers were combined, washed with brine (10 mL) and dried over MgSO_4 . The solvent was removed *in vacuo* to give **21**, as a pale yellow oil, without the need for further purification (0.25 g, 86%). $\nu_{\text{max}}/\text{cm}^{-1}$ (film): 3059 (=CH), 2834 (CH), 2358, 1594 (ring stretch), 1492 (NH), 1241 (COC), 702 (CS); δ_{H} (300 MHz): 2.00 (1H, bs, NH), 3.76 (2H, s, CH_2NHCH_2), 3.77 (3H, s, OCH_3), 3.80 (2H, s, CH_2NHCH_2), 4.05 (2H, s, $\text{CH}_2\text{SC}_6\text{H}_4$), 6.83 (1H, d, J 8.1, ArH), 6.91 (1H, td, J 7.4, 1.0, ArH), 7.14-7.28 (9H, m, ArH), 7.30-7.39 (2H, m, ArH); δ_{C} (75 MHz): 39.3 (CH_2 , $\text{CH}_2\text{SC}_6\text{H}_4$), 48.8, 51.4 (2 x CH_2 , CH_2NHCH_2), 55.2 (CH_3 , OCH_3), 110.2 (CH, aromatic CH), 120.4 (CH, aromatic CH), 126.6 (CH, aromatic CH), 127.2 (CH, aromatic CH), 127.5 (CH, aromatic CH), 128.1 (CH, aromatic CH), 128.4 (C, quaternary aromatic C), 128.5 (2 x CH, aromatic CH), 128.9 (2 x

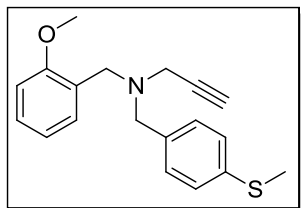
CH, aromatic CH), 129.3 (CH, aromatic CH), 129.9 (CH, aromatic CH), 130.4 (CH, aromatic CH), 135.4 (C, quaternary aromatic C), 137.4 (C, quaternary aromatic C), 140.8 (C, quaternary aromatic C), 157.7 (C, quaternary aromatic C); m/z (ESI) 350.2 [(M+H)⁺]; HRMS (ESI): exact mass calculated for C₂₂H₂₄NOS [(M+H)⁺], 350.1579. Found 350.1577.

5.2.3. Preparation of tertiary amine sulfides

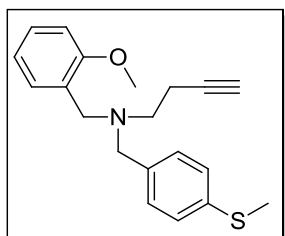
N-(3-ethoxypropyl)-*N*-[3-(methylthio)propyl]but-3-yn-1-amine (**22**)



3-Ethoxy-*N*-[3-(methylthio)propyl]propan-1-amine, **16**, (0.16 g, 0.84 mmol) was added to acetonitrile (5 mL) and solution was stirred at room temperature under nitrogen. Potassium carbonate (0.12 g, 8.4 mmol) was then added and the mixture was stirred for 5 mins before adding 4-bromo-1-butyne, **11**, (0.09 mL, 1.01 mmol) dropwise by syringe. The reaction mixture was stirred for 48 h at room temperature and the reaction progress was monitored by TLC. The temperature of the reaction could not be increased for safety reasons (F.p. 4-bromo-1-butyne, **11**: 23 °C). The mixture was diluted with CH₂Cl₂ (10 mL), washed with water (3 x 10 mL) and dried with MgSO₄. The solvent was removed *in vacuo* to yield the crude product (0.1 g, 48%), which contained a mixture (3:2) of the unreacted secondary amine, **16**, and the desired product, **22**. The crude material was purified by column chromatography using ethyl acetate as eluent, and the tertiary amine **22**, was obtained as a colourless oil (0.05 g, 25%). $\nu_{\max}/\text{cm}^{-1}$ (film): 3294 (≡C-H), 2917 (CH), 2859 (CH), 2118 (C≡C), 1122 (CN); δ_{H} (300 MHz): 1.19 (3H, t, J 7.0, OCH₂CH₃), 1.64-1.78 (4H, m, SCH₂CH₂CH₂NCH₂CH₂CH₂O), 1.94 (1H, t, J 2.6, C≡CH), 2.09 (3H, s, CH₃S), 2.30 (2H, td, J 7.4, 2.6, CH₂-C≡C), 2.48-2.56 (6H, m, 3 x CH₂N), 2.66 (2H, t, J 7.4 Hz, CH₂S), 3.42-3.51 (4H, m, CH₂OCH₂); δ_{C} (75 MHz): 15.2, 15.5 (2 x CH₃, CH₃), 17.1 (CH₂, CH₂-C≡C), 26.9, 27.7 (2 x CH₂, CH₂CH₂O and CH₂CH₂S), 32.0 (CH₂, CH₂S), 50.6, 52.6, 52.8 (3 x CH₂, 3 x NCH₂), 66.2, 68.6 (2 x CH₂, CH₂OCH₂), 68.8 (CH, C≡C-H), 83.2 (C, C≡CH); m/z (ESI) 244.2 [(M+H)⁺]; HRMS (ESI): exact mass calculated for C₁₃H₂₆NOS [(M+H)⁺], 244.1735. Found 244.1727.

***N*-(2-Methoxybenzyl)-*N*-[4-(methylthio)benzyl]prop-2-yn-1-amine (23)**

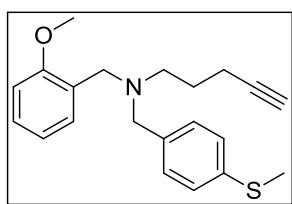
N-(2-Methoxybenzyl)-1-[4-(methylthio)phenyl]methanamine, **18**, (1.00 g, 3.66 mmol) was added to acetonitrile (20 mL) and the solution was stirred at room temperature under nitrogen. Potassium carbonate (0.51 g, 3.66 mmol) was then added and the mixture was stirred for 5 mins before the addition of propargyl bromide, **10** (0.49 mL, 0.52 g, 4.39 mmol, 80 wt. % in toluene) dropwise by syringe. The reaction mixture was heated under reflux for 24 h and the reaction progress was monitored by TLC. CH₂Cl₂ (20 mL) and water (10 mL) were then added to the reaction mixture and the phases separated. The combined organic layers were washed with water (3 x 15 mL), dried with MgSO₄ and the solvent was removed *in vacuo*. The title compound **23** was obtained as a clear oil without the need for further purification (0.80 g, 70%). (Found: C, 72.46; H, 6.59; N, 4.00%. C₁₉H₂₁NOS requires C, 73.27; H, 6.80; N, 4.50%); $\nu_{\max}/\text{cm}^{-1}$ (film): 3289 ($\equiv\text{C-H}$), 2920 (CH), 2833 (CH), ($\text{C}\equiv\text{C}$ stretch not observed), 1601 (ring stretch), 1243 (CCN), 668 ($\text{C}\equiv\text{C-H}$); δ_{H} (300 MHz): 2.27 (1H, t, *J* 2.4, $\text{C}\equiv\text{C-H}$), 2.47 (3H, s, SCH₃), 3.30 (2H, d, *J* 2.3, CH₂- $\text{C}\equiv\text{C}$), 3.68, 3.71 (2 x 2H, 2 x s, 2 x NCH₂C₆H₄), 3.81 (3H, s, OCH₃) 6.85 (1H, d, *J* 8.1, ArH), 6.93 (1H, td, *J* 7.4, 0.9, ArH), 7.18-7.26 (3H, m, ArH), 7.33 (2H, d, *J* 8.4, ArH), 7.44 (1H, dd, *J* 7.5, 1.5, ArH); δ_{C} (75 MHz): 16.1 (CH₃, SCH₃), 41.5 (CH₂, CH₂- $\text{C}\equiv\text{CH}$), 51.1 (CH₂, NCH₂C₆H₄), 55.4 (CH₃, OCH₃), 57.2 (CH₂, NCH₂C₆H₄), 73.2 (CH, $\text{C}\equiv\text{CH}$), 79.0 (C, $\text{C}\equiv\text{CH}$), 110.6 (CH, aromatic CH), 120.4 (CH, aromatic CH), 126.7 (CH, 2 x aromatic CH), 128.1 (CH, aromatic CH), 129.6 (CH, 2 x aromatic CH), 130.3 (CH, aromatic CH), 136.1 (C, quaternary aromatic C), 136.8 (C, quaternary aromatic C), 158.0 (C, 2 x quaternary aromatic C); *m/z* (ESI) 312.1 [(M+H)⁺]; HRMS (ESI): exact mass calculated for C₁₉H₂₂NOS [(M+H)⁺], 312.1422. Found 312.1416.

***N*-(2-Methoxybenzyl)-*N*-[4-(methylthio)benzyl]but-3-yn-1-amine (24)**

N-(2-Methoxybenzyl)-1-[4-(methylthio)phenyl]methanamine, **18**, (0.32 g, 1.16 mmol) was added to acetonitrile (7 mL) and the solution was stirred at room temperature under nitrogen. Potassium carbonate (0.16 g, 1.16 mmol) was then added and the mixture was stirred for 5 mins before the addition of 4-bromo-1-butyne, **11**, (0.13 mL, 1.39 mmol) slowly by syringe. The reaction mixture was stirred at room temperature for 24 h and the reaction progress was monitored by TLC. The mixture was diluted with CH₂Cl₂ (10 mL), washed with water (3 x 10 mL) and dried with MgSO₄. The solvent was removed

in vacuo and the crude product (0.30 g, 79%) was purified by column chromatography using hexane/ethyl acetate (4:1) as eluent, to give **24**, as a pale yellow oil (0.24 g, 64%). (Found: C, 73.53; H, 7.20; N, 3.43%. $C_{20}H_{23}NOS$ requires C, 73.81; H, 7.12; N, 4.30%); $\nu_{\max}/\text{cm}^{-1}$ (film): 3293 ($\equiv\text{C-H}$), 2920 (CH), 2834 (CH), 2117 ($\text{C}\equiv\text{C}$), 1600 (ring stretch), 1493 (ring stretch), 1241 (CCN), 756 (CS); δ_{H} (300 MHz): 1.92 (1H, t, J 2.6, $\text{C}\equiv\text{C-H}$), 2.38 (2H, td, J 7.4, 2.5, $\text{CH}_2\text{-C}\equiv\text{C}$), 2.47 (3H, s, SCH_3), 2.69 (2H, t, J 7.5, $\text{CH}_2\text{CH}_2\text{-C}\equiv\text{C}$), 3.61, 3.65 (2 x 2H, 2 x s, 2 x $\text{NCH}_2\text{C}_6\text{H}_5$), 3.80 (3H, s, OCH_3), 6.84 (1H, d, J 8.2, ArH), 6.93 (1H, td, J 7.5, 0.9, ArH), 7.17-7.24 (3H, m, ArH), 7.30 (2H, d, J 8.4, ArH), 7.47 (1H, dd, J 7.5, 1.5, ArH); δ_{C} (75 MHz): 16.2 (CH_3 , SCH_3), 17.0 (CH_2 , $\text{CH}_2\text{-C}\equiv\text{CH}$), 51.2, 52.3 (2 x CH_2 , 2 x NCH_2), 55.3 (CH_3 , OCH_3), 57.9 (CH_2 , NCH_2), 68.9 (CH, $\text{C}\equiv\text{CH}$), 83.2 (CH, $\text{C}\equiv\text{CH}$), 110.2 (CH, aromatic CH), 120.4 (CH, aromatic CH), 126.8 (CH, 2 x aromatic CH), 127.3 (C, quaternary aromatic C), 127.8 (CH, aromatic CH), 129.2 (CH, aromatic CH), 130.0 (CH, aromatic CH), 136.5 (C, quaternary aromatic C), 136.9 (C, quaternary aromatic C), 157.7 (C, quaternary aromatic C); m/z (ESI) 326.1 $[(\text{M}+\text{H})^+]$; HRMS (ESI): exact mass calculated for $C_{20}H_{23}NOS$ $[(\text{M}+\text{H})^+]$, 326.1579. Found 326.1570.

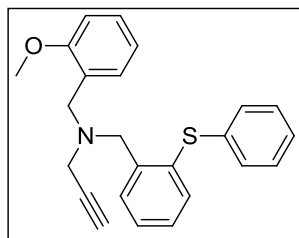
***N*-(2-Methoxybenzyl)-*N*-[4-(methylthio)benzyl]pent-4-yn-1-amine (25)**



N-(2-Methoxybenzyl)-1-[4-(methylthio)phenyl]methanamine, **18**, (0.40 g, 1.46 mmol) was added to acetonitrile (5 mL) and the solution was stirred at room temperature under nitrogen. Potassium carbonate (0.20 g, 1.46 mmol) was then added and the mixture was stirred for 5 mins before the addition of 5-iodopent-1-yne, **14**, (0.31 g, 1.61 mmol) dropwise by syringe. The reaction mixture was stirred at room temperature for 48 h and the reaction progress was monitored by TLC. Following the addition of CH_2Cl_2 (10 mL) and water (5 mL), the phases were separated. The organic extracts were combined, washed with water (3 x 10 mL), dried with MgSO_4 and the solvent was removed *in vacuo*. The crude product (0.37 g, 75%) consisted of the unreacted starting amine **18** (~20%), 5-iodopent-1-yne **14** (~8%) and the desired product **25** (~72%). Purification of the crude material was achieved by column chromatography using hexane/ethyl acetate (9:1) as eluent, to give the tertiary amine **25**, as a pale yellow oil (0.24 g, 49%). (Found: C, 74.26; H, 7.43; N, 3.92%. $C_{21}H_{25}NOS$ requires C, 74.29; H, 7.42; N, 4.13%); $\nu_{\max}/\text{cm}^{-1}$ (film): 3295 ($\equiv\text{C-H}$), 2935 (CH), 2834 (CH), 2116 ($\text{C}\equiv\text{C}$), 1600 (ring stretch), 1492 (ring stretch), 1240 (CCN), 755 (CS); δ_{H} (400 MHz): 1.70-1.78 (2H, m, $\text{NCH}_2\text{CH}_2\text{CH}_2$), 1.86 (1H, t, J 2.6, $\text{C}\equiv\text{C-H}$), 2.19 (2H, td, J 7.4, 2.5, $\text{CH}_2\text{-C}\equiv\text{C}$), 2.47 (3H, s, SCH_3), 2.50 (2H, t, J 6.9, $\text{NCH}_2\text{CH}_2\text{CH}_2$), 3.53, 3.59 (2 x 2H, 2 x s, 2 x

$\text{NCH}_2\text{C}_6\text{H}_5$), 3.81 (3H, s, OCH_3), 6.84 (1H, d, J 8.1, ArH), 6.94 (1H, td, J 7.5, 0.9, ArH), 7.18-7.23 (3H, m, ArH), 7.27 (2H, d, J 6.3, ArH), 7.45 (1H, dd, J 7.6, 1.6, ArH); δ_{C} (75 MHz): 16.2 (CH_3 , SCH_3), 16.3, 26.4 (2 x CH_2 , $\text{CH}_2\text{CH}_2\text{-C}\equiv\text{CH}$), 51.6, 52.5 (2 x CH_2 , 2 x NCH_2), 55.2 (CH_3 , OCH_3), 58.2 (CH_2 , NCH_2), 68.1 (CH , $\text{C}\equiv\text{CH}$), 84.7 (C, $\text{C}\equiv\text{CH}$), 110.2 (CH , aromatic CH), 120.3 (CH , aromatic CH), 126.7 (CH , 2 x aromatic CH), 127.6 (C, quaternary aromatic C), 127.7 (CH , aromatic CH), 129.3 (CH , 2 x aromatic CH), 129.9 (CH , aromatic CH), 136.2 (C, quaternary aromatic C), 137.2 (C, quaternary aromatic C), 157.7 (C, quaternary aromatic C); m/z (ESI) 340.2 $[(\text{M}+\text{H})^+]$; HRMS (ESI): exact mass calculated for $\text{C}_{21}\text{H}_{26}\text{NOS}$ $[(\text{M}+\text{H})^+]$, 340.1735. Found 340.1746.

***N*-(2-Methoxybenzyl)-*N*-[2-(phenylthio)benzyl]prop-2-yn-1-amine (26)**

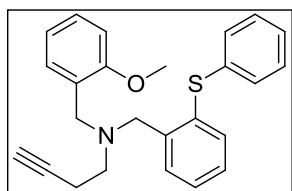


N-(2-Methoxybenzyl)-1-[2-(phenylthio)phenyl]methanamine, **19**, (0.62 g, 1.86 mmol) was added to acetonitrile (10 mL) and the solution was stirred at room temperature under nitrogen. Potassium carbonate (0.26 g, 1.86 mmol) was then added and the mixture was stirred for a further 5 mins. Propargyl bromide, **10** (0.25 mL, 2.23 mmol, 80% in toluene) was added dropwise by syringe to the vessel content. The reaction mixture was stirred at room temperature for 24 h and the reaction progress was monitored by TLC. The mixture was diluted with CH_2Cl_2 (20 mL) and washed with water (3 x 10 mL). The organic layers were combined, dried with MgSO_4 and the solvent was removed *in vacuo*. Purification by column chromatography using hexane/ethyl acetate (9:1) as eluent, afforded the title compound **26**, as a pale yellow solid (0.57 g, 82%), m.p. 77-79 °C; (Found: C, 76.80; H, 6.21; N, 3.81%. $\text{C}_{24}\text{H}_{23}\text{NOS}$ requires C, 77.18; H, 6.21; N, 3.75%); $\nu_{\text{max}}/\text{cm}^{-1}$ (film): 3292 ($\equiv\text{C-H}$), ($\text{C}\equiv\text{C}$ stretch not observed), 2834 (CH), 1587 (ring stretch), 1245 (COC), 752 (CS); δ_{H} (400 MHz): 2.26 (1H, t, J 2.4, $\text{C}\equiv\text{C-H}$), 3.30 (2H, d, J 2.4, $\text{CH}_2\text{-C}\equiv\text{C}$), 3.75 (2H, s, $\text{NCH}_2\text{C}_6\text{H}_4$), 3.79 (3H, s, OCH_3), 3.91 (2H, s, $\text{NCH}_2\text{C}_6\text{H}_4$), 6.84 (1H, dd, J 8.0, 0.8, ArH), 6.91 (1H, td, J 7.5, 1.1, ArH), 7.12-7.24 (5H, m, ArH), 7.25-7.32 (4H, m, ArH), 7.44 (1H, dd, J 7.2, 1.6, ArH), 7.56 (1H, d, J 7.2, ArH); δ_{C} (75 MHz): 41.2, 50.7 (2 x CH_2 , 2 x NCH_2), 55.3 (CH_3 , OCH_3), 56.3 (CH_2 , NCH_2), 73.1 (CH , $\text{C}\equiv\text{CH}$), 79.2 (C, $\text{C}\equiv\text{CH}$), 110.4 (CH , aromatic CH), 120.3 (CH , aromatic CH), 126.7 (CH , aromatic CH), 126.8 (C, quaternary aromatic C), 126.9 (CH , aromatic CH), 127.8 (CH , aromatic CH), 128.1 (CH , aromatic CH), 129.1 (CH , 2 x aromatic CH), 130.1 (CH , aromatic CH), 130.5 (CH , aromatic CH), 131.0 (CH , 2 x aromatic CH), 132.2 (CH , aromatic CH), 136.3 (C, quaternary aromatic C), 136.7 (C, quaternary aromatic C), 139.7 (C, quaternary aromatic C), 158.0 (C,

quaternary aromatic C); m/z (ESI) 374.1 [(M+H)⁺]; HRMS (ESI): exact mass calculated for C₂₄H₂₃NOS [(M+H)⁺], 374.1579. Found 374.1568.

Single crystals of **26** were grown on a pip by cycling the temperature above and below its melting point. Crystal data: C₂₄H₂₃NOS, $M = 373.49$, monoclinic, space group $P2_1/c$, $a = 9.538(4)$ Å, $b = 8.062(5)$ Å, $c = 26.117(15)$ Å, $\beta = 90.606(16)^\circ$, $V = 2008.2(19)$ Å³, $Z = 4$, $D_c = 1.235$ g cm⁻³, $F(000) = 792$, Mo K α radiation, $\lambda = 0.71073$ Å, $T = 296(2)$ K, $2\theta_{\max} = 24.68^\circ$, $\mu = 0.174$ mm⁻¹, 18656 reflections collected, 3356 unique ($R_{\text{int}} = 0.0855$). Final GooF = 0.999, $R_1 = 0.0464$, $wR_2 = 0.0957$ (obs. data: $I > 2\sigma(I)$); $R_1 = 0.1046$, $wR_2 = 0.1188$ (all data).

N-(2-Methoxybenzyl)-*N*-[2-(phenylthio)benzyl]but-3-yn-1-amine (**27**)

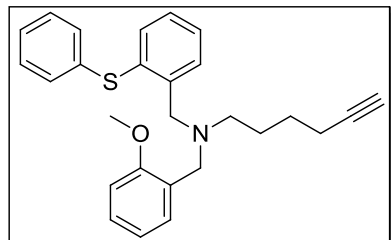


N-(2-Methoxybenzyl)-1-[2-(phenylthio)phenyl]methanamine, **19**, (0.70 g, 2.09 mmol) was added to acetonitrile (7 mL) and the solution was stirred at room temperature under nitrogen. Potassium carbonate (0.29 g, 2.09 mmol) was then added and the mixture was

stirred for 5 mins before the addition of 4-bromo-1-butyne, **11**, (0.23 mL, 2.50 mmol) dropwise by syringe. Stirring of the reaction mixture was continued at room temperature for 48 h while the reaction progress was monitored by TLC. The mixture was diluted with CH₂Cl₂ (10 mL), washed with water (3 x 10 mL), dried with MgSO₄ and the solvent was removed *in vacuo*. The crude product was purified by column chromatography using hexane/ethyl acetate (9:1) as eluent, to give the tertiary amine **27**, as a pale yellow oil (0.53 g, 65%). (Found: C, 77.00; H, 6.48; N, 3.72%. C₂₅H₂₅NOS requires C, 77.48; H, 6.50; N, 3.61%); $\nu_{\max}/\text{cm}^{-1}$ (film): 3296 ($\equiv\text{C-H}$), 2834 (CH), 2116 (C \equiv C), 1586 (ring stretch), 1241 (COC), 753 (CS); δ_{H} (300 MHz): 1.90 (1H, t, J 2.6, C \equiv C-H), 2.37-2.43 (2H, m, CH₂-C \equiv C), 2.70 (2H, t, J 7.6, CH₂CH₂-C \equiv C), 3.66 (2H, s, NCH₂C₆H₄), 3.77 (3H, s, OCH₃), 3.81 (2H, s, NCH₂C₆H₄), 6.82 (1H, d, J 8.2, ArH), 6.92 (1H, td, J 7.4, 1.0, ArH), 7.11-7.30 (9H, m, ArH), 7.45 (1H, dd, J 7.5, 1.8, ArH), 7.65 (1H, d, J 7.2, ArH); δ_{C} (75 MHz): 16.6 (CH₂, CH₂-C \equiv CH), 51.1, 52.3 (2 x CH₂, 2 x NCH₂), 55.2 (CH₃, OCH₃), 56.2 (CH₂, NCH₂), 68.8 (CH, C \equiv CH), 83.4 (C, C \equiv CH), 110.1 (CH, aromatic CH), 120.4 (CH, aromatic CH), 126.5 (CH, aromatic CH), 127.2 (C, quaternary aromatic C), 127.4 (CH, aromatic CH), 127.5 (CH, aromatic CH), 127.8 (CH, aromatic CH), 129.1 (CH, 2 x aromatic CH), 129.7 (CH, aromatic CH), 130.1 (CH, aromatic CH), 130.3 (CH, 2 x aromatic CH), 132.8 (CH, aromatic CH), 134.6 (C, quaternary aromatic C), 136.6 (C, quaternary aromatic C), 140.9 (C,

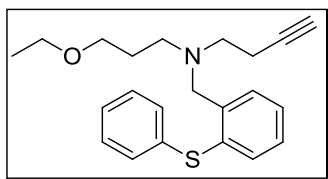
quaternary aromatic C), 157.7 (C, quaternary aromatic C); m/z (ESI) 388.2 [(M+H)⁺]; HRMS (ESI): exact mass calculated for C₂₅H₂₆NOS [(M+H)⁺], 388.1735. Found 388.1724.

***N*-(2-Methoxybenzyl)-*N*-[2-(phenylthio)benzyl]hex-5-yn-1-amine (28)**

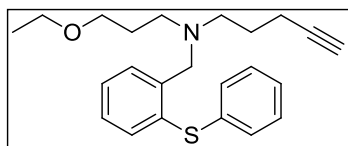


N-(2-Methoxybenzyl)-1-[2-(phenylthio)phenyl]methanamine, **19**, (0.72 g, 2.16 mmol) was added to acetonitrile (7 mL) and the solution was stirred at room temperature under a nitrogen atmosphere. Potassium carbonate (0.30 g, 2.16 mmol) was then added and the mixture was stirred for 5 mins before the addition of 6-iodohex-1-yne, **15**, (0.54 g, 2.60 mmol) dropwise by syringe. The reaction mixture was stirred at room temperature for 48 h and the reaction progress was monitored by TLC. CH₂Cl₂ (10 mL) was then added and the solution was washed with water (3 x 10 mL). The combined organic extracts were dried with MgSO₄ and the solvent was removed *in vacuo*. Purification by column chromatography using hexane/ethyl acetate (9:1) as eluent, afforded **28**, as a pale yellow oil (0.68 g, 75%). $\nu_{\max}/\text{cm}^{-1}$ (film): 3298 ($\equiv\text{C-H}$), 2940 (CH), 2834 (CH), 2116 (C \equiv C), 1601 (ring stretch), 1586 (ring stretch), 1464 (CH₂), 1439 (CH₃), 1241 (COC), 754 (CS); δ_{H} (300 MHz): 1.47-1.54, 1.59-1.67 (2 x 2H, 2 x m, NCH₂CH₂CH₂CH₂), 1.90 (1H, t, J 2.6, C \equiv C-H), 2.07 (2H, td, J 7.0, 2.5, CH₂-C \equiv C), 2.42 (2H, t, J 6.9, NCH₂CH₂), 3.61, 3.75 (2 x 2H, 2 x s, 2 x NCH₂C₆H₄), 3.78 (3H, s, OCH₃), 6.82 (1H, d, J 8.4, ArH), 6.92 (1H, td, J 7.5, 0.9, ArH), 7.10-7.29 (9H, m, ArH), 7.46 (1H, dd, J 7.5, 1.5, ArH), 7.65 (1H, d, J 7.8, ArH); δ_{C} (75 MHz): 18.2, 26.0, 26.3 (3 x CH₂, NCH₂CH₂CH₂CH₂), 51.7, 53.1 (2 x CH₂, 2 x NCH₂), 55.2 (CH₃, OCH₃), 56.4 (CH₂, NCH₂), 68.2 (CH, C \equiv CH), 84.7 (C, C \equiv CH), 110.1 (CH, aromatic CH), 120.3 (CH, aromatic CH), 126.4 (CH, aromatic CH), 127.3 (CH, aromatic CH), 127.4 (CH, aromatic CH), 127.6 (CH, aromatic CH), 127.8 (C, quaternary aromatic C), 129.1 (CH, 2 x aromatic CH), 129.7 (CH, aromatic CH), 130.1 (CH, aromatic CH), 130.2 (CH, 2 x aromatic CH), 132.7 (CH, aromatic CH), 134.4 (C, quaternary aromatic C), 136.7 (C, quaternary aromatic C), 141.4 (C, quaternary aromatic C), 157.7 (C, quaternary aromatic C); m/z (ESI) 416.2 [(M+H)⁺]; HRMS (ESI): exact mass calculated for C₂₇H₃₀NOS [(M+H)⁺], 416.2048. Found 416.2040.

* ~ 83% pure by ¹H NMR, ~ 17% of 6-iodohex-1-yne, **15**, at 1.93- 2.00 ppm (3H, m, CH₂CH₂CH₂C \equiv C-H), 2.23 ppm (2H, td, J 7.1, 2.6, CH₂-C \equiv CH), 3.21 (2H, t, J 6.9, CH₂).

***N*-(3-Ethoxypropyl)-*N*-(2-(phenylthio)benzyl)but-3-yn-1-amine (29)**

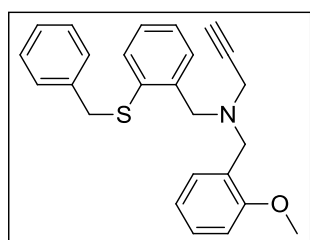
3-Ethoxy-*N*-[2-(phenylthio)benzyl]propan-1-amine, **20**, (0.35 g, 1.18 mmol) was added to acetonitrile (7 mL) and the solution was stirred at room temperature under nitrogen. Potassium carbonate (0.16 g, 1.18 mmol) was then added and the mixture was stirred for 5 mins. 4-Bromo-1-butyne, **11**, (0.13 mL, 1.41 mmol) was then added dropwise by syringe to the stirring mixture. The reaction progress was monitored by TLC and product formation was observed after 48 h. The mixture was then diluted with CH₂Cl₂ (15 mL), washed with water (3 x 7 mL), dried with MgSO₄ and the solvent was removed *in vacuo*. Due to the temperature constraints when handling 4-bromo-1-butyne, **11**, the crude mixture included unreacted secondary amine, **20** (~47%), 4-bromo-1-butyne, **11** (~20%) and the desired tertiary amine, **29** (~33%). The crude material was purified by column chromatography using hexane/ethyl acetate (7:3) as eluent, to give **29**, as a pale yellow oil (0.12 g, 29%). (Found: C, 74.31; H, 7.30; N, 4.11%. C₂₂H₂₇NOS requires C, 74.74; H, 7.70; N, 3.96%); $\nu_{\max}/\text{cm}^{-1}$ (film): 3302 (≡C-H), 2931 (CH), 2858 (CH), 2117 (C≡C), 1478 (CH₂), 1439 (CH₃), 1119 (COC), 742 (CS); δ_{H} (400 MHz): 1.15 (3H, t, *J* 7.0, OCH₂CH₃), 1.68-1.75 (2H, m, NCH₂CH₂CH₂), 1.92 (1H, t, *J* 2.6, C≡C-H), 2.32 (2H, td, *J* 7.5, 2.5, CH₂C≡C-H), 2.56 (2H, t, *J* 6.8, NCH₂CH₂), 2.70 (2H, t, *J* 7.4, NCH₂CH₂), 3.38-3.44 (4H, m, CH₂OCH₂), 3.73 (2H, s, NCH₂C₆H₄), 7.13-7.30 (8H, m, ArH), 7.53 (1H, d, *J* 7.6, ArH); δ_{C} (75 MHz): 15.2 (CH₃, CH₃), 16.7 (CH₂, CH₂-C≡CH), 27.5 (CH₂, NCH₂CH₂CH₂), 50.3, 52.6, 56.5 (3 x CH₂, 3 x NCH₂), 66.1, 68.6 (2 x CH₂, CH₂OCH₂), 68.8 (CH, C≡CH), 83.2 (C, C≡CH), 126.6 (CH, aromatic CH), 127.3 (CH, aromatic CH), 127.6 (CH, aromatic CH), 129.1 (CH, 2 x aromatic CH), 129.9 (CH, aromatic CH), 130.3 (CH, 2 x aromatic CH), 132.7 (CH, aromatic CH), 134.8 (C, quaternary aromatic C), 136.6 (C, quaternary aromatic C), 140.8 (C, quaternary aromatic C); *m/z* (ESI) 354.1 [(M+H)⁺]; HRMS (ESI): exact mass calculated for C₂₂H₂₇NOS [(M+H)⁺], 354.1892. Found 354.1886.

***N*-(3-Ethoxypropyl)-*N*-(2-(phenylthio)benzyl)pent-4-yn-1-amine (30)**

3-Ethoxy-*N*-[2-(phenylthio)benzyl]propan-1-amine, **20**, (0.12 g, 0.38 mmol) was added to acetonitrile (5 mL) and the solution was stirred at room temperature under nitrogen. Potassium carbonate (0.05 g, 0.38 mmol) was then added and the mixture was stirred for 5 mins before the addition of 5-iodopent-1-yne, **14**, (0.09 g, 0.46 mmol) dropwise by syringe. The reaction mixture was stirred at room temperature for 24 h and the reaction progress was

monitored by TLC. CH_2Cl_2 (10 mL) and water (5 mL) were then added to the reaction vessel. The phases were separated and the combined organic extracts were washed with water (3 x 10 mL), dried with MgSO_4 and the solvent was removed *in vacuo*. Purification was achieved by column chromatography using hexane/ethyl acetate (1:1) as eluent, and gave the tertiary amine **30**, as a pale yellow oil (0.10 g, 69%). (Found: C, 75.04; H, 7.84; N, 3.93%. $\text{C}_{23}\text{H}_{29}\text{NOS}$ requires C, 75.16; H, 7.95; N, 3.81%); $\nu_{\text{max}}/\text{cm}^{-1}$ (film): 3300 ($\equiv\text{C-H}$), 2938 (CH), 2861 (CH), 2116 ($\text{C}\equiv\text{C}$), 1582 (ring stretch), 1470 (CH_2), 1442 (CH_3), 1118 (CCN), 746 (CS); δ_{H} (300 MHz): 1.15 (3H, t, J 7.1, OCH_2CH_3), 1.61-1.78 (4H, m, 2 x $\text{NCH}_2\text{CH}_2\text{CH}_2$), 1.88 (1H, t, J 2.6, $\text{C}\equiv\text{C-H}$), 2.20 (2H, td, J 7.2, 2.7, $\text{CH}_2\text{C}\equiv\text{C-H}$), 2.50 (4H, td, J 7.0, 1.5 Hz, 2 x NCH_2CH_2), 3.37-3.46 (4H, m, CH_2OCH_2), 3.67 (2H, s, $\text{NCH}_2\text{C}_6\text{H}_4$), 7.11-7.31 (8H, m, ArH), 7.49 (1H, d, J 7.2, ArH); δ_{C} (75 MHz): 15.2 (CH_3 , CH_3), 16.3, 26.1, 27.3 (3 x CH_2 , $\text{CH}_2\text{CH}_2\text{-C}\equiv\text{CH}$, $\text{CH}_2\text{-C}\equiv\text{CH}$ and $\text{NCH}_2\text{CH}_2\text{CH}_2\text{O}$), 50.60, 52.65, 56.90 (3 x CH_2 , 3 x NCH_2), 66.10 (CH_2 , OCH_2), 68.17 (CH, $\text{C}\equiv\text{CH}$), 68.81 (CH_2 , OCH_2), 84.61 (C, $\text{C}\equiv\text{CH}$), 126.6 (CH, aromatic CH), 127.2 (CH, aromatic CH), 127.5 (CH, aromatic CH), 129.1 (CH, 2 x aromatic CH), 130.0 (CH, aromatic CH), 130.4 (CH, 2 x aromatic CH), 132.5 (CH, aromatic CH), 134.9 (C, quaternary aromatic C), 136.6 (C, quaternary aromatic C), 141.0 (C, quaternary aromatic C); m/z (ESI) 368.1 [($\text{M}+\text{H}$)⁺]; HRMS (ESI): exact mass calculated for $\text{C}_{23}\text{H}_{30}\text{NOS}$ [($\text{M}+\text{H}$)⁺], 368.2048. Found 368.2052.

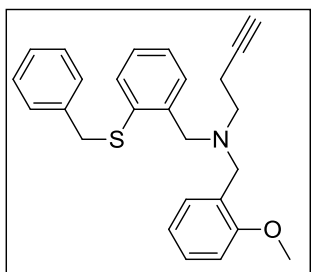
***N*-[2-(Benzylthio)benzyl]-*N*-(2-methoxybenzyl)prop-2-yn-1-amine (31)**



N-[2-(Benzylthio)benzyl]-1-(2-methoxyphenyl)methanamine, **21**, (0.50 g, 1.43 mmol) was added to acetonitrile (7 mL) and the solution was stirred at room temperature under nitrogen. Potassium carbonate (0.20 g, 1.43 mmol) was then added and the mixture was stirred for a further 5 mins. Propargyl bromide, **10** (0.19 mL, 1.72 mmol, 80% in toluene) was added dropwise by syringe to the vessel contents. The reaction progress was monitored by TLC and product formation was observed after a period of 24 h. The mixture was then diluted with CH_2Cl_2 (10 mL), washed with water (3 x 10 mL), dried with MgSO_4 . The solvent was removed *in vacuo*. The crude product was purified by column chromatography using hexane/ethyl acetate (4:1) as eluent, to give the title compound **31**, as a pale yellow oil (0.44 g, 80%). $\nu_{\text{max}}/\text{cm}^{-1}$ (film): 3291 ($\equiv\text{C-H}$), 2834 (CH), ($\text{C}\equiv\text{C}$ stretch not observed), 1493 (ring stretch), 1243 (CCN), 754 (CS); δ_{H} (300 MHz): 2.27 (1H, t, J 2.3, $\text{C}\equiv\text{C-H}$), 3.26 (2H, d, J 2.4, $\text{CH}_2\text{C}\equiv\text{C-H}$), 3.72 (2H, s, SCH_2Ph), 3.73 (3H, s, OCH_3), 3.80, 4.09 (2 x 2H, 2 x s, 2 x $\text{NCH}_2\text{C}_6\text{H}_4$), 6.80 (1H, d, J 8.1, ArH), 6.88 (1H, td, J 7.4, 1.0, ArH),

7.11-7.35 (9H, m, ArH), 7.42 (1H, dd, J 7.4, 1.7, ArH), 7.47 (1H, dd, J 6.9, 2.1, ArH); δ_C (75 MHz): 38.9, 41.1, 50.9 (3 x CH₂, 2 x NCH₂ and SCH₂Ph), 55.3 (CH₃, OCH₃), 56.0 (CH₂, NCH₂), 73.2 (CH, C≡CH), 79.2 (C, C≡CH), 110.4 (CH, aromatic CH), 120.2 (CH, aromatic CH), 125.8 (CH, aromatic CH), 126.7 (C, quaternary aromatic C), 127.1 (CH, aromatic CH), 127.5 (CH, aromatic CH), 128.1 (CH, aromatic CH), 128.4 (CH, 2 x aromatic CH), 129.1 (CH, 2 x aromatic CH), 129.3 (CH, aromatic CH), 129.9 (CH, aromatic CH), 130.6 (CH, aromatic CH), 137.2 (C, quaternary aromatic C), 137.5 (C, quaternary aromatic C), 138.7 (C, quaternary aromatic C), 158.0 (C, quaternary aromatic C); m/z (ESI) 388.2 [(M+H)⁺]; HRMS (ESI): exact mass calculated for C₂₅H₂₅NOS [(M+H)⁺], 388.1735. Found 388.1738.

***N*-[2-(Benzylthio)benzyl]-*N*-(2-methoxybenzyl)but-3-yn-1-amine (32)**



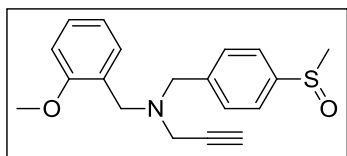
N-[2-(Benzylthio)benzyl]-1-(2-methoxyphenyl)methanamine, **21**, (0.15 g, 0.42 mmol) was added to acetonitrile (5 mL) and the solution was stirred at room temperature under nitrogen. Potassium carbonate (0.09 g, 0.63 mmol) was then added and the mixture was stirred for 5 mins before the addition of 4-bromo-1-butyne, **11** (0.05 mL, 0.51 mmol) dropwise by syringe. The reaction mixture was stirred at room temperature for 48 h and the reaction progress was monitored by TLC. The mixture was diluted with CH₂Cl₂ (10 mL), washed with water (3 x 10 mL), dried with MgSO₄ and the solvent was removed *in vacuo*. The crude mixture (0.12 g, 71%) consisted of the unreacted secondary amine and the desired product. The poor reactivity can be attributed to the temperature constraints of the reaction. Purification by column chromatography using hexane/ethyl acetate (4:1) as eluent, gave the tertiary amine **32**, as a pale yellow oil (0.08 g, 46%). $\nu_{\max}/\text{cm}^{-1}$ (film): 3295 (≡C-H), 2835 (CH), 2117 (C≡C), 1588 (ring stretch), 1493 (ring stretch), 1241 (CCN), 754 (CS); δ_H (400 MHz): 1.91 (1H, t, J 2.6, C≡C-H), 2.39 (2H, td, J 7.6, 2.4, CH₂C≡C-H), 2.67 (2H, t, J 7.6, NCH₂CH₂), 3.63, 3.69 (2 x 2H, 2 x s, NCH₂C₆H₄ or SCH₂Ph), 3.78 (3H, s, OCH₃), 4.06 (2H, s, NCH₂C₆H₄ or SCH₂Ph), 6.81 (1H, d, J 8.4, ArH), 6.91 (1H, td, J 7.4, 0.8, ArH), 7.14-7.33 (9H, m, ArH), 7.45 (1H, dd, J 7.2, 1.6, ArH), 7.52-7.55 (1H, m, ArH); δ_C (75 MHz): 16.6 (CH₂, NCH₂CH₂), 39.2 (CH₂, SCH₂Ph), 51.2, 52.4 (2 x CH₂, 2 x NCH₂), 55.2 (CH₃, OCH₃), 56.2 (CH₂, NCH₂), 68.8 (CH, C≡CH), 83.4 (C, C≡CH), 110.1 (CH, aromatic CH), 120.4 (CH, aromatic CH), 126.2 (CH, aromatic CH), 127.1 (CH, aromatic CH), 127.2 (CH, aromatic CH), 127.3 (C, quaternary aromatic C), 127.7 (CH, aromatic CH), 128.5 (CH, 2 x aromatic CH), 128.9 (CH, 2 x aromatic CH), 129.3 (CH, aromatic CH), 129.7 (CH, aromatic CH), 130.1 (CH, aromatic CH), 136.0 (C,

quaternary aromatic C), 137.5 (C, quaternary aromatic C), 139.8 (C, quaternary aromatic C), 157.7 (C, quaternary aromatic C); m/z (ESI) 402.1 [(M+H)⁺]; HRMS (ESI): exact mass calculated for C₂₆H₂₈NOS [(M+H)⁺], 402.1892. Found 402.1898.

5.2.4. Preparation of tertiary amine sulfoxides

Sulfoxides **33-34** were synthesised according to a modified version of the Golchoubian procedure.⁸ Sulfoxides **35-42** were synthesised by the Golchoubian procedure with heating as detailed by Prisinzano.⁹

N-(2-Methoxybenzyl)-*N*-[4-(methylsulfinyl)benzyl]prop-2-yn-1-amine (**33**)

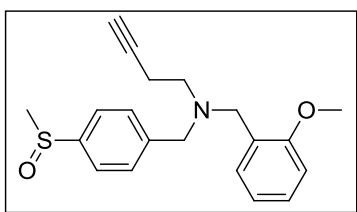


N-(2-Methoxybenzyl)-*N*-[4-(methylthio)benzyl]prop-2-yn-1-amine, **23**, (0.20 g, 0.64 mmol) was added to glacial acetic acid (1.0 mL) under nitrogen and stirred until fully dissolved.

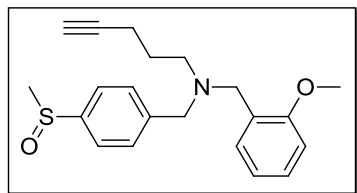
Hydrogen peroxide (0.07 mL, 30% w/v, 0.64 mmol) was then added dropwise and the reaction mixture was stirred at room temperature for 12 h. The reaction progress was monitored by TLC. The resulting solution was neutralised using aqueous NaOH (1 M) and the product was extracted CH₂Cl₂ (10 mL). The combined organic extracts were washed with water (3 x 10 mL) and dried with MgSO₄. The solvent was removed *in vacuo* to give the sulfoxide **33**, as a pale yellow solid without the need for further purification (0.19 g, 90%), m.p. 84-86 °C; (Found: C, 69.15; H, 6.45; N, 4.25%. C₁₉H₂₁NO₂S requires C, 69.69; H, 6.46; N, 4.28%); $\nu_{\max}/\text{cm}^{-1}$ (KBr): 3214 ($\equiv\text{C-H}$), 2911 (CH), 2836 (CH), 2098 ($\text{C}\equiv\text{C}$), 1494 (ring stretch), 1459 (CH₂), 1240 (COC), 1049 (S=O); δ_{H} (300 MHz): 2.30 (1H, t, J 2.3, $\text{C}\equiv\text{C-H}$), 2.73 (3H, s, SOCH₃), 3.32 (2H, d, J 2.4, CH₂- $\text{C}\equiv\text{C}$), 3.73, 3.78 (2 x 2H, 2 x s, 2 x NCH₂C₆H₄), 3.82 (3H, s, OCH₃) 6.86 (1H, d, J 8.1, ArH), 6.94 (1H, t, J 7.5, ArH), 7.21-7.28 (1H, m, ArH), 7.43 (1H, dd, J 7.5, 1.5 ArH), 7.55-7.63 (4H, m, ArH); δ_{C} (75 MHz): 41.8 (CH₂, CH₂- $\text{C}\equiv\text{CH}$), 43.8 (CH₃, SOCH₃), 51.4 (CH₂, NCH₂C₆H₄), 55.4 (CH₃, OCH₃), 57.2 (CH₂, NCH₂C₆H₄), 73.4 (CH, $\text{C}\equiv\text{CH}$), 78.7 (C, $\text{C}\equiv\text{CH}$), 110.6 (CH, aromatic CH), 120.4 (CH, aromatic CH), 123.5 (CH, 2 x aromatic CH), 126.5 (C, quaternary aromatic C), 128.4 (CH, aromatic CH), 129.9 (CH, 2 x aromatic CH), 130.3 (CH, aromatic CH), 142.8 (C, quaternary aromatic C), 144.0 (C, quaternary aromatic C), 158.0 (C, quaternary aromatic C); m/z (ESI) 328.1 [(M+H)⁺]; HRMS (ESI): exact mass calculated for C₁₉H₂₂NO₂S [(M+H)⁺], 328.1371. Found 328.1376.

Single crystals of **33** were grown on a pip by cycling the temperature above and below its melting point. Crystal data: $C_{19}H_{21}NO_2S$, $M = 327.43$, monoclinic, space group $P2_1/c$, $a = 8.9662(12) \text{ \AA}$, $b = 16.180(3) \text{ \AA}$, $c = 12.1761(15) \text{ \AA}$, $\beta = 99.871(5)^\circ$, $V = 1740.3(4) \text{ \AA}^3$, $Z = 4$, $D_c = 1.250 \text{ g cm}^{-3}$, $F(000) = 696$, Mo $K\alpha$ radiation, $\lambda = 0.71073 \text{ \AA}$, $T = 100(2) \text{ K}$, $2\theta_{\max} = 26.66^\circ$, $\mu = 0.195 \text{ mm}^{-1}$, 10233 reflections collected, 3572 unique ($R_{\text{int}} = 0.0561$). Final GooF = 1.029, $R_1 = 0.0554$, $wR_2 = 0.1322$ (obs. data: $I > 2\sigma(I)$); $R_1 = 0.0807$, $wR_2 = 0.1468$ (all data).

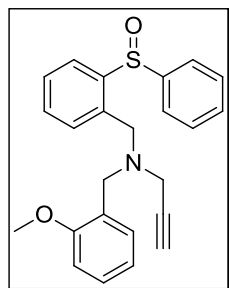
N-(2-Methoxybenzyl)-*N*-[4-(methylsulfinyl)benzyl]but-3-yn-1-amine (**34**)



N-(2-Methoxybenzyl)-*N*-[4-(methylthio)benzyl]but-3-yn-1-amine, **24**, (0.26 g, 0.79 mmol) was added to glacial acetic acid (1.2 mL) under nitrogen and stirred until fully dissolved. Hydrogen peroxide (0.09 mL, 30% w/v, 0.79 mmol) was added dropwise and the reaction mixture was stirred at room temperature for 12 h. The reaction progress was monitored by TLC. Aqueous NaOH (1 M) was added dropwise until a neutral pH was achieved. The mixture was diluted with CH_2Cl_2 (10 mL), washed with water (3 x 10 mL), dried with $MgSO_4$ and the solvent was removed *in vacuo*. The crude product was purified by column chromatography using ethyl acetate/hexane (9:1) as eluent, to give **34** as a yellow oil (0.15 g, 57%). $\nu_{\max}/\text{cm}^{-1}$ (film): 3293 ($\equiv\text{C-H}$), 2915 (CH), 2835 (CH), 2116 ($\text{C}\equiv\text{C}$), 1600 (ring stretch), 1491 (ring stretch), 1241 (COC), 1049 (S=O); δ_{H} (400 MHz): 1.95 (1H, t, J 2.8, $\text{C}\equiv\text{C-H}$), 2.41 (2H, td, J 7.3, 2.7, $\text{CH}_2\text{-C}\equiv\text{C}$), 2.71 (2H, t, J 7.2, $\text{CH}_2\text{CH}_2\text{-C}\equiv\text{C}$), 2.72 (3H, s, SOCH_3), 3.67, 3.71 (2 x 2H, 2 x s, 2 x $\text{NCH}_2\text{C}_6\text{H}_4$), 3.81 (3H, s, OCH_3), 6.85 (1H, dd, J 8.4, 0.8, ArH), 6.95 (1H, td, J 7.4, 0.9, ArH), 7.22 (1H, td, J 7.8, 1.5, ArH), 7.46 (1H, dd, J 7.6, 1.6, ArH), 7.54-7.60 (4H, m, ArH); δ_{C} (75 MHz): 17.1 (CH_2 , $\text{CH}_2\text{-C}\equiv\text{CH}$), 43.9 (CH_3 , SOCH_3), 51.4, 52.4 (2 x CH_2 , 2 x NCH_2), 55.3 (CH_3 , OCH_3), 58.0 (CH_2 , NCH_2), 69.0 (CH, $\text{C}\equiv\text{CH}$), 83.0 (C, $\text{C}\equiv\text{CH}$), 110.3 (CH, aromatic CH), 120.4 (CH, aromatic CH), 123.5 (CH, 2 x aromatic CH), 126.9 (C, quaternary aromatic C), 128.0 (CH, aromatic CH), 129.5 (CH, 2 x aromatic CH), 130.0 (CH, aromatic CH), 143.7 (C, quaternary aromatic C), 143.9 (C, quaternary aromatic C), 157.7 (C, quaternary aromatic C); m/z (ESI) 342.1 [(M+H) $^+$]; HRMS (ESI): exact mass calculated for $C_{20}H_{24}NO_2S$ [(M+H) $^+$], 342.1528. Found 342.1513.

***N*-(2-Methoxybenzyl)-*N*-[4-(methylsulfinyl)benzyl]pent-4-yn-1-amine (35)**

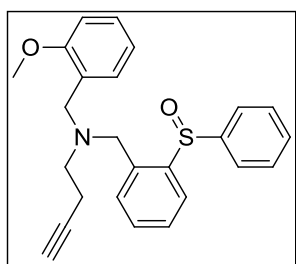
N-(2-Methoxybenzyl)-*N*-[4-(methylthio)benzyl]pent-4-yn-1-amine, **25**, (0.11 g, 0.32 mmol) was added to glacial acetic acid (0.32 mL) under nitrogen and stirred until fully dissolved. Hydrogen peroxide (0.04 mL, 30% w/v, 1.30 mmol) was then added dropwise and the reaction mixture was stirred at 40 °C for 12 h. The reaction progress was monitored by TLC. Aqueous NaOH (1 M) was added dropwise to neutralise the vessel contents. CH₂Cl₂ (10 mL) and water (5 mL) were then added. The phases were separated and the organic layers were combined, washed with water (3 x 10 mL) and dried with MgSO₄. The solvent was removed *in vacuo*. Purification by column chromatography using ethyl acetate as eluent, afforded **35**, as a yellow oil (0.05 g, 40%). (Found: C, 70.74; H, 7.13; N, 3.79 %. C₂₁H₂₅NO₂S requires C, 70.95; H, 7.09; N, 3.94%); $\nu_{\max}/\text{cm}^{-1}$ (film): 3293 ($\equiv\text{C-H}$), 2939 (CH), 2835 (CH), 2116 (C \equiv C), 1600 (ring stretch), 1491 (ring stretch), 1241 (COC), 1049 (S=O); δ_{H} (300 MHz): 1.62-1.73 (2H, m, NCH₂CH₂CH₂), 1.77 (1H, t, *J* 2.7, C \equiv C-H), 2.12 (2H, td, *J* 7.2, 2.7, CH₂-C \equiv C), 2.46 (2H, t, *J* 6.9, NCH₂CH₂CH₂), 2.63 (3H, s, SOCH₃), 3.55, 3.56 (2 x 2H, 2 x s, 2 x NCH₂C₆H₄), 3.73 (3H, s, OCH₃), 6.77 (1H, d, *J* 8.4, ArH), 6.86 (1H, td, *J* 7.4, 1.0, ArH), 7.14 (1H, td, *J* 7.8, 1.7, ArH), 7.34 (1H, dd, *J* 7.5, 1.8, ArH), 7.42-7.52 (4H, m, ArH); δ_{C} (75 MHz): 16.2, 26.4 (2 x CH₂, CH₂CH₂-C \equiv CH), 43.9 (CH₃, SOCH₃), 51.9, 52.8 (2 x CH₂, 2 x NCH₂), 55.2 (CH₃, OCH₃), 58.3 (CH₂, NCH₂), 68.2 (CH, C \equiv CH), 84.4 (C, C \equiv CH), 110.3 (CH, aromatic CH), 120.4 (CH, aromatic CH), 123.4 (CH, 2 x aromatic CH), 127.3 (C, quaternary aromatic C), 127.9 (CH, aromatic CH), 129.6 (CH, 2 x aromatic CH), 130.1 (CH, aromatic CH), 143.7 (C, quaternary aromatic C), 144.0 (C, quaternary aromatic C), 157.8 (C, quaternary aromatic C); *m/z* (ESI) 356.2 [(M+H)⁺]; HRMS (ESI): exact mass calculated for C₂₁H₂₆NO₂S [(M+H)⁺], 356.1684. Found 356.1681.

***N*-(2-Methoxybenzyl)-*N*-[2-(phenylsulfinyl)benzyl]prop-2-yn-1-amine (36)**

N-(2-Methoxybenzyl)-*N*-[2-(phenylthio)benzyl]prop-2-yn-1-amine, **26**, (0.20 g, 0.53 mmol) was added to glacial acetic acid (0.50 mL) under nitrogen and stirred until fully dissolved. Hydrogen peroxide (0.07 mL, 30% w/v, 2.14 mmol) was then added dropwise and the reaction mixture was stirred for 48 h at 40 °C. The reaction progress was monitored by TLC. Aqueous NaOH (1 M) was then added dropwise to neutralise the mixture. The vessel contents were diluted with CH₂Cl₂ (10 mL), washed with water (3 x 10 mL), dried with MgSO₄ and the solvent was removed *in vacuo*. Purification by column

chromatography using ethyl acetate/hexane (1:1) as eluent afforded the title compound, **36** as a clear oil (0.14 g, 68%). $\nu_{\max}/\text{cm}^{-1}$ (film): 3290 ($\equiv\text{C-H}$), 2934 (CH), 2834 (CH), ($\text{C}\equiv\text{C}$ stretch not observed), 1597 (ring stretch), 1493 (ring stretch), 1463 (CH_3), 1247 (COC), 1030 ($\text{S}=\text{O}$); δ_{H} (300 MHz): 2.33 (1H, t, J 2.4, $\text{C}\equiv\text{C-H}$), 3.05 (1H, A of finely split ABq, J 17.4, 2.4, $\text{CH}_2\text{-C}\equiv\text{C}$), 3.22 (1H, B of finely split ABq, J 17.4, 2.4, $\text{CH}_2\text{-C}\equiv\text{C}$), 3.65 (3H, s, OCH_3), 3.70-4.04 (4H, m, 2 x $\text{NCH}_2\text{C}_6\text{H}_4$), 6.81 (1H, d, J 8.1, ArH), 6.89 (1H, td, J 7.4, 1.0, ArH), 7.20-7.28 (1H, m, ArH), 7.29-7.50 (7H, m, ArH), 7.62-7.67 (2H, m, ArH), 7.90 (1H, dd, J 7.7, 1.4, ArH); δ_{C} (75 MHz): 40.5, 51.6, 54.7 (3 x CH_2 , 3 x NCH_2), 55.1 (CH_3 , OCH_3), 74.0 (CH, $\text{C}\equiv\text{CH}$), 78.3 (C, $\text{C}\equiv\text{CH}$), 110.4 (CH, aromatic CH), 120.2 (CH, aromatic CH), 125.56 (CH, 2 x aromatic CH), 125.63 (CH, aromatic CH), 126.0 (C, quaternary aromatic C), 128.6 (C, quaternary aromatic C), 128.8 (CH, aromatic CH), 128.9 (CH, aromatic CH), 129.0 (CH, 2 x aromatic CH), 130.3 (CH, aromatic CH), 130.5 (CH, aromatic CH), 130.8 (CH, aromatic CH), 131.3 (CH, aromatic CH), 137.1 (C, quaternary aromatic C), 145.6 (C, quaternary aromatic C), 158.1 (C, quaternary aromatic C); m/z (ESI) 390.1 $[(\text{M}+\text{H})^+]$; HRMS (ESI): exact mass calculated for $\text{C}_{24}\text{H}_{24}\text{NO}_2\text{S}$ $[(\text{M}+\text{H})^+]$, 390.1528. Found 390.1526.

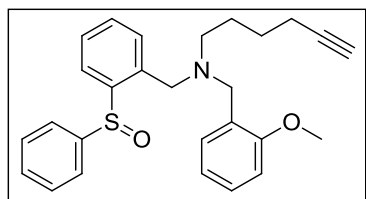
N-(2-Methoxybenzyl)-*N*-[2-(phenylsulfinyl)benzyl]but-3-yn-1-amine (**37**)



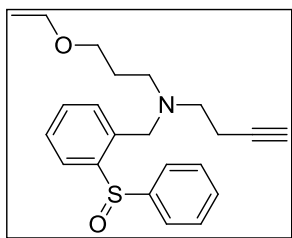
N-(2-Methoxybenzyl)-*N*-[2-(phenylthio)benzyl]but-3-yn-1-amine, **27**, (0.20g, 0.50 mmol) was added to glacial acetic acid (0.50 mL) under nitrogen and stirred until fully dissolved. Hydrogen peroxide (0.07 mL, 30% w/v, 2.02 mmol) was then added dropwise and the reaction mixture was stirred at 40 °C for 12 h. The reaction progress was monitored by TLC. The resulting solution was neutralised using aqueous NaOH (1 M) and then diluted with CH_2Cl_2 (10 mL). The phases were separated and the organic layer was washed with water (3 x 10 mL), dried with MgSO_4 and the solvent was removed *in vacuo*. Purification was achieved by column chromatography using ethyl acetate/hexane (1:1) as eluent and gave the sulfoxide **37**, as a yellow oil (0.10 g, 50%). $\nu_{\max}/\text{cm}^{-1}$ (film): 3297 ($\equiv\text{C-H}$), 2835 (CH), 2112 ($\text{C}\equiv\text{C}$), 1492 (ring stretch), 1243 (COC), 1031 ($\text{S}=\text{O}$); δ_{H} (300 MHz): 1.91 (1H, t, J 2.6, $\text{C}\equiv\text{C-H}$), 2.22-2.45, 2.52-2.75 (2 x 2H, 2 x m, $\text{CH}_2\text{CH}_2\text{-C}\equiv\text{C}$), 3.57-3.85 (4H, m, 2 x $\text{NCH}_2\text{C}_6\text{H}_4$), 3.74 (3H, s, OCH_3), 6.82 (1H, d, J 8.2, ArH), 6.90 (1H, td, J 7.4, 1.1 ArH), 7.22 (1H, td, J 7.8, 1.6, ArH), 7.29 (1H, dd, J 7.5, 1.8, ArH), 7.36-7.47 (5H, m, ArH), 7.54-7.60 (3H, m, ArH), 7.89-7.94 (1H, m, ArH); δ_{C} (75 MHz): 16.2 (CH_2 , $\text{CH}_2\text{-C}\equiv\text{CH}$), 51.1, 51.6, 54.8 (3 x CH_2 , 3 x NCH_2), 55.2 (CH_3 , OCH_3), 69.1 (CH, $\text{C}\equiv\text{CH}$), 83.0 (C, $\text{C}\equiv\text{CH}$), 110.3 (CH, aromatic CH), 120.3 (CH, aromatic CH),

125.3 (CH, aromatic CH), 125.8 (CH, 2 x aromatic CH), 126.0 (C, quaternary aromatic C), 128.4 (CH, aromatic CH), 128.5 (CH, aromatic CH), 129.1 (CH, 2 x aromatic CH), 129.9 (CH, aromatic CH), 130.7 (CH, aromatic CH), 130.8 (CH, aromatic CH), 130.9 (CH, aromatic CH), 138.1 (C, quaternary aromatic C), 144.2 (C, quaternary aromatic C), 145.3 (C, quaternary aromatic C), 157.8 (C, quaternary aromatic C); m/z (ESI) 404.1 [(M+H)⁺]; HRMS (ESI): exact mass calculated for C₂₅H₂₆NO₂S [(M+H)⁺], 404.1684. Found 404.1682.

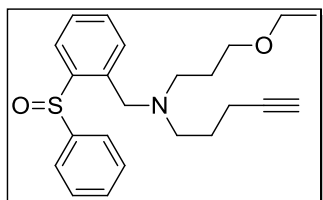
***N*-(2-Methoxybenzyl)-*N*-[2-(phenylsulfinyl)benzyl]hex-5-yn-1-amine (38)**



N-(2-Methoxybenzyl)-*N*-[2-(phenylthio)benzyl]hex-5-yn-1-amine, **28**, (0.55 g, 1.32 mmol) was added to glacial acetic acid (1.32 mL) under nitrogen and stirred until fully dissolved. Hydrogen peroxide (0.18 mL, 30% w/v, 5.29 mmol) was added dropwise and the reaction mixture was stirred at 40 °C for 12 h. The reaction progress was monitored by TLC. Aqueous NaOH (1 M) was added dropwise until neutral pH was achieved. The mixture was diluted with CH₂Cl₂ (10 mL), washed with water (3 x 10 mL), dried with MgSO₄ and the solvent was removed *in vacuo*. Purification by column chromatography using ethyl acetate/hexane (1:1) as eluent gave the title sulfoxide **38**, as a yellow oil (0.27 g, 48%). $\nu_{\max}/\text{cm}^{-1}$ (film): 3299 ($\equiv\text{C-H}$), 2940 (CH), 2835 (CH), 2115 (C=C), 1601 (ring stretch), 1493 (ring stretch), 1464 (CH₂), 1442 (CN), 1244 (COC), 1032 (S=O); δ_{H} (300 MHz): 1.37-1.48, 1.48-1.69 (2 x 2H, 2 x m, NCH₂CH₂CH₂), 1.91 (1H, t, J 2.6, C \equiv C-H), 2.08 (2H, td, J 6.9, 2.7, CH₂-C \equiv C), 2.25-2.48 (2H, m, NCH₂), 3.52-3.78 (4H, m, 2 x NCH₂), 3.74 (3H, s, OCH₃), 6.82 (1H, d, J 8.2, ArH), 6.90 (1H, td, J 7.4, 0.9, ArH), 7.21 (1H, td, J 7.8, 1.6, ArH), 7.32 (1H, dd, J 7.5, 1.5, ArH), 7.37-7.42 (5H, m, ArH), 7.54-7.60 (3H, m, ArH), 7.89-7.92 (1H, m, ArH); δ_{C} (75 MHz): 18.2, 25.5, 26.2 (3 x CH₂, NCH₂CH₂CH₂CH₂), 51.6, 52.7, 54.9 (3 x CH₂, 3 x NCH₂), 55.1 (CH₃, OCH₃), 68.4 (CH, C \equiv CH), 84.4 (C, C \equiv CH), 110.3 (CH, aromatic CH), 120.3 (CH, aromatic CH), 125.0 (CH, aromatic CH), 125.8 (CH, 2 x aromatic CH), 126.6 (C, quaternary aromatic C), 128.2 (CH, aromatic CH), 128.3 (CH, aromatic CH), 129.1 (CH, 2 x aromatic CH), 129.9 (CH, aromatic CH), 130.7 (CH, possibly for 2 x aromatic CH), 130.8 (CH, aromatic CH), 138.6 (C, quaternary aromatic C), 144.1 (C, quaternary aromatic C), 145.4 (C, quaternary aromatic C), 157.9 (C, quaternary aromatic C), (10 signals observed for 11 CH in the aromatic region); m/z (ESI) 432.1 [(M+H)⁺]; HRMS (ESI): exact mass calculated for C₂₇H₃₀NO₂S [(M+H)⁺], 432.1997. Found 432.1994.

***N*-(3-Ethoxypropyl)-*N*-[2-(phenylsulfinyl)benzyl]but-3-yn-1-amine (39)**

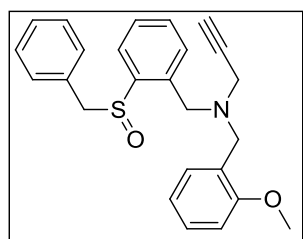
N-(3-Ethoxypropyl)-*N*-[2-(phenylthio)benzyl]but-3-yn-1-amine, **29**, (0.19 g, 0.55 mmol) was added to glacial acetic acid (0.55 mL) under nitrogen and stirred until fully dissolved. Hydrogen peroxide (0.08 mL, 30% w/v, 2.19 mmol) was then added dropwise and the reaction mixture was stirred at 40 °C for 12 h. The reaction progress was monitored by TLC. Aqueous NaOH (1 M) was then added dropwise to neutralise the solution. CH₂Cl₂ (10 mL) and water (5 mL) were then added to the reaction vessel and the phases separated. The organic extracts were combined, washed with water (3 x 10 mL), dried with MgSO₄ and the solvent was removed *in vacuo*. Purification by column chromatography using ethyl acetate/hexane (1:1) as eluent, gave **39** as a clear oil (0.15 g, 72%). $\nu_{\max}/\text{cm}^{-1}$ (film): 3297 ($\equiv\text{C-H}$), 2972 (CH), 2862 (CH), 2117 (C \equiv C), 1443 (ring stretch), 1116 (COC), 1034 (S=O); δ_{H} (300 MHz): 1.07 (3H, t, *J* 7.0, OCH₂CH₃), 1.49-1.73 (2H, m, NCH₂CH₂CH₂), 1.85 (1H, t, *J* 2.7, C \equiv C-H), 2.07-2.28 (2H, m, CH₂C \equiv C-H), 2.35-2.68 (4H, m, CH₂CH₂NCH₂CH₂), 3.26-3.37 (4H, m, CH₃CH₂OCH₂), 3.55 (1H, A of ABq, *J* 14.1, NCH₂C₆H₄), 3.73 (1H, B of ABq, *J* 13.8, NCH₂C₆H₄), 7.31-7.44 (6H, m, ArH), 7.51-7.57 (2H, m, ArH), 7.85 (1H, dd, *J* 7.5, 1.5, ArH); δ_{C} (75 MHz): 15.2 (CH₃, CH₂CH₃), 16.1 (CH₂, CH₂-C \equiv CH), 26.8 (CH₂, NCH₂CH₂CH₂), 49.9, 51.8, 55.2 (3 x CH₂, 3 x NCH₂), 66.1, 68.5 (2 x CH₂, CH₂OCH₂), 69.2 (CH, C \equiv CH), 82.8 (C, C \equiv CH), 125.7 (CH, aromatic CH), 125.8 (CH, 2 x aromatic CH), 128.6 (CH, aromatic CH), 129.1 (CH, 2 x aromatic CH), 129.9 (CH, aromatic CH), 130.8 (CH, aromatic CH), 130.9 (CH, aromatic CH), 138.1 (C, quaternary aromatic C), 144.0 (C, quaternary aromatic C), 145.4 (C, quaternary aromatic C); *m/z* (ESI) 370.2 [(M+H)⁺]; HRMS (ESI): exact mass calculated for C₂₂H₂₈NO₂S [(M+H)⁺], 370.1841. Found 370.1829.

***N*-(3-Ethoxypropyl)-*N*-[2-(phenylsulfinyl)benzyl]pent-4-yn-1-amine (40)**

N-(3-Ethoxypropyl)-*N*-[2-(phenylthio)benzyl]pent-4-yn-1-amine, **30**, (0.10 g, 0.26 mmol) was added to glacial acetic acid (0.26 mL) under nitrogen and stirred until fully dissolved. Hydrogen peroxide (0.04 mL, 30% w/v, 1.04 mmol) was then added dropwise and the reaction mixture was stirred at 40 °C for 12 h. The reaction progress was monitored by TLC. The solution was neutralised using aqueous NaOH (1 M) and then CH₂Cl₂ (10 mL) was added. The resulting mixture was washed with water (3 x 10 mL), dried with MgSO₄ and the solvent was removed *in vacuo*. Purification by column chromatography

using ethyl acetate/hexane (1:1) as eluent, yielded **40**, as a clear oil (0.03 g, 31%). (Found: C, 71.51; H, 7.52; N, 3.28%. $C_{23}H_{29}NO_2S$ requires C, 72.02; H, 7.62; N, 3.65%); $\nu_{\max}/\text{cm}^{-1}$ (film): 3299 ($\equiv\text{C-H}$), 2933 (CH), 2860 (CH), 2115 ($\text{C}\equiv\text{C}$), 1444 (ring stretch), 1374 (CH_3), 1083 (COC), 1035 (S=O); δ_{H} (300 MHz): 1.07 (3H, t, J 7.0, OCH_2CH_3), 1.42-1.73 (4H, m, $\text{OCH}_2\text{CH}_2\text{CH}_2\text{N}$ and $\text{CH}_2\text{CH}_2\text{C}\equiv\text{C-H}$), 1.81 (1H, t, J 2.6, $\text{C}\equiv\text{C-H}$), 2.06 (2H, td, J 7.1, 2.6, $\text{CH}_2\text{C}\equiv\text{C-H}$), 2.30-2.52 (4H, m, $\text{CH}_2\text{CH}_2\text{NCH}_2\text{CH}_2$), 3.26-3.37 (4H, m, CH_2OCH_2), 3.52 (1H, A of ABq, J 13.8, $\text{NCH}_2\text{C}_6\text{H}_4$), 3.67 (1H, B of ABq, J = 14.1, $\text{NCH}_2\text{C}_6\text{H}_4$), 7.30-7.42 (6H, m, ArH), 7.51-7.58 (2H, m, ArH), 7.82-7.87 (1H, m, ArH); δ_{C} (75 MHz): 14.2 (CH_3 , CH_2CH_3), 15.3, 24.3, 25.6 (3 x CH_2 , $\text{CH}_2\text{CH}_2\text{-C}\equiv\text{CH}$, $\text{CH}_2\text{-C}\equiv\text{CH}$ and $\text{NCH}_2\text{CH}_2\text{CH}_2\text{O}$), 49.2, 51.1, 54.5 (3 x CH_2 , 3 x NCH_2), 65.1 (CH_2 , CH_2O), 67.5 (CH, $\text{C}\equiv\text{CH}$), 67.7 (CH_2 , CH_2O), 83.0 (C, $\text{C}\equiv\text{CH}$), 124.5 (CH, aromatic CH), 124.8 (CH, 2 x aromatic CH), 127.5 (CH, aromatic CH), 128.1 (CH, 2 x aromatic CH), 128.9 (CH, aromatic CH), 129.7 (CH, aromatic CH), 129.9 (CH, aromatic CH), 137.5 (C, quaternary aromatic C), 143.0 (C, quaternary aromatic C), 144.4 (C, quaternary aromatic C); m/z (ESI) 384.2 [(M+H)⁺]; HRMS (ESI): exact mass calculated for $C_{23}H_{30}NO_2S$ [(M+H)⁺], 384.1997. Found 384.1995.

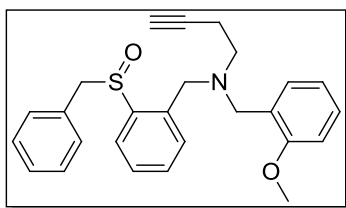
***N*-[2-(Benzylsulfinyl)benzyl]-*N*-(2-methoxybenzyl)prop-2-yn-1-amine (41)**



N-[2-(Benzylthio)benzyl]-*N*-(2-methoxybenzyl)prop-2-yn-1-amine, **31**, (0.23 g, 0.58 mmol) was added to glacial acetic acid (0.60 mL) under nitrogen and stirred until fully dissolved. Hydrogen peroxide (0.08 mL, 30% w/v, 2.34 mmol) was then added dropwise and the reaction mixture was stirred at 40 °C for 12 h. The reaction progress was monitored by TLC. Aqueous NaOH (1 M) was then added dropwise until the solution was neutralised. The mixture was then diluted with CH_2Cl_2 (10 mL), washed with water (3 x 10 mL), dried with MgSO_4 and the solvent was removed *in vacuo*. Purification was achieved by column chromatography using ethyl acetate/hexane (1:1) as eluent, and afforded the title compound **41**, as a yellow oil (0.10 g, 45%). $\nu_{\max}/\text{cm}^{-1}$ (film): 3291 ($\equiv\text{C-H}$), 2836 (CH), ($\text{C}\equiv\text{C}$ stretch not observed), 1601 (ring stretch), 1494 (ring stretch), 1455 (CH_2), 1247 (COC), 1032 (S=O); δ_{H} (300 MHz): 2.34 (1H, t, J 2.3, $\text{C}\equiv\text{C-H}$), 3.15 (1H, A of finely split ABq, J 17.1, 2.4, $\text{CH}_2\text{C}\equiv\text{C-H}$), 3.30 (1H, B of finely split ABq, J 17.1, 2.4, $\text{CH}_2\text{C}\equiv\text{C-H}$), 3.51-3.90 (4H, m, 2 x $\text{NCH}_2\text{C}_6\text{H}_4$), 3.74 (3H, s, OCH_3), 4.01 (1H, A of ABq, J 12.6, SOCH_2), 4.15 (1H, B of ABq, J 12.9, SOCH_2), 6.85 (1H, d, J 8.2, ArH), 6.89-6.96 (3H, m, ArH), 7.16-7.43 (8H, m, ArH), 7.49-7.53 (1H, m ArH); δ_{C} (75 MHz): 40.7, 51.5, 55.0 (3 x CH_2 , 3 x NCH_2), 55.2 (CH_3 , OCH_3), 61.7 (CH_2 , SOCH_2), 74.1 (CH, $\text{C}\equiv\text{CH}$), 78.4 (C,

C≡CH), 110.6 (CH, aromatic CH), 120.3 (CH, aromatic CH), 125.3 (CH, aromatic CH), 125.4 (C, quaternary aromatic C), 128.0 (CH, aromatic CH), 128.2 (CH, 2 x aromatic CH), 128.3 (CH, aromatic CH), 129.0 (CH, aromatic CH), 130.0 (CH, aromatic CH), 130.1 (C, quaternary aromatic C), 130.5 (CH, aromatic CH), 130.7 (CH, 2 x aromatic CH), 131.6 (CH, aromatic CH), 136.3 (C, quaternary aromatic C), 143.6 (C, quaternary aromatic C), 158.1 (C, quaternary aromatic C): m/z (ESI) 404.1 [(M+H)⁺]; HRMS (ESI): exact mass calculated for C₂₅H₂₆NO₂S [(M+H)⁺], 404.1684. Found 404.1698.

***N*-[2-(Benzylsulfinyl)benzyl]-*N*-(2-methoxybenzyl)but-3-yn-1-amine (42)**

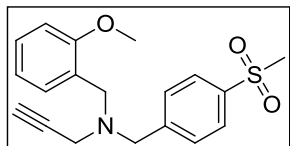


N-[2-(Benzylthio)benzyl]-*N*-(2-methoxybenzyl)but-3-yn-1-amine, **32**, (0.09 g, 0.21 mmol) was added to glacial acetic acid (0.21 mL) under nitrogen and stirred until fully dissolved. Hydrogen peroxide (0.03 mL, 30% w/v, 0.86 mmol) was then added dropwise and the reaction mixture was stirred at 40 °C for 12 h. The reaction progress was monitored by TLC. The solution was neutralised by adding aqueous NaOH (1 M) dropwise. The mixture was diluted with CH₂Cl₂ (10 mL), washed with water (3 x 10 mL), dried with MgSO₄ and the solvent was removed *in vacuo*. Purification by column chromatography using ethyl acetate/hexane (1:1) as eluent, gave the sulfoxide **42**, as a yellow oil (0.04 g, 44%). $\nu_{\max}/\text{cm}^{-1}$ (film): 3295 (≡C-H), 2836 (CH), 2116 (C≡C), 1493 (ring stretch), 1244 (COC), 1031 (S=O); δ_{H} (300 MHz): 1.93 (1H, t, J 2.6, C≡C-H), 2.30-2.50 (2H, m, CH₂C≡C-H), 2.51-2.61 (1H, m, 1 H of NCH₂), 2.70-2.81 (1H, m, 1 H of NCH₂), 3.37-3.77 (4H, m, 2 x NCH₂), 3.78 (3H, s, OCH₃), 4.04 (1H, A of ABq, J 12.6, SOCH₂), 4.09 (1H, B of ABq, J 12.6, SOCH₂), 6.86 (1H, d, J 8.2, ArH), 6.89-6.98 (3H, m, ArH), 7.18-7.46 (8H, m, ArH), 7.57-7.62 (1H, m, ArH); δ_{C} (75 MHz): 16.1 (CH₂, CH₂-C≡C-H), 51.2, 51.6, 55.0 (3 x CH₂, 3 x NCH₂), 55.2 (CH₃, OCH₃), 62.1 (CH₂, SOCH₂), 69.2 (CH, C≡CH), 82.9 (C, C≡CH), 110.4 (CH, aromatic CH), 120.4 (CH, aromatic CH), 124.9 (CH, aromatic CH), 125.8 (C, quaternary aromatic C), 128.1 (CH, aromatic CH), 128.2 (CH, aromatic CH), 128.3 (CH, 2 x aromatic CH), 128.6 (CH, aromatic CH), 129.6 (CH, aromatic CH), 129.7 (C, quaternary aromatic C), 130.6 (CH, aromatic CH), 130.6 (CH, 2 x aromatic CH), 131.0 (CH, aromatic CH), 137.3 (C, quaternary aromatic C), 142.9 (C, quaternary aromatic C), 157.9 (C, quaternary aromatic C); m/z (ESI) 418.2 [(M+H)⁺]; HRMS (ESI): exact mass calculated for C₂₆H₂₈NO₂S [(M+H)⁺], 418.1841. Found 418.1854.

5.2.5. Preparation of tertiary amine sulfones

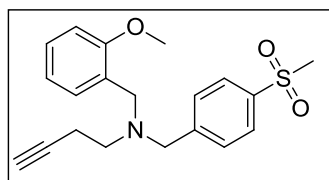
The sulfones (**43-52**) were synthesised according to a modified version of the Lehane procedure.¹⁰

N-(2-Methoxybenzyl)-*N*-[4-(methylsulfonyl)benzyl]prop-2-yn-1-amine (**43**)



A solution of oxone[®] (1.07 g, 1.73 mmol) in water (7 mL) was added dropwise over a period of 1 h to a stirred solution of the sulfide **23**, (0.27 g, 0.87 mmol) in acetone (7 mL). The reaction mixture was stirred for 16 h, concentrated *in vacuo* to half its original volume, shaken with CH₂Cl₂ (20 mL) and the layers separated. The aqueous layer was further extracted with CH₂Cl₂ (2 x 20 mL). The combined organic layers were washed with water (2 x 20 mL), brine (20 mL), dried with MgSO₄ and the solvent was removed *in vacuo*. Purification by column chromatography using ethyl acetate as eluent, yielded **43**, as a clear oil (0.17 g, 55%). $\nu_{\max}/\text{cm}^{-1}$ (film): 3275 ($\equiv\text{C-H}$), 2924 (CH), ($\text{C}\equiv\text{C}$ stretch not observed), 1600 (ring stretch), 1492 (ring stretch), 1305 (SO₂), 1243 (CN), 1150 (SO₂); δ_{H} (300 MHz): 2.23 (1H, t, J 2.3, $\text{C}\equiv\text{C-H}$), 2.97 (3H, s, SO₂CH₃), 3.24 (2H, d, J 2.4, CH₂- $\text{C}\equiv\text{C}$), 3.65 (2H, s, NCH₂C₆H₄), 3.75 (5H, s, NCH₂C₆H₄ and OCH₃), 6.79 (1H, d, J 8.4, ArH), 6.87 (1H, td, J 7.4, 1.0, ArH), 7.17 (1H, td, J 7.9, 1.6, ArH), 7.34 (1H, dd, J 7.5, 1.8, ArH), 7.54 (2H, d, J 8.7, ArH), 7.81 (2H, d, J 8.4, ArH); δ_{C} (75 MHz): 40.9 (CH₂, CH₂- $\text{C}\equiv\text{CH}$), 43.6 (CH₃, SO₂CH₃), 50.4 (CH₂, NCH₂C₆H₄), 54.4 (CH₃, OCH₃), 56.2 (CH₂, NCH₂C₆H₄), 72.5 (CH, $\text{C}\equiv\text{CH}$), 77.5 (C, $\text{C}\equiv\text{CH}$), 109.6 (CH, aromatic CH), 119.4 (CH, aromatic CH), 125.3 (C, quaternary aromatic C), 126.3 (CH, 2 x aromatic CH), 127.5 (CH, aromatic CH), 128.7 (CH, 2 x aromatic CH), 129.3 (CH, aromatic CH), 138.1 (C, quaternary aromatic C), 144.9 (C, quaternary aromatic C), 156.9 (C, quaternary aromatic C); m/z (ESI) 344.2 [(M+H)⁺]; HRMS (ESI): exact mass calculated for C₁₉H₂₂NO₃S [(M+H)⁺], 344.1320. Found 344.1317.

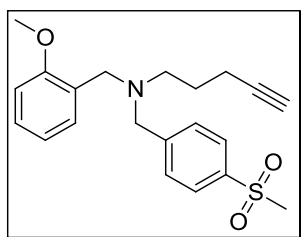
N-(2-Methoxybenzyl)-*N*-[4-(methylsulfonyl)benzyl]but-3-yn-1-amine (**44**)



A solution of oxone[®] (0.52 g, 0.84 mmol) in water (4 mL) was added dropwise over a period of 1 h to a stirred solution of the sulfide **24**, (0.14 g, 0.42 mmol) in acetone (4 mL). The reaction mixture was stirred for 16 h, concentrated *in vacuo* to half its original volume, shaken with CH₂Cl₂ (10 mL) and the layers separated. The aqueous layer was further extracted with CH₂Cl₂ (2 x 10 mL). The combined organic layers were washed

with water (2 x 10 mL), brine (10 mL), dried with MgSO₄ and the solvent was removed *in vacuo*. Purification by column chromatography using ethyl acetate/hexane (2:3) as eluent, afforded the sulfone **44**, as a clear oil (0.06 g, 42%). $\nu_{\max}/\text{cm}^{-1}$ (film): 3286 ($\equiv\text{C-H}$), 2927 (CH), 2836 (CH), 2116 ($\text{C}\equiv\text{C}$), 1600 (ring stretch), 1492 (ring stretch), 1305 (SO_2), 1242 (CN), 1150 (SO_2); δ_{H} (300 MHz): 1.96 (1H, t, J 2.7, $\text{C}\equiv\text{C-H}$), 2.41 (2H, td, J 7.2, 2.7, $\text{CH}_2\text{-C}\equiv\text{C}$), 2.71 (2H, t, J 7.4, $\text{CH}_2\text{CH}_2\text{-C}\equiv\text{C}$), 3.04 (3H, s, SO_2CH_3), 3.68, 3.74 (2 x 2H, 2 x s, 2 x $\text{NCH}_2\text{C}_6\text{H}_4$), 3.80 (3H, s, OCH_3), 6.84 (1H, d, J 8.1, ArH), 6.94 (1H, td, J 7.5, 0.9, ArH), 7.22 (1H, td, J 7.8, 1.6, ArH), 7.43 (1H, dd, J 7.5, 1.8, ArH), 7.60 (2H, d, J 8.4, ArH), 7.85 (2H, d, J 8.4, ArH); δ_{C} (75 MHz): 17.1 (CH_2 , $\text{CH}_2\text{-C}\equiv\text{CH}$), 44.6 (CH_3 , SO_2CH_3), 51.5, 52.5 (2 x CH_2 , 2 x NCH_2), 55.3 (CH_3 , OCH_3), 57.9 (CH_2 , NCH_2), 69.1 (CH, $\text{C}\equiv\text{CH}$), 82.9 (C, $\text{C}\equiv\text{CH}$), 110.3 (CH, aromatic CH), 120.4 (CH, aromatic CH), 126.7 (C, quaternary aromatic C), 127.3 (CH, 2 x aromatic CH), 128.2 (CH, aromatic CH), 129.3 (CH, 2 x aromatic CH), 130.0 (CH, aromatic CH), 139.0 (C, quaternary aromatic C), 146.8 (C, quaternary aromatic C), 157.7 (C, quaternary aromatic C); m/z (ESI) 358.1 [(M+H)⁺]; HRMS (ESI): exact mass calculated for C₂₀H₂₄NO₃S [(M+H)⁺], 358.1477. Found 344.1478.

***N*-(2-Methoxybenzyl)-*N*-[4-(methylsulfonyl)benzyl]pent-4-yn-1-amine (45)**

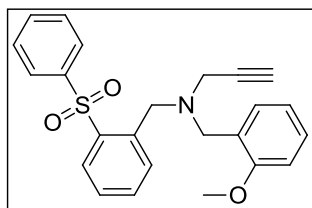


A solution of oxone[®] (0.88 g, 1.43 mmol) in water (5 mL) was added dropwise over a period of 1 h to a stirred solution of the sulfide **25**, (0.27 g, 0.72 mmol) in acetone (5 mL). The reaction mixture was stirred for 16 h and concentrated *in vacuo* to half its original volume. CH₂Cl₂ (10 mL) was then added and the layers were separated. The aqueous layer was further extracted with CH₂Cl₂ (2 x 10 mL). The combined organic layers were washed with water (2 x 10 mL), brine (10 mL), dried with MgSO₄ and the solvent was removed *in vacuo*. The crude product was purified by column chromatography using ethyl acetate/hexane (1:1) as eluent and resulted in obtaining **45**, as a white solid (0.11 g, 42%), m.p. 81-83 °C; $\nu_{\max}/\text{cm}^{-1}$ (KBr): 3279 ($\equiv\text{C-H}$), 2951 (CH), 2925 (CH), 2115 ($\text{C}\equiv\text{C}$), 1600 (ring stretch), 1494 (ring stretch), 1324 (SO_2), 1249 (CN), 1149 (SO_2); δ_{H} (300 MHz): 1.69-1.80 (2H, m, $\text{NCH}_2\text{CH}_2\text{CH}_2$), 1.85 (1H, t, J 2.5, $\text{C}\equiv\text{C-H}$), 2.20 (2H, td, J 7.2, 2.4, $\text{CH}_2\text{-C}\equiv\text{C}$), 2.54 (2H, t, J 6.9, NCH_2CH_2), 3.02 (3H, s, SO_2CH_3), 3.62, 3.65 (2 x 2H, 2 x s, 2 x $\text{NCH}_2\text{C}_6\text{H}_4$), 3.80 (3H, s, OCH_3), 6.84 (1H, d, J 7.8, ArH), 6.92 (1H, finely split t, J 7.4, ArH), 7.21 (1H, td, J 7.8, 1.4, ArH), 7.40 (2H, dd, J 7.5, 1.5, ArH), 7.55 (2H, d, J 8.1, ArH), 7.84 (2H, d, J 8.1, ArH); δ_{C} (75 MHz): 16.2, 26.4 (2 x CH_2 , $\text{CH}_2\text{CH}_2\text{-C}\equiv\text{CH}$), 44.6 (CH_3 , SO_2CH_3), 52.0, 52.8, (2 x CH_2 , 2 x NCH_2), 55.2 (CH_3 , OCH_3), 58.2

(CH₂, NCH₂), 68.4 (CH, C≡CH), 84.4 (C, C≡CH), 110.3 (CH, aromatic CH), 120.4 (CH, aromatic CH), 127.0 (C, quaternary aromatic C), 127.2 (CH, 2 x aromatic CH), 128.1 (CH, aromatic CH), 129.4 (CH, 2 x aromatic CH), 130.1 (CH, aromatic CH), 138.8 (C, quaternary aromatic C), 147.1 (C, quaternary aromatic C), 157.8 (C, quaternary aromatic C); *m/z* (ESI) 372.1 [(M+H)⁺]; HRMS (ESI): exact mass calculated for C₂₁H₂₆NO₃S [(M+H)⁺], 372.1633. Found 372.1631.

Single crystals of **45** were grown from CH₂Cl₂. Crystal data: C₂₁H₂₅NO₃S, *M* = 371.48, monoclinic, space group *P*2₁/*c*, *a* = 19.041(3) Å, *b* = 5.3401(8) Å, *c* = 20.654(3) Å, β = 111.548(5)°, *V* = 1953.3(5) Å³, *Z* = 4, *D*_c = 1.263 g cm⁻³, *F*(000) = 792, Mo Kα radiation, λ = 0.71073 Å, *T* = 300(2) K, 2θ_{max} = 25.58°, μ = 0.186 mm⁻¹, 12060 reflections collected, 3644 unique (*R*_{int} = 0.0429). Final GooF = 1.181, *R*₁ = 0.0482, *wR*₂ = 0.1262 (obs. data: *I* > 2σ(*I*)); *R*₁ = 0.0759, *wR*₂ = 0.1402 (all data).

N-(2-Methoxybenzyl)-*N*-[2-(phenylsulfonyl)benzyl]prop-2-yn-1-amine (**46**)

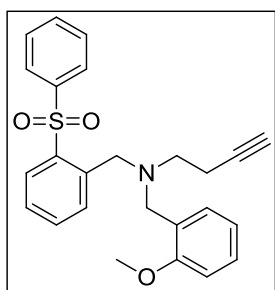


To a stirred solution of the sulfide **26**, (0.53 g, 1.42 mmol) in acetone (7 mL), was added dropwise over a 1 h, a solution of oxone[®] (1.74 g, 2.83 mmol) in water (7 mL). The reaction mixture was stirred for 16 h, concentrated *in vacuo* to half its original volume, shaken with CH₂Cl₂ (20 mL) and the layers separated. The aqueous layer was further washed with CH₂Cl₂ (2 x 20 mL). The combined organic layers were then washed with water (2 x 20 mL), brine (20 mL), dried with MgSO₄ and the solvent was removed *in vacuo*. Purification by column chromatography using ethyl acetate/hexane (2:3) as eluent, gave the title compound **46**, as a white solid (0.16 g, 28%), m.p. 92-94 °C; *v*_{max}/cm⁻¹ (KBr): 3284 (≡C-H), 2940 (CH), 2832 (CH), (C≡C stretch not observed), 1600 (ring stretch), 1493 (ring stretch), 1312 (SO₂), 1245 (CN), 1150 (SO₂); δ_H (300 MHz): 2.18 (1H, t, *J* 2.4, C≡C-H), 3.16 (2H, d, *J* 2.4, CH₂-C≡C), 3.49 (2H, s, NCH₂C₆H₄), 3.76 (3H, s, OCH₃), 4.01 (2H, s, NCH₂C₆H₄), 6.82 (1H, d, *J* 8.4, ArH), 6.87 (1H, td, *J* 7.4, 1.0, ArH), 7.17-7.28 (2H, m, ArH), 7.40-7.49 (3H, m, ArH), 7.52-7.62 (2H, m, ArH), 7.86-7.92 (2H, m, ArH), 7.97 (1H, d, *J* 7.5, ArH), 8.20 (1H, dd, *J* 8.0, 1.4, ArH); δ_C (75 MHz): 42.1, 50.9, 54.1 (3 x CH₂, 3 x NCH₂), 55.2 (CH₃, OCH₃), 73.0 (CH, C≡CH), 79.2 (C, C≡CH), 110.4 (CH, aromatic CH), 120.3 (CH, aromatic CH), 126.2 (C, quaternary aromatic C), 127.2 (CH, aromatic CH), 127.7 (CH, 2 x aromatic CH), 128.3 (CH, aromatic CH), 129.0 (CH, 2 x aromatic CH), 129.5 (CH, aromatic CH), 130.4 (CH, aromatic CH), 130.6 (CH, aromatic CH), 132.9 (CH, aromatic CH), 133.6 (CH, aromatic CH), 138.6 (C, quaternary aromatic C), 139.5 (C,

quaternary aromatic C), 141.8 (C, quaternary aromatic C), 157.9 (C, quaternary aromatic C); m/z (ESI) 406.14 [(M+H)⁺]; HRMS (ESI): exact mass calculated for C₂₄H₂₄NO₃S [(M+H)⁺], 406.1477. Found 406.1476.

Single crystals of **46** were grown from CH₂Cl₂. Crystal data: C₂₄H₂₃NO₃S, $M = 405.49$, monoclinic, space group $P2_1/c$, $a = 14.2356(14)$ Å, $b = 9.2099(10)$ Å, $c = 16.7855(17)$ Å, $\beta = 109.255(2)^\circ$, $V = 2077.6(4)$ Å³, $Z = 4$, $D_c = 1.296$ g cm⁻³, $F(000) = 856$, Mo K α radiation, $\lambda = 0.71073$ Å, $T = 100(2)$ K, $2\theta_{\max} = 28.15^\circ$, $\mu = 0.181$ mm⁻¹, 25323 reflections collected, 5036 unique ($R_{\text{int}} = 0.0613$). Final GooF = 1.151, $R_1 = 0.1019$, $wR_2 = 0.2072$ (obs. data: $I > 2\sigma(I)$); $R_1 = 0.1247$, $wR_2 = 0.2189$ (all data).

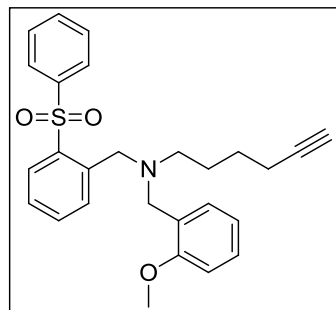
N-(2-Methoxybenzyl)-*N*-[2-(phenylsulfonyl)benzyl]but-3-yn-1-amine (**47**)



A solution of oxone[®] (0.22 g, 0.36 mmol) in water (5 mL) was added dropwise over a period of 1 h to a stirred solution of the sulfide **27**, (0.07 g, 0.18 mmol) in acetone (5 mL). The reaction mixture was stirred for 16 h and concentrated *in vacuo* to half its original volume. CH₂Cl₂ (10 mL) was then added and the layers separated. The aqueous layer was further extracted with CH₂Cl₂ (2 x 10 mL). The combined organic layers were washed with water (2 x 10 mL), brine (10 mL), dried with MgSO₄ and the solvent was removed *in vacuo*. Purification by column chromatography using ethyl acetate/hexane (1:1) as eluent, afforded **47**, as a clear oil (0.07 g, 88%). $\nu_{\max}/\text{cm}^{-1}$ (film): 3293 ($\equiv\text{C-H}$), 2937 (CH), 2836 (CH), 2117 (C \equiv C), 1492 (ring stretch), 1446 (CH₂), 1307 (SO₂), 1243 (CN), 1154 (SO₂); δ_{H} (300 MHz): 1.88 (1H, t, J 2.6, C \equiv C-H), 2.19 (2H, td, J 7.3, 2.6, CH₂-C \equiv C), 2.43 (2H, t, J 7.4, CH₂CH₂-C \equiv C), 3.48 (2H, s, NCH₂C₆H₄), 3.77 (3H, s, OCH₃), 3.88 (2H, s, NCH₂C₆H₄), 6.81 (1H, d, J 8.1, ArH), 6.87 (1H, td, J 7.4, 1.0, ArH), 7.17 (1H, td, J 7.8, 1.5, ArH), 7.28 (1H, dd, J 7.5, 1.8, ArH), 7.37-7.49 (3H, m, ArH), 7.52-7.60 (2H, m, ArH), 7.79-7.84 (2H, m, ArH), 8.02 (1H, d, J 7.8, ArH), 8.17 (1H, dd, J 8.0, 1.4, ArH); δ_{C} (75 MHz): 16.8 (CH₂, CH₂-C \equiv CH), 51.7, 52.1, 54.1 (3 x CH₂, 3 x NCH₂), 55.2 (CH₃, OCH₃), 68.9 (CH, C \equiv CH), 83.0 (C, C \equiv CH), 110.3 (CH, aromatic CH), 120.3 (CH, aromatic CH), 126.6 (C, quaternary aromatic C), 127.0 (CH, aromatic CH), 127.5 (CH, 2 x aromatic CH), 128.1 (CH, aromatic CH), 129.0 (CH, 2 x aromatic CH), 129.2 (CH, aromatic CH), 130.0 (CH, aromatic CH), 130.5 (CH, aromatic CH), 133.0 (CH, aromatic CH), 133.7 (CH, aromatic CH), 138.3 (C, quaternary aromatic C), 140.4 (C, quaternary aromatic C), 141.7 (C, quaternary aromatic C), 157.7 (C, quaternary aromatic C); m/z (ESI) 420.1

[(M+H)⁺]; HRMS (ESI): exact mass calculated for C₂₅H₂₆NO₃S [(M+H)⁺], 420.1633. Found 420.1638.

***N*-(2-Methoxybenzyl)-*N*-[2-(phenylsulfonyl)benzyl]hex-5-yn-1-amine (48)**

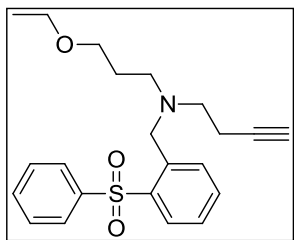


A solution of oxone[®] (0.46 g, 0.76 mmol) in water (5 mL) was added dropwise to a stirred solution of the sulfide **28**, (0.16 g, 0.38 mmol) in acetone (5 mL) over a period of 1 h. The reaction mixture was stirred for 16 h, concentrated *in vacuo* to half its original volume, shaken with CH₂Cl₂ (10 mL) and the layers separated. The aqueous layer was further extracted with CH₂Cl₂ (2 x 10 mL). The combined organic layers were washed with water (2 x 10 mL) and brine (10 mL), dried with MgSO₄ and the solvent was removed *in vacuo*. The crude product was purified by column chromatography using ethyl acetate/hexane (1:4) as eluent and **48** was obtained, as a pale yellow oil (0.03 g, 19%). $\nu_{\max}/\text{cm}^{-1}$ (film): 3289 ($\equiv\text{C-H}$), 2940 (CH), 2116 (C \equiv C), 1492 (ring stretch), 1446 (CH₂), 1307 (SO₂), 1243 (CN), 1154 (SO₂); δ_{H} (300 MHz): 1.33-1.50 (4H, m, NCH₂CH₂CH₂CH₂), 1.89 (1H, t, *J* 2.7, C \equiv C-H), 2.02 (2H, td, *J* 6.8, 2.6, CH₂-C \equiv C), 2.16 (2H, t, *J* 6.8, NCH₂CH₂), 3.40 (2H, s, NCH₂C₆H₄), 3.78 (3H, s, OCH₃), 3.81 (2H, s, NCH₂C₆H₄), 6.81 (1H, d, *J* 8.1, ArH), 6.86 (1H, td, *J* 7.4, 0.9, ArH), 7.18 (1H, td, *J* 7.8, 1.7, ArH), 7.27 (1H, dd, *J* 7.5, 1.5, ArH), 7.36-7.50 (3H, m, ArH), 7.52-7.60 (2H, m, ArH), 7.80-7.85 (2H, m, ArH), 8.00 (1H, d, *J* 7.2, ArH), 8.17 (1H, dd, *J* 8.1, 1.2, ArH); δ_{C} (75 MHz): 18.2, 26.1, 26.3 (3 x CH₂, NCH₂CH₂CH₂CH₂), 52.2, 53.1, 54.4 (3 x CH₂, 3 x NCH₂), 55.2 (CH₃, OCH₃), 68.2 (CH, C \equiv CH), 84.5 (C, C \equiv CH), 110.2 (CH, aromatic CH), 120.3 (CH, aromatic CH), 126.8 (CH, aromatic CH), 127.2 (C, quaternary aromatic C), 127.6 (CH, 2 x aromatic CH), 127.8 (CH, aromatic CH), 129.0 (CH, 2 x aromatic CH), 129.1 (CH, aromatic CH), 129.9 (CH, aromatic CH), 130.4 (CH, aromatic CH), 132.9 (CH, aromatic CH), 133.6 (CH, aromatic CH), 138.3 (C, quaternary aromatic C), 141.1 (C, quaternary aromatic C), 141.8 (C, quaternary aromatic C), 157.7 (C, quaternary aromatic C); *m/z* (ESI) 448.1 [(M+H)⁺]; HRMS (ESI): exact mass calculated for C₂₇H₃₀NO₃S [(M+H)⁺], 448.1946. Found 448.1964.

Single crystals of **48** were grown from CH₂Cl₂. The structure was obtained as a solvate, with uncertainty surrounding the exact nature of the solvate, and the structure is clearly not publishable at this point. Crystal data: C₂₈HCl₃NO₁₂S₃, *M* = 745.83, triclinic, space group *P*1, *a* = 12.1294(15) Å, *b* = 12.5317(16) Å, *c* = 13.1686(16) Å, α = 65.324(3)°, β = 74.818(3)°, γ = 84.251(3)°, *V* = 1755.3(4) Å³, *Z* = 2, *D*_c = 1.411 g cm⁻³, *F*(000) = 742, *Mo*

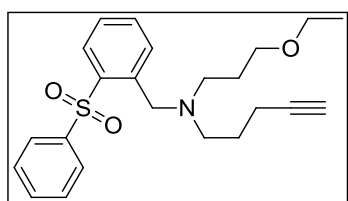
K α radiation, $\lambda = 0.71073 \text{ \AA}$, $T = 159(2) \text{ K}$, $2\theta_{\max} = 26.45^\circ$, $\mu = 0.497 \text{ mm}^{-1}$, 39234 reflections collected, 7075 unique ($R_{\text{int}} = 0.0399$). Final GooF = 2.085, $R_1 = 0.1344$, $wR_2 = 0.4371$ (obs. data: $I > 2\sigma(I)$); $R_1 = 0.1509$, $wR_2 = 0.4573$ (all data).

N-(3-Ethoxypropyl)-N-[2-(phenylsulfonyl)benzyl]but-3-yn-1-amine (49)



A solution of oxone[®] (0.35 g, 0.58 mmol) in water (5 mL) was added dropwise over a period of 1 h to a stirred solution of the sulfoxide **39**, (0.11 g, 0.29 mmol) in acetone (5 mL). The reaction mixture was stirred for 16 h, concentrated at reduced pressure to half its original volume, shaken with CH₂Cl₂ (10 mL) and the layers separated. The aqueous layer was further extracted with CH₂Cl₂ (2 x 10 mL). The combined organic layers were washed with water (2 x 10 mL) and brine (10 mL), dried with MgSO₄ and the solvent was removed *in vacuo*. Purification by column chromatography using ethyl acetate/hexane (1:4) as eluent, gave the sulfone **49**, as a pale yellow oil (0.03 g, 25%). (Found: C, 68.24; H, 7.02; N, 3.54%. C₂₂H₂₇NO₃S requires C, 68.54; H, 7.06; N, 3.63%); $\nu_{\max}/\text{cm}^{-1}$ (film): 3285 ($\equiv\text{C-H}$), 2863 (CH), 2117 (C \equiv C), 1447 (CH₃), 1307 (SO₂), 1154 (SO₂); δ_{H} (300 MHz): 1.15 (3H, t, J 6.9, OCH₂CH₃), 1.50-1.61 (2H, m, NCH₂CH₂CH₂), 1.89 (1H, t, J 2.6, C \equiv C-H), 2.12 (2H, td, J 7.4, 2.7, CH₂C \equiv C-H), 2.37 (2H, t, J 7.1, NCH₂CH₂), 2.47 (2H, t, J 7.4, NCH₂CH₂), 3.31-3.44 (4H, m, CH₂OCH₂), 3.81 (2H, s, NCH₂C₆H₄), 7.43 (1H, td, J 7.7, 1.1, ArH), 7.46-7.62 (4H, m, ArH), 7.82-7.87 (2H, m, ArH), 7.93 (1H, d, J 7.8, ArH), 8.18 (1H, dd, J 8.0, 1.4, ArH); δ_{C} (75 MHz): 15.20 (CH₃, CH₂CH₃), 16.9, 27.5 (2 x CH₂, CH₂-C \equiv CH and NCH₂CH₂CH₂), 50.7, 52.7, 54.4 (3 x CH₂, 3 x NCH₂), 66.1, 68.4 (2 x CH₂, CH₂OCH₂), 68.9 (CH, C \equiv CH), 82.9 (C, C \equiv CH), 127.0 (CH, aromatic CH), 127.4 (CH, 2 x aromatic CH), 129.1 (CH, 2 x aromatic CH), 129.3 (CH, aromatic CH), 130.5 (CH, aromatic CH), 133.1 (CH, aromatic CH), 133.7 (CH, aromatic CH), 138.1 (C, quaternary aromatic C), 140.5 (C, quaternary aromatic C), 141.7 (C, quaternary aromatic C); m/z (ESI) 386.1 [(M+H)⁺]; HRMS (ESI): exact mass calculated for C₂₂H₂₈NO₃S [(M+H)⁺], 386.1790. Found 386.1789.

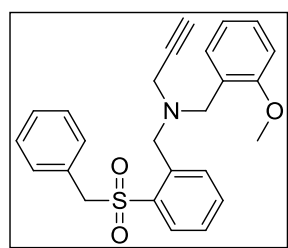
N-(3-Ethoxypropyl)-N-[2-(phenylsulfonyl)benzyl]pent-4-yn-1-amine (50)



A solution of oxone[®] (0.20 g, 0.32 mmol) in water (3 mL) was added dropwise over a period of 1 h to a stirred solution of the sulfide **30**, (0.06 g, 0.16 mmol) in acetone (3 mL). The reaction

mixture was stirred for 16 h, concentrated *in vacuo* to half its original volume, shaken with CH_2Cl_2 (10 mL) and the layers separated. The aqueous layer was further extracted with CH_2Cl_2 (2 x 10 mL). The combined organic layers were washed with water (2 x 10 mL) and brine (10 mL), dried with MgSO_4 and the solvent was removed *in vacuo*. Purification by column chromatography using ethyl acetate/hexane (1:4) as eluent, yielded **50**, as a pale yellow oil (0.02 g, 30%). $\nu_{\text{max}}/\text{cm}^{-1}$ (film): 3285 ($\equiv\text{C-H}$), 2963 (CH), 2865 (CH), 2116 ($\text{C}\equiv\text{C}$), 1447 (CH_3), 1307 (SO_2), 1154 (SO_2), 1091 (COC); δ_{H} (300 MHz): 1.08 (3H, t, J 7.1, CH_3), 1.35-1.53 (4H, m, 2 x NCH_2CH_2), 1.79 (1H, t, J 2.7, $\text{C}\equiv\text{C-H}$), 2.01 (2H, td, J 7.2, 2.7, $\text{CH}_2\text{C}\equiv\text{C-H}$), 2.19-2.28 (4H, m, 2 x NCH_2CH_2), 3.26 (2H, t, J 6.5, $\text{CH}_2\text{CH}_2\text{O}$), 3.32 (2H, q, J 7.0, OCH_2CH_3), 3.69 (1H, s, $\text{NCH}_2\text{C}_6\text{H}_4$), 7.31-7.55 (5H, m, ArH), 7.75-7.84 (3H, m, ArH), 8.11 (1H, dd, J 8.1, 1.2, ArH); δ_{C} (75 MHz): 14.2 (CH_3 , CH_2CH_3), 15.2, 25.0, 26.4 (3 x CH_2 , $\text{CH}_2\text{CH}_2\text{-C}\equiv\text{CH}$, $\text{CH}_2\text{-C}\equiv\text{CH}$ and $\text{NCH}_2\text{CH}_2\text{CH}_2\text{O}$), 50.0, 51.9, 53.6 (3 x CH_2 , 3 x NCH_2), 65.1, 67.3 (2 x CH_2 , CH_2OCH_2), 67.5 (CH, $\text{C}\equiv\text{CH}$), 83.2 (C, $\text{C}\equiv\text{CH}$), 125.9 (CH, aromatic CH), 126.5 (CH, 2 x aromatic CH), 128.0 (CH, 2 x aromatic CH), 128.2 (CH, aromatic CH), 129.3 (CH, aromatic CH), 132.0 (CH, aromatic CH), 132.6 (CH, aromatic CH), 137.1 (C, quaternary aromatic C), 139.9 (C, quaternary aromatic C), 140.7 (C, quaternary aromatic C); m/z (ESI) 400.4 $[(\text{M}+\text{H})^+]$; HRMS (ESI): exact mass calculated for $\text{C}_{23}\text{H}_{30}\text{NO}_3\text{S}$ $[(\text{M}+\text{H})^+]$, 400.1946. Found 400.1933.

***N*-[2-(Benzylsulfonyl)benzyl]-*N*-(2-methoxybenzyl)prop-2-yn-1-amine (51)**

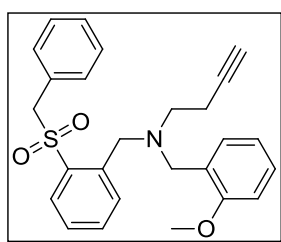


A solution of oxone[®] (1.28 g, 2.08 mmol) in water (7 mL) was added dropwise over a period of 1 h to a stirred solution of the sulfide **31**, (0.40 g, 1.04 mmol) in acetone (7 mL). The reaction mixture was stirred for 16 h and concentrated *in vacuo* to half its original volume. CH_2Cl_2 (20 mL) was then added to the mixture and the phases were separated. The aqueous layer was further extracted with CH_2Cl_2 (2 x 20 mL). The combined organic extracts were washed with water (2 x 20 mL), brine (20 mL), dried with MgSO_4 and the solvent was removed *in vacuo*. Purification by column chromatography using ethyl acetate/hexane (1:4) as eluent, gave the title compound **51**, as a clear viscous oil (0.18 g, 33%). $\nu_{\text{max}}/\text{cm}^{-1}$ (film): 3287 ($\equiv\text{C-H}$), 2837 (CH), ($\text{C}\equiv\text{C}$ stretch not observed), 1602 (ring stretch), 1494 (ring stretch), 1311 (SO_2), 1248 (C-O), 1153 (SO_2), 1121 (COC); δ_{H} (300 MHz): 2.31 (1H, t, J 2.4, $\text{C}\equiv\text{C-H}$), 3.27 (2H, d, J 2.1, $\text{CH}_2\text{C}\equiv\text{C-H}$), 3.65 (3H, s, OCH_3), 3.81, 4.19 (2 x 2H, 2 x s, 2 x $\text{NCH}_2\text{C}_6\text{H}_4$), 4.64 (2H, s, SO_2CH_2), 6.76 (1H, d, J 8.1, ArH), 6.84 (1H, td, J 7.5, 0.9, ArH), 6.97-7.03 (2H, m, ArH), 7.09-7.22 (5H,

m, ArH), 7.31 (1H, dd, J 7.5, 1.8, ArH), 7.45 (1H, td, J 7.5, 1.5, ArH), 7.54 (1H, dd, J 8.0, 1.4, ArH), 7.63 (1H, d, J 7.5, ArH); δ_{C} (75 MHz): 40.9, 52.2, 55.0 (3 x CH₂, 3 x NCH₂), 55.1 (CH₃, OCH₃), 62.2 (CH₂, SO₂CH₂), 74.4 (CH, C≡CH), 78.6 (C, C≡CH), 110.5 (CH, aromatic CH), 120.3 (CH, aromatic CH), 125.6 (C, quaternary aromatic C), 127.6 (CH, aromatic CH), 128.4 (CH, aromatic CH), 128.5 (CH, 2 x aromatic CH), 128.6 (C, quaternary aromatic C), 128.9 (CH, aromatic CH), 130.9 (CH, 2 x aromatic CH), 131.4 (CH, aromatic CH), 131.8 (CH, aromatic CH), 132.4 (CH, aromatic CH), 133.4 (CH, aromatic CH), 137.1 (C, quaternary aromatic C), 138.8 (C, quaternary aromatic C), 158.1 (C, quaternary aromatic C); m/z (ESI) 420.2 [(M+H)⁺]; HRMS (ESI): exact mass calculated for C₂₅H₂₅NO₃S [(M+H)⁺], 420.1633. Found 420.1634.

Single crystals of the HCl salt of **51** were obtained. Ethereal aqueous HCl [ether (8 ml), conc. HCl (2 ml)] was added dropwise to a solution of **51** in CH₂Cl₂ (2 ml) until the salt crashed out. Crystal data: C₂₆H₂₈Cl₂NO₄S, $M = 521.45$, monoclinic, space group $P1$, $a = 9.0798(10)$ Å, $b = 9.4984(10)$ Å, $c = 15.5218(17)$ Å, $\alpha = 76.019(3)^\circ$, $\beta = 80.617(3)^\circ$, $\gamma = 76.068(3)^\circ$, $V = 1252.9(2)$ Å³, $Z = 2$, $D_{\text{c}} = 1.382$ g cm⁻³, $F(000) = 546$, Mo K α radiation, $\lambda = 0.71073$ Å, $T = 100(2)$ K, $2\theta_{\text{max}} = 27.27^\circ$, $\mu = 0.376$ mm⁻¹, 29991 reflections collected, 5589 unique ($R_{\text{int}} = 0.0406$). Final GooF = 1.061, $R_1 = 0.0574$, $wR_2 = 0.1610$ (obs. data: $I > 2\sigma(I)$); $R_1 = 0.0682$, $wR_2 = 0.1707$ (all data).

***N*-[2-(Benzylsulfonyl)benzyl]-*N*-(2-methoxybenzyl)but-3-yn-1-amine (**52**)**



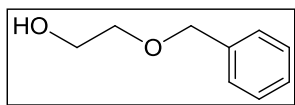
A solution of oxone[®] (0.17 g, 0.28 mmol) in water (3 mL), was added dropwise over a period of 1 h to a stirred solution of the sulfide **32** (0.06 g, 0.14 mmol) in acetone (3 mL). The reaction mixture was stirred for 16 h, concentrated *in vacuo* to half its original volume, shaken with CH₂Cl₂ (10 mL) and the layers separated. The aqueous layer was further extracted with CH₂Cl₂ (2 x 10 mL). The combined organic layers were washed with water (2 x 10 mL) and brine (10 mL), dried with MgSO₄ and the solvent was removed *in vacuo*. The crude product was purified by column chromatography using ethyl acetate/hexane (1:4) as eluent, which afforded the sulfone **52**, as a clear viscous oil (0.02 g, 38%). $\nu_{\text{max}}/\text{cm}^{-1}$ (film): 3293 (≡C-H), 2918 (CH), 2837 (CH), 2116 (C≡C), 1601 (ring stretch), 1493 (ring stretch), 1312 (SO₂), 1243 (C-O), 1152 (SO₂); δ_{H} (300 MHz): 1.93 (1H, t, J 2.7, C≡C-H), 2.44 (2H, td, J 7.4, 2.7, CH₂C≡C-H), 2.73 (2H, t, J 7.5, NCH₂CH₂), 3.74, (2H, s, NCH₂C₆H₄), 3.79 (3H, s, OCH₃), 4.02 (2H, s, NCH₂C₆H₄), 4.50 (2H, s, SO₂CH₂), 6.85 (1H, d, J 8.4, ArH), 6.91 (1H, td, J 7.5, 0.9, ArH), 7.06 (2H, dd,

J 8.1, 1.5, ArH), 7.19-7.32 (5H, m, ArH), 7.38 (1H, dd, *J* 7.5, 1.5, ArH), 7.54 (1H, td, *J* 7.5, 1.5, ArH), 7.68 (1H, dd, *J* 8.0, 1.4, ArH), 7.81 (1H, d, *J* 7.5, ArH); δ_{C} (75 MHz): 16.5 (CH₂, NCH₂CH₂), 51.7, 52.1, (2 x CH₂, 2 x NCH₂), 55.2 (CH₃, OCH₃), 55.4 (CH₂, NCH₂), 62.8 (CH₂, SO₂CH₂), 69.1 (CH, C≡CH), 83.1 (C, C≡CH), 110.3 (CH, aromatic CH), 120.4 (CH, aromatic CH), 126.3 (C, quaternary aromatic C), 127.3 (CH, aromatic CH), 128.1 (C, quaternary aromatic C), 128.3 (CH, aromatic CH), 128.5 (CH, 2 x aromatic CH), 128.7 (CH, aromatic CH), 130.5 (CH, aromatic CH), 131.0 (CH, 2 x aromatic CH), 131.3 (CH, aromatic CH), 131.4 (CH, aromatic CH), 133.6 (CH, aromatic CH), 136.5 (C, quaternary aromatic C), 140.5 (C, quaternary aromatic C), 157.8 (C, quaternary aromatic C); *m/z* (ESI) 434.1 [(M+H)⁺]. HRMS (ESI): exact mass calculated for C₂₆H₂₈NO₃S [(M+H)⁺], 434.1790. Found 434.1791.

5.3. Aromatic based systems

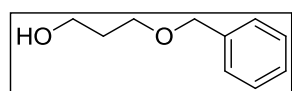
5.3.1. Arms D, E and F

2-(Benzyloxy)ethanol (**60**)¹¹



Neat benzyl bromide, **65**, (41 mL, 0.35 mol) was added dropwise to a stirring solution of ethylene glycol **59** (86 mL, 1.40 mol) and potassium hydroxide (40.0 g, 0.70 mol) under nitrogen. The reaction mixture was then heated to 80 °C for 24 h. Then the mixture was cooled to room temperature and diluted with ethyl acetate (200 mL). Water (150 mL) was added and the phases were separated. The aqueous layer was extracted with ethyl acetate (2 x 200 mL). The organic layers were combined, dried over MgSO₄, filtered, and the solvent was removed *in vacuo* to afford **60**, as a clear oil which was sufficiently pure to use without further purification (37.79 g, 72%). $\nu_{\text{max}}/\text{cm}^{-1}$ (film): 3328 (OH), 2931 (CH), 2868 (CH), 1719 (ring stretch), 1454 (CH₂), 1277 (COC), 1116 (C-O); δ_{H} (300 MHz): 2.76 (1H, bs, OH), 3.52-3.57, 3.67-3.73 (2 x 2H, 2 x m, CH₂OBn and CH₂OH), 4.52 (2H, s, OCH₂Ph), 7.21-7.37 (5H, m, ArH); Spectral characteristics were in agreement with those previously reported.¹¹

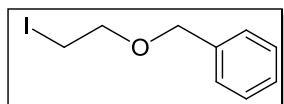
3-(Benzyloxy)propan-1-ol (**63**)¹²



Neat benzyl bromide, **65**, (59.85 g, 0.45 mol) was added dropwise to a stirring solution of 1,3-propanediol **62** (107 mL, 1.40 mol) and potassium hydroxide (40 g, 0.70 mol) under nitrogen. The reaction mixture was then heated to 80 °C while stirring for 24 h. After 24 h, the mixture was cooled to room temperature and

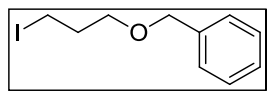
diluted with ethyl acetate (150 mL). Water (200 mL) was added and the layers were separated. The aqueous layer was extracted with ethyl acetate (3 x 300 mL). The organic layers were combined, dried over MgSO_4 , filtered, and the solvent was removed *in vacuo*. The title compound **63**, was obtained as a clear oil which was sufficiently pure to use without further purification (39.27 g, 68%). ν_{max} (film): 3316 (OH), 2947 (CH), 2872 (CH), 1716 (ring stretch), 1453 (CH_2), 1277 (COC), 1098 (C-O), 1072 (COC); δ_{H} (300 MHz) 1.79-1.89 (2H, m, $\text{CH}_2\text{CH}_2\text{OH}$), 2.70 (1H, bs, OH), 3.62 (2H, t, J 6.0, CH_2OBn or CH_2OH), 3.73 (2H, t, J 5.9, CH_2OBn or CH_2OH), 4.50 (2H, s, CH_2Ph), 7.23-7.37 (5H, m, ArH); Spectral characteristics were in agreement with those previously reported.¹²

[(2-Iodoethoxy)methyl]benzene (**61**)⁵

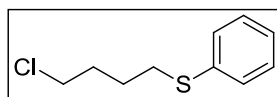


This compound was prepared with a modification of the method published by Borbas.⁵ Triphenylphosphine (10.75 g, 41.0 mmol), imidazole (2.79 g, 31.0 mmol) and CH_2Cl_2 (50 mL) were added to a two-necked round bottom flask under a flow of nitrogen and stirred at room temperature until the solids had dissolved resulting in a clear solution. The reaction mixture was cooled to 0 °C using an ice bath and iodine (10.4 g, 41.0 mmol) was then added portionwise to the mixture. Once all the iodine had dissolved, 2-benzyloxyethanol, **60**, (3.1 mL, 31.0 mmol) in CH_2Cl_2 (10 mL) was added slowly by syringe over 10-15 minutes. Stirring of the reaction mixture was continued for 24 h. The mixture was then washed with portions of aqueous sodium thiosulfate (1 M, 4 x 20 mL) and the phases separated. The organic extracts were washed repeatedly with water until colourless, dried over MgSO_4 , filtered, and the solvent was removed *in vacuo*. Purification by column chromatography using hexane/ethyl acetate (3:2) as eluent, gave **61**, as a pale yellow oil (3.98 g, 46%). $\nu_{\text{max}}/\text{cm}^{-1}$ (film): 2860 (CH), 1496 (ring stretch), 1454 (CH_2), 1107 (COC); δ_{H} (300 MHz): 3.25 (2H, t, J 6.8, CH_2I), 3.75 (2H, t, J 6.8, CH_2OBn), 4.55 (2H, s, CH_2Ph), 7.23-7.36 (5H, m, ArH); δ_{C} (75 MHz): 2.6 (CH_2 , CH_2I), 70.4 (CH_2 , CH_2OCH_2), 72.6 (CH_2 , CH_2OCH_2), 127.4 (CH, 2 x aromatic CH), 127.5 (CH, aromatic CH), 128.1 (CH, 2 x aromatic CH), 137.5 (C, quaternary aromatic C); Spectral characteristics were in agreement with those previously reported.⁵

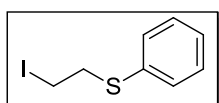
* Unassigned signals were observed in δ_{C} at: 20.5, 69.2, 72.9, 127.3, 128.0.

[(3-Iodopropoxy)methyl]benzene (64)¹³

Triphenylphosphine (10.75 g, 41.0 mmol), imidazole (2.79 g, 31.0 mmol), CH₂Cl₂ (50 mL), iodine (10.4 g, 41.0 mmol) and 3-(benzyloxy)propan-1-ol, **63**, (4.57 mL, 31 mmol) were used in the same way as described in **61** to give **64**, as a pale yellow oil after column chromatography (3.60 g, 42%). $\nu_{\max}/\text{cm}^{-1}$ (film): 2858 (CH), 1454 (CH₂), 1102 (COC); δ_{H} (300 MHz): 2.02-2.14 (2H, m, ICH₂CH₂), 3.30 (2H, t, *J* 6.9, ICH₂), 3.53 (2H, t, *J* 5.9, CH₂OBn), 4.51 (2H, s, CH₂Ph), 7.23-7.39 (5H, m, ArH); δ_{C} (75 MHz): 3.5 (CH₂, CH₂I), 33.5 (CH₂, OCH₂CH₂CH₂), 69.6 (CH₂, CH₂OCH₂), 73.2 (CH₂, CH₂OCH₂), 127.7 (CH, 3 x aromatic CH), 128.4 (CH, 2 x aromatic CH), 138.3 (C, quaternary aromatic C); Spectral characteristics were in agreement with those previously reported.¹³

(4-Chlorobutyl)(phenyl)sulfide (67)¹⁴

Sodium (1.13 g, 49.0 mmol) was added to methanol (30 ml) while stirring at 0 °C in a three-necked round bottom flask under nitrogen. Thiophenol, **4** (5.0 mL, 49.0 mmol) and 1-bromo-4-chlorobutane, **66**, (5.3 mL, 46 mmol) were then added dropwise to the solution. The reaction mixture was stirred under a nitrogen atmosphere for 4 h. Aqueous NaOH (1 M, 10 mL) was added and the mixture extracted with CH₂Cl₂ (3 x 50 mL). The combined organic layers were dried over MgSO₄, filtered, and the solvent was removed *in vacuo* providing **67**, as a colourless oil, which was sufficiently pure to use without further purification (7.83 g, 80%). $\nu_{\max}/\text{cm}^{-1}$ (film): 2882 (CH), 1688 (ring stretch), 1600 (ring stretch), 759 (C-Cl); δ_{H} (300 MHz): 1.73-1.85 (2H, m, CH₂CH₂Cl or CH₂CH₂SPh), 1.86-1.97 (2H, m, CH₂CH₂Cl or CH₂CH₂SPh), 2.94 (2H, t, *J* 7.0, CH₂SPh), 3.52 (2H, t, *J* 6.5, CH₂Cl), 7.13-7.21 (1H, m, ArH), 7.24-7.36 (4H, m, ArH); δ_{C} (75 MHz): 26.3 (CH₂, CH₂CH₂CH₂S), 31.4 (CH₂, CH₂CH₂CH₂S), 33.0 (CH₂, CH₂CH₂CH₂S), 44.4 (CH₂Cl), 126.0 (CH, aromatic CH), 128.9 (CH, 2 x aromatic CH), 129.3 (CH, 2 x aromatic CH), 136.3 (C, quaternary aromatic C); Spectral characteristics were in agreement with those previously reported.¹⁴

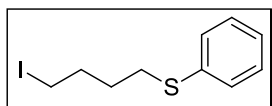
(2-Iodoethyl)(phenyl)sulfide (69)¹⁵

This compound was synthesised using a modified version of the Coleman procedure.¹⁶ Sodium iodide (4.10 g, 27.4 mmol) was added to acetone (40 mL) and stirred at room temperature under nitrogen until a clear solution was observed. (2-Chloroethyl)(phenyl)sulfide, **68**, (2.00 mL, 13.7 mmol) was then added

dropwise using a syringe and the mixture was heated under reflux for 16 h. 30 mL of acetone was then removed *in vacuo*. Water (20 mL) was added and the product was extracted by washing with ether (3 x 20 mL). Aqueous sodium thiosulfate (1 M, 30 mL) was then added to the mixture. The combined organic phases were dried over MgSO₄, filtered, and the solvent was removed *in vacuo*. Purification of the title compound **69**, was attempted by column chromatography using hexane/ethyl acetate (9:1) as eluent to give a pale yellow liquid (2.75 g, 76%). The product contained a mixture of (2-chloroethyl)(phenyl)sulfide (~33%) and the desired product, **69**, (~67%) which were inseparable by column chromatography. $\nu_{\max}/\text{cm}^{-1}$ (film): 1583 (ring stretch), 1481 (ring stretch), 1439 (CH₂), 739 (C-S); δ_{H} (300 MHz): 3.16-3.36 (4H, m, CH₂I and CH₂SPh), 7.20-7.41 (5H, m, ArH); δ_{C} (75 MHz): 2.7 (CH₂, CH₂I), 37.0 (CH₂, CH₂CH₂I), 127.2 (CH, aromatic CH), 129.3 (CH, 2 x aromatic CH), 130.6 (CH, 2 x aromatic CH), 134.1 (C, quaternary aromatic C).

* Signals for the starting chloride were observed at δ_{H} 3.16-3.36 (2H, m, CH₂SPh), 3.57-3.64 (2H, m, CH₂Cl), 7.20-7.41 (5H, m, ArH); δ_{C} 36.2 (CH₂), 42.3 (CH₂), 127.1 (CH, aromatic CH), 129.25 (CH, 2 x aromatic CH), 130.5 (CH, 2 x aromatic CH), 134.2 (C, quaternary aromatic C).

(4-Iodobutyl)(phenyl)sulfide (**70**)¹⁷

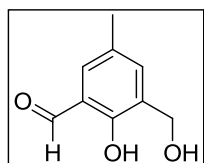


This compound was synthesised using a modified version of the Coleman procedure.¹⁶ Sodium iodide (2.0 g, 13.5 mmol) was added to acetone (25 mL) and stirred at room temperature under nitrogen until a clear solution was observed. (4-Chlorobutyl)(phenyl)sulfide, **67**, (1.40 g, 6.7 mmol) was then added dropwise using a syringe and the mixture was heated under reflux for 16 h. 10 mL of acetone was then removed *in vacuo*. Water (20 mL) was added and the product was extracted by washing with ether (3 x 20 mL). Aqueous sodium thiosulfate (1 M, 20 mL) was subsequently added to the mixture. The combined organic layers were dried over MgSO₄, filtered, and the solvent was removed *in vacuo* to give **70**, as a pale yellow liquid which was sufficiently pure to use without further purification (1.17 g, 60%). The product obtained consisted of a mixture of the starting material, **67** (~53%) and the desired product, **70** (~47%) which were inseparable by column chromatography. ¹H and ¹³C NMR signals for **67** were identical to those described earlier and the characteristic signals for **70** are detailed below. $\nu_{\max}/\text{cm}^{-1}$ (film): 2953 (CH), 1584 (ring stretch), 1480 (ring stretch), 1438 (CH₂); δ_{H} (300 MHz): 1.70-1.86 (2H, m, CH₂CH₂I or CH₂CH₂SPh), 1.86-2.03 (2H, m, CH₂CH₂I or CH₂CH₂SPh), 2.90-2.98 (2H, m, CH₂S), 3.19 (2H, t, *J* 6.9, CH₂I), 7.15-7.22 (1H, m, ArH), 7.25-7.36 (4H, m, ArH);

δ_C (75 MHz): 5.9 (CH₂, CH₂I), 29.8, 32.3, 32.6 (CH₂, CH₂CH₂CH₂S), 126.1 (CH, aromatic CH), 128.9 (CH, 2 x aromatic CH), 129.34 (CH, 2 x aromatic CH), 136.22 (C, quaternary aromatic C).

5.3.2. Synthetic Strategy I

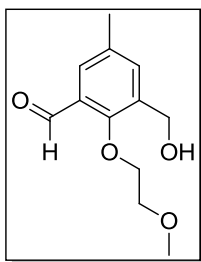
2-Hydroxy-3-(hydroxymethyl)-5-methylbenzaldehyde (**71**)¹⁸



2,6-Bis(hydroxymethyl)-4-methylphenol, **57**, (1.0 g, 5.95 mmol) was placed in a 50 mL round bottom flask and stirred with a suspension of electronic grade MnO₂ (5.17 g, 59.5 mmol) in dry THF (20 mL) for 24 h at room temperature. The mixture was filtered through celite[®] and washed with THF several times until the filtrate became colourless. The solvent was then removed *in vacuo*. Purification by column chromatography using hexane/ethyl acetate/triethylamine (9:0.9:0.1) as eluent, gave **71**, as a pale yellow solid (0.46 g, 47%). m.p: 72-74 °C (Lit.¹⁹ 72-73 °C); (Found: C, 65.17; H, 6.08%. C₉H₁₀O₃ requires C, 65.05; H, 6.07%); $\nu_{\max}/\text{cm}^{-1}$ (KBr): 3287 (OH), 2853 (CH), 1645 (C=O), 1456 (ring stretch), 1380 (H-C=O); δ_H (300 MHz): 1.55 (2H, bs, 2 x OH), 2.35 (3H, s, CH₃), 4.74 (2H, s, CH₂OH), 7.30 (1H, s, ArH), 7.41 (1H, s, ArH), 9.87 (1H, s, CHO); δ_C (75 MHz): 20.3 (CH₃, ArCH₃), 60.7 (CH₂, CH₂OH), 120.1 (C, quaternary aromatic C), 129.0 (C, quaternary aromatic C), 129.2 (C, quaternary aromatic C), 132.6 (CH, aromatic CH), 136.9 (CH, aromatic CH), 157.4 (C, quaternary aromatic C), 196.7 (C, C=O); Spectral characteristics were in agreement with those previously reported.¹⁹ Single crystals of **71** were grown from THF. Crystal data: C₉H₁₀O₃, $M = 166.17$, monoclinic, space group $P2_1/n$, $a = 4.6657(4)$, $b = 14.8397(11)$, $c = 24.217(2)$ Å, $\beta = 92.875(2)^\circ$, $V = 1674.6(2)$ Å³, $Z = 8$, $D_c = 1.318$ g cm⁻³, $F(000) = 704$, Mo K α radiation, $\lambda = 0.71073$ Å, $T = 296(2)$ K, $2\theta_{\max} = 26.47^\circ$, $\mu = 0.099$ mm⁻¹, 19565 reflections collected, 3432 unique ($R_{\text{int}} = 0.0580$). Final GooF = 1.025, $R_1 = 0.0509$, $wR_2 = 0.1187$ (obs. data: $I > 2\sigma(I)$); $R_1 = 0.1155$, $wR_2 = 0.1490$ (all data).

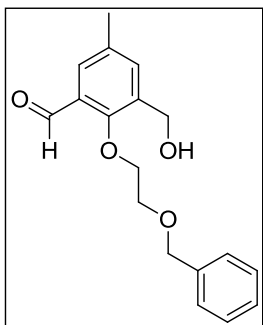
The following compounds (**72-74**) were prepared according to a modified version of the Sarju procedure.²⁰

3-(Hydroxymethyl)-2-(2-methoxyethoxy)-5-methylbenzaldehyde (**72**)



The aldehyde **71** (0.3 g, 1.77 mmol), anhydrous potassium carbonate (0.25 g, 1.77 mmol), 2-bromoethyl methyl ether, **58**, (0.20 mLs, 2.12 mmol), methanol (1.5 mL) were added to a pyrex[®] cylindrical reaction tube containing a magnetic stirrer bar. The tube was septum-sealed and irradiated with microwaves while stirring, at a set temperature of 150 °C for 80 mins. The temperature was maintained constant by modulated irradiation of 300 W. The reaction mixture was cooled to room temperature and the solvent was removed *in vacuo*. The solid residue was extracted with CH₂Cl₂ (3 x 20 mL), dried over MgSO₄, filtered, and the solvent removed *in vacuo*. Purification by column chromatography using hexane/ethyl acetate (3:2) as eluent, gave **72**, as an orange oil (0.19 g, 47%). $\nu_{\max}/\text{cm}^{-1}$ (film): 3428 (OH), 2882 (CH), 1688 (C=O), 1455 (CH₃), 1212 (COC); δ_{H} (300 MHz): 1.61 (1H, bs, OH), 2.36 (3H, s, Ar-CH₃), 3.46 (3H, s, OCH₃), 3.74-3.79, 4.19-4.23 (2 x 2H, 2 x m, OCH₂CH₂O), 4.68 (2H, d, *J* 5.4, CH₂OH), 7.40 (1H, finely split s, ArH), 7.56 (1H, finely split s, ArH), 10.30 (1H, s, CHO); δ_{C} (75 MHz): 20.6 (CH₃, Ar-CH₃), 59.1 (CH₃, OCH₃), 61.0, 71.85, 76.0 (3 x CH₂, CH₂OH, CH₂OC₆H₂, CH₂OCH₃), 129.0 (C, quaternary aromatic C), 129.7 (CH, aromatic CH), 134.4 (C, quaternary aromatic C), 135.4 (C, quaternary aromatic C), 137.2 (CH, aromatic CH), 158.2 (C, quaternary aromatic C), 190.1 (C, CHO). *m/z* (ESI) 225.1 [(M+H)⁺].

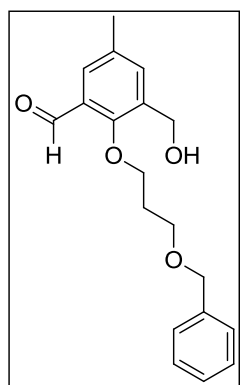
2-[2-(Benzyloxy)ethoxy]-3-(hydroxymethyl)-5-methylbenzaldehyde (**73**)



A pyrex[®] cylindrical reaction tube was charged with the aldehyde **71** (0.2 g, 1.20 mmol), anhydrous potassium carbonate (0.17 g, 1.20 mmol), (2-iodoethoxy)methylbenzene, **61**, (0.38 g, 1.44 mmol), methanol (1.5 mL) and a magnetic stirrer bar. The tube was septum-sealed and irradiated with microwaves while stirring, at a set temperature of 150 °C for 60 mins. The temperature was maintained constant by modulated irradiation of 300 W. The reaction mixture was cooled to room temperature, the solvent was removed *in vacuo* and the solid residue extracted with CH₂Cl₂ (3 x 20 mL). The organic extracts were dried over MgSO₄, filtered, and the solvent removed *in vacuo*. Purification by column chromatography using hexane/ethyl acetate (4:1) as eluent, gave the title compound **73**, as a brown oil (0.19 g, 47%) which was ~70-80% pure as

determined by ^1H NMR. $\nu_{\text{max}}/\text{cm}^{-1}$ (film): 3435 (OH), 2865 (CH), 1683 (C=O), 1471 (ring stretch), 1455 (CH_2), 1210 (COC); δ_{H} (300 MHz): 1.61 (1H, bs, OH), 2.35 (3H, s, Ar- CH_3), 3.80-3.85, 4.20-4.24 (2 x 2H, 2 x m, $\text{OCH}_2\text{CH}_2\text{O}$), 4.64 (2H, s, CH_2Ph), 4.69 (2H, d, J 6.6, CH_2OH), 7.28-7.38 (5H, m, ArH), 7.39 (1H, finely split s, ArH), 7.57 (1H, finely split s, ArH), 10.31 (1H, s, CHO); δ_{C} (75 MHz): 20.6 (CH_3 , Ar- CH_3), 60.9, 69.2, 73.5, 76.1 (4 x CH_2 , CH_2OH , CH_2OBn , $\text{CH}_2\text{OC}_6\text{H}_2$, CH_2Ph), 128.0 (CH, 2 x aromatic CH), 128.1 (CH, aromatic CH), 128.6 (CH, 2 x aromatic CH), 129.0 (C, quaternary aromatic C), 129.6 (CH, aromatic CH), 134.4 (C, quaternary aromatic C), 135.4 (C, quaternary aromatic C), 137.1 (CH, aromatic CH), 137.2 (C, quaternary aromatic C), 158.2 (C, quaternary aromatic C), 190.1 (CHO); m/z (ESI) 301.1 [(M+H) $^+$].

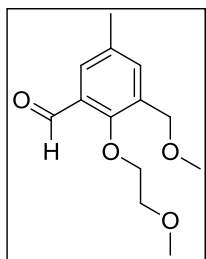
2-[3-(Benzyloxy)propoxy]-3-(hydroxymethyl)-5-methylbenzaldehyde (**74**)



A pyrex[®] cylindrical reaction tube was charged with the aldehyde **71** (0.05 g, 0.32 mmol), anhydrous potassium carbonate (0.05 g, 0.32 mmol), [(3-iodopropoxy)methyl]benzene, **64**, (0.11 g, 0.39 mmol), methanol (1.0 mL) and a magnetic stirrer bar. The tube was septum-sealed and irradiated with microwaves while stirring, at a set temperature of 150 °C for 40 mins. The temperature was maintained constant by modulated irradiation of 300 W. The reaction mixture was cooled to room temperature, the solvent was evaporated under reduced pressure and the solid residue extracted with CH_2Cl_2 (3 x 20 mL), dried over MgSO_4 , filtered, and the solvent removed *in vacuo*. Purification by column chromatography using hexane/ethyl acetate (1:1) as eluent, gave **74**, as a brown oil (0.05 g, 53%) which was ~80% pure as determined by ^1H NMR. $\nu_{\text{max}}/\text{cm}^{-1}$ (film): 3436 (OH), 2867 (CH), 1686 (C=O), 1459 (ring stretch), 1209 (COC), 1074 (C-O); δ_{H} (300 MHz): 2.08-2.17 (2H, m, $\text{CH}_2\text{CH}_2\text{OBn}$), 2.34 (3H, s, Ar- CH_3), 3.76 (2H, t, J 5.9, CH_2OBn or $\text{CH}_2\text{OC}_6\text{H}_2$), 4.08 (2H, t, J 6.2, CH_2OBn or $\text{CH}_2\text{OC}_6\text{H}_2$), 4.56 (2H, s, CH_2Ph), 4.68 (2H, s, CH_2OH), 7.25-7.37 (5H, m, ArH), 7.45 (1H, finely split s, ArH), 7.57 (1H, finely split s, ArH), 10.30 (1H, s, CHO); δ_{C} (75 MHz): 20.7 (CH_3 , Ar- CH_3), 30.3 (CH_2 , $\text{CH}_2\text{CH}_2\text{OC}_6\text{H}_2$), 60.4, 66.4, 73.2, 74.6 (4 x CH_2 , CH_2OH , CH_2OBn , $\text{CH}_2\text{OC}_6\text{H}_2$, OCH_2Ph), 127.8 (CH, aromatic CH), 127.9 (CH, 2 x aromatic CH), 128.5 (CH, 2 x aromatic CH), 128.7 (CH, aromatic CH), 129.1 (C, quaternary aromatic C), 134.4 (C, quaternary aromatic C), 135.0 (C, quaternary aromatic C), 136.5 (CH, aromatic CH), 138.0 (C, quaternary aromatic C), 158.3 (C, quaternary aromatic C), 190.1 (C, CHO); m/z (ESI) 315.4

[(M+H)⁺]; HRMS (ESI): exact mass calculated for C₁₉H₂₃O₄ [(M+H)⁺], 315.1596. Found 315.1597.

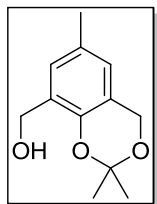
2-(2-Methoxyethoxy)-3-(methoxymethyl)-5-methylbenzaldehyde (**75**)



3-(Hydroxymethyl)-2-(2-methoxyethoxy)-5-methylbenzaldehyde, **72**, (0.03 g, 0.14 mmol) in DMF (1.0 mL) was stirred at room temperature under nitrogen. Sodium hydride (60% dispersed in mineral oil, 0.007 g, 0.164 mmol) was added to the solution at 0 °C and the reaction mixture was stirred for 5 mins. Methyl iodide (0.01 mL, 0.16 mmol) was then added dropwise using a syringe over 10 mins. The reaction mixture was allowed to gradually rise to room temperature and then heated under reflux for 120 h. The reaction progress was monitored by TLC. Diethyl ether (10 mL) was added to dilute the reaction mixture which was then subsequently washed with water (3 x 15 mL), brine (20 mL), dried over MgSO₄, filtered, and the solvent removed *in vacuo*. The crude material (0.016 g, 50%) contained a mixture of unreacted starting material **72**, (~21%), unknown impurity (~25%), and the desired product (~54%). Purification by column chromatography using hexane/ethyl acetate (3:2) as eluent, gave **75** as a clear oil (0.003 g, 10%). $\nu_{\max}/\text{cm}^{-1}$ (film): 2924 (CH), 1687 (C=O), 1128 (COC); δ_{H} (300 MHz): 2.36 (3H, s, Ar-CH₃), 3.44, 3.45 (2 x 3H, 2 x s, 2 x OCH₃), 3.70-3.73, 4.12-4.15 (2 x 2H, 2 x m, OCH₂CH₂O), 4.52 (2H, s, CH₂C₆H₂), 7.48 (1H, finely split s, ArH), 7.59 (1H, finely split s, ArH), 10.40 (1H, s, CHO); δ_{C} (75 MHz): 20.7 (CH₃, Ar-CH₃), 58.5, 59.1 (2 x CH₃, 2 x OCH₃), 68.9, 71.5, 76.4 (3 x CH₂, CH₂C₆H₂, CH₂OC₆H₂, CH₂CH₂OCH₃), 128.5 (CH, aromatic CH), 132.3 (C, quaternary aromatic C), 134.3 (C, quaternary aromatic C), 135.3 (C, quaternary aromatic C), 137.0 (CH, aromatic CH), 190.5 (C, CHO), 3 signals seen for 4 quaternary aromatic C; m/z (ESI) 239.1 [(M+H)⁺]; HRMS (ESI): exact mass calculated for C₁₃H₁₉O₄ [(M+H)⁺], 239.1283. Found 239.1273.
* ~ 70% pure by ¹H NMR, ~ 30% of unknown impurity at δ_{H} 2.42 (s), 3.39 (s), 7.90 (s), 10.42 (s).

5.3.3. Synthetic Strategy II

(2,2,6-Trimethyl-4*H*-benzo[*d*][1,3]dioxin-8-yl)-methanol (**82**)²¹

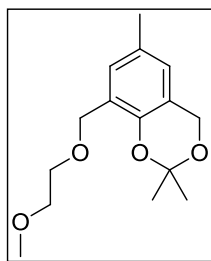


The procedure was followed as described by Clark for a similar triol.²² 2,2-Dimethoxypropane, **81**, (6.46 mL, 52.5 mmol) and camphorsulfonic acid (0.35 g, 1.5 mmol) were added to a solution of 2,6-bis(hydroxymethyl)-4-methylphenol, **57**, (2.5 g, 15.0 mmol) in acetone (15 mL) under nitrogen. The mixture was stirred for 30 mins at room temperature, water (15 mL) was added and then the product was extracted with ethyl acetate (3 x 20 mL). The organic layers were combined, washed with brine (50 mL), dried over MgSO₄, filtered, and the solvent removed *in vacuo*. The crude material was stirred with acetic acid/water (15 mL/15 mL) for 3.5 h. The mixture was then dissolved with ethyl acetate (50 mL) and washed with saturated aqueous NaHCO₃ solution until no effervescence was observed. The organic layer was washed with water (2 x 20 mL), brine (50 mL), dried over MgSO₄, filtered and the solvent removed *in vacuo*, to afford **82** as a white solid, which was sufficiently pure to use without further purification (1.97 g, 64%). m.p. 56-58 °C; (Found: C, 69.05; H, 7.76%. C₁₂H₁₆O₃ requires C, 69.21; H, 7.74%); $\nu_{\max}/\text{cm}^{-1}$ (KBr): 3462 (OH), 2999 (CH), 2947 (CH), 1475 (ring stretch), 1381 (CH₃), 1247 (COC), 1078 (C-O); δ_{H} (400 MHz): 1.55 (6H, s, 2 x OCCH₃), 2.26 (3H, s, Ar-CH₃), 4.62 (2H, d, *J* 6.4, CH₂OH), 4.82 (2H, s, CH₂OC), 6.73 (1H, finely split s, ArH), 6.97 (1H, finely split s, ArH). Spectral characteristics were in agreement with those previously reported.²¹

Single crystals of **82** were grown from CH₂Cl₂. Crystal data: C₁₂H₁₆O₃, *M* = 208.25, monoclinic, space group *P*2₁/*c*, *a* = 8.894(4), *b* = 16.220(8), *c* = 7.742(3) Å, β = 90.214(14)°, *V* = 1116.9(9) Å³, *Z* = 4, *D_c* = 1.238 g cm⁻³, *F*(000) = 448, Mo K α radiation, λ = 0.71073 Å, *T* = 300(2) K, $2\theta_{\max}$ = 25.01°, μ = 0.088 mm⁻¹, 7217 reflections collected, 1944 unique (*R*_{int} = 0.0427). Final GooF = 1.062, *R*₁ = 0.0462, *wR*₂ = 0.1222 (obs. data: *I* > 2 σ (*I*)); *R*₁ = 0.0852, *wR*₂ = 0.1646 (all data).

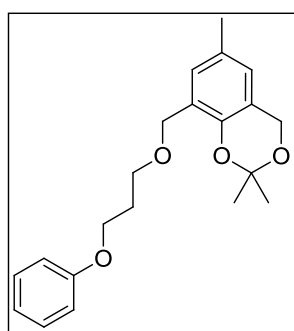
The following compounds (**77-80**) were prepared according to a modified version of Singh's procedure.²³

8-[(2-Methoxyethoxy)methyl]-2,2,6-trimethyl-4H-benzo[d][1,3]-dioxine (**77**)



The acetal **82** (1.76 g, 8.46 mmol) was added to a suspension of sodium hydride (60% dispersed in mineral oil, 1.50 g, 37.5 mmol), in THF (30 mL) and the reaction mixture was heated under reflux for 3 h, while stirring under nitrogen. The mixture was then cooled to room temperature and 2-bromoethyl methyl ether, **58**, (2.49 mL, 25.4 mmol) in THF (5 mL) was added dropwise over 5 mins to the vessel contents. The resulting mixture was further heated under reflux for 12 h. After completion of the reaction (TLC), the mixture was brought to room temperature and quenched with cold water (30 mL). It was then saturated with sodium chloride after which two layers formed. The layers were then separated and the aqueous layer was extracted with ethyl acetate (3 x 25 mL). The combined organic extracts were washed with brine (2 x 10 mL), dried over MgSO₄, filtered and the solvent removed *in vacuo*, to give **77**, as a dark orange oil, which was sufficiently pure to use without further purification (2.17 g, 96%). $\nu_{\max}/\text{cm}^{-1}$ (film): 2925 (CH), 2859 (CH), 1482 (ring stretch), 1135 (COC); δ_{H} (300 MHz): 1.52 (6H, s, 2 x OCCH₃), 2.26 (3H, s, ArCH₃), 3.41 (3H, s, OCH₃), 3.56-3.61, 3.63-3.68 (2 x 2H, 2 x m, OCH₂CH₂O), 4.54, 4.81 (2 x 2H, 2 x s, 2 x C₆H₂CH₂O), 6.69 (1H, s, ArH), 7.09 (1H, s, ArH); δ_{C} (75 MHz): 20.7 (CH₃, ArCH₃), 22.7 (CH₃, 2 x OCCH₃), 59.1 (CH₃, CH₂OCH₃), 61.0, 67.1, 69.5, 72.0 (4 x CH₂, 4 x CH₂O), 99.4 [C, C(CH₃)₂], 118.7 (C, quaternary aromatic C), 124.1 (CH, aromatic CH), 125.9 (C, quaternary aromatic C), 128.3 (CH, aromatic CH), 129.2 (C, quaternary aromatic C), 146.6 (C, quaternary aromatic C).

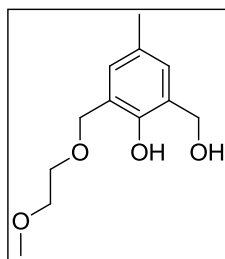
2,2,6-Trimethyl-8-[(3-phenoxypropoxy)methyl]-4H-benzo[d][1,3]dioxine (**78**)



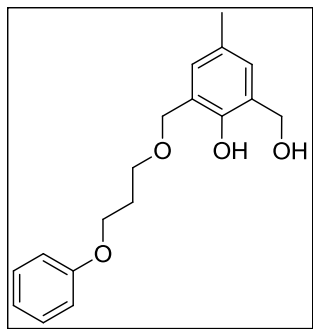
The acetal **82** (2.00 g, 9.61 mmol) was added to a suspension of sodium hydride (60% dispersed in mineral oil, 1.70 g, 42.6 mmol) in THF (60 mL) and the reaction mixture was heated under reflux for 4 h under nitrogen. 3-Phenoxypropyl bromide, **76**, (4.54 mL, 28.8 mmol) in THF (10 mL) was then added dropwise over 5 mins and the reaction mixture was heated under reflux for an additional 12 h. After completion of the reaction (TLC), the mixture was brought to room temperature and quenched with cold water (30 mL). It was then saturated with sodium chloride after which two layers were formed. The layers were separated and the aqueous layer was

extracted with ethyl acetate (3 x 25 mL). The combined organic extracts were washed with brine (2 x 10 mL), dried over MgSO₄, filtered and the solvent was removed *in vacuo*. The crude product was purified by column chromatography using hexane:ethyl acetate (19:1) as eluent, and the acetal **78**, was obtained as a clear viscous oil (1.03 g, 31%). (Found: C, 73.17; H, 7.56%. C₂₁H₂₆O₄ requires C, 73.66; H, 7.65%); $\nu_{\max}/\text{cm}^{-1}$ (film): 2941 (CH), 2863 (CH), 1601 (ring stretch), 1482 (ring stretch), 1246 (COC), 1135 (COC); δ_{H} (300 MHz): 1.50 (6H, s, 2 x CCH₃), 2.04-2.14 (2H, m, OCH₂CH₂CH₂OAr), 2.23 (3H, s, ArCH₃), 3.69 (2H, t, *J* 6.2, OCH₂CH₂), 4.09 (2H, t, *J* 6.3, OCH₂CH₂), 4.49, 4.79 (2 x 2H, 2 x s, 2 x C₆H₂CH₂O), 6.68 (1H, s, ArH), 6.88-6.96 (3H, m, ArH), 7.05 (1H, s, ArH), 7.22-7.30 (2H, m, ArH); δ_{C} (75 MHz): 20.6 (CH₃, ArCH₃), 24.8 (CH₃, 2 x CCH₃), 29.8 (CH₂, ArOCH₂CH₂CH₂O), 61.0, 64.9, 66.9, 67.0 (4 x CH₂, 4 x CH₂O), 99.4 [C, C(CH₃)₂], 114.5 (CH, 2 x aromatic CH), 118.8 (C, quaternary aromatic C), 120.6 (CH, aromatic CH), 124.0 (CH, aromatic CH), 126.2 (C, quaternary aromatic C), 128.0 (CH, aromatic CH), 129.2 (C, quaternary aromatic C), 129.4 (CH, 2 x aromatic CH), 146.6 (C, quaternary aromatic C), 159.1 (C, quaternary aromatic C).

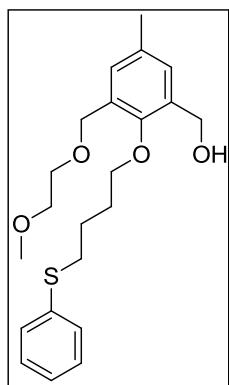
2-(Hydroxymethyl)-6-[(2-methoxyethoxy)methyl]-4-methylphenol (**79**)



Aqueous HCl (1 M, 10 mL) was added to a solution of the acetal, **77** (0.35 g, 1.32 mmol) in THF (10 mL) and the reaction mixture was stirred for 12 h at room temperature. The organic solvent was then removed *in vacuo*. The aqueous solution was extracted with ethyl acetate (3 x 20 mL). The combined organic layers were washed with saturated NaHCO₃ solution (2 x 10 mL), brine (2 x 10 mL) and dried over MgSO₄, filtered and the solvent removed *in vacuo*, to give **79**, as an orange oil, which was sufficiently pure to use without further purification (0.25 g, 85%). $\nu_{\max}/\text{cm}^{-1}$ (film): 3365 (OH), 2923 (CH), 1484 (ring stretch), 1084 (C-O); δ_{H} (300 MHz): 2.24 (3H, s, Ar-CH₃), 2.51 (1H, bs, OH), 3.43 (3H, s, OCH₃), 3.57-3.62, 3.69-3.74 (2 x 2H, 2 x m, 2 x OCH₂CH₂), 4.69, 4.70 (2 x 2H, 2 x s, 2 x C₆H₂CH₂), 6.83 (1H, s, ArH), 6.98 (1H, s, ArH), 7.78 (1H, s, OH); δ_{C} (75 MHz): 20.4 (CH₃, Ar-CH₃), 29.7 (CH₂, CH₂OH), 59.0 (CH₃, CH₂OCH₃), 62.5, 69.4, 71.5 (3 x CH₂, 3 x CH₂O), 122.7 (C, quaternary aromatic C), 127.2 (C, quaternary aromatic C), 128.7 (CH, aromatic CH), 128.8 (C, quaternary aromatic C), 129.0 (CH, aromatic CH), 152.1 (C, quaternary aromatic C); *m/z* (ESI) 225.1 [(M-H)⁻]; HRMS (ESI): exact mass calculated for C₁₂H₁₇O₄ [(M-H)⁻], 225.1127. Found 225.1128.

2-(Hydroxymethyl)-4-methyl-6-[(3-phenoxypropoxy)methyl]phenol (80)

Aqueous HCl (1 M, 10 mL) was added to a solution of the acetal, **78** (0.95 g, 2.77 mmol) in THF (10 mL) and the reaction mixture was stirred for 12 h at room temperature under nitrogen. The organic solvent was removed *in vacuo*. The aqueous solution was extracted with ethyl acetate (3 x 20 mL). The combined organic layers were washed with saturated NaHCO₃ solution (2 x 10 mL), brine (2 x 10 mL), dried over MgSO₄, filtered and the solvent removed *in vacuo*, to give **80**, as an orange oil which was sufficiently pure to use without further purification (0.47 g, 56%). $\nu_{\max}/\text{cm}^{-1}$ (film): 3349 (OH), 2928 (CH), 2873 (CH), 1600 (ring stretch), 1487 (ring stretch), 1244 (COC), 1082 (C-O); δ_{H} (300 MHz): 2.07-2.17 (2H, m, OCH₂CH₂CH₂O), 2.24 (3H, s, ArCH₃), 3.75 (2H, t, *J* 6.2, OCH₂CH₂), 4.08 (2H, t, *J* 6.0, OCH₂CH₂), 4.675 (2H, s, C₆H₂CH₂OCH₂), 4.678 (2H, d, *J* 6.0, C₆H₂CH₂OH), 6.82 (1H, s, ArH), 6.87-6.98 (4H, m, ArH), 7.24-7.32 (2H, m, ArH), 7.76 (1H, s, OH); δ_{C} (75 MHz): 20.4 (CH₃, ArCH₃), 29.5 (CH₂, ArOCH₂CH₂CH₂O), 62.7, 64.6, 67.7, 71.8 (4 x CH₂, 4 x CH₂O), 114.5 (CH, 2 x aromatic CH), 120.8 (CH, aromatic CH), 122.4 (C, quaternary aromatic C), 127.2 (C, quaternary aromatic C), 128.3 (CH, aromatic CH), 128.9 (C, quaternary aromatic C), 129.0 (CH, aromatic CH), 129.5 (CH, 2 x aromatic CH), 152.1 (C, quaternary aromatic C), 158.8 (C, quaternary aromatic C).

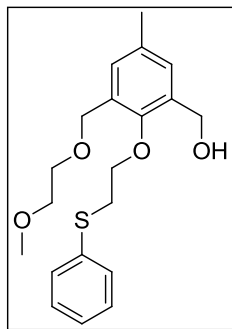
3-[(2-Methoxyethoxy)methyl]-5-methyl-2-[4-(phenylthio)butoxy]phenyl-methanol (84)

2-(Hydroxymethyl)-6-[(2-methoxyethoxy)methyl]-4-methylphenol, **79**, (0.30 g, 1.33 mmol) was added to acetonitrile (10 mL) and stirred at room temperature under nitrogen until fully dissolved. Anhydrous potassium carbonate (0.18 g, 1.33 mmol) was then added and the reaction mixture was stirred for 5 mins at room temperature. (4-Iodobutyl)(phenyl)sulfide, **70**, (0.78 g, estimated as 2.65 mmol) [which consisted of a mixture of **67** (~53%) and **70** (~47%)], was added dropwise by syringe over 5 mins. The reaction mixture was stirred under reflux for 24 h and the reaction progress monitored by TLC. The reaction mixture was then cooled to room temperature and CH₂Cl₂ was added (20 mL). The mixture was then washed with water (3 x 20 mL), brine (15 mL), dried over MgSO₄, filtered and the solvent was removed *in vacuo*. Purification by column chromatography using ethyl acetate/hexane (1:4) as eluent, yielded the title compound **84** as an orange oil (0.30 g, 59%). $\nu_{\max}/\text{cm}^{-1}$ (film): 3445 (OH), 2925

(CH), 2865 (CH), 1481 (ring stretch), 1439 (CH₃), 1093 (C-O); δ_{H} (300 MHz): 1.80-2.00 (4H, m, CH₂CH₂CH₂S), 2.30 (3H, s, Ar-CH₃), 3.01 (2H, t, J 7.1, CH₂S), 3.37 (3H, s, OCH₃), 3.53-3.58, 3.61-3.66 (2 x 2H, 2 x m, OCH₂CH₂O), 3.87 (2H, t, J 6.2, C₆H₂OCH₂), 4.54 (2H, s, C₆H₂CH₂OCH₂), 4.65 (2H, d, J 6.0, C₆H₂CH₂OH), 7.10 (1H, s, ArH), 7.14-7.21 (2H, m, ArH), 7.25-7.38 (4H, m, ArH); δ_{C} (75 MHz): 20.8 (CH₃, Ar-CH₃), 25.8, 29.5, 33.6 (3 x CH₂, CH₂CH₂CH₂S), 59.1 (CH₃, OCH₃), 61.3, 68.1, 69.6, 72.0, 74.7 (5 x CH₂, 5 x CH₂O), 126.0 (CH, aromatic CH), 128.9 (CH, aromatic CH), 129.2 (CH, aromatic CH), 129.5 (CH, aromatic CH), 130.4 (CH, aromatic CH), 131.0 (C, quaternary aromatic C), 133.6 (C, quaternary aromatic C), 133.9 (C, quaternary aromatic C), 136.5 (C, quaternary aromatic C), 153.2 (C, quaternary aromatic C); m/z (ESI) 389.3 [(M-H)⁻]; HRMS (ESI): exact mass calculated for C₂₂H₂₉O₄S [(M-H)⁻], 389.1787. Found 389.1777.

3-[(2-Methoxyethoxy)methyl]-5-methyl-2-[2-(phenylthio)ethoxy]phenylmethanol (**83**)

2-(Hydroxymethyl)-6-[(2-methoxyethoxy)methyl]-4-methylphenol, **79**, (1.08 g, 4.77 mmol)

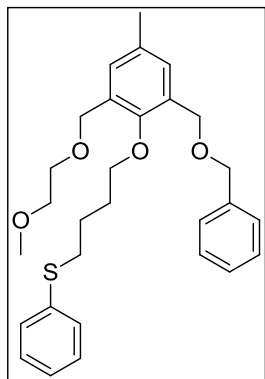


was added to acetonitrile (20 mL) and stirred at room temperature under nitrogen until fully dissolved. Anhydrous potassium carbonate (0.66 g, 4.77 mmol) was then added and the reaction mixture was stirred for 5 mins at room temperature. (2-Iodoethyl)(phenyl)sulfide, **69**, (2.52 g, estimated as 9.55 mmol) [which consisted of a mixture of (2-chloroethyl)(phenyl)sulfide (~33%) and **69** (~67%)], was added

dropwise by syringe over 5 mins. The reaction mixture was stirred under reflux for 24 h and the reaction progress monitored by TLC. The reaction mixture was cooled to room temperature and CH₂Cl₂ was added (20 mL). The mixture was then washed with water (3 x 20 mL) and brine (15 mL). The organic layer was dried over MgSO₄, filtered and the solvent was removed *in vacuo*. The crude product which consisted of a complex mixture was purified by column chromatography using ethyl acetate/hexane (1:1) as eluent, and **83** was obtained as an orange oil (0.24 g, 14%). $\nu_{\text{max}}/\text{cm}^{-1}$ (film): 3410 (OH), 2876 (CH₂), 1584 (ring stretch), 1481 (ring stretch), 1355 (CH₃), 1287 (CO), 1210 (COC), 1088 (CO), 1006 (ring stretch); δ_{H} (300 MHz): 1.65 (1H, bs, OH), 2.29 (3H, s, ArCH₃), 3.33 (2H, t, J 6.5, CH₂S), 3.37 (3H, s, OCH₃), 3.51-3.56, 3.59-3.64 (2 x 2H, 2 x m, OCH₂CH₂O), 4.08 (2H, t, J 6.5, OCH₂CH₂S), 4.55 (2H, s, C₆H₂CH₂OCH₂), 4.63 (2H, d, J 5.7 Hz, C₆H₂CH₂OH), 7.08 (1H, finely split s, ArH), 7.16 (1H, finely split s, ArH), 7.18-7.23 (1H, m, ArH), 7.25-7.33 (2H, m, ArH), 7.37-7.44 (2H, m, ArH); δ_{C} (75 MHz): 20.8 (CH₃, Ar-CH₃), 33.9 (CH₂, CH₂S), 59.1 (CH₃, OCH₃), 61.4, 68.2, 69.6, 71.9, 73.0 (5 x CH₂, 5 x CH₂O), 126.4 (CH, aromatic

CH), 129.1 (2 x CH, aromatic CH), 129.5 (2 x CH, aromatic CH), 129.8 (CH, aromatic CH), 130.6 (CH, aromatic CH), 131.0 (C, quaternary aromatic C), 133.7 (C, quaternary aromatic C), 134.2 (C, quaternary aromatic C), 135.6 (C, quaternary aromatic C), 153.0 (C, quaternary aromatic C); m/z (ESI) 363.1 [(M+H)⁺]; HRMS (ESI): exact mass calculated for C₂₀H₂₇O₄S [(M+H)⁺], 363.1630. Found 363.1622.

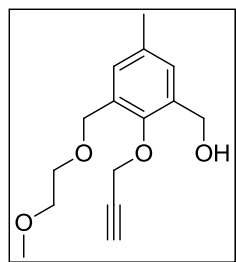
4-[2-(Benzyloxy)methyl]-6-[(2-methoxyethoxy)methyl-4-methylphenoxy]butyl (phenyl)sulfane (**85**)



The alcohol **84** (0.10 g, 0.26 mmol) was added to a suspension of sodium hydride (60% dispersed in mineral oil, 0.05 g, 1.13 mmol) in dry THF (5 mL) under nitrogen. The reaction mixture was heated under reflux for 3 h after which benzyl bromide, **65**, (0.09 mL, 0.77 mmol) in THF (2 mL) was added dropwise to the reaction mixture over 5 mins. The mixture was heated under reflux for a further 12 h. After completion of the reaction (TLC), the mixture was brought to room temperature and quenched with cold water (10 mL). It was then saturated with sodium chloride after which two layers were formed. The layers were separated and the aqueous layer was extracted with ethyl acetate (3 x 10 mL). The combined organic extracts were washed with brine (2 x 5 mL), dried over MgSO₄, filtered and the solvent was removed *in vacuo*. Purification by column chromatography using ethyl acetate/hexane (1:4) as eluent, afforded the trisubstituted compound **85**, as an orange oil (0.03 g, 26%). $\nu_{\max}/\text{cm}^{-1}$ (film): 2920 (CH), 2868 (CH), 1481 (ring stretch), 1094 (COC), 738 (C-S); δ_{H} (300 MHz): 1.73-1.92 (4H, m, CH₂CH₂CH₂S), 2.30 (3H, s, Ar-CH₃), 2.97 (2H, t, *J* 7.1, CH₂S), 3.37 (3H, s, OCH₃), 3.52-3.57, 3.60-3.65 (2 x 2H, 2 x m, OCH₂CH₂O), 3.79 (2H, t, *J* 6.2, C₆H₂OCH₂), 4.52, 4.54, 4.59 (3 x 2H, 3 x s, 3 x ArCH₂O), 7.14-7.20 (3H, m, ArH), 7.24-7.38 (9H, m, ArH); δ_{C} (75 MHz): 20.9 (CH₃, Ar-CH₃), 25.9, 29.4, 33.6 (3 x CH₂, CH₂CH₂CH₂S), 59.1 (CH₃, OCH₃), 67.1, 68.2, 69.6, 72.0, 72.6, 74.8 (6 x CH₂, 6 x CH₂O), 125.9 (CH, aromatic CH), 127.7 (CH, aromatic CH), 127.9 (CH, aromatic CH), 128.4 (CH, aromatic CH), 128.9 (CH, aromatic CH), 129.1 (CH, aromatic CH), 130.3 (CH, aromatic CH), 130.4 (CH, aromatic CH), 130.9 (C, quaternary aromatic C), 130.9 (C, quaternary aromatic C), 133.6 (C, quaternary aromatic C), 136.7 (C, quaternary aromatic C), 138.3 (C, quaternary aromatic C), 153.5 (C, quaternary aromatic C); m/z (ESI) 479.3 [(M-H)⁻]; HRMS (ESI): exact mass calculated for C₂₉H₃₇O₄S [(M+H)⁺], 481.2413. Found 481.2424.

5.3.4. Synthetic Strategy III

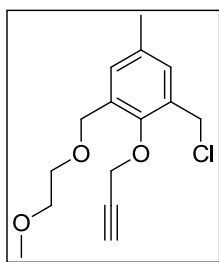
3-[(2-Methoxyethoxy)methyl]-5-methyl-2-(prop-2-yn-1-yloxy)phenylmethanol (**86**)



This compound was synthesised using a modified version of the Amato procedure.²⁴ A stirred mixture of 2-(hydroxymethyl)-6-[(2-methoxyethoxy)methyl]-4-methylphenol, **79**, (0.20 g, 0.88 mmol), propargyl bromide, **10** (0.20 mL, 1.77 mmol, 80% in toluene) and anhydrous potassium carbonate (0.12 g, 0.88 mmol) in acetonitrile (3 mL) was heated under reflux for 1.5 h. After evaporation of the solvent, the residue was partitioned between aqueous HCl (0.1 M, 10 mL) and CH₂Cl₂ (15 mL). The organic layer was washed with water (15 mL), dried over MgSO₄, filtered and the solvent was removed *in vacuo*. Purification by column chromatography using diethyl ether/ethyl acetate (5:1) as eluent, gave **86**, as a white solid (0.14 g, 60%); m.p. 59-61 °C; (Found: C, 67.94; H, 7.60%. C₁₅H₂₀O₄ requires C, 68.16; H, 7.63%); $\nu_{\max}/\text{cm}^{-1}$ (KBr): 3240 ($\equiv\text{C-H}$), 2119 (C \equiv C), 1462 (CH₃), 1353 (CH₃), 1205 (C-O), 1096 (C-O); δ_{H} (300 MHz): 2.31 (3H, s, Ar-CH₃), 2.55 (1H, t, *J* 2.4, C \equiv C-H), 3.39 (3H, s, OCH₃), 3.55-3.61, 3.64-3.70 (2 x 2H, 2 x m, OCH₂CH₂O), 4.59 (2H, s, C₆H₂CH₂), 4.67 (2H, d, *J* 2.4, CH₂C \equiv CH), 4.74 (2H, s, C₆H₂CH₂), 7.15 (1H, s, ArH), 7.18 (1H, s, ArH); δ_{C} (75 MHz): 20.8 (CH₃, Ar-CH₃), 59.0 (CH₃, OCH₃), 61.2, 62.6, 68.5, 69.6, 71.9 (5 x CH₂, 5 x OCH₂), 75.6 (CH, C \equiv CH), 79.3 (C, C \equiv CH), 130.0 (CH, aromatic CH), 130.9 (CH, aromatic CH), 131.1 (C, quaternary aromatic C), 134.1 (C, quaternary aromatic C), 134.6 (C, quaternary aromatic C), 152.7 (C, quaternary aromatic C); NMR spectral assignment was aided by HSQC 2D NMR experiment; *m/z* (ESI) 287.4 [(M+Na+H)⁺]; HRMS (ESI): exact mass calculated for C₁₅H₂₀O₄Na [(M+Na+H)⁺], 287.1259. Found 287.1251.

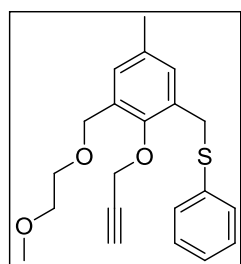
Single crystals of **86** were grown from CH₂Cl₂. Crystal data: C₁₅H₂₀O₄, *M* = 264.31, monoclinic, space group *P*2₁/*c*, *a* = 8.5342(16) Å, *b* = 38.781(7) Å, *c* = 4.6175(9) Å, β = 104.966(4)°, *V* = 1476.4(5) Å³, *Z* = 4, *D*_c = 1.189 g cm⁻³, *F*(000) = 568, Mo K α radiation, λ = 0.71073 Å, *T* = 296.(2) K, $2\theta_{\max}$ = 25.61°, μ = 0.085 mm⁻¹, 14677 reflections collected, 2755 unique (*R*_{int} = 0.0567). Final GooF = 1.041, *R*₁ = 0.0506, *wR*₂ = 0.1182 (obs. data: *I* > 2 σ (*I*)); *R*₁ = 0.1367, *wR*₂ = 0.1498 (all data).

1-(Chloromethyl)-3-[(2-methoxyethoxy)methyl]-5-methyl-2-(prop-2-yn-1-yloxy)benzene (87)



This compound was synthesised using a modified version of the Amato procedure.²⁴ A solution of thionyl chloride (0.28 mL, 3.86 mmol) in CH₂Cl₂ (5 mL) was added dropwise over a period of 10 mins to a solution of the alcohol, **86**, (0.40 g, 1.53 mmol) in CH₂Cl₂ (15 mL) under nitrogen. The mixture was stirred at room temperature for 12 h. After removal of most of the solvent, toluene (5 mL) was added and the mixture was concentrated *in vacuo* to dryness. Brine (15 mL) was added to the oily residue and the product was extracted with CH₂Cl₂ (3 x 15 mL), dried over MgSO₄, filtered and the solvent was removed *in vacuo*. Purification by column chromatography using diethyl ether as eluent, gave **87**, as a pale yellow oil (0.24 g, 55%). $\nu_{\max}/\text{cm}^{-1}$ (film): 3290 ($\equiv\text{C-H}$), 2924 (CH), 2123 (C \equiv C), 1476 (ring stretch), 1140 (COC), 1094 (COC); δ_{H} (400 MHz): 2.31 (3H, s, Ar-CH₃), 2.56 (1H, t, J 2.0, C \equiv C-H), 3.39 (3H, s, OCH₃), 3.56-3.61, 3.66-3.71 (2 x 2H, 2 x m, OCH₂CH₂), 4.59, 4.69 (2 x 2H, 2 x s, 2 x C₆H₂CH₂), 4.70 (2H, d, J 2.4, CH₂C \equiv CH), 7.19 (1H, s, ArH), 7.21 (1H, s, ArH); δ_{C} (75 MHz): 20.8 (CH₃, Ar-CH₃), 41.3 (CH₂, CH₂Cl), 59.0 (CH₃, OCH₃), 62.8, 68.4, 69.7, 71.9 (4 x CH₂, 4 x OCH₂), 75.8 (CH, C \equiv CH), 79.0 (C, C \equiv CH), 131.1 (C, quaternary aromatic C), 131.3 (CH, aromatic CH), 131.6 (C, quaternary aromatic C), 131.8 (CH, aromatic CH), 134.8 (C, quaternary aromatic C), 152.7 (C, quaternary aromatic C); m/z (ESI) 283.3 [(M+H)⁺]; HRMS (ESI): exact mass calculated for C₁₅H₂₀O₃Cl [(M+H)⁺], 283.1101. Found 283.1080.

3-[(2-Methoxyethoxy)methyl]-5-methyl-2-(prop-2-yn-1-yloxy)benzylphenylsulfane (88)

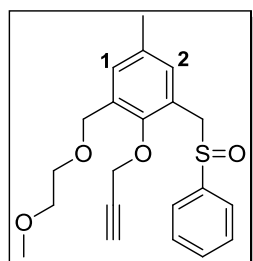


This compound was synthesised using a procedure similar to Cronin.²⁵ Freshly cut sodium (0.02 g, 0.65 mmol) was cautiously added portionwise over 15 min to dry ethanol (4 mL) while stirring under nitrogen. When the sodium had dissolved completely, the solution was cooled to room temperature and a solution of thiophenol, **4**, (0.07 mL, 0.65 mmol) in dry ethanol (0.2 mL) was added dropwise over 15 min. Stirring was continued for 30 min, then a solution of the chloride **87**, (0.17 g, 0.65 mmol) in dry ethanol (1 mL) was added dropwise over 10 mins. The reaction mixture was heated to 50 °C with stirring for 16 h after which time the cloudy solution was cooled to room temperature and the ethanol removed *in vacuo*. The residual oil was diluted with ethyl acetate (20 mL), washed with water (3 x 10 mL), dried over MgSO₄ and concentrated *in vacuo*. Purification by column chromatography using CH₂Cl₂/ethyl acetate (19:1) as eluent, yielded the sulfide **88**, as a pale

orange oil (0.07 g, 32%), which consisted of a mixture of the chloride **87** (~15%) and the desired product **88** (~85%) as determined by ^1H and ^{13}C NMR. $\nu_{\text{max}}/\text{cm}^{-1}$ (film): 3288 ($\equiv\text{C-H}$), 2922 (CH), 2874 (CH), 2123 ($\text{C}\equiv\text{C}$), 1480 (ring stretch), 1439 (CH_3), 1203 (COC), 1134 (COC), 740 (CS); δ_{H} (400 MHz): 2.16 (3H, s, ArCH_3), 2.46 (1H, t, J 2.4, $\text{C}\equiv\text{C-H}$), 3.31 (3H, s, OCH_3), 3.48-3.52, 3.58-3.62 (2 x 2H, 2 x m, OCH_2CH_2), 4.12, 4.51 (2 x 2H, 2 x s, 2 x $\text{C}_6\text{H}_2\text{CH}_2$), 4.60 (2H, d, J 2.4, $\text{CH}_2\text{C}\equiv\text{CH}$), 6.94 (1H, s, ArH), 7.05 (1H, s, ArH), 7.08-7.15 (1H, m, ArH), 7.16-7.23 (2H, m, ArH), 7.28 (2H, d, J 8.0, ArH); δ_{C} (75 MHz): 20.8 (CH_3 , ArCH_3), 33.5 (CH_2 , CH_2S), 59.0 (CH_3 , OCH_3), 62.7, 68.6, 69.7, 71.9 (4 x CH_2 , 4 x CH_2O), 75.6 (CH, $\text{C}\equiv\text{CH}$), 79.3 (C, $\text{C}\equiv\text{CH}$), 126.4 (CH, aromatic CH), 128.9 (2 x CH, aromatic CH), 129.9 (2 x CH, aromatic CH), 130.4 (CH, aromatic CH), 130.5 (C, quaternary aromatic C), 131.2 (CH, aromatic CH), 131.3 (C, quaternary aromatic C), 134.3 (C, quaternary aromatic C), 136.6 (C, quaternary aromatic C), 152.8 (C, quaternary aromatic C); m/z (ESI) 281.3, 357.4 $[(\text{M}+\text{H})^+]$; 281.3 $[(\text{M}+\text{H})^+]$ identified as $\text{C}_{15}\text{H}_{20}\text{O}_3\text{S}$; HRMS (ESI): exact mass calculated for $\text{C}_{21}\text{H}_{25}\text{O}_3\text{S}$ $[(\text{M}+\text{H})^+]$, 357.1524. Found 357.1519.

* δ_{C} signals observed for **87** were identical to those as described earlier, including the characteristic signal of the chloride at δ_{C} 41.3.

1-(2-Methoxyethoxy)methyl-5-methyl-3-(phenylsulfinyl)methyl-2-(prop-2-yn-1-yloxy)benzene (**89**)

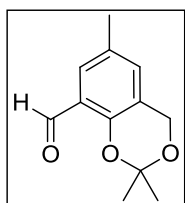


A solution of sodium periodate (0.04 g, 0.17 mmol) in water (3 mL) was added over 5 mins to a stirred solution of the sulfide, **88** (~85% pure), (0.03 g, estimated as 0.08 mmol) in methanol (3 mL) cooled to 0 °C. The reaction mixture was stirred for 12 h at room temperature and then concentrated *in vacuo*. The residue was partitioned between CH_2Cl_2 (10 mL) and water (10 mL). The layers were separated and the aqueous layer further extracted with CH_2Cl_2 (2 x 10 mL). The combined organic layers were washed with water (2 x 10 mL), brine (10 mL), dried over MgSO_4 and the solvent removed *in vacuo*. Purification of the residue by column chromatography, using the eluent hexane/ethyl acetate (3:2) yielded the title sulfoxide **89**, as a clear oil (0.025 g, 80%); (Found: C, 67.04; H, 6.41%. $\text{C}_{21}\text{H}_{24}\text{O}_4\text{S}$ requires C, 67.72; H, 6.49%); $\nu_{\text{max}}/\text{cm}^{-1}$ (film): 3237 ($\equiv\text{C-H}$), 2876 (CH), 2116 ($\text{C}\equiv\text{C}$), 1475 (ring stretch), 1086 (COC), 1045 (S=O); δ_{H} (400 MHz): 2.24 (3H, s, Ar-CH_3), 2.56 (1H, t, J 2.4, $\text{C}\equiv\text{C-H}$), 3.39 (3H, s, OCH_3), 3.56-3.60 (2H, m, CH_2OCH_3), 3.64-3.68 (2H, m, $\text{C}_6\text{H}_2\text{CH}_2\text{OCH}_2$), 4.12 (1H, A of ABq, J 12.4, CH_2SO), 4.16 (1H, B of ABq, J 12.4, CH_2SO), 4.55 (2H, s, $\text{C}_6\text{H}_2\text{CH}_2\text{O}$), 4.59 (1H, A of finely split ABq, J 15.6, 2.4, $\text{CH}_2\text{C}\equiv\text{CH}$),

4.65 (1H, B of finely split ABq, J 15.6, 2.4, $\text{CH}_2\text{C}\equiv\text{CH}$), 6.82 [1H, s, C_6H_2 (**1**)], 7.19 [1H, s, C_6H_2 (**2**)], 7.45-7.50 (3H, m, ArH), 7.53-7.57 (2H, m, ArH); δ_{C} (75 MHz): 20.7 (CH_3 , Ar- CH_3), 59.0 (CH_3 , OCH_3), 59.5 (CH_2 , CH_2SO), 62.9 (CH_2 , $\text{C}_6\text{H}_2\text{OCH}_2$), 68.5 (CH_2 , $\text{C}_6\text{H}_2\text{CH}_2\text{O}$), 69.7 (CH_2 , $\text{C}_6\text{H}_2\text{CH}_2\text{OCH}_2$), 71.9 (CH_2 , CH_2OCH_3), 75.9 (CH , $\text{C}\equiv\text{CH}$), 79.2 (C , $\text{C}\equiv\text{CH}$), 124.1 (C , quaternary aromatic C), 124.4 (2 x CH, aromatic CH), 128.9 (2 x CH, aromatic CH), 131.1 (CH , aromatic CH), 131.2 (C , quaternary aromatic C), 131.8 (CH , aromatic CH), 132.4 (CH , aromatic CH), 134.4 (C , quaternary aromatic C), 143.9 (C , quaternary aromatic C), 153.7 (C , quaternary aromatic C); NMR spectral assignment was aided by HMBC and NOESY 2D NMR experiments; m/z (ESI) 373.14 [($\text{M}+\text{H}$)⁺]; HRMS (ESI): exact mass calculated for $\text{C}_{21}\text{H}_{25}\text{O}_4\text{S}$ [($\text{M}+\text{H}$)⁺], 373.1474. Found 373.1464.

5.4. Combination of tertiary amine and aromatic scaffolds

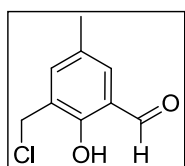
2,2,6-Trimethyl-4*H*-benzo[*d*][1,3]dioxine-8-carbaldehyde (**90**)²⁶



This compound was synthesised using a modified version of the Chirakul procedure.²⁶ Pyridinium chlorochromate (3.11 g, 14.4 mmol) was suspended in CH_2Cl_2 (20 mL). At 0 °C, (2,2,6-trimethyl-4*H*-benzo[1,3]dioxin-8-yl)-methanol, **82**, (2.00 g, 9.61 mmol) was added in one portion to the solution.

The mixture was stirred at room temperature for 2 h, then ether was added (50 mL) and the supernatant was decanted from a black gum. The insoluble residue was washed with ether (3 x 10 mL). The ether extracts were passed through celite[®] and concentrated *in vacuo*. The residue was purified by column chromatography using hexane/ethyl acetate (1:1) as eluent, to afford the aldehyde **90**, as a cream sticky solid (1.65 g, 83%). $\nu_{\text{max}}/\text{cm}^{-1}$ (film): 1683 ($\text{C}=\text{O}$), 1478 (ring stretch), 1133 (COC); δ_{H} (300 MHz): 1.60 (6H, s, 2 x CCH_3), 2.29 (3H, s, Ar- CH_3), 4.86 (2H, s, CH_2), 7.02 (1H, s, ArH), 7.52 (1H, s, ArH), 10.38 (1H, s, CHO). Spectral characteristics were in agreement with those previously reported.²⁶

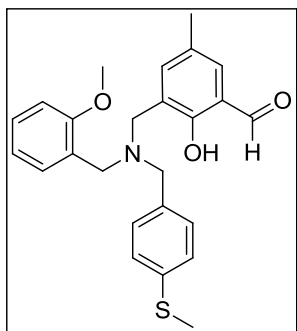
3-(Chloromethyl)-2-hydroxy-5-methylbenzaldehyde (**91**)²⁶



A modified version of the Chirakul procedure was used to prepare this compound.²⁶ The aldehyde **90**, (1.60 g, 7.76 mmol) was added to concentrated HCl (37% w/w, 23 mL) under nitrogen. After 12 h, the product was filtered and washed several times with water. The crude product was recrystallised from hexane and **91**, was obtained as a white solid (1.26 g, 88%). m.p. 93-95 °C (Lit.²⁶ 94-95 °C); $\nu_{\text{max}}/\text{cm}^{-1}$ (KBr): 3183 (OH), 1663 ($\text{C}=\text{O}$), 1600 (ring stretch), 1471 (CH_2), 1257 (CO), 613

(CCl₄); δ_{H} (300 MHz): 2.35 (3H, s, CH₃), 4.67 (2H, s, CH₂Cl), 7.35 (1H, s, ArH), 7.46 (1H, s, ArH), 9.87 (1H, s, CHO). Spectral characteristics were in agreement with those previously reported.²⁶

2-Hydroxy-3-[(2-methoxybenzyl)(4-(methylthio)benzyl)amino]methyl-5-methylbenzaldehyde (**92**)

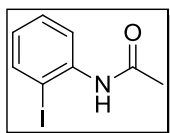


This compound was synthesised using a modified version of the Boudalis procedure.²⁷ The secondary amine **18**, (0.40 g, 1.46 mmol) was dissolved in THF (50 mL) and 3-(chloromethyl)-2-hydroxy-5-methylbenzaldehyde, **91**, (0.86 g, 1.87 mmol) was added to the stirring solution. Triethylamine (0.78 mL, 5.60 mmol) was added dropwise over 5 mins and the formation of a pale yellow precipitate was observed. The mixture was stirred for 12 h, gravity filtered and the solvent removed *in vacuo*, resulting in a yellow oil. Water (20 mL) was then added and the mixture was extracted using CH₂Cl₂ (3 x 20 mL). The combined organic layers were dried over MgSO₄, filtered and the solvent was removed *in vacuo*. Purification by column chromatography using hexane/ethyl acetate (4:1) as eluent, gave the tertiary amine **92**, as a yellow oil (0.44 g, 71%). $\nu_{\text{max}}/\text{cm}^{-1}$ (film): 2920 (CH), 2836 (CH), 1679 (C=O), 1602 (ring stretch), 1494 (ring stretch), 1472 (CH₂), 1247 (COC), 755 (CS); δ_{H} (300 MHz): 2.25, 2.48 (2 x 3H, 2 x s, ArCH₃, SCH₃), 3.60, 3.63, 3.70 (3 x 2H, 3 x s, 3 x NCH₂), 3.81 (3H, s, OCH₃), 6.84-6.96 (2H, m, ArH), 7.14 (1H, s, ArH), 7.24 (6H, s, ArH), 7.40 (1H, s, ArH), 10.35 (1H, s, CHO); δ_{C} (75 MHz): 15.9, 20.3 (2 x CH₃, ArCH₃, SCH₃), 53.0, (CH₂, NCH₂), 55.1 (CH₃, OCH₃), 55.1, 57.8 (2 x CH₂, 2 x NCH₂), 110.6 (CH, aromatic CH), 120.4 (CH, aromatic CH), 122.5 (C, quaternary aromatic C), 124.6 (C, quaternary aromatic C), 125.1 (C, quaternary aromatic C), 126.5 (2 x CH, aromatic CH), 127.7 (CH, aromatic CH), 128.1 (C, quaternary aromatic C), 129.2 (CH, aromatic CH), 130.0 (2 x CH, aromatic CH), 131.3 (CH, aromatic CH), 134.0 (C, quaternary aromatic C), 136.3 (CH, aromatic CH), 137.6 (C, quaternary aromatic C), 158.0 (C, quaternary aromatic C), 159.3 (C, quaternary aromatic C), 191.6 (C, C=O); m/z (ESI) 422.2 [(M+H)⁺]; HRMS (ESI): exact mass calculated for C₂₅H₂₈NOS₂ [(M+S+H)⁺], 422.1612. Found 422.1622.

5.5. Diphenylacetylene Scaffold

5.5.1. Iodoamide precursors

N-(2-Iodophenyl)acetamide (**115**)²⁸



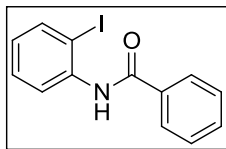
This compound was prepared according to a modified version of the Kotha procedure.²⁸ One drop of concentrated sulfuric acid was added to a stirred solution of 2-iodoaniline, **99**, (1.00 g, 4.57 mmol) in acetic anhydride (5 mL) under nitrogen. The resulting mixture was stirred at room temperature for 30 min, then quenched with water (10 mL) and extracted with CH₂Cl₂ (3 x 20 mL). The combined organic layers were washed with water (20 mL), brine (20 mL) and dried with MgSO₄. The solvent was removed *in vacuo* and the crude product was recrystallised from hexane to give the amide, **115**, as a white crystalline solid (0.71 g, 59%); m.p. 109-110 °C (Lit.²⁹ 109-111 °C); $\nu_{\max}/\text{cm}^{-1}$ (KBr): 3274 (NH), 1660 (C=O), 1531 (NH), 1433 (CH₃), 1294 (CN), 1015 (ring stretch), 751 (CH); δ_{H} (300 MHz): 2.25 (3H, s, CH₃), 6.85 (1H, t, *J* 7.1, ArH), 7.35 (1H, td, *J* 7.2, 1.2 ArH), 7.42 (1H, bs, NH), 7.77 (1H, d, *J* 8.0, ArH), 8.21 (1H, d, *J* 7.8, ArH). Spectral characteristics were in agreement with those previously reported.³⁰

Single crystals of **115** were grown from CH₂Cl₂. Crystal data: C₈H₈INO, *M* = 261.05, orthorhombic, space group *P*2₁2₁2₁, *a* = 4.7545(15) Å, *b* = 6.965(3) Å, *c* = 26.955(9) Å, *V* = 892.6(5) Å³, *Z* = 4, *D*_c = 1.943 g cm⁻³, *F*(000) = 496, Mo K α radiation, λ = 0.71073 Å, *T* = 296.(2) K, $2\theta_{\max}$ = 26.42°, μ = 3.531 mm⁻¹, 7184 reflections collected, 1825 unique (*R*_{int} = 0.0437). Final GooF = 1.006, *R*₁ = 0.0294, *wR*₂ = 0.0533 (obs. data: *I* > 2 σ (*I*)); *R*₁ = 0.0380, *wR*₂ = 0.0562 (all data).

Crystals of **115** were obtained after purification of the Sonogashira product, **131**. Crystal data: C₈H₈INO, *M* = 261.05, triclinic, space group *P*1, *a* = 4.7876(11) Å, *b* = 9.753(2) Å, *c* = 10.905(4) Å, α = 112.792(7)°, β = 92.464(7)°, γ = 103.434(5)°, *V* = 451.5(2) Å³, *Z* = 2, *D*_c = 1.920 g cm⁻³, *F*(000) = 248, Mo K α radiation, λ = 0.71073 Å, *T* = 296.(2) K, $2\theta_{\max}$ = 26.86°, μ = 3.490 mm⁻¹, 4837 reflections collected, 1877 unique (*R*_{int} = 0.0444). Final GooF = 0.989, *R*₁ = 0.0436, *wR*₂ = 0.0973 (obs. data: *I* > 2 σ (*I*)); *R*₁ = 0.0653, *wR*₂ = 0.1062 (all data).

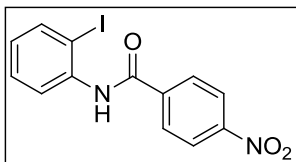
The following iodoamides (**116-119**) were synthesised according to a modified version of the Barbero procedure.³¹

N-(2-Iodophenyl)benzamide (**116**)³¹

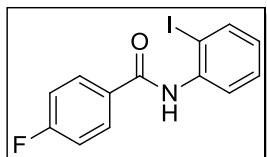


Benzoyl chloride, **111**, (0.29 mL, 2.51 mmol) was added to a solution of 2-iodoaniline, **99**, (0.50 g, 2.28 mmol) in dry THF (5 mL) and the resulting mixture was stirred at room temperature for 12 h under nitrogen. Then ethyl acetate (10 mL) was added and the organic layer was washed with NaHCO₃ (5% aq. sol., 2 x 10 mL), brine (10 mL), HCl (5 % aq. sol., 2 x 10 mL), dried over MgSO₄ and the solvent was removed *in vacuo*. The crude product was recrystallised from hexane which yielded **116**, as a white crystalline solid (0.37 g, 50%); m.p. 132-133 °C (Lit.³² 133-134 °C); $\nu_{\max}/\text{cm}^{-1}$ (KBr): 3216 (NH), 1661 (C=O), 1516 (ring stretch), 1466 (NH), 1299 (CN), 748, 689; δ_{H} (300 MHz): 6.89 (1H, td, *J* 7.7, 1.7, ArH), 7.42 (1H, td, *J* 7.2, 1.4, ArH), 7.51-7.63 (3H, m, ArH), 7.83 (1H, dd *J* 8.1, 1.5, ArH), 7.97-8.00 (2H, m, ArH), 8.30 (1H, bs, NH), 8.47 (1H, dd, *J* 8.1, 1.5, ArH). Spectral characteristics were in agreement with those previously reported.³³

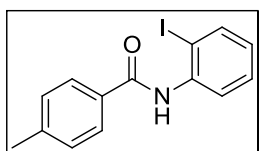
N-(2-Iodophenyl)-4-nitrobenzamide (**117**)³⁴



4-Nitrobenzoyl chloride, **112**, (0.47 g, 2.51 mmol) was added to a solution of 2-iodoaniline, **99**, (0.50 g, 2.28 mmol) in dry THF (5 mL), and the resulting mixture was stirred at room temperature for 12 h under nitrogen. Then ethyl acetate (10 mL) was added and the organic layer was washed with NaHCO₃ (5% aq. sol., 2 x 10 mL), brine (10 mL), HCl (5 % aq. sol., 2 x 10 mL), dried over MgSO₄ and the solvent was removed *in vacuo*. The title compound, **117**, was obtained as a pale purple crystalline solid which was sufficiently pure to use without further purification (0.68 g, 82%); m.p. 147-148 °C (Lit.³⁴ 147-149 °C); $\nu_{\max}/\text{cm}^{-1}$ (KBr): 3281 (NH), 1655 (C=O), 1575 (ring stretch), 1520 (NO₂), 1434 (CN), 1347 (NO₂), 1300 (NO₂), 1015 (ring stretch), 760, 649; δ_{H} (300 MHz): 6.94 (1H, td, *J* 7.7, 1.5, ArH), 7.44 (1H, td, *J* 7.2, 1.2, ArH), 7.85 (1H, dd, *J* 8.0, 1.4, ArH), 8.10-8.17 (2H, m, ArH), 8.35-8.44 (3H, m, ArH). Spectral characteristics were in agreement with those previously reported.³⁴

4-Fluoro-N-(2-iodophenyl)benzamide (118)

4-Fluorobenzoyl chloride, **113**, (0.31 mL, 2.60 mmol) was added to a solution of 2-iodoaniline, **99**, (0.52 g, 2.40 mmol) in dry THF (5.2 mL), and the resulting mixture was stirred at room temperature for 12 h under nitrogen. The reaction mixture was then diluted with ethyl acetate (10 mL) and the organic layer was washed with NaHCO₃ (5% aq. sol., 2 x 10 mL), brine (10 mL), HCl (5 % aq. sol., 2 x 10 mL), dried over MgSO₄ and the solvent was removed *in vacuo*. Purification was achieved by column chromatography using hexane/ethyl acetate (4:1) as eluent to afford the iodoamide **118**, as a white solid (0.49 g, 60%); m.p. 138-139 °C; (Found: C, 45.76; H, 2.74; N, 3.40%. C₁₃H₉FINO requires C, 45.77; H, 2.66; N, 4.11%); $\nu_{\max}/\text{cm}^{-1}$ (KBr): 3198 (NH), 1645 (C=O), 1500 (NH), 1314 (CN); δ_{H} (300 MHz): 6.89 (1H, td, *J* 7.7, 1.7, ArH), 7.18-7.24 (2H, m, ArH), 7.41 (1H, td *J* 7.2, 1.2, ArH), 7.82 (1H, dd, *J* 7.8, 1.4, ArH), 7.95-8.02 (2H, m, ArH), 8.21 (1H, bs, NH), 8.42 (1H, dd *J* 8.1, 1.5, ArH); δ_{C} (75 MHz): 90.3 (C, quaternary aromatic C-I), 116.1 (CH, d, ²*J*_{C-F} 22.0, aromatic CH), 121.8 (CH, aromatic CH), 126.2 (CH, aromatic CH), 129.5 (CH, d, ³*J*_{C-F} 4.2, aromatic CH), 129.7 (CH, aromatic CH), 130.7 (C, quaternary aromatic C), 138.1 (C, quaternary aromatic C), 138.8 (CH, aromatic CH), 164.2 (C, C=O), 165.2 (C, ¹*J*_{C-F} 253.0, aromatic C-F); *m/z* (ESI) 141.3 (identified as C₇H₆NOF), 342.2 [(M+H)⁺]; HRMS (ESI): exact mass calculated for C₁₃H₁₀NOFI [(M+H)⁺], 341.9791. Found 341.9792.

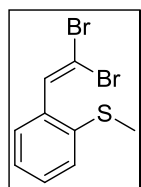
N-(2-Iodophenyl)-4-methylbenzamide (119)

4-Methylbenzoyl chloride, **114**, (0.34 mL, 2.60 mmol) was added to a solution of 2-iodoaniline, **99**, (0.52 g, 2.30 mmol) in dry THF (5.0 mL), and the resulting mixture was stirred at room temperature for 24 h. Then ethyl acetate (10 mL) was added and the organic layer was washed with NaHCO₃ (5% aq. sol., 2 x 10 mL), brine (10 mL), HCl (5 % aq. sol., 2 x 10 mL), dried over MgSO₄ and the solvent was removed *in vacuo*. The iodoamide, **119**, was purified by column chromatography using hexane/ethyl acetate (9:1) as eluent and isolated as a white solid (0.42 g, 54%); m.p. 116-118 °C; $\nu_{\max}/\text{cm}^{-1}$ (KBr): 3268 (NH), 1650 (C=O), 1521 (NH), 1305 (CN), 1016 (ring stretch), 754, 650; δ_{H} (300 MHz): 6.87 (1H, td, *J* 7.7, 1.7, ArH), 7.32 (2H, d, *J* 7.8, ArH), 7.39 (1H, td, *J* 7.2, 1.2, ArH), 7.81 (1H, dd, *J* 7.8, 1.5, ArH), 7.86 (2H, d, *J* 8.4, ArH), 8.26 (1H, bs, NH), 8.46 (1H, dd, *J* 8.3, 1.7, ArH); δ_{C} (75 MHz): 21.5 (CH₃, Ar-CH₃), 90.1 (C, quaternary aromatic C-I), 121.7 (CH, aromatic CH), 125.9 (CH, aromatic CH), 127.2 (CH, 2 x aromatic CH), 129.4 (CH, aromatic CH), 129.6 (CH, 2 x aromatic CH),

131.7 (C, quaternary aromatic C), 138.4 (C, quaternary aromatic C), 138.8 (CH, aromatic CH), 142.8 (C, quaternary aromatic C), 165.3 (C, C=O); m/z (ESI) 100.2, 338.2 [(M+H)⁺]; HRMS (ESI): exact mass calculated for C₁₄H₁₃NOI [(M+H)⁺], 338.0042. Found 338.0043.

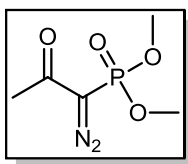
5.5.2. Terminal alkyne precursors

1,1-Dibromo-2-(2-methylthiophenyl)ethene (**122**)¹⁰

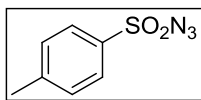


This compound was synthesised using Lehane's procedure.¹⁰ Triphenylphosphine (6.90 g, 26.2 mmol) was added to a well stirred solution of zinc powder (1.71 g, 26.2 mmol) and carbon tetrabromide (6.53 g, 19.7 mmol) in CH₂Cl₂ (40 mL) at 0 °C. The mixture was stirred for 10 mins and then a solution of 2-methylthiobenzaldehyde, **121**, (1.00 g, 6.56 mmol) in CH₂Cl₂ (30 mL) was added. Stirring was continued at 0 °C for 2 h and the reaction mixture was then stirred at room temperature for a further 16 h. Isolation of the crude dibromo-olefin, **122**, was accomplished by addition of hexane (20 mL) to the reaction mixture, filtration to remove insoluble material and concentration of the filtrate *in vacuo*, to give a yellow-brown semi-solid. Purification by column chromatography, using hexane as eluent, afforded the title compound **122**, as a white solid (1.47 g, 73%). m.p. 107-108 °C; $\nu_{\max}/\text{cm}^{-1}$ (KBr): 3060 (=C-H), 2996 (CH), 2913 (CH), 1582 (ring stretch), 1434 (CH₃), 875 (=CH), 738 (C-S), 541 (C-Br); δ_{H} (300 MHz): 2.45 (3H, s, CH₃), 7.18 (1H, td, J 7.4, 1.4, ArH), 7.24-7.36 (2H, m, ArH), 7.48 (1H, d, J 7.5, ArH), 7.54 (1H, s, HC=CBr₂); Spectral characteristics were in agreement with those previously reported, although Lehane had reported **122** as an oil.¹⁰

Single crystals of **122** were grown from CH₂Cl₂. Crystal data: C₉H₈Br₂S, $M = 308.03$, monoclinic, space group $P2_1/n$, $a = 4.133(2)$ Å, $b = 9.547(5)$ Å, $c = 26.270(13)$ Å, $\beta = 93.497(13)^\circ$, $V = 1034.6(9)$ Å³, $Z = 4$, $D_c = 1.978$ g cm⁻³, $F(000) = 592$, Mo K α radiation, $\lambda = 0.71073$ Å, $T = 296(2)$ K, $2\theta_{\max} = 28.15^\circ$, $\mu = 7.981$ mm⁻¹, 23829 reflections collected, 2498 unique ($R_{\text{int}} = 0.1158$). Final GooF = 1.016, $R_1 = 0.0428$, $wR_2 = 0.0934$ (obs. data: $I > 2\sigma(I)$); $R_1 = 0.0894$, $wR_2 = 0.1110$ (all data).

Dimethyl (1-diazo-2-oxopropyl)phosphonate (125)³⁵

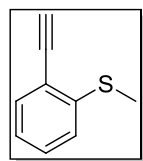
The Bestmann–Ohira reagent was prepared according to literature procedure.³⁵ Dimethyl (2-oxopropyl)phosphonate, **124**, (1.50 g, 9.03 mmol) was added to dry CH₂Cl₂ (15 mL) and cooled to 0 °C (icebath) under nitrogen. Anhydrous potassium carbonate (1.37 g, 9.93 mmol) and then tosyl azide (1.96 g, 9.93 mmol) were added sequentially in single portions and the resulting mixture was stirred at room temperature for 16 h. The mixture was then dissolved with diethyl ether (30 mL) and filtered through celite[®] which was subsequently washed several times with ether. The solvent was eliminated *in vacuo* and the crude product was purified by column chromatography, using ethyl acetate/hexane (7:3) as eluent. The Bestmann–Ohira reagent, **125**, was isolated as a yellow oil (1.36 g, 78%). $\nu_{\max}/\text{cm}^{-1}$ (film): 2960 (CH), 2126 (N≡N), 1661 (C=O), 1271 (P=O), 1025 (P–O–C); δ_{H} (300 MHz): 2.28 (3H, s, CH₃C=O), 3.85 (6H, d, *J* 8.0, 2 x OCH₃); Spectral characteristics were in agreement with those previously reported.³⁶

***p*-Toluenesulfonyl azide (*p*-Tosyl azide) (168)**³⁷

A solution of *p*-toluenesulfonyl chloride (11.22 g, 58.9 mmol) in acetone (30 mL) was added rapidly to a solution of sodium azide (4.21 g, 64.8 mmol) in water (20 mL) and acetone (30 mL) at 0 °C. The reaction mixture was stirred for 2 h and then concentrated *in vacuo*. CH₂Cl₂ (25 mL) was added and the layers separated. The organic layer was washed with water (2 x 25 mL), dried over MgSO₄, filtered, and the solvent removed *in vacuo* to give the azide, **168**, (8.94 g, 77%) as a colourless oil which solidifies upon storage at low temperature.

Note:

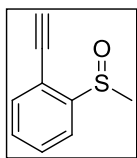
1. As all azides are potentially explosive caution was exercised in their handling. *p*-Tosyl azide, **168**, was stored in the freezer and transferred as an oil due to its high impact sensitivity.
2. Previous researchers^{38,39} have reported recrystallising *p*-toluenesulfonyl chloride before use. Recrystallisation was not conducted in this research with no apparent impact on the use of *p*-tosyl azide, **168**, for diazo transfer.

1-Ethynyl-2-methylthiobenzene (123)¹⁰Method 1:

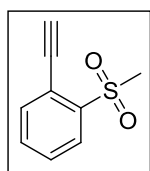
This compound was synthesised using Lehane's procedure.¹⁰ 1,1-Dibromo-2-(2-methylthiophenyl)ethene, **122**, (1.47 g, 4.80 mmol) was dissolved in dry THF (20 mL) and the solution cooled to -78 °C under nitrogen. *N*-Butyl lithium (1.6 M in hexanes, 5.25 mL, 8.40 mmol) was added to the stirred solution. Stirring was continued at -78 °C for 1 h after which time the cooling bath was removed and the reaction mixture stirred at room temperature for 1.5 h. The reaction was quenched with water (20 mL) and extracted with hexane (3 x 20 mL). The combined organic extracts were dried over MgSO₄, filtered, and the solvent was removed *in vacuo*. Purification by column chromatography using hexane/ethyl acetate (9:1) as eluent gave **123**, as a brown oil (0.38 g, 54%) which was (~60%) pure by ¹H NMR.

Method 2:

Mueller's procedure was followed as an alternative synthesis for this compound.⁴⁰ To a solution of 2-methylthiobenzaldehyde, **121**, (0.11 mL, 0.87 mmol) and anhydrous potassium carbonate (0.29 g, 2.08 mmol) in dry methanol (15 mL) under nitrogen, was added dimethyl (1-diazo-2-oxopropyl)phosphonate, **125**, (0.20 g, 1.04 mmol). The reaction mixture was stirred at room temperature for 12 h. It was then diluted with ether (25 mL), washed with sodium bicarbonate (5% aqueous solution, 50 mL), brine (50 mL), dried over MgSO₄, filtered, and the solvent was removed *in vacuo*. Purification by column chromatography using hexane/ethyl acetate (9:1) as eluent gave **123**, as a clear oil (0.11 g, 86%). $\nu_{\max}/\text{cm}^{-1}$ (film): 3286 ($\equiv\text{C-H}$), 2956 (CH), 2926 (CH), 2103 (C \equiv C), 1463 (ring stretch), 750 (C-S); δ_{H} (300 MHz): 2.49 (3H, s, CH₃), 3.47 (1H, s, C \equiv C-H), 7.09 (1H, td J 7.5, 1.2, ArH), 7.17 (1H, d, J 8.1, ArH), 7.31 (1H, td, J 7.7, 1.5, ArH), 7.45 (1H, dd, J 7.7, 1.4, ArH); δ_{C} (150 MHz): 15.7 (CH₃, SCH₃), 81.1 (C, C \equiv CH), 83.6 (CH, C \equiv CH), 120.2 (C, quaternary aromatic C), 124.3 (CH, 2 x aromatic CH), 129.3, 133.2 (2 x CH, 2 x aromatic CH), 141.9 (C, quaternary aromatic C); NMR spectral assignment was aided by HSQC 2D NMR experiment; Spectral characteristics were in agreement with those previously reported.¹⁰

1-Ethynyl-2-(methylsulfinyl)benzene (126)

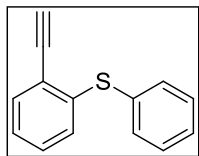
This compound was synthesised using Lehane's procedure.¹⁰ A solution of sodium periodate (0.58 g, 2.70 mmol) in water (7 mL) was added over 5 min to a stirred solution of the sulfide, **123**, (0.20 g, 1.35 mmol) in methanol (7 mL) cooled to 0 °C. The reaction mixture was stirred for 16 h at room temperature and concentrated *in vacuo* to a colourless residue. The residue was partitioned between CH₂Cl₂ (20 mL) and water (10 mL). The layers were separated and the aqueous layer further extracted with CH₂Cl₂ (2 x 20 mL). The combined organic layers were washed with water (2 x 20 mL) and brine (20 mL), dried over MgSO₄, filtered, and the solvent was removed *in vacuo*. The crude product was purified by column chromatography, using hexane/ethyl acetate (1:1) as eluent, and afforded **126** as a clear oil (0.20 g, 90%). $\nu_{\max}/\text{cm}^{-1}$ (film): 3205 ($\equiv\text{C-H}$), 2100 (C \equiv C), 1463 (ring stretch), 1070 (S=O), 1039 (S=O), 762 (C-S); δ_{H} (400 MHz): 2.84 (3H, s, CH₃), 3.52 (1H, s, C \equiv C-H), 7.46 (1H, td, J 7.2, 1.2, ArH), 7.55 (1H, d, J 7.6, ArH), 7.62 (1H, td, J 7.6, 1.4, ArH), 7.98 (1H, d, J 8.0, ArH); δ_{C} (75 MHz): 42.1 (CH₃, SOCH₃), 78.6 (C, C \equiv C-H), 85.9 (CH, C \equiv C-H), 118.0 (C, quaternary aromatic C), 123.3 (CH, aromatic CH), 130.2 (CH, aromatic CH), 130.3 (CH, aromatic CH), 133.3 (CH, aromatic CH), 148.0 (C, quaternary aromatic C); m/z (ESI) 165.03 [(M+H)⁺]; HRMS (ESI): exact mass calculated for C₉H₉OS [(M+H)⁺], 165.0374. Found 165.0361.

1-Ethynyl-2-(methylsulfonyl)benzene (127)¹⁰

This compound was synthesised using Lehane's procedure.¹⁰ A solution of oxone[®] (2.18 g, 3.55 mmol) in water (10 mL) was added dropwise to a stirred solution of the sulfide **123**, (0.26 g, 1.78 mmol) in acetone (10 mL). The reaction mixture was stirred for 16 h, then concentrated *in vacuo*, shaken with CH₂Cl₂ (20 mL) and the layers separated. The aqueous layer was further extracted with CH₂Cl₂ (2 x 20 mL). The combined organic layers were washed with water (2 x 20 mL), brine (20 mL), dried over MgSO₄, filtered, and the solvent was removed *in vacuo*. Purification by column chromatography using ethyl acetate/hexane (3:2) as eluent, gave **127**, as a white solid (0.29 g, 91%). m.p: 97-99 °C (Lit.¹⁰ 97-99 °C); $\nu_{\max}/\text{cm}^{-1}$ (KBr): 3280 ($\equiv\text{C-H}$), 2956 (CH), 2112 (C \equiv C), 1467 (ring stretch), 1310 (SO₂), 1153 (SO₂), 761 (C-S); δ_{H} (300 MHz): 3.30 (3H, s, CH₃), 3.64 (1H, s, C \equiv C-H), 7.52-7.65 (2H, m, ArH), 7.72 (1H, dd, J 7.5, 1.5, ArH), 8.12 (1H, dd, J 7.4, 1.8, ArH); δ_{C} (75 MHz): 42.4 (CH₃, SO₂CH₃), 79.6 (C, C \equiv C-H), 86.5 (CH, C \equiv C-H), 128.7 (CH, aromatic CH), 129.3 (CH, aromatic CH), 133.2 (CH, aromatic CH), 135.5 (CH, aromatic CH), signals not observed for 2 x quaternary aromatic C;

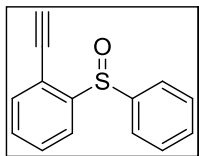
NMR spectral assignment was aided by HSQC 2D NMR experiment; Spectral characteristics were in agreement with those previously reported.¹⁰

(2-Ethynylphenyl)(phenyl)sulfane (**128**)⁴¹



Mueller's procedure was followed for the synthesis of this compound.⁴⁰ Dimethyl (1-diazo-2-oxopropyl)phosphonate, **125**, (0.43 g, 2.23 mmol) was added to a solution of 2-(phenylthio)benzaldehyde, **6**, (0.40 g, 1.86 mmol) and anhydrous potassium carbonate (0.51 g, 3.71 mmol) in dry methanol (20 mL) under nitrogen. The reaction mixture was stirred for 12 h. It was then diluted with ether (25 mL), washed with sodium bicarbonate (5% aqueous solution, 50 mL), brine (50 mL), dried over MgSO₄, filtered, and the solvent was removed *in vacuo*. Purification by column chromatography using hexane/ethyl acetate (9:1) as eluent, gave **128**, as a pale yellow oil (0.30 g, 77%). $\nu_{\max}/\text{cm}^{-1}$ (film): 3288 ($\equiv\text{C-H}$), 2956 (CH), 2928 (CH), 2099 ($\text{C}\equiv\text{C}$), 1438 (ring stretch), 755 (C-S); δ_{H} (300 MHz): 3.42 (1H, s, $\text{C}\equiv\text{C-H}$), 6.96 (1H, dd, J 7.5, 1.7, ArH), 7.08-7.21 (2H, m, ArH), 7.29-7.40 (3H, m, ArH), 7.41-7.53 (3H, m, ArH); Spectral characteristics were in agreement with those previously reported.⁴¹

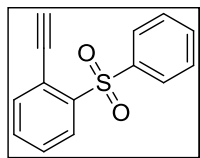
1-Ethynyl-2-(phenylsulfinyl)benzene (**129**)



This compound was synthesised using Lehane's procedure.¹⁰ A solution of sodium periodate (1.02 g, 4.76 mmol) in water (10 mL) was added over 5 min to a stirred solution of the sulfide, **128**, (0.50 g, 2.38 mmol) in methanol (10 mL) cooled to 0 °C. The reaction mixture was stirred for 16 h at room temperature and then concentrated *in vacuo* to a colourless residue. The residue was partitioned between CH₂Cl₂ (20 mL) and water (10 mL). The layers were separated and the aqueous layer further extracted with CH₂Cl₂ (2 x 20 mL). The combined organic layers were washed with water (2 x 20 mL), brine (20 mL), dried over MgSO₄, filtered, and the solvent was removed *in vacuo*. Purification by column chromatography using hexane/ethyl acetate (4:1) as eluent, gave **129** as a pale pink solid (0.23 g, 43%). m.p. 89-91 °C; (Found: C, 74.00; H, 4.50%. C₁₄H₁₀OS requires C, 74.31; H, 4.45%); $\nu_{\max}/\text{cm}^{-1}$ (KBr): 3172 ($\equiv\text{C-H}$), 2098 ($\text{C}\equiv\text{C}$), 1463 (ring stretch), 1079 (S=O), 1030 (S=O); δ_{H} (300 MHz): 3.50 (1H, s, $\text{C}\equiv\text{C-H}$), 7.36-7.46 (4H, m, ArH), 7.48-7.60 (2H, m, ArH), 7.74-7.79 (2H, m, ArH), 8.03 (1H, dd, J 8.0, ArH); δ_{C} (75 MHz): 79.4 (C, $\text{C}\equiv\text{CH}$), 85.6 (CH, $\text{C}\equiv\text{CH}$), 119.4 (C, quaternary aromatic C), 123.7 (CH, aromatic CH), 125.4 (CH, 2 x aromatic CH), 129.2 (CH, 2 x aromatic CH), 130.1 (CH, aromatic CH), 130.6 (CH, aromatic CH), 131.2 (CH, aromatic

CH), 133.6 (CH, aromatic CH), 145.2 (C, quaternary aromatic C), 147.8 (C, quaternary aromatic C); m/z (ESI) 227.05 [(M+H)⁺]; HRMS (ESI): exact mass calculated for C₁₄H₁₁OS [(M+H)⁺], 227.0531. Found 227.0533.

1-Ethynyl-2-(phenylsulfonyl)benzene (**130**)



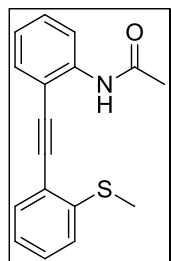
This compound was synthesised using Lehane's procedure.¹⁰ A solution of oxone[®] (2.01 g, 3.27 mmol) in water (10 mL) was added dropwise to a stirred solution of the sulfide **128**, (0.34 g, 1.64 mmol) in acetone (10 mL).

The reaction mixture was stirred for 16 h, then concentrated *in vacuo*, shaken with CH₂Cl₂ (20 mL) and the layers separated. The aqueous layer was further extracted with CH₂Cl₂ (2 x 20 mL). The combined organic layers were washed with water (2 x 20 mL), brine (20 mL), dried over MgSO₄, filtered, and the solvent was removed *in vacuo*. Purification by column chromatography using CH₂Cl₂ as eluent, gave **130**, as a pale pink solid (0.21 g, 52%). m.p. 110-112 °C; (Found: C, 69.34; H, 4.18%. C₁₄H₁₀O₂S requires C, 69.40; H, 4.16%); $\nu_{\max}/\text{cm}^{-1}$ (KBr): 3251 ($\equiv\text{C-H}$), 2106 (C \equiv C), 1447 (ring stretch), 1307 (SO₂), 1156 (SO₂); δ_{H} (300 MHz): 3.48 (1H, s, C \equiv C-H), 7.46-7.63 (6H, m, ArH), 7.98-8.01 (2H, m, ArH), 8.27-8.31 (1H, m, ArH); δ_{C} (75 MHz): 79.6 (C, C \equiv C-H), 86.4 (CH, C \equiv C-H), 121.4 (C, quaternary aromatic C), 128.5 (CH, 2 x aromatic CH), 128.7 (CH, 2 x aromatic CH), 129.1 (CH, aromatic CH), 129.2 (CH, aromatic CH), 133.0 (CH, aromatic CH), 133.4 (CH, aromatic CH), 135.8 (CH, aromatic CH), 140.4 (C, quaternary aromatic C), 142.1 (C, quaternary aromatic C); m/z (ESI) 243.04 [(M+H)⁺]; HRMS (ESI): exact mass calculated for C₁₄H₁₁O₂S [(M+H)⁺], 243.0480. Found 243.0473.

5.5.3. Sonogashira coupled products

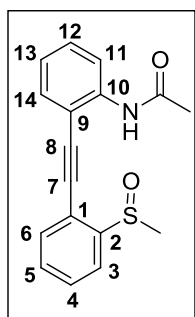
The following compounds (**131**, **133-149**) were synthesised according to a modified version of Jones procedure.⁴²

N-2-[2-(Methylthio)phenylethynyl]phenylacetamide (**131**)



N-(2-Iodophenyl)acetamide, **115**, (0.55 g, 2.11 mmol), 1-ethynyl-2-methylthiobenzene, **123**, (0.16 g, 1.11 mmol), triethylamine (3 mL) and DMF (2 mL) were stirred under nitrogen at room temperature for 10 min, then copper iodide (0.04 g, 0.2 mmol) and bis(triphenylphosphine)-palladium(II) dichloride (0.05 g, 0.05 mmol) were added sequentially. The resulting mixture was heated to 60 °C and stirred for 18 h under nitrogen. The solution was then cooled to room temperature, poured onto water (5 mL) and extracted with EtOAc (3 x 5 mL). The organic layers were combined and washed with brine (10 mL), dried over MgSO₄ and concentrated *in vacuo*. The crude solid was purified by column chromatography using hexane/ethyl acetate (9:1) as eluent to give, **131**, as a dark orange solid (0.22 g, 70%); $\nu_{\max}/\text{cm}^{-1}$ (KBr): 3363 (NH), 2918 (CH), (C≡C stretch not observed), 1688 (C=O), 1576 (ring stretch), 1514 (NH), 1435 (CH₃), 1300 (C-N), 744 (C-S); δ_{H} (300 MHz): 2.30 (3H, s, COCH₃), 2.57 (3H, s, SCH₃), 7.07 (1H, td, *J* 7.5, 1.2, ArH), 7.18 (1H, td, *J* 7.5, 1.2, ArH), 7.25 (1H, d, *J* 7.8, ArH), 7.32-7.40 (2H, m, ArH), 7.49-7.55 (2H, m, ArH), 8.50 (1H, d, *J* 8.4, ArH), 8.55 (1H, bs, NH); δ_{C} (75 MHz): 15.3 (CH₃, SCH₃), 25.2 (CH₃, COCH₃), 91.3 (C, C≡C), 93.7 (C, C≡C), 119.3 (CH, aromatic CH), 121.1 (C, quaternary aromatic C), 123.2 (CH, aromatic CH), 124.6 (CH, aromatic CH), 125.0 (CH, aromatic CH), 129.3 (CH, aromatic CH), 129.9 (CH, aromatic CH), 131.5 (CH, aromatic CH), 132.1 (CH, aromatic CH), 139.3 (C, quaternary aromatic C), 140.3 (C, quaternary aromatic C), 168.7 (C, C=O), 3 signals observed for 4 quaternary aromatic C; *m/z* (ESI) 282.2 [(M+H)⁺]; HRMS (ESI): exact mass calculated for C₁₇H₁₆NOS [(M+H)⁺], 282.0953. Found 282.0942.

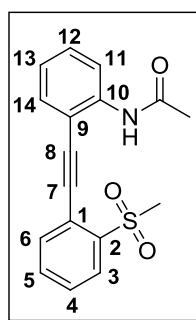
Single crystals of **131** were grown from acetonitrile. Crystal data: C₁₇H₁₅NOS, *M* = 281.37, monoclinic, space group *P*2₁/*c*, *a* = 34.021(9) Å, *b* = 5.0948(11) Å, *c* = 17.202(4) Å, β = 103.853(6)°, *V* = 2894.9(12) Å³, *Z* = 8, *D_c* = 1.291 g cm⁻³, *F*(000) = 1184, Mo K α radiation, λ = 0.71073 Å, *T* = 296(2) K, $2\theta_{\max}$ = 25.02°, μ = 0.218 mm⁻¹, 28420 reflections collected, 5090 unique (*R_{int}* = 0.0570). Final GooF = 1.265, *R*₁ = 0.0478, *wR*₂ = 0.1210 (obs. data: *I* > 2 σ (*I*)); *R*₁ = 0.0760, *wR*₂ = 0.1390 (all data).

***N*-2-[2-(Methylsulfinyl)phenylethynyl]phenylacetamide (132)**

A solution of sodium periodate (0.50 g, 2.35 mmol) in water (7 mL) was added dropwise over 5 min to a stirred solution of the sulfide, **131**, (0.22 g, 0.78 mmol) in methanol (7 mL) cooled to 0 °C. The reaction mixture was stirred for 16 h at room temperature and then concentrated *in vacuo* to give a colourless residue. The residue was partitioned between CH₂Cl₂ (20 mL) and water (10 mL). The layers were separated and the aqueous layer was

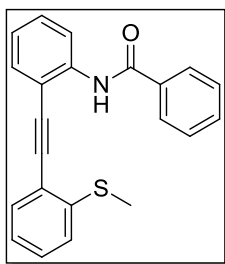
further extracted with CH₂Cl₂ (2 x 10 mL). The combined organic layers were washed with water (2 x 10 mL), brine (10 mL), dried using MgSO₄ and the solvent removed *in vacuo*. Purification of the residue was achieved by column chromatography using hexane/ethyl acetate (1:1) as eluent, to yield the sulfoxide **132**, as a pale yellow solid (0.20 g, 88%).
 $\nu_{\max}/\text{cm}^{-1}$ (KBr): 3378 (NH), 2987 (CH), 2210 (C≡C), 1694 (C=O), 1519 (ring stretch), 1305 (C-N), 1071 (S=O), 1039 (S=O), 767 (C-S); δ_{H} (600 MHz): 2.32 (3H, s, COCH₃), 2.93 (3H, s, SOCH₃), 7.09 [1H, td, *J* 7.6, 1.1, C(13)H], 7.40 [1H, td, *J* 7.5, 1.2, C(12)H], 7.51 [1H, dd, *J* 7.8, 1.2 C(14)H], 7.54 [1H, td, *J* 7.5, 1.4, C(5)H], 7.58 [1H, td, *J* 7.5, 1.4, C(4)H], 7.65 [1H, dd, *J* 7.2, 1.2, C(6)H], 7.86 [1H, d, *J* 7.2, C(3)H], 8.47 [1H, d, *J* 8.4, C(11)H], 8.53 (1H, bs, NH); δ_{C} (150 MHz): 24.9 (CH₃, COCH₃), 41.5 (CH₃, SOCH₃), 90.5 [C, C(7)], 93.8 [C, C(8)], 110.8 [C, quaternary aromatic C(9)], 119.6 [C, quaternary aromatic C(1)], 120.1 [CH, aromatic C(11)H], 123.4 [CH, aromatic C(13)H], 124.8 [CH, aromatic C(3)H], 129.6 [CH, aromatic C(4)H], 130.7 [CH, aromatic C(12)H], 131.2 [CH, aromatic C(5)H], 131.9 [CH, aromatic C(14)H], 133.4 [CH, aromatic C(6)H], 139.9 [C, quaternary aromatic C(10)], 145.6 [C, quaternary aromatic C(2)], 169.2 (C, C=O); NMR spectral assignment was aided by COSY, HSQC, HMBC and NOESY 2D NMR experiments; *m/z* (ESI) 298.1 [(M+H)⁺]; HRMS (ESI): exact mass calculated for C₁₇H₁₆NO₂S [(M+H)⁺], 298.0902. Found 298.0914.

Single crystals of **132** were grown from acetonitrile. Crystal data: C₁₇H₁₅NO₂S, *M* = 297.36, monoclinic, space group *P*2₁/*n*, *a* = 11.6773(18) Å, *b* = 5.7157(8) Å, *c* = 22.940(4) Å, β = 104.148(4)°, *V* = 1484.7(4) Å³, *Z* = 4, *D_c* = 1.330 g cm⁻³, *F*(000) = 624, Mo K α radiation, λ = 0.71073 Å, *T* = 296(2) K, $2\theta_{\max}$ = 26.32°, μ = 0.221 mm⁻¹, 15857 reflections collected, 3009 unique (*R_{int}* = 0.0307). Final GooF = 1.042, *R*₁ = 0.0541, *wR*₂ = 0.1389 (obs. data: *I* > 2 σ (*I*)); *R*₁ = 0.0652, *wR*₂ = 0.1476 (all data).

N-2-[2-(Methylsulfonyl)phenylethynyl]phenylacetamide (133)

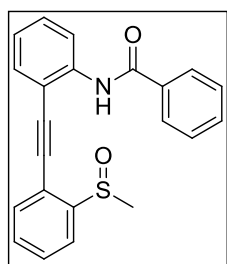
N-(2-Iodophenyl)acetamide, **115**, (0.07 g, 0.25 mmol), 2-methylsulfonyl ethynyl benzene, **127**, (0.05 g, 0.28 mmol), triethylamine (2 mL) and DMF (2 mL) were stirred under nitrogen at room temperature for 10 min, then copper iodide (0.01 g, 0.05 mmol) and bis(triphenylphosphine)palladium(II) dichloride (0.02 g, 0.03 mmol) were added sequentially. The resulting mixture was heated to 60 °C and stirred for 18 h under nitrogen. The solution was then cooled to room temperature, poured onto water (5 mL) and extracted with EtOAc (3 x 5 mL). The organic layers were combined and washed with brine (10 mL), dried over MgSO₄ and concentrated *in vacuo*. The crude solid was purified by column chromatography using CH₂Cl₂/ethyl acetate (9:1) as eluent yielding the sulfone, **133** as a pale yellow solid (0.03 g, 34%); (Found: C, 64.33; H, 4.26; N, 3.11%. C₁₇H₁₅NO₃S requires C, 65.16; H, 4.82; N, 4.47%); $\nu_{\max}/\text{cm}^{-1}$ (KBr): 3344 (NH), 2215 (C≡C), 1696 (C=O), 1578 (ring stretch), 1520 (NH), 1305 (SO₂), 1153 (SO₂); δ_{H} (600 MHz): 2.32 (3H, s, COCH₃), 3.23 (3H, s, SO₂CH₃), 7.07 [1H, td, *J* 7.5, 0.8, C(13)H], 7.41 [1H, td, *J* 7.2, 1.5, C(12)H], 7.51 [1H, dd, *J* 7.8, 1.2, C(14)H], 7.58 [1H, td, *J* 7.8, 1.2, C(4)H], 7.68 [1H, td, *J* 7.5, 1.4, C(5)H], 7.77 [1H, dd, *J* 7.5, 0.9, C(6)H], 8.13 [1H, dd, *J* 8.1, 0.9, C(3)H], 8.55 (1H, d, *J* 8.4, C(11)H], 8.79 (1H, bs, NH); δ_{C} (600 MHz): 24.7 (CH₃, COCH₃), 42.8 (CH₃, SO₂CH₃), 90.9 [C, C(7)], 94.4 [C, C(8)], 110.3 [C, quaternary aromatic C(9)], 120.2 [CH, aromatic C(11)H], 121.9 [C, quaternary aromatic C(1)], 123.0 [CH, aromatic C(13)H], 129.0 [CH, aromatic C(4)H], 129.1 [CH, aromatic C(3)H], 130.9 [CH, aromatic C(12)H], 132.2 [CH, aromatic C(14)H], 133.6 [CH, aromatic C(5)H], 134.2 [CH, aromatic C(6)H], 140.1 [C, quaternary aromatic C(2)], 141.1 [C, quaternary aromatic C(10)], 170.2 (C, C=O); NMR spectral assignment was aided by COSY, HSQC, HMBC and NOESY 2D NMR experiments; *m/z* (ESI) 314.3 [(M+H)⁺]; HRMS (ESI): exact mass calculated for C₁₇H₁₆NO₃S [(M+H)⁺], 314.0851. Found 314.0840.

Single crystals of **133** were grown from acetonitrile. Crystal data: C₁₇H₁₅NO₃S, *M* = 313.36, monoclinic, space group *P*2₁/*c*, *a* = 10.673(2) Å, *b* = 14.691(3) Å, *c* = 9.918(2) Å, β = 96.285(4)°, *V* = 1545.8(5) Å³, *Z* = 4, *D_c* = 1.346 g cm⁻³, *F*(000) = 656, Mo K α radiation, λ = 0.71073 Å, *T* = 296(2) K, $2\theta_{\max}$ = 26.30°, μ = 0.221 mm⁻¹, 8797 reflections collected, 3102 unique (*R_{int}* = 0.0540). Final GooF = 0.966, *R*₁ = 0.0490, *wR*₂ = 0.1083 (obs. data: *I* > 2 σ (*I*)); *R*₁ = 0.1157, *wR*₂ = 0.1370 (all data).

N-2-[2-(Methylthio)phenylethynyl]phenylbenzamide (134)

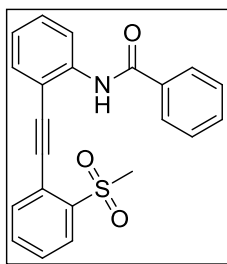
N-(2-Iodophenyl)benzamide, **116**, (1.22 g, 3.76 mmol), 1-ethynyl-2-methylthiobenzene, **123**, (0.30 g, 1.99 mmol), triethylamine (3 mL) and DMF (3 mL) were stirred under nitrogen at room temperature for 10 min, then copper iodide (0.07 g, 0.36 mmol) and bis(triphenylphosphine)palladium(II) dichloride (0.08 g, 0.12 mmol) were added sequentially. The resulting mixture was heated to 60 °C and stirred for 18 h under nitrogen. The solution was then cooled to room temperature, poured onto water (5 mL) and extracted with EtOAc (3 x 5 mL). The organic layers were combined and washed with brine (10 mL), dried over MgSO₄ and concentrated *in vacuo*. Purification was achieved by column chromatography using hexane/ethyl acetate (9:1) as eluent to afford the title compound **134**, as a dark brown solid (0.10 g, 15%); m.p. 70-72 °C; $\nu_{\max}/\text{cm}^{-1}$ (KBr): 3366 (NH), 2917 (CH), (C≡C stretch not observed), 1673 (C=O), 1511 (ring stretch), 1437(CH₃), 1302 (C-N), 747 (C-S); δ_{H} (300 MHz): 2.12 (3H, s, SCH₃), 7.03-7.11 (3H, m, ArH), 7.22-7.54 (7H, m, ArH), 7.88-7.93 (2H, m, ArH), 8.50 (1H, d, *J* 8.4, ArH), 8.94 (1H, bs, NH); δ_{C} (75 MHz): 14.7 (CH₃, SCH₃), 91.2 (C, C≡C), 93.9 (C, C≡C), 112.4 (C, quaternary aromatic C), 119.9 (CH, aromatic CH), 120.6 (C, quaternary aromatic C), 123.6 (CH, aromatic CH), 124.1 (CH, aromatic CH), 124.5 (CH, aromatic CH), 127.9 (CH, 2 x aromatic CH), 128.5 (CH, 2 x aromatic CH), 129.3 (CH, aromatic CH), 129.9 (CH, aromatic CH), 131.7 (CH, aromatic CH), 131.9 (CH, aromatic CH), 132.1 (CH, aromatic CH), 135.3 (C, quaternary aromatic C), 139.3 (C, quaternary aromatic C), 141.2 (C, quaternary aromatic C), 166.4 (C, C=O); *m/z* (ESI) 344.1 [(M+H)⁺]; HRMS (ESI): exact mass calculated for C₂₂H₁₇NOS [(M+H)⁺], 344.1109. Found 344.1100.

Single crystals of **134** were grown from acetonitrile. Crystal data: C₂₂H₁₇NOS, *M* = 343.43, monoclinic, space group *P*2₁/*c*, *a* = 12.1161(17) Å, *b* = 15.091(2) Å, *c* = 9.8508(14) Å, β = 91.810(4)°, *V* = 1800.3(4) Å³, *Z* = 4, *D_c* = 1.267 g cm⁻³, *F*(000) = 720, Mo K α radiation, λ = 0.71073 Å, *T* = 296(2) K, $2\theta_{\max}$ = 26.70°, μ = 0.188 mm⁻¹, 17883 reflections collected, 3482 unique (*R_{int}* = 0.0592). Final GooF = 1.129, *R*₁ = 0.0457, *wR*₂ = 0.1166 (obs. data: *I* > 2 σ (*I*)); *R*₁ = 0.0867, *wR*₂ = 0.1371 (all data).

N-2-[2-(Methylsulfinyl)phenylethynyl]phenylbenzamide (135)

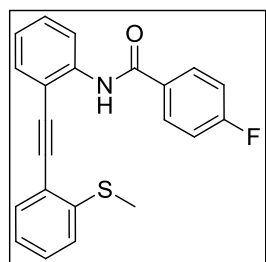
N-(2-Iodophenyl)benzamide, **116**, (0.08 g, 0.25 mmol), 1-ethynyl-2-(methylsulfinyl)benzene, **126**, (0.05 g, 0.27 mmol), triethylamine (2 mL) and DMF (2 mL) were stirred under nitrogen at room temperature for 10 min, then copper iodide (0.01 g, 0.05 mmol) and bis(triphenylphosphine)palladium(II) dichloride (0.02 g, 0.03 mmol) were added sequentially. The resulting mixture was heated to 60 °C and stirred for 18 h under nitrogen. The solution was then cooled to room temperature, poured onto water (5 mL) and extracted with EtOAc (3 x 5 mL). The organic layers were combined and washed with brine (10 mL), dried over MgSO₄ and concentrated *in vacuo*. The crude solid was purified by column chromatography using CH₂Cl₂/ethyl acetate (1:1) as eluent. The title sulfoxide, **135** was obtained as a pale yellow solid (0.03 g, 15%); m.p. 133-135 °C; $\nu_{\max}/\text{cm}^{-1}$ (KBr): 3393 (NH), 2212 (C≡C), 1668 (C=O), 1518 (ring stretch), 1300 (C-N), 1021 (S=O); δ_{H} (300 MHz): 2.57 (3H, s, SOCH₃), 7.09 (1H, td, *J* 7.6, 1.1, ArH), 7.36-7.59 (8H, m, ArH), 7.86-7.93 (3H, m, ArH), 8.46 (1H, d, *J* 8.1, ArH), 8.62 (1H, bs, NH); δ_{C} (75 MHz): 42.1 (CH₃, SOCH₃), 91.1 (C, C≡C), 93.1 (C, C≡C), 111.6 (C, quaternary aromatic C), 118.6 (C, quaternary aromatic C), 120.3 (CH, aromatic CH), 123.7 (CH, aromatic CH), 124.0 (CH, aromatic CH), 127.2 (CH, 2 x aromatic CH), 128.2 (CH, aromatic CH), 129.1 (CH, 2 x aromatic CH), 130.2 (CH, aromatic CH), 130.8 (CH, aromatic CH), 132.1 (CH, aromatic CH), 132.4 (CH, aromatic CH), 132.6 (CH, aromatic CH), 134.7 (C, quaternary aromatic C), 139.1 (C, quaternary aromatic C), 146.9 (C, quaternary aromatic C), 165.8 (C, C=O); *m/z* (ESI) 359.1 [(M+H)⁺]; HRMS (ESI): exact mass calculated for C₂₂H₁₈NO₂S [(M+H)⁺], 360.1058. Found 360.1041.

Single crystals of **135** were grown from acetonitrile. Crystal data was obtained for acetonitrile solvate: C₂₄H₂₀N₂O₂S, *M* = 400.48, monoclinic, space group *P*2₁/*c*, *a* = 21.71(2) Å, *b* = 5.313(5) Å, *c* = 17.898(16) Å, β = 96.69(3)°, *V* = 2050.(3) Å³, *Z* = 4, *D_c* = 1.298 g cm⁻³, *F*(000) = 840, Mo K α radiation, λ = 0.71073 Å, *T* = 300(2) K, $2\theta_{\max}$ = 24.80°, μ = 0.180 mm⁻¹, 7989 reflections collected, 3483 unique (*R*_{int} = 0.1289). Final GooF = 1.416, *R*₁ = 0.2026, *wR*₂ = 0.4416 (obs. data: *I* > 2 σ (*I*)); *R*₁ = 0.2787, *wR*₂ = 0.4805 (all data).

***N*-2-[2-(Methylsulfonyl)phenylethynyl]phenylbenzamide (136)**

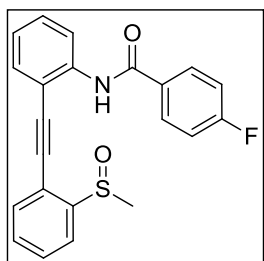
N-(2-Iodophenyl)benzamide, **116**, (0.06 g, 0.19 mmol), 2-methylsulfonyl ethynylbenzene, **127**, (0.04 g, 0.20 mmol), triethylamine (2 mL) and DMF (2 mL) were stirred under nitrogen at room temperature for 10 min, then copper iodide (0.007 g, 0.04 mmol) and bis(triphenylphosphine)palladium(II) dichloride (0.01 g, 0.02 mmol) were added sequentially. The resulting mixture was heated to 60 °C and stirred for 18 h under nitrogen. The solution was then cooled to room temperature, poured onto water (5 mL) and extracted with EtOAc (3 x 5 mL). The organic layers were combined and washed with brine (10 mL), dried over MgSO₄ and concentrated *in vacuo*. The crude material was purified by column chromatography using CH₂Cl₂/ethyl acetate (9:1) as eluent. The sulfone **136** was obtained as a pale yellow solid (0.04 g, 55%); m.p. 141-143 °C; (Found: C, 70.57; H, 4.66; N, 3.63%. C₂₂H₁₇NO₃S requires C, 70.38; H, 4.56; N, 3.73%); $\nu_{\max}/\text{cm}^{-1}$ (KBr): 3340 (NH), 2215 (C≡C), 1679 (C=O), 1576 (ring stretch), 1311 (SO₂), 1152 (SO₂); δ_{H} (300 MHz): 2.92 (3H, s, SO₂CH₃), 7.15 (1H, td, *J* 7.7, 1.1, ArH), 7.43-7.67 (7H, m, ArH), 7.72 (1H, dd, *J* 7.7, 1.4, ArH), 7.97-8.02 (2H, m, ArH), 8.07 (1H, dd, *J* 8.0, 1.4, ArH), 8.42 (1H, d, *J* 8.1, ArH), 9.06 (1H, bs, NH); δ_{C} (75 MHz): 42.3 (CH₃, SO₂CH₃), 91.3 (C, C≡C), 94.0 (C, C≡C), 112.3 (C, quaternary aromatic C), 121.7 (C, quaternary aromatic C), 121.8 (CH, aromatic CH), 123.9 (CH, aromatic CH), 128.1 (CH, 2 x aromatic CH), 128.5 (CH, 2 x aromatic CH), 129.1 (CH, aromatic CH), 130.6 (CH, aromatic CH), 132.1 (CH, aromatic CH), 132.5 (CH, aromatic CH), 133.4 (CH, aromatic CH), 134.3 (CH, aromatic CH), 134.6 (C, quaternary aromatic C), 140.0 (C, quaternary aromatic C), 140.6 (C, quaternary aromatic C), 166.9 (C, C=O); 10 signals observed for 11 aromatic CH signals; *m/z* (ESI) 376.3 [(M+H)⁺]; HRMS (ESI): exact mass calculated for C₂₂H₁₈NO₃S [(M+H)⁺], 376.1007. Found 376.0991.

Single crystals of **136** were grown from acetonitrile. Crystal data: C₂₂H₁₇NO₃S, *M* = 375.43, monoclinic, space group *P*2₁/*c*, *a* = 19.613(2) Å, *b* = 5.0559(6) Å, *c* = 19.507(3) Å, β = 107.915(3)°, *V* = 1840.6(4) Å³, *Z* = 4, *D*_c = 1.355 g cm⁻³, *F*(000) = 784, Mo K α radiation, λ = 0.71073 Å, *T* = 296(2) K, $2\theta_{\max}$ = 25.14°, μ = 0.198 mm⁻¹, 9962 reflections collected, 3253 unique (*R*_{int} = 0.0952). Final GooF = 0.964, *R*₁ = 0.0518, *wR*₂ = 0.0848 (obs. data: *I* > 2 σ (*I*)); *R*₁ = 0.1429, *wR*₂ = 0.1099 (all data).

4-Fluoro-*N*-2-[2-(methylthio)phenylethynyl]phenylbenzamide (137)

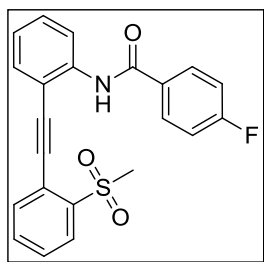
4-Fluoro-*N*-(2-iodophenyl)benzamide, **118**, (0.22 g, 0.65 mmol), 1-ethynyl-2-methylthiobenzene, **123**, (0.11 g, 0.72 mmol), triethylamine (2 mL) and DMF (2 mL) were stirred under nitrogen at room temperature for 10 min, then copper iodide (0.03 g, 0.13 mmol) and bis(triphenyl-phosphine)palladium(II) dichloride (0.05 g, 0.07 mmol) were added sequentially. The resulting mixture was heated to 60 °C and stirred for 18 h under nitrogen. The solution was then cooled to room temperature, poured onto water (5 mL) and extracted with EtOAc (3 x 5 mL). The organic layers were combined and washed with brine (10 mL), dried over MgSO₄ and concentrated *in vacuo*. Purification of the crude material was achieved by column chromatography using CH₂Cl₂ as eluent. The title compound, **137** was obtained as a white solid (0.08 g, 33%) and consisted of a mixture of the starting material **118** (~7%) and the desired product **137** (~93%) as determined by ¹H and ¹³C NMR; m.p. 90.5-92.5 °C; $\nu_{\max}/\text{cm}^{-1}$ (KBr): 3336 (NH), (C≡C stretch not observed), 1660 (C=O), 1504 (ring stretch), 1313 (C-N), 757 (C-S); δ_{H} (300 MHz): 2.24 (3H, s, SCH₃), 7.09-7.16 (5H, m, ArH), 7.33 (1H, td, *J* 7.7, 1.4, ArH), 7.41 (1H, td, *J* 7.1, 1.7, ArH), 7.49 (1H, d, *J* 8.1, ArH), 7.56 (1H, dd, *J* 7.8, 1.5, ArH), 7.96-8.01 (2H, m, ArH), 8.54 (1H, d, *J* 8.4, ArH), 8.94 (1H, bs, NH); δ_{C} (75 MHz): 14.8 (CH₃, SCH₃), 91.1 (C, C≡C), 94.0 (C, C≡C), 112.5 (C, quaternary aromatic C), 115.5 (CH, d, ²*J*_{C-F} 21.9, 2 x aromatic CH), 119.8 (CH, aromatic CH), 120.6 (C, quaternary aromatic C), 123.7 (CH, aromatic CH), 124.2 (CH, aromatic CH), 124.6 (CH, aromatic CH), 129.4 (CH, aromatic CH), 129.9 (CH, aromatic CH), 130.3 (CH, d, ³*J*_{C-F} 8.8, 2 x aromatic CH), 131.9 (CH, aromatic CH), 132.1 (CH, aromatic CH), 139.1 (C, quaternary aromatic C), 141.0 (C, quaternary aromatic C), 164.9 (C, ¹*J*_{C-F} 252.5, quaternary aromatic C-F), 165.1 (C, C=O); 5 signals observed for 6 quaternary aromatic C; *m/z* (ESI) 362.09 [(M+H)⁺]; HRMS (ESI): exact mass calculated for C₂₂H₁₇NOFS [(M+H)⁺], 362.1015. Found 362.1014.

Single crystals of **137** were grown from acetonitrile. Crystal data: C₂₂H₁₆FNOS, *M* = 361.42, monoclinic, space group *P*2₁/*n*, *a* = 17.33(2) Å, *b* = 5.176(5) Å, *c* = 20.89(2) Å, β = 102.06(2)°, *V* = 1832.(3) Å³, *Z* = 4, *D*_c = 1.310 g cm⁻³, *F*(000) = 752, Mo K α radiation, λ = 0.71073 Å, *T* = 296(2) K, $2\theta_{\max}$ = 24.92°, μ = 0.196 mm⁻¹, 10219 reflections collected, 2998 unique (*R*_{int} = 0.0403). Final GooF = 1.123, *R*₁ = 0.0428, *wR*₂ = 0.1073 (obs. data: *I* > 2 σ (*I*); *R*₁ = 0.0816, *wR*₂ = 0.1257 (all data).

4-Fluoro-*N*-2-[2-(methylsulfinyl)phenylethynyl]phenylbenzamide (138)

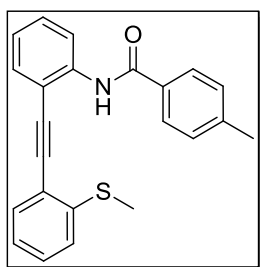
4-Fluoro-*N*-(2-iodophenyl)benzamide, **118**, (0.09 g, 0.25 mmol), 1-ethynyl-2-(methylsulfinyl)benzene, **126**, (0.05 g, 0.28 mmol), triethylamine (2 mL) and DMF (2 mL) were stirred under nitrogen at room temperature for 10 min, then copper iodide (0.01 g, 0.05 mmol) and bis(triphenyl-phosphine)palladium(II) dichloride (0.02 g, 0.03 mmol) were added sequentially. The resulting mixture was heated to 60 °C and stirred for 18 h under nitrogen. The solution was then cooled to room temperature, poured onto water (5 mL) and extracted with EtOAc (3 x 5 mL). The organic layers were combined and washed with brine (10 mL), dried over MgSO₄ and concentrated *in vacuo*. The crude solid was purified by column chromatography using CH₂Cl₂/ethyl acetate (7:3) as eluent to give the sulfoxide **138**, as a white solid (0.08 g, 81%). m.p. 143-145 °C; $\nu_{\max}/\text{cm}^{-1}$ (KBr): 3264 (NH), 2207 (C≡C), 1671 (C=O), 1578 (ring stretch), 1447 (CH₃), 1310 (C-N), 1065 (S=O), 1024 (S=O); δ_{H} (300 MHz): 2.70 (3H, s, SOCH₃), 7.13-7.25 (3H, m, ArH), 7.43-7.66 (5H, m, ArH), 7.94-8.02 (3H, m, ArH), 8.49 (1H, d, *J* 7.8, ArH), 8.67 (1H, bs, NH); δ_{C} (75 MHz): 42.1 (CH₃, SOCH₃), 91.1 (C, C≡C), 93.1 (C, C≡C), 111.7 (C, quaternary aromatic C), 116.2 (CH, d, ²*J*_{C-F} 22.1, 2 x aromatic CH), 118.7 (C, quaternary aromatic C), 120.5 (CH, aromatic CH), 123.9 (CH, aromatic CH), 124.1 (CH, aromatic CH), 129.6 (CH, aromatic CH), 129.7 (CH, aromatic CH), 130.2 (CH, aromatic CH), 130.8 (CH, d, ³*J*_{C-F} 6.9, 2 x aromatic CH), 132.1 (CH, aromatic CH), 132.6 (CH, aromatic CH), 139.1 (C, quaternary aromatic C), 146.9 (C, quaternary aromatic C), 164.7 (C, C=O), 165.2 (C, ¹*J*_{C-F} 253.7, quaternary aromatic C-F); 5 signals observed for 6 quaternary aromatic C; *m/z* (ESI) 378.3 [(M+H)⁺]; HRMS (ESI): exact mass calculated for C₂₂H₁₇NO₂FS [(M+H)⁺], 378.0964. Found 378.0970.

Single crystals of **138** were grown from acetonitrile. Crystal data: C₂₂H₁₆FNO₂S, *M* = 377.42, monoclinic, space group *P*2₁/*n*, *a* = 11.660(7) Å, *b* = 9.166(5) Å, *c* = 17.978(10) Å, β = 103.976(11)°, *V* = 1864.5(18) Å³, *Z* = 4, *D*_c = 1.345 g cm⁻³, *F*(000) = 784, Mo K α radiation, λ = 0.71073 Å, *T* = 296.(2) K, $2\theta_{\max}$ = 27.62°, μ = 0.200 mm⁻¹, 10505 reflections collected, 4059 unique (*R*_{int} = 0.1132). Final GooF = 0.910, *R*₁ = 0.0815, *wR*₂ = 0.1556 (obs. data: *I* > 2 σ (*I*); *R*₁ = 0.2596, *wR*₂ = 0.2237 (all data).

4-Fluoro-*N*-2-[2-(methylsulfonyl)phenylethynyl]phenylbenzamide (139)

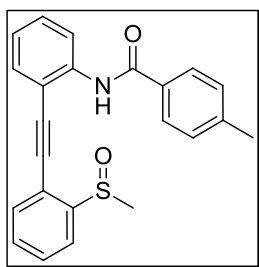
4-Fluoro-*N*-(2-iodophenyl)benzamide, **118**, (0.13 g, 0.39 mmol), 2-methylsulfonyl ethynylbenzene, **127**, (0.08 g, 0.43 mmol), triethylamine (2 mL) and DMF (2 mL) were stirred under nitrogen at room temperature for 10 min, then copper iodide (0.02 g, 0.08 mmol) and bis(triphenyl-phosphine)palladium(II) dichloride (0.03 g, 0.04 mmol) were added sequentially. The resulting mixture was heated to 60 °C and stirred for 18 h under nitrogen. The solution was then cooled to room temperature, poured onto water (5 mL) and extracted with EtOAc (3 x 5 mL). The organic layers were combined and washed with brine (10 mL), dried over MgSO₄ and concentrated *in vacuo*. The crude solid was purified by column chromatography using CH₂Cl₂/ethyl acetate (19:1) as eluent. The sulfone **139**, was obtained as a white solid (0.04 g, 26%); m.p. 155-157 °C; (Found: C, 66.99; H, 4.40; N, 3.34%. C₂₂H₁₆FNO₃S requires C, 67.16; H, 4.10; N, 3.56%); $\nu_{\max}/\text{cm}^{-1}$ (KBr): 3323 (NH), 2211 (C≡C), 1658 (C=O), 1604 (ring stretch), 1445 (C-N), 1309 (SO₂), 1153 (SO₂); δ_{H} (300 MHz): 3.00 (3H, s, SO₂CH₃), 7.09-7.19 (3H, m, ArH), 7.47 (1H, td, *J* 7.1, 1.7, ArH), 7.52-7.60 (2H, m, ArH), 7.65 (1H, td, *J* 7.6, 1.4, ArH), 7.74 (1H, dd, *J* 7.7, 1.4, ArH), 7.98-8.06 (2H, m, ArH), 8.08 (1H, dd, *J* 8.0, 1.4, ArH), 8.41 (1H, d, *J* 8.1, ArH), 9.03 (1H, bs, NH); δ_{C} (75 MHz): 42.5 (CH₃, SO₂CH₃), 91.3 (C, C≡C), 94.0 (C, C≡C), 112.1 (C, quaternary aromatic C), 115.5 (CH, d, ²*J*_{C-F} 22.0, 2 x aromatic CH), 121.6 (C, quaternary aromatic C), 121.8 (CH, aromatic CH), 123.9 (CH, aromatic CH), 129.1 (CH, d, ³*J*_{C-F} 5.1, 2 x aromatic CH), 130.5 (CH, aromatic CH), 130.7 (CH, 2 x aromatic CH), 132.5 (CH, aromatic CH), 133.5 (CH, aromatic CH), 134.3 (CH, aromatic CH), 140.1 (C, quaternary aromatic C), 140.6 (C, quaternary aromatic C), 165.1 (C, ¹*J*_{C-F} 252.8, quaternary aromatic C-F), 165.9 (C, C=O); 5 signals observed for 6 quaternary aromatic C, 9 signals observed for 10 aromatic CH signals; *m/z* (ESI) 394.4 [(M+H)⁺]; HRMS (ESI): exact mass calculated for C₂₂H₁₇NO₃FS [(M+H)⁺], 394.0913. Found 394.0913.

Single crystals of **139** were grown from acetonitrile. Crystal data: C₂₂H₁₇FNO₃S, *M* = 393.42, orthorhombic, space group *P*2₁2₁2₁, *a* = 5.0988(8) Å, *b* = 11.1272(18) Å, *c* = 32.779(5) Å, *V* = 1859.7(5) Å³, *Z* = 4, *D*_c = 1.405 g cm⁻³, *F*(000) = 816, Mo Kα radiation, λ = 0.71073 Å, *T* = 296(2) K, $2\theta_{\max}$ = 26.88°, μ = 0.207 mm⁻¹, 21470 reflections collected, 3980 unique (*R*_{int} = 0.0499). Final GooF = 1.017, *R*₁ = 0.0383, *wR*₂ = 0.0805 (obs. data: *I* > 2σ(*I*)); *R*₁ = 0.0543, *wR*₂ = 0.0875 (all data).

4-Methyl-N-2-[2-(methylthio)phenylethynyl]phenylbenzamide (140)

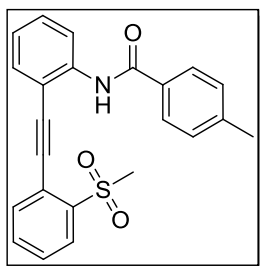
N-(2-Iodophenyl)-4-methylbenzamide, **119**, (0.12 g, 0.37 mmol), 1-ethynyl-2-methylthiobenzene, **123**, (0.06 g, 0.41 mmol), triethylamine (2 mL) and DMF (2 mL) were stirred under nitrogen at room temperature for 10 min, then copper iodide (0.01 g, 0.07 mmol) and bis(triphenylphosphine)palladium(II)dichloride (0.03 g, 0.04 mmol) were added sequentially. The resulting mixture was heated to 60 °C and stirred for 18 h under nitrogen. The solution was then cooled to room temperature, poured onto water (5 mL) and extracted with EtOAc (3 x 5 mL). The organic layers were combined and washed with brine (10 mL), dried over MgSO₄ and concentrated *in vacuo*. Purification was achieved by column chromatography using CH₂Cl₂ as eluent to afford **140**, as a dark brown solid (0.07 g, 56%). m.p. 130-132 °C; $\nu_{\max}/\text{cm}^{-1}$ (KBr): 3364 (NH), (C≡C stretch not observed), 1670 (C=O), 1506 (ring stretch), 1435 (CH₃), 1300 (C-N), 742 (C-S); δ_{H} (300 MHz): 2.23 (3H, s, ArCH₃), 2.42 (3H, s, SCH₃), 7.07-7.19 (3H, m, ArH), 7.25 (2H, d, *J* 7.8, ArH), 7.29-7.36 (1H, m, ArH), 7.37-7.45 (1H, m, ArH), 7.50 (1H, dd, *J* 7.5, 1.5, ArH), 7.56 (1H, dd, *J* 7.7, 1.4, ArH), 7.87 (2H, d, *J* 8.4, ArH), 8.57 (1H, d, *J* 8.3, ArH), 8.96 (1H, bs, NH); δ_{C} (75 MHz): 14.8 (CH₃, SCH₃), 21.5 (CH₃, ArCH₃), 91.2 (C, C≡C), 93.9 (C, C≡C), 112.4 (C, quaternary aromatic C), 119.8 (CH, aromatic CH), 120.7 (C, quaternary aromatic C), 123.4 (CH, aromatic CH), 124.2 (CH, aromatic CH), 124.5 (CH, aromatic CH), 127.9 (CH, 2 x aromatic CH), 129.2 (CH, 2 x aromatic CH), 129.2 (CH, aromatic CH), 129.9 (CH, aromatic CH), 131.9 (CH, aromatic CH), 132.1 (CH, aromatic CH), 132.4 (C, quaternary aromatic C), 139.4 (C, quaternary aromatic C), 141.3 (C, quaternary aromatic C), 142.2 (C, quaternary aromatic C), 166.2 (C, C=O); *m/z* (ESI) 358.47 [(M+H)⁺]; HRMS (ESI): exact mass calculated for C₂₃H₂₀NOS [(M+H)⁺], 358.1266. Found 358.1277.

Single crystals of **140** were grown from acetonitrile. Crystal data: C₂₃H₁₉NOS, *M* = 357.45, orthorhombic, space group *Pna*2₁, *a* = 18.196(7) Å, *b* = 24.721(7) Å, *c* = 4.0080(17) Å, *V* = 1802.9(11) Å³, *Z* = 4, *D_c* = 1.317 g cm⁻³, *F*(000) = 752, Mo Kα radiation, λ = 0.71073 Å, *T* = 300(2) K, $2\theta_{\max}$ = 25.84°, μ = 0.191 mm⁻¹, 12012 reflections collected, 3303 unique (*R_{int}* = 0.0420). Final GooF = 1.035, *R*₁ = 0.0399, *wR*₂ = 0.0871 (obs. data: *I* > 2σ(*I*)); *R*₁ = 0.0581, *wR*₂ = 0.0934 (all data).

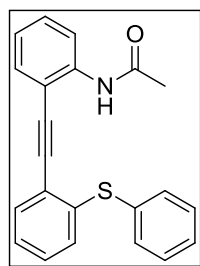
4-Methyl-N-2-[2-(methylsulfinyl)phenylethynyl]phenylbenzamide (141)

N-(2-Iodophenyl)-4-methylbenzamide, **119**, (0.08 g, 0.24 mmol), 1-ethynyl-2-(methylsulfinyl)benzene, **126**, (0.04 g, 0.27 mmol), triethylamine (2 mL) and DMF (2 mL) were stirred under nitrogen at room temperature for 10 min, then copper iodide (0.005 g, 0.02 mmol) and bis(triphenylphosphine)palladium(II) dichloride (0.01 g, 0.01 mmol) were added sequentially. The resulting mixture was heated to 60 °C and stirred for 18 h under nitrogen. The solution was then cooled to room temperature, poured onto water (5 mL) and extracted with EtOAc (3 x 5 mL). The organic layers were combined and washed with brine (10 mL), dried over MgSO₄ and concentrated *in vacuo*. The crude solid was purified by column chromatography using the eluent CH₂Cl₂/ethyl acetate (7:3). The resulting sulfoxide **141**, was obtained as a white solid (0.04 g, 48%). m.p. 168.8-170 °C; $\nu_{\max}/\text{cm}^{-1}$ (KBr): 3306 (NH), 3001 (CH), 2213 (C≡C), 1668 (C=O), 1572 (ring stretch), 1445 (CH₃), 1305 (S=O); δ_{H} (300 MHz): 2.36 (3H, s, ArCH₃), 2.59 (3H, s, SOCH₃), 7.07 (1H, td, *J* 7.6, 1.1, ArH), 7.25 (2H, d, *J* 7.8, ArH), 7.37-7.60 (5H, m, ArH), 7.79 (2H, d, *J* 8.1, ArH), 7.91 (1H, dd, *J* 7.8, 0.9, ArH), 8.46 (1H, d, *J* 7.8, ArH), 8.59 (1H, bs, NH); δ_{C} (75 MHz): 21.6 (CH₃, ArCH₃), 42.1 (CH₃, SOCH₃), 91.1 (C, C≡C), 93.2 (C, C≡C), 111.5 (C, quaternary aromatic C), 118.6 (C, quaternary aromatic C), 120.3 (CH, aromatic CH), 123.7 (CH, aromatic CH), 123.8 (CH, aromatic CH), 127.2 (CH, 2 x aromatic CH), 129.7 (CH, 2 x aromatic CH), 130.1 (CH, aromatic CH), 130.7 (CH, aromatic CH), 130.8 (CH, aromatic CH), 131.8 (C, quaternary aromatic C), 132.1 (CH, aromatic CH), 132.6 (CH, aromatic CH), 139.3 (C, quaternary aromatic C), 143.0 (C, quaternary aromatic C), 147.0 (C, quaternary aromatic C), 165.7 (C, C=O); *m/z* (ESI) 374.3 [(M+H)⁺]; HRMS (ESI): exact mass calculated for C₂₃H₂₀NO₂S [(M+H)⁺], 374.1215. Found 374.1197.

Single crystals of **141** were grown from acetonitrile. Crystal data: C₂₃H₁₉NO₂S, *M* = 373.45, monoclinic, space group *P*2₁/*c*, *a* = 21.597(16) Å, *b* = 5.319(4) Å, *c* = 18.133(13) Å, β = 113.493(14)°, *V* = 1910.(2) Å³, *Z* = 4, *D_c* = 1.299 g cm⁻³, *F*(000) = 784, Mo K α radiation, λ = 0.71073 Å, *T* = 296(2) K, $2\theta_{\max}$ = 21.15°, μ = 0.187 mm⁻¹, 6800 reflections collected, 2088 unique (*R_{int}* = 0.1403). Final GooF = 0.999, *R*₁ = 0.0577, *wR*₂ = 0.0892 (obs. data: *I* > 2 σ (*I*)); *R*₁ = 0.1549, *wR*₂ = 0.1264 (all data).

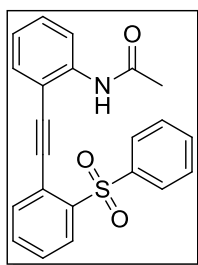
4-Methyl-N-2-[2-(methylsulfonyl)phenylethynyl]phenylbenzamide (142)

N-(2-Iodophenyl)-4-methylbenzamide, **119**, (0.08 g, 0.22 mmol), 2-methylsulfonyl ethynylbenzene, **127**, (0.04 g, 0.24 mmol), triethylamine (2 mL) and DMF (2 mL) were stirred under nitrogen at room temperature for 10 min, then copper iodide (0.008 g, 0.04 mmol) and bis(triphenylphosphine)palladium(II) dichloride (0.02 g, 0.02 mmol) were added sequentially. The resulting mixture was heated to 60 °C and stirred for 18 h under nitrogen. The solution was then cooled to room temperature, poured onto water (5 mL) and extracted with EtOAc (3 x 5 mL). The organic layers were combined and washed with brine (10 mL), dried over MgSO₄ and concentrated *in vacuo*. The crude solid was purified by column chromatography using CH₂Cl₂ as eluent to yield the title sulfone **142**, as a white solid (0.03 g, 28%). m.p. 154-156 °C; (Found: C, 70.72; H, 4.93; N, 2.93%. C₂₃H₁₉NO₃S requires C, 70.93; H, 4.92; N, 3.60%); $\nu_{\max}/\text{cm}^{-1}$ (KBr): 3339 (NH), 3014 (CH), 2216 (C≡C), 1655 (C=O), 1524 (ring stretch), 1300 (SO₂), 1153 (SO₂); δ_{H} (300 MHz): 2.41 (3H, s, ArCH₃), 2.97 (3H, s, SO₂CH₃), 7.14 (1H, td, *J* 7.6, 1.0, ArH), 7.27 (2H, d, *J* 8.4, ArH), 7.46 (1H, td, *J* 7.2, 1.5, ArH), 7.50-7.60 (2H, m, ArH), 7.63 (1H, td, *J* 7.6, 1.3, ArH), 7.72 (1H, dd, *J* 7.7, 1.4, ArH), 7.90 (2H, d, *J* 8.1, ArH), 8.08 (1H, dd, *J* 7.8, 1.2, ArH), 8.42 (1H, d, *J* 8.4, ArH), 9.00 (1H, bs, NH); δ_{C} (75 MHz): 21.5 (CH₃, ArCH₃), 42.3 (CH₃, SO₂CH₃), 91.3 (C, C≡C), 94.1 (C, C≡C), 112.2 (C, quaternary aromatic C), 121.8 (CH, aromatic CH), 123.8 (CH, aromatic CH), 128.1 (CH, 2 x aromatic CH), 129.0 (CH, 2 x aromatic CH), 129.2 (CH, 2 x aromatic CH), 129.4 (C, quaternary aromatic C), 130.6 (CH, aromatic CH), 131.7 (C, quaternary aromatic C), 132.5 (CH, aromatic CH), 133.4 (CH, aromatic CH), 134.3 (CH, aromatic CH), 140.1 (C, quaternary aromatic C), 140.7 (C, quaternary aromatic C), 142.6 (C, quaternary aromatic C), 167.7 (C, C=O); 9 signals observed for 10 aromatic CH signals *m/z* (ESI) 182.4, 390.3, 530.4 [(M+H)⁺]; 182.4 identified as C₉H₈O₂S; HRMS (ESI): exact mass calculated for C₂₃H₂₀NO₃S [(M+H)⁺], 390.1164. Found 390.1165.

N-2-[2-(Phenylthio)phenylethynyl]phenylacetamide (143)

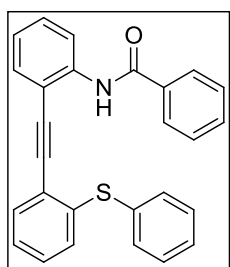
N-(2-Iodophenyl)acetamide, **115**, (0.09 g, 0.35 mmol), (2-ethynylphenyl)(phenyl)sulfane, **128**, (0.08 g, 0.38 mmol), triethylamine (2 mL) and DMF (2 mL) were stirred under nitrogen at room temperature for 10 min, then copper iodide (0.007 g, 0.35 mmol) and bis(triphenylphosphine)palladium(II) dichloride (0.01 g, 0.02 mmol) were added sequentially. The resulting mixture was heated to 60 °C and stirred for 2.5 h under nitrogen. The solution was then cooled to room temperature, poured onto water (5 mL) and extracted with EtOAc (3 x 5 mL). The organic layers were combined, washed with brine (10 mL), dried over MgSO₄ and concentrated *in vacuo*. The crude solid was purified by column chromatography using CH₂Cl₂ as eluent to give **143** as a dark brown solid (0.03 g, 22%). m.p. 91-93 °C; (Found: C, 76.99; H, 5.16; N, 3.75%. C₂₂H₁₇NOS requires C, 76.94; H, 4.99; N, 4.08%); $\nu_{\max}/\text{cm}^{-1}$ (KBr): 3367 (NH), 2206 (C≡C), 1690 (C=O), 1576 (ring stretch), 1519 (NH), 1443 (CH₃), 1301 (C-N), 751 (C-S); δ_{H} (300 MHz): 2.19 (3H, s, COCH₃), 7.02-7.09 (2H, m, ArH), 7.18-7.25 (2H, m, ArH), 7.31-7.42 (4H, m, ArH), 7.44-7.52 (3H, m, ArH), 7.54-7.61 (1H, m, ArH), 8.48 (1H, d, *J* 8.4, ArH), 8.56 (1H, bs, NH); δ_{C} (75 MHz): 25.1 (CH₃, COCH₃), 90.7 (C, C≡C), 94.0 (C, C≡C), 111.5 (C, quaternary aromatic C), 119.4 (CH, aromatic CH), 122.5 (C, quaternary aromatic C), 123.2 (CH, aromatic CH), 126.4 (CH, aromatic CH), 128.6 (CH, aromatic CH), 129.0 (CH, aromatic CH), 129.3 (CH, aromatic CH), 129.8 (CH, 2 x aromatic CH), 130.0 (CH, aromatic CH), 131.6 (CH, aromatic CH), 132.2 (CH, aromatic CH), 132.6 (C, quaternary aromatic C), 133.1 (CH, aromatic CH), 139.2 (C, quaternary aromatic C), 139.5 (C, quaternary aromatic C), 168.8 (C, C=O); *m/z* (ESI) 344.3 [(M+H)⁺]; HRMS (ESI): exact mass calculated for C₂₂H₁₈NOS [(M+H)⁺], 344.1109. Found 344.1118.

Single crystals of **143** were grown from acetonitrile. Crystal data: C₂₂H₁₇NOS, *M* = 343.43, monoclinic, space group *P*2₁/*c*, *a* = 19.8741(16) Å, *b* = 5.1206(4) Å, *c* = 18.8843(16) Å, β = 111.922(2)°, *V* = 1782.8(3) Å³, *Z* = 4, *D_c* = 1.279 g cm⁻³, *F*(000) = 720, Mo K α radiation, λ = 0.71073 Å, *T* = 296(2) K, $2\theta_{\max}$ = 27.76°, μ = 0.190 mm⁻¹, 21585 reflections collected, 4197 unique (*R_{int}* = 0.0343). Final GooF = 1.050, *R*₁ = 0.0659, *wR*₂ = 0.1699 (obs. data: *I* > 2 σ (*I*)); *R*₁ = 0.1076, *wR*₂ = 0.2011 (all data).

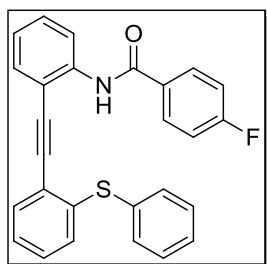
***N*-2-[2-(Phenylsulfonyl)phenylethynyl]phenylacetamide (144)**

N-(2-Iodophenyl)acetamide, **115**, (0.07 g, 0.25 mmol), 1-ethynyl-2-(phenylsulfonyl)benzene, **128**, (0.07 g, 0.28 mmol), triethylamine (2 mL) and DMF (2 mL) were stirred under nitrogen at room temperature for 10 min, then copper iodide (0.01 g, 0.05 mmol) and bis(triphenylphosphine)palladium(II) dichloride (0.02 g, 0.03 mmol) were added sequentially. The resulting mixture was heated to 60 °C and stirred for 2.5 h under nitrogen. The solution was then cooled to room temperature, poured onto water (5 mL) and extracted with EtOAc (3 x 5 mL). The organic layers were combined and washed with brine (10 mL), dried over MgSO₄ and concentrated *in vacuo*. The crude solid was purified by column chromatography, using CH₂Cl₂/ethyl acetate (9:1) as eluent to afford **144**, as a white solid (0.09 g, 95%). m.p. 125-127 °C; (Found: C, 70.15; H, 4.49; N, 3.63%. C₂₂H₁₇NO₃S requires C, 70.38; H, 4.56; N, 3.73%); $\nu_{\max}/\text{cm}^{-1}$ (KBr): 3295 (NH), 2212 (C≡C), 1666 (C=O), 1575 (ring stretch), 1528 (NH), 1446 (C-N), 1302 (SO₂), 1154 (SO₂); δ_{H} (300 MHz): 2.25 (3H, s, COCH₃), 6.97 (1H, td, *J* 7.6, 1.1, ArH), 7.29-7.37 (4H, m, ArH), 7.40-7.53 (3H, m, ArH), 7.58 (1H, dd, *J* 7.7, 1.4, ArH), 7.81-7.87 (2H, m, ArH), 8.11 (1H, dd, *J* 7.7, 1.4, ArH), 8.53 (1H, d, *J* 8.4, ArH), 8.94 (1H, bs, NH); δ_{C} (75 MHz): 24.7 (CH₃, COCH₃), 91.8 (C, C≡C), 93.8 (C, C≡C), 110.6 (C, quaternary aromatic C), 120.0 (CH, aromatic CH), 122.0 (C, quaternary aromatic C), 123.0 (CH, aromatic CH), 127.6 (CH, 2 x aromatic CH), 129.0 (CH, aromatic CH), 129.2 (CH, 2 x aromatic CH), 129.5 (CH, aromatic CH), 130.7 (CH, aromatic CH), 132.1 (CH, aromatic CH), 133.3 (CH, aromatic CH), 133.6 (CH, aromatic CH), 134.6 (CH, aromatic CH), 140.6 (C, quaternary aromatic C), 140.9 (C, quaternary aromatic C), 141.0 (C, quaternary aromatic C), 170.3 (C, C=O); *m/z* (ESI) 376.3 [(M+H)⁺]; HRMS (ESI): exact mass calculated for C₂₂H₁₈NO₃S [(M+H)⁺], 376.1007. Found 376.0999.

Single crystals of **144** were grown from acetonitrile. Crystal data: C₂₂H₁₇NO₃S, *M* = 375.43, monoclinic, space group *P*2₁/*c*, *a* = 18.7171(7) Å, *b* = 10.3330(4) Å, *c* = 9.6906(3) Å, β = 90.532(2)°, *V* = 1874.12(12) Å³, *Z* = 4, *D*_c = 1.331 g cm⁻³, *F*(000) = 784, Mo K α radiation, λ = 0.71073 Å, *T* = 296(2) K, $2\theta_{\max}$ = 66.10°, μ = 1.717 mm⁻¹, 15687 reflections collected, 3189 unique (*R*_{int} = 0.0307). Final GooF = 1.055, *R*₁ = 0.0365, *wR*₂ = 0.1025 (obs. data: *I* > 2 σ (*I*)); *R*₁ = 0.0404, *wR*₂ = 0.1062 (all data).

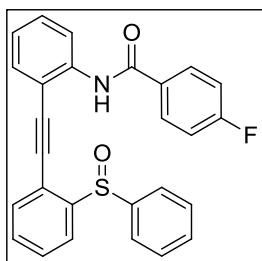
***N*-2-[2-(Phenylthio)phenylethynyl]phenylbenzamide (145)**

N-(2-Iodophenyl)benzamide, **116**, (0.16 g, 0.49 mmol), (2-ethynylphenyl)(phenyl)sulfane, **128**, (0.11 g, 0.53 mmol), triethylamine (2 mL) and DMF (2 mL) were stirred under nitrogen at room temperature for 10 min, then copper iodide (0.02 g, 0.10 mmol) and bis(triphenylphosphine)palladium(II) dichloride (0.04 g, 0.05 mmol) were added sequentially. The resulting mixture was heated to 60 °C and stirred for 18 h under nitrogen. The solution was then cooled to room temperature, poured onto water (5 mL) and extracted with EtOAc (3 x 5 mL). The organic layers were combined and washed with brine, dried over MgSO₄ and concentrated *in vacuo*. Purification was achieved by column chromatography using CH₂Cl₂/ethyl acetate (7:3) as eluent. The title compound, **145** was obtained as a dark brown solid (0.10 g, 15%); m.p. 96-98 °C; $\nu_{\max}/\text{cm}^{-1}$ (film): 3369 (NH), (C≡C stretch not observed), 1679 (C=O), 1516 (ring stretch), 1303 (C-N), 751 (C-S); δ_{H} (300 MHz): 6.90-6.97 (1H, m, ArH), 7.11 (1H, td, *J* 7.6, 1.1, ArH), 7.14-7.19 (2H, m, ArH), 7.24-7.37 (8H, m, ArH), 7.41 (1H, td, *J* 7.2, 1.7, ArH), 7.51-7.57 (2H, m, ArH), 7.91-7.97 (2H, m, ArH), 8.57 (1H, d, *J* 8.1, ArH), 8.97 (1H, bs, NH); δ_{C} (75 MHz): 90.8 (C, C≡C), 94.2 (C, C≡C), 112.4 (C, quaternary aromatic C), 119.9 (CH, aromatic CH), 121.7 (C, quaternary aromatic C), 123.6 (CH, aromatic CH), 125.9 (CH, aromatic CH), 127.6 (CH, 2 x aromatic CH), 128.3 (CH, aromatic CH), 128.5 (CH, aromatic CH), 128.6 (CH, 2 x aromatic CH), 129.3 (CH, aromatic CH), 129.5 (CH, 2 x aromatic CH), 130.0 (CH, aromatic CH), 131.7 (CH, aromatic CH), 132.1 (CH, aromatic CH), 132.4 (C, quaternary aromatic C), 132.4 (CH, aromatic CH), 133.5 (CH, 2 x aromatic CH), 135.1 (C, quaternary aromatic C), 139.2 (C, quaternary aromatic C), 140.2 (C, quaternary aromatic C), 166.3 (C, C=O); *m/z* (ESI) 406.3 [(M+H)⁺]; HRMS (ESI): exact mass calculated for C₂₇H₂₀NOS [(M+H)⁺], 406.1266. Found 406.1251.

4-Fluoro-*N*-2-[2-(phenylthio)phenylethynyl]phenylbenzamide (146)

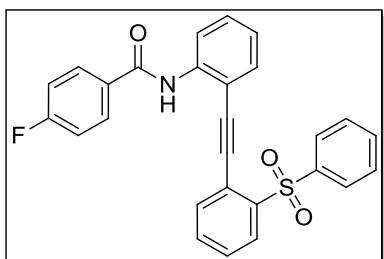
4-Fluoro-*N*-(2-iodophenyl)benzamide, **118**, (0.23 g, 0.68 mmol), (2-ethynylphenyl)(phenyl)sulfane, **128**, (0.16 g, 0.75 mmol), triethylamine (2 mL) and DMF (2 mL) were stirred under nitrogen at room temperature for 10 min, then copper iodide (0.03 g, 0.14 mmol) and bis(triphenylphosphine)palladium(II) dichloride (0.05 g, 0.08 mmol) were added sequentially. The resulting mixture was heated to 60 °C and stirred for 18 h under nitrogen. The solution was then cooled to room temperature, poured onto water (5 mL) and extracted with EtOAc (3 x 5 mL). The organic layers were combined and washed with brine (10 mL), dried over MgSO₄ and concentrated *in vacuo*. The crude solid was purified by column chromatography using the eluent CH₂Cl₂/ethyl acetate (1:1) to afford the title compound, **146**, as a pale yellow solid (0.11 g, 37%). m.p. 113-115 °C; $\nu_{\max}/\text{cm}^{-1}$ (KBr): 3202 (NH), (C≡C stretch not observed), 1646 (C=O), 1601 (ring stretch), 1501 (ring stretch), 1232 (C-N), 754 (C-S); δ_{H} (300 MHz): 6.95 (2H, t, *J* 8.6, ArH), 7.07 (1H, td, *J* 7.6, 1.1, ArH), 7.20-7.26 (3H, m, ArH), 7.32-7.40 (2H, m, ArH), 7.41-7.53 (5H, m, ArH), 7.73-7.86 (3H, m, ArH), 8.40 (1H, d, *J* 8.1, ArH), 8.67 (1H, bs, NH); δ_{C} (75 MHz): 92.0 (C, C≡C), 92.7 (C, C≡C), 111.9 (C, quaternary aromatic C), 115.9 (CH, d, ²*J*_{C-F} 22.0, aromatic CH), 120.2 (C, quaternary aromatic C), 120.5 (CH, aromatic CH), 124.1 (CH, aromatic CH), 124.7 (CH, aromatic CH), 124.9 (CH, 2 x aromatic CH), 129.2 (CH, 2 x aromatic CH), 129.6 (CH, d, ³*J*_{C-F} 9.1, aromatic CH), 130.1 (CH, aromatic CH), 130.7 (CH, aromatic CH), 131.1 (CH, aromatic CH), 131.2 (CH, aromatic CH), 132.1 (CH, aromatic CH), 132.8 (CH, aromatic CH), 139.2 (C, quaternary aromatic C), 144.5 (C, quaternary aromatic C), 146.9 (C, quaternary aromatic C), 164.8 (C, C=O), 165.0 (C, ¹*J*_{C-F} 253.2, quaternary aromatic C-F); 6 signals observed for 7 quaternary aromatic C; *m/z* (ESI) 342.2, 424.1 [(M+H)⁺]; HRMS (ESI): exact mass calculated for C₂₇H₁₉NOFS [(M+H)⁺], 424.1171. Found 424.1173.

Single crystals of **146** were grown from acetonitrile. Crystal data: C₂₇H₁₈FNOS, *M* = 423.48, monoclinic, space group *P*2₁/*n*, *a* = 5.095(2) Å, *b* = 27.806(12) Å, *c* = 14.648(6) Å, β = 90°, *V* = 2075.2(15) Å³, *Z* = 4, *D*_c = 1.356 g cm⁻³, *F*(000) = 880, Mo K α radiation, λ = 0.71073 Å, *T* = 296(2) K, $2\theta_{\max}$ = 24.56°, μ = 0.185 mm⁻¹, 21862 reflections collected, 3399 unique (*R*_{int} = 0.1940). Final GooF = 0.970, *R*₁ = 0.0570, *wR*₂ = 0.0844 (obs. data: *I* > 2 σ (*I*)); *R*₁ = 0.1668, *wR*₂ = 0.1005 (all data).

4-Fluoro-*N*-2-[2-(phenylsulfinyl)phenylethynyl]phenylbenzamide (147)

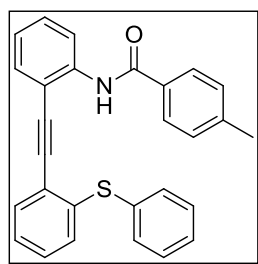
4-Fluoro-*N*-(2-iodophenyl)benzamide, **118**, (0.08 g, 0.24 mmol), 1-ethynyl-2-(phenylsulfinyl)benzene, **129**, (0.06 g, 0.27 mmol), triethylamine (2 mL) and DMF (2 mL) were stirred under nitrogen at room temperature for 10 min, then copper iodide (0.009 g, 0.05 mmol) and bis(triphenylphosphine)palladium(II) dichloride (0.02 g, 0.03 mmol) were added sequentially. The resulting mixture was heated to 60 °C and stirred for 18 h under nitrogen. The solution was then cooled to room temperature, poured onto water (5 mL) and extracted with EtOAc (3 x 5 mL). The organic layers were combined and washed with brine (10 mL), dried over MgSO₄ and concentrated *in vacuo*. The crude solid was purified by column chromatography using the eluent CH₂Cl₂/ethyl acetate (19:1). The sulfoxide **147** was obtained as a white solid (0.40 g, 37%). m.p. 165-167 °C; $\nu_{\max}/\text{cm}^{-1}$ (KBr): 3300 (NH), 2211 (C≡C), 1648 (C=O), 1505 (ring stretch), 1237 (C-N), 1041 (S=O); δ_{H} (300 MHz): 7.06 (2H, t, *J* 8.5, ArH), 7.18 (1H, td, *J* 7.6, 1.1, ArH), 7.30-7.37 (3H, m, ArH), 7.43-7.57 (2H, m, ArH), 7.52-7.62 (5H, m, ArH), 7.82-7.90 (2H, m, ArH), 7.92-7.96 (1H, m, ArH), 8.52 (1H, d, *J* 8.1, ArH), 8.73 (1H, bs, NH); δ_{C} (75 MHz): 92.1 (C, C≡C), 92.7 (C, C≡C), 111.8 (C, quaternary aromatic C), 116.0 (CH, d, $^2J_{\text{C-F}}$ 22.0, aromatic CH), 120.2 (C, quaternary aromatic C), 120.4 (CH, aromatic CH), 124.0 (CH, aromatic CH), 124.7 (CH, aromatic CH), 125.0 (CH, 2 x aromatic CH), 129.3 (CH, 2 x aromatic CH), 129.6 (CH, d, $^3J_{\text{C-F}}$ 9.1, aromatic CH), 130.1 (CH, aromatic CH), 130.7 (CH, aromatic CH), 131.1 (CH, aromatic CH), 131.2 (CH, aromatic CH), 132.1 (CH, aromatic CH), 132.8 (CH, aromatic CH), 139.2 (C, quaternary aromatic C), 144.5 (C, quaternary aromatic C), 146.9 (C, quaternary aromatic C), 164.8 (C, C=O), 165.0 (C, $^1J_{\text{C-F}}$ 253.2, quaternary aromatic C-F); 6 signals observed for 7 quaternary aromatic C; *m/z* (ESI) 440.1 [(M+H)⁺]; HRMS (ESI): exact mass calculated for C₂₇H₁₉NO₂FS [(M+H)⁺], 440.1121. Found 440.1111.

Single crystals of **147** were grown from acetonitrile. Crystal data: C₂₇H₁₈FNO₂S, *M* = 439.48, monoclinic, space group *P*2₁/*n*, *a* = 4.7664(8) Å, *b* = 29.372(5) Å, *c* = 15.354(3) Å, β = 94.982(4)°, *V* = 2141.4(7) Å³, *Z* = 4, *D_c* = 1.363 g cm⁻³, *F*(000) = 912, Mo K α radiation, λ = 0.71073 Å, *T* = 296(2) K, $2\theta_{\max}$ = 25.11°, μ = 0.185 mm⁻¹, 22498 reflections collected, 3816 unique (*R_{int}* = 0.0405). Final GooF = 1.008, *R*₁ = 0.0338, *wR*₂ = 0.0775 (obs. data: *I* > 2 σ (*I*)); *R*₁ = 0.0506, *wR*₂ = 0.0859 (all data).

4-Fluoro-*N*-2-[2-(phenylsulfonyl)phenyl]ethynylphenylbenzamide (148)

4-Fluoro-*N*-(2-iodophenyl)benzamide, **118**, (0.08 g, 0.24 mmol), 1-ethynyl-2-(phenylsulfonyl)benzene, **130**, (0.06 g, 0.26 mmol), triethylamine (2 mL) and DMF (2 mL) were stirred under nitrogen at room temperature for 10 min, then copper iodide (0.009 g, 0.05 mmol) and bis(triphenylphosphine)palladium(II) dichloride (0.02 g, 0.03 mmol) were added sequentially. The resulting mixture was heated to 60 °C and stirred for 18 h under nitrogen. The solution was then cooled to room temperature, poured onto water (5 mL) and extracted with EtOAc (3 x 5 mL). The organic layers were combined and washed with brine (10 mL), dried over MgSO₄ and concentrated *in vacuo*. The crude material was purified by column chromatography using CH₂Cl₂/ethyl acetate (19:1) as eluent, to yield **148**, as a pale yellow solid (0.09 g, 82%). m.p. 160-162 °C; $\nu_{\max}/\text{cm}^{-1}$ (KBr): 3414 (NH), 2207 (C≡C), 1677 (C=O), 1505 (ring stretch), 1315 (SO₂), 1235 (C-N), 1041 (SO₂); δ_{H} (300 MHz): 7.04 (2H, t, *J* 8.6, ArH), 7.14 (1H, td, *J* 7.6, 1.1, ArH), 7.33 (2H, t, *J* 7.7, ArH), 7.44-7.65 (6H, m, ArH), 7.80-7.85 (2H, m, ArH), 7.96-8.04 (2H, m, ArH), 8.17-8.22 (1H, m, ArH), 8.52 (1H, d, *J* 8.7, ArH), 9.12 (1H, bs, NH); δ_{C} (75 MHz): 92.0 (C, C≡C), 93.4 (C, C≡C), 112.1 (C, quaternary aromatic C), 115.4 (CH, d, ²*J*_{C-F} 21.9, aromatic CH), 121.1 (CH, aromatic CH), 121.8 (C, quaternary aromatic C), 123.8 (CH, aromatic CH), 127.8 (CH, 2 x aromatic CH), 128.9 (CH, 2 x aromatic CH), 129.1 (CH, aromatic CH), 129.5 (CH, aromatic CH), 130.4 (CH, d, ³*J*_{C-F} 9.2, aromatic CH), 130.5 (CH, aromatic CH), 132.2 (CH, aromatic CH), 133.2 (CH, aromatic CH), 133.4 (CH, aromatic CH), 134.6 (CH, aromatic CH), 140.0 (C, quaternary aromatic C), 140.5 (C, quaternary aromatic C), 141.6 (C, quaternary aromatic C), 165.0 (C, ¹*J*_{C-F} 252.5, quaternary aromatic C-F), 165.6 (C, C=O); 6 signals observed for 7 quaternary aromatic C; *m/z* (ESI) 456.1 [(M+H)⁺]; HRMS (ESI): exact mass calculated for C₂₇H₁₉NO₃FS [(M+H)⁺], 456.1070. Found 456.1057.

Single crystals of **148** were grown from acetonitrile. Crystal data: C₂₇H₁₈FNO₃S, *M* = 455.48, monoclinic, space group *P*2₁/*n*, *a* = 12.251(2) Å, *b* = 7.5687(13) Å, *c* = 23.787(4) Å, β = 99.304(5)°, *V* = 2176.6(7) Å³, *Z* = 4, *D*_c = 1.390 g cm⁻³, *F*(000) = 944, Mo K α radiation, λ = 0.71073 Å, *T* = 296(2) K, $2\theta_{\max}$ = 26.47°, μ = 0.188 mm⁻¹, 24227 reflections collected, 4473 unique (*R*_{int} = 0.0764). Final GooF = 1.001, *R*₁ = 0.0465, *wR*₂ = 0.0960 (obs. data: *I* > 2 σ (*I*)); *R*₁ = 0.0988, *wR*₂ = 0.1183 (all data).

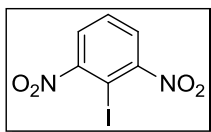
4-Methyl-N-2-[2-(phenylthio)phenyl]ethynylphenylbenzamide (149)

N-(2-Iodophenyl)-4-methylbenzamide, **119**, (0.15 g, 0.43 mmol), (2-ethynylphenyl)(phenyl)sulfane, **128**, (0.1 g, 0.48 mmol), triethylamine (2 mL) and DMF (2 mL) were stirred under nitrogen at room temperature for 10 min, then copper iodide (0.02 g, 0.09 mmol) and bis(triphenylphosphine)palladium(II) dichloride (0.03 g, 0.05 mmol) were added sequentially. The resulting mixture was heated to 60 °C and stirred for 18 h under nitrogen. The solution was then cooled to room temperature, poured onto water (5 mL) and extracted with EtOAc (3 x 5 mL). The organic layers were combined and washed with brine, dried over MgSO₄ and concentrated *in vacuo*. The crude solid was purified by column chromatography using CH₂Cl₂ as eluent to yield **149**, as an orange solid (0.02 g, 9%). m.p. 92-93 °C; $\nu_{\max}/\text{cm}^{-1}$ (KBr): 3389 (NH), (C≡C stretch not observed), 1678 (C=O), 1505 (ring stretch), 1431 (CH₃), 1300 (C-N), 749 (C-S); δ_{H} (300 MHz): 2.18 (3H, s, ArCH₃), 6.81-6.89 (1H, m, ArH), 6.97 (2H, d, *J* 8.1, ArH), 7.03 (1H, td, *J* 7.5, 1.2, ArH), 7.06-7.14 (2H, m, ArH), 7.19-7.28 (5H, m, ArH), 7.33 (1H, td, *J* 7.2, 1.5, ArH), 7.43-7.50 (2H, m, ArH), 7.75 (2H, d, *J* 8.4, ArH), 8.48 (1H, d, *J* 7.8, ArH), 8.86 (1H, bs, NH); δ_{C} (75 MHz): 21.4 (CH₃, ArCH₃), 90.9 (C, C≡C), 94.1 (C, C≡C), 112.3 (C, quaternary aromatic C), 119.9 (CH, aromatic CH), 121.6 (C, quaternary aromatic C), 123.4 (CH, aromatic CH), 125.8 (CH, aromatic CH), 127.6 (CH, 2 x aromatic CH), 128.1 (CH, aromatic CH), 128.4 (CH, aromatic CH), 129.2 (C, quaternary aromatic C), 129.2 (CH, 2 x aromatic CH), 129.5 (CH, 2 x aromatic CH), 129.9 (CH, aromatic CH), 132.0 (CH, aromatic CH), 132.3 (C, quaternary aromatic C), 132.4 (CH, aromatic CH), 132.4 (C, quaternary aromatic C), 133.7 (CH, 2 x aromatic CH), 139.4 (C, quaternary aromatic C), 140.3 (C, quaternary aromatic C), 142.1 (C, quaternary aromatic C), 166.3 (C, C=O); *m/z* (ESI) 100.2, 142.3, 420.1 [(M+H)⁺]; HRMS (ESI): exact mass calculated for C₂₈H₂₂NOS [(M+H)⁺], 420.1422. Found 420.1440.

Single crystals of **149** were grown from acetonitrile. Crystal data: C₂₈H₂₁NOS, *M* = 419.53, monoclinic, space group *P*2₁/*c*, *a* = 12.823(4) Å, *b* = 9.727(3) Å, *c* = 17.598(6) Å, β = 91.015(7)°, *V* = 2194.6(12) Å³, *Z* = 4, *D_c* = 1.270 g cm⁻³, *F*(000) = 880, Mo K α radiation, λ = 0.71073 Å, *T* = 296(2) K, $2\theta_{\max}$ = 26.54°, μ = 0.168 mm⁻¹, 12264 reflections collected, 4512 unique (*R_{int}* = 0.0272). Final GooF = 1.212, *R*₁ = 0.0425, *wR*₂ = 0.1107 (obs. data: *I* > 2σ(*I*)); *R*₁ = 0.0693, *wR*₂ = 0.1230 (all data).

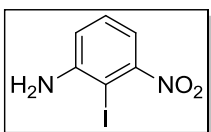
5.6. Introduction of competing hydrogen bond donor

2-Iodo-1,3-dinitrobenzene (**158**)⁴³

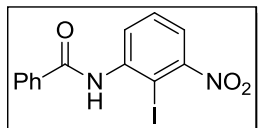


2,6-Dinitroaniline, **157**, was first diazotised using the Gunstone method.⁴⁴ Sodium nitrate (0.84 g, 12.1 mmol) was added slowly over a period of 10-15 mins to concentrated sulphuric acid (10 mL) under nitrogen. The solution was heated to 70 °C and stirred until the sodium nitrate was fully dissolved. The resulting mixture was then cooled to 25 °C and a solution of 2,6-dinitroaniline, **157**, (2.00 g, 11.0 mmol) in hot glacial acetic acid (25 mL) was added slowly to the mixture maintaining the temperature at 25 °C. The mixture was then stirred at 40 °C for 1 h. Diazotised 2,6-dinitroaniline was treated with a solution of potassium iodide (3.65 g, 22.0 mmol) in water (20 mL) and resulted in the formation 2-iodo-1,3-dinitrobenzene, **158**, as a dark orange solid which was subsequently filtered and dried (2.67 g, 82%). m.p: 115-117 °C (Lit.⁴³ 115-117 °C); $\nu_{\max}/\text{cm}^{-1}$ (KBr): 3088 (=C-H), 1543 (NO₂), 1349 (NO₂); δ_{H} (300 MHz): 7.63-7.68 (1H, m, ArH), 7.82 (1H, s, ArH), 7.85 (1H, s).

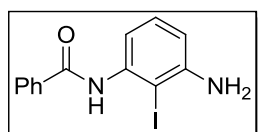
2-Iodo-3-nitroaniline (**159**)⁴²



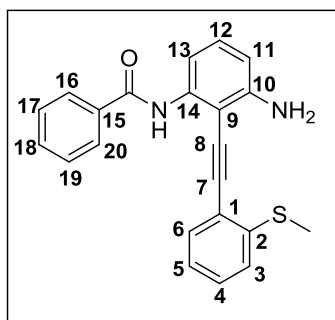
This compound was prepared according to a modified version of Jones procedure.⁴² A mixture of 2-iodo-1,3-dinitrobenzene, **158**, (5.40 g, 18.0 mmol) and acetic acid (60 mL) was heated to 110 °C under nitrogen. Iron powder (< 212 micron, 2.97 g, 53.0 mmol) was added in small portions to the solution. The mixture was then heated under reflux with vigorous stirring for 2.5 h and poured onto cold water (250 mL). The product was extracted with CH₂Cl₂ (3 x 100 mL), dried over MgSO₄ and concentrated *in vacuo*. Purification was achieved by column chromatography using hexane/ethyl acetate (2:1), as eluent to afford 2-iodo-3-nitroaniline, **159**, as an orange solid (2.04 g, 43%). m.p: 84-85 °C (Lit.⁴⁵ 84-85 °C); $\nu_{\max}/\text{cm}^{-1}$ (KBr): 3460 (NH), 3367 (NH₂), 1619 (ring stretch), 1513 (NO₂), 1350 (NO₂); δ_{H} (300 MHz): 4.54 (2H, bs, NH₂), 6.88 (1H, dd, *J* 8.1, 1.5, ArH), 7.05 (1H, dd, *J* 7.8, 1.5, ArH), 7.21 (1H, t, *J* 8.0, ArH). Spectral characteristics were in agreement with those previously reported.⁴²

***N*-(2-Iodo-3-nitrophenyl)benzamide (160)**⁴²

This compound was prepared according to a modified version of Jones procedure.⁴² 2-Iodo-3-nitroaniline, **159**, (2.03 g, 7.68 mmol), DMAP (ca. 1.0 mg) and CH₂Cl₂ (60 mL) were stirred under nitrogen. Pyridine (0.67 mL, 8.37 (mmol)) was added and the solution was stirred for 5 min and then benzoyl chloride, **111**, (1.95 mL, 16.8 mmol) was added dropwise over 5 min. The resulting solution was stirred for 6 h and then poured over aqueous HCl (2 M, 20 mL). The organic layer was extracted with CH₂Cl₂ (3 x 10 mL), dried over MgSO₄ and concentrated *in vacuo*. The crude product was purified by column chromatography using hexane/ethyl acetate (2:1) as eluent. The title compound **160**, was obtained as a yellow solid (2.13 g, 75%). $\nu_{\max}/\text{cm}^{-1}$ (KBr): 3368 (NH), 1650 (C=O), 1530 (NO₂); δ_{H} (300 MHz): 7.50-7.68 (5H, m, ArH), 7.97-8.03 (2H, m, ArH), 8.64 (1H, bs, NH), 8.68-8.75 (1H, m, ArH). Spectral characteristics were in agreement with those previously reported.⁴²

***N*-(2-Iodo-3-aminophenyl)benzamide (161)**⁴²

Tin(II) chloride dihydrate (6.64 g, 29.0 mmol) was added portionwise to a stirring solution of *N*-(2-iodo-3-nitrophenyl)benzamide, **160**, (2.13 g, 5.79 mmol) in EtOAc (20 mL) under nitrogen. The mixture was stirred for 5 h and then saturated NaHCO₃ (20 mL) was added. The suspension was filtered through celite[®] and washed several times with EtOAc. The organic filtrate was extracted with EtOAc (3 x 50 mL), dried over MgSO₄ and concentrated *in vacuo*. The crude product was purified by column chromatography, using hexane/ethyl acetate (2:1) as eluent to afford *N*-(2-iodo-3-aminophenyl)benzamide, **161**, as a cream coloured solid (1.72 g, 88%). m.p. 121-123 °C; $\nu_{\max}/\text{cm}^{-1}$ (KBr): 3358 (NH), 3221 (NH₂), 1615 (C=O), 1464 (ring stretch); δ_{H} (300 MHz): 4.19 (2H, bs, NH₂), 6.59 (1H, dd, *J* 8.1, 1.5, ArH), 7.19 (1H, t, *J* 8.0, ArH), 7.49-7.62 (3H, m, ArH), 7.82 (1H, dd, *J* 8.1, 1.5, ArH), 7.95-8.01 (2H, m, ArH), 8.27 (1H, bs, CONH). Spectral characteristics were in agreement with those previously reported.⁴²

***N*-3-Amino-2-[2-(methylthio)phenylethynyl]phenylbenzamide (162)**

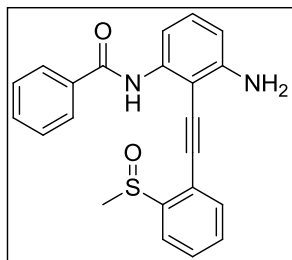
N-(2-Iodo-3-aminophenyl)benzamide, **161**, (0.13 g, 0.39 mmol), 1-ethynyl-2-methylthiobenzene, **123**, (0.06 g, 0.43 mmol), triethylamine (2 mL) and DMF (2 mL) were stirred under nitrogen at room temperature for 10 min, then copper iodide (0.007 g, 0.04 mmol) and bis(triphenylphosphine)-palladium(II) dichloride (0.015 g, 0.02 mmol) were added sequentially. The

resulting mixture was heated to 60 °C and stirred for 2.5 h under nitrogen. The solution was then cooled to room temperature, poured onto water (5 mL) and extracted with EtOAc (3 x 5 mL). The organic layers were combined and washed with brine (10 mL), dried over MgSO₄ and concentrated *in vacuo*. Purification was achieved by column chromatography using the eluent system CH₂Cl₂/ethyl acetate (9:1). The sulfide **162**, was obtained as a white solid (0.045 g, 34%). m.p. 120-122 °C; (Found: C, 73.12; H, 4.68; N, 6.52%. C₂₂H₁₈N₂OS requires C, 73.71; H, 5.06; N, 7.82%); $\nu_{\max}/\text{cm}^{-1}$ (KBr): 3479 (NH), 3371 (NH), 3314 (NH₂), 2203 (C≡C), 1652 (C=O), 1611 (NH₂), 1532 (NH), 1469 (ring stretch), 1306 (C-N), 743 (C-S); δ_{H} (600 MHz): 2.33 (3H, s, SCH₃), 4.48 (2H, bs, NH₂), 6.54 [1H, d (finely split), *J* 7.8, C(11)H], 7.15 [1H, td, *J* 7.5, 1.0, C(5)H], 7.18-7.23 [2H, m, C(3)H and C(12)H], 7.33 [1H, td, *J* 7.8, 1.2, C(4)H], 7.45-7.50 [3H, m, C(6)H, C(17)H and C(19)H], 7.55 [1H, t, *J* 7.2, C(18)H], 7.95-7.99 [3H, m, C(13)H, C(16)H and C(20)H], 8.88 (1H, bs, NH); δ_{C} (150 MHz): 15.0 (CH₃, SCH₃), 88.1 [C, C(8)], 97.8 [C, quaternary aromatic C(9)], 99.7 [C, C(7)], 109.2 [CH, aromatic C(13)], 109.8 [CH, aromatic C(11)], 120.8 [C, quaternary aromatic C(1)], 124.4 [CH, aromatic C(3)H], 124.6 [CH, aromatic C(5)H], 127.6 [2 x CH, aromatic C(16)H and aromatic C(20)H], 128.6 [2 x CH, aromatic C(17)H and aromatic C(19)H], 129.1 [CH, aromatic C(4)H], 130.7 [CH, aromatic C(12)H], 131.4 [CH, aromatic C(6)H], 131.7 [CH, aromatic C(18)H], 135.4 [C, quaternary aromatic C(15)], 139.4 [C, quaternary aromatic C(14)], 140.7 [C, quaternary aromatic C(2)], 148.4 [C, quaternary aromatic C(10)], 165.8 (C, C=O); NMR spectral assignment was aided by COSY, HSQC, HMBC and NOESY 2D NMR experiments; *m/z* (ESI) 359.1 [(M+H)⁺]; HRMS (ESI): exact mass calculated for C₂₂H₁₉N₂OS [(M+H)⁺], 359.1218. Found 359.1218.

Single crystals of **162** were grown from CH₂Cl₂. Crystal data: C₂₂H₁₈N₂OS, *M* = 358.44, orthorhombic, space group *Pna*2₁, *a* = 18.140(3) Å, *b* = 5.0400(9) Å, *c* = 19.369(3) Å, *V* = 1770.8(5) Å³, *Z* = 4, *D_c* = 1.334 g cm⁻³, *F*(000) = 752, Mo K α radiation, λ = 0.71073 Å, *T* = 300(2) K, 2 θ_{\max} = 25.10°, μ = 0.196 mm⁻¹, 13743 reflections collected, 3012 unique (*R_{int}* =

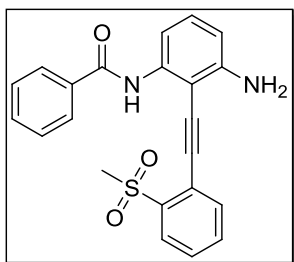
0.0631). Final GooF = 1.136, $R_1 = 0.0548$, $wR_2 = 0.1413$ (obs. data: $I > 2\sigma(I)$); $R_1 = 0.0757$, $wR_2 = 0.1638$ (all data).

***N*-3-Amino-2-[2-(methylsulfinyl)phenylethynyl]phenylbenzamide (163)**



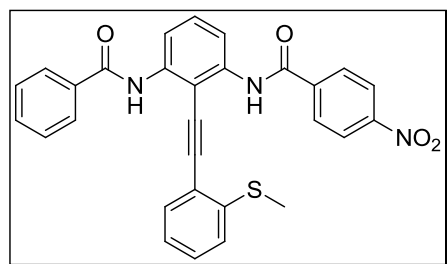
A solution of sodium periodate (0.03 g, 0.13 mmol) in water (2 mL) was added over 5 min to a stirred solution of *N*-3-amino-2-[2-(methylthio)phenylethynyl]phenylbenzamide, **162**, (0.02 g, 0.07 mmol) in methanol (3 mL) cooled to 0 °C. The reaction mixture was stirred for 16 h at room temperature and concentrated *in vacuo* to afford a colourless residue. The residue was partitioned between CH₂Cl₂ (20 mL) and water (10 mL). The layers were separated and the aqueous layer was further extracted with CH₂Cl₂ (2 x 10 mL). The combined organic layers were washed with water (2 x 10 mL), brine (10 mL), dried using MgSO₄ and concentrated *in vacuo*. Purification of the residue by column chromatography, using CH₂Cl₂/ethyl acetate (1:1) as eluent yielded the sulfoxide **163**, as a white solid (0.02 g, 65%). $\nu_{\max}/\text{cm}^{-1}$ (KBr): 3433 (NH), 3337 (NH), 2924 (CH), 2208 (C≡C), 1658 (C=O), 1624 (NH₂), 1523 (NH), 1470 (ring stretch), 1300 (C-N), 1026 (S=O); δ_{H} (600 MHz): 2.74 (3H, s, SOCH₃), 4.50 (2H, bs, NH₂), 6.54 (1H, dd, J 8.4, 0.6, ArH), 7.25 (1H, t, J 7.8, ArH), 7.50-7.57 (4H, m, ArH), 7.58-7.62 (2H, m, ArH), 7.91 (1H, d, J 8.4, ArH), 7.94-7.98 (3H, m, ArH), 8.61 (1H, bs, NH); δ_{C} (150 MHz): 41.9 (CH₃, SOCH₃), 90.5 (C, C≡C or quaternary aromatic C), 96.78 (C, C≡C or quaternary aromatic C), 96.84 (C, C≡C or quaternary aromatic C), 109.4 (CH, aromatic CH), 110.1 (CH, aromatic CH), 119.1 (C, quaternary aromatic C), 124.2 (CH, aromatic CH), 127.1 (CH, 2 x aromatic CH), 129.0 (CH, 2 x aromatic CH), 129.8 (CH, aromatic CH), 131.0 (CH, aromatic CH), 131.6 (CH, aromatic CH), 132.17 (CH, aromatic CH), 132.21 (CH, aromatic CH), 135.1 (C, quaternary aromatic C), 139.4 (C, quaternary aromatic C), 145.9 (C, quaternary aromatic C), 149.0 (C, quaternary aromatic C), 165.5 (C, C=O); m/z (ESI) 375.1 [(M+H)⁺]; HRMS (ESI): exact mass calculated for C₂₂H₁₉N₂OS [(M+H)⁺], 375.1167. Found 375.1169.

Single crystals of **163** were grown from CH₂Cl₂. Crystal data: C₂₂H₁₈N₂O₂S, $M = 374.44$, monoclinic, space group $P2_1/c$, formula $a = 8.8488(15)$ Å, $b = 21.149(4)$ Å, $c = 10.0801(17)$ Å, $\beta = 98.541(4)^\circ$, $V = 1865.5(5)$ Å³, $Z = 4$, $D_c = 1.333$ g cm⁻³, $F(000) = 784$, Mo K α radiation, $\lambda = 0.71073$ Å, $T = 296(2)$ K, $2\theta_{\max} = 25.05^\circ$, $\mu = 0.193$ mm⁻¹, 19006 reflections collected, 3277 unique ($R_{\text{int}} = 0.0763$). Final GooF = 1.027, $R_1 = 0.0571$, $wR_2 = 0.1463$ (obs. data: $I > 2\sigma(I)$); $R_1 = 0.1075$, $wR_2 = 0.1747$ (all data).

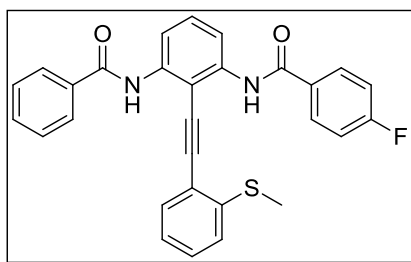
N-3-Amino-2-[2-(methylsulfonyl)phenylethynyl]phenylbenzamide (164)

N-(2-Iodo-3-aminophenyl)benzamide, **161**, (0.35 g, 1.03 mmol), 2-methylsulfonyl ethynylbenzene, **127**, (0.20 g, 1.13 mmol), triethylamine (2 mL) and DMF (2 mL) were stirred under nitrogen at room temperature for 10 min, then copper iodide (0.04 g, 0.20 mmol) and bis(triphenylphosphine)palladium(II) dichloride (0.08 g, 0.11 mmol) were added sequentially. The resulting mixture was heated to 60 °C and stirred for 18 h under nitrogen. The solution was then cooled to room temperature, poured onto water (5 mL) and extracted with EtOAc (3 x 5 mL). The organic layers were combined and washed with brine (10 mL), dried over MgSO₄ and concentrated *in vacuo*. Purification was achieved by column chromatography, using CH₂Cl₂/ethyl acetate (19:1) as eluent, to afford the sulfone **164**, as a white solid (0.14 g, 34%). m.p. 160-161 °C; $\nu_{\max}/\text{cm}^{-1}$ (KBr): 3450 (NH₂), 3360 (NH), 2201 (C≡C), 1673 (C=O), 1472 (ring stretch), 1304 (SO₂), 1151 (SO₂); δ_{H} (300 MHz): 3.19 (3H, s, SO₂CH₃), 4.87 (2H, bs, NH₂), 6.49 (1H, dd, *J* 8.1, 0.6, ArH), 7.23 (1H, t, *J* 8.3, ArH), 7.49-7.65 (7H, m, ArH), 7.85 (1H, d, *J* 7.8, ArH), 7.95-8.01 (2H, m, ArH), 8.12 (1H, d, *J* 7.8, ArH), 8.74 (1H, bs, NH); δ_{C} (75 MHz): 42.4 (CH₃, SO₂CH₃), 91.7 (C, C≡C or quaternary aromatic C), 96.3 (C, C≡C or quaternary aromatic C), 97.7 ((C, C≡C or quaternary aromatic C), 109.0 (CH, aromatic CH), 110.0 (CH, aromatic CH), 121.9 (C, quaternary aromatic C), 127.2 (CH, 2 x aromatic CH), 128.7 (CH, aromatic CH), 128.8 (CH, 2 x aromatic CH), 129.3 (CH, aromatic CH), 131.9 (CH, aromatic CH), 132.1 (CH, aromatic CH), 133.2 (CH, aromatic CH), 133.5 (CH, aromatic CH), 135.2 (C, quaternary aromatic C), 139.8 (C, quaternary aromatic C), 139.9 (C, quaternary aromatic C), 150.4 (C, quaternary aromatic C), 165.5 (C, C=O); *m/z* (ESI) 391.1 [(M+H)⁺]; HRMS (ESI): exact mass calculated for C₂₂H₁₉N₂O₃S [(M+H)⁺], 391.1116. Found 391.1108.

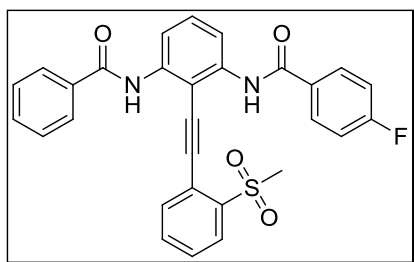
Single crystals of **164** were grown from CH₂Cl₂. Crystal data: C₂₂H₁₈N₂O₃S, *M* = 390.44, monoclinic, space group *P*2₁/*c*, *a* = 10.511(2) Å, *b* = 34.171(8) Å, *c* = 11.778(3) Å, β = 113.517(5)°, *V* = 3879.0(15) Å³, *Z* = 8, *D_c* = 1.337 g cm⁻³, *F*(000) = 1632, Mo K α radiation, λ = 0.71073 Å, *T* = 296(2) K, $2\theta_{\max}$ = 25.84°, μ = 0.192 mm⁻¹, 21664 reflections collected, 7387 unique (*R_{int}* = 0.0505). Final GooF = 1.003, *R*₁ = 0.0504, w*R*₂ = 0.1066 (obs. data: *I* > 2 σ (*I*)); *R*₁ = 0.1043, w*R*₂ = 0.1279 (all data).

***N*-[3-Benzamido-2-2-(methylthio)phenylethynylphenyl]-4-nitrobenzamide (165)**

DMAP (<0.001 g) was added to a stirring solution of the amine **162** (0.02 g, 0.07 mmol) in CH₂Cl₂ (2 mL), under nitrogen. Pyridine (0.01 mL, 0.16 mmol) was then added and the resulting solution was stirred for 10 mins at room temperature. 4-Nitrobenzoyl chloride, **112**, (0.03 g, 0.14 mmol) was then added and the mixture was stirred for 18 h. The reaction mixture was poured onto aqueous HCl (2 M, 10 mL) and extracted with CH₂Cl₂ (3 x 5 mL). The combined organic phases were washed with aqueous NaOH (2 M, 10 mL), dried over MgSO₄ and concentrated *in vacuo*. The amide **165** was obtained as a white solid which was sufficiently pure to use without further purification (0.03 g, 79%). m.p. 209-210 °C; (Found: C, 68.68; H, 4.17; N, 7.02%. C₂₉H₂₁N₃O₄S requires C, 68.62; H, 4.17; N, 8.28%); $\nu_{\max}/\text{cm}^{-1}$ (KBr): 3392 (NH), 3366 (NH), (C≡C stretch not observed), 1682 (C=O), 1512 (NH), 1467 (NO₂), 1300 (CN); δ_{H} (300 MHz): 2.20 (3H, s, SCH₃), 7.16-7.23 (2H, m, ArH), 7.38-7.45 (2H, m, ArH), 7.47-7.51 (3H, m, ArH), 7.56-7.63 (1H, m, ArH), 7.96-8.02 (2H, m, ArH), 8.13-8.19 (2H, m, ArH), 8.31-8.38 (3H, m, ArH), 8.42 (1H, dd, *J* 8.4, 0.6, ArH), 8.88 (2H, d, *J* 9.0, 2 x NH); δ_{C} (75 MHz): 14.7 (CH₃, SCH₃), 86.3 (C, C≡C or quaternary aromatic C), 101.8 (C, C≡C or quaternary aromatic C), 102.5 (C, C≡C or quaternary aromatic C), 115.2 (CH, aromatic CH), 115.8 (CH, aromatic CH), 119.4 (C, quaternary aromatic C), 123.9 (CH, 2 x aromatic CH), 124.5 (CH, aromatic CH), 124.9 (CH, aromatic CH), 127.5 (CH, 2 x aromatic CH), 128.80 (CH, 2 x aromatic CH), 128.81 (CH, 2 x aromatic CH), 130.2 (CH, aromatic CH), 131.0 (CH, aromatic CH), 131.4 (CH, aromatic CH), 132.2 (CH, aromatic CH), 134.9 (C, quaternary aromatic C), 138.5 (C, quaternary aromatic C), 139.4 (C, quaternary aromatic C), 140.5 (C, quaternary aromatic C), 141.1 (C, quaternary aromatic C), 149.8 (C, quaternary aromatic C), 163.7 (C, C=O), 165.7 (C, C=O); *m/z* (ESI) 508.1 [(M+H)⁺]; HRMS (ESI): exact mass calculated for C₂₉H₂₂N₃O₄S [(M+H)⁺], 508.1331. Found 508.1326.

N-[3-Benzamido-2-2-(methylthio)phenylethynylphenyl]-4-fluorobenzamide (166)

The amine, **162**, (0.06 g, 0.15 mmol) was stirred in CH_2Cl_2 (2 mL) under nitrogen. DMAP (<0.001 g) and pyridine (0.03 mL, 0.35 mmol) were then added and the resulting solution was stirred for 10 mins at room temperature. 4-Fluorobenzoyl chloride, **113**, (0.04 mL, 0.32 mmol) was then added dropwise over 1 min to the reaction vessel and the mixture was stirred for 18 h. The reaction mixture was poured onto aqueous HCl (2 M, 10 mL) and extracted with CH_2Cl_2 (3 x 5 mL). The combined organic phases were washed with aqueous NaOH (2 M, 10 mL), dried over MgSO_4 and concentrated *in vacuo*. The amide, **166**, was obtained as white solid without the need for further purification (0.07 g, 98%). (Found: C, 72.30; H, 4.46; N, 5.80%. $\text{C}_{29}\text{H}_{21}\text{FN}_2\text{O}_2\text{S}$ requires C, 72.48; H, 4.40; N, 5.83%); $\nu_{\text{max}}/\text{cm}^{-1}$ (KBr): 3385 (NH), 3375 (NH), 2196 ($\text{C}\equiv\text{C}$), 1684 ($\text{C}=\text{O}$), 1501 (NH), 1298 (CN); δ_{H} (300 MHz): 2.19 (CH_3 , SCH_3), 7.18 (4H, t, J 8.6, ArH), 7.36-7.45 (2H, m, ArH), 7.46-7.54 (3H, m, ArH), 7.55-7.62 (1H, m, ArH), 7.96-8.05 (4H, m, ArH), 8.30-8.40 (2H, m, ArH), 8.81 (1H, bs, NH), 8.87 (1H, bs, NH); δ_{C} (75 MHz): 14.7 (CH_3 , SCH_3), 86.6 (C, $\text{C}\equiv\text{C}$ or quaternary aromatic C), 101.6 (C, $\text{C}\equiv\text{C}$ or quaternary aromatic C), 102.2 (C, $\text{C}\equiv\text{C}$ or quaternary aromatic C), 115.1 (CH, aromatic CH), 115.2 (CH, aromatic CH), 115.6 (CH, d, $^2J_{\text{C-F}}$ 21.9, aromatic CH), 119.7 (C, quaternary aromatic C), 124.4 (CH, aromatic CH), 124.8 (CH, aromatic CH), 127.5 (CH, 2 x aromatic CH), 128.8 (CH, 2 x aromatic CH), 129.9 (C, quaternary aromatic C), 130.0 (CH, d, $^3J_{\text{C-F}}$ 21.9, aromatic CH), 130.9 (CH, aromatic CH), 131.4 (CH, aromatic CH), 132.0 (CH, aromatic CH), 135.0 (C, quaternary aromatic C), 139.1 (C, quaternary aromatic C), 139.3 (C, quaternary aromatic C), 141.3 (C, quaternary aromatic C), 164.7 (C, $\text{C}=\text{O}$), 165.8 (C, $\text{C}=\text{O}$); 11 signals seen for 12 aromatic CH; 7 signals seen for 8 quaternary aromatic C (C-F not observed); m/z (ESI) 481.2 [(M+H) $^+$]; HRMS (ESI): exact mass calculated for $\text{C}_{29}\text{H}_{21}\text{FN}_2\text{O}_2\text{S}$ [(M+H) $^+$], 481.1386. Found 481.1374.

***N*-[3-Benzamido-2-2-(methylsulfonyl)phenylethynylphenyl]-4-fluorobenzamide (167)**

DMAP (<0.001 g) and pyridine (0.02 mL, 0.18 mmol) were added to a stirred solution of the sulfone, **164**, (0.03 g, 0.08 mmol) in CH₂Cl₂ (2mL) under nitrogen and the resulting solution was stirred for 15 min at room temperature. 4-Fluorobenzoyl chloride, **113**, (0.02 mL, 0.17 mmol) was then added to the solution dropwise over 1 min and the vessel contents were stirred for 18 h. The reaction mixture was poured onto aqueous HCl (2 M, 10 mL) and extracted with CH₂Cl₂ (3 x 5 mL). The combined organic phases were washed with aqueous NaOH (2 M, 10 mL), dried over MgSO₄ and concentrated *in vacuo*. Purification was achieved by column chromatography using CH₂Cl₂/ethyl acetate (1:1) as eluent, to afford the amide, **164**, as a white solid (0.04 g, 97%). m.p. 212-214 °C; (Found: C, 67.24; H, 4.28; N, 4.59%. C₂₉H₂₁FN₂O₄S requires C, 67.96; H, 4.13; N, 5.47%); $\nu_{\max}/\text{cm}^{-1}$ (KBr): 3306 (NH), 2210 (C≡C), 1647 (C=O), 1312 (SO₂), 1155 (SO₂); δ_{H} (300 MHz): 2.85 (CH₃, SO₂CH₃), 7.18 (2H, t, *J* 8.7, ArH), 7.48-7.70 (7H, m, ArH), 7.95-8.04 (4H, m, ArH), 8.09 (1H, d, *J* 7.8, ArH), 8.20 (1H, dd, *J* 8.4, 0.9, ArH), 8.26 (1H, dd, *J* 8.3, 0.8, ArH), 8.88 (1H, bs, NH), 8.91 (1H, bs, NH); δ_{C} (75 MHz): 42.5 (CH₃, SO₂CH₃), 89.4 (C, C≡C or quaternary aromatic C), 98.8 (C, C≡C or quaternary aromatic C), 102.5 (C, C≡C or quaternary aromatic C), 115.8 (CH, d, ²*J*_{C-F} 21.8, aromatic CH), 116.4 (CH, aromatic CH), 116.8 (CH, aromatic CH), 120.9 (C, quaternary aromatic C), 127.5 (CH, 2 x aromatic CH), 128.8 (CH, 2 x aromatic CH), 129.6 (CH, aromatic CH), 129.8 (CH, aromatic CH), 130.3 (CH, d, ³*J*_{C-F} 9.0, aromatic CH), 130.7 (C, quaternary aromatic C), 131.6 (CH, aromatic CH), 132.3 (CH, aromatic CH), 133.5 (CH, aromatic CH), 133.7 (CH, aromatic CH), 134.7 (C, quaternary aromatic C), 140.1 (C, quaternary aromatic C), 140.2 (C, quaternary aromatic C), 140.5 (C, quaternary aromatic C), 165.4 (C, C=O), 166.0 (C, C=O); 7 signals seen for 8 quaternary aromatic C (C-F not observed); *m/z* (ESI) 513.2 [(M+H)⁺]; HRMS (ESI): exact mass calculated for C₂₉H₂₂FN₂O₄S [(M+H)⁺], 513.1284. Found 513.1280.

5.7. References

1. Heynderickx, A.; Samat, A.; Guglielmetti, R. *J. Heterocycl. Chem.*, **2001**, *38*, 737-742.
2. Creed, T.; Leardini, R.; McNab, H.; Nanni, D.; Nicolson, I. S.; Reed, D. *J. Chem. Soc., Perkin Trans. I*, **2001**, 1079-1085.
3. Crawford, L. A.; McNab, H. *Collect. Czech. Chem. Commun.*, **2009**, *74*, 995-1009.
4. Jackson, P. M.; Moody, C. J.; Shah, P. *J. Chem. Soc., Perkin Trans. I*, **1990**, 2909-2918.
5. Borbas, K. E.; Chandrashaker, V.; Muthiah, C.; Kee, H. L.; Holten, D.; Lindsey, J. S. *J. Org. Chem.*, **2008**, *73*, 3145-3158.
6. Abdel-Magid, A. F.; Carson, K. G.; Harris, B. D.; Maryanoff, C. A.; Shah, R. D. *J. Org. Chem.*, **1996**, *61*, 3849-3862.
7. Baxter, E. W.; Reitz, A. B. *Org. React.*, **2002**, *59*, No.
8. Golchoubian, H.; Hosseinpour, F. *Molecules*, **2007**, *12*, 304-310.
9. Prisinzano, T.; Podobinski, J.; Tidgewell, K.; Luo, M.; Swenson, D. *Tetrahedron: Asymmetry*, **2004**, *15*, 1053-1058.
10. Lehane, K. N.; Moynihan, E. J. A.; Brondel, N.; Lawrence, S. E.; Maguire, A. R. *CrystEngComm*, **2007**, *9*, 1041-1050.
11. Cloarec, J. M.; Charette, A. B. *Org. Lett.*, **2004**, *6*, 4731-4734.
12. Micali, E.; Chehade, K. A. H.; Isaacs, R. J.; Andres, D. A.; Spielmann, H. P. *Biochemistry*, **2001**, *40*, 12254-12265.
13. Munoz, L.; Bosch, M. P.; Rosell, G.; Guerrero, A. *Tetrahedron: Asymmetry*, **2009**, *20*, 420-424.
14. Martin, R. E.; Plancq, B.; Gavelle, O.; Wagner, B.; Fischer, H.; Bendels, S.; Muller, K. *ChemMedChem*, **2007**, *2*, 285-287.
15. Chantar, H.; Wilhelm, J. C.; Georges, J.; Schneider, M.; Mieloszynski, J. L.; Paquer, D. *Sulfur Lett.*, **1994**, *17*, 63-68.
16. Coleman, G. H.; Hauser, C. R. *J. Am. Chem. Soc.*, **1928**, *50*, 1193-1196.
17. Cere, V.; Pollicino, S.; Fava, A. *Tetrahedron*, **1996**, *52*, 5989-5998.
18. Carlsson, H.; Haukka, M.; Bousseksou, A.; Latour, J. M.; Nordlander, E. *Inorg. Chem.*, **2004**, *43*, 8252-8262.
19. Sun, G. C.; He, Z. H.; Li, Z. J.; Yuan, X. D.; Yang, Z. J.; Wang, G. X.; Wang, L. F.; Liu, C. R. *Molecules*, **2001**, *6*, 1001-1005.

20. Sarju, J.; Danks, T. N.; Wagner, G. *Tetrahedron Lett.*, **2004**, *45*, 7675-7677.
21. Abe, A. M. M.; Helaja, J.; Koskinen, A. M. P. *Org. Lett.*, **2006**, *8*, 4537-4540.
22. Clark, D. A.; Riccardis, F. D.; Nicolaou, K. C. *Tetrahedron*, **1994**, *50*, 11391-11426.
23. Singh, V.; Alam, S. Q.; Praveena, G. D. *Tetrahedron*, **2002**, *58*, 9729-9736.
24. Amato, M. E.; Ballistreri, F. P.; Pappalardo, A.; Sciotto, D.; Tomaselli, G. A.; Toscano, R. M. *Tetrahedron*, **2007**, *63*, 9751-9757.
25. Cronin, M. *Ph.D. Thesis, NUI 1998*.
26. Chirakul, P.; Hampton, P. D.; Bencze, Z. *J. Org. Chem.*, **2000**, *65*, 8297-8300.
27. Boudalis, A. K.; Aston, R. E.; Smith, S. J.; Mirams, R. E.; Riley, M. J.; Schenk, G.; Blackman, A. G.; Hanton, L. R.; Gahan, L. R. *Dalton Trans.*, **2007**, 5132-5139.
28. Kotha, S.; Shah, V. R. *Eur. J. Org. Chem.*, **2008**, 1054-1064.
29. Larock, R. C.; Yum, E. K.; Refvik, M. D. *J. Org. Chem.*, **1998**, *63*, 7652-7662.
30. Kabalka, G. W.; Wang, L.; Pagni, R. M. *Tetrahedron*, **2001**, *57*, 8017-8028.
31. Barbero, N.; Carril, M.; San, M.; Dominguez, E. *Tetrahedron*, **2007**, *63*, 10425-10432.
32. Evindar, G.; Batey, R. A. *J. Org. Chem.*, **2006**, *71*, 1802-1808.
33. Ganton, M. D.; Kerr, M. A. *Org. Lett.*, **2005**, *7*, 4777-4779.
34. Gimbert, C.; Vallribera, A. *Org. Lett.*, **2009**, *11*, 269-271.
35. Quesada, E.; Raw, S. A.; Reid, M.; Roman, E.; Taylor, R. J. K. *Tetrahedron*, **2006**, *62*, 6673-6680.
36. Belanger, D.; Tong, X.; Soumare, S.; Dory, Y. L.; Zhao, Y. *Chem. --Eur. J.*, **2009**, *15*, 4428-4436, S4428-1.
37. Curphey, T. J. *Org. Prep. Proced. Int.*, **1981**, *13*, 112-115.
38. Kelleher, L. L. *Ph.D. Thesis, NUI 1997*.
39. O'Keefe, E. *Ph.D. Thesis, NUI 2002*.
40. Mueller, S.; Liepold, B.; Roth, G. J.; Bestmann, H. J. *Synlett*, **1996**, 521-522.
41. Kitamura, T.; Takachi, T.; Soda, S.; Kawasato, H.; Taniguchi, H. *Chem. Lett.*, **1992**, 1357-1360.
42. Jones, I. M.; Hamilton, A. D. *Org. Lett.*, **2010**, *12*, 3651-3653.
43. Parker, R. E.; Read, T. O. *J. Chem. Soc.*, **1962**, 3149-3153.
44. Gunstone, F. D.; Tucker, S. H. *Org. Synth.*, **1952**, *32*, No.

45. Xu, Z.; Hu, W.; Liu, Q.; Zhang, L.; Jia, Y. *J. Org. Chem.*, **2010**, *75*, 7626-7635.

Appendices

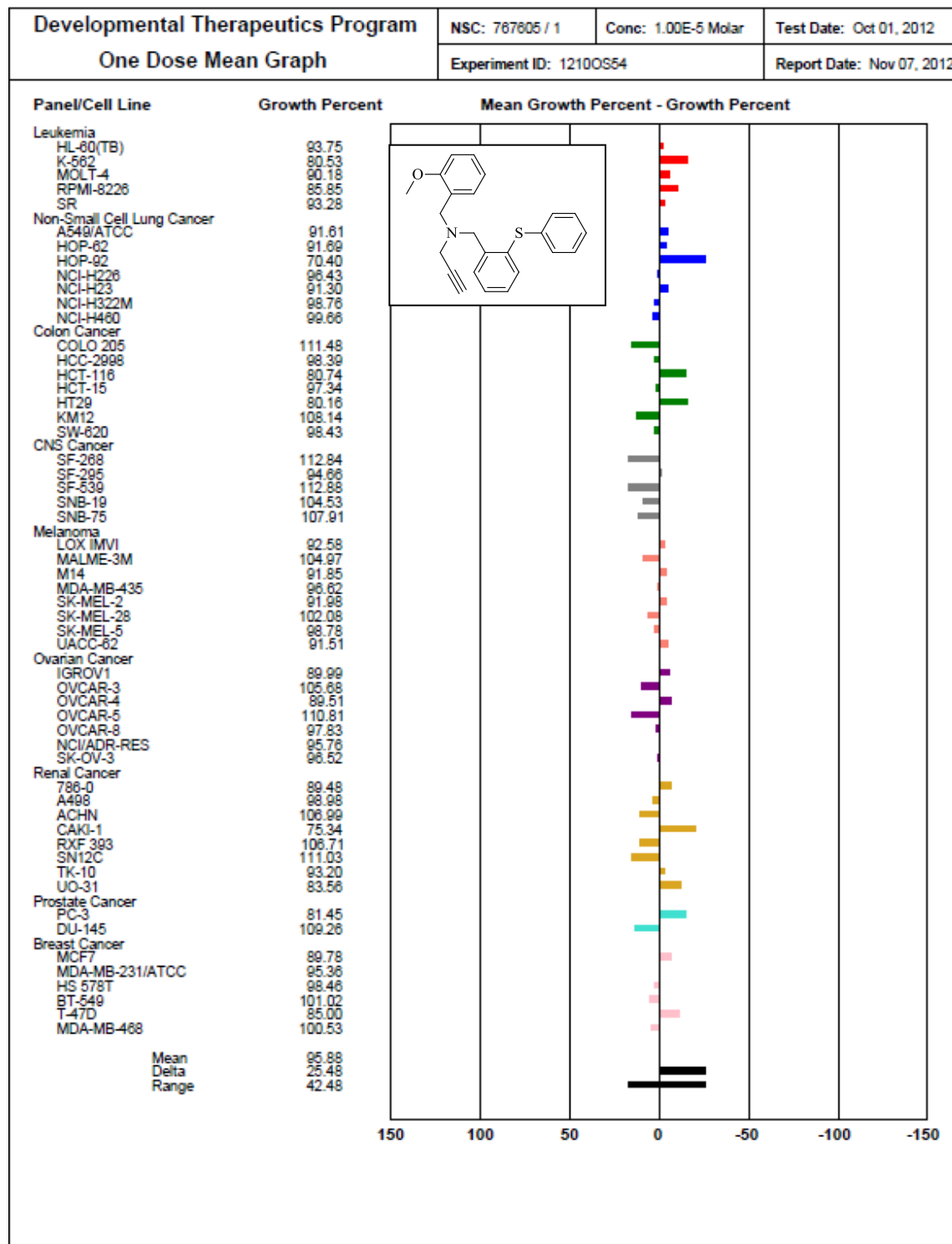
Appendix I: List of Abbreviations

Å	angstroms
°	degrees
Δ	heat
Ar	aryl
Bu	butyl
BuLi	butyllithium
Bn	benzyl
bp	boiling point
COSY	correlation spectroscopy
CSA	camphorsulfonic acid
CSD	Cambridge Structural Database
DEPT	distortionless enhancement of polarisation transfer
DMAP	(dimethylamino)pyridine
DMF	dimethylformamide
DMSO	dimethylsulfoxide
Et	ethyl
EWG	electron-withdrawing group
equiv	equivalents
FAD	flavin adenine dinucleotide
g	gram
h	hour(s)
HCl	hydrochloric acid
HMBC	heteronuclear multiple-bond correlation spectroscopy
HPLC	high performance liquid chromatography
HRMS	high resolution mass spectrometry
HSQC	heteronuclear single quantum coherence spectroscopy
IR	infrared
lit	literature
LSD1	lysine specific demethylase 1
<i>m</i> -	meta
M	molar
Me	methyl
MEP	molecular electrostatic potential
MHz	megahertz
min	minute(s)
mmol	millimole
mp	melting point
m.w	microwave
NCI	National Cancer Institute
NMR	nuclear magnetic resonance
NOE	nuclear overhauser effect
NOESY	nuclear overhauser effect spectroscopy
<i>p</i> -	para
PCC	pyridinium chlorochromate
2-PCPA	2-phenylcyclopropyl-amine
Ph	phenyl
rt	room temperature

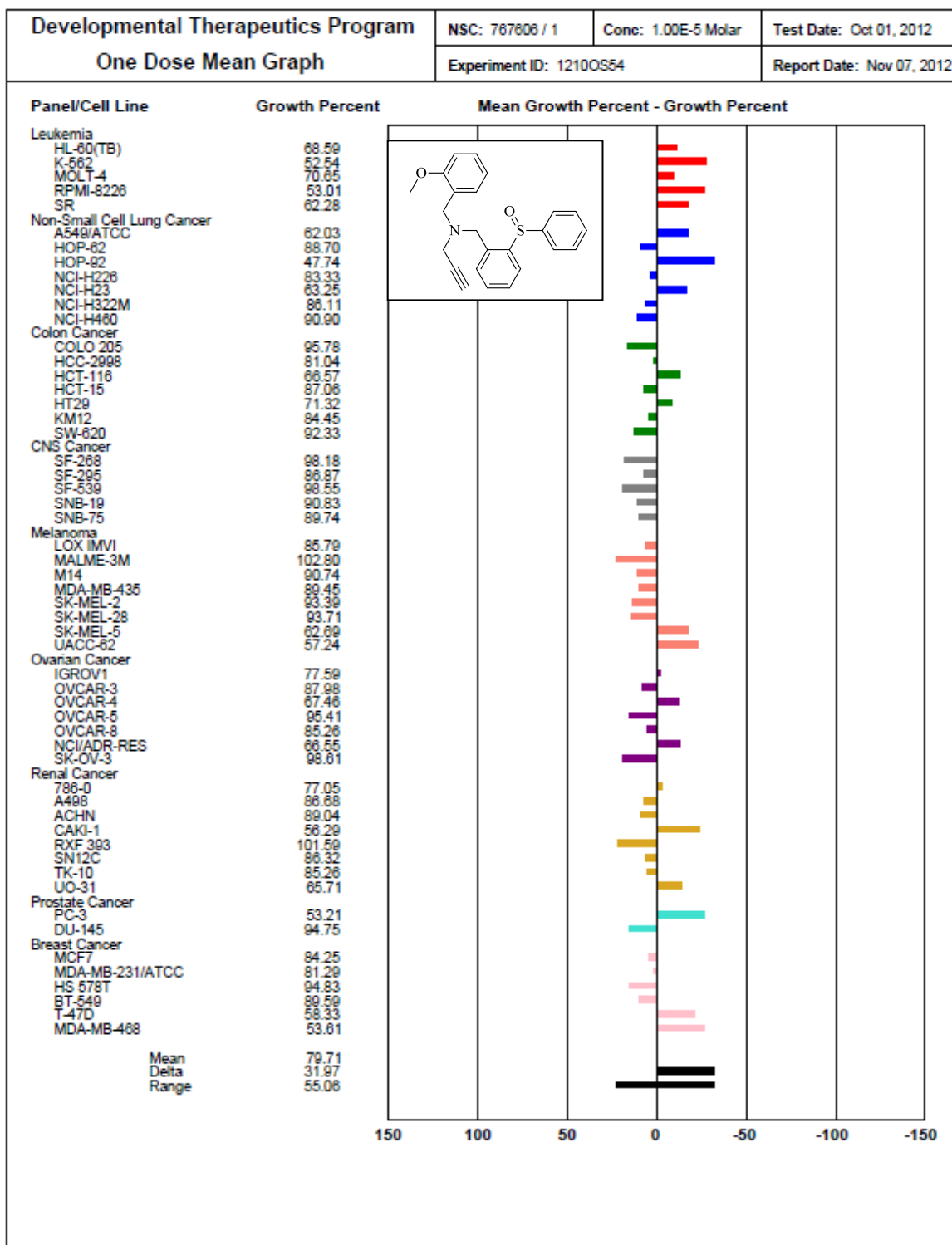
THF	tetrahydrofuran
TLC	thin layer chromatography
TMS	trimethylsilyl
U.V	ultra-violet

Appendix II: NCI-60 one dose results 'Mean Graph'

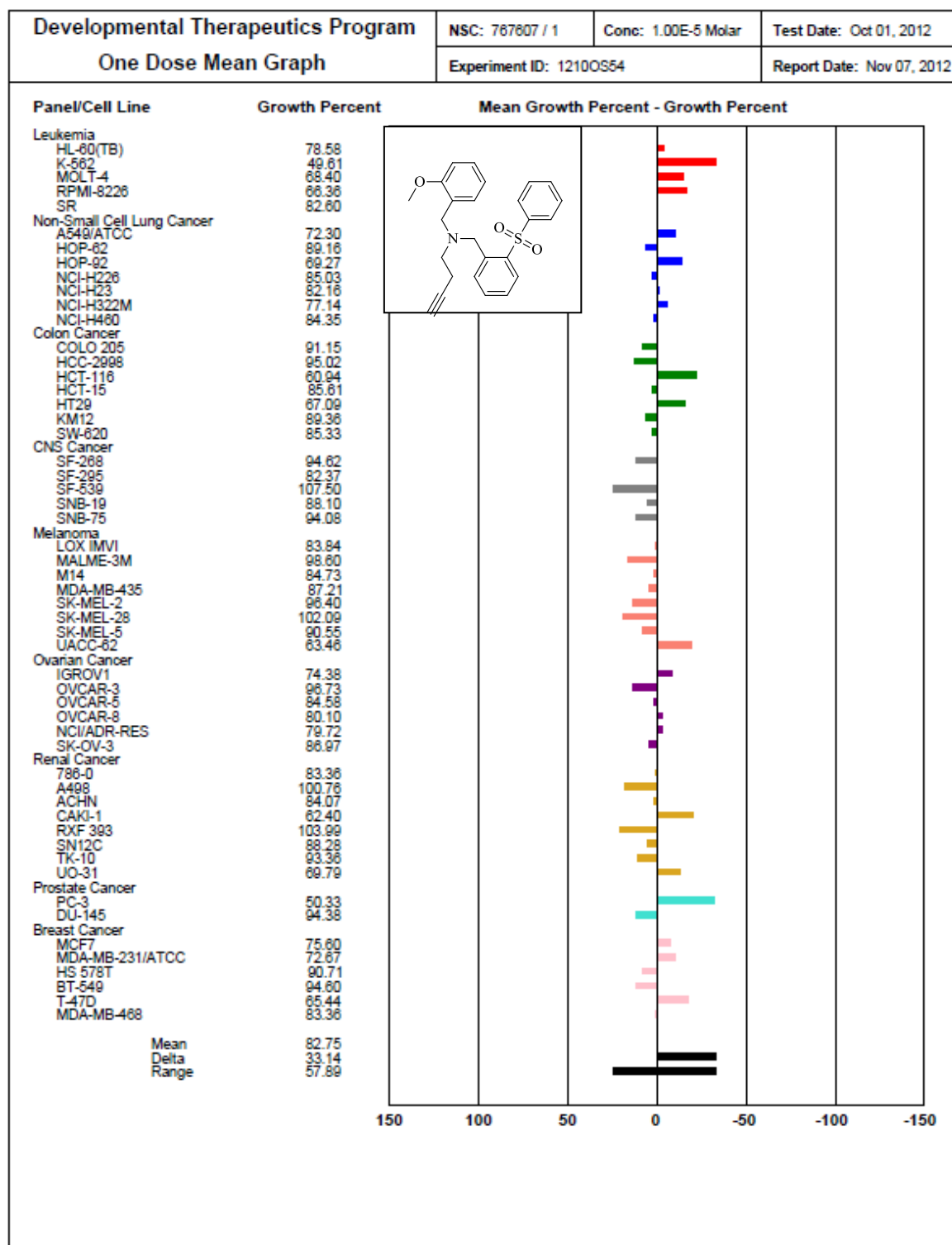
NSC: 767605/1 (26; 10 µM)



NSC: 767606/1 (36; 10 μM)



NSC: 767607/1 (47; 10 μ M)



NSC: 767608/1 (45; 10 μM)

